brain sciences

Deep Brain Stimulation (DBS) Applications

Edited by
Tipu Aziz and Alex Green

Printed Edition of the Special Issue Published in *Brain Sciences*

www.mdpi.com/journal/brainsci

MDPI

Deep Brain Stimulation (DBS) Applications

Special Issue Editors
Tipu Aziz
Alex Green

MDPI • Basel • Beijing • Wuhan • Barcelona • Belgrade

Special Issue Editors
Tipu Aziz
University of Oxford
UK

Alex Green
University of Oxford
UK

Editorial Office
MDPI AG
St. Alban-Anlage 66
Basel, Switzerland

This edition is a reprint of the Special Issue published online in the open access journal *Brainsciences* (ISSN 2076-3425) from 2016–2017 (available at: http://www.mdpi.com/journal/brainsci/special_issues/dbs).

For citation purposes, cite each article independently as indicated on the article page online and as indicated below:

Author 1; Author 2. Article title. *Journal Name* **Year**, *Article number*, page range.

First Edition 2017

ISBN 978-3-03842-538-0 (Pbk)
ISBN 978-3-03842-539-7 (PDF)

Table of Contents

Section 3: Deep Brain Stimulation for Pain and Autonomic Dysfunction

Section 4: Brain Stimulation for Psychiatric Disease

About the Special Issue Editors

Tipu Z. Aziz, Ph. D., is the founder and head of Oxford functional neurosurgery. His primate work was central to confirming the subthalamic nucleus as a possible surgical target for deep brain stimulation in Parkinson's disease and more recently the pedunculopontine nucleus. OFN is currently one of the busiest centres for such surgery in the UK and academically very productive. Research Interests are the role of the upper brain stem in the control of movement, the clinical neurophysiology of movement disorders and neuropathic pain and autonomic responses to deep brain stimulation, use of MR and MEG imaging in functional neurosurgery.

Alexander L. Green, Ph.D., has been looking at the neurocircuitry underlying autonomic function and pain in humans undergoing Deep Brain Stimulation (DBS) over the past ten years. There are several aims of this research. Firstly, he wishes to understand both the mechanisms underlying the pathophysiology of neuropathic pain as well as why some patients get much better than results than others. Secondly, by understanding the autonomic nervous system, it may be possible to control diseases such as hypertension, respiratory and bladder disease by brain manipulation in the future. Most of the research to date has involved stimulating brain areas under different experimental conditions and also recording local field potentials to understand the underlying neurophysiology. This work has resulted in a number of publications including improvement in peak expiratory flow with stimulation, the effect of stimulation on blood pressure and baroreceptors sensitivity and novel electrical signals associated with pain states.

Preface to "Deep Brain Stimulation (DBS) Application"

This special issue looks at some of the developments taking place in the field of brain stimulation, with a particular emphasis on deep brain stimulation. The broad nature of the manuscripts reflects the ever broadening nature of the field of Brain Stimulation. The papers in this issue reflect cutting edge research and clinical practice and range from preliminary concept to clinical trials i.e., work that is already being translated. The reader will see that the field of DBS which was very focused on movement disorders for a thirty year period until around 2000–2005 now includes treatment of obesity, Huntington's disease, Tourette's syndrome and there are explorations into other realms such as spinal cord injury and schizophrenia. Fast improving technology and developments in other areas of Neuroscience is being applied to DBS to make it better and to expand the indications. Whilst the early applications of DBS involved psychiatric disorders and pain, these indications are now being revisited. We hope that this collection of articles will be both informative and inspiring to the reader, who will, in turn, contribute to the ever increasing knowledge and development of this technique.

Tipu Aziz and Alex Green
Special Issue Editors

Section 1:
Deep Brain Stimulation for Movement and Neurodegenerative Disorders

brain sciences

MDPI

Article

Improvement of Advanced Parkinson's Disease Manifestations with Deep Brain Stimulation of the Subthalamic Nucleus: A Single Institution Experience

Ahmed Rabie [1,2], Leo Verhagen Metman [3], Mazen Fakhry [2], Ayman Youssef Ezeldin Eassa [4], Wael Fouad [2], Ahmed Shakal [5] and Konstantin V. Slavin [1,*]

1 Department of Neurosurgery, University of Illinois at Chicago, Chicago, IL 60612, USA; dr_a_rabie@hotmail.com
2 Department of Neurosurgery, Alexandria University, Alexandria, Egypt; mazenfakhry56@yahoo.com (M.F.); waelfouad_67@hotmail.com (W.F.)
3 Department of Neurological Sciences, Rush University Medical Center, Chicago, IL 60612, USA; lverhage@rush.edu
4 Department of Neurology, Alexandria University, Alexandria, Egypt; af_eassa@yahoo.com
5 Department of Neurosurgery, Tanta University, Tanta, Egypt; ahmedshakal@yahoo.com
* Correspondence: kslavin@uic.edu; Tel.: +1-312-996-4842; Fax +1-312-996-9018

Academic Editors: Tipu Aziz and Alex Green
Received: 9 September 2016; Accepted: 5 December 2016; Published: 13 December 2016

Abstract: We present our experience at the University of Illinois at Chicago (UIC) in deep brain stimulation (DBS) of the subthalamic nucleus (STN), describing our surgical technique, and reporting our clinical results, and morbidities. Twenty patients with advanced Parkinson's disease (PD) who underwent bilateral STN-DBS were studied. Patients were assessed preoperatively and followed up for one year using the Unified Parkinson's Disease Rating Scale (UPDRS) in "on" and "off" medication and "on" and "off" stimulation conditions. At one-year follow-up, we calculated significant improvement in all the motor aspects of PD (UPDRS III) and in activities of daily living (UPDRS II) in the "off" medication state. The "off" medication UPDRS improved by 49.3%, tremors improved by 81.6%, rigidity improved by 50.0%, and bradykinesia improved by 39.3%. The "off" medication UPDRS II scores improved by 73.8%. The Levodopa equivalent daily dose was reduced by 54.1%. The UPDRS IVa score (dyskinesia) was reduced by 65.1%. The UPDRS IVb score (motor fluctuation) was reduced by 48.6%. Deep brain stimulation of the STN improves the cardinal motor manifestations of the idiopathic PD. It also improves activities of daily living, and reduces medication-induced complications.

Keywords: subthalamic nucleus; deep brain stimulation; Parkinson's disease; neuromodulation; clinical outcome

1. Introduction

The deep brain stimulation (DBS) system consists of a lead that is implanted into a specific deep brain target. The lead is connected to an implantable pulse generator (IPG), which is the power source of the system. The lead and the IPG are connected by an extension wire that is tunneled under the skin between both of them. This system is used to chronically stimulate the deep brain target by delivering a high-frequency current to this target [1,2].

James Parkinson was the first to describe Parkinson's disease (PD) in 1817; he described it as a combination of tremor, rigidity, postural abnormalities, and bradykinesia [3]. The main step that marked the onset of stereotactic surgery and the surgical treatment of different movement disorders was in 1947, when Ernest Spiegel and Henry Wycis invented the first frame-based stereotactic apparatus

"stereoencephalotome". This was the first device to be used for localization of targets in the living human brain [4]. They performed the first stereotactic thalamotomy and pallidotomy, but the clinical effects were disappointing [5,6].

The credit goes to Leksell for using the posteroventral pallidum as the target for lesioning [7]. At the same time, the ventrolateral (VL) nucleus of the thalamus emerged as a target for lesioning, and with time it replaced pallidotomy for the treatment of tremors [8–10].

The discovery of Levodopa in the late 1960s led to a decline in surgeries for PD. Lesioning of the ventral intermediate (Vim) nucleus of the thalamus and the globus pallidus internus (GPi) continued to be the major surgical targets.

The first published work describing the use of DBS in the treatment of PD was by Benabid et al. in Montreal, France in 1987. They proved that high-frequency DBS was able to mimic, in a reversible and adjustable manner, the effects of ablation of Vim as the target to control tremors [11–13]. The first attempt to use the GPi as the target of DBS to treat PD was by Siegfried and Lippitz, published in 1994. DBS of the GPI proved efficiency in controlling tremors, bradykinesia, and drug-induced dyskinesias [14–16]. The subthalamic nucleus (STN) was investigated in animal studies as a target for Parkinson's disease surgery [17]. Lesioning of the STN in humans proved to be effective in reducing the three cardinal symptoms of PD [18,19]. Again, Benabid and the Grenoble group were the pioneers in using DBS of the STN for the treatment of PD in 1994, based on findings from animal studies [20,21]. This led to the approval of DBS by the FDA as a method of treatment of PD. Since then the STN has been the target of choice for DBS in PD patients. It proved to be superior to medical therapy in controlling tremors, rigidity, and dyskinesia in advanced stages of PD [22–26].

Shakal et al. reported the first use of STN-DBS for the management of PD in Egypt in 2011 [27]. At the University of Illinois at Chicago (UIC), USA, DBS surgeries started with the work of the senior author (KVS) in early 2001. The work we are presenting here is a collaborative work between the Neurosurgery Department of Alexandria, Egypt and that of UIC. Here we present the STN-DBS experience at UIC, describe our surgical technique, and report our clinical results and morbidities. Our objectives are to evaluate the clinical outcome of STN-DBS in PD and share our experience in this field.

2. Methods

After obtaining an appropriate IRB approval, we retrospectively analyzed the data of 20 patients diagnosed with advanced PD who underwent bilateral STN-DBS at the UIC in the period from 2013 to 2014. Patients who qualified for surgery had idiopathic PD and showed sustained response to levodopa, with a minimum of 30% improvement in Unified Parkinson's Disease Rating Scale (UPDRS) motor subscore following a levodopa challenge. Most patients had severe levodopa-related motor response despite optimal dose adjustment, and/or disabling tremors. We excluded patients with atypical Parkinsonism as multiple system atrophy (MSA), progressive supranuclear palsy (PSP), corticobasal degeneration, vascular, and drug-induced parkinsonism. We also excluded patients with severe cognitive impairment or dementia (Mattis Dementia Rating Scale <130 or Mini Mental Status examination $\leq$24), patients with severe uncontrolled psychiatric illness or depression (Beck Depression Inventory II score >19), and patients with magnetic resonance imaging (MRI) features of moderate to severe cortical atrophy, ventricular enlargement, and significant white matter changes or other significant intracranial lesions such as tumor, arteriovenous malformations, etc. We also excluded patients with other significant illnesses.

2.1. Pre-Operative Patient Assessment and Selection

The first step of the patient assessment was to confirm the diagnosis of primary PD and exclude other forms of movement disorders and atypical forms of parkinsonism. To make the diagnosis, the patient must have at least two of the three motor features (rest tremors, bradykinesia, and rigidity), and bradykinesia must be one of those two features. The patient must have a good response to

dopaminergic drugs, as poor response suggests an atypical parkinsonian syndrome. We only included patients who had the disease for more than five years; this is to follow the recommendation of the core assessment program for surgical interventional therapies in PD (CAPSIT-PD) committee [28–31].

Each patient was asked to come for a second appointment after being off medications for 12 h to be evaluated for surgery. At this visit, the patient was assessed for mental state, behavior, and mood (part I of the UPDRS) [32–35]. Then the patient was assessed for activities of daily living (ADL), using part II of the UPDRS in both the "on" and "off" states. Then the patient was evaluated for levodopa-related complications using the UPDRS part IV [33,34,36], including the duration of motor fluctuation (items 36–39) and the severity of levodopa-induced dyskinesia (items 32–35). In the early phase of PD, symptoms can be controlled with dopaminergic medications [37,38]. After five or more years of dopaminergic therapy, about 50% of patients begin to experience motor fluctuations and dyskinesia and may become candidates for DBS [37,38]. In the late phase of PD, some patients become unresponsive to levodopa. Those patients are not considered surgical candidates for DBS [37,38]. Then the patient was assessed using the levodopa challenge test and the UPDRS motor scoring (part III) and video recorded. First, the scale was performed in an "off" state. Then the patient was given a supra-therapeutic dose of levodopa (1.5 times the patient's current dose) and the UPDRS motor scale was assessed again during the "best on state". At this visit, we also calculated the axial score by summing the motor subscores: speech, gait, posture, and postural stability (items 18, 28, 29, and 30 of the UPDRS part III). We also assessed the Modified Hoehn and Yahr Rating Scale (HYRS) [39], and the Schwab and England Rating Scale (SERS) [40]. Both of them were done in the "off" state. We also calculated the levodopa equivalent daily dose (LEDD) [41].

2.2. Neuropsychological and Psychiatric Evaluation

A dedicated psychologist then assessed the patient during the best "on" state.

The tests used for assessment were: Mattis Dementia Rating Scale (MDRS) [42], Beck Depression Inventory II (BDI-II) [43,44], Independent Living Scale (ILS)—Health and Safety, Mini Mental Status Exam (MMSE) [45,46], Peabody Picture Vocabulary Test—Fourth Edition (PPVT-4), Wechsler Adult Intelligence Scale for DSM-IV (WAIS-IV)—Digit Span, Wisconsin Card Sorting Test (WCST), Hopkins' Verbal Learning Test—Revised (HVLT-R), and Frontal System Behavior Scale (FrSBe).

This assessment is a mandatory step before surgery. It helps to exclude any patient with severe cognitive and or behavioral impairments (Mattis Dementia Rating Scale <130 or Mini Mental Status examination $\leq$24), severe uncontrolled psychiatric illness or depression (Beck Depression Inventory II score >19). This assessment also helped to establish the baseline of the mental, verbal, and frontal lobe functions for further follow-up.

2.3. Surgery

The surgery was done in two stages. In the first stage, we implanted DBS electrodes under local anesthesia using the frame-based stereotactic technique. The patient was instructed to stop all anti-Parkinsonian medications 12 h before surgery to facilitate microelectrode recording (MER), and allow clinical assessment during stimulation. The first step was the application of the Leksell frame Model G (Elekta Instruments, Inc., Atlanta, GA, USA) to the patient's head (Figure 1).

A high-resolution MRI of the patient's brain with 3-tesla scanner (Signa 3T94 VHi; General Electric Medical Systems, Milwaukee, WI, USA) was done. Two main sequences were obtained. The first is a 3D T1-weighted, spoiled gradient echo imaging of the entire head (section thickness: 2 mm; field of view: 26 $\times$ 26 cm; TR: 7.0–8.0 ms; TE: ~400 ms; flip angle: 12; band width: 31.25 KHz; acquisition time: <7 min). The second sequence is high-resolution, contiguous, T2-weighted, fast spin-echo imaging through the region of the midbrain and basal ganglia (section thickness: 1.5 mm; slice interval: 0 mm; matrix size: 512 $\times$ 512; field of view: 26 $\times$ 26 cm; TR: 4600–6200 ms; TE: 95–108 ms; acquisition time: <5 min) (Figure 2).

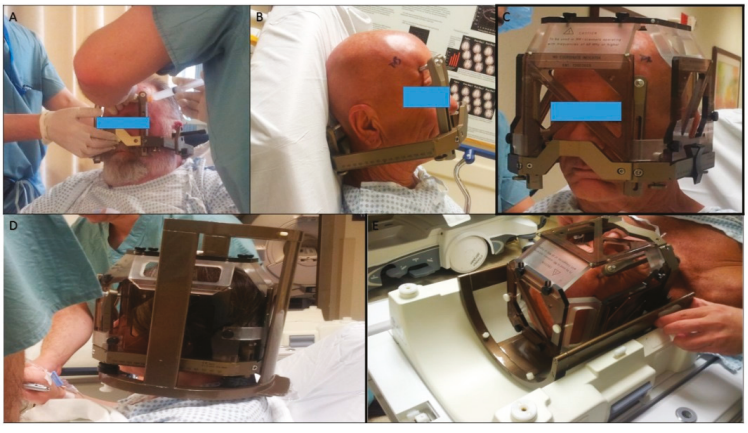

Figure 1. Different steps of Leksell frame application. (**A**) Application of the frame with the ear bars; note that the assistant is holding the frame in position with a lateral bar parallel to the intercommissural line while the senior surgeon is injecting a local anesthetic at the site of pin fixation; (**B**) position of the frame after its application; (**C**) the magnetic resonance imaging (MRI) localizer attached to the frame base; (**D**) the MRI localizer and the table adaptor attached to the frame base; (**E**) the table adaptor fitting to the MRI table.

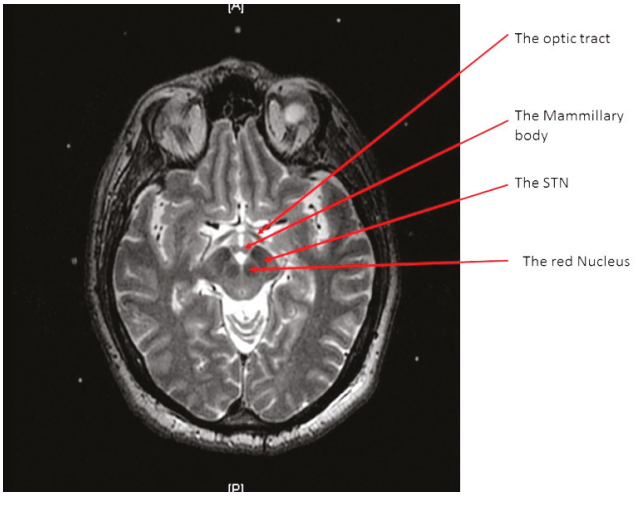

Figure 2. An axial T2 weighted magnetic resonance imaging (MRI) image at the level of the subthalamic nuclei (STN).

At the end of the scan, we chose an axial T2 image (or two adjacent images) in which both the AC and the PC are seen (Figure 3). With simple arithmetic equations based on the Leksell frame coordinates system, we were able to calculate the stereotactic coordinates of the mid-commissural point (MCP), and the STN directly from the MRI coordinates of the AC and the PC (Figure 4). Based on the known anatomical relationship of the STN to MCP from the previous anatomical studies and stereotactic atlases [36,47–54], we selected the STN target at 12 mm lateral, 3 mm posterior, and 6 mm inferior to the MCP.

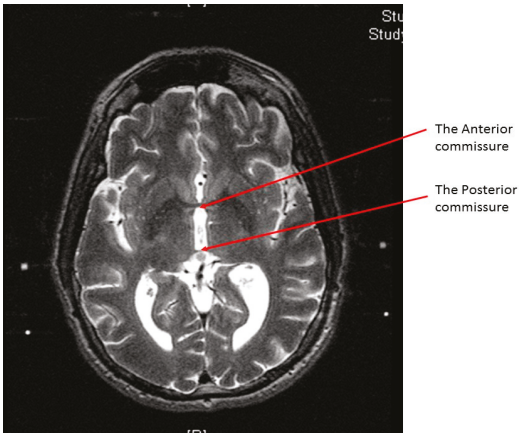

Figure 3. An axial T2 weighted magnetic resonance imaging (MRI) image showing the anterior commissure and the posterior commissure.

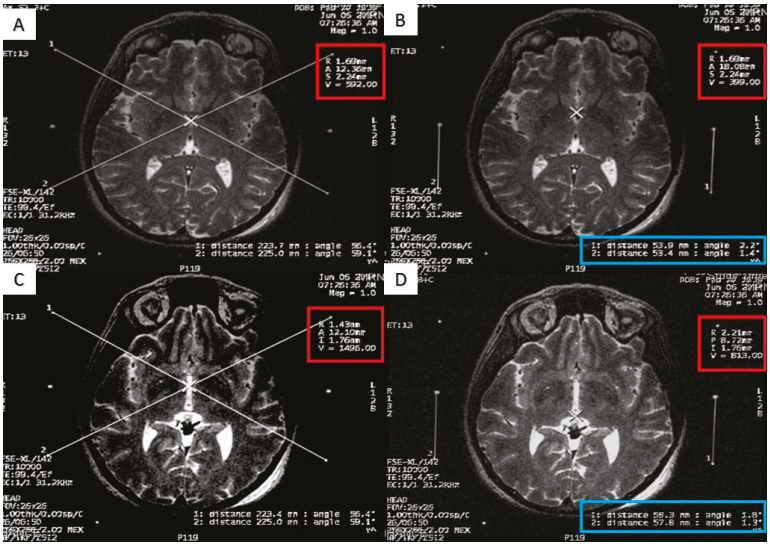

Figure 4. Calculating the anterior commissure (AC) and posterior commissure (PC) coordinates using the magnetic resonance console. (**A**) Two diagonal lines intersecting at the center of the frame at the AC level with the magnetic resonance imaging (MRI) coordinates of the center of the frame shown inside the red square; (**B**) a crosshair at the posterior margin of the AC, with the MRI coordinates of the AC shown inside the red square. Two lines are drawn between the middle and the lower fiducials on both sides of the frame and their lengths (in the blue rectangle) are used to calculate the Z coordinate of the AC. (**C**) Two diagonal lines intersecting at the center of the frame at the PC level with the MRI coordinates of the center of the frame shown inside the red square; (**D**) a crosshair at the anterior margin of the PC, with the MRI coordinates of the PC shown inside the red square. Two lines are drawn between the middle and the lower fiducials on both sides of the frame and their lengths (in the blue rectangle) are used to calculate the Z coordinates of the PC.

The second method we used to calculate the STN coordinates was direct visualization of the STN on a T2 weighted MRI (Figure 5) [55]. The STN is the almond-shaped hypointense structure located lateral and anterior to the red nucleus. We identified an axial T2 image that showed the largest red nuclei circumference, and then we drew a line from the midline, medial to lateral, along the anterior edge of RN. The center of the STN was chosen at the extension of this straight line about 12 mm from the midline. Then the coordinates were calculated using the same Excel worksheet. Another method of the STN coordinates localization was done in the OR, using the FrameLink software, which is a part of the StealthStation navigation system (Medtronic, Minneapolis, MN, USA) (Figure 6). The software compensates for head and frame tilt in any direction. It allows calculation of the STN coordinates and planning of suitable entry point and trajectory of the DBS electrode that avoid going through the cortical sulci, the ventricles, or any cerebral blood vessels. The final coordinates for the procedure were derived from all the previous techniques and subsequently adjusted using intraoperative electrical microrecording and macrostimulation.

In the operating room, the patient was placed on the operating table with a Leksell frame secured to the table using a Mayfield adapter. The C-arm was placed around the patient in order to use intraoperative fluoroscopy for electrode tracking and positioning (Figure 7). We used transparent sterile drapes to allow easier communication with the patient and observation of the patient's symptoms during this awake procedure (Figure 8). Two semicircular incisions were made on both sides of the midline (Figure 9). Then we drilled two burr holes, one on each side, 1 cm anterior to the coronal suture and 2–3 cm lateral to the midline. We started the surgeries with the left side and then shifted to the right side.

We performed microelectrode recording (MER) of the brain activity using a NeuroNav microelectrode recording system (AlphaOmega, Nazareth, Israel) (Figure 10). Fluoroscopic confirmation of the target approach was obtained at 5 mm intervals, 2 mm above the target, and at the target (Figure 11).

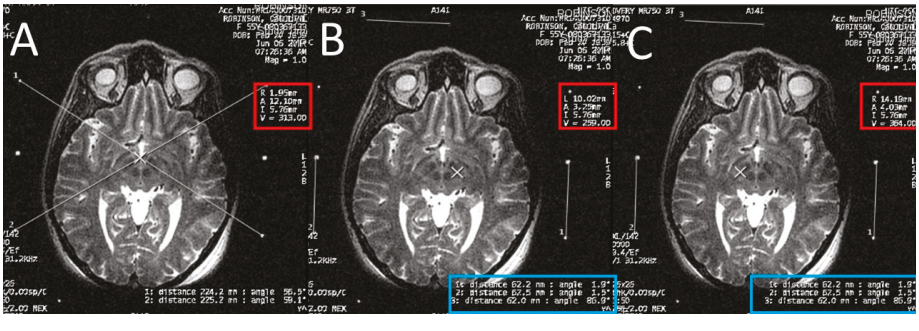

Figure 5. Calculating the subthalamic nucleus (STN) coordinates from the magnetic resonance imaging (MRI) console. (**A**) Two diagonal lines intersecting at the center of the frame at the STN level with MRI coordinates of the center of the frame shown inside the red square; (**B**) a crosshair at the center of the left STN, with its MRI coordinates shown inside the red square; two lines are drawn between the middle and lower fiducials on both sides of the frame and their lengths (in the blue rectangle) are used to calculate the Z coordinate; (**C**) a crosshair at the center of the right STN, with its MRI coordinates shown inside the red square; two line are drawn between the middle and lower fiducials on both sides of the frame and their lengths (in the blue rectangle) are used to calculate the Z coordinate.

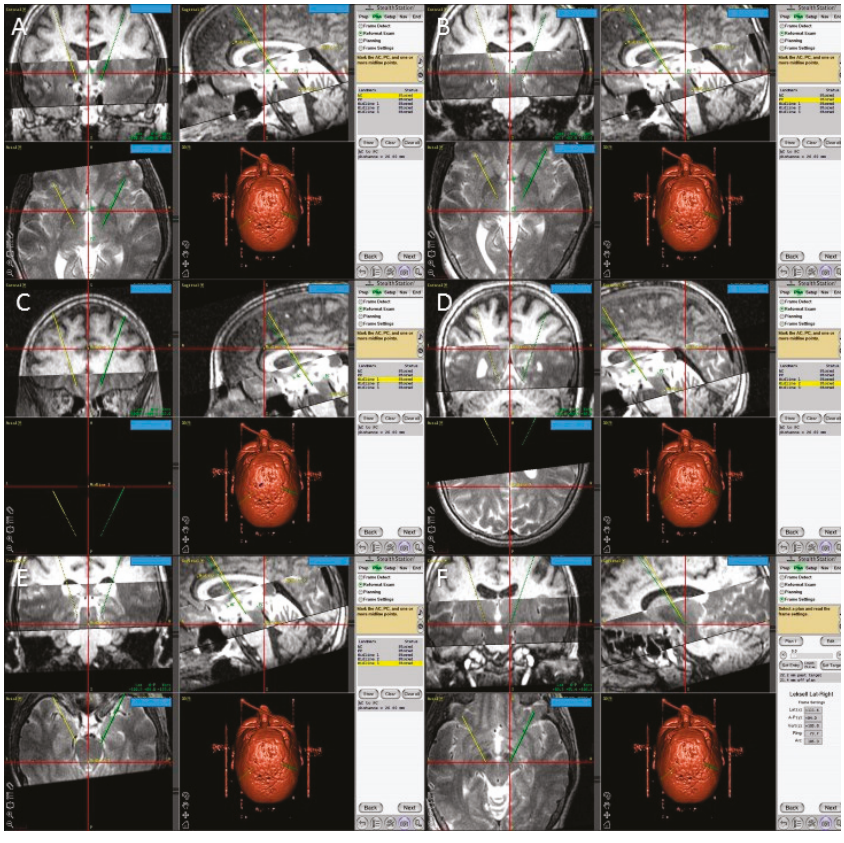

Figure 6. Screen shots from the FrameLink software of the StealthStation showing fused T1 and T2 magnetic resonance imaging (MRI) images of the patient and the planning process with identification of the posterior edge of the anterior commissure (**A**); the anterior edge of the posterior commissure PC (**B**); three midline points (**C**–**E**); and the final coordinates of the right subthalamic nucleus (**F**).

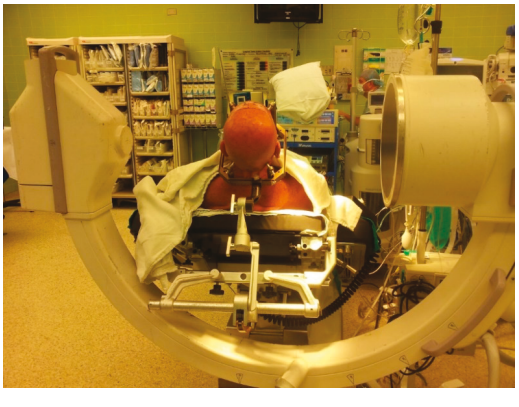

Figure 7. Position of the patient on the operating room table with the Leksell frame fixed to the table through a Mayfield adaptor and the C- arm positioned around the patient.

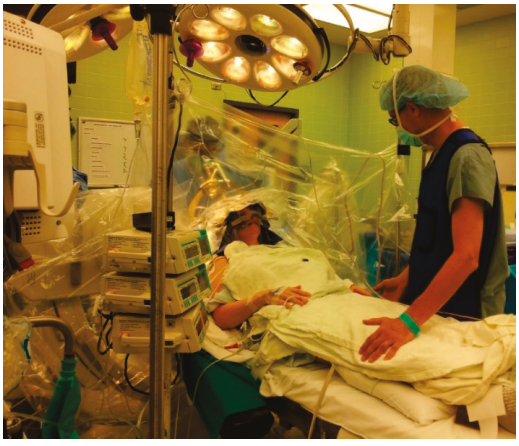

Figure 8. The final position of the patient. Note the transparent draping to allow better communication.

Figure 9. The site of the two semicircular incisions marked on both sides of the midline; with the two burr holes' positions marked with an X.

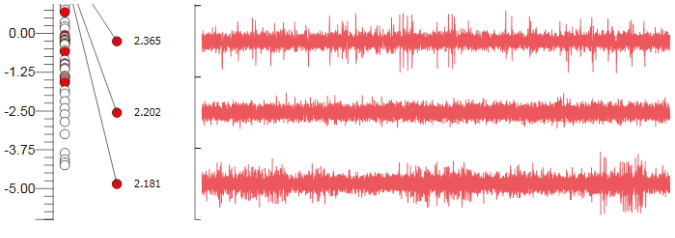

Figure 10. Microelectrode recording appearance of the subthalamic nucleus signal; note the increase in background activity, with high amplitude irregular firing.

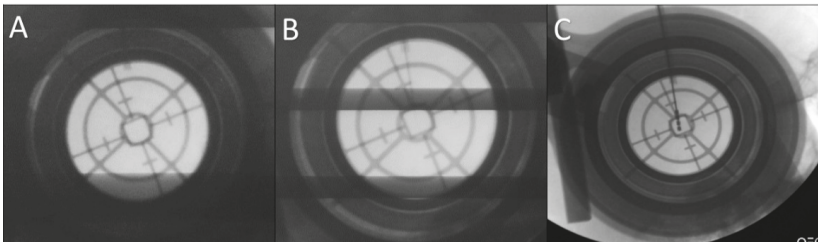

Figure 11. Fluoroscopic confirmation of the target approach. (**A**) Confirmation of the position of the stereotactic cannula; (**B**) the microelectrode is advanced to the target under fluoroscopic guidance; (**C**) the final position of the deep brain stimulation electrode confirmed.

After identification of the STN borders and depth by the MER, we started high-frequency macrostimulation. The aim of the stimulation was to confirm the optimal target, which provided adequate control of the Parkinsonian symptoms (specifically tremors), without undesirable effects from stimulation below 4 volts. Once we reached our desired target, we removed the microelectrode and replaced it with a standard four-contact (0–3) deep brain stimulation electrode (Medtronic DBS lead 3389). Generally, we placed the deepest electrode contact (0) at or just beyond the target point. We repeated the testing using this electrode in order to confirm the reproducibility of the effects. We locked the electrode in place using a Stimloc device (Medtronic, Minneapolis, MN, USA) (Figure 12). The excess of the electrode was coiled around the burr hole to create a strain relief loop (Figure 13). Then the same procedure was repeated on the right side.

The patient returned to hospital after one week for the second-stage surgery, in which the IPG was implanted in the sub-clavicular region under general anesthesia. After surgery, the IPG was interrogated. We checked the impedance of all eight contacts and programmed the pulse width, frequency, and amplitude of stimulation. By the end of the programming, we confirmed that the amplitude was set at zero and that the voltage of the battery was in the expected range.

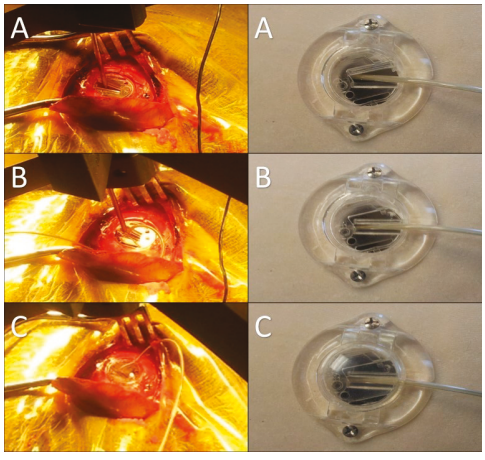

Figure 12. Intraoperative pictures and corresponding model images showing the steps of electrode fixation using the Stimloc device. (**A**) A special locking piece placed onto the Stimloc base with the electrode passing through it; (**B**) the electrode is locked in place with this piece after removing the stylet and moving the electrode out of the cannula; (**C**) the final step of the electrode fixation: the Stimloc cap is placed and fixed over its base.

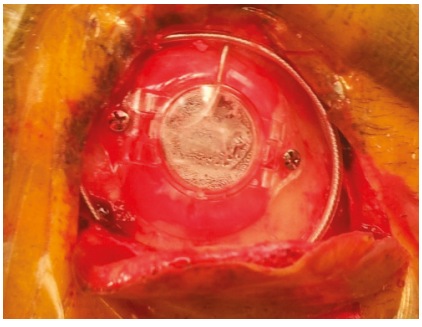

Figure 13. The final appearance of the electrode fixed using the Stimloc device; the excess of the electrode is coiled around the burr hole to create a strain relief loop.

2.4. Post-Operative Patient Assessment

Immediately after the first stage of surgery, all patients had a CT scan of the head to rule out hemorrhage. All of them had an MRI of the brain on the same day of surgery or the next day before discharge to confirm accurate electrode placement.

An experienced neurologist performed the first postoperative programming session one month after surgery. This interval was given to allow the brain to recover from the surgery and the micro-lesioning effect of the electrode placement. The patient was programmed to the best setting that gave the best clinical improvement at the lowest stimulation intensity and largest therapeutic range before inducing undesirable effects. At the same time, drug doses were reduced.

Comprehensive neurological evaluation was done 12 months after surgery. At this visit, each patient came after 12 h without medical treatment. The patient was reassessed for parts I, II, and IV of the UPDRS. After this, each patient was assessed using the UPDRS III and video recorded in four conditions: "on" stimulation and "off" medication; then "off" stimulation and "off" medication, after switching off the stimulation for at least 1 hour; then "off" stimulation and "on" medication, after administration of a supra-threshold dose of levodopa and waiting for the "best on state"; then "on" stimulation and "on" medication, after turning on stimulation using the chronic stimulation parameters. We also calculated the axial score, MMSE and SERS [40]. We recalculated the LEDD for the patient's recent anti-Parkinsonism medications. We documented any surgical-, device-, or stimulation-related undesirable effects.

2.5. Data Collection and Statistical Analysis

The collected data were coded, tabulated, and statistically analyzed using the IBM SPSS statistics software version 22.0 (IBM Corp., Chicago, IL, 2013). Descriptive statistics were done for quantitative data as minimum & maximum of the range, median and first & third inter-quartile range, as well as mean $\pm$ SD (standard deviation). We calculated the number and percentages for qualitative data. Inferential analyses were done for quantitative variables using the two-tailed paired t-test for two dependent groups with parametric data, and the Wilcoxon signed rank test for two dependent groups with non-parametric data. Correlations were calculated using the two-tailed Pearson correlation for numerical parametric data, the two-tailed Spearman's rho test for numerical non-parametric and qualitative data, and the two-tailed partial correlation when controlling for a HYRS. The level of significance was taken at p value <0.05.

3. Results

Twenty patients were included in this study; six were men (30%), and 14 were women (70%). The age of the patients at the time of surgery ranged from 48 to 82 years, with a mean age of 61.1 years.

The duration of illness before surgery ranged from five to 30 years, with a mean duration of 11.7 years. The mean ± SD of HYRS of PD stage was 3.6 ± 0.7 with a range from 2.5 to 5.0. No correlation was found between age, sex, family history, or the preoperative associated medical conditions and the one-year follow-up results (Table 1).

The total surgical time of the first-stage surgery ranged from 133 to 280 min, with a mean ± SD of 214.8 ± 44.3 min. The average number of MER tracks used for mapping the STN at a single side was 1.4.

Table 1. Preoperative demographic and medical characteristics.

Variables		Mean ± SD	Range
Age (years)		61.1 ± 8.7	48.0–82.0
HYRS		3.6 ± 0.7	2.5–5.0
Duration of illness (years)		11.7 ± 6.4	5.0–30.0
		Number	**Percentage (%)**
Sex	Male	6	30.0
	Female	14	70.0
Family history of PD		4	20.0
Smoking		3	15.0
Alcohol intake		4	20.0
Drugs addiction		2	10.0
Hypertension		5	25.0
Coronary artery diseases		1	5.0
Diabetes Mellitus		2	10.0

Total = 20; HYRS Hoehn and Yahr Rating Scale; PD Parkinson's disease; SD standard deviation; % percentage of change

3.1. Motor Scores (UPDRS III)

UPDRS III motor score improved by mean ± SD of 20.3 ± 8.9 (49.3%) from the preoperative "off" medication to the one-year follow-up of the "off" medication "on" stimulation score ($p < 0.001$). Tremors improved by mean ± SD of 8.0 ± 5.9 (81.6%) with $p < 0.001$. Rigidity improved by mean ± SD of 3.5 ± 2.1 (50.0%) with $p < 0.001$. Bradykinesia improved by mean ± SD of 5.7 ± 2.7 (39.3%) with $p < 0.001$. The axial score improved by mean ± SD of 2.0 ± 1.2 (38.5%) with $p < 0.001$ (Table 2, Figure 14).

Table 2. Changes in the "off" medications UPDRS III and UPDRS II scores.

Score (Range)	Measures	Preoperative	One Year	Δ Change	%	^ *p*
UPDRSIII "off" (0–108)	Mean ± SD Median (IQR) Range	40.0 ± 12.4 36.3 (31.3–54.0) 20.0–59.0	19.7 ± 7.1 18.0 (13.4–26.8) 9.0–33.0	−20.3 ± 8.9 −19.5 (−26.0–−16.3) −36.0–2.0	49.3%	<0.001 *
Tremors "off" (0–28)	Mean ± SD Median (IQR) Range	9.8 ± 6.9 10.0 (3.0–16.8) 0.0–19.0	1.8 ± 1.7 1.3 (0.0–3.0) 0.0–5.0	−8.0 ± 5.9 −7.5 (−14.4–−3.0) −17.0–0.0	81.6%	<0.001 *
Rigidity "off" (0–20)	Mean ± SD Median (IQR) Range	7.0 ± 3.4 8.0 (4.0–9.8) 1.0–12.0	3.5 ± 2.4 3.3 (2.0–5.0) 0.0–10.0	−3.5±2.1 −3.0 (−4.9–−2.0) −9.0–−1.0	50.0%	<0.001 *
Bradykinesia "off" (0–32)	Mean ± SD Median (IQR) Range	14.5 ± 4.4 14.0 (12.0–17.8) 7.5–23.0	8.8 ± 3.4 7.8 (6.3–11.8) 5.0–16.0	−5.7±2.7 −6.0 (−7.8–−4.5) −9.5–2.0	39.3%	<0.001 *
Axial "off" (0–16)	Mean ± SD Median (IQR) Range	5.2 ± 1.3 5.3 (4.3–6.0) 3.0–7.0	3.3 ± 1.5 3.0 (2.1–3.9) 1.5–8.0	−2.0 ± 1.2 −2.0 (−2.5–−1.6) −3.5–2.5	38.5%	<0.001 *
UPDRSII "off" (0–52)	Mean ± SD Median (IQR) Range	20.1 ± 4.2 21.0 (16.0–23.0) 13.0–27.0	11.2 ± 6.4 10.5 (7.3–13.0) 5.0–35.0	−8.8 ± 4.5 −9.5 (−12.0–−8.0) −13.0–8.0	73.8%	<0.001 *

Total = 20; Δ Change from before to after (negative values indicate a reduction); *p* probability (*p*-value); SD standard deviation; UPDRS Unified Parkinson's Disease Rating Scale; % percentage of change; ^ Wilcoxon Signed Ranks Test; * Significant.

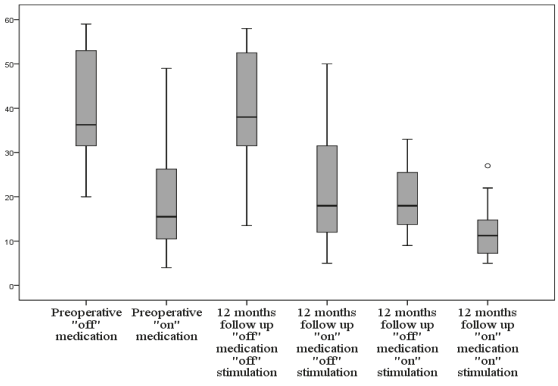

Figure 14. Graph showing the changes of UPDRS III score preoperatively and at 12-month follow-up in different medication and stimulation combinations; UPDRS Unified Parkinson's Disease Rating Scale.

We did not find a correlation between the preoperative improvement in the UPDRS III score, bradykinesia, and axial score after levodopa intake and the one-year follow-up values. A positive correlation was found between the preoperative improvement in tremors score ($r = 0.563$, $p = 0.010$) and rigidity score ($r = 0.485$, $p = 0.030$) with the postoperative tremors and rigidity, respectively.

Regarding the "on" medication state, a total improvement by mean ± SD of 7.0 ± 9.7 (36.5%) from the preoperative "on" medication motor subscore to the one-year follow-up "on" medication "on" stimulation score ($p < 0.001$). Tremors improved by mean ± SD of 2.5 ± 3.8 (78.1%) with $p = 0.002$. Rigidity improved by mean ± SD of 1.6 ± 1.6 (61.5%) with $p < 0.001$. Bradykinesia improved by mean ± SD of 2.7 ± 3.9 (31.4%) with $p = 0.002$. The axial score improved by mean ± SD of 0.3 ± 1.4 (10.7%) with $p = 0.046$ (Table 3).

The "off" medication "off" stimulation score at one year decreased by a mean of 0.4 (1%) compared to the preoperative "off" medication score. This change was found to be non-significant ($p = 0.452$). The "on" medication "off" stimulation at one year increased compared to the preoperative "on" score by a mean of 1.6 (8.3%) with $p = 0.13$.

Table 3. Changes in the "on" medications UPDRS III and UPDRS II scores.

Score (Range)	Measures	Preoperative	One Year	Δ Change	%	^ *p*
UPDRS III "on" (0–108)	Mean ± SD Median (IQR) Range	19.2 ± 11.7 15.5 (10.3–28.1) 4.0–49.0	12.2 ± 5.5 11.3 (7.1–15.1) 5.0–27.0	−7.0 ± 9.7 −4.0 (−14.1–1.6) −27.0–15.0	36.5%	<0.001 *
Tremors "on" (0–28)	Mean ± SD Median (IQR) Range	3.2 ± 4.1 1.5 (0.0–5.8) 0.0–14.0	0.7 ± 1.3 0.0 (0.0–1.0) 0.0–4.0	−2.5 ± 3.8 −1.0 (−2.5–0.0) −13.0–0.0	78.1%	0.002 *
Rigidity "on" (0–20)	Mean ± SD Median (IQR) Range	2.6 ± 2.1 2.0 (1.0–4.5) 0.0–7.0	1.0 ± 1.1 1.0 (0.0–1.0) 0.0–4.0	−1.6 ± 1.6 −1.0 (−2.0–−1.0) −5.0–0.0	61.5 %	<0.001 *
Bradykinesia "on" (0–32)	Mean ± SD Median (IQR) Range	8.6 ± 4.6 7.0 (6.0–13.0) 1.5–18.0	6.0 ± 2.9 5.0 (4.1–6.8) 1.0–14.0	−2.7 ± 3.9 −2.0 (−5.5–−0.6) −9.0–8.0	31.4%	0.002 *
Axial "on" (0–16)	Mean ± SD Median (IQR) Range	2.8 ± 1.4 3.0 (1.6–3.0) 1.0–6.0	2.5 ± 1.7 2.0 (1.0–3.0) 1.0–8.0	−0.3 ± 1.4 −0.3 (−1.0–0.0) −2.0–5.0	10.7%	0.046 *
UPDRSII "on" (0–52)	Mean ± SD Median (IQR) Range	9.5 ± 5.5 9.0 (5.3–14.4) 0.0–17.5	7.8 ± 5.4 7.8 (5.3–9.5) 0.0–26.0	−1.7 ± 5.5 −0.3 (−4.9–0.0) −11.0–16.0	17.9%	0.073

Total = 20, Δ Change from before to after (negative values indicate a reduction); *p* probability (*p*-value); SD standard deviation; UPDRS Unified Parkinson's Disease Rating Scale; % percentage of change; ^ Wilcoxon Signed Ranks Test; * Significant.

3.2. Activity of Daily Living

The "off" medication UPDRS II improved by mean ± SD of 8.8 ± 4.5 (73.8%) with $p < 0.001$ (Figure 15). The "on" medication UPDRS II improved by mean ± SD of 1.7 ± 5.5 (17.9%), but this improvement did not prove to be statistically significant. The "off" medication SERS improved at the one-year follow-up by mean ± SD of 37.5 ± 15.9 (104.2%) with $p < 0.001$.

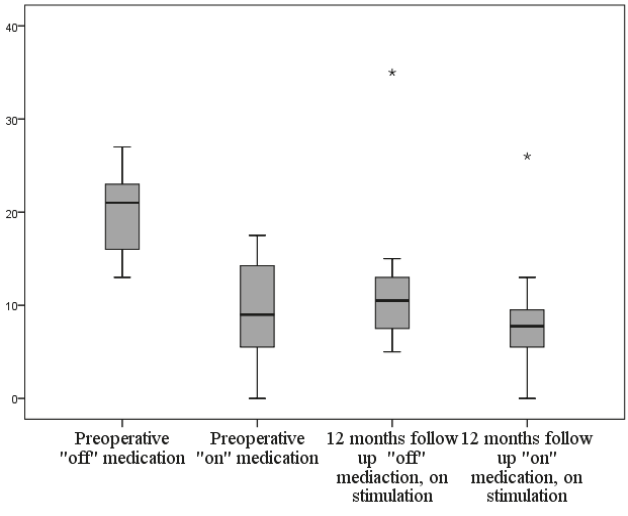

Figure 15. Graph showing the changes of UPDRS II score preoperatively and at 12-month follow-up in "on" and "off" medication conditions; UPDRS Unified Parkinson's Disease Rating Scale.

3.3. Mental State

The UPDRS I score showed non-significant change from a preoperative score of 1.7 ± 1.2 to a one-year score of 1.9 ± 1.3 (Table 4). The MMSE also showed non-significant change (Table 4).

Table 4. Changes in UPDRS I and MMSE scores.

Score (Range)	Measures	Preoperative	One Year	Δ Change	^ *p*
UPDRS I (2–16)	Mean ± SD	1.7 ± 1.2	1.9 ± 1.3	0.2 ± 0.7	^ 0.059
	Median (IQR)	2.0 (1.0–2.8)	2.0 (1.0–3.0)	0.0 (0.0–0.8)	
	Range	0.0–4.0	0.0–4.0	0.0–2.0	
MMSE (0–30)	Mean ± SD	29.2±1.0	28.9 ± 1.3	−0.3 ± 1.1	# 0.249
	Median (IQR)	29.0 (29.0–30.0)	29.0 (28.0–30.0)	0.0 (−1.0–0.0)	
	Range	27.0–30.0	25.0–30.0	−4.0–2.0	

Total = 20, Δ Change from before to after (negative values indicate a reduction); IQR interquartile range; *p* probability (*p*-value); MMSE Mini Mental Status Exam; SD standard deviation; UPDRS Unified Parkinson's Disease Rating Scale; ^ Wilcoxon Signed Ranks Test, # Paired *t*-test.

3.4. Medications

LEDD decreased in the one-year follow-up by mean ± SD of 849.4 ± 448.1 mg/dL (54.1%) with $p < 0.001$. The UPDRS IVa score improved at the one-year follow-up by mean ± SD of 2.8 ± 2.1 (65.1%) from the preoperative score with $p < 0.001$. The UPDRS IVb score improved at the one-year follow-up by mean ± SD of 1.7 ± 1.1 (48.6%) from the preoperative score with $p < 0.001$ (Table 5, Figure 16).

Table 5. Changes in the LEDD and UPDRS IV score.

Score	Measures	Preoperative	One Year	Δ Change	%	^ *p*
LEDD (mg/dL)	Mean ± SD	1570.8 ± 662.9	721.4 ± 312.4	−849.4 ± 448.1	54.1%	<0.001 *
	Median (IQR)	1675.0 (832.5–2175.0)	691.0 (416.5–975.0)	−800.0 (−1287.5–−360.0)		
	Range	616.0–2500.0	300.0–1200.0	−1514.0–−270.0		
UPDRS IVa	Mean ± SD	4.3 ± 2.9	1.6 ± 1.5	−2.8 ± 2.1	65.1%	<0.001 *
	Median (IQR)	5.0 (1.3–7.0)	1.3 (0.3–2.0)	−3.0 (−4.9–−1.0)		
	Range	0.0–8.0	0.0–5.0	−6.0–1.0		
UPDRS IVb	Mean ± SD	3.5 ± 1.8	1.8 ± 1.0	−1.7 ± 1.1	48.6%	<0.001 *
	Median (IQR)	4.0 (2.3–5.0)	2.0 (1.0–2.9)	−2.0 (−2.0–−1.0)		
	Range	0.0–6.0	0.0–3.0	−4.0–0.0		

Total = 20, Δ Change from before to after (negative values indicate a reduction, which is an indicator of improvement); LEDD levodopa equivalent daily dose; *p* probability (*p*-value); SD standard deviation; UPDRS Unified Parkinson's Disease Rating Scale; % percentage of change; ^ Wilcoxon Signed Ranks Test; * Significant.

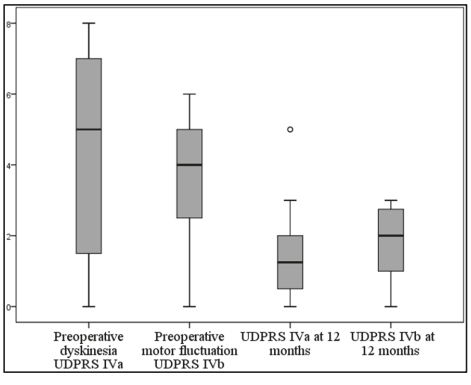

Figure 16. Graph showing the preoperative and 12-month follow-up of UPDRS IVa and IVb; UPDRS Unified Parkinson's Disease Rating Scale.

3.5. Complications

All patients reported a postoperative headache that was relieved within a few days. This headache may be attributed to the surgical intervention itself or to the small film of pneumocephalus that appeared on the postoperative CT scans of all the patients. This pneumocephalus was transient and disappeared within days on follow-up CT scans. Three patients complained of memory difficulties; one patient experienced a worsening of his daytime hallucinations, one patient experienced numbness of the scalp at the incision site, and one patient experienced an increase in his depressive symptoms. These adverse events were transient and disappeared within a few weeks. One patient suffered a worsening of speech when turning the stimulation on. One patient developed postoperative right frontal hemorrhage at the site of the cortical penetration by the electrode, and she suffered deterioration of the level of consciousness. The hematoma was evacuated and she achieved complete recovery within one month. One patient suffered from wound dehiscence at the IPG implantation site. The IPG was removed and replaced with a new one in a subcutaneous pocket in the anterior abdominal wall.

4. Discussion

In this study we present a snapshot of our experience at UIC in the management of advanced PD using STN-DBS by reporting our preoperative and intraoperative methods as well as the clinical outcomes of 20 patients who were operated on from 2013 to 2014 and followed up for a year. Our experience with DBS started in 2001, and over the years we have modified and improved our techniques [55–57].

We have done our preoperative target calculations using a combination of the standard indirect atlas-based X, Y, and Z coordinates of the STN at 12 mm lateral, 3 mm posterior, and 6 mm inferior to the MCP, and direct visualization of the STN on T2 weighted images.

We believe that intra-operative physiological and clinical confirmation of the target is crucial in the final position confirmation. The initial anatomical and radiological planning is also essential in target selection. Accurate preoperative planning would decrease the intra-operative time needed for the MER and the number of the microelectrodes tracks needed to reach the target, and subsequently decrease the complications. This fact is supported by our results, as our average number of MER tracks was 1.4 tracks and our average surgical time was 214.8 min.

Twenty patients were included in the current study; their demographic characteristics are similar to those of the patients included in other studies (Table 6). We only included patients who had the disease for more than five years; this time period is recommended by CAPSIT-PD guidelines to improve the accuracy of diagnosing idiopathic PD, because the defining features of some of the atypical Parkinsonian syndromes may appear late in the course of the disease, e.g., eye movement abnormalities in PSP and autonomic dysfunction in MSA [28–31]. This time interval is agreed upon by most authors in the literature, as the mean duration of the disease before surgery in previous studies ranged from 6.8 to 16.4 years. The mean ± SD HYRS was 3.6 ± 0.7, ranging from 2.5 to 5.0.

Table 6. Demographic characteristics of patients in previous studies of bilateral subthalamic nucleus stimulation in PD.

Study	*N*	F/U (Months)	Mean Age at Surgery (Years)	Mean Disease Duration before Surgery (Years)	Mean "off" HYRS
Limousin et al. [58]	20	12	56 ± 8	14 ± 5	4.6 ± 0.5
Ostergaard et al. [59]	26	12	59 ± 8 (30–75)	15 ± 5	3.7
Simuni et al. [60]	12	12	58 ± 11	12 ± 4	3.8
Thobois et al. [61]	14	12	56.9 ± 6	13.5 ± 4.4	3.6
Vesper et al. [62]	38	12	55.6 (47–72)	13	3.5
Vingerhoets et al. [63]	20	21 ± 8	63 ± 8	16 ± 5	*
Volkmann et al. [64]	16	12	60.2 ± 9.8	13.1 ± 5.9	*
Herzog et al. [65]	20	24	60 ± 6	15 ± 5	3.7
Krause et al. [66]	24	29.8 ± 8.5	57.7	14.4 ± 5.8	4.3
Fraix et al. [67]	24	12	55.7 ± 7.3	16.3 ± 5.4	4.5
Kleiner-Fisman et al. [68]	25	24	57.2 ± 11.7	13.4 ± 4.3	*
Krack et al. [69]	42	60	55 (34–68)	14.6 ± 5	*
Romito et al. [70]	33	25.7 ± 13.5	56.8 ± 7.1	13.8 ± 5.5	*
Visser-Vandewalle et al. [71]	20	48	60.9 ± 8.1	15.0 ± 4.4	*
Rodrguez-Oroz et al. [72]	10	48	62.0 (53–73)	13 (4–23)	*
Rodrguez-Oroz et al. [73]	49	48	*	*	*
Wider et al. [74]	37	60	64.9 ± 7.6	14.4 ± 4.9	*
Gervais-Bernard et al. [75]	23	48	55.1 ± 7.2	12.9 ± 3.2	*
Castrioto et al. [26]	18	120	52.9 ± 7.9	13.4 ± 4.8	*
Weaver et al. [76]	70	36	60.7 ± 8.9	11.3 ± 4.7	3.3 ± 0.8
Li et al. [77]	195	60	58.2 ± 10	6.8 (5–15)	*
Tabbal et al. [78]	72	6	48.4 ± 9.8 (28–69)	14.5 ± 6.5 (4–29)	*
This study	20	12	61.1±8.7 (48–82)	11.7 ± 6.4 (5–30)	3.6 ± 0.7 (2.5–5)

N: number of patients; F/U: duration of follow-up; HYRS Hoehn and Yahr Rating Scale; PD: Parkinson's disease; UPDRS: Unified Parkinson's Disease Rating Scale; *: no available data

In this study, we report significant improvement in all the motor aspects of PD (UPDRS III) and in ADL (UPDRS II) in the "off" medication state following bilateral STN stimulation. This was accompanied by significant reduction of both medication doses and medication-related adverse effects. This improvement of motor function was significant for the total UPDRS III score and for all the motor subscores (tremor, rigidity, bradykinesia, and the axial score). The change in UPDRS motor scores following surgery in the stimulation "on", medication "off" condition compared to the baseline medication "off" condition was used as the primary outcome measure in many previous studies (Table 7). The improvement of UPDRS III score ranged from 38.3% to 66.5% [26,27,63,67–69,71,73–77,79–81] at one-year follow-up; with longer follow-up the beneficial

effect of stimulation tends to decrease but scores remain significantly better than preoperative scores [22,26,68,69,71,77,79,80]. The deterioration seems to involve the axial manifestations of PD more than the appendicular motor symptoms. This may be caused by the difference in the pathogenesis of the axial symptoms from the other motor manifestations of PD [82]. The improvement of the UPDRS II "off" score in other studies ranged from 17% to 68.5% and this improvement also tends to decrease with a longer follow-up period [58,59,72,77,83].

Table 7. Motor and activity of daily living outcomes of patients in previous studies of bilateral subthalamic nucleus stimulation in PD.

Study	% of Change of UPDRS III "off"	% of Change of UPDRS III "on"	% of Change of UPDRS II "off"
Limousin et al. [58]	−60%	−10%	−60%
Ostergaard et al. [59]	−64.3%	*	−66.3%
Simuni et al. [62]	−47.1%	−2%	*
Thobois et al. [64]	−55%	*	−52.8%
Vesper et al. [60]	−48%	−39%	−38%
Vingerhoets et al. [63]	−45%	*	−37%
Volkmann et al. [65]	−60.3%	*	−55.9%
Herzog et al. [61]	−57.2%	−35%	−43.6%
Krause et al. [66]	−38.3%	*	−17%
Fraix et al. [67]	−66.5	−16%	*
Kleiner-Fisman et al. [68]	−39%	*	−26%
Krack et al. [69]	−54%	+47.6	−49%
Romito et al. [70]	−51.6%	*	−68.5%
Visser-Vandewalle et al. [71]	−42.8%	−22.6%	−59.4%
Rodrguez-Oroz et al. [72]	−62.0%	*	−62.0%
Rodrguez-Oroz et al. [73]	−50%	−12.3%	−43.1%
Wider et al. [74]	−25.5%	+26%	*
Gervais-Bernard et al. [75]	−55%	−11.2%	−38.1%
Castrioto et al. [26]	−25.3%	+44.7	−23%
Weaver et al. [76]	−30.1%	+11.1%	−6.25%
Li et al. [77]	−60.3%	*	−54.2%
Tabbal et al. [78]	−47%	*	*
This study	−49.3%	−36.5%	−73.8%

%: percentage, *: no available data, UPDRS: Unified Parkinson's Disease Rating Scale, PD: Parkinson's disease.

The "on" medication, "on" stimulation total UPDRS III score and all the motor subscores showed significant improvement compared to the preoperative "on" medication. Some of the previous studies showed significant improvement at one-year UPDRS III "on" score [60,61], others non-significant improvement [58,62,71], but most studies showed deterioration (increase) of this score at longer follow-up periods [26,32,69,74,76]. The UPDRS II "on" score showed little improvement compared to the preoperative "on" state and it was statistically non-significant. Few studies described significant improvement in this score [71]. Most of the previous studies showed non-significant improvement in the "on" state ADL [58–62,64–66]. After longer follow-up, previous studies showed significant deterioration in ADL (increase in score) [26,69,72,74,75]. The less obvious effect of stimulation on the UPDRS III and UPDRS II in the medication "on" state in these studies can be explained by an increase in bradykinesia and the axial sub-scores at the one-year follow-up. The insignificant change of the "off" stimulation UPDRS III in both the "on" and the "off" medication states confirms that the improvement in the "on" stimulation scores is attributed to the DBS effect. Medication doses and medication-induced side effects (dyskinesia and motor fluctuations) were reduced by 65.1% and 48.6%, respectively. These results are in agreement with previous studies (Table 8). The reduction of the LEDD in previous studies ranged from 19.5% to 80.7% (Table 8).

Table 8. Change of LEDD and medication-induced complications in patients in previous studies of bilateral subthalamic nucleus stimulation in PD.

Study	% of Change of LEDD	% of Change of Dyskinesia	% of Change of Motor Fluctuation
Limousin et al. [58]	*	−60%	*
Ostergaard et al. [59]	−19.5%	−86%	−79%
Simuni et al. [62]	−55%	−64.3%	−32.4%
Thobois et al. [64]	−65.5%	−76%	*
Vesper et al. [60]	−53%	−71.9%	−35%
Vingerhoets et al. [63]	−79%	−92%	−95%
Volkmann et al. [65]	−65.3%	−83.3%	*
Herzog et al. [61]	−67%	−85%	*
Krause et al. [66]	−30%	−70%	−16%
Fraix et al. [67]	−80.7%	−86.7%	*
Kleiner-Fisman et al. [68]	−42%	−65.5%	−58%
Krack et al. [69]	−63%	−65%	*
Romito et al. [70]	−56.2%	−83.9%	−94.2%
Visser-Vandewalle et al. [71]	−47.2%	−79%	−78.4%
Rodrguez-Oroz et al. [72]	−50.0%	−53%	*
Rodrguez-Oroz et al. [73]	−35%	−59%	*
Wider et al. [74]	−56.9%	−85.4%	−84.2%
Gervais-Bernard et al. [75]	−54.4%	−60%	*
Castrioto et al. [26]	−36.3%	−68.8%	−46.9%
Weaver et al. [76]	−35.7%	−75%	*
Tabbal et al. [78]	45%	*	*
This study	−54.1%	−65.1%	−48.6%

LEDD levodopa equivalent daily dose; PD: Parkinson's disease, UPDRS: Unified Parkinson's Disease Rating Scale, %: percentage, *: no available data.

The adverse events encountered in this group of patients were within the accepted complication rate for DBS [84]. While we had one patient with ICH and one with wound dehiscence, both fortunately recovered, one without permanent deficits. While DBS is generally considered a safe procedure, complications can occur and are usually classified into procedure-related, hardware-related, and stimulation–related types [84]. The overall incidence of adverse effects related to surgery is 11%, but it is highly variable between studies [85]. Death is very rare after DBS surgery [62,86]. Procedure-related complications include intracranial hemorrhage (0%–3.9%) and sub-optimal electrode placement (0%–2.5%). Hardware related complications account for 5%–18.5% of the complications; they include lead fracture (0%–5%), lead migration (0%–3.5%), infections, and erosions (1%–9.7%). Stimulation-related complications are the most common problems encountered after DBS surgery, but most of them are reversible or can be avoided by adequate adjustment of the stimulation parameters [69,87–89]. They include transient confusion and mood changes. Several studies found that the effect of STN-DBS on overall cognitive functions is non-significant and reversible [27,90–92], consistent with the lack of changes from baseline in both the UPDRS I and MMSE scores in our study. A commonly observed complication after DBS is weight gain (8.4%), which can be attributed to the decrease in energy output due to the control of the abnormal movements [84,85,89,93]. Other, reversible, stimulation-related adverse events include contralateral numbness, facial pulling, eye deviation, dysphonia, and speech disturbances. Stimulation may also cause serious psychiatric adverse events such as acute depression but they are reversible upon changing the stimulation parameters. In addition, DBS may induce exacerbation of pre-existing mood disturbances and it is recommended that all patients are screened preoperatively for psychiatric problems [92,94,95]. Nevertheless, patients should not be flat-out denied surgery based on a history of psychiatric illness. In some cases preoperative psychosis or depressive symptoms may be caused by medications, and may therefore improve with dose reduction after surgery [96].

5. Conclusions

Despite the limitations of this study as the assessments were not blinded to before vs. after surgery, to medication status, or to DBS status, we can conclude that bilateral deep brain stimulation of the subthalamic nucleus significantly improves motor symptoms, activities of daily living, and medication-induced complications in patients with advanced PD.

Acknowledgments: We would like to thank Hazem El-Hariri who helped us with the statistics.

Author Contributions: Ahmed Rabie, the first author, came up with the idea of the research and shared in all phases of the research. Konstantin V. Slavin and Leo Verhagen Metman shared in conducting the research, analyzing the data, and writing the paper. Mazen Fakhry, Ezeldin Eassa, Ahmed Shakal, and Wael Fouad shared in data analysis, paper writing and revision.

Conflicts of Interest: The authors declare no conflict of interest.

References

1. Awan, N.R.; Lozano, A.; Hamani, C. Deep brain stimulation: Current and future perspectives. *Neurosurg. Focus* **2009**, *27*, E2. [CrossRef] [PubMed]
2. Benabid, A.L.; Chabardes, S.; Mitrofanis, J.; Pollak, P. Deep brain stimulation of the subthalamic nucleus for the treatment of Parkinson's disease. *Lancet Neurol.* **2009**, *8*, 67–81. [CrossRef]
3. Critchley, M. *James Parkinson (1755–1824): A Bicentenary Volume of Papers Dealing with Parkinson's Disease, Incorporating the Original "Essay on the Shaking Palsy"*; St. Martin's Press: New York, NY, USA, 1955.
4. Spiegel, E.; Wycis, H.; Marks, M.; Lee, A. Stereotactic apparatus for operations on the human brain. *Science* **1947**, *10*, 349–350. [CrossRef] [PubMed]
5. Wycis, H.T.; Spiegel, E.A. The effect of thalamotomy and pallidotomy upon involuntary movements in chorea and athetosis. *Surg. Forum* **1950**, *1*, 329–332.
6. Spiegel, E.A.; Wycis, H.T. Thalamotomy and pallidotomy for treatment of choreic movements. *Acta Neurochir.* **1952**, *2*, 417–422. [CrossRef] [PubMed]
7. Svennilson, E.; Torvik, A.; Lowe, R.; Leksell, L. Treatment of Parkinsonism by stereotatic thermolesions in the pallidal region. A clinical evaluation of 81 cases. *Acta Psychiatr. Scand.* **1960**, *35*, 358–377. [CrossRef] [PubMed]
8. Hassler, R.; Riechert, T.; Mundinger, F.; Umbach, W.; Ganglberger, J.A. Physiological observations in stereotaxic operations in extrapyramidal motor disturbances. *Brain* **1960**, *83*, 337–350. [CrossRef] [PubMed]
9. Laitinen, L. Thalamic targets in the stereotaxic treatment of Parkinson's disease. *J. Neurosurg.* **1966**, *24*, 82–85. [CrossRef] [PubMed]
10. Riechert, T. Stereotaxic operations for extrapyramidal motor disturbances with particular regard to age groups. *Confin. Neurol.* **1965**, *26*, 213–217. [PubMed]
11. Benabid, A.L.; Pollak, P.; Louveau, A.; Henry, S.; de Rougemont, J. Combined (thalamotomy and stimulation) stereotactic surgery of the VIM thalamic nucleus for bilateral Parkinson disease. *Appl. Neurophysiol.* **1987**, *50*, 344–346. [CrossRef] [PubMed]
12. Benabid, A.L.; Pollak, P.; Gervason, C.; Hoffmann, D.; Gao, D.M.; Hommel, M.; Perret, J.E.; de Rougemont, J. Long-term suppression of tremor by chronic stimulation of the ventral intermediate thalamic nucleus. *Lancet* **1991**, *337*, 403–406. [CrossRef]
13. Kumar, K.; Kelly, M.; Toth, C. Deep brain stimulation of the ventral intermediate nucleus of the thalamus for control of tremors in Parkinson's disease and essential tremor. *Stereotact. Funct. Neurosurg.* **1999**, *72*, 47–61. [CrossRef] [PubMed]
14. Siegfried, J.; Lippitz, B. Bilateral chronic electrostimulation of ventroposterolateral pallidum: A new therapeutic approach for alleviating all parkinsonian symptoms. *Neurosurgery* **1994**, *35*, 1126–1129. [CrossRef] [PubMed]
15. Gross, C.; Rougier, A.; Guehl, D.; Boraud, T.; Julien, J.; Bioulac, B. High-frequency stimulation of the globus pallidus internalis in Parkinson's disease: A study of seven cases. *J. Neurosurg.* **1997**, *87*, 491–498. [CrossRef] [PubMed]

16. Kumar, R.; Lang, A.E.; Rodriguez-Oroz, M.C.; Lozano, A.M.; Limousin, P.; Pollak, P.; Benabid, A.L.; Guridi, J.; Ramos, E.; van der Linden, C.; et al. Deep brain stimulation of the globus pallidus pars interna in advanced Parkinson's disease. *Neurology* **2000**, *55*, S34–S39. [PubMed]
17. Aziz, T.Z.; Peggs, D.; Sambrook, M.A.; Crossman, A.R. Lesion of the subthalamic nucleus for the alleviation of 1-methyl-4-phenyl-1,2,3,6-tetrahydropyridine (MPTP)-induced parkinsonism in the primate. *Mov. Disord.* **1991**, *6*, 288–292. [CrossRef] [PubMed]
18. Obeso, J.A.; Guridi, J.; Obeso, J.A.; DeLong, M. Surgery for Parkinson's disease. *J. Neurol. Neurosurg. Psychiatr.* **1997**, *62*, 2–8. [CrossRef] [PubMed]
19. Alvarez, L.; Macias, R.; Guridi, J.; Lopez, G.; Alvarez, E.; Maragoto, C.; Teijeiro, J.; Torres, A.; Pavon, N.; Rodriguez-Oroz, M.C.; et al. Dorsal subthalamotomy for Parkinson's disease. *Mov. Disord.* **2001**, *16*, 72–78. [CrossRef]
20. Benabid, A.L.; Pollak, P.; Gross, C.; Hoffmann, D.; Benazzouz, A.; Gao, D.M.; Laurent, A.; Gentil, M.; Perret, J. Acute and long-term effects of subthalamic nucleus stimulation in Parkinson's disease. *Stereotact. Funct. Neurosurg.* **1994**, *62*, 76–84. [CrossRef] [PubMed]
21. Pollak, P.; Benabid, A.L.; Gross, C.; Gao, D.M.; Laurent, A.; Benazzouz, A.; Hoffmann, D.; Gentil, M.; Perret, J. Effects of the stimulation of the subthalamic nucleus in Parkinson disease. *Rev. Neurol.* **1993**, *149*, 175–176. [PubMed]
22. Weaver, F.M.; Follett, K.; Stern, M.; Hur, K.; Harris, C.; Marks, W.J., Jr.; Rothlind, J.; Sagher, O.; Reda, D.; Moy, C.S.; et al. Bilateral deep brain stimulation vs. best medical therapy for patients with advanced Parkinson disease: A randomized controlled trial. *JAMA* **2009**, *301*, 63–73. [CrossRef] [PubMed]
23. Williams, A.; Gill, S.; Varma, T.; Jenkinson, C.; Quinn, N.; Mitchell, R.; Scott, R.; Ives, N.; Rick, C.; Daniels, J.; et al. Deep brain stimulation plus best medical therapy versus best medical therapy alone for advanced Parkinson's disease (PD SURG trial): A randomised, open-label trial. *Lancet Neurol.* **2010**, *9*, 581–591. [CrossRef]
24. Antonini, A.; Isaias, I.U.; Rodolfi, G.; Landi, A.; Natuzzi, F.; Siri, C.; Pezzoli, G. A 5-year prospective assessment of advanced Parkinson disease patients treated with subcutaneous apomorphine infusion or deep brain stimulation. *J. Neurol.* **2011**, *258*, 579–585. [CrossRef] [PubMed]
25. Deuschl, G.; Schade-Brittinger, C.; Krack, P.; Volkmann, J.; Schafer, H.; Botzel, K.; Daniels, C.; Deutschlander, A.; Dillmann, U.; Eisner, W.; et al. A randomized trial of deep-brain stimulation for Parkinson's disease. *N. Engl. J. Med.* **2006**, *355*, 896–908. [CrossRef] [PubMed]
26. Castrioto, A.; Lozano, A.M.; Poon, Y.Y.; Lang, A.E.; Fallis, M.; Moro, E. Ten-year outcome of subthalamic stimulation in Parkinson disease: A blinded evaluation. *Arch. Neurol.* **2011**, *68*, 1550–1556. [CrossRef] [PubMed]
27. Shakal, A.; Ramadan, E.; Fouad, W. Effect of deep brain stimulation on motor and mental status of Parkinson's disease patients: A preliminary Egyptian study. *Egypt. J. Neurol. Psychiatr. Neurosurg.* **2011**, *48*, 257–264.
28. Defer, G.L.; Widner, H.; Marie, R.M.; Remy, P.; Levivier, M. Core assessment program for surgical interventional therapies in Parkinson's disease (CAPSIT-PD). *Mov. Disord.* **1999**, *14*, 572–584. [CrossRef]
29. Scaravilli, T.; Tolosa, E.; Ferrer, I. Progressive supranuclear palsy and corticobasal degeneration: Lumping versus splitting. *Mov. Disord.* **2005**, *20*, S21–S28. [CrossRef] [PubMed]
30. Quinn, N.P. How to diagnose multiple system atrophy. *Mov. Disord.* **2005**, *20*, S5–S10. [CrossRef] [PubMed]
31. Pahwa, R.; Lyons, K.E. Early diagnosis of Parkinson's disease: Recommendations from diagnostic clinical guidelines. *Am. J. Manag. Care* **2010**, *16*, S94–S99. [PubMed]
32. The Deep-Brain Stimulation for Parkinson's Disease Study Group. Deep-brain stimulation of the subthalamic nucleus or the pars interna of the globus pallidus in Parkinson's disease. *N. Engl. J. Med.* **2001**, *345*, 956–963.
33. Goetz, C.G.; Fahn, S.; Martinez-Martin, P.; Poewe, W.; Sampaio, C.; Stebbins, G.T.; Stern, M.B.; Tilley, B.C.; Dodel, R.; Dubois, B.; et al. Movement Disorder Society-sponsored revision of the unified Parkinson's Disease Rating Scale (MDS-UPDRS): Process, format, and clinimetric testing plan. *Mov. Disord.* **2007**, *22*, 41–47. [CrossRef] [PubMed]
34. Goetz, C.G.; Tilley, B.C.; Shaftman, S.R.; Stebbins, G.T.; Fahn, S.; Martinez-Martin, P.; Poewe, W.; Sampaio, C.; Stern, M.B.; Dodel, R.; et al. Movement Disorder Society-sponsored revision of the unified Parkinson's Disease Rating Scale (MDS-UPDRS): Scale presentation and clinimetric testing results. *Mov. Disord.* **2008**, *23*, 2129–2170. [CrossRef] [PubMed]

35. Goetz, C.G.; Stebbins, G.T.; Chmura, T.A.; Fahn, S.; Poewe, W.; Tanner, C.M. Teaching program for the movement disorder society-sponsored revision of the Unified Parkinson's Disease Rating Scale: (MDS-UPDRS). *Mov. Disord.* **2010**, *25*, 1190–1194. [CrossRef] [PubMed]
36. Starr, P.A.; Vitek, J.L.; DeLong, M.; Bakay, R.A. Magnetic resonance imaging-based stereotactic localization of the globus pallidus and subthalamic nucleus. *Neurosurgery* **1999**, *44*, 303–313. [CrossRef] [PubMed]
37. Lyons, M.K. Deep brain stimulation: Current and future clinical applications. *Mayo Clin. Proc.* **2011**, *86*, 662–672. [CrossRef] [PubMed]
38. Kluger, B.M.; Foote, K.D.; Jacobson, C.E.; Okun, M.S. Lessons learned from a large single center cohort of patients referred for DBS management. *Parkinsonism Relat. Disord.* **2011**, *17*, 236–239. [CrossRef] [PubMed]
39. Hoehn, M.M.; Yahr, M.D. Parkinsonism: Onset, progression and mortality. *Neurology* **1967**, *17*, 427–442. [CrossRef] [PubMed]
40. Schwab, R.; England, A. Projection technique for evaluating surgery in Parkinson's disease. In *Third Symposium on Parkinson's Disease*; Gillingham and Donaldson: Edinburgh, UK, 1969.
41. Tomlinson, C.L.; Stowe, R.; Patel, S.; Rick, C.; Gray, R.; Clarke, C.E. Systematic review of levodopa dose equivalency reporting in Parkinson's disease. *Mov. Disord.* **2010**, *25*, 2649–2653. [CrossRef] [PubMed]
42. Coblentz, J.M.; Mattis, S.; Zingesser, L.H.; Kasoff, S.S.; Wisniewski, H.M.; Katzman, R. Presenile dementia. Clinical aspects and evaluation of cerebrospinal fluid dynamics. *Arch. Neurol.* **1973**, *29*, 299–308. [CrossRef] [PubMed]
43. Bech, P. Rating scales for affective disorders: Their validity and consistency. *Acta Psychiatr. Scand. Suppl.* **1981**, *295*, 1–101. [PubMed]
44. Beck, A.T.; Ward, C.H.; Mendelson, M.; Mock, J.; Erbaugh, J. An inventory for measuring depression. *Arch. Gen. Psychiatr.* **1961**, *4*, 561–571. [CrossRef] [PubMed]
45. Folstein, M. Mini-mental and son. *Int. J. Geriatr. Psychiatry* **1998**, *13*, 290–294. [PubMed]
46. Folstein, M.F.; Folstein, S.E.; McHugh, P.R. "Mini-mental state". A practical method for grading the cognitive state of patients for the clinician. *J. Psychiatr. Res.* **1975**, *12*, 189–198. [CrossRef]
47. Talairach, J.; Tournoux, P.; Szikla, G.; Bonis, A.; Bancaud, J. surgical treatment of Parkinson's disease. Methodologic remarks and surgical technic. *Int. J. Neurol.* **1961**, *2*, 76–91. [PubMed]
48. Talairach, J.; Tournoux, P. *Co-Planar Stereotaxic Atlas of the Human Brain: 3-Dimensional Proportional System: An Approach to Cerebral Imaging*; Georg Thieme: New York, NY, USA, 1988; p. 122.
49. Talairach, J.; Tournoux, P.; Missir, O. *Referentially Oriented Cerebral MRI Anatomy: An Atlas of Stereotaxic Anatomical Correlations for Gray and White Matter*; Thieme Medical Publishers: Stuttgart; New York, NY, USA, 1993.
50. Niemann, K.; Mennicken, V.R.; Jeanmonod, D.; Morel, A. The morel stereotactic atlas of the human thalamus: Atlas-to-MR registration of internally consistent canonical model. *Neuroimage* **2000**, *12*, 601–616. [CrossRef] [PubMed]
51. Schaltenbrand, G. Stereotactic methods. *Ther. Ggw.* **1961**, *100*, 383–392. [PubMed]
52. Schaltenbrand, G.; Woolsey, C.N.; World Federation of Neurology. Cerebral Localization and Organization. In Proceedings of the Symposium Sponsored by the World Federation of Neurology, Lisbon, Portugal, October 1960; University of Wisconsin Press: Madison, WI, USA, 1964.
53. Schaltenbrand, G. Personal observations on the development of stereotaxy. *Confin. Neurol.* **1975**, *37*, 410–416. [CrossRef] [PubMed]
54. Schaltenbrand, G.; Wahren, W. *Atlas for Stereotaxy of the Human Brain*; Thieme: Stuttgart, Germany, 1977.
55. Slavin, K.V.; Thulborn, K.R.; Wess, C.; Nersesyan, H. Direct visualization of the human subthalamic nucleus with 3T MR imaging. *AJNR Am. J. Neuroradiol.* **2006**, *27*, 80–84. [PubMed]
56. Sukul, V.V.; Slavin, K.V. Deep brain and motor cortex stimulation. *Curr. Pain Headache Rep.* **2014**, *18*, 427. [CrossRef] [PubMed]
57. Colpan, M.E.; Slavin, K.V. Subthalamic and red nucleus volumes in patients with Parkinson's disease: Do they change with disease progression? *Parkinsonism Relat. Disord.* **2010**, *16*, 398–403. [CrossRef] [PubMed]
58. Limousin, P.; Krack, P.; Pollak, P.; Benazzouz, A.; Ardouin, C.; Hoffmann, D.; Benabid, A.L. Electrical stimulation of the subthalamic nucleus in advanced Parkinson's disease. *N. Engl. J. Med.* **1998**, *339*, 1105–1111. [CrossRef] [PubMed]
59. Ostergaard, K.; Sunde, N.; Dupont, E. Effects of bilateral stimulation of the subthalamic nucleus in patients with severe Parkinson's disease and motor fluctuations. *Mov. Disord.* **2002**, *17*, 693–700. [CrossRef] [PubMed]

60. Vesper, J.; Klostermann, F.; Stockhammer, F.; Funk, T.; Brock, M. Results of chronic subthalamic nucleus stimulation for Parkinson's disease: A 1-year follow-up study. *Surg. Neurol.* **2002**, *57*, 306–311. [CrossRef]
61. Herzog, J.; Volkmann, J.; Krack, P.; Kopper, F.; Potter, M.; Lorenz, D.; Steinbach, M.; Klebe, S.; Hamel, W.; Schrader, B.; et al. Two-year follow-up of subthalamic deep brain stimulation in Parkinson's disease. *Mov. Disord.* **2003**, *18*, 1332–1337. [CrossRef] [PubMed]
62. Simuni, T.; Jaggi, J.L.; Mulholland, H.; Hurtig, H.I.; Colcher, A.; Siderowf, A.D.; Ravina, B.; Skolnick, B.E.; Goldstein, R.; Stern, M.B.; et al. Bilateral stimulation of the subthalamic nucleus in patients with Parkinson disease: A study of efficacy and safety. *J. Neurosurg.* **2002**, *96*, 666–672. [CrossRef] [PubMed]
63. Vingerhoets, F.J.; Villemure, J.G.; Temperli, P.; Pollo, C.; Pralong, E.; Ghika, J. Subthalamic DBS replaces levodopa in Parkinson's disease: Two-year follow-up. *Neurology* **2002**, *58*, 396–401. [CrossRef] [PubMed]
64. Thobois, S.; Mertens, P.; Guenot, M.; Hermier, M.; Mollion, H.; Bouvard, M.; Chazot, G.; Broussolle, E.; Sindou, M. Subthalamic nucleus stimulation in Parkinson's disease: Clinical evaluation of 18 patients. *J. Neurol.* **2002**, *249*, 529–534. [CrossRef] [PubMed]
65. Volkmann, J.; Allert, N.; Voges, J.; Weiss, P.H.; Freund, H.J.; Sturm, V. Safety and efficacy of pallidal or subthalamic nucleus stimulation in advanced PD. *Neurology* **2001**, *56*, 548–551. [CrossRef] [PubMed]
66. Krause, M.; Fogel, W.; Mayer, P.; Kloss, M.; Tronnier, V. Chronic inhibition of the subthalamic nucleus in Parkinson's disease. *J. Neurol. Sci.* **2004**, *219*, 119–124. [CrossRef] [PubMed]
67. Fraix, V.; Pollak, P.; Van Blercom, N.; Xie, J.; Krack, P.; Koudsie, A.; Benabid, A.L. Effect of subthalamic nucleus stimulation on levodopa-induced dyskinesia in Parkinson's disease. 2000. *Neurology* **2001**, *57*, S60–S62. [PubMed]
68. Kleiner-Fisman, G.; Fisman, D.N.; Sime, E.; Saint-Cyr, J.A.; Lozano, A.M.; Lang, A.E. Long-term follow up of bilateral deep brain stimulation of the subthalamic nucleus in patients with advanced Parkinson disease. *J. Neurosurg.* **2003**, *99*, 489–495. [CrossRef] [PubMed]
69. Krack, P.; Batir, A.; Van Blercom, N.; Chabardes, S.; Fraix, V.; Ardouin, C.; Koudsie, A.; Limousin, P.D.; Benazzouz, A.; LeBas, J.F.; et al. Five-year follow-up of bilateral stimulation of the subthalamic nucleus in advanced Parkinson's disease. *N. Engl. J. Med.* **2003**, *349*, 1925–1934. [CrossRef] [PubMed]
70. Romito, L.M.; Scerrati, M.; Contarino, M.F.; Iacoangeli, M.; Bentivoglio, A.R.; Albanese, A. Bilateral high frequency subthalamic stimulation in Parkinson's disease: Long-term neurological follow-up. *J. Neurosurg. Sci.* **2003**, *47*, 119–128. [PubMed]
71. Visser-Vandewalle, V.; van der Linden, C.; Temel, Y.; Celik, H.; Ackermans, L.; Spincemaille, G.; Caemaert, J. Long-term effects of bilateral subthalamic nucleus stimulation in advanced Parkinson disease: A four year follow-up study. *Parkinsonism Relat. Disord.* **2005**, *11*, 157–165. [CrossRef] [PubMed]
72. Rodriguez-Oroz, M.C.; Zamarbide, I.; Guridi, J.; Palmero, M.R.; Obeso, J.A. Efficacy of deep brain stimulation of the subthalamic nucleus in Parkinson's disease 4 years after surgery: Double blind and open label evaluation. *J. Neurol. Neurosurg. Psychiatr.* **2004**, *75*, 1382–1385. [CrossRef] [PubMed]
73. Rodriguez-Oroz, M.C.; Obeso, J.A.; Lang, A.E.; Houeto, J.L.; Pollak, P.; Rehncrona, S.; Kulisevsky, J.; Albanese, A.; Volkmann, J.; Hariz, M.I.; et al. Bilateral deep brain stimulation in Parkinson's disease: A multicentre study with 4 years follow-up. *Brain* **2005**, *128*, 2240–2249. [CrossRef] [PubMed]
74. Wider, C.; Pollo, C.; Bloch, J.; Burkhard, P.R.; Vingerhoets, F.J. Long-term outcome of 50 consecutive Parkinson's disease patients treated with subthalamic deep brain stimulation. *Parkinsonism Relat. Disord.* **2008**, *14*, 114–119. [CrossRef] [PubMed]
75. Gervais-Bernard, H.; Xie-Brustolin, J.; Mertens, P.; Polo, G.; Klinger, H.; Adamec, D.; Broussolle, E.; Thobois, S. Bilateral subthalamic nucleus stimulation in advanced Parkinson's disease: Five year follow-up. *J. Neurol.* **2009**, *256*, 225–233. [CrossRef] [PubMed]
76. Weaver, F.M.; Follett, K.A.; Stern, M.; Luo, P.; Harris, C.L.; Hur, K.; Marks, W.J., Jr.; Rothlind, J.; Sagher, O.; Moy, C.; et al. Randomized trial of deep brain stimulation for Parkinson disease: Thirty-six-month outcomes. *Neurology* **2012**, *79*, 55–65. [CrossRef] [PubMed]
77. Li, J.; Zhang, Y.; Li, Y. Long-term follow-up of bilateral subthalamic nucleus stimulation in Chinese Parkinson's disease patients. *Br. J. Neurosurg.* **2015**, *29*, 329–333. [CrossRef] [PubMed]
78. Tabbal, S.D.; Revilla, F.J.; Mink, J.W.; Schneider-Gibson, P.; Wernle, A.R.; de Erausquin, G.A.; Perlmutter, J.S.; Rich, K.M.; Dowling, J.L. Safety and efficacy of subthalamic nucleus deep brain stimulation performed with limited intraoperative mapping for treatment of Parkinson's disease. *Neurosurgery* **2007**, *61*, 119–127. [PubMed]

79. Romito, L.M.; Scerrati, M.; Contarino, M.F.; Bentivoglio, A.R.; Tonali, P.; Albanese, A. Long-term follow up of subthalamic nucleus stimulation in Parkinson's disease. *Neurology* **2002**, *58*, 1546–1550. [CrossRef] [PubMed]
80. Zabek, M.; Sobstyl, M.; Koziara, H.; Kadziolka, B.; Mossakowski, Z.; Dzierzecki, S. Bilateral subthalamic nucleus stimulation in the treatment of advanced Parkinson's disease. Five years' personal experience. *Neurol. Neurochir. Polska* **2010**, *44*, 3–12. [CrossRef]
81. Gan, J.; Xie-Brustolin, J.; Mertens, P.; Polo, G.; Klinger, H.; Mollion, H.; Benatru, I.; Henry, E.; Broussolle, E.; Thobois, S. Bilateral subthalamic nucleus stimulation in advanced Parkinson's disease: Three years follow-up. *J. Neurol.* **2007**, *254*, 99–106. [CrossRef] [PubMed]
82. Hamani, C.; Richter, E.; Schwalb, J.M.; Lozano, A.M. Bilateral subthalamic nucleus stimulation for Parkinson's disease: A systematic review of the clinical literature. *Neurosurgery* **2005**, *56*, 1313–1321. [CrossRef] [PubMed]
83. Ji, S.; Hartov, A.; Roberts, D.; Paulsen, K. Data assimilation using a gradient descent method for estimation of intraoperative brain deformation. *Med. Image Anal.* **2009**, *13*, 744–756. [CrossRef] [PubMed]
84. Chan, D.T.; Zhu, X.L.; Yeung, J.H.; Mok, V.C.; Wong, E.; Lau, C.; Wong, R.; Poon, W.S. Complications of deep brain stimulation: A collective review. *Asian J. Surg.* **2009**, *32*, 258–263. [CrossRef]
85. Kleiner-Fisman, G.; Herzog, J.; Fisman, D.N.; Tamma, F.; Lyons, K.E.; Pahwa, R.; Lang, A.E.; Deuschl, G. Subthalamic nucleus deep brain stimulation: Summary and meta-analysis of outcomes. *Mov. Disord.* **2006**, *21*, S290–S304. [CrossRef] [PubMed]
86. Valldeoriola, F.; Pilleri, M.; Tolosa, E.; Molinuevo, J.L.; Rumia, J.; Ferrer, E. Bilateral subthalamic stimulation monotherapy in advanced Parkinson's disease: Long-term follow-up of patients. *Mov. Disord.* **2002**, *17*, 125–132. [CrossRef] [PubMed]
87. Fenoy, A.J.; Simpson, R.K., Jr. Risks of common complications in deep brain stimulation surgery: Management and avoidance. *J. Neurosurg.* **2014**, *120*, 132–139. [CrossRef] [PubMed]
88. Voges, J.; Waerzeggers, Y.; Maarouf, M.; Lehrke, R.; Koulousakis, A.; Lenartz, D.; Sturm, V. Deep-brain stimulation: Long-term analysis of complications caused by hardware and surgery—Experiences from a single centre. *J. Neurol. Neurosurg. Psychiatr.* **2006**, *77*, 868–872. [CrossRef] [PubMed]
89. Hariz, M.I. Complications of deep brain stimulation surgery. *Mov. Disord.* **2002**, *17*, S162–S166. [CrossRef] [PubMed]
90. Ardouin, C.; Pillon, B.; Peiffer, E.; Bejjani, P.; Limousin, P.; Damier, P.; Arnulf, I.; Benabid, A.L.; Agid, Y.; Pollak, P. Bilateral subthalamic or pallidal stimulation for Parkinson's disease affects neither memory nor executive functions: A consecutive series of 62 patients. *Ann. Neurol.* **1999**, *46*, 217–223. [CrossRef]
91. Vingerhoets, G.; van der Linden, C.; Lannoo, E.; Vandewalle, V.; Caemaert, J.; Wolters, M.; Van den Abbeele, D. Cognitive outcome after unilateral pallidal stimulation in Parkinson's disease. *J. Neurol. Neurosurg. Psychiatry* **1999**, *66*, 297–304. [CrossRef] [PubMed]
92. Witt, K.; Daniels, C.; Reiff, J.; Krack, P.; Volkmann, J.; Pinsker, M.O.; Krause, M.; Tronnier, V.; Kloss, M.; Schnitzler, A.; et al. Neuropsychological and psychiatric changes after deep brain stimulation for Parkinson's disease: A randomised, multicentre study. *Lancet Neurol.* **2008**, *7*, 605–614. [CrossRef]
93. Macia, F.; Perlemoine, C.; Coman, I.; Guehl, D.; Burbaud, P.; Cuny, E.; Gin, H.; Rigalleau, V.; Tison, F. Parkinson's disease patients with bilateral subthalamic deep brain stimulation gain weight. *Mov. Disord.* **2004**, *19*, 206–212. [CrossRef] [PubMed]
94. Bejjani, B.P.; Damier, P.; Arnulf, I.; Thivard, L.; Bonnet, A.M.; Dormont, D.; Cornu, P.; Pidoux, B.; Samson, Y.; Agid, Y. Transient acute depression induced by high-frequency deep-brain stimulation. *N. Engl. J. Med.* **1999**, *340*, 1476–1480. [CrossRef] [PubMed]
95. Kulisevsky, J.; Berthier, M.L.; Gironell, A.; Pascual-Sedano, B.; Molet, J.; Pares, P. Mania following deep brain stimulation for Parkinson's disease. *Neurology* **2002**, *59*, 1421–1424. [CrossRef] [PubMed]
96. Black, K.J. Psychiatric screening for DBS. *Parkinsonism Relat. Disord.* **2007**, *13*, 546. [CrossRef] [PubMed]

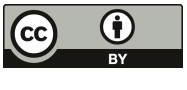

brain sciences

MDPI

Article

Long-Term Task- and Dopamine-Dependent Dynamics of Subthalamic Local Field Potentials in Parkinson's Disease

Sara J. Hanrahan [1], Joshua J. Nedrud [1], Bradley S. Davidson [2], Sierra Farris [3], Monique Giroux [3], Aaron Haug [4], Mohammad H. Mahoor [5], Anne K. Silverman [6], Jun Jason Zhang [5] and Adam Olding Hebb [1,*]

1 Colorado Neurological Institute, Englewood, CO 80113, USA; shanrahan@thecni.org (S.J.H.); jnedrud@thecni.org (J.J.N.)
2 Department of Mechanical and Materials Engineering, University of Denver, Denver, CO 80208, USA; Bradley.Davidson@du.edu
3 Movement and Neuroperformance Center of Colorado, Englewood, CO 80113, USA; sierrafarris@gmail.com (S.F.); giroux_ml@yahoo.com (M.G.)
4 Blue Sky Neurology, Englewood, CO 80113, USA; aaronhaug@gmail.com
5 Department of Electrical and Computer Engineering, University of Denver, CO 80208, USA; Mohammad.Mahoor@du.edu (M.H.M.); Jun.Zhang@du.edu (J.J.Z.)
6 Department of Mechanical Engineering, Colorado School of Mines, Golden, CO 80401, USA; asilverm@mines.edu
* Correspondence: adam.hebb@aoh.md

Academic Editors: Tipu Aziz and Alex Green
Received: 16 August 2016; Accepted: 17 November 2016; Published: 29 November 2016

Abstract: Subthalamic nucleus (STN) local field potentials (LFP) are neural signals that have been shown to reveal motor and language behavior, as well as pathological parkinsonian states. We use a research-grade implantable neurostimulator (INS) with data collection capabilities to record STN-LFP outside the operating room to determine the reliability of the signals over time and assess their dynamics with respect to behavior and dopaminergic medication. Seven subjects were implanted with the recording augmented deep brain stimulation (DBS) system, and bilateral STN-LFP recordings were collected in the clinic over twelve months. Subjects were cued to perform voluntary motor and language behaviors in on and off medication states. The STN-LFP recorded with the INS demonstrated behavior-modulated desynchronization of beta frequency (13–30 Hz) and synchronization of low gamma frequency (35–70 Hz) oscillations. Dopaminergic medication did not diminish the relative beta frequency oscillatory desynchronization with movement. However, movement-related gamma frequency oscillatory synchronization was only observed in the medication on state. We observed significant inter-subject variability, but observed consistent STN-LFP activity across recording systems and over a one-year period for each subject. These findings demonstrate that an INS system can provide robust STN-LFP recordings in ambulatory patients, allowing for these signals to be recorded in settings that better represent natural environments in which patients are in a variety of medication states.

Keywords: Parkinson's disease (PD); local field potential (LFP); deep brain stimulation (DBS); beta frequency oscillations; subthalamic nucleus; closed-loop

1. Introduction

The subthalamic nucleus (STN) is a common target for deep brain stimulation (DBS) therapy in patients with Parkinson's disease (PD). DBS alleviates the motor symptoms of PD [1], but may

lead to side effects, such as impaired cognition [2], speech [3,4], gait [5] and balance [6]. An adaptive DBS system with active modulation of stimulation by appropriate physiological control variables may reduce these side effects, while providing maximum therapeutic benefit of PD motor symptoms [7–11]. Local field potentials (LFP) recorded from the STN have the potential to be a robust control signal to indicate a change in a patient's state [12–15]. STN-LFPs have been shown to correlate with a patient's Parkinson's disease symptom state [16], levodopa medication level [17,18], behavior [19–21] and neurostimulation intensity [8]. Furthermore, LFP signals are stable over long periods of time, as evidenced by recordings from the motor cortex [22] and STN [23,24], a necessary characteristic for a feedback signal in a closed-loop DBS system.

In PD patients, the loss of nigral dopaminergic input to the striatum leads to the symptoms of rigidity and bradykinesia [25] that are related to increased beta frequency oscillatory power (β power). Decreased dopaminergic inputs to the basal ganglia promote synchronized oscillatory activity in the beta frequency (13–30 Hz) of STN-LFP recordings [26–29] and have been shown to correlate with worsening of rigidity and bradykinesia [16]. Prominent beta frequency oscillations can also be observed from the cortical surface using EEG [17,30] and ECoG electrodes [31]. In concurrence with the reduction of PD motor symptoms, dopaminergic therapy has been shown to suppress synchronized beta frequency oscillations [17,18] and resulted in a new peak in the gamma frequency from 60 to 80 Hz [18] and in the high frequency oscillation of 300 Hz in STN-LFPs [32].

Beta frequency oscillations in the STN-LFP are reduced before and during voluntary movements [21,27,33]. This event-related desynchronization (ERD) in the beta frequency behaves in a manner consistent with movement-related processing in the cortex, specifically the supplementary motor cortex [33]. Beta frequency desynchronization with movement suggests that beta suppression may be a prerequisite of voluntary movement [34–36]. Levodopa therapy has been shown to increase the duration and magnitude of relative pre-movement beta frequency ERD [37], strengthening the hypothesis that beta ERD is a non-pathological phenomenon. Event-related synchronization (ERS), or increases in power, occurs in subjects performing voluntary movements in the gamma frequency (>35 Hz) of EEG signals recorded from the motor cortex [38]. This gamma ERS (increased γ power) is felt to represent increased local neuronal computation and thus to reflect normal neural processes necessary for movement. Synchronous gamma frequency oscillations also develop in STN-LFPs and supplementary motor area activity in PD patients only after patients have been treated with levodopa medication (medication "on" state) [17]. As this STN-LFP gamma ERS is only observed in a medication on state, it is assumed to reflect normal neural processes, as in motor cortex.

STN-LFP activity in PD patients is traditionally recorded directly from the macroelectrodes on the DBS lead intraoperatively or postoperatively, in the interval between lead implantation and subsequent connection to the subcutaneous implantable neurostimulator (INS). In these controlled environments, brief recordings are performed with subjects in a reclined operating table or hospital bed and may not be representative of the variable recordings that will be present in a real-world setting. As PD symptoms are dependent on the patient's attention, alertness and behavior, the STN-LFP activity likely varies with these factors, as well [39–43]. Therefore, inter-day variability will be a challenge that must be addressed in a closed-loop DBS system. In this paper, we chronically record STN-LFP in PD subjects in the medication on and off state while the subject is at rest and performing motor and speech behavioral tasks using a DBS system that is augmented with LFP recording capability [24,44,45]. Reliable chronic recording of neural activity with a fully-implanted system is an imperative first step towards developing a closed-loop DBS system.

2. Materials and Methods

2.1. Recruitment

Seven subjects undergoing DBS as standard of care for the treatment of idiopathic PD were enrolled in this study (Table 1). All subjects provided informed consent for participation in this research

study, in a manner approved by the HealthOne Institutional Review Board (approval code 418262) and the Food and Drug Administration Investigational Device Exemption regulation (Clinical Trial Number NCT02115802).

Table 1. Subject demographics.

Subject	Age (years)	Sex	Handedness	Pre-op UPDRS III [1]	Post-op UPDRS III [2]	Diagnosis and Predominant Symptom	Clinical DBS Settings Left STN	Clinical DBS Settings Right STN	Bipolar Channels for Behavioral Recording
1	59	F	R	37/22	35/24/16/13	PD, bradykinesia	E3, E2$^-$, 3.6 V, 60 μs, 130 Hz	C, E1$^-$, 3.6 V, 60 us, 130 Hz	L: 2/3, R: 0/1
2	65	M	R	48/14	49/23/17/16	PD, rigidity	E1, E2$^-$, 2.6 V, 60 μs, 150 Hz	C, E2$^-$, 2.4 V, 60 us, 150 Hz	L: 2/3, R: 2/3
3	63	F	R	23/6	32/25/24/16	PD, dyskinesias	E3, E2$^-$, 2.4 V, 60 μs, 130 Hz	E3, E2$^-$, 2.5 V, 60 us, 130 Hz	L: 1/2, R: 2/3
4	71	M	R	31/7	38/37/21/20	PD, gait disturbance	E3, E2$^-$, 3.6 V, 60 μs, 130 Hz	E3, E2$^-$, 3.6 V, 60 μs, 130 Hz	L: 2/3, R: 2/3
5	44	M	R	38/20	36/16/29/11	PD, tremor	C, E1$^-$, E2$^-$, 2.9 V, 60 μs, 130 Hz	C, E2$^-$, 3.2 V, 60 μs, 130 Hz	L: 1/2, R: 2/3
6	62	M	L	31/20	24/16/21/14	PD, tremor	C, E1$^-$, 2.6 V, 60 μs, 130 Hz	C, E1$^-$, 3.9 V, 70 μs, 135 Hz	L: 1/2, R: 2/3
7	68	M	R	67/40	-/-/-/-	PD, bradykinesia	C, E1$^-$, 2.2 V, 60 μs, 130 Hz	C, E2$^-$, 2.0 V, 60 μs, 130 Hz	L: 2/3, R: 2/3

[1] Pre-op UPDRS III listed in order of Medication off/Medication on; [2] Post-op UPDRS III listed in order of Medication off-DBS off/Medication off-DBS on/Medication on-DBS off/Medication on-DBS on. PD, Parkinson's disease. UPDRS, unified Parkinson's disease rating scale. STN, subthalamic nucleus. M, male. F, female. L, left. R, right.

2.2. DBS Surgery

Subjects underwent DBS surgery in the off medication state per clinical routine. DBS lead implantation surgery was performed with a Leksell (Elekta, Stockholm, Sweden) stereotactic head frame and Surgiplan (Elekta, Stockholm, Sweden) targeting software. Targeting of the dorsolateral STN was based on a combination of formula-based and indirect coordinates. We used an a priori, formula-based target of (x, y, z): ($\pm$12 mm, $-$2 mm, $-$4 mm) with respect to the mid-commissural point and anterior commissure (AC)–posterior commissure (PC) plane. Targeting was then adjusted based on indirect targeting from the borders of the red nucleus (RN) for (x, y, z): (3 mm lateral to the RN border, at the anterior border of RN, 2 mm inferior to the superior border of RN). The prescribed sagittal trajectory angle was 60 degrees from the AC-PC plane, and the coronal angle was 15 degrees from a parasagittal plane, with minor adjustments for cortical sulci and blood vessels. Microelectrodes (Alpha Omega, Nazareth, Israel) were positioned in the center and anterior positions or the center, anterior and lateral positions of a BenGun trajectory guide, with a parallel separation of 2 mm. Moderate propofol anesthesia was used without a protected airway only during placement of the burr hole. Clinical microelectrode recording was performed from 15 mm above to approximately 2 mm below the target. Whereas subjects may have had residual effects from propofol during the initial microelectrode recording though thalamic nuclei, we did not proceed with recording in the STN region until patients were fully awake and conversant. After localization of the STN, the microelectrodes were removed, and a permanent 4-electrode DBS lead (Medtronic 3389, Minneapolis, MN, USA) was implanted in the optimal BenGun trajectory.

In a separate surgery, an implantable neurostimulator (INS) with additional voltage recording capabilities [44] (Activa PC + S, Medtronic, Inc., Minneapolis, MN, USA) was implanted subcutaneously to provide both standard therapeutic stimulation and bilateral local field potential (LFP) recordings.

2.3. Data Collection

Simultaneous bilateral recordings were performed in all subjects. All recordings used a subset of the 4 macroelectrodes of each DBS lead. The DBS lead electrode is platinum/iridium, has a surface area of 6.0 mm^2 and an impedance of 1.7 kΩ (mean; 95% CI = 1.1–2.4 kΩ) [21].

All subjects underwent an intraoperative (OR) data recording session during the initial implantation surgery. Signals were amplified and digitized with a sampling frequency (Fs) of 4.8 kHz (g.USBamp, g.tec, Graz, Austria) and combined with event markers and subject response signals [46]. Skin surface electrodes were used for ground and linked bilateral mastoid common reference. LFP electrodes consisted of linearly-ordered contacts, with 0 being the most ventral and 3 being the most dorsal. Channels were bipolar re-referenced (0–1, 1–2, 2–3) prior to analysis for each brain hemisphere.

Two types of postoperative INS recordings were performed: non-behavioral montage signal review and behavioral dual bipolar recording. During the non-behavioral montage signal review, all bipolar channel pairs from each hemisphere were amplified and digitized with a Fs of 422 Hz by the INS for 30 s sequentially. During the behavioral recording, two bipolar re-referenced LFP signals, one from each hemisphere, were amplified and digitized (Fs 422 Hz) by the INS (Table 2). Using the initial montage signal review, the bipolar pair of channels that contained the most prominent peak in beta frequency oscillations was selected for further behavioral recordings. This selection method emphasized a relative strength of beta power over other frequencies. Simultaneously, the biopotential of the skin over the INS was amplified and digitized (Fs 4.8 kHz) (g.USBamp, g.tec, Graz, Austria) and combined with event markers and subject response signals [46]. The INS was used to produce a 5-Hz, 2-V, 90-μs non-therapeutic stimulation signal at the beginning and end of each recording. Digitized signals were then downloaded from the INS and synchronized to the external signals using the artifacts produced by the non-therapeutic stimulation. Recordings were performed at 1, 3, 6 and 12 months after DBS lead implantation. Montage signal review was performed at each recording session, and behavioral recordings were performed at Months 3 and 6. All postoperative recording sessions were performed in the medication on state, except for the 6-month recording (Table 3). Subject 1 did not have a postoperative recording session in the medication off state. At the time of publication, all subjects have undergone the 1-, 3-, and 6-month sessions, and 5 of the 7 subjects have undergone the 12-month session. Medication off recording sessions were performed after subjects refrained from taking their prescribed levodopa medications for at least 12 h. Medication on recordings sessions were performed while the subjects were administered their prescribed levodopa medication dosage. All recordings were performed with the stimulation off.

Table 2. Comparison of amplifier settings for intraoperative and postoperative recording sessions.

	OR	INS
Input impedance	>100 MOhm	1 MOhm
Range	−250 mV–250 mV	−10 V–10 V
Filters used	0.5–2000 Hz	0.5–100 Hz
Sampling Rate	4800 Hz	422 Hz
Noise Floor	<0.3 μV RMS (0.1–10 Hz)	Min signal to detect 1 μV RMS differential with noise floor <0.3 μV RMS

OR, operating room. INS, implantable neurostimulator. MOhm, megaohm. RMS, root mean square.

Table 3. Timing and type of recording sessions performed.

Recording Session	Intra-Operative	1 Month	3 Month	6 Month	12 Month
Recording Type	OR	INS	INS	INS	INS
Medication State	Off	On	On	Off	On
Non-behavioral Montage Recording	6 bipolar channels	6 bipolar channels	6 bipolar channels	6 bipolar channels	6 bipolar channels
Behavioral Recording	-	-	2 bipolar channels	2 bipolar channels	-

2.4. Behavioral Tasks

Behavioral tasks were performed postoperatively and included motor and speech tasks. The motor tasks were cued button pressing, a one out of eight target reaching for both the left and right arm/hand and a cued tongue extension. The speech task was a cued reading aloud of one word presented on a computer screen. Tasks were selected to evoke language- and motor-based neural activity in the STN with precise and consistent timing for robust analysis. More specifically, button press was chosen as a simple motor task that models finger tapping [21,47]. A reach task was selected as an alternative motor task requiring larger muscle recruitment and coordination [48,49]. A brief speech task was chosen because it was consistent in timing with the movement tasks, but similar tasks have been previously used [21,50]. A mouth movement task was used as a comparison to the speech tasks. Each task was repeated with a period of 5 s with a $\pm$ 0.5 s jitter in blocks of 11 trials for neurostimulator recordings due to the memory constraints of the INS system with 10 s of reset between each block. The subject was instructed to return to a comfortable resting position between each trial, so the period immediately preceding the cue could be used as a baseline resting state. The entire paradigm was performed up to three times during each session based on subject fatigue. For task initiation, subjects received an audio and visual cue from a presentation computer running a custom Python application (Python Software Foundation, version 3.5, Wilmington, DE, USA). A random time factor ($\pm$ 0.5 s) was programmed into the trial period length to reduce any effect of anticipation.

2.5. Analysis

Time series data of subject response channels were reviewed to mark motor and speech onset and offset times for tasks. Button press responses were extracted from the digital input channel using a threshold algorithm. Reaching motor responses were extracted from the touch-screen monitor digital input channel using a threshold algorithm. Both button and touch-screen inputs were recorded as digital channels; using a threshold of 0.5, values above this threshold (1) indicate a response, while values below this threshold (0) indicate no response. The sensitivities of the button and the touch-screen were left at their factory set defaults. Tongue extension responses were marked from the first time synced video frame the tongue was visible until the last video frame the tongue was visible. Speech responses were manually marked from the start of the first audible syllable above the noise floor until the end of the last audible syllable above the noise floor in the time-synced audio channel.

Power spectral density estimates were calculated using a custom Welch's method with 50% overlapping Hanning windowed segments of 256 samples padded to 1024 samples for a frequency resolution of 422/1024 (~0.412 Hz). Time-dependent power spectral density estimates were calculated using both wavelet analysis and a fixed-window short time Fourier transform technique [51,52]. Wavelet analysis utilized complex Morlet wavelets and operated on time-by-trial event matrices based on subject response time markers. Button press motor action onset and offset were determined by the digital input channel. For reach motor action, trials were aligned by touch-screen response timing (i.e., at the completion of the reach motion, when the subject hits the target). To measure ERDs, the number of pixels of significant desynchronization in the area of interest around the event were summed. Ratios between two different ERD measures were then computed to compare spectrograms and remove the dependence on pixel density; Student's *t*-tests were used to compare these ratios against 1 as a significance test.

2.6. Statistics

Permutation (bootstrap) analyses were applied to the spectrogram response matrices to determine significant deviation from the baseline of ERS or ERD [21]. These matrices were built using entire-record normalized log transformed data, baselined on a trial-by-trial basis. A time window of 500-ms duration, terminating 100 ms before the cue, was used for baseline data for all tasks. A permutation "sign-test" was performed using randomly-sampled trials without replacement using a custom Python script.

For each permutation, the sign of half of the trials was inverted and a new average generated. The null hypothesis states that no ERSs or ERDs are significantly different from zero, and therefore, inversion of the sign would be expected to increase the absolute value of the average for a substantial number of permutations. For the alternate hypothesis, ERSs or ERDs are significantly different from zero, and inversion would be expected to decrease the absolute value of the average.

To correct for multiple comparisons, we conservatively assumed that each 50-ms segment could be considered an independent sample. We calculated the number of permutations, such that the resolution of our *p*-value was 1/5 of the corrected significance value for an alpha error of 5%. This calculation was 5 × (((spectrogram duration)/50 ms)/5%) permutations, which gives corrected *p*-value resolutions of 1/permutations. The spectrogram duration used for statistical analysis and the number of permutations for each task are as follows: button press task, 4 s and 8000 permutations; reach task, 5 s and 10,000 permutations; tongue extension task, 4 s and 8000 permutations; speech task, 4 s and 8000 permutations. To calculate our *p*-value, we counted the number of permutations that created a new mean greater than the original mean and multiplied this count by the resolution of our *p*-value, producing a statistical matrix. If the permutation mean was greater than the original mean, no more than the 5/permutations fraction, the null hypothesis was rejected for that pixel, and it was deemed significant.

The Pearson product-moment correlation coefficient was applied to pairs of calculated power spectral density (PSD) estimations to test for significant spectral correlation between STN-LFP recordings at different times or in different states. Bonferroni correction was applied when testing multiple pairs.

3. Results

STN-LFP activity from fourteen hemispheres of seven PD subjects was analyzed. The mean age of the subjects at DBS lead implant was 61 ± 9 years. Two subjects were female. All subjects were evaluated preoperatively using the unified Parkinson's disease rating scale (UPDRS) III in the medication on and off state. Six of seven subjects were evaluated postoperatively using the UPDRS III in the medication on and off state and DBS stimulation on and off state. Predominant PD symptoms with a notably high value in the initial UPDRS evaluation prior to DBS implantation included bradykinesia, rigidity, dyskinesias, gait disturbances and tremor. Clinical DBS settings from the last recording session can be viewed in Table 1.

STN-LFPs recorded with an external amplifier in the operating room and an INS system in the clinic at six months post lead implantation both yield signals with similar characteristics. Peaks in the beta frequency were visible in 19 out of 36 PSD estimates in the OR recordings and 15 out of 36 PSD estimates in the six-month INS recordings. Beta frequency peaks varied in amplitude and specific frequency range by subject. Figure 1 demonstrates the PSD estimation of representative bipolar channel pairs in the acute and chronic setting for each subject. Although the INS was set at a lower sampling rate of 422 Hz compared to 4.8 kHz (Table 2), the spectral content of the signals was comparable with a characteristic one/frequency curve common in LFP signals. A peak at 60 Hz was visible in two of the six subjects in the intraoperative recording session due to environmental line noise. No 60-Hz artifacts were visible in the postoperative recording sessions with the INS system. Across the full set of bipolar channel pairs, 33 of 36 recordings showed significant correlation between PSD estimations derived from recordings in the acute and chronic setting (multiple correlation tests with Bonferroni correction, $\alpha = 0.05/36$ (~0.0014)). Channel pairs that had PSD estimations that were significantly different included one channel pair with an impedance consistent with an electrical short (Subject 3) and two channel pairs with a large amount of 60-Hz line noise due to a lack of stable ground connection in the OR recording (Subject 5).

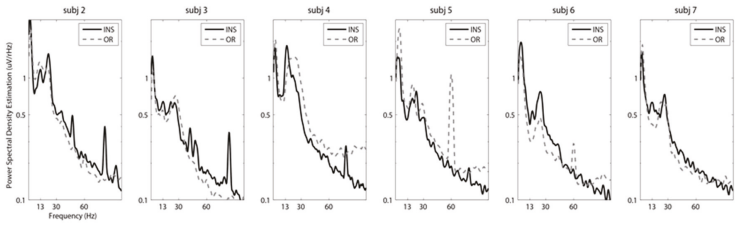

Figure 1. Stability of subthalamic nucleus (STN) local field potential (LFP) signals across recording systems in acute and chronic environments. Representative power spectral density (PSD) estimations of 30-s STN-LFP epochs with subjects at rest in the medication off state are presented. One bipolar channel pair was selected for each subject as an exemplar PSD. The selected bipolar channel pairs for Subjects 2, 3, 5 and 6 were left hemisphere Channels 1 and 2. The selected bipolar channel pairs for Subjects 4 and 7 were right hemisphere Channels 1 and 2. Implantable neurostimulator (INS) digitized signals were recorded at six months post deep brain stimulation (DBS) lead implantation in the medication off state, and STN-LFP signals were recorded in the operating room (OR) during DBS lead implantation. Prominent peaks in the beta frequency were observable in both types of recordings. Subject 1 did not have a recording in the medication off state.

STN-LFPs recorded while each subject was at rest were compared across one year. Similar to the comparison of recording amplifiers, the spectral content in STN-LFP signals varied across subjects, but remained consistent across sessions within subjects (Figure 2). Prominent peaks in beta frequency were visible in 18 out of 36 PSD estimations in the on medication state (Month 3) and 15 of 36 of PSD estimations in the off medication state (Month 6). Peaks in beta frequency varied in amplitude and specific frequency range by subject. The average beta frequency (13–30 Hz) maximum for each subject across all recording sessions ranged from 16.0–25.5 Hz with an average across all subjects of 20.4 $\pm$ 4.1 Hz. In early recording sessions, the power analysis subsystem of the INS recording system was programmed to a suboptimal setting that led to a contaminate signal in the recording at the 25, 50 and 75 Hz as seen in PSD estimation for the 1-, 3- and 6-month session for Subject 2, the 1-, 3- and 6-month sessions for Subject 3 and the one-month session for Subjects 1 and 5. This contamination was later avoided by configuring the power analysis subsystem into lower priority frequencies to minimize its impact on the recording. Within subjects, all but one channel pair showed significant correlation between INS PSD estimations over time (multiple correlation tests with Bonferroni correction, $\alpha = 0.05/216$ (~0.0002))) (Table S1). The inconsistent channel pair was due to an electrical short in one channel pair in Subject 3.

STN-LFP activity was further examined for differences between therapeutic and nontherapeutic contacts, as well as differences from the medication on and off state. The spectral content of STN-LFP activity recorded from therapeutic and non-therapeutic contacts while the subjects were at rest in the medication off state at six months was compared (Figure 3). Therapeutic contacts were the active (negative) contact selected by the subject's neurologist. The therapeutic electrode was deduced after testing each cathode using 60 μs, 130 Hz and selecting the cathode that was most effective in reducing rigidity, bradykinesia and/or tremor with priority given to the efficacious cathode requiring the lowest amplitude to reach the most effective symptom reduction. Side effects were not a factor in selecting the most effective (therapeutic) cathode; however, stimulation-induced side effects were a factor in selecting polarity and pulse width. Clinical DBS settings are listed in Table 1. For Subject 5, a double cathode was used to expand the area of activation when side effects limited the increase in amplitude and pulse width. Therapeutic bipolar channel pairs consisted of at least one therapeutic contact. A prominent peak in beta frequency power was observed in 16 of the 25 therapeutic bipolar channel pairs, although the size and shape of the beta frequency peak was inconsistent across subjects. Notably, eight of 11 non-therapeutic bipolar channel pairs

lacked prominent peaks in the beta frequency. Examining only therapeutic bipolar channel pairs across all subjects, there was not a significant decrease in total beta frequency power in the STN-LFP activity recorded at three months post lead implantation with subjects in the medication on state compared to the STN-LFP activity recorded at six months post lead implantation in the medication off state (paired *t*-test with Bonferroni correction, $\alpha = 0.05/6$ (~0.0083)). Furthermore, there were no significant interactions between therapeutic/non-therapeutic bipolar channels and medication or the laterality of the bipolar channels and medication when measuring total beta power (two-factor ANOVA, $\alpha = 0.05$). The overall change in total beta power from the on medication to off medication state was $-0.28\% \pm -0.1\%$. If subjects who exhibited an increase in beta frequency power in the on medication state were excluded, there remained a minimal effect with an average $9\% \pm 3\%$ decrease in beta frequency power in the on medication state in comparison to the off medication state (Figure S1).

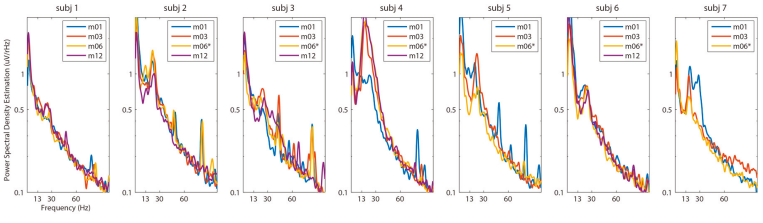

Figure 2. Stability of subthalamic nucleus (STN) local field potential (LFP) signals recorded with an implantable neurostimulator over one year. Representative PSD estimations of 30-s STN-LFP epochs with subjects at rest over one year are presented. One bipolar channel pair was selected for each subject as an exemplar PSD. The selected bipolar channel pairs for Subjects 1, 2, 3, 4, 5 and 6 were left hemisphere Channels 1 and 2. The selected bipolar channel pair for Subject 7 was right hemisphere Channels 1 and 2. Figure S4 provides the PSDs for all bipolar channel pairs. STN-LFP frequency content was visibly consistent across multiple recording sessions. Legends denote recording date in months post-surgical implantation * Denotes recording sessions in which the subject was in the medication off state.

STN-LFP event-related power changes were examined in the medication on and off state at three and six months post DBS lead implantation. All subjects completed six different cued tasks in four categories, left and right button press with a combined reaction time of 0.49 ± 0.18 s, left and right reaching with a combined reaction time of 1.37 ± 0.38, tongue extension with a reaction time of 0.61 ± 0.28 and cued reading with a reaction time of 0.75 ± 0.22. Significant changes in relative power were generally limited to beta (13–30 Hz) and low gamma (35–70 Hz) frequencies, although some significant changes in relative power were visible in frequencies below 13 Hz (Figure 4). The relative ERD of beta and the ERS of gamma frequency oscillations were present in all behaviors, but significant changes in gamma oscillations were not consistently present in all subjects. Gamma ERS was only observed in the medication on state. Dopaminergic medication did not diminish the magnitude of the beta ERD. Across all subjects, dopaminergic medication produced a significant increase in the relative magnitude and duration of beta frequency ERD for all behaviors, except right button press; see Figure S2 (paired *t*-test, $\alpha = 0.05$). Event-related power change patterns over time were variable across behaviors. Left and right arm reach to target movement had the longest duration of relative power change. Unlike the other behavioral tasks, time zero marked when the subject completed the reach at the highlighted target, prior to moving back to resting position. Brief, relative significant changes in power occurred with left and right hand movement. Similar to limb movements, speech and mouth movement showed significant beta ERD and gamma ERS.

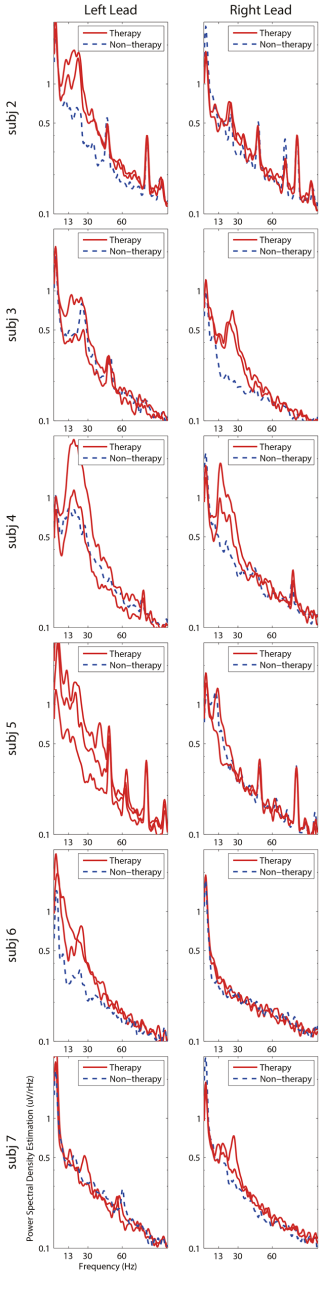

Figure 3. Spectral content of subthalamic nucleus (STN) local field potentials (LFP) signals recorded with an implantable neurostimulator (INS) from therapeutic and non-therapeutic contacts. PSD estimation of 30-s STN-LFP epochs of all bipolar channel pairs for each subject at rest at six months post deep brain stimulation lead implant in the medication off state are presented. Therapeutic bipolar channel pairs consisted of at least one therapeutic (negative) contact for stimulation. Subject 1 did not have a recording in the medication off state.

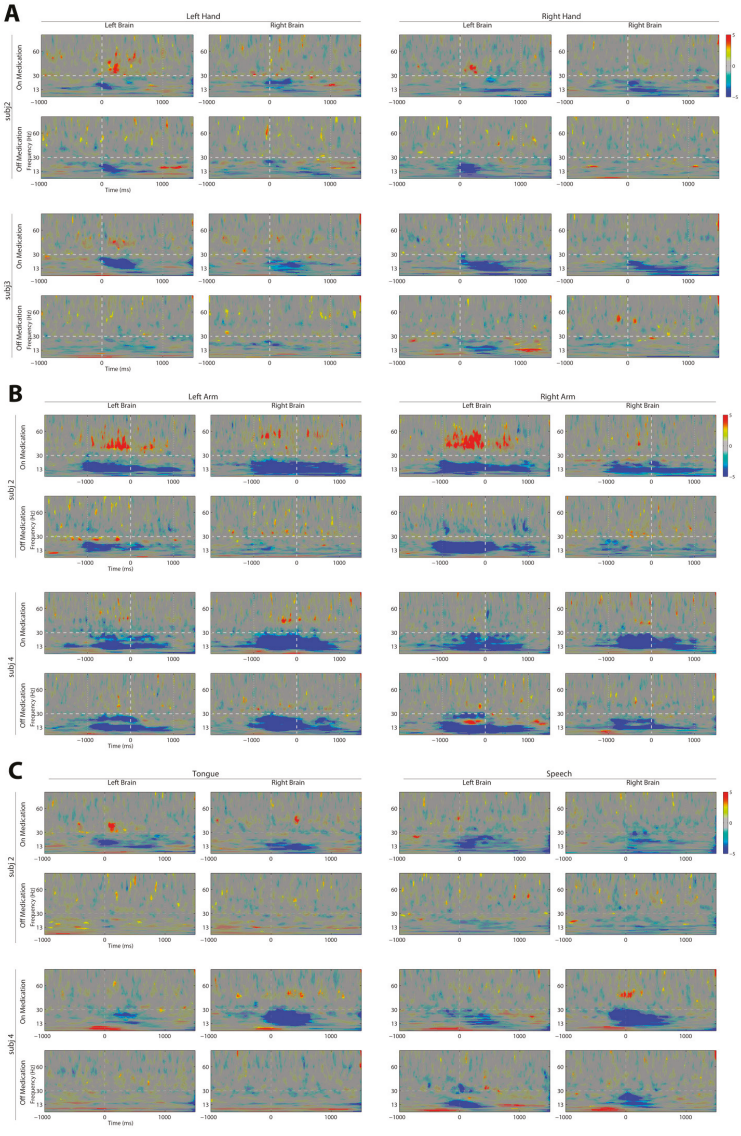

Figure 4. Dopamine-dependent dynamics of subthalamic nucleus (STN) local field potential (LFP) activity recorded with an implantable neurostimulator (INS) with behavioral events. Subjects performed (**A**) left and right button press, Time 0 ms indicates digital response; (**B**) left and right reach, Time 0 ms indicates detection of reaching target by a touch-screen monitor; (**C**) tongue extension, Time 0 ms indicates first observance of tongue with a time-synced video recording; and speech, Time 0 ms indicates the onset of speech as detected by a time synced audio recording. Medication on recordings were performed at three months post DBS lead implant. Medication off recordings were performed at six months post DBS lead implant. STN-LFP event-related desynchronization (ERD) in beta (13–30 Hz) frequencies was observed in the medication off state. STN-LFP ERD in beta frequencies and event-related synchronization in low gamma (35–70 Hz) frequencies were observed in the medication on state. One bipolar channel pair was selected from each hemisphere for behavioral recordings (listed in Table 1). Figure S3 provides the spectrograms for all subjects performing each behavior.

4. Discussion

In this study, we examine the influence of medication and behavior on STN-LFP features in PD subjects over one year. With the expected ongoing development of closed-loop DBS systems that utilize features of the LFP as a control signal, the stability of this feature modulation in response to patient factors (behavior, medication) is critical to establish.

The INS system used in this study is an early step in the development of a closed-loop DBS system. The significant advantage of this system is the ability to chronically record STN-LFP. As an implanted system, advantages include the absence of movement artifacts and line noise that contaminate traditional LFP recordings, as seen in Figure 1, and the ability to record LFP signals in a variety of environments and medication states. The INS system utilized in this study is the first of its kind to be implanted in patients [24,44,45]. Two previous studies have utilized the same INS system to examine STN-LFP activity while subjects were performing different behaviors and with varying amplitudes of deep brain stimulation. Although one study was performed in non-human primates [45] and the other in human subjects [24], both studies were able to record reliable LFP signals that were comparable to intraoperative STN-LFP signals. Behavioral recording sessions with the INS are limited in length, number of channels and sampling rate. Recording sessions are stored to an internal memory and retrieved as a second step. The two-step procedure also increases the amount of time that our subjects give to the project. For our recording sessions, we configured the device to record two time-domain channels at Fs 422 Hz without compression, and internal memory restrictions limited recordings to 15 min. Next generation devices may address many of these limitations by increasing the number of simultaneous recording channels and streaming the data in real time, eliminating the recording time limit and decreasing the time needed for each subject visit.

The INS device used in this study is powered by a non-rechargeable battery that is shared with the neurostimulation circuitry. Thus, utilization of the sensing technology potentially reduces the lifetime of the stimulator. Furthermore, the power analysis subsystem circuitry of the INS system produces a crossover signal in the time domain recording at the configured frequency. By changing the configured power analysis frequency, this contamination can be moved into lower priority frequencies to minimize its impact on the recording. However, our site had noticeable peaks in their PSD at 25, 50 and 75 Hz in early recordings. These artifacts at 25, 50 and 75 Hz did not affect our analysis of beta power at rest or with an event. All our INS recordings were performed with the stimulation off. Active stimulation would create more artifacts in DBS lead recordings, but setting recording parameters, such as the INS recording gain and channel configuration, can limit the influence of stimulation artifact on the recording signal. Furthermore, many groups are examining methods to remove stimulation artifacts [53–55] from STN-LFP.

The STN-LFP activity varied between subjects, but was consistent within subjects across recording systems and over a one-year time period. In our study, we found consistent spectral content of LFP activity less than 100 Hz across the one year of recordings. The stability of LFPs has been previously examined up to a span of seven years post DBS implantation. Similar to our findings, beta band amplitude was consistent at three weeks post DBS lead. However, the amplitude decreased at two to seven years after the DBS implant [23]. In the medication on and off states, we observed a prominent peak in beta frequency power spectral density. Beta power from STN-LFP recorded from therapeutic contacts while the subject was at rest did not significantly vary with medication state. Therapeutic contacts were selected for this analysis because they have been found to have higher beta power in comparison to non-therapeutic contacts in previous studies and in our results [56,57]. The suppression of beta frequency activity in the resting state with dopaminergic medication has been observed in other studies [17,18,37], but was inconsistent in our study.

Similar to previous work, beta ERD was demonstrated to be coincident with a behavioral task [23]. The amplitude of this modulation, relative to a baseline period immediately preceding the cue to start movement, was greater in the medication on state in five of six tasks. This phenomenon, although counter to the pathological hypothesis of beta frequency rhythms in Parkinson's disease, has been

previously observed [24]. This work reinforces the theory that dopaminergic mechanisms facilitate movement-related beta desynchronization. The gamma ERS was, as expected, present only in the medication on state, but was inconsistently observed. However, the frequency of gamma ERS in our study was in a lower gamma range than has been observed in previous studies [32,33,58]. Left and right reaching movements elicited the largest difference between medication on and off states, likely because this behavior involved sustained gross motor movement of the entire arm, where other behaviors were more restricted.

We acknowledge that there are limitations of the current study with respect to our findings on the medication effect on beta power. We demonstrated that there was no significant medication effect on overall beta power present at rest. Furthermore, the on medication state had a significant influence on the strength and duration of beta ERD, when compared to the pre-activity baseline. However, comparing STN-LFP activity during the medication on state at three months to the medication off state at six months would be dependent on a time factor, as well as the medication state. It is possible the recordings at six months could be influenced by a degradation of the signal. We were not able to collect on and off medication data at each three- and six-month encounter. In designing the study, we wanted to preserve the lifetime of the generator and limit the number of recording sessions we performed, while extending the recording to 12 months after DBS implant. We do not believe that our results were due to overall degradation of recording over time. As seen in Figure S4, for the channels chosen for behavioral recordings (Table 1), the prominent beta peak was consistent across 3, 6 and 12 months. Furthermore, the increase in impedance from 3–6 months was minimal at 2.6% $\pm$ 18%. We believe this small change in impedance is within the typical range of variability seen in DBS systems [59] and, therefore, demonstrates that the impedances were stable between the two recording sessions. The current study was designed to explore changes in frequency with behavioral tasks, but not to fully elucidate the medication effect. Investigations particularly designed to address this question are planned for future studies.

The magnitude and time course of beta and low gamma power modulation in response to behavior were variable between subjects. This synchronization/desynchronization modulation did not reach significance for certain subjects. Sources for variation between subjects may stem from differences in DBS lead location within the STN, the level of patient's PD progression, prescribed medication, predominant PD symptoms and unknown factors. This variability has direct implications for the development of closed loop systems. From our work, only a subset of subjects had reliably significant movement-related synchronization patterns for targeting as a control signal for DBS [11]. Strategies for surgical targeting regions of the STN where control signals are optimum may be required for closed loop systems. In this study, surgical targeting was not considered for optimal STN-LFP signals, as the utilization of these signals is not standard clinical practice.

5. Conclusions

Our study examined the influence of medication and behavior on STN-LFP activity in PD patients over one year. Many groups are currently investigating appropriate neurophysiological biomarkers to be used as a feedback signal in a closed-loop DBS system [11,49,60–62]. The INS system in our study was able to consistently record LFP power fluctuations with behavior, demonstrating an ability to utilize STN-LFP signals as a surrogate for behavioral program activation in a closed-loop DBS system. Although the number of simple behavioral tasks performed by subjects was limited, STN-LFP activity was sensitive to the particular type of motor program. Patterns within STN-LFP signals have been determined to be specific to different motor programs allowing for high classification rates [20]. The data presented demonstrate that STN-LFP activity may be an appropriate feedback signal that is stable over time, providing relevant patient-specific information on a subject's behavior and medication level.

Supplementary Materials: The following are available online at http://www.mdpi.com/2076-3425/6/4/57/s1. Figure S1: Beta frequency power of STN-LFP activity recorded from therapeutic contacts with subjects in the medication on and off states at rest; Figure S2: Event-related beta frequency desynchronization of STN-LFP signals in the medication on state relative to the medication off state; Figure S3. Dopamine-dependent dynamics of STN-LFP activity recorded with an INS with behavioral events for all subjects; Figure S4. Stability of STN-LFP recorded with an INS over one year; Table S1. Correlation coefficients and associated *p*-values for longitudinal PSD stability over one year.

Acknowledgments: The authors gratefully acknowledge support from the Colorado Neurological Institute, Swedish Medical Center (Englewood, Colorado), and Medtronic, Inc., for providing the DBS systems. The authors would like to thank Cara Dobbertin for performing UPDRS assessments and Kevin Reilly for performing neuropsychological assessments.

Author Contributions: A.O.H., J.J.N. and S.J.H. conceived of and designed the experiments. J.J.N. and S.J.H. performed the experiments. J.J.N. analyzed the data. S.F., M.G. and A.H., contributed relevant clinical evaluations and data points. B.S.D., M.H.M., A.K.S. and J.J.Z. provided technical expertise in data collection and analysis. S.J.H., J.J.N. and A.O.H. wrote the paper.

Conflicts of Interest: A.O.H. receives consulting and research support from Medtronic, Inc. The other authors declare no conflict of interest.

References

1. Li, Q.; Qian, Z.-M.; Arbuthnott, G.W.; Ke, Y.; Yung, W.-H. Cortical effects of deep brain stimulation: Implications for pathogenesis and treatment of Parkinson disease. *JAMA Neurol.* **2014**, *71*, 100–103. [CrossRef] [PubMed]
2. Bordini, B.J.; Garg, A.; Gallagher, C.L.; Bell, B.; Garell, P.C. Neuropsychological effects of bilateral deep brain stimulation of the subthalamic nucleus in Parkinson's disease. *Stereotact. Funct. Neurosurg.* **2007**, *85*, 113–120. [CrossRef] [PubMed]
3. Tripoliti, E.; Zrinzo, L.; Martinez-Torres, I.; Frost, E.; Pinto, S.; Foltynie, T.; Holl, E.; Petersen, E.; Roughton, M.; Hariz, M.I.; et al. Effects of subthalamic stimulation on speech of consecutive patients with Parkinson disease. *Neurology* **2011**, *76*, 80–86. [CrossRef] [PubMed]
4. Morrison, C.E.; Borod, J.C.; Perrine, K.; Beric, A.; Brin, M.F.; Rezai, A.; Kelly, P.; Sterio, D.; Germano, I.; Weisz, D.; et al. Neuropsychological functioning following bilateral subthalamic nucleus stimulation in Parkinson's disease. *Arch. Clin. Neuropsychol.* **2004**, *19*, 165–181. [CrossRef]
5. Fleury, V.; Pollak, P.; Gere, J.; Tommasi, G.; Romito, L.; Combescure, C.; Bardinet, E.; Chabardes, S.; Momjian, S.; Krainik, A.; et al. Subthalamic stimulation may inhibit the beneficial effects of levodopa on akinesia and gait. *Mov. Disord.* **2016**, *31*, 1389–1397. [CrossRef] [PubMed]
6. Hariz, M.I.; Rehncrona, S.; Quinn, N.P.; Speelman, J.D.; Wensing, C.; Multicentre Advanced Parkinson's Disease Deep Brain Stimulation Group. Multicenter study on deep brain stimulation in Parkinson's disease: An independent assessment of reported adverse events at 4 years. *Mov. Disord.* **2008**, *23*, 416–421. [CrossRef] [PubMed]
7. Arlotti, M.; Rossi, L.; Rosa, M.; Marceglia, S.; Priori, A. An external portable device for adaptive deep brain stimulation (aDBS) clinical research in advanced Parkinson's disease. *Med. Eng. Phys.* **2016**, *38*, 498–505. [CrossRef] [PubMed]
8. Beudel, M.; Little, S.; Pogosyan, A.; Ashkan, K.; Foltynie, T.; Limousin, P.; Zrinzo, L.; Hariz, M.; Bogdanovic, M.; Cheeran, B.; et al. Tremor Reduction by Deep Brain Stimulation Is Associated With Gamma Power Suppression in Parkinson's Disease. *Neuromodulation* **2015**, *18*, 349–354. [CrossRef] [PubMed]
9. Mahlknecht, P.; Limousin, P.; Foltynie, T. Deep brain stimulation for movement disorders: Update on recent discoveries and outlook on future developments. *J. Neurol.* **2015**, *262*, 2583–2595. [CrossRef] [PubMed]
10. Mohammed, A.; Zamani, M.; Bayford, R.; Demosthenous, A. Patient specific Parkinson's disease detection for adaptive deep brain stimulation. In Proceedings of the 2015 37th Annual International Conference of the IEEE Engineering in Medicine and Biology Society, Milan, Italy, 25–29 August 2015; pp. 1528–1531.
11. Hebb, A.O.; Zhang, J.J.; Mahoor, M.H.; Tsiokos, C.; Matlack, C.; Chizeck, H.J.; Pouratian, N. Creating the Feedback Loop. *Neurosurg. Clin. N. Am.* **2014**, *25*, 187–204. [CrossRef] [PubMed]
12. Giannicola, G.; Rosa, M.; Servello, D.; Menghetti, C.; Carrabba, G.; Pacchetti, C.; Zangaglia, R.; Cogiamanian, F.; Scelzo, E.; Marceglia, S.; et al. Subthalamic local field potentials after seven-year deep brain stimulation in Parkinson's disease. *Exp. Neurol.* **2012**, *237*, 312–317. [CrossRef] [PubMed]

13. Friston, K.J.; Bastos, A.M.; Pinotsis, D.; Litvak, V. LFP and oscillations-what do they tell us? *Curr. Opin. Neurobiol.* **2015**, *31*, 1–6. [CrossRef] [PubMed]
14. Little, S.; Brown, P. What brain signals are suitable for feedback control of deep brain stimulation in Parkinson's disease? *Ann. N. Y. Acad. Sci.* **2012**, *1265*, 9–24. [CrossRef] [PubMed]
15. Gmel, G.E.; Parker, J.L.; Hamilton, T.J. A new biomarker for closed-loop deep brain stimulation in the subthalamic nucleus for patients with Parkinson's disease. In Proceedings of the 2014 IEEE Biomedical Circuits and Systems Conference (BioCAS), Lausanne, Switzerland, 22–24 October 2014; pp. 500–503.
16. Timmermann, L.; Florin, E. Parkinson's disease and pathological oscillatory activity: Is the beta band the bad guy?—New lessons learned from low-frequency deep brain stimulation. *Exp. Neurol.* **2012**, *233*, 123–125. [CrossRef] [PubMed]
17. Williams, D.; Tijssen, M.; Van Bruggen, G.; Bosch, A.; Insola, A.; Di Lazzaro, V.; Mazzone, P.; Oliviero, A.; Quartarone, A.; Speelman, H.; et al. Dopamine-dependent changes in the functional connectivity between basal ganglia and cerebral cortex in humans. *Brain J. Neurol.* **2002**, *125*, 1558–1569. [CrossRef]
18. Brown, P.; Oliviero, A.; Mazzone, P.; Insola, A.; Tonali, P.; Lazzaro, V.D. Dopamine Dependency of Oscillations between Subthalamic Nucleus and Pallidum in Parkinson's Disease. *J. Neurosci.* **2001**, *21*, 1033–1038. [PubMed]
19. Loukas, C.; Brown, P. Online prediction of self-paced hand-movements from subthalamic activity using neural networks in Parkinson's disease. *J. Neurosci. Methods* **2004**, *137*, 193–205. [CrossRef] [PubMed]
20. Niketeghad, S.; Hebb, A.O.; Nedrud, J.; Hanrahan, S.J.; Mahoor, M.H. Single trial behavioral task classification using subthalamic nucleus local field potential signals. In Proceedings of the 2014 36th Annual International Conference of the IEEE Engineering in Medicine and Biology Society, Chicago, IL, USA, 26–30 August 2014; pp. 3793–3796.
21. Hebb, A.O.; Darvas, F.; Miller, K.J. Transient and state modulation of beta power in human subthalamic nucleus during speech production and finger movement. *Neuroscience* **2012**, *202*, 218–233. [CrossRef] [PubMed]
22. Flint, R.D.; Wright, Z.A.; Scheid, M.R.; Slutzky, M.W. Long term, stable brain machine interface performance using local field potentials and multiunit spikes. *J. Neural Eng.* **2013**, *10*, 56005. [CrossRef] [PubMed]
23. Abosch, A.; Lanctin, D.; Onaran, I.; Eberly, L.; Spaniol, M.; Ince, N.F. Long-term recordings of local field potentials from implanted deep brain stimulation electrodes. *Neurosurgery* **2012**, *71*, 804–814. [CrossRef] [PubMed]
24. Quinn, E.J.; Blumenfeld, Z.; Velisar, A.; Koop, M.M.; Shreve, L.A.; Trager, M.H.; Hill, B.C.; Kilbane, C.; Henderson, J.M.; Brontë-Stewart, H. Beta oscillations in freely moving Parkinson's subjects are attenuated during deep brain stimulation. *Mov. Disord.* **2015**, *30*, 1750–1758. [CrossRef] [PubMed]
25. Ribeiro, M.-J.; Vidailhet, M.; Loc'h, C.; Dupel, C.; Nguyen, J.P.; Ponchant, M.; Dollé, F.; Peschanski, M.; Hantraye, P.; Cesaro, P.; et al. Dopaminergic function and dopamine transporter binding assessed with positron emission tomography in Parkinson disease. *Arch. Neurol.* **2002**, *59*, 580–586. [CrossRef] [PubMed]
26. Bronte-Stewart, H.; Barberini, C.; Koop, M.M.; Hill, B.C.; Henderson, J.M.; Wingeier, B. The STN beta-band profile in Parkinson's disease is stationary and shows prolonged attenuation after deep brain stimulation. *Exp. Neurol.* **2009**, *215*, 20–28. [CrossRef] [PubMed]
27. Levy, R.; Ashby, P.; Hutchison, W.D.; Lang, A.E.; Lozano, A.M.; Dostrovsky, J.O. Dependence of subthalamic nucleus oscillations on movement and dopamine in Parkinson's disease. *Brain J. Neurol.* **2002**, *125*, 1196–1209. [CrossRef]
28. Marceglia, S.; Foffani, G.; Bianchi, A.M.; Baselli, G.; Tamma, F.; Egidi, M.; Priori, A. Dopamine-dependent non-linear correlation between subthalamic rhythms in Parkinson's disease. *J. Physiol.* **2006**, *571*, 579–591. [CrossRef] [PubMed]
29. Weinberger, M.; Mahant, N.; Hutchison, W.D.; Lozano, A.M.; Moro, E.; Hodaie, M.; Lang, A.E.; Dostrovsky, J.O. Beta oscillatory activity in the subthalamic nucleus and its relation to dopaminergic response in Parkinson's disease. *J. Neurophysiol.* **2006**, *96*, 3248–3256. [CrossRef] [PubMed]
30. Marsden, J.F.; Limousin-Dowsey, P.; Ashby, P.; Pollak, P.; Brown, P. Subthalamic nucleus, sensorimotor cortex and muscle interrelationships in Parkinson's disease. *Brain J. Neurol.* **2001**, *124*, 378–388. [CrossRef]
31. De Hemptinne, C.; Ryapolova-Webb, E.S.; Air, E.L.; Garcia, P.A.; Miller, K.J.; Ojemann, J.G.; Ostrem, J.L.; Galifianakis, N.B.; Starr, P.A. Exaggerated phase-amplitude coupling in the primary motor cortex in Parkinson disease. *Proc. Natl. Acad. Sci. USA* **2013**, *110*, 4780–4785. [CrossRef] [PubMed]

32. Foffani, G.; Priori, A.; Egidi, M.; Rampini, P.; Tamma, F.; Caputo, E.; Moxon, K.A.; Cerutti, S.; Barbieri, S. 300-Hz subthalamic oscillations in Parkinson's disease. *Brain J. Neurol.* **2003**, *126*, 2153–2163. [CrossRef] [PubMed]
33. Cassidy, M.; Mazzone, P.; Oliviero, A.; Insola, A.; Tonali, P.; Di Lazzaro, V.; Brown, P. Movement-related changes in synchronization in the human basal ganglia. *Brain J. Neurol.* **2002**, *125*, 1235–1246. [CrossRef]
34. Jenkinson, N.; Brown, P. New insights into the relationship between dopamine, beta oscillations and motor function. *Trends Neurosci.* **2011**, *34*, 611–618. [CrossRef] [PubMed]
35. Paradiso, G.; Cunic, D.; Saint-Cyr, J.A.; Hoque, T.; Lozano, A.M.; Lang, A.E.; Chen, R. Involvement of human thalamus in the preparation of self-paced movement. *Brain J. Neurol.* **2004**, *127*, 2717–2731. [CrossRef] [PubMed]
36. Meziane, H.B.; Moisello, C.; Perfetti, B.; Kvint, S.; Isaias, I.U.; Quartarone, A.; Di Rocco, A.; Ghilardi, M.F. Movement preparation and bilateral modulation of beta activity in aging and Parkinson's disease. *PLoS ONE* **2015**, *10*, e0114817. [CrossRef] [PubMed]
37. Doyle, L.M.F.; Kühn, A.A.; Hariz, M.; Kupsch, A.; Schneider, G.-H.; Brown, P. Levodopa-induced modulation of subthalamic beta oscillations during self-paced movements in patients with Parkinson's disease. *Eur. J. Neurosci.* **2005**, *21*, 1403–1412. [CrossRef] [PubMed]
38. Pfurtscheller, G.; Lopes da Silva, F.H. Event-related EEG/MEG synchronization and desynchronization: Basic principles. *Clin. Neurophysiol.* **1999**, *110*, 1842–1857. [CrossRef]
39. Chomiak, T.; Pereira, F.V.; Meyer, N.; de Bruin, N.; Derwent, L.; Luan, K.; Cihal, A.; Brown, L.A.; Hu, B. A new quantitative method for evaluating freezing of gait and dual-attention task deficits in Parkinson's disease. *J. Neural Transm.* **2015**, *122*, 1523–1531. [CrossRef] [PubMed]
40. Nocera, J.R.; Roemmich, R.; Elrod, J.; Altmann, L.J.P.; Hass, C.J. Effects of cognitive task on gait initiation in Parkinson disease: Evidence of motor prioritization? *J. Rehabil. Res. Dev.* **2013**, *50*, 699–708. [CrossRef] [PubMed]
41. Wessel, J.R.; Jenkinson, N.; Brittain, J.-S.; Voets, S.H.E.M.; Aziz, T.Z.; Aron, A.R. Surprise disrupts cognition via a fronto-basal ganglia suppressive mechanism. *Nat. Commun.* **2016**, *7*, 11195. [CrossRef] [PubMed]
42. Powell, D.; Hanson, N.; Threlkeld, A.J.; Fang, X.; Xia, R. Enhancement of parkinsonian rigidity with contralateral hand activation. *Clin. Neurophysiol.* **2011**, *122*, 1595–1601. [CrossRef] [PubMed]
43. Rektor, I.; Baláz, M.; Bocková, M. Cognitive activities in the subthalamic nucleus. Invasive studies. *Parkinsonism Relat. Disord.* **2009**, *15* (Suppl. S3), S83–S86. [CrossRef]
44. Stanslaski, S.; Afshar, P.; Cong, P.; Giftakis, J.; Stypulkowski, P.; Carlson, D.; Linde, D.; Ullestad, D.; Avestruz, A.-T.; Denison, T. Design and validation of a fully implantable, chronic, closed-loop neuromodulation device with concurrent sensing and stimulation. *IEEE Trans. Neural Syst. Rehabil. Eng.* **2012**, *20*, 410–421. [CrossRef] [PubMed]
45. Connolly, A.T.; Muralidharan, A.; Hendrix, C.; Johnson, L.; Gupta, R.; Stanslaski, S.; Denison, T.; Baker, K.B.; Vitek, J.L.; Johnson, M.D. Local field potential recordings in a non-human primate model of Parkinsons disease using the Activa PC + S neurostimulator. *J. Neural Eng.* **2015**, *12*, 66012. [CrossRef] [PubMed]
46. Schalk, G.; McFarland, D.J.; Hinterberger, T.; Birbaumer, N.; Wolpaw, J.R. BCI2000: A general-purpose brain-computer interface (BCI) system. *IEEE Trans. Biomed. Eng.* **2004**, *51*, 1034–1043. [CrossRef] [PubMed]
47. Oswal, A.; Litvak, V.; Brücke, C.; Huebl, J.; Schneider, G.-H.; Kühn, A.A.; Brown, P. Cognitive Factors Modulate Activity within the Human Subthalamic Nucleus during Voluntary Movement in Parkinson's Disease. *J. Neurosci.* **2013**, *33*, 15815–15826. [CrossRef] [PubMed]
48. Waldert, S.; Vigneswaran, G.; Philipp, R.; Lemon, R.N.; Kraskov, A. Modulation of the Intracortical LFP during Action Execution and Observation. *J. Neurosci.* **2015**, *35*, 8451–8461. [CrossRef] [PubMed]
49. Johnson, L.A.; Nebeck, S.D.; Muralidharan, A.; Johnson, M.D.; Baker, K.B.; Vitek, J.L. Closed-Loop Deep Brain Stimulation Effects on Parkinsonian Motor Symptoms in a Non-Human Primate—Is Beta Enough? *Brain Stimul.* **2016**, *9*, 892–896. [CrossRef] [PubMed]
50. Watson, P.; Montgomery, E.B. The relationship of neuronal activity within the sensori-motor region of the subthalamic nucleus to speech. *Brain Lang.* **2006**, *97*, 233–240. [CrossRef] [PubMed]
51. Van der Walt, S.; Colbert, S.C.; Varoquaux, G. The NumPy Array: A Structure for Efficient Numerical Computation. *Comput. Sci. Eng.* **2011**, *13*, 22–30. [CrossRef]
52. Jones, E.; Oliphant, T.; Peterson, P. SciPy: Open Source Scientific Tools for Python. Available online: http://www.scipy.org/ (accessed on 5 November 2014).

53. Allen, D.P.; Stegemöller, E.L.; Zadikoff, C.; Rosenow, J.M.; Mackinnon, C.D. Suppression of deep brain stimulation artifacts from the electroencephalogram by frequency-domain Hampel filtering. *Clin. Neurophysiol.* **2010**, *121*, 1227–1232. [CrossRef] [PubMed]
54. Erez, Y.; Tischler, H.; Moran, A.; Bar-Gad, I. Generalized framework for stimulus artifact removal. *J. Neurosci. Methods* **2010**, *191*, 45–59. [CrossRef] [PubMed]
55. Hashimoto, T.; Elder, C.M.; Vitek, J.L. A template subtraction method for stimulus artifact removal in high-frequency deep brain stimulation. *J. Neurosci. Methods* **2002**, *113*, 181–186. [CrossRef]
56. Thompson, J.A.; Lanctin, D.; Ince, N.F.; Abosch, A. Clinical Implications of Local Field Potentials for Understanding and Treating Movement Disorders. *Stereotact. Funct. Neurosurg.* **2014**, *92*, 251–263. [CrossRef] [PubMed]
57. Holdefer, R.N.; Cohen, B.A.; Greene, K.A. Intraoperative local field recording for deep brain stimulation in Parkinson's disease and essential tremor. *Mov. Disord.* **2010**, *25*, 2067–2075. [CrossRef] [PubMed]
58. Alegre, M.; Alonso-Frech, F.; Rodríguez-Oroz, M.C.; Guridi, J.; Zamarbide, I.; Valencia, M.; Manrique, M.; Obeso, J.A.; Artieda, J. Movement-related changes in oscillatory activity in the human subthalamic nucleus: Ipsilateral vs. contralateral movements. *Eur. J. Neurosci.* **2005**, *22*, 2315–2324. [CrossRef] [PubMed]
59. Cheung, T.; Nuño, M.; Hoffman, M.; Katz, M.; Kilbane, C.; Alterman, R.; Tagliati, M. Longitudinal Impedance Variability in Patients with Chronically Implanted DBS Devices. *Brain Stimul.* **2013**, *6*, 746–751. [CrossRef] [PubMed]
60. Beudel, M.; Brown, P. Adaptive deep brain stimulation in Parkinson's disease. *Parkinsonism Relat. Disord.* **2016**, *22*, S123–S126. [CrossRef] [PubMed]
61. Swann, N.C.; de Hemptinne, C.; Miocinovic, S.; Qasim, S.; Wang, S.S.; Ziman, N.; Ostrem, J.L.; San Luciano, M.; Galifianakis, N.B.; Starr, P.A. Gamma Oscillations in the Hyperkinetic State Detected with Chronic Human Brain Recordings in Parkinson's Disease. *J. Neurosci.* **2016**, *36*, 6445–6458. [CrossRef] [PubMed]
62. Liu, C.; Wang, J.; Deng, B.; Wei, X.; Yu, H.; Li, H.; Fietkiewicz, C.; Loparo, K. Closed-loop Control of Tremor-predominant Parkinsonian State Based on Parameter Estimation: A Computational Study. *IEEE Trans. Neural Syst. Rehabil. Eng.* **2016**, *24*, 1109–1121. [CrossRef] [PubMed]

brain sciences

MDPI

Review

Rescue Procedures after Suboptimal Deep Brain Stimulation Outcomes in Common Movement Disorders

Adam M. Nagy and Christopher M. Tolleson *

Department of Neurology, Vanderbilt University Medical Center, 1161 21st Avenue South, A-0118 Medical Center North, Nashville, TN 37232, USA; adam.nagy@vanderbilt.edu
* Correspondence: christopher.tolleson@vanderbilt.edu; Tel.: +1-615-936-2025; Fax: +1-615-936-1229

Academic Editors: Tipu Aziz and Alex Green
Received: 3 July 2016; Accepted: 28 September 2016; Published: 8 October 2016

Abstract: Deep brain stimulation (DBS) is a unique, functional neurosurgical therapy indicated for medication refractory movement disorders as well as some psychiatric diseases. Multicontact electrodes are placed in "deep" structures within the brain with targets varying depending on the surgical indication. An implanted programmable pulse generator supplies the electrodes with a chronic, high frequency electrical current that clinically mimics the effects of ablative lesioning techniques. DBS's efficacy has been well established for its movement disorder indications (Parkinson's disease, essential tremor, and dystonia). However, clinical outcomes are sometimes suboptimal, even in the absence of common, potentially reversible complications such as hardware complications, infection, poor electrode placement, and poor programming parameters. This review highlights some of the rescue procedures that have been explored in suboptimal DBS cases for Parkinson's disease, essential tremor, and dystonia. To date, the data is limited and difficult to generalize, but a large majority of published reports demonstrate positive results. The decision to proceed with such treatments should be made on a case by case basis. Larger studies are needed to clearly establish the benefit of rescue procedures and to establish for which patient populations they may be most appropriate.

Keywords: Parkinson's disease; essential tremor; dystonia; deep brain stimulation; treatment failure; rescue leads

1. Introduction

Deep brain stimulation (DBS) is a unique and exciting functional neurosurgical therapy, allowing for easily adjustable post-surgical changes to an implanted programmable device, which maximizes long-term clinical outcomes. It involves neurosurgical implantation of multicontact electrodes either unilaterally or bilaterally in specific anatomical areas "deep" within the brain. Targets vary depending on the indication for surgery. These electrodes are connected by a tunneled extension wire to a pulse generator, or neurostimulator, typically implanted in a subcutaneous pocket below the clavicle. The neurostimulator provides a modifiable, high frequency electrical current that modulates the neurocircuitry surrounding the electrodes, clinically mimicking the effects of ablative stereotactic lesioning techniques [1,2]. The stimulation parameters (amplitude, pulse width and frequency) as well as activated contact(s) can be easily adjusted by the treating physician in the clinic. Depending on the comfort level of the physician, patients can also be given varying levels of control over their programming settings. DBS has Food and Drug Administration (FDA) approval in two conditions, Parkinson's disease (PD) and essential tremor (ET). DBS also has a humanitarian device exemption for dystonia and obsessive compulsive disorder. Outside of these approved indications, DBS has

been used for a variety of conditions including Parkinson's plus disorders, Huntington's disease, Tourette's, Alzheimer's, epilepsy, chronic pain, major depression, post-traumatic stress disorder, and schizophrenia among others [3]. In general, DBS is indicated in all its approved conditions when prospective patients are symptomatically severe and refractory to medical treatment, or when medication adverse effects become intolerable [4].

The process of selecting proper candidates for DBS, successfully implanting the electrode(s) in the proper location, and appropriately programming the DBS device is complex. When done correctly, the efficacy of DBS is well established [5–8]. However, in some instances, even under optimal circumstances with a multidisciplinary team approach, DBS can lead to suboptimal results either immediately after the initial surgery or, later, as symptom benefit declines [9–11]. When common and reversible complications such as hardware issues, improper lead positioning and inadequate programming are ruled out, the patient and clinicians are left with the difficult decision of what to do next. DBS centers have trialed various options including the use of additional or "rescue" DBS lead(s), moving the established lead to another location, or subsequently using lesioning therapy. Given a paucity of data, it can be difficult for centers to make decisions. It can also be difficult to counsel patients and their families as outcomes are not clear. Obtaining consent and appropriately detailing out risks and benefits in such situations comes with inherent difficulties and should be given careful attention by the DBS team [12,13]. This review will highlight the available data on some of the techniques used after suboptimal DBS results in PD, ET, and dystonia patients.

2. Parkinson's Disease

Parkinson's disease (PD) is a neurodegenerative disorder characterized by the progressive loss of dopaminergic neurons and the buildup of intracellular inclusions called Lewy bodies composed of alpha synuclein. Clinically, it manifests as both the diagnostic motor features (tremor, bradykinesia, rigidity, and postural instability) as well as a myriad of non-motor features (autonomic instability, neuropsychiatric decline, sleep disorders, pain, etc.). PD medications primarily involve modulation of the dopaminergic pathway and target motor features, whereas non-motor features are much more difficult to treat.

DBS is a proven adjunctive surgical therapy for treatment of the motor symptoms of PD [6,14,15]. It is currently approved for levodopa-responsive PD patients with at least 4 years of disease not adequately controlled with medication or whose treatment is complicated by medication-related side effects (i.e., motor fluctuations, dyskinesias). The surgery has been approved for PD since 2002 with recent indications suggesting that earlier usage in the disease may be effective [16]. Compared to best medical therapy alone, DBS in conjunction with medication has been proven far superior. Studies have demonstrated a notable improvement in quality of life, motor scores, and a reduction of wearing off in patients who have received DBS [17–19]. Overall benefits have been maintained for up to 11 years according to long-term follow-up studies [20–22] although there is some concern that any initial benefit in gait or posture may deteriorate more quickly [23].

The most commonly used targets are the subthalamic nucleus (STN) and globus pallidus internus (GPi). Large comparative trials have demonstrated equal benefit in regards to the overall treatment of PD motor symptoms between targets [6,24]. However, there were subtle differences identified, which are still continuously being explored. For example, STN stimulation classically has allowed for greater medication reduction post-surgery, and GPi stimulation has seemed more advantageous for patients with depression, greater balance difficulty, and impairments in verbal fluency [6,24,25]. The longest follow-up in the large trials directly comparing the two targets was 24 months [6,24]. There is still no unifying consensus on specific criteria for favoring one target over the other with the current data. Different DBS centers still differ on their approaches for target selection and often will use the target with which they have the most experience and comfort.

DBS in these two targets can be said to have "failed" for many reasons. Some of the more common reasons include improper patient selection, suboptimal electrode placement, suboptimal management

(programming and medications), hardware complications (infection, lead fracture, dead battery), and progression of PD such that symptoms not modified by DBS become the patient's primary disability [11]. Exclusive of these more common reasons for failure of PD DBS, patients can still have inadequate or progressively lessening motor benefit despite good lead positioning and programming parameters [10,11]. This can manifest as reemergence of dystonia, worsening in motor fluctuations and dyskinesias, and progression in the cardinal motor symptoms (tremor, bradykinesia, rigidity) initially modified by DBS [10,11]. In certain patients, up titration of dopaminergics in attempts to adequately control breakthrough symptoms can also lead to disabling side effects (neuropsychiatric changes, fatigue, sleep disruption, impulse control disorders, orthostatic hypotension, and dyskinesia among others). Case studies and series have reported using additional leads in the other primary PD DBS target (i.e., STN stimulation to rescue failed GPi stimulation and vice versa) in these circumstances with some success [15,26–30].

Published cases where patients underwent GPi stimulation for failed STN stimulation generally report patients with a young age of disease onset (average age 41) and a long interval of success with their initial STN surgery (average of 8 years until rescue surgery) [26,27,29,30]. In all reviewed cases, the reason for failure was disabling dyskinesia or dystonia. Discontinuation of STN stimulation after initiation of GPi stimulation sometimes led to worse control of cardinal motor features, leading to continued STN stimulation in four of seven cases reviewed [26,27,29,30]. Of the seven cases, six achieved a clinically significant benefit with the addition of GPi stimulation [26,27,29,30]. Benefits included reduction in the dystonia, dyskinesia, and levodopa equivalent daily dose (i.e., total medication needed) [26,27,29,30].

In the six cases reviewed where STN stimulation was used to rescue failed GPi stimulation, the reason for failure was worsening motor symptoms soon after surgery (within the first 2–3 years) [15,28]. Average age at disease onset was also in the 40s (exact ages at onset unavailable from one study). Notably, in three of the six cases, there were hardware complications that necessitated the removal of at least one GPi electrode prior to the use of rescue leads [15,28]. In all cases, STN stimulation replaced GPi stimulation, rather than stimulation of both regions, as the GPi leads were already removed in all patients [15,28]. STN stimulation led to improved United Parkinson's disease Rating Scale Part III (UPDRS-III) scores, decreased levodopa daily dose, and cessation of or improvement in dyskinesia [15,28].

Another interesting rescue procedure reported by Deligny et al. was that of a bilateral subthalamotomy performed through DBS electrodes prior to their removal due to hardware infection [31]. In this case, radiofrequency subthalamotomy through the leads led to a durable benefit in measured motor scores, dyskinesia and off times [31]. Unfortunately, after the procedure, there were some mild cognitive and motivation side effects witnessed as well [31].

Finally, other targets besides the STN and GPi have been explored in PD DBS such as the pedunculopontine nucleus (PPN). This target has primarily been used for PD patients suffering from freezing of gait (FOG) and other gait disturbances, either as the sole target or in combination with STN DBS. It has the potential to be used as a rescue target in the future but further study is needed. The PPN was initially chosen as a potential DBS target given work in animal models which has shown the PPN plays a significant role in the normal operation of axial muscles which help regulate posture and gait [32–34]. FOG is a disabling symptom commonly seen in PD where patients literally "freeze" to the floor when they attempt to ambulate. It commonly occurs with the initiation of gait, with turning or when maneuvering in tight spaces such as doorways and crowds [35,36]. FOG is generally refractory to medications and STN/GPi DBS [37]. Several studies were reviewed that looked at the PPN as the sole target in PD patients with postural instability and gait symptoms (PIGD). A recent meta-analysis was performed on 10 such studies [37]. While there was a statistically significant improvement in motor symptoms and postural instability, the meta-analysis did not find a significant improvement in FOG [37]. The improvement in motor symptoms was also less substantial with PPN stimulation than has been found with STN or GPi stimulation [37]. In contrast, an interesting study

by Stefani et al. looked at six PD patients with axial signs simultaneously implanted in the PPN and STN [38]. Patients were analyzed 2–6 months after surgery in ON/OFF medication states with either or both targets activated. The PPN was particularly effective for gait and posture, and the combination of the targets being "on" was superior to one alone [38]. Liu et al. also report a case of a PD patient with FOG implanted simultaneously with bilateral PPN and STN leads [39]. The investigators did not test the leads in both targets simultaneously due to problems with dizziness when all leads were activated. However, on testing individual targets, sole stimulation of the PPN leads did show some benefit in the gait problems whereas the STN leads did not [39].

In summary, case reports of rescue procedures for PD have been generally positive, though follow-up has been short. Typically, rescue procedures have involved stimulation of the approved target that was not originally implanted (i.e., STN for failed GPi or vice versa). Subthalamotomy performed through existing DBS electrodes has also been attempted. Rescue procedures seem to be more common in those with a young age of disease onset. Stimulation of the PPN is also an intriguing idea both as an initial therapy and a rescue therapy for those with more axial symptoms and FOG, but currently further study is still needed.

3. Essential Tremor

Essential tremor (ET) is the most commonly seen movement disorder [40]. Clinically, it typically manifests as a bilateral action and postural tremor. The disease commonly runs in families, suggesting a hereditary component, yet a specific genetic cause has not been identified [40]. Common therapeutic medications include primidone, beta blockers, topiramate and gabapentin.

DBS is a proven surgical option for medication refractory ET. The accepted target is the ventral intermediate (VIM) nucleus of the thalamus. Unilateral DBS for ET received FDA approval in 1997 although it is commonly used bilaterally. Response to stimulation is often robust, with studies demonstrating >80% tremor improvement [7,8]. Studies have also demonstrated that this benefit can be persistent over a long period of time (>12 years) [41–43].

In some cases, however, the benefits of DBS either are suboptimal or diminish irrespective of inaccurate lead placement, hardware complications or other device issues [11,44]. Possible reasons for diminishing response include disease progression and tolerance to stimulation. Several different rescue techniques have been attempted to improve tremor control in these patients. Some DBS centers have attempted to either add additional leads or reposition in a second target. These other targets have primarily included the STN, caudal zona inserta (cZI), or the ventralis oralis anterior nucleus of the thalamus (VOA) [9,45,46]. Many of these newer targets were selected to see if stimulation of the subthalamic areas (STN, cZI, prelemniscal radiations) would produce similar results to previously used lesioning approaches. Subthalamotomy has been an efficacious surgical option for tremor dating back to the 1960s [47–49]. Our institution has also tried adding a second thalamic lead anterior to the VIM, using the combination of the VOA and VIM leads together to direct current away from structures causing stimulation-induced side effects and allow for more aggressive stimulation parameters [50–52].

In a case series by Blomstedt et al., patients who had failed VIM stimulation underwent re-implantation in the cZI [9]. In this series, they reported a 57% improvement in tremor control with cZI stimulation, compared to a 25% improvement in tremor control with prior VIM stimulation [9]. Within their cohort (n = 5), however, two of the patients had relatively immediate failure of their VIM leads (<6 months) [9]. This may suggest an initial improper positioning of the leads as opposed to true superiority of the cZI over VIM. The other three patients received their cZI lead implantation an average of 9 years after VIM implantation with benefit [9].

In two series by Mehanna et al. and Oyama et al., a total of seven patients underwent a second operation into the VOA, STN, or prelemniscal radiations for failed VIM stimulation [45,46]. Six of the seven patients had mild to moderate improvement after reoperation [45,46]. In some patients, the physicians used simultaneous stimulation of both the new target and VIM, while others had stimulation of the new target alone [45,46]. A shortcoming of these series is the heterogeneity of the patient

population and treatment strategies. Four of the seven patients did not have ET [45,46]. Rather, two had multiple sclerosis induced tremor, one had tremor from a treated thalamic anteriovenous malformation and one had an atypical tremor of unknown cause [45,46]. In the three patients with ET, one had maximal tremor control with the VOA rescue lead stimulated alone. The other two had maximal tremor control with simultaneous stimulation of VIM and the new target (one in the VOA and one in the prelemniscal radiations). The varying treatment strategies (different targets and different combinations of stimulation) make this data difficult to interpret.

Yu et al., Isaacs et al. and Sukul et al. from our institution [50–52] published a series in which they used the placement of a second electrode in the thalamus antero-medially to the VIM to direct stimulation away from structures causing stimulation-induced side effects (such as the internal capsule and ventralis caudalis nucleus of the thalamus) [50–52]. Limiting side effects from the initial lead included severe paresthesias, diplopia, dysarthria, and dizziness. The leads were connected in parallel to a common voltage source allowing more control over the field of stimulation [50–52]. Directing the stimulation away from unintended targets allowed for more aggressive stimulation parameters with essentially equivalent or better tremor control and reduced side effects in all patients [50–52].

Bahgat et al. retrospectively reviewed seven patients with ET who underwent unilateral thalamotomy as a rescue procedure after failed VIM DBS [53]. Reasons for failure in these patients included intolerable side effects, malpositioned electrodes, and symptom progression [53]. After thalamotomy, six of the seven patients reported symptomatic improvement, though only three of those six reported corresponding functional improvement and one patient reported no improvement at all [53]. However, only one patient had a significant persistent adverse effect in the form of facial numbness from thalamotomy after DBS [53].

In summary, case reports of rescue procedures for ET have also been generally positive, though cohorts have been notably heterogeneous. Several newer targets have been tried in combination with and as a replacement for VIM stimulation, which has raised the possibility of a synergistic effect of stimulating different regions. Thalamotomy for failed DBS had modest success. An alternative rescue approach with favorable results has been implanting additional thalamic leads to direct stimulation away from structures responsible for intolerable side effects.

4. Dystonia

Dystonia is an unusual movement disorder characterized by sustained and repetitive muscle contraction, often resulting in abnormal posturing [54]. The exact pathophysiology is not known, but the origin appears to be in the basal ganglia. Dystonia can be from a variety of causes such as genetic abnormalities, neurodegenerative conditions, structural changes or insults to the brain, chemical exposures, or medications among others [55,56]. It also has a varied clinical presentation, presenting either as a focal dystonia (i.e., isolated to one body part) versus a more generalized or segmental dystonia [55,56]. Common non-surgical treatments for dystonia include botulinum toxin injections, anticholinergic medications, and benzodiazepines.

DBS is a proven surgical treatment for dystonia refractory to medication and botulinum toxin injections, particularly primary generalized dystonia (i.e., genetic or idiopathic) [5]. This treatment received Humanitarian Device Exemption from the FDA in 2003. The primary target has been the GPi in the majority of cases due to prior experience with lesioning therapies and the use of the target in the PD population [57]. More recent DBS cases have used the STN target as well, most commonly with focal cervical dystonia [5,58]. Some studies report up to a 60%–70% improvement on dystonia rating scales in generalized dystonia post GPi DBS [5,58–61]. Results in focal dystonias are more variable. The most common dystonia, cervical dystonia, does tend to have good response post DBS [62–64]. The responses to DBS in other types of focal or segmental dystonia are less well defined and reported less in the literature [5]. Post-surgical programming in this population can also often be challenging compared to PD and ET. Unlike these movement disorders where stimulation results in immediate

clinical results, there is a long latency between programming adjustments and resulting clinical benefit that can be months in duration.

Like the other movement disorders already discussed, dystonia patients can have a suboptimal response to DBS despite good lead positioning and a lack of detectable reversible complications such as hardware malfunction or poor programming parameters [46,65]. Various techniques have been applied in the dystonia population. A case series by Oyama et al. reported two patients who underwent rescue lead placement for dystonia [46]. The first was a patient with cervical dystonia who had incomplete benefit from bilateral GPi stimulation and underwent implantation of a second rescue lead into the left GPi [46]. The rationale was that the patient's original left GPi lead was 2.4 mm more anterior than the right on repeat imaging. The second was a tardive dyskinesia/dystonia patient who had incomplete benefit from bilateral GPi stimulation and underwent implantation of bilateral STN rescue leads two years later [46]. Both patients had complete symptom resolution with stimulation of both the original and rescue leads [46]. In the first case, the authors stimulated all contacts immediately after the addition of the third lead with excellent results. In the second case, the authors attempted to reduce GPi stimulation in favor of purely STN stimulation but only with activation of all four leads did the patient achieve maximum benefit. Benefit was sustained at 17 months for the left GPi rescue operation and 15 months for the bilateral STN rescue procedure at the time of publication [46].

No other case series were found that specifically addressed rescue leads for suboptimal DBS results in dystonia. There was one report where bilateral STN DBS was used as a rescue procedure for a failed unilateral pallidotomy [65]. Also, Schjerling et al. did perform a study directly comparing the STN to the GPi as targets for dystonia [66]. Part of the study did address simultaneous stimulation of the two targets. The study was a randomized, double-blind crossover study, and all patients received both STN and GPi leads [66]. The study included 13 patients and was quite heterogeneous; ages ranged from 12 to 57 years, disease duration ranged from 3 to 30 years, and it was roughly half generalized and half focal dystonia [66]. While the results did not demonstrate a statistically significant difference between GPi and STN stimulation, there was a trend toward greatest improvement with simultaneous stimulation of both targets, followed by STN alone and then GPi alone [66]. As with the single case report mentioned above, there may be a role for simultaneous stimulation of the STN and GPi targets in patients who have failed to achieve beneficial results with a single target.

In summary, there is little available data regarding rescue lead implantation for dystonia patients. In the one case report reviewed in addition to the study employing simultaneous GPi and STN stimulation, the increased benefit of combined STN and GPi stimulation is intriguing and could be looked at more intensely in additional studies with larger populations. The published number of cases is currently extremely limited. Studies of DBS in dystonia are complicated by the variety of clinical presentations and underlying causes of dystonia. Studies are also complicated by the delay in benefit from stimulation which can take several months to manifest, if not longer. This makes programming inherently difficult as well as determining what qualifies as a DBS failure.

5. Discussion and Conclusions

As described, published rescue procedures for failed DBS in PD, ET, and dystonia have been performed with generally positive reported results and do have a role in cases of suboptimal DBS outcomes. However, the data is still quite difficult to apply to any general population for several reasons. There is a high degree of individualization that takes place between institutions and patients when it comes to such procedures. The amount of data is still very limited, and is currently entirely in the form of case reports and series. Further, there is little incentive to write or publish case reports of negative outcomes after rescue procedures, likely creating significant publication bias.

Ultimately, more established guidelines, utilizing more concrete data, are needed for performing rescue therapies in suboptimal DBS outcomes in each of the indications discussed. However, a consensus set of guidelines based on better data from prospective blinded, randomized clinical trials may be difficult to achieve given the ethics of performing a blinded randomized trial

of a rescue surgical therapy as well as the multiple differing variables present in situations where rescue leads are required. Nonetheless, with the uncertainty of the current data and the difficulty of putting a patient through another surgery with poorly established outcomes, it is a given that rescue procedures should only be performed as a last resort, after every attempt to optimize the current DBS lead has been undertaken. Postoperative imaging should be performed to verify proper lead placement, hardware checked to make sure its functioning appropriately, medications optimized to the fullest, and programming adjustments exhausted as much as possible. There should be multidisciplinary discussions between experienced DBS neurologists and neurosurgeons before undertaking these procedures where targets and procedural options are discussed and weighed. The risks, ethics, and potential emotional distress of putting patients and their families through another brain surgery should never be taken lightly.

This review summarizes the available data on rescue therapies post DBS. More information and experience from DBS centers, both good and bad, is needed to better establish future guidelines and techniques. Still, available data does suggest that some patients can achieve benefits with rescue procedures. The decision to proceed with such treatment should be undertaken with caution and involve open discussions with a team of DBS physicians, patients and their families, fully explaining the uncertainty of results.

Author Contributions: A.N. and C.T. both contributed to the conception of the review topic, and shared in the writing of this manuscript. A.N. was the primary writer with C.T. providing guidance and editing.

Conflicts of Interest: A.N. declares no conflict of interest. C.T. has done consulting for Medtronic, Acadia and Teva. The mentioned entities had no role in the topics of the invited review; in the writing of the manuscript, and in the decision to publish.

References

1. Volkmann, J.; Herzog, J.; Kopper, F.; Deuschl, G. Introduction to the programming of deep brain stimulators. *Mov. Disord.* **2002**, *17*, S181–S187. [CrossRef] [PubMed]
2. Volkmann, J. Surgery for Parkinson's disease. In *Therapeutics of Parkinson's Disease and Other Movement Disorders*; Hallet, M., Poewe, W., Eds.; John Wiley and Sons: Chichester, UK, 2008; pp. 121–136.
3. Ostergard, T.; Miller, J.P. Deep brain stimulation: New directions. *J. Neurosurg. Sci.* **2014**, *58*, 191–198. [PubMed]
4. Siddiqui, M.S.; Haq, I.U.; Okun, M.S. Deep brain stimulation in movement disorders. *CONTINUUM Lifelong Learn. Neurol.* **2010**, *16*, 110–130. [CrossRef] [PubMed]
5. Crowell, J.L.; Shah, B.B. Surgery for dystonia and tremor. *Curr. Neurol. Neurosci. Rep.* **2016**, *16*, 1–13. [CrossRef] [PubMed]
6. Follett, K.A.; Weaver, F.M.; Stern, M.; Hur, K.; Harris, C.L.; Luo, P.; Marks, W.J., Jr.; Rothlind, J.; Sagher, O.; Moy, C.; et al. Pallidal versus subthalamic deep-brain stimulation for Parkinson's disease. *N. Engl. J. Med.* **2010**, *362*, 2077–2091. [CrossRef] [PubMed]
7. Nazzaro, J.M.; Pahwa, R.; Lyons, K.E. Long-term benefits in quality of life after unilateral thalamic deep brain stimulation for essential tremor: Clinical article. *J. Neurosurg.* **2012**, *117*, 156–161. [CrossRef] [PubMed]
8. Ondo, W.; Jankovic, J.; Schwartz, K.; Almaguer, M.; Simpson, R.K. Unilateral thalamic deep brain stimulation for refractory essential tremor and Parkinson's disease tremor. *Neurology* **1998**, *51*, 1063–1069. [CrossRef] [PubMed]
9. Blomstedt, P.; Lindvall, P.; Linder, J.; Olivecrona, M.; Forsgren, L.; Hariz, M.I. Reoperation after failed deep brain stimulation for essential tremor. *World Neurosurg.* **2012**, *78*, e1–e5. [CrossRef] [PubMed]
10. Granziera, C.; Pollo, C.; Russmann, H.; Staedler, C.; Ghika, J.; Villemure, J.G.; Burkhard, P.R.; Vingerhoets, F.J.G. Sub-acute delayed failure of subthalamic DBS in Parkinson's disease: The role of micro-lesion effect. *Parkinsonism Relat. Disord.* **2008**, *14*, 109–113. [CrossRef] [PubMed]
11. Okun, M.S.; Tagliati, M.; Pourfar, M.; Fernandez, H.H.; Rodriguez, R.L.; Alterman, R.L.; Foote, K.D. Management of referred deep brain stimulation failures: A retrospective analysis from 2 movement disorders centers. *Arch. Neurol.* **2005**, *62*, 1250–1255. [CrossRef] [PubMed]

12. Gilbert, F. Self-estrangement and deep brain stimulation: Ethical issues related to forced explantation. *Neuroethics* **2014**, *8*, 107–114. [CrossRef]
13. Unterrainer, M.; Oduncu, F.S. The ethics of deep brain stimulation (DBS). *Med. Health Care Philos.* **2015**, *18*, 475–485. [CrossRef] [PubMed]
14. Kleiner-Fisman, G.; Herzog, J.; Fisman, D.N.; Tamma, F.; Lyons, K.E.; Pahwa, R.; Lang, A.E.; Deuschl, G. Subthalamic nucleus deep brain stimulation: Summary and meta-analysis of outcomes. *Mov. Disord.* **2006**, *21*, S290–S304. [CrossRef] [PubMed]
15. Volkmann, J.; Allert, N.; Voges, J.; Sturm, V.; Schnitzler, A.; Freund, H.J. Long term results of bilateral pallidal stimulation in Parkinson's disease. *Ann. Neurol.* **2004**, *55*, 871–875. [CrossRef] [PubMed]
16. Schuepbach, W.M.M.; Rau, J.; Knudsen, K.; Volkmann, J.; Krack, P.; Timmermann, L.; Hälbig, T.D.; Hesekamp, H.; Navarro, S.M.; Meier, N.; et al. Neurostimulation for Parkinson's disease with early motor complications. *N. Engl. J. Med.* **2013**, *368*, 610–622. [CrossRef] [PubMed]
17. Sharma, A.; Szeto, K.; Desilets, A.R. Efficacy and safety of deep brain stimulation as an adjunct to pharmacotherapy for the treatment of Parkinson disease. *Ann. Pharmacother.* **2012**, *46*, 248–254. [CrossRef] [PubMed]
18. Weaver, F.M.; Follett, K.; Stern, M.; Hur, K.; Harris, C.; Marks, W.J.; Rothlind, J.; Sagher, O.; Reda, D.; Moy, C.S.; et al. Bilateral deep brain stimulation vs. best medical therapy for patients with advanced Parkinson disease: A randomized controlled trial. *JAMA* **2009**, *301*, 63–73. [CrossRef] [PubMed]
19. Williams, A.; Gill, S.; Varma, T.; Jenkinson, C.; Quinn, N.; Mitchell, R.; Scott, R.; Ives, N.; Rick, C.; Daniels, J.; et al. Deep brain stimulation plus best medical therapy versus best medical therapy alone for advanced Parkinson's disease (PD SURG trial): A randomised, open-label trial. *Lancet Neurol.* **2010**, *9*, 581–591. [CrossRef]
20. Castrioto, A.; Lozano, A.M.; Poon, Y.Y.; Lang, A.E.; Fallis, M.; Moro, E. Ten-year outcome of subthalamic stimulation in Parkinson disease: A blinded evaluation. *Arch. Neurol.* **2011**, *68*, 1550–1556. [CrossRef] [PubMed]
21. Rizzone, M.G.; Fasano, A.; Daniele, A.; Zibetti, M.; Merola, A.; Rizzi, L.; Piano, C.; Piccininni, C.; Romito, L.M.; Lopiano, L.; et al. Long-term outcome of subthalamic nucleus DBS in Parkinson's disease: From the advanced phase towards the late stage of the disease? *Parkinsonism Relat. Disord.* **2014**, *20*, 376–381. [CrossRef] [PubMed]
22. Zibetti, M.; Merola, A.; Rizzi, L.; Ricchi, V.; Angrisano, S.; Azzaro, C.; Artusi, C.A.; Arduino, N.; Marchisio, A.; Lanotte, M.; et al. Beyond nine years of continuous subthalamic nucleus deep brain stimulation in Parkinson's disease. *Mov. Disord.* **2011**, *26*, 2327–3234. [CrossRef] [PubMed]
23. George, R.S.; Nutt, J.G.; Burchiel, K.J.; Horak, F.B. A meta-regression of the long-term effects of deep brain stimulation on balance and gait in PD. *Neurology* **2010**, *75*, 1292–1299. [CrossRef] [PubMed]
24. Liu, Y.; Li, W.; Tan, C.; Liu, X.; Wang, X.; Gui, Y.; Qin, L.; Deng, F.; Hu, C.; Chen, L. Meta-analysis comparing deep brain stimulation of the globus pallidus and subthalamic nucleus to treat advanced Parkinson disease: A review. *J. Neurosurg.* **2014**, *121*, 709–718. [CrossRef] [PubMed]
25. Martinez-Ramirez, D.; Hu, W.; Bona, A.R.; Okun, M.S.; Wagle Shukla, A. Update on deep brain stimulation in Parkinson's disease. *Transl. Neurodegener.* **2015**, *4*, 12. [CrossRef] [PubMed]
26. Allert, N.; Schnitzler, A.; Sturm, V.; Maarouf, M. Failure of long-term subthalamic nucleus stimulation corrected by additional pallidal stimulation in a patient with Parkinson's disease. *J. Neurol.* **2012**, *259*, 1244–1246. [CrossRef] [PubMed]
27. Cook, R.J.; Jones, L.; Fracchia, G.; Anderson, N.; Miu, J.; Meagher, L.J.; Silburn, P.A.; Silberstein, P. Globus pallidus internus deep brain stimulation as rescue therapy for refractory dyskinesias following effective subthalamic nucleus stimulation. *Stereotact. Funct. Neurosurg.* **2015**, *93*, 25–29. [CrossRef] [PubMed]
28. Houeto, J.L.; Bejjani, P.B.; Damier, P.; Staedler, C.; Bonnet, A.M.; Pidoux, B.; Dormont, D.; Cornu, P.; Agid, Y. Failure of long-term pallidal stimulation corrected by subthalamic stimulation in PD. *Neurology* **2000**, *55*, 728–730. [CrossRef] [PubMed]
29. Matias, C.M.; Silva, D.; Machado, A.G.; Cooper, S.E. "Rescue" of bilateral subthalamic stimulation by bilateral pallidal stimulation: Case report. *J. Neurosurg.* **2016**, *124*, 417–421. [CrossRef] [PubMed]
30. Minafra, B.; Fasano, A.; Pozzi, N.G.; Zangaglia, R.; Servello, D.; Pacchetti, C. Eight-years failure of subthalamic stimulation rescued by globus pallidus implant. *Brain Stimul.* **2014**, *7*, 179–181. [CrossRef] [PubMed]

31. Deligny, C.; Drapier, S.; Verin, M.; Lajat, Y.; Raoul, S.; Damier, P. Bilateral subthalamotomy through dbs electrodes: A rescue option for device-related infection. *Neurology* **2009**, *73*, 1243–1244. [CrossRef] [PubMed]
32. Ferraye, M.U.; Debû, B.; Fraix, V.; Goetz, L.; Ardouin, C.; Yelnik, J.; Henry-Lagrange, C.; Seigneuret, E.; Piallat, B.; Krack, P.; et al. Effects of pedunculopontine nucleus area stimulation on gait disorders in Parkinson's disease. *Brain* **2010**, *133*, 205–214. [CrossRef] [PubMed]
33. Stein, J.F. Akinesia, motor oscillations and the pedunculopontine nucleus in rats and men. *Exp. Neurol.* **2009**, *215*, 1–4. [CrossRef] [PubMed]
34. Mazzone, P.; Lozano, A.; Stanzione, P.; Galati, S.; Scarnati, E.; Peppe, A.; Stefani, A. Implantation of human pedunculopontine nucleus: A safe and clinically relevant target in Parkinson's disease. *Neuroreport* **2005**, *16*, 1877–1881. [CrossRef] [PubMed]
35. Morris, M.E.; Iansek, R.; Galna, B. Gait festination and freezing in Parkinson's disease: Pathogenesis and rehabilitation. *Mov. Disord.* **2008**, *23*, S451–S460. [CrossRef] [PubMed]
36. Vercruysse, S.; Spildooren, J.; Heremans, E.; Vandenbossche, J.; Levin, O.; Wenderoth, N.; Swinnen, S.P.; Janssens, L.; Vandenberghe, W.; et al. Freezing in Parkinson's disease: A spatiotemporal motor disorder beyond gait. *Mov. Disord.* **2012**, *27*, 254–263. [CrossRef] [PubMed]
37. Golestanirad, L.; Elahi, B.; Graham, S.J.; Das, S.; Wald, L.L. Efficacy and safety of pedunculopontine nuclei (PPN) deep brain stimulation in the treatment of gait disorders: A meta-analysis of clinical studies. *Can. J. Neurol. Sci.* **2016**, *43*, 120–126. [CrossRef] [PubMed]
38. Stefani, A.; Lozano, A.M.; Peppe, A.; Stanzione, P.; Galati, S.; Tropepi, D.; Pierantozzi, M.; Brusa, L.; Scarnati, E.; Mazzone, P. Bilateral deep brain stimulation of the pedunculopontine and subthalamic nuclei in severe Parkinson's disease. *Brain* **2007**, *130*, 1596–1607. [CrossRef] [PubMed]
39. Liu, H.G.; Zhang, K.; Yang, A.C.; Zhang, J.G. Deep brain stimulation of the subthalamic and pedunculopontine nucleus in a patient with Parkinson's disease. *J. Korean Neurosurg. Soc.* **2015**, *57*, 303–306. [CrossRef] [PubMed]
40. Chunling, W.; Zheng, X. Review on clinical update of essential tremor. *Neurol. Sci.* **2016**, *37*, 495–502. [CrossRef] [PubMed]
41. Baizabal-Carvallo, J.F.; Kagnoff, M.N.; Jimenez-Shahed, J.; Fekete, R.; Jankovic, J. The safety and efficacy of thalamic deep brain stimulation in essential tremor: 10 years and beyond. *J. Neurol. Neurosurg. Psychiatry* **2014**, *85*, 567–572. [CrossRef] [PubMed]
42. Børretzen, M.N.; Bjerknes, S.; Sæhle, T.; Skjelland, M.; Skogseid, I.M.; Toft, M.; Dietrichs, E. Long-term follow-up of thalamic deep brain stimulation for essential tremor—Patient satisfaction and mortality. *BMC Neurol.* **2014**, *14*, 120. [CrossRef] [PubMed]
43. Pilitsis, J.G.; Metman, L.V.; Toleikis, J.R.; Hughes, L.E.; Sani, S.B.; Bakay, R.A. Factors involved in long-term efficacy of deep brain stimulation of the thalamus for essential tremor. *J. Neurosurg.* **2008**, *109*, 640–646. [CrossRef] [PubMed]
44. Ellis, T.M.; Foote, K.D.; Fernandez, H.H.; Sudhyadhom, A.; Rodriguez, R.L.; Zeilman, P.; Jacobson, C.E., IV; Okun, M.S. Reoperation for suboptimal outcomes after deep brain stimulation surgery. *Neurosurgery* **2008**, *63*, 754–761. [CrossRef] [PubMed]
45. Mehanna, R.; Machado, A.G.; Oravivattanakul, S.; Genc, G.; Cooper, S.E. Comparing two deep brain stimulation leads to one in refractory tremor. *Cerebellum* **2014**, *13*, 425–432. [CrossRef] [PubMed]
46. Oyama, G.; Foote, K.D.; Hwynn, N.; Jacobson, C.E.; Malaty, I.A.; Rodriguez, R.L.; Zeilman, P.; Okun, M.S. Rescue leads: A salvage technique for selected patients with a suboptimal response to standard DBS therapy. *Parkinsonism Relat. Disord.* **2011**, *17*, 451–455. [CrossRef] [PubMed]
47. Mundinger, F. Results of 500 subthalamotomies in the region of the zona incerta. In *Third Symposium on Parkinson's Disease*; E & S Livingstone: Edinburgh, UK; London, UK, 1969; pp. 261–265.
48. Velasco, F.; Jiménez, F.; Pérez, M.L.; Carrillo-Ruiz, J.D.; Velasco, A.L.; Ceballos, J.; Velasco, M. Electrical stimulation of the prelemniscal radiation in the treatment of Parkinson's disease: An old target revised with new techniques. *Neurosurgery* **2001**, *49*, 293–308. [CrossRef] [PubMed]
49. Wertheimer, P.; Bourret, J.; Lapras, C. Apropos of the treatment of a dyskinesia by stereotaxic leucotomy. *Lyon Med.* **1960**, *92*, 885–889. [PubMed]
50. Isaacs, D.; Butler, J.; Sukul, V.; Tolleson, C.; Fang, J.; Phibbs, F.; Hedera, P.; Yu, H.; Konrad, P. Confined thalamic stimulation in refractory essential tremor. Presented at the 20th International Congress of Parkinson's Disease and Movement Disorders, Berlin, Germany, 19–23 June 2016.

51. Yu, H.; Hedera, P.; Fang, J.; Davis, T.L.; Konrad, P.E. Confined stimulation using dual thalamic deep brain stimulation leads rescues refractory essential tremor: Report of three cases. *Stereotact. Funct. Neurosurg.* **2009**, *87*, 309–313. [CrossRef] [PubMed]
52. Sukul, V.; Isaacs, D.A.; Pallavaram, S.; Rodriguez, W.; Butler, J.; Yu, H.; Neimat, J.S.; Konrad, P. Field-steering rescue lead therapy for patients with essential tremor refractory to ventralis intermedius deep brain stimulation. *Neurosurgery* **2016**, *63*, 155–156. [CrossRef] [PubMed]
53. Bahgat, D.; Magill, S.T.; Berk, C.; McCartney, S.; Burchiel, K.J. Thalamotomy as a treatment option for tremor after ineffective deep brain stimulation. *Stereotact. Funct. Neurosurg.* **2012**, *91*, 18–23. [CrossRef] [PubMed]
54. Albanese, A.; Bhatia, K.; Bressman, S.B.; DeLong, M.R.; Fahn, S.; Fung, V.S.; Hallett, M.; Jankovic, J.; Jinnah, H.A.; Klein, C.; et al. Phenomenology and classification of dystonia: A consensus update. *Mov. Disord.* **2013**, *28*, 863–873. [CrossRef] [PubMed]
55. Geyer, H.L.; Bressman, S.B. The diagnosis of dystonia. *Lancet Neurol.* **2006**, *5*, 780–790. [CrossRef]
56. Tarsy, D.; Simon, D.K. Dystonia. *N. Engl. J. Med.* **2006**, *355*, 818–829. [CrossRef] [PubMed]
57. Vitek, J.L.; DeLong, M.R.; Starr, P.A.; Hariz, M.I.; Metman, L.V. Intraoperative neurophysiology in DBS for dystonia. *Mov. Disord.* **2011**, *26*, S31–S36. [CrossRef] [PubMed]
58. Ostrem, J.L.; Starr, P.A. Treatment of dystonia with deep brain stimulation. *Neurotherapeutics* **2008**, *5*, 320–330. [CrossRef] [PubMed]
59. Kupsch, A.; Benecke, R.; Müller, J.; Trottenberg, T.; Schneider, G.H.; Poewe, W.; Eisner, W.; Wolters, A.; Müller, J.U.; Deuschl, G.; et al. Pallidal deep-brain stimulation in primary generalized or segmental dystonia. *N. Engl. J. Med.* **2006**, *355*, 1978–1990. [CrossRef] [PubMed]
60. Speelman, J.D.; Contarino, M.F.; Schuurman, P.R.; Tijssen, M.A.J.; de Bie, R.M.A. Deep brain stimulation for dystonia: Patient selection and outcomes. *Eur. J. Neurol.* **2010**, *17*, 102–106. [CrossRef] [PubMed]
61. Vidailhet, M.; Vercueil, L.; Houeto, J.L.; Krystkowiak, P.; Benabid, A.L.; Cornu, P.; Lagrange, C.; du Tézenas Montcel, S.; Dormont, D.; Grand, S.; et al. Bilateral deep-brain stimulation of the globus pallidus in primary generalized dystonia. *N. Engl. J. Med.* **2005**, *352*, 459–467. [CrossRef] [PubMed]
62. Kiss, Z.H.; Doig-Beyaert, K.; Eliasziw, M.; Tsui, J.; Haffenden, A.; Suchowersky, O. The Canadian multicentre study of deep brain stimulation for cervical dystonia. *Brain* **2007**, *130*, 2879–2886. [CrossRef] [PubMed]
63. Skogseid, I.M.; Ramm-Pettersen, J.; Volkmann, J.; Kerty, E.; Dietrichs, E.; Røste, G.K. Good long-term efficacy of pallidal stimulation in cervical dystonia: A prospective, observer-blinded study. *Eur. J. Neurol.* **2012**, *19*, 610–615. [CrossRef] [PubMed]
64. Walsh, R.A.; Sidiropoulos, C.; Lozano, A.M.; Hodaie, M.; Poon, Y.Y.; Fallis, M.; Moro, E. Bilateral pallidal stimulation in cervical dystonia: Blinded evidence of benefit beyond 5 years. *Brain* **2013**, *136*, 761–769. [CrossRef] [PubMed]
65. Novak, K.E.; Nenonene, E.K.; Bernstein, L.P.; Vergenz, S.; Cozzens, J.W.; Rezak, M. Successful bilateral subthalamic nucleus stimulation for segmental dystonia after unilateral pallidotomy. *Stereotact. Funct. Neurosurg.* **2007**, *86*, 80–86. [CrossRef] [PubMed]
66. Schjerling, L.; Hjermind, L.E.; Jespersen, B.; Madsen, F.F.; Brennum, J.; Jensen, S.R.; Løkkegaard, A.; Karlsborg, M. A randomized double-blind crossover trial comparing subthalamic and pallidal deep brain stimulation for dystonia: Clinical article. *J. Neurosurg.* **2013**, *119*, 1537–1545. [CrossRef] [PubMed]

brain sciences

MDPI

Article

Vocal Tremor: Novel Therapeutic Target for Deep Brain Stimulation

Vinod K. Ravikumar *, Allen L. Ho, Jonathon J. Parker, Elizabeth Erickson-DiRenzo and Casey H. Halpern

Department of Neurosurgery, Stanford University, 300 Pasteur Dr., Edwards Bldg. R-293, Stanford, CA 94305, USA; aho5@stanford.edu (A.L.H.); parkerjo@stanford.edu (J.J.P.); edirenzo@ohns.stanford.edu (E.E.); chalpern@stanford.edu (C.H.H.)

* Correspondence: vinod.rr@gmail.com

Academic Editors: Tipu Aziz and Alex Green

Received: 27 July 2016; Accepted: 3 October 2016; Published: 10 October 2016

Abstract: Tremulous voice is characteristically associated with essential tremor, and is referred to as essential vocal tremor (EVT). Current estimates suggest that up to 40% of individuals diagnosed with essential tremor also present with EVT, which is associated with an impaired quality of life. Traditional EVT treatments have demonstrated limited success in long-term management of symptoms. However, voice tremor has been noted to decrease in patients receiving deep brain stimulation (DBS) with the targeting of thalamic nuclei. In this study, we describe our multidisciplinary procedure for awake, frameless DBS with optimal stimulation targets as well as acoustic analysis and laryngoscopic assessment to quantify tremor reduction. Finally, we investigate the most recent clinical evidence regarding the procedure.

Keywords: deep brain stimulation; awake DBS; ventral intermediate nucleus; VIM; dysphonia; essential tremor; essential vocal tremor; EVT; voice; tremulous voice; laryngoscopy; acoustic analysis; microelectrode recording

1. Introduction

Tremulous voice is a distinguishing feature of many neurologic disorders including Parkinson's Disease (PD), stroke, orofacial dystonia, spasmodic dysphonia, myasthenia gravis, and progressive supranuclear palsy [1–3]. Tremulous voice is characteristically associated with essential tremor (ET), and is referred to as essential vocal tremor (EVT). EVT is thus a manifestation of the oscillatory and rhythmic features of ET in the phonatory apparatus. Current estimates suggest that up to 40% of individuals diagnosed with essential tremor also present with EVT [4]. EVT is characterized by increased vocal effort, particularly during periods of anxiety or stress, causing significant social embarrassment. Patients with severe cases of EVT may feel obliged to reduce social commitments, extricating themselves from employment and hobbies. Though discernable in many forms of vocal interaction, irregularities are most noticeable with sustained phonation of vowels. Thus, EVT may significantly impair quality of life, and patients are in need of a durable solution [5].

Tremulous voice is a symptom of laryngeal tremor. The antagonistic contractions of pharyngeal, laryngeal, and/or palatal muscles cause rhythmic oscillations of the laryngeal apparatus at a rate of 4–8 Hz in EVT patients. Such oscillations alter voice pitch and intensity, corresponding to acoustic changes in fundamental frequency (f_0) and amplitude, respectively [5]. Symptoms may be exacerbated by involuntary movements of vocal accessory muscles such as chest wall muscles, abdominal muscles, and the diaphragm. Regularity and intensity of acoustic changes are subject to considerable variability between EVT patients [6].

2. Patient Evaluation/Assessment of EVT

The multidisciplinary outpatient evaluation of EVT includes an otolaryngologist specialized in voice disorders as well as a speech language pathologist. Patients will present with debilitating, progressive vocal tremor that is refractory to medication and causing a significant reduction in quality of life. Other tremors such as head or upper extremity tremor may also be present.

If the patient should present de novo to the neurosurgeon for consideration of deep brain stimulation (DBS) for tremor, normal preoperative DBS work-up and clearance should be completed. The patient must also consult a laryngologist and speech language pathologist for a full tremor work-up. Diagnosis and characterization of EVT is performed by a laryngologist with fiberoptic nasolaryngoscopic examination of the pharynx and larynx, also known as flexible distal-chip laryngoscopy, during tasks that emphasize prolonged phonation [5]. The preoperative examination by the speech language pathologist serves to characterize instrumental and acoustic qualities of the vocal tremor, to develop behavioral strategies for patients to reduce phonatory collision forces at the region of identified pathology. These objective measures also establish a baseline from which to measure intra- and postoperative alterations in voice with DBS [6].

Additional, objective acoustic measures may concomitantly be used to assist with diagnosis [7]. Though transnasal and oral endoscopic approaches are used in EVT diagnosis, the transnasal approach is preferred since it permits a more thorough investigation of the musculature while keeping the patient in a natural posture. Laryngeal tremor may be diagnosed on transnasal endoscopy upon identification of characteristic rhythmic oscillations of the vocal folds during speech. This rhythmic oscillation may be complemented with craniocaudal laryngeal oscillations and/or contractions of the palate as well as the pharynx. Tremor is noticeable both on prolonged vowel phonation as well as during quiet respiration [5,8].

An acoustical examination, comprised of sustained and short sentences as well as sustained vowel sounds, should be utilized to supplement findings and conclusions drawn from a direct laryngeal exam [9]. During the evaluation, it is essential that the patient sustain phonation of vowels since connected speech may conceal the presence or severity of EVT. The rates of f_0 and intensity change are measured, recorded, and used to describe the acoustic characteristics of EVT. Changes in these two rate parameters are typically synchronous, and are the most noticeable features of vocal tremor. Additionally, the magnitude of change in intensity and f_0 may also be utilized in describing EVT acoustic characteristics. Magnitude values are determined by calculating the ranges of both intensity and f_0 oscillations. High voice intensity is characteristic of an ET patient, and successful intervention will likely result in a reduction [10]. Investigation of other acoustic measures such as shimmer, jitter, and harmonic-to-noise ratio, speech rate (syllables per second), and voice aerodynamics (e.g., s-to-z ratio and maximum phonation time) may also be used to preoperatively evaluate patients or assess vocal changes [7]. EVT patients experience increases in shimmer and jitter, as well as a reduction in harmonic-to-noise ratio (voice quality), s-to-z ratio, and maximum phonation time. Therefore, a shift in these parameters can signify reduction of ET symptoms and may be used as markers to verify accurate lead and electrode placement in vocal tremor patients.

3. Treatment of EVT

Traditional EVT treatments have demonstrated limited success in long-term management of symptoms. First-line pharmacologic treatment with agents such as primidone and propranolol yield varied outcomes [11]. Alternatively, EVT patients whose tremor originates in the thryroarytenoid and extralaryngeal muscles have received targeted injections of Botulinum A toxin (Botox). Such targeted Botox therapies have demonstrated a significant reduction in tremor amplitude in up to 80% of this subset of patients [12]. However, it should be noted that patients rarely experience complete tremor resolution, despite the transient nature of this treatment and need for periodic injections over the patient's lifetime. Botox injections may also present with adverse effects including dysphagia, coughing, choking, and breathiness. This side effect profile limits use of the treatment in elderly patients [13].

Currently, there are promising avenues for behavioral modification treatment by working with a speech language pathologist [6]. However, it is evident that an enduring and effective treatment for EVT is required.

4. DBS for EVT

Despite shortcomings of pharmacological and behavioral treatments for EVT, Deep Brain Stimulation (DBS) is known to be a safe and reputed method of reducing nonspecific tremor severity for patients who are refractory to medication [7]. However, there remains little research or evidence in the literature that has systematically investigated symptom improvement EVT upon DBS intervention, and many laryngologists remain under-informed regarding the therapeutic potential of DBS [3].

In 2002, Sataloff et al. reported the first case report for the application of DBS in treating vocal tremor [14]. The study examined two patients who were implanted with stimulators bilaterally in the ventral intermediate nucleus (Vim) of the thalamus. Voice analysis and strobovideolaryngoscopy revealed elimination of symptoms in one patient and significant decrease in voice tremor in the other [14]. Most studies since that time are comprised of results from small number of participants or are in the form of case reports [15–19].

Voice tremor has been noted to decrease in patients receiving DBS treatment for other indications including dystonia, essential hand tremor, and PD-associated tremor due to the targeting of nearby thalamic nuclei [2,15,20]. For example, DBS targeting the STN for treatment of PD demonstrates improvement in voice tremor symptoms, albeit inconsistent [2]. Patients without Vim targeting did not experience as great a reduction in voice tremor as other regions with tremor [15,16,21].

Of note, patient eligibility and selection should account for potential worsening of gait especially following bilateral Vim DBS implantation, as noted in certain studies [21]. However, gait imbalances can be partially or fully resolved with reprogramming.

5. Vim Target for DBS

In 1987, Benabid et al. was first to suggest that tremor symptoms could be alleviated by stimulating the Vim region of the thalamus [22]. The Vim is organized in a somatotopic fashion, with cerebellar afferents from the face positioned most medially, and progressing to hands then feet, laterally. Since the precise location of Vim may be difficult to discern on, microelectrode recording and stereotactic referencing are utilized for physiological mapping and indirect targeting, respectively. The coordinates of the Vim are different for each individual, but as a general rule, direct Vim targeting proceeds 6 mm posterior to the midpoint of the anterior commissure-posterior commissure (AC-PC) and 12–14 mm lateral to the AC-PC line [7]. Microelectrode unit activation occurs more frequently with passive kinesthetic movement of extremity joints, as it passes from the skull entry point caudally to the Vim.

Receptive fields in the thalamus are arranged in a somatotopic map with fields corresponding to the face located medially, upper extremity located ventromedially, and lower extremity located dorsolaterally. As the electrode descends in the customary dorsolateral-to-ventromedial track into the Vim, it will pass leg and subsequently arm kinesthetic receptive fields [6]. Therefore, suppression of voice tremor is contingent on stimulator positioning 1–2 mm medial the typical essential tremor (ET) target [23,24].

Since vocal tremor must be continually monitored by a speech language pathologist, surgery is always conducted in the awake state. Tremor can be monitored in regions associated with vocal tremor and which demonstrate tremor symptoms, such as the head and limbs. Before electrode insertion, depth of the target in the Vim is determined. The microelectrode is initially set to a point 15 mm proximal to the target to test and confirm its impedance range.

The microelectrode is then moved incrementally towards the target, while continuously recording. Single unit recordings when the electrode passes through the thalamus are typically excellent. As the electrode nears the target, macrostimulation is accompanied by meticulous documentation of tremor reduction and careful monitoring for paresthesias. A neurophysiologist will help record

kinesthetic responses the corresponding extremity, proximal motor groups, and macrostimulation via the microcannula. Additionally, a speech language pathologist will perform both an intraoperative acoustic assessment and a speech assessment for the patient.

Accuracy in electrode implantation at an appropriate distance from certain nuclei is contingent on proper identification of surrounding structures. Slightly anterior to the Vim are the ventrooralis posterior and anterior nuclei, which are activated by movement of the contralateral extremities. By contrast, the ventral caudalis nucleus is located posteriorly to the Vim. It can be distinguished from the Vim as it contains a narrow somatotopic area of receptive fields reacting to light touch [25]. Electrode implantation is considered safe if it is sufficiently far from the ventral caudalis nucleus (>2 mm). In ET patients, the DBS electrode is usually targeted to the kinesthetic fields, which are linked to the hands. Successful or near-complete tremor suppression will require macroelectrode stimulation with currents as low as 0.2 mA and microelectrode stimulation with currents up to 100 microAmps. If the electrode is implanted distally from the Vim and proximally to the ventral caudalis nucleus, the patient will experience paresthesia in place of tremor suppression. Thus, successful stimulation will manifest as decreased tremor without any sustained sensation of paresthesia [26].

Following successful electrode insertion and verification with macrostimulation and microrecording, the lead should be implanted utilizing the same track. Optimal placement of the electrode will necessitate several passes, introducing a possibility of morbidity. Upon observation of tremor reduction, a Medtronic 3389 DBS electrode, sized to the correct length, may be relayed to the target point along the track. Following test simulations that confirm tremor reduction and rule out the presence of harmful side effects, the lead is secured. This entire process is repeated in the contralateral side for bilateral tremor patients. After one week, the patient returns to have a pulse generator implanted infraclavicularly. Two weeks post-implantation, the patient returns for a programming visit, and will also receive both speech and neurophysiologic analysis.

6. Discussion

EVT is a type of tremulous voice disorder that is highly refractory to treatment, and results in significantly compromised quality of life for patients. Though a decade has passed since DBS had been hypothesized as a therapeutic avenue for patients with EVT, the literature remains sparse with respect to systematic studies. DBS has been proposed as a more permanent treatment modality for EVT patients, but few comprehensive studies exist in the literature investigating DBS use for this particular indication. The first of these studies was performed by Sataloff et al. and utilized objective voice analysis and strobovideolaryngoscopy to evaluate patient outcomes. Both patients in the study experienced significant reductions in vocal tremor, with one patient emerging symptom-free after treatment [14]. Most other studies examining DBS-induced vocal tremor reduction feature patients with an assortment of other pathologies and utilization of differing techniques of intervention [15,16,18,21,27]. Additionally, tremor assessments are not complete and often contain varied time intervals during which recordings were made. Furthermore, qualitative assessment protocols introduce variation between stimulator settings, resulting in more variation in methodology. Moreover, certain tremor evaluations conducted alone, such as subjective speech evaluations without any other examination, have little reliability [7].

In this article, we aim to provide a detailed account of the comprehensive and multidisciplinary use of awake, frameless DBS in treating EVT, beginning with the pre-operative evaluation. Characteristic features of our procedure include designation of the Vim as the neurophysiological target and utilization of real-time physiologic feedback to track changes in vocal tremor while in the operating room. Utilization of a frameless system provides added benefits in comparison to the stereotactic frame equivalent, including ease of intraoperative neurological examinations, improved patient comfort, greater accuracy, as well as real-time electrode tracking by synthesizing multiple information sources. These benefits are demonstrated in the clinical setting without compromising either stability or accuracy [28].

Notably, our procedure is successful in reducing symptoms of EVT without minimizing the positive effects of DBS on tremor in the concurrent extremities. DBS intervention results in an increased harmonic-to-noise ratio (improved voice quality) and decreased f_0 [7]. More investigation is required to uncover the prime electrode targets to concurrently treat multiple tremor types. Moreover, Vogel et al. found that optimal stimulator settings, including the Pitch Floors/Ceilings and Time Steps, are superior in function when compared to baseline, clinical settings [7]. However, we believe that this effort will help influence and inspire the development of new treatments for this previously refractory group of patients.

Despite their limitations, these studies exhibit positive results of DBS treatment, including decreases in both tremor severity and the rate of F0 modulation [6,15]. It is imperative that further prospective investigations are conducted to validate the positive effects of DBS in EVT patients. Furthermore, it is important to distinguish the difference between successful tremor reduction and speech outcomes. While DBS has demonstrated promise and consistent success in reducing tremor, the correlation between tremor decrease and speech improvement is unclear [7,29]. A recent study examining the use of DBS for EVT in a different brain region found that vocal tremor treatment significantly reduced symptoms in only half of the patient cohort [30]. This suggests the possibility of vocal tremor symptoms that originate in other parts of the body, from sources outside of the direct phonatory apparatus. Hence, careful evaluation of the source of tremor by a trained otolaryngologist is essential.

Future studies should incorporate larger patient cohorts studied over long periods of time in order to truly examine efficacy and complications of DBS as a treatment for vocal tremor. The focal, reportable metric in these studies will be a complete voice and larynx examination pre-, intra-, and post-operatively, which will help in the production of evidence-based guidelines. This examination should incorporate nasal endoscopy for direct laryngeal visualization as well as vocal analysis, such as aerodynamics, review by both patient and physician, and acoustics. Results from such studies will have the potential to shape future therapies for this group of medication-refractory patients.

7. Conclusions

In this study, we describe our multidisciplinary procedure for awake, frameless DBS with optimal stimulation targets as well as acoustic analysis and laryngoscopic assessment to quantify tremor reduction.

Acknowledgments: The Authors thank Stanford University School of Medicine.

Author Contributions: Casey Halpern, Elizabeth Erickson-DiRenzo, and Allen Ho contributed to the conception of the topic. Vinod Ravikumar was the primary writer with Allen Ho providing guidance and editing. Jonathon Parker provided critical input.

Conflicts of Interest: The Authors declare no conflict of interest.

References

1. Limousin-Dowsey, P.; Pollak, P.; Van Blercom, N.; Krack, P.; Benazzouz, A.; Benabid, A.L. Thalamic, subthalamic nucleus and internal pallidum stimulation in Parkinson's disease. *J. Neurol.* **1999**, *246*, II42–II45. [CrossRef] [PubMed]
2. D'Alatri, L.; Paludetti, G.; Contarino, M.F.; Galla, S.; Marchese, M.R.; Bentivoglio, A.R. Effects of bilateral subthalamic nucleus stimulation and medication on Parkinsonian speech impairment. *J. Voice* **2008**, *22*, 365–372. [CrossRef] [PubMed]
3. Hawkshaw, M.J.; Sataloff, R.T. Deep brain stimulation for treatment of voice disorders. *J. Voice* **2012**, *26*, 769–771. [CrossRef] [PubMed]
4. Wolraich, D.; Vasile Marchis-Crisan, C.; Redding, N.; Khella, S.L.; Mirza, N. Laryngeal tremor: Co-occurrence with other movement disorders. *ORL J. Otorhinolaryngol. Relat. Spec.* **2010**, *72*, 291–294. [CrossRef] [PubMed]

5. Merati, A.L.; Heman-Ackah, Y.D.; Abaza, M.; Altman, K.W.; Sulica, L.; Belamowicz, S. Common movement disorders affecting the larynx: A report from the neurolaryngology committee of the AAO-HNS. *Otolaryngol. Head Neck Surg.* **2005**, *133*, 654–665. [CrossRef] [PubMed]
6. Ho, A.L.; Erickson-Direnzo, E.; Pendharkar, A.V.; Sung, C.K.; Halpern, C.H. Deep brain stimulation for vocal tremor: A comprehensive, multidisciplinary methodology. *Neurosurg. Focus* **2015**, *38*, E6. [CrossRef] [PubMed]
7. Vogel, A.P.; McDermott, H.J.; Perera, T.; Jones, M.; Peppard, R.; McKay, C.M. The feasibility of using acoustic markers of speech for optimizing patient outcomes during randomized amplitude variation in deep brain stimulation: A proof of principle methods study. *Front. Bioeng. Biotechnol.* **2015**, *3*, 98. [CrossRef] [PubMed]
8. Barkmeier-Kraemer, J.; Lato, A.; Wiley, K. Development of a speech treatment program for a client with essential vocal tremor. *Semin. Speech Lang.* **2011**, *32*, 43–57. [CrossRef] [PubMed]
9. Gamboa, J.; Jiménez-Jiménez, F.J.; Nieto, A.; Montojo, J.; Ortí-Pareja, M.; Molina, J.A.; García-Albea, E.; Cobeta, I. Acoustic voice analysis in patients with Parkinson's disease treated with dopaminergic drugs. *J. Voice* **1997**, *11*, 314–320. [CrossRef]
10. Gamboa, J.; Jiménez-Jiménez, F.J.; Nieto, A.; Cobeta, I.; Vegas, A.; Ortí-Pareja, M.; Gasalla, T.; Molina, J.A.; García-Albea, E. Acoustic voice analysis in patients with essential tremor. *J. Voice* **1998**, *12*, 444–452. [CrossRef]
11. Kendall, K.A. Vocal tremor. In *Mechanisms and Emerging Therapies in Tremor Disorders*; Grimaldi, G., Manto, M., Eds.; Springer: New York, NY, USA, 2013; pp. 235–248.
12. Gurey, L.E.; Sinclair, C.F.; Blitzer, A. A new paradigm for the management of essential vocal tremor with botulinum toxin. *Laryngoscope* **2013**, *123*, 2497–2501. [CrossRef] [PubMed]
13. Warrick, P.; Dromey, C.; Irish, J.C.; Durkin, L.; Pakiam, A.; Lang, A. Botulinum toxin for essential tremor of the voice with multiple anatomical sites of tremor: A crossover design study of unilateral versus bilateral injection. *Laryngoscope* **2000**, *110*, 1366–1374. [CrossRef] [PubMed]
14. Sataloff, R.T.; Heuer, R.J.; Munz, M.; Yoon, M.S.; Spiegel, J.R. Vocal tremor reduction with deep brain stimulation: A preliminary report. *J. Voice* **2002**, *16*, 132–135. [PubMed]
15. Carpenter, M.A.; Pahwa, R.; Miyawaki, K.L.; Wilkinson, S.B.; Searl, J.P.; Koller, W.C. Reduction in voice tremor under thalamic stimulation. *Neurology* **1998**, *50*, 796–798. [PubMed]
16. Moringlane, J.R.; Pützer, M.; Barry, W.J. Bilateral high-frequency electrical impulses to the thalamus reduce voice tremor: Acoustic and electroglottographic analysis. A case report. *Eur. Arch. Otorhinolaryngol.* **2004**, *261*, 334–336. [CrossRef] [PubMed]
17. Mure, H.; Morigaki, R.; Koizumi, H.; Okita, S.; Kawarai, T.; Miyamoto, R.; Kaji, R.; Nagahiro, S.; Goto, S. Deep brain stimulation of the thalamic ventral lateral anterior nucleus for DYT6 dystonia. *Stereotact. Funct. Neurosurg.* **2014**, *92*, 393–396. [CrossRef] [PubMed]
18. Yoon, M.S.; Munz, M.; Sataloff, R.T.; Spiegel, J.R.; Heuer, R.J. Vocal tremor reduction with deep brain stimulation. *Stereotact. Funct. Neurosurg.* **1999**, *72*, 241–244. [CrossRef] [PubMed]
19. Ho, A.L.; Choudhri, O.; Sung, C.K.; DiRenzo, E.E.; Halpern, C.H. Deep brain stimulation for essential vocal tremor: A technical report. *Cureus* **2015**, *7*, e256. [CrossRef] [PubMed]
20. Groen, J.L.; Ritz, K.; Contarino, M.F.; van de Warrenburg, B.P.; Aramideh, M.; Foncke, E.M.; van Hilten, J.J.; Schuurman, P.R.; Speelman, J.D.; Koelman, J.H.; et al. DYT6 dystonia: Mutation screening, phenotype, and response to deep brain stimulation. *Mov. Disord.* **2010**, *25*, 2420–2427. [CrossRef] [PubMed]
21. Taha, J.M.; Janszen, M.A.; Favre, J. Thalamic deep brain stimulation for the treatment of head, voice, and bilateral limb tremor. *J. Neurosurg.* **1999**, *91*, 68–72. [CrossRef] [PubMed]
22. Benabid, A.; Pollak, P.; Louveau, A.; Henry, S.; de Rougemont, J. Combined (thalamotomy and stimulation) stereotactic surgery of the VIM thalamic nucleus for bilateral Parkinson disease. *Appl. Neurophysiol.* **1987**, *50*, 1–6. [CrossRef]
23. Vitek, J.L.; Ashe, J.; DeLong, M.R.; Alexander, G.E. Physiologic properties and somatotopic organization of the primate motor thalamus. *J. Neurophysiol.* **1994**, *71*, 1498–1513. [PubMed]
24. Vitek, J.L.; Ashe, J.; DeLong, M.R.; Kaneoke, Y. Microstimulation of primate motor thalamus: Somatotopic organization and differential distribution of evoked motor responses among subnuclei. *J. Neurophysiol.* **1996**, *75*, 2486–2495. [PubMed]
25. Macchi, G.; Jones, E.G. Toward an agreement on terminology of nuclear and subnuclear divisions of the motor thalamus. *J. Neurosurg.* **1997**, *86*, 77–92. [CrossRef] [PubMed]

26. Benabid, A.L.; Pollak, P.; Gao, D.; Hoffmann, D.; Limousin, P.; Gay, E.; Payen, I.; Benazzouz, A. Chronic electrical stimulation of the ventralis intermedius nucleus of the thalamus as a treatment of movement disorders. *J. Neurosurg.* **1996**, *84*, 203–214. [CrossRef] [PubMed]
27. Halpern, C.H.; Torres, N.; Hurtig, H.I.; Wolf, J.A.; Stephen, J.; Oh, M.Y.; Williams, N.N.; Dichter, M.A.; Jaggi, J.L.; Caplan, A.L.; et al. Expanding applications of deep brain stimulation: A potential therapeutic role in obesity and addiction management. *Acta Neurochir.* **2011**, *153*, 2293–2306. [CrossRef] [PubMed]
28. Holloway, K.L.; Gaede, S.E.; Starr, P.A.; Rosenow, J.M.; Ramakrishnan, V.; Henderson, J.M. Frameless stereotaxy using bone fiducial markers for deep brain stimulation. *J. Neurosurg.* **2005**, *103*, 404–413. [CrossRef] [PubMed]
29. King, N.O.; Anderson, C.J.; Dorval, A.D. Deep brain stimulation exacerbates hypokinetic dysarthria in a rat model of Parkinson's disease. *J. Neurosci. Res.* **2016**, *94*, 128–138. [CrossRef] [PubMed]
30. Hägglund, P.; Sandström, L.; Blomstedt, P.; Karlsson, F. Voice tremor in patients with essential tremor: Effects of deep brain stimulation of caudal zona incerta. *J. Voice* **2016**, *30*, 228–233. [CrossRef] [PubMed]

brain sciences

MDPI

Review

Deep Brain Stimulation in Huntington's Disease—Preliminary Evidence on Pathophysiology, Efficacy and Safety

Lars Wojtecki [1,2,*], Stefan Jun Groiss [1,2], Christian Johannes Hartmann [1,2], Saskia Elben [1,2], Sonja Omlor [2], Alfons Schnitzler [1,2] and Jan Vesper [3]

1 Department of Neurology, Medical Faculty, Heinrich-Heine University Düsseldorf, Moorenstrasse 5, Düsseldorf 40225, Germany; groiss@uni-duesseldorf.de (S.J.G.); christian-hartmann@uni-duesseldorf.de (C.J.H.); saskia.elben@med.uni-duesseldorf.de (S.E.); Sonja.Omlor@uni-duesseldorf.de (S.O.); schnitza@uni-duesseldorf.de (A.S.)

2 Institute of Clinical Neuroscience & Medical Psychology, Medical Faculty, Heinrich-Heine University Düsseldorf, Moorenstrasse 5, Düsseldorf 40225, Germany

3 Department of Functional Neurosurgery and Stereotaxy, Medical Faculty, Heinrich-Heine University Düsseldorf, Moorenstrasse 5, Düsseldorf 40225, Germany; jan.vesper@med.uni-duesseldorf.de

* Correspondence: lars.wojtecki@med.uni-duesseldorf.de; Tel.: +49-211-811-6756; Fax: +49-211-811-6525

Academic Editors: Tipu Aziz and Alex Green
Received: 15 July 2016; Accepted: 22 August 2016; Published: 30 August 2016

Abstract: Huntington's disease (HD) is one of the most disabling degenerative movement disorders, as it not only affects the motor system but also leads to cognitive disabilities and psychiatric symptoms. Deep brain stimulation (DBS) of the pallidum is a promising symptomatic treatment targeting the core motor symptom: chorea. This article gives an overview of preliminary evidence on pathophysiology, safety and efficacy of DBS in HD.

Keywords: chorea; Huntington; deep brain stimulation; DBS; safety pathophysiology; recordings; globus pallidus

1. Introduction

In this manuscript, the authors update a recent perspective article on brain stimulation in Huntington's disease (HD), [1] focusing especially on deep brain stimulation (DBS) and its preliminary evidence on safety and efficacy.

HD is an autosomal dominant inherited neurodegenerative disorder [2]. As a consequence of an expanded CAG repeat in the HD gene motor symptoms, psychiatric symptoms and cognitive decline progressively develop. Even though cellular pathology is evident in the whole body, medium spiny neurons in the circumscribed area of the striatum are considered to selectively degenerate in the course of HD and thereby lead to motor symptoms [3], typically including chorea, dystonia and bradykinesia. Especially, choreatic symptoms commonly occur in early stages of HD [4]. Here, the disinhibition of one basal ganglia network circuit is considered to be pivotal [4]. Degeneration of striatal neurons, which project to the indirect pathway of the basal ganglia circuit, cause decreased basal ganglia output [5] and the aforementioned disinhibition. Furthermore, pathological changes in the direct pathway of the basal ganglia circuit have to be taken into account. Structural alterations in the substantia nigra and the cerebellum could also play a crucial role in dystonic or hypokinetic-rigid symptoms [6,7].

The status quo in HD treatment has offered no approved neuroprotective or causal treatment so far. As a consequence, the therapeutic options for HD rely on symptom treatment, which often is not sufficiently effective or causes side effects.

2. Evolution of Deep Brain Stimulation for HD

Chronic electric stimulation of deep brain structures (see Figure 1) is a well-established therapeutic method using stereotactic techniques to pinpoint the target regions of interest, such as certain parts of the basal ganglia network [8,9]. In 1987, Benabid and colleagues paved the way for the broader DBS application with an implanted impulse generator in different movement disorders and other disorders in the field of neurology and psychiatry [10]. Previous to this, DBS predominantly was (sometimes abusively) proposed for psychiatric disorders [11–13]. Subsequent DBS findings in movement disorders such as tremor and dystonia however indicated the first benefits for patients [14–16]. The underlying mechanisms of DBS are still not sufficiently identified and therefore the extensive current assumptions about DBS functional principles are discussed elsewhere in more detail [17,18].

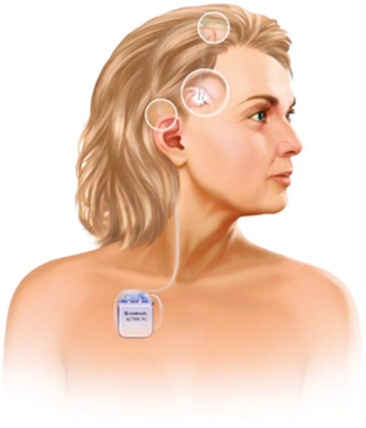

Figure 1. DBS components. Subcutaneous implanted impulse generator (IPG), lead extension and stereotactically implanted stimulation electrodes. Image provided by Medtronic.

In short, underlying mechanisms include local and network-wide effects and might even range to neuroprotective and neurogenesis effects, even though evidence is preliminary here. While high frequency stimulation seems to mimic a lesion in the targeted area [19,20], the frequency of the action's potential output in this certain region increases [18]. Therefore, no one unified mechanism such as the inhibition of neuronal activity can explain the DBS overall effect on the region of interest. A dissociation between the somatic and axonal activity of the neurons may explain these contradicting patterns. As a consequence of different thresholds for somatic and axonal neuronal activity, DBS might inhibit the soma near to the stimulated electrode, but activate axons and dendrites in the stimulated area, which results in an increase of the action potential output frequency [18]. Notwithstanding, these inhibition and activation effects are merely two out of several mechanisms contributing to the impact of DBS.

The overall effect of DBS in the globus pallidus internus (GPi) is beneficial to hyperkinetic movement disorders like dyskinesia in Parkinson's disease (PD) [21,22], primary dystonia [23,24], tardive dyskinesia [25,26] and other disorders like neurodegeneration with Brain Iron Accumulation [27], chorea-akanthocytosis [28,29] or dystonia–choreoathetosis in cerebral palsy [30–32]. As an alternative method to pallidotomy as a treatment option for HD, DBS (especially of the GPI) has been of growing interest during the last 12 years [33,34].

3. Invasive Assessment of the Basal Ganglia Network in HD

The disruption of the cortico-striato-thalamo-cortical (CSTC) networks is assumed to be the underlying functional mechanism of HD and presumably is linked to cellular degeneration [35]. Three parallel arranged circuits—an associative, motor and limbic circuit—can be distinguished [36]. Due to the evolution of the three systems, a functional segregation of these networks is assumed. Nevertheless, a shared hierarchic CSTC-architecture can be found (see Figure 2): Cortical glutamatergic projections reach the associative striatal areas, from where a direct and an indirect pathway reach the output nuclei of the basal ganglia system [37]. The direct pathway comprises the following circuit: Distinct neurons of the associative striatal areas project via inhibitory (GABA-ergic) transmission to output nuclei of the basal ganglia system [38], which connects again via GABA-ergic projections to certain parts of the thalamus, that eventually indicate glutamatergic efferents to cortical areas. Depending on the certain function of a circuit the involved anatomical structures of striatum, output nuclei, and thalamic nuclei vary, e.g., the motor circuit involves the putamen, GPi and the anterior ventral thalamic nucleus. On the other hand, the indirect pathway comprises different stations: either it solely passes the globus pallidus externus (GPe; GABA-ergic) or the indirect pathway reaches the output nuclei by transversing both the GPe and subthalamic nucleus (STN, glutamatergic) [38]. The loss of striatal neurons, which reach the GPe within the "indirect pathway", is characteristic and probably pivotal in early stages of HD [39,40]. The consequences are, firstly, the relatively overactive GPe, secondly, the increased inhibition of the STN [41,42], thirdly, the suppression of the output nuclei and, eventually, the disinhibition of thalamic nuclei. Hence, the loss of striatal neurons results in a thalamic overactivity. Choreatic movements derive from the increased thalamic output in the basal ganglia motor loop. In contrast to this, early cognitive impairment, e.g., the inhibition of error control, may arise from the impairment of the associative CSTC circuit [43]. With respect to an affection of the third basal ganglia loop, i.e., the limbic circuit, findings suggest altered affectivity in HD, such as agitation, irritability, anxiety, or euphoria [44]. As HD progresses, alteration of striatal efferents of the direct pathway play a more significant role. Concurrently, hyperkinetic-rigid symptoms aggravate at the expense of initial choreatic symptoms, so that this shift of symptoms could relate to the direct pathway affection [45]. The assumption of open connections between the different circuits is an additional concept to the aforementioned closed loop projections. This concept facilitates interaction at different hierarchical levels of the CSTC network [46] such as directional input from the associative CSTC circuit to both the motor and limbic loops. Findings in histology as well as in morphometry indicate an early affection of the associative CSTC loop. Assuming a (relative) functional integrity of the three main CSTC circuits, the idea of an open connection between those offers an explanation for the motor and limbic symptoms, which manifest subsequently [46].

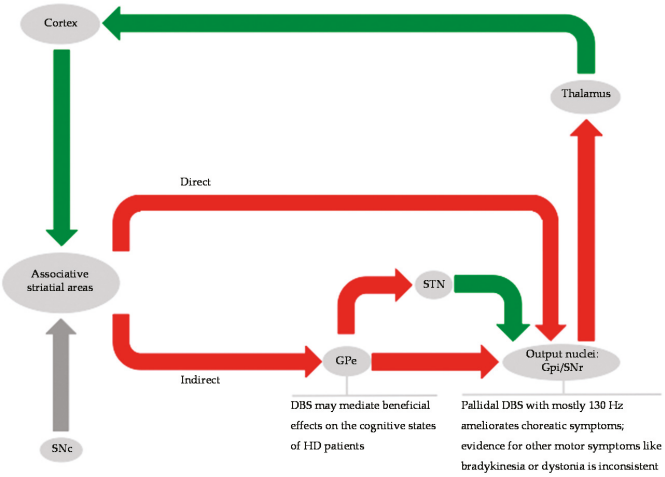

Figure 2. Basal ganglia network and targets for DBS in HD. Red arrows indicate inhibitory, green arrows indicate excitatory connections.

Prior to the implantation of the DBS electrodes, one method to determine the precise, circumscribed target position is the invasive electrical recording of multi-unit recordings of action potentials. On the other hand, these microelectrode recordings are also useful in the research of dysfunctional electrophysiological processes in e.g., movement disorders [47]. As such, they serve to uncover circumscribed characteristic neuronal patterns. The comparison of invasive electrical recordings without sedation between PD and idiopathic dystonia indicates disease-specific pallidal activation patterns. While the measured average GPe discharge rates for dystonia and for PD are almost identical (~55 Hz), both diseases differ distinctly in the GPi discharge rates (PD ~95 Hz, Dystonia ~55 Hz) [48]. Findings of invasive electrical recordings in HD patients are comparatively scarce up to now. Heterogeneous study conditions and populations (such as anesthesia or disease type) result in divergent neuronal firing patterns [34,49]. In contrast to the first published study of HD GPi firing patterns, which investigates one juvenile HD patient under general sedation [34], later studies also focus on discharge rates in non-anesthetized patients [49,50]. In terms of the discharge rate, the findings are inconsistent: While the neurons in the GP indicate a dorsoventral (GPe to GPi) gradient in their discharge rate in DBS surgery in one awake HD patient (~51 to ~73 Hz) [50]. In two non-anaesthetized patients with severe HD, the firing rate of GPi was almost identical to PD: above 80 Hz [49]. Findings with anesthesia [34,51] indicate slower firing of the GPi, around and below 20 Hz, as the use of sedatives is a decisive factor suppressing the discharge rate.

Another method for the electrophysiological characterization of neural networks is the assessment of oscillatory activity via local field potentials (LFP), which reflect synchronized activity of neural clusters in the vicinity of the recording electrode. The analysis of LFP oscillations s by Starr et al. revealed less synchronized neuronal activity in the surrounding of the electrode for the 2–35 Hz frequency range in resting, non-anesthetized HD patients in contrast to PD patients [50]. In another study of one HD patient without sedation from our own group, LFP recordings indicate dorsoventral gradients in the target area [52]. While approaching the GPi center, the power increases in the alpha-theta range (4–12 Hz). We concluded that this alpha-theta dominance could reflect a general characteristic of unvoluntary movements due to corresponding findings in other diseases such as dystonia, levodopa-induced dyskinesia and Tourette's syndrome. Furthermore, our group observed an even more evident dorsoventral gradient for the low gamma range (35–45 Hz), which intensified when

reaching the GPi ventral border. This dorsoventral gradient was considered as crucial pathophysiology for exaggerated motor drive [52].

4. Clinical Implications of DBS in HD

4.1. Clinical Implications of DBS on Hyperkinetic and Hypokinetic Symptoms

To date, there is only one prospective randomized, double-blind study on the impact of DBS on HD symptoms [53]. Two HD patients with juvenile onset (Westphal variant) and four HD patients with later onset underwent pallidal DBS. Dystonic and bradykinetic symptoms predominated in the Westphal patients, while chorea symptoms were more pronounced in the HD patients with adult onset. In contrast to the two Westphal HD patients, the four other patients could profit extensively from pallidal (GPi or GPe) DBS, as the choreatic symptoms significantly decreased by 60% compared to symptoms' baseline within the six month DBS treatment. The 60% reduction in choreatic symptoms derives from the acquisition of the UHDRS chorea subscore (Unified Huntington Disease Rating Scale) at baseline and six months after surgery. Although not significant over group, in three out of four non-Westphal patients, marked improvement of dystonia could be observed. In another study with seven HD patients, the 60% reduction in choreatic symptoms could even been measured by the UHDRS one year after implantation [54]. Tables 1 and 2 illustrate case reports and series with distinct chorea symptom reduction. A total number of 36 patients are reported. As a meta-analysis, chorea reduction can be estimated at around 56%, whereas improvement of Dystonia (scores available from 20 patients) is minor (1%).

Table 1. Case reports (n = number of patients) of DBS in HD.

Study	n	FUP (Months)	Age (Years)	DisDur (Years)	Chorea	Bradykinesia	Dystonia	Total Motor	Comments
Moro et al. [55]	1	8	43	8	44%	14%	38%	31%	DBS frequency of 130 Hz but not 40 Hz worsened bradykinesia. Increased regional cerebral blood flow in cortical motor regions.
Fawcett et al. [56]	1	4	42	n.a.	56%	n.a.	60%	26%	Moderate improvement of speech, swallowing and gait, task-specific improvement of oculomotor function.
Hebb et al. [57]	1	12	41	13	57%	n.a.	n.a.	15%	Chorea improves with higher stimulation frequency (180 Hz), no frequency-dependent effect of bradykinesia
Fasano et al. [58]	1	12	72	17	77%	60%	100%	n.a.	Worsening of gait, apathy, cognitive decline, functional gain minimal, turning off at 11 months did not induce chorea
Biolsi et al. [59]	1	48	60	10	21%	n.a.	n.a.	5%	Chorea reduced by 56%, when comparing DBS-on vs. DBS-off. L-Dopa-responsive worsening of bradykinesia. Cognition stable.
Groiss et al. [52]	1	12	65	n. a.	47%	n.a.	31%	n.a	Primary focus on local field potentials. Hypokinesia observed at 180 Hz stimulation improved from 40 Hz DBS
Garcia-Ruiz et al. [60]	1	12	30	10	n.a.	n.a.	n.a.	48%	Marked improvement of vocalization. No effect of DBS on hypokinesia and rigidity. Facilitated activities of daily living.
Spielberger et al. [61]	1	48	30	9	75%	5%	70%	−4%	Worsening of chorea with 40 Hz DBS, best results with 130 Hz DBS. Progression of bradykinesia compatible with natural course.
Huys et al. [62]	1	12	40	3				16%	Improved cognition 6 months after surgery followed by a decline at 12 months (but improved results compared to baseline assessment)
Velez-Lago et al. [63]	1	60	60	2	56%	n.a.	−40%	−98%	Chorea (69%), dystonia (40%), and overall motor score (37%) improved up to 24 months after surgery. Stable cognition.
Cislaghi et al. [64]	1	48	31	16	67%	n.a.	n.a.	n.a.	Significant improvement in chorea in juvenile HD. Impairment of bradykinesia. No effect on cognitive function.
Gruber et al. [65]	1	48	41	9	60%	42%	50%	19%	GPI DBS-induced bradykinesia alleviated with STN DBS. Cognitive decline compatible with the natural course of HD.
Loutfi et al. [66]	1	12	59	12	27%	n.a.	−40%	12%	Stable cognition, modest improvement of verbal fluency, marked improvement of behavioral assessment.

Improvement is indicated as percentage of baseline scores (negative values indicate impairment). FUP = Follow-up period. DisDur = disease duration. Table adapted from [1].

Table 2. Case series and trials (n = number of patients) of pallidal DBS in HD.

Study	n	FUP (Months)	Age (Years)	DisDur (Years)	Chorea	Bradykinesia	Dystonia	Total Motor	Comments
Kang et al. [67]	2	24	57	10	63%	−11%	n.a.	22%	Best results on chorea with either 40 Hz (patient 1) or 130 Hz (patient 2) DBS. Cognitive decline compatible with natural disease progression
		24	50	5	59%	0%	0 to 6	4%	
Velez-Lago et al. [63]	2	12	27	7	74%	n.a.	n.a.	43%	Despite good effect on chorea, there was no improvement for a patient with predominant dystonia. Worsening of bradykinesia and rigidity
		9	19	6	n.a.	n.a.	20%	−24%	
Gonzales et al. [54]	7	36	78	5	65%	n.a.	n.a.	−10%	Bradykinesia worsened over time. Additionally, DBS-dependent effects could be observed. Reduction of pulse width reduced bradykinesia. Non-significant worsening of dystonia over time. Despite progressive decline of cognition, cognitive levels were not significantly worse compared to baseline
		36	39	8	69%			14%	
		36	74	4	20%			−11%	
		36	54	8	79%			−30%	
		36	37	3	67%			33%	
		12	30	3	70%			40%	
		12	36	3	80%			−64%	
Wojtecki et al. [53]	6	6	52	3	66%	5%	56%	42%	First randomized, double-blind study up to date. First study comparing GPE and GPI DBS. Patients 4 and 5 suffered from juvenile variant of HD and therefore exclusively presented with hypokinetic-rigid symptoms and dystonia. DBS of GPE and GPI did not lead to significantly different results. Heterogeneous results concerning functional outcome.
		6	71	21	63%	−9%	85%	27%	
		6	38	10	46%	−22%	55%	11%	
		6	25	11	n. a.	−19%	−44%	−3%	
		6	23	8	n. a.	−10%	−37%	−9%	
		6	29	4	66%	17%	0%	28%	
Zittel et al. [68]	3	36	54	5	50%	−36%	100%	11%	Heterogeneous results concerning DBS effects on bradykinesia and dystonia. Mini-mental status examination stable over time, while more complex tests revealed diverging results
		12	35	4	58%	11%	−250%	25%	
		12	45	7	40%	39%	−100%	20%	
Delorme et al. [51]	3	30	56	10	15%	−100%	0 to 1	−18%	Greater effect size (with mean improvement of 55% of chorea and 32% for the total score), if not compared to baseline but DBS off assessment at follow-up. DBS via ventral electrode contacts was more effective than DBS via dorsal contacts
		24	24	3	67%	0 to 4	0 to 6	20%	
		12	50	10	29%	−33%	−140%	−2%	

Improvement is indicated as percentage of baseline scores (negative values indicate impairment). If a percentage could not be calculated, since the initial value was 0, raw data are provided. FUP = Follow-up period. DisDur = disease duration. Table adapted from [1].

In one patient with four implanted electrodes in the bilateral GPi and STN, solely STN DBS failed to reduce the chorea symptoms [65]. On the other hand, STN DBS could play a major role for hypokinesia, as GPi DBS side effects of increased hypokinetic symptoms could be reduced with additional STN DBS in one HD patient [65]. DBS of the GPi seems to cause these hypokinetic side effects such as gait disturbances [69–71] and of more pronounced bradykinesia [54,55,64,67]. As a meta-analysis from available bradykinesia-scores in 17 from 36 HD patients, the impairment by GP-DBS is minor (around 3%).

Thus, the few findings in HD patients with DBS on hyperkinetic symptoms of dystonia and hypokinetic symptoms of bradykinesia do not admit an unambiguous recommendation for the stimulation of the pallidum. Beneficial therapeutic effects of well-established pallidal DBS on primary dystonia cannot be transferred to the impact on dystonic symptoms in HD. The few existing studies suggest pallidal DBS to be beneficial [72] or ineffective [54] or negatively impacting [63] on the dystonic symptoms. These heterogeneous findings are also supported in our prospective trial [53] and the above mentioned meta-analysis. Due to the small amount of case reports here, individual pathophysiology could contribute to those contradicting, inconsistent findings of pallidal DBS on dystonic symptoms of HD. Furthermore, depending on the stimulated area of the pallidum, opposite motor effects are known [21].

In terms of unwanted effects, a lower frequency stimulation of 40 Hz could be superior to a higher frequency stimulation of 130 Hz, as choreatic symptoms ameliorated in the same amount under both stimulation frequencies, but hypokinetic symptoms only became less pronounced under the 40 Hz stimulation in three case reports [52,55,58]. Nevertheless, those preliminary results of only three patients have to be interpreted with caution as the overall findings on the optimal stimulation frequency for minimal side effects are inconsistent: High frequency stimulation of more than 100 Hz does not always lead to a worsening of induced hypokinesia [57,60] and DBS of approximately 40 Hz does not always result in a reduction of those hypokinetic symptoms [67,68]. Along with the optimal stimulation area, the precise, most beneficial stimulation frequency is of particular interest for the clinical treatment. According to the few, preliminary existing findings, chorea tends to be suppressed more with higher frequency stimulation compared to lower frequency stimulation. High frequencies of 130 Hz are mostly applied in treatment studies of HD chorea symptoms and, according to some findings, the benefits even increase when using 180 Hz frequencies [57,67,72].

4.2. Clinical Implications of DBS on Non-Motor-Functions

Prior to the HD diagnosis based on motoric symptoms, cognitive abilities can decline. Simultaneously, striking physiological changes such as cerebral atrophy become evident [73]. Various cognitive domains such as processing speed, working memory and attention can be affected and the cognitive impairment is progressive in the course of the HD [74]. Deficits in error feedback control mechanisms are regarded as a key problem for cognitive but also motor malfunctions. The improvement of the early cognitive deficits by DBS would contribute to therapeutic treatment, but also to an understanding of physiological dysfunctional mechanisms, as cognitive conspicuities precede motor symptoms [75,76]. In early HD stages, the striatal neurons projecting to the GPe predominantly degenerate, thus positing a major role of the GPe for the cognitive deficits in HD. As such, Ayalon et al. lesioned different parts of the indirect pathway in rats and their results suggest the GPe in primates as a valuable stimulation area to treat cognitive in addition to motor symptoms [77]. Another study sheds light on the cognitive ability of response inhibition in the first transgenic HD rat model. The primate GPe equivalent in rats was stimulated and effectively improved the deficits in the response inhibition [78]. Findings in humans by our own group might point in the same direction, as pallidal DBS in HD patients with preponderant choreatic symptoms over six months was followed by a stable level in cognitive abilities instead of a progressive decline in cognition. Results were slightly, but not significantly better in the GPe-DBS group than in the GPi-DBS group in terms of cognitive effects. This could suggest that pallidal DBS in HD slows down

progressive cognitive decline and keeps cognitive abilities on a stable level to some extent [53]. In a recent DBS imaging study, stimulation of the GPe was highlighted with respect to cognitive networks. Nevertheless, this study lacks cognitive tests in order to validate the imaging data [79]. In another experimental study, GPe-DBS had beneficial effects on cognitive control and, here, behavioral as well as electrophysiological data were collected for identification of cognitive effects. Two patients performed an error monitoring task ON and OFF GPe-stimulation: A flanker paradigm was applied to investigate adaptive behavior in response to committed errors. Error-related-behavioral adaptation was compared via the error-related-negativity (ERN) and the post error slowing in the DBS and control group. In addition to this, general response monitoring was measured via the correct-related negativity (CRN/Nc) amplitude for both groups. The findings suggest that GP-DBS positively impacts both aspects, the adaptive behavior as a response to error processing and also the general response monitoring. Smaller ERN, less pronounced post-error-slowing and less pronounced Nc could be observed in manifest HD patients OFF DBS, but their behavioral and electrophysiological measures aligned with the healthy control group when GPe DBS was applied [80]. These are promising findings, which highlight the GPe as a valuable DBS target and suggest cognitive benefits. However, it has to be noted that up to date no placebo-controlled prospective clinical data on GPe-DBS is available. On the other hand, DBS stimulation of the GPi led to far more inconsistent effects, up to now. The effects of GPi-DBS on patients cognition range from a progressive decline similar to non-stimulated HD patients [58,61,67] to stable cognitive functions for at least 4 years [59] and even to alleviation in distinct cognitive abilities [62,68]. Various causes have been discussed for the numerous observed effects of GPi-DBS. According to animal-based findings and studies with humans, it is suggested that GPi-DBS treatment benefits on cognition could derive from electric fields in the GPi, which extend to the GPe. Evidence on other non-motor functions and quality-of life (QoL) is sparse up to date. Existing data from the prospective protocol might suggest some improvement of sub-scales of QoL and depression [70].

5. Safety of DBS in HD

In our executed pilot study, the implantation of the DBS electrodes into the GP proved to be a safe procedure and lacked procedure-related side effects. However, these preliminary data have to be treated with caution as they included only six HD patients [53]. Nevertheless, this pilot study is the only one available up to date with a prospective design, which corresponds to the CONSORT criteria with adverse events (AE) entirely reported by using an independent data and safety monitoring board (DSMB). Besides the side effects described in Sections 4.1 and 4.2, here we focus on the formal safety report of the prospective trial. One might anticipate that DBS causes three main types of adverse device effects (ADE): (1) transient due to electrical stimulation; (2) transient due to technical problems/complication/infections and, finally, (3) transient or permanent due to implantation complications. Concerning all types of AE including ADE, the data from our pilot trial showed the following: AEs that where actually reported within 6 months: eight adverse events were recorded. All AE resolved without sequelae. AEs unrelated to stimulation but possibly due to hospitalization: thrombophlebitis, MRSA nose infection, superficial nose abrasion. AEs related to treatment—thus ADE—were: possibly related to stimulation (Type 1 ADE, exclusively reported with GPi- but not GPe- stimulation): bradykinesia, hyperthermia, gait impairment, increased chorea and possibly related to stimulation system: deactivation of impulse generator (Type 2 ADE). In addition, two serious adverse events (SAE) were reported: gait impairment and hyperkinesia after reprogramming (SAE criterion: leading to hospital admission and requiring reprogramming) and postoperative malignant hyperthermia possibly related to stimulation (SAE criterion: life-threatening and leading to prolonged hospital stay). Both SAE were judged as SADE (Serious Adverse Device Effects) with Type 1. No procedure-related complication or bleeding occurred (Type 3 ADE). In the prospective trial, no side effects on cognition and mood were present.

6. Outlook

Preliminary findings in HD patients reveal overall positive effects of pallidal stimulation on chorea. Beside the motor effect on chorea by GPi-stimulation, the presumably better effect-side-effect ratio and the promising findings of GPe-DBS for cognition ought to be further validated. The GPi/GPe border zone might be a suitable target for DBS. One evident difficulty is the progressive atrophy of the GP which might prevent the precise identification of distinct pallidal parts. On the other hand, the atrophic altered GP might lead to the unintended impairment of areas in the surroundings of the target site and thereby provoke unwanted side effects as a consequence of DBS surgery. To overcome these aspects, technical advanced stimulation programming can be used. To identify an optimal treatment of motor symptoms, a systematic investigation of the stimulation frequency is needed, as chorea and bradykinesia treatments were shown to have different, opposing optimal stimulation frequencies. Another further step ought to systemically study the DBS pulse width. As a standard, 60–450 μs were implemented in most cases and, up to now, not much attention has been paid to variations of the pulse width [59,60]. However, an optimal pulse width could warrant larger therapeutic windows and might avoid side effects, as revealed by studies of STN DBS in parkinsonism, in which 30 μs was beneficial [81,82]. Furthermore, the newest DBS devices allow new possibilities concerning pulse width, current steering and directional stimulation [83,84]. The most beneficial treatment approach of direct DBS in HD might be attained by identifying the optimal parameters corresponding to the predominating symptoms in each individual. Optimal stimulation programs could also be achieved by algorithms and models taking into account the volume of tissue active (VTA) and tailored parameters automatically based on anticipated side effects (see Figure 3).

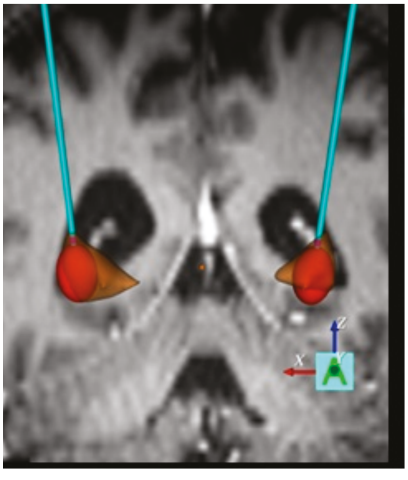

Figure 3. Stimulated target. Example visualization on 3D coronary MRI-view of individual electrodes and volume of tissue activated (VTA, in red) in relation to the pallidum (in brown). Image source: authors' own contribution.

Moreover, sensing neurostimulators will be valuable devices in therapeutic treatment and research. However, contrary to other movement disorders [85], as stated in Section 3, LFP recording data as a possible biomarker in HD is sparse up to date.

In order to create a higher level of evidence for DBS in HD, the next major step is a prospective, randomized, double blind, parallel group, sham-controlled, multi-center (MC) superiority trial which is currently recruiting in Europe (ClinicalTrials.gov: NCT02535884). Based on the evidence outlined in this review article, the ongoing MC-randomized controlled trial is focusing on the efficacy of GP-DBS

on chorea as a primary endpoint while considering several motor functions such as dystonia and bradykinesia, cognition, mood and quality of life as secondary endpoints. Patients with predominant chorea despite best medical treatment (UHDRS chorea sub score $\geq$ 10) with only minor cognitive and psychiatric disturbances are selected. Postural instability is considered as exclusion criteria for DBS. In terms of risk management, based on the preliminary data, the HD cohort does not seem to be at special risk due to DBS when all inclusion/exclusion criteria of patients are carefully addressed. This assumption is based on the data with three Type 1 and one Type 2 ADE and no Type 3 ADE in the pilot data [70]. For the most serious Type 3 complications, we propose the following risk stratification: Risk of brain bleeding is stratified with grade of brain atrophy:

(1) No significant atrophy;
(2) Mild cortical atrophy as common in neurodegenerative disorders;
(3) Severe cortical atrophy and additional atrophy periventricular and of the target basal ganglia structures.

Grade 1 atrophy is not expected in neurodegenerative diseases such as Parkinson's and Huntington's disease. Grade 2 is common in these diseases and results in a risk of bleeding of (5%–7%) during implantation [86]. As Grade 3 atrophy makes a surgical approach more difficult due to the atrophy of the target area, it is assumed that these patients have higher operative risks. However, no systematic data on these patients is available. Grade 3 atrophy is more common in HD patients at moderate stages than in PD patients. Thus, these patients are excluded in order to keep the implantation risk at the level of PD of 5%–7%. Thus, due to the mentioned risk assessment and calculation, it is assumed that the implantation risk in HD patients with brain atrophy Grade 2 is at the level of already approved and CE marked indication of DBS.

7. Conclusions

There is preliminary evidence for the usefulness of pallidal DBS for chorea suppression in HD from a number of cases, case series and smaller trials (with fewer than 10 patients per trial) and from one prospective randomized, double-blinded trial lacking a placebo control group. DBS procedure was demonstrated to be a safe treatment option in the above mentioned trial. Cognitive functions might benefit from stimulation of the external part of the pallidum. Up to date, DBS effects on chorea and other motor symptoms such as dystonia and on QoL are examined in a larger and placebo (OFF-stimulation) controlled trial.

Acknowledgments: No funding sources for this review.

Author Contributions: L.W., C.J.H., S.J.G., S.O. wrote the paper, S.E., A.S., J.V. reviewed the draft of the manuscript.

Conflicts of Interest: Related to Huntington's Disease and/or deep brain stimulation: L.W. received consultant honoraria and travel grants from Medtronic, St. Jude Medical, Inomed and Desitin. S.J.G. received coverage of travel expenses and honoraria from Medtronic and Boston Scientific. C.J.H., S.E. and S.O. declare no conflicts of interest. A.S. and J.V. received consultant honoraria and travel grants from Medtronic. The authors have no other relevant affiliations or financial involvement with any organization or entity with a financial interest in or financial conflict with the subject matter or materials discussed in the manuscript apart from those disclosed. No writing assistance was utilized in the production of this manuscript. Trial NCT02535884 is supported by Medtronic. Medtronic had no role in the design of the review, in the collection, analyses, or interpretation of data, in the writing of the manuscript, or in the decision to publish the results. Medtronic provided Figure 1 for this manuscript on request of the authors.

References

1. Hartmann, C.J.; Groiss, S.J.; Vesper, J.; Schnitzler, A.; Wojtecki, L. Brain stimulation in Huntington's disease. *Neurodegener. Dis. Manag.* **2016**, *6*, 223–236. [CrossRef] [PubMed]
2. Walker, F.O. Huntington's disease. *Semin. Neurol.* **2007**, *27*, 143–150. [CrossRef] [PubMed]

3. Mitchell, I.J.; Cooper, A.J.; Griffiths, M.R. The selective vulnerability of striatopallidal neurons. *Prog. Neurobiol.* **1999**, *59*, 691–719. [CrossRef]
4. Albin, R.L.; Reiner, A.; Anderson, K.D.; Penney, J.B.; Young, A.B. Striatal and nigral neuron subpopulations in rigid huntington's disease: Implications for the functional anatomy of chorea and rigidity-akinesia. *Ann. Neurol.* **1990**, *27*, 357–365. [CrossRef] [PubMed]
5. Wichmann, T.; DeLong, M.R. Functional and pathophysiological models of the basal ganglia. *Curr. Opin. Neurobiol.* **1996**, *6*, 751–758. [CrossRef]
6. Louis, E.D.; Anderson, K.E.; Moskowitz, C.; Thorne, D.Z.; Marder, K. Dystonia-predominant adult-onset huntington disease: Association between motor phenotype and age of onset in adults. *Arch. Neurol.* **2000**, *57*, 1326–1330. [CrossRef] [PubMed]
7. Thompson, P.D.; Berardelli, A.; Rothwell, J.C.; Day, B.L.; Dick, J.P.; Benecke, R.; Marsden, C.D. The coexistence of bradykinesia and chorea in huntington's disease and its implications for theories of basal ganglia control of movement. *Brain J. Neurol.* **1988**, *111*, 223–244. [CrossRef]
8. Spiegel, E.A.; Wycis, H.T.; Marks, M.; Lee, A.J. Stereotaxic apparatus for operations on the human brain. *Science* **1947**, *106*, 349–350. [CrossRef] [PubMed]
9. Gildenberg, P.L. History repeats itself. *Stereotact. Funct. Neurosurg.* **2003**, *80*, 61–75. [CrossRef] [PubMed]
10. Benabid, A.L.; Pollak, P.; Louveau, A.; Henry, S.; de Rougemont, J. Combined (thalamotomy and stimulation) stereotactic surgery of the VIM thalamic nucleus for bilateral parkinson disease. *Appl. Neurophysiol.* **1987**, *50*, 344–346. [CrossRef] [PubMed]
11. Delgado, J.M.; Hamlin, H.; Chapman, W.P. Technique of intracranial electrode implacement for recording and stimulation and its possible therapeutic value in psychotic patients. *Confin. Neurol.* **1952**, *12*, 315–319. [CrossRef] [PubMed]
12. Delgado, J.M.; Mark, V.; Sweet, W.; Ervin, F.; Weiss, G.; Bach, Y.R.G.; Hagiwara, R. Intracerebral radio stimulation and recording in completely free patients. *J. Nerv. Ment. Dis.* **1968**, *147*, 329–340. [CrossRef] [PubMed]
13. Sem-Jacobsen, C.W. Depth-electrographic observations in psychotic patients: A system related to emotion and behavior. *Acta Psychiatr. Scand.* **1959**, *34*, 412–416. [CrossRef]
14. Alberts, W.W.; Wright, E.W., Jr.; Levin, G.; Feinstein, B.; Mueller, M. Threshold stimulation of the lateral thalamus and globus pallidus in the waking human. *Electroencephalogr. Clin. Neurophysiol.* **1961**, *13*, 68–74. [CrossRef]
15. Sem-Jacobsen, C.W. Depth-electrographic observations related to Parkinson's disease. Recording and electrical stimulation in the area around the third ventricle. *J. Neurosurg.* **1966**, *24*, S388–S402.
16. Mundinger, F. New stereotactic treatment of spasmodic torticollis with a brain stimulation system (author's transl.). *Med. Klin.* **1977**, *72*, 1982–1986.
17. Miocinovic, S.; Somayajula, S.; Chitnis, S.; Vitek, J.L. History, applications, and mechanisms of deep brain stimulation. *JAMA Neurol.* **2013**, *70*, 163–171. [CrossRef] [PubMed]
18. Herrington, T.M.; Cheng, J.J.; Eskandar, E.N. Mechanisms of deep brain stimulation. *J. Neurophysiol.* **2016**, *115*, 19–38. [CrossRef] [PubMed]
19. Benabid, A.L.; Pollak, P.; Gervason, C.; Hoffmann, D.; Gao, D.M.; Hommel, M.; Perret, J.E.; de Rougemont, J. Long-term suppression of tremor by chronic stimulation of the ventral intermediate thalamic nucleus. *Lancet* **1991**, *337*, 403–406. [CrossRef]
20. Grill, W.M.; Snyder, A.N.; Miocinovic, S. Deep brain stimulation creates an informational lesion of the stimulated nucleus. *Neuroreport* **2004**, *15*, 1137–1140. [CrossRef] [PubMed]
21. Krack, P.; Pollak, P.; Limousin, P.; Hoffmann, D.; Benazzouz, A.; Le Bas, J.F.; Koudsie, A.; Benabid, A.L. Opposite motor effects of pallidal stimulation in Parkinson's disease. *Ann. Neurol.* **1998**, *43*, 180–192. [CrossRef] [PubMed]
22. Kumar, R.; Lang, A.E.; Rodriguez-Oroz, M.C.; Lozano, A.M.; Limousin, P.; Pollak, P.; Benabid, A.L.; Guridi, J.; Ramos, E.; van der Linden, C.; et al. Deep brain stimulation of the globus pallidus pars interna in advanced Parkinson's disease. *Neurology* **2000**, *55*, S34–S39. [PubMed]
23. Volkmann, J.; Mueller, J.; Deuschl, G.; Kuhn, A.A.; Krauss, J.K.; Poewe, W.; Timmermann, L.; Falk, D.; Kupsch, A.; Kivi, A.; et al. Pallidal neurostimulation in patients with medication-refractory cervical dystonia: A randomised, sham-controlled trial. *Lancet Neurol.* **2014**, *13*, 875–884. [CrossRef]

24. Vidailhet, M.; Jutras, M.F.; Grabli, D.; Roze, E. Deep brain stimulation for dystonia. *J. Neurol. Neurosurg. Psychiatry* **2013**, *84*, 1029–1042. [CrossRef] [PubMed]
25. Damier, P.; Thobois, S.; Witjas, T.; Cuny, E.; Derost, P.; Raoul, S.; Mertens, P.; Peragut, J.C.; Lemaire, J.J.; Burbaud, P.; et al. Bilateral deep brain stimulation of the globus pallidus to treat tardive dyskinesia. *Arch. Gen. Psychiatry* **2007**, *64*, 170–176. [CrossRef] [PubMed]
26. Trottenberg, T.; Paul, G.; Meissner, W.; Maier-Hauff, K.; Taschner, C.; Kupsch, A. Pallidal and thalamic neurostimulation in severe tardive dystonia. *J. Neurol. Neurosurg. Psychiatry* **2001**, *70*, 557–559. [CrossRef] [PubMed]
27. Timmermann, L.; Pauls, K.A.; Wieland, K.; Jech, R.; Kurlemann, G.; Sharma, N.; Gill, S.S.; Haenggeli, C.A.; Hayflick, S.J.; Hogarth, P.; et al. Dystonia in neurodegeneration with brain iron accumulation: Outcome of bilateral pallidal stimulation. *Brain* **2010**, *133*, 701–712. [CrossRef] [PubMed]
28. Miquel, M.; Spampinato, U.; Latxague, C.; Aviles-Olmos, I.; Bader, B.; Bertram, K.; Bhatia, K.; Burbaud, P.; Burghaus, L.; Cho, J.W.; et al. Short and long term outcome of bilateral pallidal stimulation in chorea-acanthocytosis. *PLoS ONE* **2013**, *8*, e79241. [CrossRef] [PubMed]
29. Guehl, D.; Cuny, E.; Tison, F.; Benazzouz, A.; Bardinet, E.; Sibon, Y.; Ghorayeb, I.; Yelnick, J.; Rougier, A.; Bioulac, B.; et al. Deep brain pallidal stimulation for movement disorders in neuroacanthocytosis. *Neurology* **2007**, *68*, 160–161. [CrossRef] [PubMed]
30. Krauss, J.K.; Loher, T.J.; Weigel, R.; Capelle, H.H.; Weber, S.; Burgunder, J.M. Chronic stimulation of the globus pallidus internus for treatment of non-dYT1 generalized dystonia and choreoathetosis: 2-year follow up. *J. Neurosurg.* **2003**, *98*, 785–792. [CrossRef] [PubMed]
31. Gill, S.; Curran, A.; Tripp, J.; Melarickas, L.; Hurran, C.; Stanley, O. Hyperkinetic movement disorder in an 11-year-old child treated with bilateral pallidal stimulators. *Dev. Med. Child Neurol.* **2001**, *43*, 350–353. [CrossRef] [PubMed]
32. Vidailhet, M.; Yelnik, J.; Lagrange, C.; Fraix, V.; Grabli, D.; Thobois, S.; Burbaud, P.; Welter, M.L.; Xie-Brustolin, J.; Braga, M.C.; et al. Bilateral pallidal deep brain stimulation for the treatment of patients with dystonia-choreoathetosis cerebral palsy: A prospective pilot study. *Lancet Neurol.* **2009**, *8*, 709–717. [CrossRef]
33. Spiegel, E.A.; Wycis, H.T. Thalamotomy and pallidotomy for treatment of choreic movements. *Acta Neurochir.* **1952**, *2*, 417–422. [CrossRef] [PubMed]
34. Cubo, E.; Shannon, K.M.; Penn, R.D.; Kroin, J.S. Internal globus pallidotomy in dystonia secondary to Huntington's disease. *Mov. Disord.* **2000**, *15*, 1248–1251. [CrossRef]
35. Tobin, A.J.; Signer, E.R. Huntington's disease: The challenge for cell biologists. *Trends Cell Biol.* **2000**, *10*, 531–536. [CrossRef]
36. Alexander, G.E.; DeLong, M.R.; Strick, P.L. Parallel organization of functionally segregated circuits linking basal ganglia and cortex. *Annu. Rev. Neurosci.* **1986**, *9*, 357–381. [CrossRef] [PubMed]
37. Alexander, G.E.; Crutcher, M.D.; DeLong, M.R. Basal ganglia-thalamocortical circuits: Parallel substrates for motor, oculomotor, "prefrontal" and "limbic" functions. *Prog. Brain Res.* **1990**, *85*, 119–146. [PubMed]
38. Smith, Y.; Bevan, M.D.; Shink, E.; Bolam, J.P. Microcircuitry of the direct and indirect pathways of the basal ganglia. *Neuroscience* **1998**, *86*, 353–387. [PubMed]
39. Reiner, A.; Albin, R.L.; Anderson, K.D.; D'Amato, C.J.; Penney, J.B.; Young, A.B. Differential loss of striatal projection neurons in huntington disease. *Proc. Natl. Acad. Sci. USA* **1988**, *85*, 5733–5737. [CrossRef] [PubMed]
40. Albin, R.L.; Reiner, A.; Anderson, K.D.; Dure, L.S.; Handelin, B.; Balfour, R.; Whetsell, W.O., Jr.; Penney, J.B.; Young, A.B. Preferential loss of striato-external pallidal projection neurons in presymptomatic huntington's disease. *Ann. Neurol.* **1992**, *31*, 425–430. [CrossRef] [PubMed]
41. Albin, R.L.; Young, A.B.; Penney, J.B. The functional anatomy of basal ganglia disorders. *Trends Neurosci.* **1989**, *12*, 366–375. [CrossRef]
42. Penney, J.B., Jr.; Young, A.B. Striatal inhomogeneities and basal ganglia function. *Mov. Disord.* **1986**, *1*, 3–15. [CrossRef] [PubMed]
43. Georgiou, N.; Bradshaw, J.L.; Phillips, J.G.; Bradshaw, J.A.; Chiu, E. The Simon effect and attention deficits in Gilles de la Tourette's syndrome and Huntington's disease. *Brain J. Neurol.* **1995**, *118*, 1305–1318. [CrossRef]
44. Litvan, I.; Paulsen, J.S.; Mega, M.S.; Cummings, J.L. Neuropsychiatric assessment of patients with hyperkinetic and hypokinetic movement disorders. *Arch. Neurol.* **1998**, *55*, 1313–1319. [CrossRef] [PubMed]

45. Raymond, L.A.; Andre, V.M.; Cepeda, C.; Gladding, C.M.; Milnerwood, A.J.; Levine, M.S. Pathophysiology of Huntington's disease: Time-dependent alterations in synaptic and receptor function. *Neuroscience* **2011**, *198*, 252–273. [CrossRef] [PubMed]
46. Joel, D. Open interconnected model of basal ganglia-thalamocortical circuitry and its relevance to the clinical syndrome of Huntington's disease. *Mov. Disord.* **2001**, *16*, 407–423. [CrossRef] [PubMed]
47. Gross, R.E.; Krack, P.; Rodriguez-Oroz, M.C.; Rezai, A.R.; Benabid, A.L. Electrophysiological mapping for the implantation of deep brain stimulators for Parkinson's disease and tremor. *Mov. Disord.* **2006**, *21*, S259–S283. [CrossRef] [PubMed]
48. Starr, P.A.; Rau, G.M.; Davis, V.; Marks, W.J., Jr.; Ostrem, J.L.; Simmons, D.; Lindsey, N.; Turner, R.S. Spontaneous pallidal neuronal activity in human dystonia: Comparison with Parkinson's disease and normal macaque. *J. Neurophysiol.* **2005**, *93*, 3165–3176. [CrossRef] [PubMed]
49. Tang, J.K.; Moro, E.; Lozano, A.M.; Lang, A.E.; Hutchison, W.D.; Mahant, N.; Dostrovsky, J.O. Firing rates of pallidal neurons are similar in Huntington's and Parkinson's disease patients. *Exp. Brain Res.* **2005**, *166*, 230–236. [CrossRef] [PubMed]
50. Starr, P.A.; Kang, G.A.; Heath, S.; Shimamoto, S.; Turner, R.S. Pallidal neuronal discharge in Huntington's disease: Support for selective loss of striatal cells originating the indirect pathway. *Exp. Neurol.* **2008**, *211*, 227–233. [CrossRef] [PubMed]
51. Delorme, C.; Rogers, A.; Lau, B.; Francisque, H.; Welter, M.L.; Fernandez Vidal, S.; Yelnik, J.; Durr, A.; Grabli, D.; Karachi, C. Deep brain stimulation of the internal pallidum in Huntington's disease patients: Clinical outcome and neuronal firing patterns. *J. Neurol.* **2016**, *263*, 290–298. [CrossRef] [PubMed]
52. Groiss, S.J.; Elben, S.; Reck, C.; Voges, J.; Wojtecki, L.; Schnitzler, A. Local field potential oscillations of the globus pallidus in Huntington's disease. *Mov. Disord.* **2011**, *26*, 2577–2578. [CrossRef] [PubMed]
53. Wojtecki, L.; Groiss, S.J.; Ferrea, S.; Elben, S.; Hartmann, C.J.; Dunnett, S.B.; Rosser, A.; Saft, C.; Sudmeyer, M.; Ohmann, C.; et al. A prospective pilot trial for pallidal deep brain stimulation in Huntington's disease. *Front. Neurol.* **2015**, *6*, 177. [CrossRef] [PubMed]
54. Gonzalez, V.; Cif, L.; Biolsi, B.; Garcia-Ptacek, S.; Seychelles, A.; Sanrey, E.; Descours, I.; Coubes, C.; de Moura, A.M.; Corlobe, A.; et al. Deep brain stimulation for Huntington's disease: Long-term results of a prospective open-label study. *J. Neurosurg.* **2014**, *121*, 114–122. [CrossRef] [PubMed]
55. Moro, E.; Lang, A.E.; Strafella, A.P.; Poon, Y.Y.; Arango, P.M.; Dagher, A.; Hutchison, W.D.; Lozano, A.M. Bilateral globus pallidus stimulation for Huntington's disease. *Ann. Neurol.* **2004**, *56*, 290–294. [CrossRef] [PubMed]
56. Fawcett, A.P.; Moro, E.; Lang, A.E.; Lozano, A.M.; Hutchison, W.D. Pallidal deep brain stimulation influences both reflexive and voluntary saccades in Huntington's disease. *Mov. Disord.* **2005**, *20*, 371–377. [CrossRef] [PubMed]
57. Hebb, M.O.; Garcia, R.; Gaudet, P.; Mendez, I.M. Bilateral stimulation of the globus pallidus internus to treat choreathetosis in Huntington's disease: Technical case report. *Neurosurgery* **2006**, *58*, E383. [CrossRef] [PubMed]
58. Fasano, A.; Mazzone, P.; Piano, C.; Quaranta, D.; Soleti, F.; Bentivoglio, A.R. GPi-DBS in Huntington's disease: Results on motor function and cognition in a 72-year-old case. *Mov. Disord.* **2008**, *23*, 1289–1292. [CrossRef] [PubMed]
59. Biolsi, B.; Cif, L.; Fertit, H.E.; Robles, S.G.; Coubes, P. Long-term follow-up of Huntington disease treated by bilateral deep brain stimulation of the internal globus pallidus. *J. Neurosurg.* **2008**, *109*, 130–132. [CrossRef] [PubMed]
60. Garcia-Ruiz, P.J.; Ayerbe, J.; del Val, J.; Herranz, A. Deep brain stimulation in disabling involuntary vocalization associated with Huntington's disease. *Parkinsonism Relat. Disord.* **2012**, *18*, 803–804. [CrossRef] [PubMed]
61. Spielberger, S.; Hotter, A.; Wolf, E.; Eisner, W.; Muller, J.; Poewe, W.; Seppi, K. Deep brain stimulation in Huntington's disease: A 4-year follow-up case report. *Mov. Disord.* **2012**, *27*, 806–807. [CrossRef] [PubMed]
62. Huys, D.; Bartsch, C.; Poppe, P.; Lenartz, D.; Huff, W.; Prutting, J.; Timmermann, L.; Klosterkotter, J.; Maarouf, M.; Rommel, T.; et al. Management and outcome of pallidal deep brain stimulation in severe Huntington's disease. *Fortschr. Neurol. Psychiatr.* **2013**, *81*, 202–205. [CrossRef] [PubMed]

63. Velez-Lago, F.M.; Thompson, A.; Oyama, G.; Hardwick, A.; Sporrer, J.M.; Zeilman, P.; Foote, K.D.; Bowers, D.; Ward, H.E.; Sanchez-Ramos, J.; et al. Differential and better response to deep brain stimulation of chorea compared to dystonia in Huntington's disease. *Stereotact. Funct. Neurosurg.* **2013**, *91*, 129–133. [CrossRef] [PubMed]
64. Cislaghi, G.; Capiluppi, E.; Saleh, C.; Romano, L.; Servello, D.; Mariani, C.; Porto, M. Bilateral globus pallidus stimulation in westphal variant of Huntington disease. *Neuromodul. J. Int. Neuromodul. Soc.* **2014**, *17*, 502–505. [CrossRef] [PubMed]
65. Gruber, D.; Kuhn, A.A.; Schoenecker, T.; Kopp, U.A.; Kivi, A.; Huebl, J.; Lobsien, E.; Mueller, B.; Schneider, G.H.; Kupsch, A. Quadruple deep brain stimulation in Huntington's disease, targeting pallidum and subthalamic nucleus: Case report and review of the literature. *J. Neural* **2014**, *121*, 1303–1312. [CrossRef] [PubMed]
66. Loutfi, G.; Linder, J.; Hariz, G.-M.; Hariz, M.; Blomstedt, P. Pallidal deep brain stimulation in the treatment of Huntington's chorea. *Brain Disord. Ther.* **2014**, *3*. [CrossRef]
67. Kang, G.A.; Heath, S.; Rothlind, J.; Starr, P.A. Long-term follow-up of pallidal deep brain stimulation in two cases of Huntington's disease. *J. Neurol. Neurosurg. Psychiatry* **2011**, *82*, 272–277. [CrossRef] [PubMed]
68. Zittel, S.; Moll, C.K.; Gulberti, A.; Tadic, V.; Rasche, D.; Baumer, T.; Fellbrich, A.; Bruggemann, N.; Engel, A.K.; Tronnier, V.; et al. Pallidal deep brain stimulation in Huntington's disease. *Parkinsonism Relat. Disord.* **2015**, *21*, 1105–1108. [CrossRef] [PubMed]
69. Amtage, F.; Feuerstein, T.J.; Meier, S.; Prokop, T.; Piroth, T.; Pinsker, M.O. Hypokinesia upon pallidal deep brain stimulation of dystonia: Support of a gabaergic mechanism. *Front. Neurol.* **2013**, *4*, 198. [CrossRef] [PubMed]
70. Berman, B.D.; Starr, P.A.; Marks, W.J., Jr.; Ostrem, J.L. Induction of bradykinesia with pallidal deep brain stimulation in patients with cranial-cervical dystonia. *Stereotact. Funct. Neurosurg.* **2009**, *87*, 37–44. [CrossRef] [PubMed]
71. Schrader, C.; Capelle, H.H.; Kinfe, T.M.; Blahak, C.; Bazner, H.; Lutjens, G.; Dressler, D.; Krauss, J.K. GPi-DBS may induce a hypokinetic gait disorder with freezing of gait in patients with dystonia. *Neurology* **2011**, *77*, 483–488. [CrossRef] [PubMed]
72. Lopez-Sendon Moreno, J.L.; Garcia-Caldentey, J.; Regidor, I.; del Alamo, M.; Garcia de Yebenes, J. A 5-year follow-up of deep brain stimulation in Huntington's disease. *Parkinsonism Relat. Disord.* **2014**, *20*, 260–261. [CrossRef] [PubMed]
73. Paulsen, J.S. Cognitive impairment in huntington disease: Diagnosis and treatment. *Curr. Neurol. Neurosci. Rep.* **2011**, *5*, 474–483. [CrossRef] [PubMed]
74. Beglinger, L.J.; O'Rourke, J.J.; Wang, C.; Langbehn, D.R.; Duff, K.; Paulsen, J.S. Earliest functional declines in Huntington disease. *Psychiatry Res.* **2010**, *178*, 414–418. [CrossRef] [PubMed]
75. Smith, M.A.; Brandt, J.; Shadmehr, R. Motor disorder in Huntington's disease begins as a dysfunction in error feedback control. *Nature* **2000**, *403*, 544–549. [CrossRef] [PubMed]
76. Beste, C.; Saft, C.; Andrich, J.; Gold, R.; Falkenstein, M. Error processing in Huntington's disease. *PLoS ONE* **2006**, *1*, e86. [CrossRef] [PubMed]
77. Ayalon, L.; Doron, R.; Weiner, I.; Joel, D. Amelioration of behavioral deficits in a rat model of Huntington's disease by an excitotoxic lesion to the globus pallidus. *Exp. Neurol.* **2004**, *186*, 46–58. [CrossRef]
78. Temel, Y.; Cao, C.; Vlamings, R.; Blokland, A.; Ozen, H.; Steinbusch, H.W.; Michelsen, K.A.; von Horsten, S.; Schmitz, C.; Visser-Vandewalle, V. Motor and cognitive improvement by deep brain stimulation in a transgenic rat model of Huntington's disease. *Neurosci. Lett.* **2006**, *406*, 138–141. [CrossRef] [PubMed]
79. Ligot, N.; Krystkowiak, P.; Simonin, C.; Goldman, S.; Peigneux, P.; Van Naemen, J.; Monclus, M.; Lacroix, S.F.; Devos, D.; Dujardin, K.; et al. External globus pallidus stimulation modulates brain connectivity in Huntington's disease. *J. Cereb. Blood Flow Metab.* **2011**, *31*, 41–46. [CrossRef] [PubMed]
80. Beste, C.; Muckschel, M.; Elben, S.; C, J.H.; McIntyre, C.C.; Saft, C.; Vesper, J.; Schnitzler, A.; Wojtecki, L. Behavioral and neurophysiological evidence for the enhancement of cognitive control under dorsal pallidal deep brain stimulation in Huntington's disease. *Brain Struct. Funct.* **2015**, *220*, 2441–2448. [CrossRef] [PubMed]
81. Reich, M.M.; Steigerwald, F.; Sawalhe, A.D.; Reese, R.; Gunalan, K.; Johannes, S.; Nickl, R.; Matthies, C.; McIntyre, C.C.; Volkmann, J. Short pulse width widens the therapeutic window of subthalamic neurostimulation. *Ann. Clin. Transl. Neurol.* **2015**, *2*, 427–432. [CrossRef] [PubMed]

82. Volkmann, J.; Stiegerwald, S.; Reich, M. Deep brain stimulation at short pulse width results in superior therapeutic windows for treatment of Parkinson's disease: A randomized, controlled, double-blind neurostimulation trial (CUSTOM-DBS). In Proceedings of the 18th International Congress of Parkinson's Disease and Movement Disorders, Stockholm, Sweden, 8–12 June 2014.
83. Contarino, M.F.; Bour, L.J.; Verhagen, R.; Lourens, M.A.; de Bie, R.M.; van den Munckhof, P.; Schuurman, P.R. Directional steering: A novel approach to deep brain stimulation. *Neurology* **2014**, *83*, 1163–1169. [CrossRef] [PubMed]
84. Pollo, C.; Kaelin-Lang, A.; Oertel, M.F.; Stieglitz, L.; Taub, E.; Fuhr, P.; Lozano, A.M.; Raabe, A.; Schupbach, M. Directional deep brain stimulation: An intraoperative double-blind pilot study. *Brain J. Neurol.* **2014**, *137*, 2015–2026. [CrossRef] [PubMed]
85. Quinn, E.J.; Blumenfeld, Z.; Velisar, A.; Koop, M.M.; Shreve, L.A.; Trager, M.H.; Hill, B.C.; Kilbane, C.; Henderson, J.M.; Bronte-Stewart, H. Beta oscillations in freely moving Parkinson's subjects are attenuated during deep brain stimulation. *Mov. Disord.* **2015**, *30*, 1750–1758. [CrossRef] [PubMed]
86. Fenoy, A.J.; Simpson, R.K., Jr. Risks of common complications in deep brain stimulation surgery: Management and avoidance. *J. Neurosurg.* **2014**, *120*, 132–139. [CrossRef] [PubMed]

Section 2:
DBS: Technical Considerations

brain sciences

MDPI

Article

Using "Functional" Target Coordinates of the Subthalamic Nucleus to Assess the Indirect and Direct Methods of the Preoperative Planning: Do the Anatomical and Functional Targets Coincide?

Ahmed Rabie [1,2], Leo Verhagen Metman [3] and Konstantin V. Slavin [1,*]

1 Department of Neurosurgery, University of Illinois at Chicago, Chicago, IL 60612, USA; dr_a_rabie@hotmail.com
2 Department of Neurosurgery, Alexandria University, Alexandria, Egypt
3 Department of Neurological Sciences, Rush University Medical Center, Chicago, IL 60612, USA; Leonard_A_Verhagen@rush.edu
* Correspondence: kslavin@uic.edu; Tel.: +1-312-996-4842; Fax: +1-312-996-9018

Academic Editors: Tipu Aziz and Alex Green
Received: 9 September 2016; Accepted: 12 December 2016; Published: 21 December 2016

Abstract: Objective: To answer the question of whether the anatomical center of the subthalamic nucleus (STN), as calculated indirectly from stereotactic atlases or by direct visualization on magnetic resonance imaging (MRI), corresponds to the best functional target. Since the neighboring red nucleus (RN) is well visualized on MRI, we studied the relationships of the final target to its different borders. Methods: We analyzed the data of 23 PD patients (46 targets) who underwent bilateral frame-based STN deep brain stimulation (DBS) procedure with microelectrode recording guidance. We calculated coordinates of the active contact on DBS electrode on postoperative MRI, which we referred to as the final "functional/optimal" target. The coordinates calculated by the atlas-based "indirect" and "direct" methods, as well as the coordinates of the different RN borders were compared to these final coordinates. Results: The mean ± SD of the final target coordinates was 11.7 ± 1.5 mm lateral (X), 2.4 ± 1.5 mm posterior (Y), and 6.1 ± 1.7 mm inferior to the mid-commissural point (Z). No significant differences were found between the "indirect" X, Z coordinates and those of the final targets. The "indirect" Y coordinate was significantly posterior to Y of the final target, with mean difference of 0.6 mm ($p = 0.014$). No significant differences were found between the "direct" X, Y, and Z coordinates and those of the final targets. Conclusions: The functional STN target is located in direct proximity to its anatomical center. During preoperative targeting, we recommend using the "direct" method, and taking into consideration the relationships of the final target to the mid-commissural point (MCP) and the different RN borders.

Keywords: subthalamic nucleus; deep brain stimulation; targeting; Parkinson's disease; planning

1. Introduction

Deep brain stimulation (DBS) is the gold standard surgical treatment of advanced Parkinson's disease (PD). The subthalamic nucleus (STN) has been used for the last two decades as the target of choice for this procedure [1].

The STN is a small gray matter structure located at the junction of the midbrain and diencephalon. It has anatomic relationships to the internal capsule and the Globus Pallidus Internus (GPi) anterolaterally, the Zona Incerta (ZI) and the thalamus superiorly, fibers of the third nerve anteromedially, the red nucleus (RN) posteromedially, and the cerebral peduncle and the Substantia

Nigra (SN) ventrally [2,3]. The target of DBS is the sensorimotor (dorsolateral) part of the STN [4,5]. This complex anatomy of the STN necessitates precise targeting during DBS surgeries.

There are two conventional methods for pre-operative localization of the STN [6]. The first is the indirect targeting; in which a brain atlas is used to define the coordinates of the STN in relation to the midcommissural point (MCP). The second is the direct method, which was developed by the work of Bejjani et al. in 2000 [7] in which the STN is directly visualized as a hypointense structure on T2 weighted images. Direct localization became easier with the improvements of magnetic resonance imaging (MRI) sequences and the use of special stereotactic software to perform 3D image reconstruction and help in the calculations [8–12]. Many studies assessed the direct coordinates and compared them to the coordinates obtained by the indirect method [13–17]. Yet, the exact correlation between these two conventional methods and the postoperative final (functional) target has not been established.

In this paper, we considered the final position of the best active electrode contact on the postoperative MRI images as the "true functional stimulation site" or the "final target". This final target position is confirmed by the intra-operative microelectrode recording (MER) and the postoperative improvement of the Parkinsonian symptoms. We compared these final coordinates to the initial coordinates calculated by both the direct and indirect methods.

2. Objectives

Assessment of the accuracy of the conventional methods of "direct" and "indirect" localization of STN target vs. the final functional target. This may help us to determine the optimal coordinates for the STN DBS target. We also aim to study the relationships of the final functional target coordinates to the coordinates of the different borders of the RN, in attempt to find any new relationships that can improve the preoperative planning. This may eventually increase the accuracy of the preoperative targeting, and subsequently decrease the intra-operative time needed for the MER and the number of microelectrode insertion tracks needed to reach the target, and consequently reducing the rate of complications.

3. Methods

After obtaining an appropriate institutional review board (IRB) approval, we retrospectively analyzed the data of all patients diagnosed with advanced Parkinson's disease who underwent bilateral STN-DBS at the University of Illinois at Chicago (UIC) in the period from January 2013 to December 2014. From a total of 40 bilateral STN-DBS procedures that were performed over this period, we included in this analysis 23 patients (46 targets) who had available postoperative MRI images, and a minimum follow up period of 6 months with documented clinical improvement on fixed stimulation parameters. We excluded the patients with postoperative complications causing abnormalities in the electrode position (1 patient), those who did not get a beneficial clinical effect from the stimulation (1 patient), and those whose follow-up visits (15 patients) took place in other institutions.

3.1. The Preoperative Planning and the Surgical Procedure

The surgery was done in two stages. The first stage involves implantation of the DBS electrodes under local anesthesia. Procedure starts with application of Leksell stereotactic frame Model G (Elekta Instruments, Atlanta, GA, USA) to the patient's head.

A high-resolution MRI of the patient's brain with a 3 Tesla scanner (Signa 3T94 VHi; General Electric Medical Systems, Milwaukee, WI, USA) was done. Two main sequences were obtained. The first is a 3D T1-weighted, spoiled gradient echo imaging of the entire head (section thickness: 2 mm; field of view: 26 × 26 cm; TR: 7.0–8.0 milliseconds; TE: ~400 milliseconds; flip angle: 12; band width: 31.25 KHz; acquisition time: <7 min). The second is high-resolution, contiguous, T2-weighted, fast spin-echo imaging through the region of the midbrain and basal ganglia (section thickness: 1.5 mm;

slice interval: 0 mm; matrix size: 512 × 512; field of view: 26 × 26 cm; TR: 4600–6200 milliseconds; TE: 95–108 milliseconds; acquisition time: <5 min) (Figure 1).

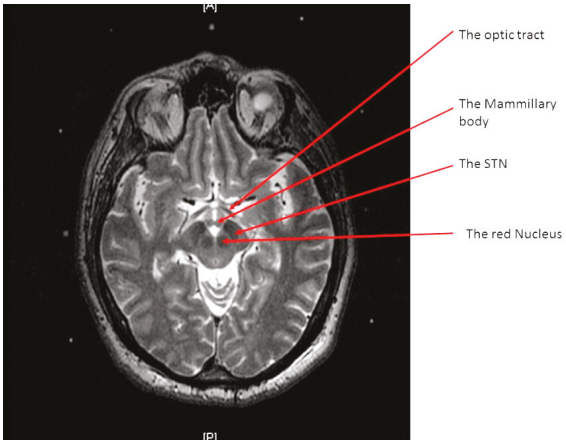

Figure 1. An axial T2 weighted magnetic resonance image (MRI) at the level of the midbrain showing the two subthalamic nuclei (STN).

3.1.1. The "Indirect" Method of the STN Coordinates Calculation

At the end of the scan, we chose the axial T2 image (or two adjacent images) in which the anterior commissure (AC) and the posterior commissure (PC) are identified (Figure 2). Then, we measured the distance between the middle and lower fiducials on both sides of the frame, and a maximum of 2 mm difference was allowed. The X and Y MR coordinate of the center of the frame was obtained at the point of meeting of two diagonal lines drawn on the MR console between the opposing anterior and posterior fiducials. After that, the X and Y MR coordinates of both the AC, the PC, and the center of the frame (Figure 3) were obtained from the MR console, and entered into a simple Excel worksheet (Microsoft, Redmond, WA, USA) designed by the senior author.

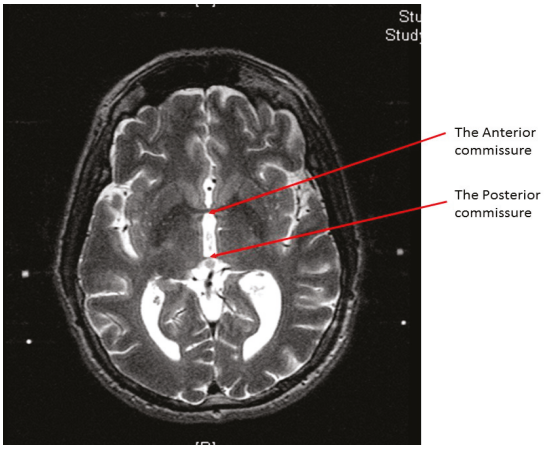

Figure 2. An axial T2 weighted magnetic resonance image showing the anterior commissure and the posterior commissure at the same cut.

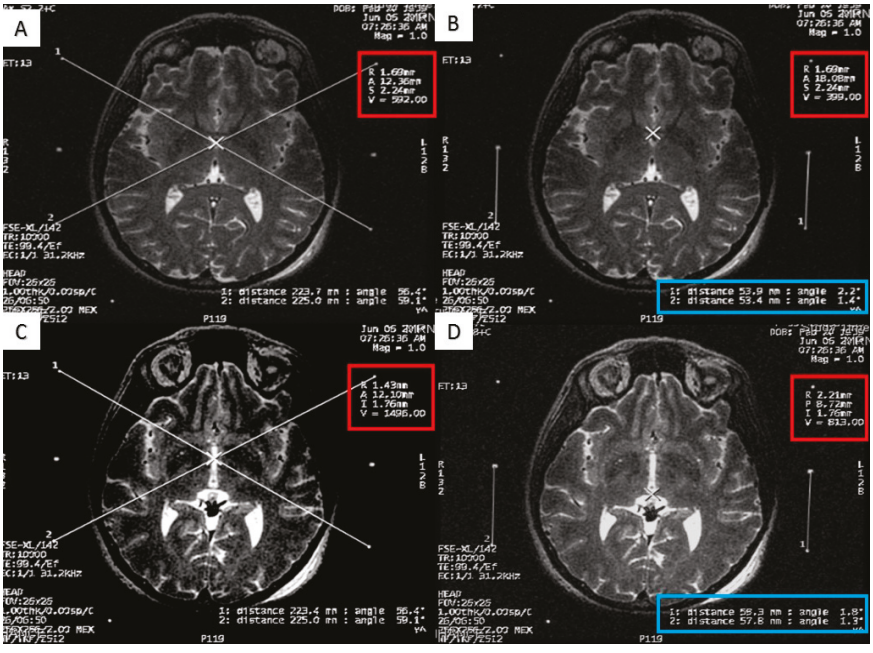

Figure 3. Calculating the anterior commissure (AC) and posterior commissure (PC) coordinates using the magnetic resonance scanner console. (**A**) Two diagonal lines intersecting at the center of the frame at the AC level with the magnetic resonance imaging (MRI) coordinates of the center of the frame shown inside the red square; (**B**) a crosshair at the posterior margin of the AC, with the MRI coordinates of the AC shown inside the red square. Two lines are drawn between the middle and the lower fiducials on both sides of the frame and their lengths (in the blue rectangle) are used to calculate the Z coordinate of the AC; (**C**) two diagonal lines intersecting at the center of the frame at the PC level with the MRI coordinates of the center of the frame shown inside the red square; (**D**) a crosshair at the anterior margin of the PC, with the MRI coordinates of the PC shown inside the red square. Two lines are drawn between the middle and the lower fiducials on both sides of the frame and their lengths (in the blue rectangle) are used to calculate the Z coordinates of the PC.

Afterwards, the frame coordinates of the AC, PC, the mid-commissural point (MCP), and the intercommissural distance (should be from 21 to 28 mm) were calculated with the help of this Excel worksheet by using the following formulas:

$$\text{X coordinates of the AC} = 100 + \text{MRI scanner X coordinates of the AC} - \text{MRI scanner X coordinates of the center of the frame} \quad (1)$$

$$\text{Y coordinates of the AC} = 100 + \text{MRI scanner Y coordinates of the AC} - \text{MRI scanner Y coordinates of the center of the frame} \quad (2)$$

$$\text{Z coordinates of the AC} = 40 + \text{distance between the lower and middle fiducials at the AC-PC plane} \quad (3)$$

$$\text{Intercommisural distance} = \sqrt{[(X_{AC} - X_{PC}) \times (X_{AC} - X_{PC}) + (Y_{AC} - Y_{PC}) \times (Y_{AC} - Y_{PC}) + (Z_{AC} - Z_{PC}) \times (Z_{AC} - Z_{PC})]} \quad (4)$$

$$X_{MCP} = (X_{AC} + X_{PC})/2 \quad (5)$$

$$Y_{MCP} = (Y_{AC} + Y_{PC})/2 \quad (6)$$

$$Z_{MCP} = (Z_{AC} + Z_{PC})/2 \quad (7)$$

Based on the known anatomical relationship of the STN to the MCP from previous anatomical studies and stereotactic atlases [18–21], we selected the STN target at 12 mm lateral, 3 mm posterior, and 6 mm inferior to the MCP. We used the following formulas to do the calculations:

$$X_{STN} = X_{MCP} \pm \mathbf{12\ mm} \quad (8)$$

Subtract for the right STN and add for the left STN

$$Y_{STN} = Y_{MCP} - \mathbf{3\ mm} \quad (9)$$

$$Z_{STN} = Z_{MCP} \mathbf{+\ 6\ mm} \quad (10)$$

The base of the STN.

3.1.2. The "Direct" Method of the STN Coordinates Calculation

The STN is the hypointense structure located lateral and anterior to the red nucleus on axial T2 MRI (Figure 4) [8]. The center of the STN hypointensity was identified at the extension of a straight line drawn at the anterior margin of the RN bisecting the STN. Then, the coordinates were calculated using the same Excel worksheet.

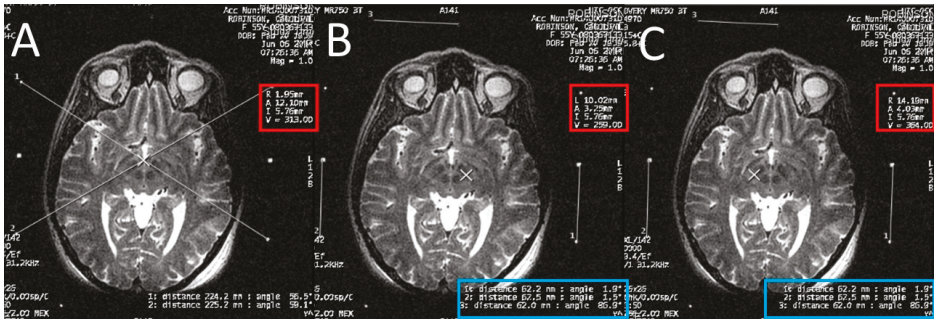

Figure 4. Calculating the subthalamic nucleus (STN) coordinates from the magnetic resonance imaging (MRI) console. (**A**) two diagonal lines intersecting at the center of the frame at the STN level with MRI coordinates of the center of the frame shown inside the red square; (**B**) a crosshair at the center of the left STN, with its MRI coordinates shown inside the red square, two line are drawn between the middle and lower fiducials on both sides of the frame and their lengths (in the blue rectangle) are used to calculate the Z coordinate; (**C**) a crosshair at the center of the right STN, with its MRI coordinates shown inside the red square, two line are drawn between the middle and lower fiducials on both sides of the frame and their lengths (in the blue rectangle) are used to calculate the Z coordinate.

In the operation room, we used the FrameLink software, which is a part of StealthStation navigation system (Medtronic, Minneapolis, MN, USA) to confirm our calculations of the direct STN coordinates (Figure 5). This software compensates for head and frame tilt in any direction. The final coordinates for the procedure were derived from the two techniques, and subsequently adjusted using intraoperative electrical microrecording and macrostimulation.

During surgery, we performed microelectrode recording (MER) of the brain activity using a NeuroNav microelectrode recording system (AlphaOmega, Nazareth, Israel). Fluoroscopic confirmation of the target approach was obtained at 5 mm intervals, 2 mm above the target, and at the target (Figure 6).

During MER, the STN is the most electrically active structure encountered during the recording. An indicator of entry into the STN is the increase of the background activity (Figure 7). The STN cells have a mean firing rate of 37 $\pm$ 17 Hz with high amplitude and irregular firing pattern [22]. We used the following criteria for choosing an ideal STN target:

- The length of the STN, measured along its trajectory, is 4–5 mm.
- Dense discharge patterns recorded in the STN.
- The presence of an identifiable region of increased neuronal firing at the STN on sensorimotor stimulation of the contralateral limbs.

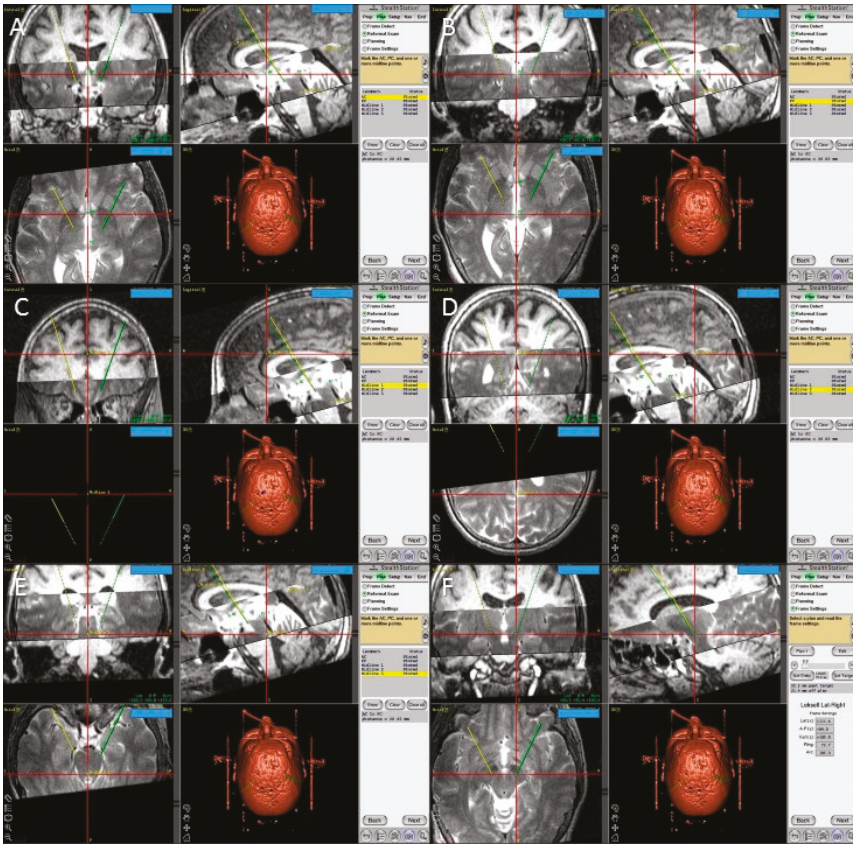

Figure 5. Screen shots from the Framelink software of the Stealthstation showing fused T1 and T2 MRI images of the patient and the planning process with identification of the posterior edge of the anterior commissure (AC) (**A**); the anterior edge of the posterior commissure (PC) (**B**); three midline points (**C**–**E**); and the final coordinates of the right subthalamic nucleus (**F**).

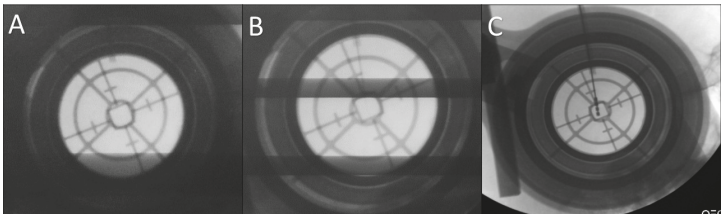

Figure 6. Fluoroscopic confirmation of the target approach. (**A**) Confirmation of the position of the stereotactic cannula; (**B**) the microelectrode is advanced to the target under fluoroscopic guidance; (**C**) the final position of the deep brain stimulation (DBS) electrode confirmed.

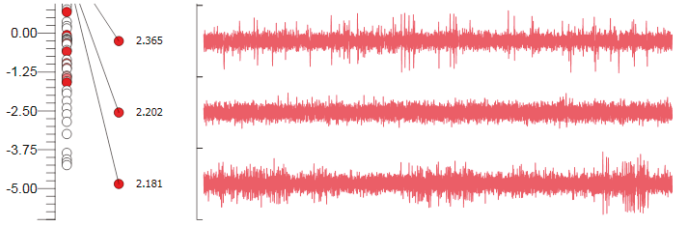

Figure 7. Microelectrode recording appearance of the subthalamic nucleus signal; note the increase in background activity, with high amplitude irregular firing.

After identification of the STN borders and depth by the MER, we started high frequency macrostimulation. The aim of the stimulation was to confirm the optimal target, which provides adequate control of the parkinsonian symptoms (most identifiable is the tremor), with no undesirable effects from stimulation below 4 V.

We tried to minimize the number of the tracks used for recording and stimulation to reach the STN as possible (Figure 6). The maximum number of tracks we used for a single side target was three (Figure 8).

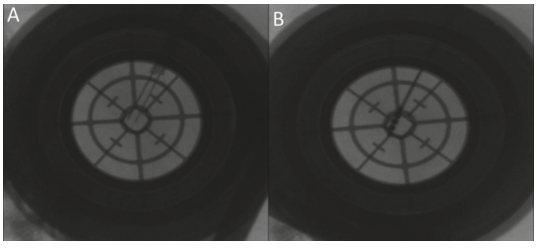

Figure 8. Fluoroscopic confirmation of the electrode position showing (**A**) a second microelectrode is inserted posterior to the original one due to suboptimal subthalamic nucleus (STN) signal during mapping along the original trajectory; (**B**) the final position of the deep brain stimulation (DBS) electrode in the new posterior trajectory.

Once we reached our desired target, we removed the microelectrode and replaced it with a standard four contact (0–3) deep brain stimulation electrode (Medtronic DBS lead 3389). Generally, we placed the deepest electrode contact (0) at or just beyond the target point. Then, we repeated the testing using this electrode in order to confirm the reproducibility of the beneficial effects and high thresholds for the undesirable effects (Figures 6 and 8). We locked the

electrode in place using a Stimloc device (Medtronic, Minneapolis, MN, USA). Then, the same procedure was repeated again for the opposite side electrode.

After removal of the stereotactic frame, the patient was transferred to the intensive care unit. Upon arrival, all patients had a CT scan of the head to rule out the presence of intracerebral hemorrhage. They all had an MRI of the brain in the same day of surgery or the next day to check the position of the electrodes prior to discharge home.

The patient returned to hospital after one week for the second stage, in which the implantable pulse generator (IPG) was implanted under general anesthesia.

3.2. Postoperative Calculation of the Active Contact Coordinates

Postoperative MRI images of the patients were loaded to the Medtronic Stealth station and the Framelink stereotactic software was used to perform fusion of the pre and the postoperative MRI images. This allowed us to get the coordinates of the active DBS electrode in relation to the mid commissural point (MCP). The first step after image fusion was to identify the tip of the DBS electrode. We chose a point at the center of the hypointense signal representing the tip of the electrode in all the three orthogonal planes and we marked it as our target. Then, we identified and marked the entry point of the electrode into the brain. The computer software then was able to draw a trajectory overlapping the electrode's pathway through the brain. Then, using a probe eye view we could move along this trajectory from the distal tip upwards. We moved by 0.25 mm increments until we reached the predetermined position of the active contact and we got its coordinates in relation to the MCP coordinates.

As all our patients were followed up for at least a period of 6 months, in our study, we collected the data of the stimulating electrodes combinations that gave them optimal clinical response and no undesirable effects at the lowest stimulation voltage. The Medtronic 3389 electrode which we used has four contacts that can be named 0, 1, 2, 3 (or 4, 5, 6, 7 or 8, 9, 10, 11) with contacts 0, 4 or 8 being the most distal and they are located 1.5 mm proximal to the tip of the electrode (Figure 9). The contacts are 1.5 mm in length and are separated by 0.5 mm intervals. We used a previously published methodology to calculate the coordinates of the active contact [23,24]. The midpoint of the first contact (0, 4, or 8) is located 2.25 mm cranial to the tip of the electrode, the midpoints of the second contact (1, 5, or 9) is located 4.25 mm cranial to the tip, the midpoint of the third contact (2, 6, or 10) is located 6.25 mm cranial to the tip, and the midpoint of the fourth contact (3, 7, or 11) is located 8.25 mm cranial to the tip. If the patient had a double monopolar electrodes combination, we chose our target to be the midpoint between the two cathodes. If he had a bipolar combination, we chose the cathode as our target [23,24].

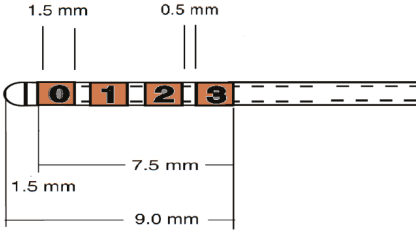

Figure 9. An illustration showing the geometry of the distal end of the 3389 deep brain stimulation (DBS) electrode model (Medtronic, Minneapolis, MN, USA).

We also calculated X coordinate of the lateral RN border, Y coordinate of the anterior RN border, and Z coordinate of the superior RN border to compare them with X, Y, and Z coordinates of the active contact respectively.

3.3. Data Processing and Statistical Analysis

The final active contact coordinates, being confirmed intra-operatively in all the patients as the STN functional target, and with documented postoperative beneficial clinical effect, were compared to the coordinates obtained by the preoperative indirect atlas based calculations and to those obtained by direct visualization. All coordinates were recorded based on the relationships of the target to the MCP, and all the distances were measured in millimeters. Data were initially recorded using a Microsoft Excel work sheet. We subtracted X, Y, and Z of the final active electrode coordinates from the corresponding X, Y, and Z of direct and indirect STN coordinates. We also calculated the distances between X coordinate of the lateral RN border, Y coordinate of the anterior RN border, and Z coordinate of the superior RN border and the final coordinates. We also calculated the Euclidean distances between the final active contact coordinates and the preoperative direct and indirect targets coordinates in three dimensions. The Euclidean distance is the "ordinary" (i.e., straight-line) distance between two points (p and q) in the Euclidean space. With this distance, the Euclidean space becomes a metric space. In a three-dimensional system with p at (p_1, p_2, p_3) and q at (q_1, q_2, q_3). The Euclidean distance is calculated by using the formula $[d(p,q) = \sqrt{(p_1 - q_1)^2 + (p_2 - q_3)^2 + (p_3 - q_3)^2}]$.

We coded, tabulated, and statistically analyzed our data using the IBM SPSS statistics software version 22.0 (IBM Corp., Chicago, IL, USA). Descriptive statistics were done for quantitative data as minimum & maximum of the range, mean ± SD (standard deviation), median, and confidence interval (CI) while we calculated numbers and percentages for qualitative data, as well as well as 95% confidence interval for both. Inferential analyses were done using the one-sample t-test and the paired t-test. The null hypothesis was that there is no difference between the direct, the indirect STN targets, the borders of RN, and the final electrode coordinates. The level of significance was taken at p-value < 0.05.

4. Results

The most commonly used electrode contacts for stimulation were the second (1, 5, 9) and the third contacts (2, 6, 10), and each of them was used in used in 15 targets (32.6%). The most commonly used double monopolar combination was between the second and the third contact (N = 4, 8.7%) (Figure 10).

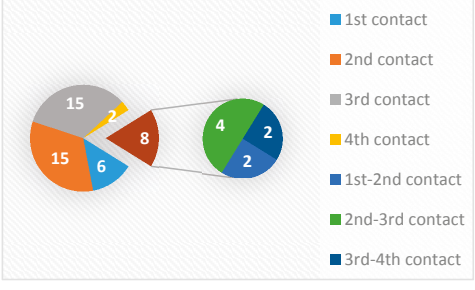

Figure 10. The distribution of the active contacts used as the final targets.

4.1. X Coordinates

The mean value of X coordinate of the final active contact was 11.7 mm lateral to MCP, with SD of 1.5 mm, median of 11.5, range 8.2–16.0 mm, and 95% CI of 11.2–12.2 mm (Figure 11). Comparison of the direct X coordinate to the final X coordinate showed no statistically significant difference with the mean value of the difference (X direct-X final) is −0.2 mm (95% CI −0.7–0.2 mm) (Table 1). The number of the direct X coordinates that lie within 1 mm lateral and 1 mm medial to the final X coordinates was 24/46 (52.2%, 95% CI = 37.2%–67.2%) (Table 2). Comparison of the indirect X coordinate to the final X coordinate also showed no statistically significant difference with the mean value of the

difference (X indirect-X final) was 0.3 mm (95% CI = −0.2–0.8 mm). The number of the indirect X coordinates that lie within 1 mm lateral and 1 mm medial to the final X coordinates was 23/46 (50.0%, 95% CI = 35.0%–65.0%) (Table 2).

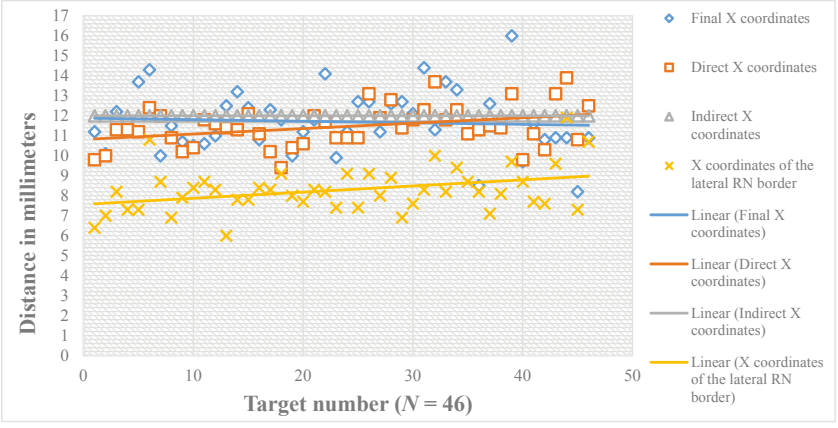

Figure 11. The X coordinates in relation to the mid-commissural point (MCP).

Table 1. The differences between the direct and indirect coordinates of STN from the final active electrode coordinates.

Method	Directions	Mean ± SD (mm)	Variance (mm)	Range (mm)	95% CI (mm)	*p*
Direct	X	−0.2 ± 1.5	2.2	−2.9–3.0	−0.7–0.2	0.271
	Y	−0.4 ± 1.9	3.6	−4.9–6.5	−0.9–0.2	0.205
	Z	−0.1 ± 1.7	3.0	−3.5–4.6	−0.6–0.4	0.650
	ED	2.7 ± 1.2	1.5	0.4–6.8	2.4–3.1	<0.001 *
Indirect	X	0.3 ± 1.5	2.3	−4.0–3.8	−0.2–0.8	0.186
	Y	0.6 ± 1.5	2.3	−3.2–3.0	0.1–1.0	0.014 *
	Z	−0.1 ± 1.7	2.9	−3.0–4.5	−0.6–0.4	0.810
	ED	2.6 ± 0.9	0.8	0.9–4.5	2.4–2.9	<0.001 *

Total = 46 targets, SD: standard deviation, CI: Confidence interval, *p*: *p*-value of one sample *t*-test, ED: Euclidean distance, * Significant: Differences are direct/indirect—final: Positive-X = lateral to the final X, Negative-X = medial to the final X; Positive-Y = posterior to the final Y, Negative-Y = anterior to the final Y; Positive-Z = inferior to the final Z, Negative-Z = superior to the final Z.

Table 2. Numbers and percentages of the coordinates of the direct, indirect and RN borders within ±1.0 mm of the final targets.

Method	Coordinates	*N* (%)	95% CI
Direct	X	24 (52.2%)	37.2%–67.2%
	Y	26 (56.5%)	41.6%–71.4%
	Z	22 (47.8%)	32.8%–62.8%
	ED	1 (2.2%)	0.0%–6.6%
Indirect	X	23 (50.0%)	35.0%–65.0%
	Y	19 (41.3%)	26.5%–56.1%
	Z	22 (47.8%)	32.8%–62.8%
	ED	2 (4.3%)	0.0%–10.5%
Y coordinate of the anterior RN border		22 (47.8%)	32.8%–62.8%

Total = 46 targets, CI: Confidence interval, ED: Euclidean distance, RN: red nucleus.

The mean value of X coordinate of the lateral RN border was 8.3 mm lateral to MCP (SD of 1.1 mm, median of 8.2, range 6.0–11.9 mm). The mean distance between X coordinates of the lateral RN border and X coordinate of the final target (X of the RN-X final) was 3.4 mm on the medial side (95% CI −4.0–−2.9 mm, $p < 0.001$) (Table 3).

Table 3. The distances between the different RN borders and the final active electrode coordinates.

Coordinates	Mean ± SD (mm)	Variance (mm)	Range (mm)	95% CI (mm)	*p*
X of the lateral RN border	−3.4 ± 1.8	3.3	−6.5–1.0	−4.0–−2.9	<0.001 *
Y of the anterior RN border	−0.2 ± 1.9	3.7	−5.2–4.1	−0.7–0.4	0.562
Z of the superior RN border	−3.5 ± 1.8	3.3	−6.8–1.0	−4.0–−2.9	<0.001 *

Total = 46 targets, SD: standard deviation, CI: Confidence interval, *p*: *p*-value of one sample *t*-test, * Significant: Differences are direct/indirect—final: Positive-X = lateral to the final X, Negative-X = medial to the final X; Positive-Y = posterior to the final Y, Negative-Y = anterior to the final Y; Positive-Z = inferior to the final Z, Negative-Z = superior to the final Z.

4.2. Y Coordinates

The mean value of Y coordinate of the final active contact is 2.4 mm posterior to MCP (SD of 1.5 mm, median of 2.1, range 0–6.2 mm, 95% CI 2.0–2.9 mm) (Figure 12). Comparison of the direct Y coordinate to the final Y coordinate showed no statistically significant difference with the mean value of the difference (Y direct-Y final) was −0.4 mm (95% CI −0.9–0.2 mm) (Figure 13). The number of the direct Y coordinates that lie within 1 mm anterior and 1 mm posterior to the final Y coordinates was 26/46 (56.5%, 95% CI = 41.6%–71.4%). Comparison of the indirect Y coordinate to the final Y coordinate showed a statistically significant difference with the mean value of the difference (Y indirect-Y final) was 0.6 mm (95% CI 0.1–1.0 mm, $p = 0.014$). The number of the indirect Y coordinates that lie within 1 mm anterior and 1 mm posterior to the final Y coordinates was 19/46 (41.3%, 95% CI = 26.5%–56.1%).

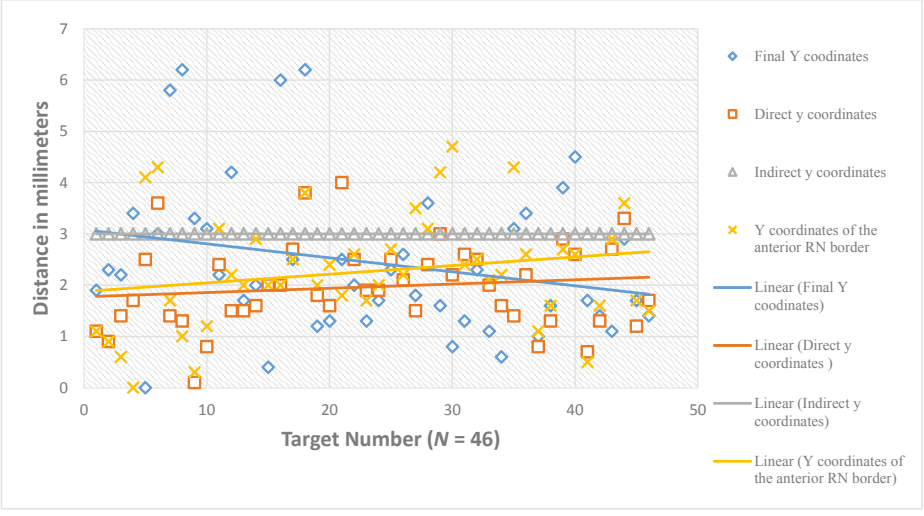

Figure 12. The Y coordinates in relation to the mid-commissural point (MCP).

The mean value of Y coordinate of the anterior RN border was 2.3 mm lateral to MCP (SD of 1.1 mm, range 0–4.7 mm). There was no statistically significant difference between Y coordinate of the anterior RN border and Y coordinate of the final target with the mean value of the difference (Y of RN-Y final) was −0.2 mm (95% CI −0.7–0.4 mm. $p = 0.562$).

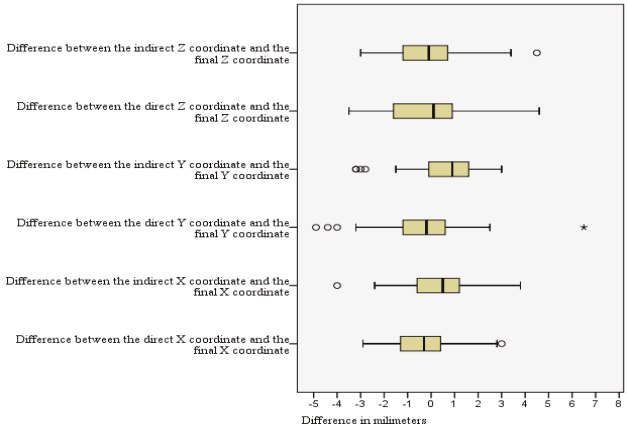

Figure 13. The differences between the direct and indirect coordinates of the subthalamic nucleus from the final active electrode coordinates. °: outliers.

4.3. Z Coordinates

The mean value of Z coordinate of the final active contact is 6.1 mm inferior to MCP (SD of 1.7 mm, median of 6.1, range 1.5–9.0 mm, 95% CI 5.6–6.6 mm) (Figure 14). Comparison of the direct Z coordinate to the final Z coordinate showed no statistically significant difference with the mean value of the difference (Z direct-Z final) was −0.1 mm(95% CI −0.6–0.4 mm). The number of the direct Z coordinates that lie within 1 mm superior and 1 mm inferior to the final Z coordinates is 22/46 (47.8%, 95% CI = 32.8%–62.8%). Comparison of the indirect Z coordinate to the final Z coordinate showed no statistically significant difference with the mean value of the difference (Z indirect-Z final) was −0.1 mm (95% CI −0.6–0.4 mm). The number of the indirect Z coordinates that lie within 1 mm superior and 1 mm inferior to the final Z coordinates is 22/46 (47.8%, 95% CI = 32.8%–62.8%).

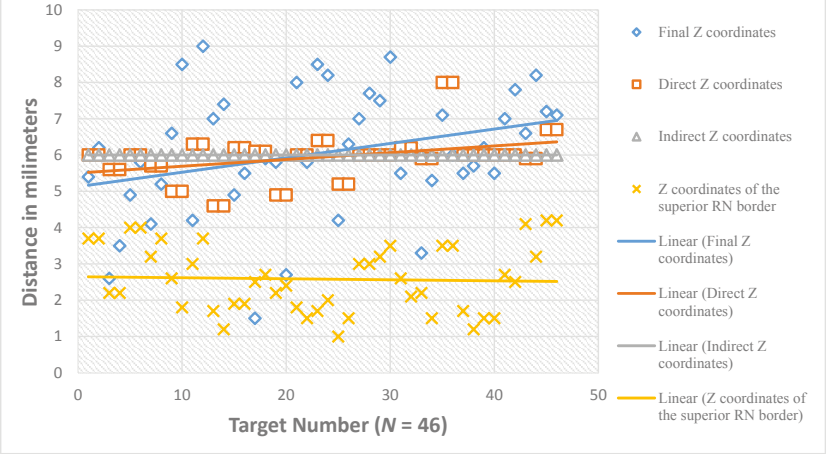

Figure 14. The Z coordinates in relation to the mid-commissural point (MCP).

The mean value of Z coordinates of the superior RN border was 2.6 mm inferior to MCP (SD of 0.9 mm, range 1.0–4.2 mm). The mean distance of Z coordinates of the superior border of RN superior

to the STN and Z coordinates of the final contact (Z of RN-Z final) was −3.5 mm (95% confidence interval −4.0–−2.9 mm, $p < 0.001$) (Figure 15).

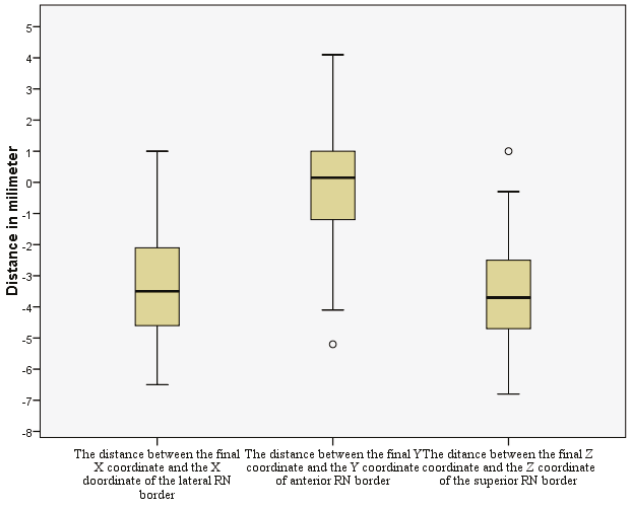

Figure 15. The distances between the different red nuleus (RN)borders and the final active electrode coordinates. °: outliers.

4.4. The Euclidean Distances

The Euclidean distance (ED) between the final position of the active contact and the preoperative planned position of STN by the direct visualization method was found to be statistically significant with a mean of 2.7 mm (95% confidence interval 2.4–3.1 mm, and $p < 0.001$). The number of the direct STN targets that lie within 1 mm in any direction of the final targets is only 1/46 (2.2%, 95% CI = 0%–6.6%).

ED between the final position of the active contact and the preoperative planned position of STN by indirect method was found to be statistically significant with a mean of 2.6 mm (95% confidence interval 2.4–2.9 mm, and $p < 0.001$). The number of the indirect STN targets that lie within 1 mm in any direction of the final targets was only 2/46 (4.3%, 95% CI = 0%–10.5%).

There was no statistically significant difference in ED of the final active contact to the direct target vs. the distance of the final active contact to the indirect target with the mean difference 0.08 mm (95% confidence interval −0.3–0.4 mm, and $p = 0.674$).

5. Discussion

In our practice, we use both the direct and the indirect methods for the preoperative planning. However, it is not unusual to move the electrode into different coordinates of STN based on intraoperative neurophysiological findings. This may happen when our planned target does not exhibit an adequate pattern of the STN signal on MER or it turns out to be too close to the nearby structures causing undesired effects. Therefore, we may move the electrode position a few millimeters away from the originally planned one to reach a better functioning stimulation site (Figure 8). Hamani et al. [25] compared the coordinates of the different borders of STN as identified on MRI to the coordinates identified by MER of STN activity. In their results, 15 tracks (52% of the tracks) had STN-like activity outside the identified borders of STN on MRI (mostly by 1 mm) [25].

This study comes as a continuation of our previous efforts to define the optimal method to calculate the coordinates for the different DBS procedures [6,26]. We considered the final position of the active electrode contact on the postoperative MRI as the "true functional stimulation site" or the

"final target". This final target position is confirmed by the intra-operative MER and the postoperative improvement of the parkinsonian symptoms. We compared these final coordinates to the initial coordinates calculated by both the direct and indirect methods. We also studied the relations of the final functional target coordinates to the coordinates of the different borders of RN in attempt to find any new relations that can improve the preoperative planning. The reason why we chose RN is its close proximity to STN, and the fact that the borders of RN are well visualized on MRI even better than those of STN.

In our results, both the direct X and the indirect X coordinates did not show a statistically significant difference from the final X coordinate. These results confirm that X of the final functional target of STN corresponds to X of the anatomical center calculated by either of the two methods. The difference between the direct X coordinate calculation and the final X had smaller mean, variance, and narrower range, and CI than the difference between the indirect and the final X (Table 1). The mean value of X coordinate of the final active contact was 11.7 mm lateral to MCP with 95% CI = 11.2–12.2 mm. The mean distance between X coordinates of the lateral RN border and X coordinate of the final target (X of RN-X final) was 3.4 mm on the medial side, with 95% CI = 4.0–2.9 mm. Accordingly, we suggest for preoperative calculation of X coordinate to choose our X at the center of the hypointensity range representing STN on an axial MRI image, taking into consideration that most of the functional STN targets lie 11–12.5 mm lateral to MCP, and 3–4 mm lateral to the lateral RN border.

In regard to Y coordinate, comparison of the direct Y coordinate to the final Y coordinate showed no statistically significant difference. In addition, there was no statistically significant difference between the Y coordinate of the anterior RN border and the Y coordinate of the active contact. Meanwhile, a comparison of the indirect Y coordinate to the final Y coordinate showed a statistically significant difference. These results confirm that Y of the final functional target of the STN corresponds to Y of the anatomical center calculated by direct visualization on MRI at the extension of a straight line drawn at the anterior margin of the RN, as suggested by Bejjani et al. in 2000 [7]. The mean value of the Y coordinate of the final target was 2.4 mm posterior to the MCP with 95% CI = 2.0–2.9 mm. Accordingly, we suggest for the preoperative calculation of the Y coordinate to choose our Y at the center of the hypointensity range representing the STN in an axial MRI image. During the calculation, we should take into consideration that most of the functional STN targets lie 2–3 mm posterior to the MCP, and at the same Y of a straight line drawn at the anterior margin of the RN.

In regard to the Z coordinate, both the direct Z and the indirect Z coordinates did not show a statistically significant difference from the final Z coordinate. These results confirm that Z of the final functional target of STN corresponds to the Z of the anatomical center calculated by either of the two methods. The mean value of the Z coordinate of the final active contact was 6.1 mm inferior to MCP with a 95% CI = 5.6–6.6 mm. The mean distance of the Z coordinate of the superior RN border and the Z coordinate of the final contact (Z of RN-Z final) was 3.5 mm more superior, with the 95% CI = 4.0–2.9 mm. Accordingly, we suggest for the preoperative calculation of the Z coordinate to choose our Z at the center of the hypointensity representing STN on coronal MRI, taking into consideration that most of the STN functional targets lie between 5.5 and 6.6 mm inferior to MCP, and 3–4 mm inferior to the superior RN border.

The results of this study show that both the indirect and the direct methods of localization correspond largely to the final functional target in calculating X and Z coordinates, with the direct visualization being more accurate. Nevertheless, the indirect Y coordinate was significantly posterior to Y of the final optimal target. Ashkan et al. [13] calculated the indirect STN coordinates at 12 mm lateral, 2 mm posterior, and 4 mm inferior to MCP. They compared these indirect coordinates with those obtained by direct visualization. Their results showed that, on average, the directly visualized target compared to the atlas target was 1.7 mm more medial ($p < 0.0001$), 0.7 mm more anterior ($p < 0.001$) and 0.7 mm more ventral ($p < 0.0001$).

In our indirect calculations, we used the Z coordinate at 6 mm inferior to MCP. Our results showed that there was no significant difference between this Z coordinate and the final Z value. This is different

from other studies that used other values of Z coordinates such as 3 [27], 4 [13,28–31], or 5 [16] mm inferior to MCP. These studies found a significant difference in the Z coordinate calculation between the indirect and the direct [16,31] targeting or between the indirect and the final target [27,30].

To our best knowledge, no studies calculated the difference in the distance between the final STN coordinates and the coordinates of the different RN borders. Andrade-Souza et al. [27] used coordinates derived from the stereotactic atlases to preoperatively plan STN targets based on the coordinates of different RN borders. They defined an X coordinate 3 mm lateral to the lateral RN border, a Y coordinate at the same Y of the anterior RN border, and a Z coordinate as 2 mm inferior to the superior RN border. They calculated the mean ± SD of the differences between the preoperative RN based calculations and the final targets; X = 1.82 ± 1.38 mm, Y = 1.62 ± 1.05 mm, and Z = 1.37 ± 0.93 mm. Houshmand et al. [16] used the same parameters used by Andrade-Souza et al. [27] to calculate STN target coordinates based on the coordinates of different RN borders. They calculated the distances between different RN borders and the STN anatomical center seen on 3T MRI. They calculated the mean ± SD of the differences between the preoperative RN based calculation and the final targets; X = 0.67 ± 0.45 mm, Y = 0.77 ± 0.54 mm, and Z = 0.56 ± 0.40 mm. Both of those studies found that the RN base targeting was closer to the optimal target, than the direct or the indirect calculations. Starr et al. [29] considered the center of the DBS electrode array in the postoperative MRI as the final target, and they calculated the mean distance between its coordinates and X and Y coordinates of the center of RN (X = 6.5 mm lateral, Y = 3.5 mm anterior).

Despite the great similarities of the final coordinates to that of the preoperatively planned direct and indirect coordinates, the Euclidean distances between the final targets and both the direct and indirect targets were found to have statistically significantly differences. This in addition to the wide range of values of the different coordinates of the final targets in relation to MCP (X = 8.2–16.0, Y = 0.0–6.2, Z = 1.5–9.0) exclude the possibility of depending on the preoperative planning as the sole method of targeting STN. We believe that the intra-operative physiological and clinical confirmation of the target is crucial in the final position confirmation. Still, initial anatomical and radiological planning is also essential in target selection. Accurate preoperative planning would decrease the intra-operative time needed for MER, and the number of microelectrodes tracks needed to reach the target, and subsequently prevent additional complication. This fact is supported by our experience, as our average number of MER tracks was 1.4 tracks.

6. Conclusions

The functional target of STN corresponds to the anatomical center of STN as seen in the three orthogonal planes of MRI images. During the preoperative calculation of the STN target, we prefer using the direct method, and taking into consideration that most of the functional targets are located: (1) 11–12.5 mm lateral to MCP, and 3–4 mm lateral to the lateral RN border; (2) 2–3 mm posterior to MCP, and at the same Y of a straight line drawn at the anterior margin of the red nuclei; (3) 5.5–6.6 mm inferior to MCP, and 3–4 mm inferior to the superior RN border. It seems that the preoperative anatomical/radiological planning cannot be used as the sole method of targeting the STN, intra-operative physiological and clinical confirmation is crucial in the final position confirmation.

Acknowledgments: We would like to thank Hazem El-Hariri and Ahmed Hussein who helped us with the statistics.

Author Contributions: Ahmed Rabie, the first author, came up with the idea of the research and shared in all phases of the research. Konstantin V. Slavin and Leo Verhagen Metman shared in conducting the research, analyzing and revising the data, and writing the paper.

Conflicts of Interest: The authors declare no conflict of interest.

References

1. Sukul, V.V.; Slavin, K.V. Deep brain and motor cortex stimulation. *Curr. Pain Headache Rep.* **2014**, *18*, 427. [CrossRef] [PubMed]
2. Parent, A.; Hazrati, L.N. Functional anatomy of the basal ganglia. II. The place of subthalamic nucleus and external pallidum in basal ganglia circuitry. *Brain Res. Brain Res. Rev.* **1995**, *20*, 128–154. [CrossRef]
3. Hamani, C.; Saint-Cyr, J.A.; Fraser, J.; Kaplitt, M.; Lozano, A.M. The subthalamic nucleus in the context of movement disorders. *Brain* **2004**, *127*, 4–20. [CrossRef] [PubMed]
4. Rodriguez-Oroz, M.C.; Rodriguez, M.; Guridi, J.; Mewes, K.; Chockkman, V.; Vitek, J.; DeLong, M.R.; Obeso, J.A. The subthalamic nucleus in Parkinson's disease: Somatotopic organization and physiological characteristics. *Brain* **2001**, *124*, 1777–1790. [CrossRef] [PubMed]
5. Levy, R.; Hutchison, W.D.; Lozano, A.M.; Dostrovsky, J.O. High-frequency synchronization of neuronal activity in the subthalamic nucleus of parkinsonian patients with limb tremor. *J. Neurosci.* **2000**, *20*, 7766–7775. [PubMed]
6. Slavin, K.V.; Anderson, G.J.; Burchiel, K.J. Comparison of three techniques for calculation of target coordinates in functional stereotactic procedures. *Stereotact. Funct. Neurosurg.* **1999**, *72*, 192–195. [CrossRef] [PubMed]
7. Bejjani, B.P.; Dormont, D.; Pidoux, B.; Yelnik, J.; Damier, P.; Arnulf, I.; Bonnet, A.M.; Marsault, C.; Agid, Y.; Philippon, J.; et al. Bilateral subthalamic stimulation for Parkinson's disease by using three-dimensional stereotactic magnetic resonance imaging and electrophysiological guidance. *J. Neurosurg.* **2000**, *92*, 615–625. [CrossRef] [PubMed]
8. Slavin, K.V.; Thulborn, K.R.; Wess, C.; Nersesyan, H. Direct visualization of the human subthalamic nucleus with 3T MR imaging. *Am. J. Neuroradiol.* **2006**, *27*, 80–84. [PubMed]
9. Hariz, M.I.; Krack, P.; Melvill, R.; Jorgensen, J.V.; Hamel, W.; Hirabayashi, H.; Lenders, M.; Wesslen, N.; Tengvar, M.; Yousry, T.A. A quick and universal method for stereotactic visualization of the subthalamic nucleus before and after implantation of deep brain stimulation electrodes. *Stereotact. Funct. Neurosurg.* **2003**, *80*, 96–101. [CrossRef] [PubMed]
10. Dormont, D.; Ricciardi, K.G.; Tande, D.; Parain, K.; Menuel, C.; Galanaud, D.; Navarro, S.; Cornu, P.; Agid, Y.; Yelnik, J. Is the subthalamic nucleus hypointense on T2-weighted images? A correlation study using MR imaging and stereotactic atlas data. *Am. J. Neuroradiol.* **2004**, *25*, 1516–1523. [PubMed]
11. Wippold, F.J., 2nd; Brown, D.C.; Broderick, D.F.; Burns, J.; Corey, A.S.; Deshmukh, T.K.; Douglas, A.C.; Holloway, K.; Jagadeesan, B.D.; Jurgens, J.S.; et al. ACR appropriateness criteria dementia and movement disorders. *J. Am. Coll. Radiol.* **2015**, *12*, 19–28. [CrossRef] [PubMed]
12. Chandran, A.S.; Bynevelt, M.; Lind, C.R. Magnetic resonance imaging of the subthalamic nucleus for deep brain stimulation. *J. Neurosurg.* **2016**, *124*, 96–105. [CrossRef] [PubMed]
13. Ashkan, K.; Blomstedt, P.; Zrinzo, L.; Tisch, S.; Yousry, T.; Limousin-Dowsey, P.; Hariz, M.I. Variability of the subthalamic nucleus: The case for direct MRI guided targeting. *Br. J. Neurosurg.* **2007**, *21*, 197–200. [CrossRef] [PubMed]
14. Littlechild, P.; Varma, T.R.; Eldridge, P.R.; Fox, S.; Forster, A.; Fletcher, N.; Steiger, M.; Byrne, P.; Tyler, K.; Flintham, S. Variability in position of the subthalamic nucleus targeted by magnetic resonance imaging and microelectrode recordings as compared to atlas co-ordinates. *Stereotact. Funct. Neurosurg.* **2003**, *80*, 82–87. [CrossRef] [PubMed]
15. Patel, N.K.; Khan, S.; Gill, S.S. Comparison of atlas- and magnetic-resonance-imaging-based stereotactic targeting of the subthalamic nucleus in the surgical treatment of Parkinson's disease. *Stereotact. Funct. Neurosurg.* **2008**, *86*, 153–161. [CrossRef] [PubMed]
16. Houshmand, L.; Cummings, K.S.; Chou, K.L.; Patil, P.G. Evaluating indirect subthalamic nucleus targeting with validated 3-Tesla magnetic resonance imaging. *Stereotact. Funct. Neurosurg.* **2014**, *92*, 337–345. [CrossRef] [PubMed]
17. Caire, F.; Ouchchane, L.; Coste, J.; Gabrillargues, J.; Derost, P.; Ulla, M.; Durif, F.; Lemaire, J.J. Subthalamic nucleus location: Relationships between stereotactic AC-PC-based diagrams and MRI anatomy-based contours. *Stereotact. Funct. Neurosurg.* **2009**, *87*, 337–347. [CrossRef] [PubMed]
18. Talairach, J.; Tournoux, P. *Co-Planar Stereotaxic Atlas of the Human Brain: 3-Dimensional Proportional System: An Approach to Cerebral Imaging*; Georg Thieme: Stuttgart, Germany; New York, NY, USA, 1988; p. 122.

19. Starr, P.A.; Vitek, J.L.; DeLong, M.; Bakay, R.A. Magnetic resonance imaging-based stereotactic localization of the globus pallidus and subthalamic nucleus. *Neurosurgery* **1999**, *44*, 303–313. [CrossRef] [PubMed]
20. Niemann, K.; Mennicken, V.R.; Jeanmonod, D.; Morel, A. The Morel stereotactic atlas of the human thalamus: Atlas-to-MR registration of internally consistent canonical model. *Neuroimage* **2000**, *12*, 601–616. [CrossRef] [PubMed]
21. Schaltenbrand, G.; Wharen, W. *Atlas for Stereotaxy of the Human Brain*; Thieme: Stuttgart, Germany, 1977.
22. Hutchison, W.D.; Allan, R.J.; Opitz, H.; Levy, R.; Dostrovsky, J.O.; Lang, A.E.; Lozano, A.M. Neurophysiological identification of the subthalamic nucleus in surgery for Parkinson's disease. *Ann. Neurol.* **1998**, *44*, 622–628. [CrossRef] [PubMed]
23. Saint-Cyr, J.A.; Hoque, T.; Pereira, L.C.; Dostrovsky, J.O.; Hutchison, W.D.; Mikulis, D.J.; Abosch, A.; Sime, E.; Lang, A.E.; Lozano, A.M. Localization of clinically effective stimulating electrodes in the human subthalamic nucleus on magnetic resonance imaging. *J. Neurosurg.* **2002**, *97*, 1152–1166. [CrossRef] [PubMed]
24. Vergani, F.; Landi, A.; Antonini, A.; Parolin, M.; Cilia, R.; Grimaldi, M.; Ferrarese, C.; Gaini, S.M.; Sganzerla, E.P. Anatomical identification of active contacts in subthalamic deep brain stimulation. *Surg. Neurol.* **2007**, *67*, 140–146. [CrossRef] [PubMed]
25. Hamani, C.; Richter, E.O.; Andrade-Souza, Y.; Hutchison, W.; Saint-Cyr, J.A.; Lozano, A.M. Correspondence of microelectrode mapping with magnetic resonance imaging for subthalamic nucleus procedures. *Surg. Neurol.* **2005**, *63*, 249–253. [CrossRef] [PubMed]
26. Colpan, M.E.; Slavin, K.V. Subthalamic and red nucleus volumes in patients with Parkinson's disease: Do they change with disease progression? *Parkinsonism Relat. Disord.* **2010**, *16*, 398–403. [CrossRef] [PubMed]
27. Andrade-Souza, Y.M.; Schwalb, J.M.; Hamani, C.; Eltahawy, H.; Hoque, T.; Saint-Cyr, J.; Lozano, A.M. Comparison of three methods of targeting the subthalamic nucleus for chronic stimulation in Parkinson's disease. *Neurosurgery* **2005**, *56*, 360–368. [CrossRef] [PubMed]
28. Benabid, A.L.; Pollack, P.; Benazzouz, A. Grenoble guidelines for deep brain stimulation. In *First European Symposium on Stimulation in Parkinson Disease*; Universite Joseph Fourier de Grenoble: Grenoble, France, 1998.
29. Starr, P.A.; Christine, C.W.; Theodosopoulos, P.V.; Lindsey, N.; Byrd, D.; Mosley, A.; Marks, W.J., Jr. Implantation of deep brain stimulators into the subthalamic nucleus: Technical approach and magnetic resonance imaging-verified lead locations. *J. Neurosurg.* **2002**, *97*, 370–387. [CrossRef] [PubMed]
30. Hamid, N.A.; Mitchell, R.D.; Mocroft, P.; Westby, G.W.; Milner, J.; Pall, H. Targeting the subthalamic nucleus for deep brain stimulation: Technical approach and fusion of pre- and postoperative MR images to define accuracy of lead placement. *J. Neurol. Neurosurg. Psychiatry* **2005**, *76*, 409–414. [CrossRef] [PubMed]
31. Savas, A.; Bozkurt, M.; Akbostanci, C. A comparison between stereotactic targeting methods of the subthalamic nucleus in cases with Parkinson's disease. *Acta Neurochir. Suppl.* **2013**, *117*, 35–41. [PubMed]

brain sciences

MDPI

Article

Investigation into Deep Brain Stimulation Lead Designs: A Patient-Specific Simulation Study

Fabiola Alonso [1,*], Malcolm A. Latorre [1], Nathanael Göransson [1,2], Peter Zsigmond [2,3] and Karin Wårdell [1]

1 Department of Biomedical Engineering, Linköping University, Linköping 58185, Sweden; malcolm.latorre@liu.se (M.A.L.); Nathanael.Goransson@regionostergotland.se (N.G.); karin.wardell@liu.se (K.W.)

2 Department of Neurosurgery, Linköping University Hospital, Region Östergötland, Linköping 58185, Sweden; Peter.Zsigmond@regionostergotland.se

3 Department of Clinical and Experimental Medicine, Linköping University, Linköping 58185, Sweden

* Correspondence: fabiola.alonso@liu.se; Tel.: +46-101-030-000

Academic Editors: Tipu Aziz and Alex Green
Received: 30 June 2016; Accepted: 30 August 2016; Published: 7 September 2016

Abstract: New deep brain stimulation (DBS) electrode designs offer operation in voltage and current mode and capability to steer the electric field (EF). The aim of the study was to compare the EF distributions of four DBS leads at equivalent amplitudes (3 V and 3.4 mA). Finite element method (FEM) simulations (n = 38) around cylindrical contacts (leads 3389, 6148) or equivalent contact configurations (leads 6180, SureStim1) were performed using homogeneous and patient-specific (heterogeneous) brain tissue models. Steering effects of 6180 and SureStim1 were compared with symmetric stimulation fields. To make relative comparisons between simulations, an EF isolevel of 0.2 V/mm was chosen based on neuron model simulations (n = 832) applied before EF visualization and comparisons. The simulations show that the EF distribution is largely influenced by the heterogeneity of the tissue, and the operating mode. Equivalent contact configurations result in similar EF distributions. In steering configurations, larger EF volumes were achieved in current mode using equivalent amplitudes. The methodology was demonstrated in a patient-specific simulation around the zona incerta and a "virtual" ventral intermediate nucleus target. In conclusion, lead design differences are enhanced when using patient-specific tissue models and current stimulation mode.

Keywords: deep brain stimulation (DBS); steering; patient-specific; electric field; finite element method; neuron model; brain model; zona incerta (ZI); electrode design

1. Introduction

Deep brain stimulation (DBS) is an established technique to alleviate the symptoms caused by several movement disorders such as Parkinson's disease and essential tremor. DBS is now also expanding towards other symptoms such as psychiatric illness [1]. The technique has been proven to be successful even though the mechanisms of action are still uncertain, which makes it difficult to have complete control on the desired effect and avoid side effects.

Traditionally, DBS systems have operated in voltage mode using conventional ring-shaped electrodes generating a symmetrical stimulation field around the lead. Recently, new electrode designs offer the capability to steer the stimulation field allowing some compensation for a possible lead misplacement [2,3]. The operating mode has also been modified delivering current instead of voltage stimulation. Current controlled systems, in comparison to voltage, automatically adjust the voltage to changes in the surrounding tissue impedance, in order to deliver a constant current [4]. Brain tissue is an electrically conductive medium in which the distribution of the electric field (EF) can be calculated

and visualized with computer models that solve the corresponding differential equation. In this study, the finite element method (FEM) has been used to evaluate and compare the EF from four different leads used in DBS systems.

Numerous computational models have been used to predict and visualize the first derivative of the electric potential, i.e., the EF [5–8] or the second derivative of the electric potential generated by DBS systems [9,10]. However, these are usually employed using traditional leads with voltage control operating mode. We have previously compared the conventional leads *Medtronic 3389* and *St. Jude Medical 6148* in different operating modes and time points [11]. Other simulations studied the influence from heterogeneity and anisotropy for the 3389 lead [12,13]. This study extends the comparisons to include two steering field leads, *St. Jude Medical 6180* and *Medtronic SureStim1*. When comparing FEM simulations, a fixed isolevel EF has been useful in making relative simulation comparisons for the 3389 lead [5,6,8]. In a previous study [14], neuron model simulations were run for a range of stimulation amplitudes, pulse lengths and axon diameters. These settings and physiological parameters should be taken into account in the choice of isolevel.

The aim of the study was to compare four DBS lead EF distributions in both voltage and current modes as presented in homogenous and heterogeneous, i.e., patient-specific, tissue models for the zona incerta (ZI) and the ventral intermediate nucleus (VIM) brain targets. Furthermore, steering effect simulations were investigated and compared with conventional 3389 lead EF. Visualization of the 3389 EF for the implanted ZI target with the patient-specific stimulation settings was demonstrated.

2. Materials and Methods

2.1. Patient Data, Surgery and Imaging

DBS data and images from one patient with tremor dominant Parkinson's disease implanted in the ZI at the Department of Neurosurgery, Linköping University Hospital were included in the study. An additional "virtual target", VIM, along the planned trajectory was used for the simulations. Informed written consent was received from the patient and the study was approved by the local ethics committee in Linköping (2012/434-31).

Prior to surgery and under general anaesthesia, the Leksell Stereotactic System (G frame, Elekta Instrument AB, Linköping, Sweden) was attached. Thereafter, a 3 Tesla, T2-weigthed magnetic resonance imaging (MRI) Philips Intera, Eindhoven, The Netherlands) with 2 mm contiguous axial slices ($2 \times 0.5 \times 0.5$) mm^3 was performed. Direct anatomical targeting was planned using Surgiplan® (Elekta Instrument AB). Surgery followed the routine protocol [15] for DBS implantation and was completed in a single procedure. The probe's position was verified by intraoperative fluoroscopy (Philips BV Pulsera, Philips Medical Systems, Eindhoven, The Netherlands). A postoperative computer tomography (CT) was performed to confirm the lead's positioning the day after surgery, and a second CT was taken after 4.5 weeks (chronic time point). These CT images were separately co-registered with the preoperative MRI using Surgiplan®. From the postoperative image artefacts, the surgeon noted the Leksell® coordinates (x, y, z) of a point at the lowest contact and another reference point 10 mm above the AC-PC line along the lead axis. These coordinates were used to place the lead within the brain model. The electrode position at the chronic time point was considered for the simulations in this study. The Leksell® coordinates for ZI and VIM targets were also identified for simulations.

2.2. FEM Modelling and Simulation

The leads and brain tissue were modelled in the FEM software COMSOL Multiphysics 5.2 (Comsol AB, Stockholm, Sweden).

2.2.1. DBS Leads

The lead geometry was based on the specifications from the corresponding manufacturing companies (Figure 1). Lead 3389 (Medtronic Inc., Minneapolis, MN, USA) and lead 6148

(St. Jude Medical Inc., Saint Paul, MN, USA) consist of four cylindrical platinum iridium alloy electrodes or contacts separated by 0.5 mm of insulating material. The contacts are 1.5 mm long except for lead 6148's distal contact which is 3 mm long and covers the tip of the lead. The lead 3389 has a diameter of 1.27 mm and a contact surface of 6 mm^2 while lead 6148 is 1.4 mm, with a contact surface area of 6.6 mm^2. The steering lead 6180 (St. Jude Medical Inc., Saint Paul, MN, USA) has the same dimensions as lead 3389 and similar disposition of the contacts except for the two middle contacts which are partitioned axially into three sections; a single segment of the split-ring contact has a surface area of 1.8 mm^2. SureStim1 lead (Medtronic Eindhoven Design Centre BV, Eindhoven, The Netherlands) also has a diameter of 1.27 mm and consists of 40 elliptical contacts of 0.66 × 0.74 mm^2 arranged on 10 rows of four contacts each, along the lead; each contact surface area is 0.39 mm^2 [2]. The stereotactic coordinates obtained from Surgiplan® from the co-registered postoperative CT along with the fiducial points of the preoperative MRI were used to calculate the Cartesian coordinates and the angle of the lead for the FEM mode. The first contact of the lead 3389 was placed at the lower point noted by the surgeon; lead 6148 and the steering leads' locations were adjusted to match the middle point of the active contacts.

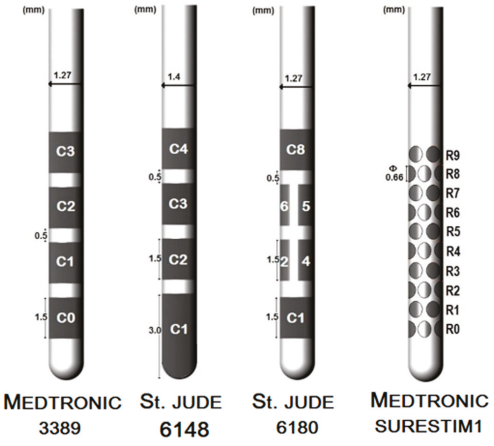

Figure 1. Representation of the conventional and the steering field leads.

2.2.2. Brain Tissue Model

Patient-specific brain tissue models were based on preoperative MRI. An in-house developed program (ELMA) [16,17] was used to convert the medical images into COMSOL FEM software readable files. With the ELMA tool, the preoperative image was cropped to a region of interest (Figure 2a), including the VIM and the ZI. Within that region, the tissue was classified into grey matter, white matter, blood or cerebrospinal fluid based on the image intensity values. Average intensity values were calculated from three slices of the preoperative image set. Finally, the electrical conductivity, σ, was assigned according to grey matter (σ = 0.123 S/m), white matter (σ = 0.075 S/m), blood (σ = 0.7 S/m) and cerebrospinal fluid (σ = 2.0 S/m). The corresponding electric conductivities for each tissue type were obtained from tabulated values [18,19] weighted with the spectral distribution of the pulse shape [20]. The conductivity for each voxel was calculated by an interpolation function which takes into account the effects of partial volumes, thus voxels with intensity levels between grey and white matter receive an electrical conductivity between grey and white matter. The result was a cuboid of about 100 mm per side (Figure 2b) containing the electrical conductivity values for each classified voxel of the preoperative MR image. The model included a peri-electrode space (PES) of 0.25 mm to mimic the electrode–tissue interface at the chronic stage [21]. The electrical conductivity assigned

to the PES corresponded to the white matter assuming its similarity to fibrous tissue (σ = 0.075 S/m) which is believed to wrap around the lead at the chronic stage [22].

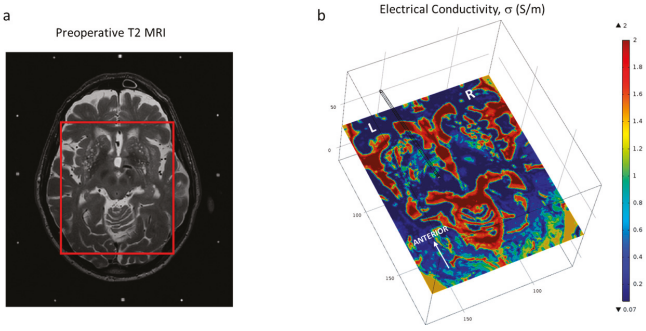

Figure 2. (**a**) Demarcation of the region of interest on the patient T2 MRI dataset (cauda-cranial point of view) and (**b**) Brain model displaying one slice of the interpolated conductivity matrix (cranio-caudal point of view) and the trajectory of the lead. Axial images displayed at the level of the ZI.

The electric field was calculated by the equation for steady currents:

$$\nabla \cdot \boldsymbol{J} = -\nabla \cdot (\sigma \nabla V) = 0 \ (\mathrm{A/m^3}) \quad (1)$$

where $\boldsymbol{J}$ is the current density ($\mathrm{A/m^2}$), V is the electric potential (V). For patient-specific models, σ corresponds to the interpolation matrix extracted by ELMA. For the homogeneous model, a single σ value corresponding to grey matter conductivity was considered for the whole brain tissue. The electrodes were set in a monopolar configuration where the active contact is considered as a voltage or current source and the outer boundaries are grounded (V = 0 V). For the conventional leads, the third contact (C2 and C3, for Medtronic 3389 and St. Jude 6148 respectively) was active. For SureStim1 eight consecutive electrodes corresponding to ring 6 and 7 were selected, and for the St. Jude 6180 lead the contacts 5, 6, 7 constituting the third ring were active. The active contacts of each lead were driven with either 3 V or 3.4 mA which is the equivalent current amplitude for Medtronic 3389 lead in a homogeneous model (σ = 0.123 S/m). The equivalent stimulation current value was considered as that required to achieve the same electric field to the one obtained with voltage control [11]. The inactive contacts were set to floating potential ($\int -\boldsymbol{n} \cdot \sigma \nabla V dS = 0 \ (A)$; $\boldsymbol{n} \times (-\nabla V) = 0 \ (V/m)$) and the non-conductive surfaces of the lead were set to electric insulation ($\boldsymbol{n} \cdot \nabla V = 0 \ (V/m)$) where $\boldsymbol{n}$ is the surface normal vector. The mesh applied was physics-controlled with a denser distribution around the leads. The mesh was set to the finest resolution available resulting in more than 2,000,000 tetrahedral elements (minimum element size of 0.026 mm). For the steering configuration, a single contact (C5) was selected for lead 6180 while for lead SureStim1, four contacts in a diamond configuration (two adjacent contacts from ring 6 and one contact from ring 5 and 7 anteriorly oriented) were active. The 3D models with ~3 million degrees of freedom were solved using the iterative COMSOL built-in conjugate gradients solver.

2.3. Neuron Model Simulations

An axon cable model was used in combination with the FEM model. A complete description of the neuron model is found in Åström et al. 2015 [14]. FEM modelling was completed for each lead design (n = 16) with a stimulation amplitude of 1 V or 1 mA for both homogenous and patient-specific brain tissue models for the VIM target. The electric potential was evaluated at the axial plane around the lead's third contact (Figure 3a). The potential lines were extracted from the medial, lateral, posterior and anterior locations from the axial plane. The potential along the 62 parallel lines separated

by 0.1 mm was exported and used as input data to the cable model to calculate the neuron activation distances. Simulations (n = 832) were performed for a fixed pulse width (60 μs) with variation in amplitudes (0.5–5 V in steps of 0.5 V; and 0.5–5 mA in steps of 0.5 mA) and variation in axon diameters (1.5–7.5 μm in steps of 0.5 μm) (Figure 3b).

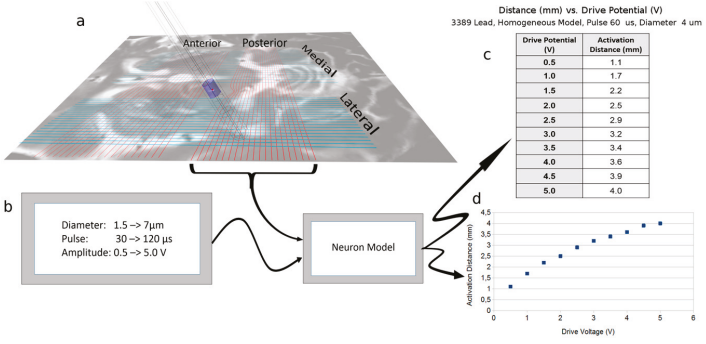

Figure 3. Neuron model application and single calculation run. (**a**) The voltage gradient extraction lines generated from FEM (COMSOL) simulation. The posterior lines have been replaced by the real potential values along the lines, as can be seen by the deviation of the line close to the electrode; (**b**) Input to the neuron model and the model block [14]; (**c**) Data points output from the Neuron model for the 3389 lead, with the specific input parameters of FEM output (homogeneous model and 3389 lead), pulse length of 60 μs, and neuronal diameter of 4 μm. The output is the distance from the surface of the lead to the distance where activation no longer happens; (**d**) The graphical implementation of the one data set.

2.4. Electric Field Simulations

FEM simulations of the electric field (n = 38) were performed in different stages setting to 3 V or 3.4 mA the third contact or equivalent as previously described. First, homogenous and patient-specific tissue models were investigated solely with lead 3389 (n = 6). Patient-specific simulations included two targets, the ZI and the VIM. Secondly, patient-specific models (one for each target, moving the leads accordingly, approximately 4 mm along the trajectory) were used to compare the electric field achieved by the four leads (n = 16) for the two operating modes. The patient-specific model of the actual implantation site in ZI was also used to investigate the EF achieved by lead 3389 with the actual stimulation 1.6 V, set four and a half weeks after implantation, which relieved the patient's symptoms. Simulations were also performed for the corresponding equivalent value in current mode (n = 4). At last, simulations with steering configurations for lead 6180 and SureStim1 were performed (n = 8). For investigation of the steering function, additional simulations (n = 4) were performed for St. Jude 6180 and SureStim1 and compared with the Medtronic 3389 lead.

2.5. Data Analysis

The neuron model simulation output is a table of activation distances (mm) which can be presented as plots against the stimulation amplitudes (Figure 3c,d). The average deviation in activation distances between the leads was calculated as mean ± standard deviation (S.D.) for 3 V and 3.4 mA stimulation amplitudes for all axon diameters simulated. An EF isolevel of 0.2 V/mm corresponding to an axon diameter of approximately 4 μm was selected to compare the activation distances between the leads.

The EF isolevel 0.2 V/mm was superimposed on the preoperative 3T MRI, and visualized at the axial, sagittal and coronal planes. The isocontours for each simulation were extracted in order to measure the maximal distance (mm) from the isocontour to the centre of the active electrode. A program in MatLab was developed for this purpose. COMSOL's integration function was used to

calculate the volumes (mm^3) inside the 0.2 V/mm EF isosurfaces for all leads. Relative differences in percentages were calculated for voltage and current control in order to compare the results for (I) homogeneous vs. patient-specific models; (II) 3389 lead vs. leads 6148, 6180 and SureStim1.

3. Results

3.1. Neuron Model Simulations

The selection of an EF isolevel of 0.2 V/mm was supported by the neuron model simulations (Figure 3) for an axonal diameter of 4.0 μm in both homogenous and heterogeneous tissue models (Figure 4a,b).

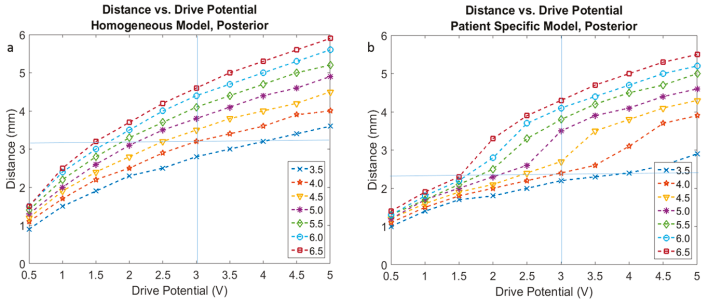

Figure 4. Activation distance plots based on FEM analysis for voltage driven lead 3389 with fixed parameters of 60 μs pulse width, drive potentials range of 0.5 to 5 V, and neuron diameters ranging from 3.5 μm to 6.5 μm. (**a**) Homogeneous tissue model and (**b**) patient-specific tissue model.

Figure 5 presents the activation distances at the posterior direction for all four leads in voltage (Figure 5a,c) and current modes (Figure 5b,d), as well as homogeneous (Figure 5a,b) and patient-specific (Figure 5c,d) brain models. Plots of the other three directions (anterior, lateral, medial) are part of the Appendix A (Figures A1–A3).

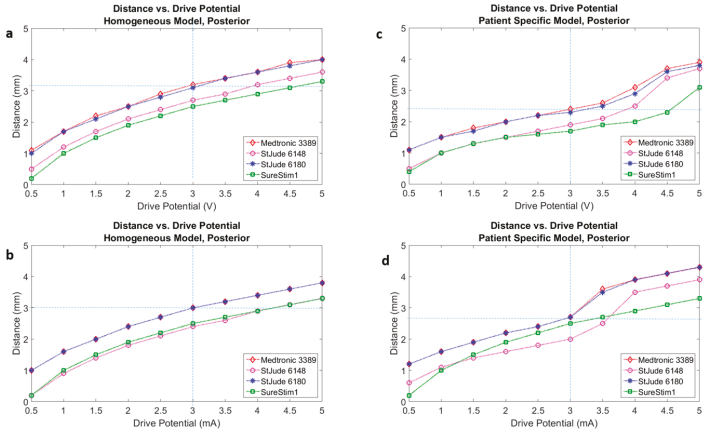

Figure 5. Activation distances for four leads mapped onto a single plot under the same test conditions of 60 μs pulse width, neuron diameter of 4 μm, configuration of all leads in 3389 lead single ring equivalent. (**a**) Homogeneous tissue model with voltage driven electrode; (**b**) Homogeneous tissue model with current driven electrode; (**c**) Patient-specific tissue model with voltage driven electrode; (**d**) Patient-specific tissue model with current driven electrode.

3.2. Homogenous vs. Patient-Specific Models

The electric field around the 3389 lead was compared for homogeneous and patient-specific models at the ZI and the VIM. Figure 6 shows the influence of the heterogeneity of the tissue. The EF extension for homogeneous tissue model was 3.3, 3.6 and 3.4 mm at the axial, sagittal and coronal planes, respectively, while for the patient-specific model the extension varied from 3.3 to 3.9 mm. The average EF distribution was 12% larger in current mode. This was valid for the three directions explored, in both anatomical regions investigated. The EF volumes achieved at the ZI were larger than those at VIM. The volumetric difference between targets (Table 1) was higher in current mode (12%) than in voltage mode (5%).

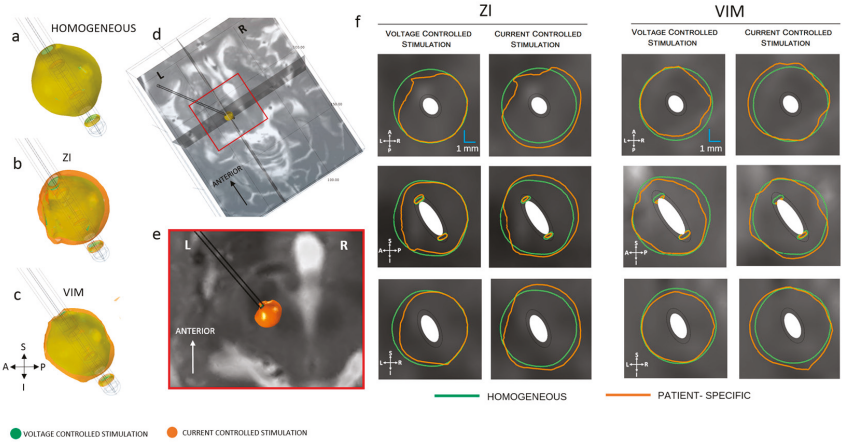

Figure 6. Electric field (EF) distribution (0.2 V/mm) in voltage and current control stimulation mode. (**a**) Homogeneous model (**b**) patient-specific model, ZI and (**c**) VIM; (**d**) Axial, sagittal and coronal cut planes, crossing at the middle point of the active contact (**e**) closer view of the axial plane of the preoperative MRI at the ZI and (**f**) electric field isocontours (0.2 V/mm) of lead 3389 for homogeneous and patient-specific brain models. EF obtained at 3 V (first and third column) and 3.4 mA (second and fourth column). A: anterior, P: posterior, S: superior, I: inferior, L: left, R: right.

Table 1. Homogeneous and patient-specific electric field (EF) volumes (<0.2 V/mm isosurface) achieved with different operating modes and the relative difference between each target and the homogeneous volumes.

Model	Voltage	Current	Voltage	Current
	Volumes (mm^3)	Volumes (mm^3)	Difference (%)	Difference (%)
HOMOGENEOUS	144	144	0	0
ZI	118.0	177.4	−18.0	22.9
VIM	111.0	160.5	−23.2	11.4

3.3. Lead Comparison

The EF volumes (Figures 7 and 8) within the 0.2 V/mm isosurface were approximately 49% larger for current controlled stimulation than for voltage mode. The relative difference of the EF volumes between the ZI and the VIM are shown in Table 2, for voltage and current controlled stimulation, respectively.

The electric field simulated for the four different lead designs was visualized at axial, sagittal and coronal planes crossing at the centre of each lead in the middle of the active contacts (Figure 9). The maximum extension of the 0.2 V/mm isocontour in voltage mode was achieved with lead 6148

while for current lead SureStim1 presented the largest EF extension. An example of the maximum EF spatial extension at the ZI, measured from the lead axis, is shown in Table 3.

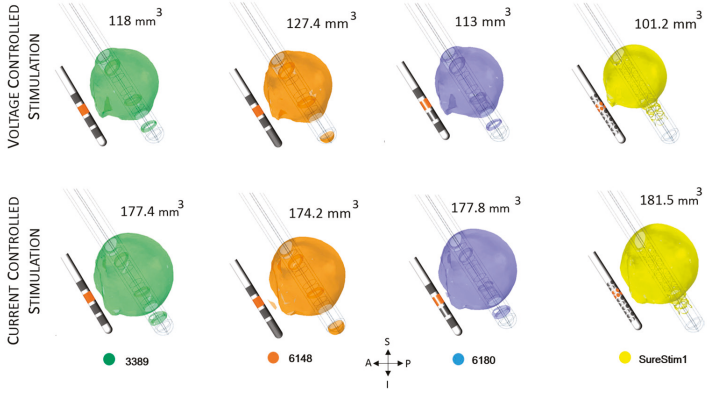

Figure 7. Electric field (EF) simulated at ZI for each lead depicted with an isosurface of 0.2 V/mm. Active contacts (shown in orange in each lead schematic) set to 3 V (first row) and 3.4 mA (bottom row). EF volume within the selected isosurface shown to the right of the lead. A: anterior, P: posterior, S: superior, I: inferior, L: left, R: right.

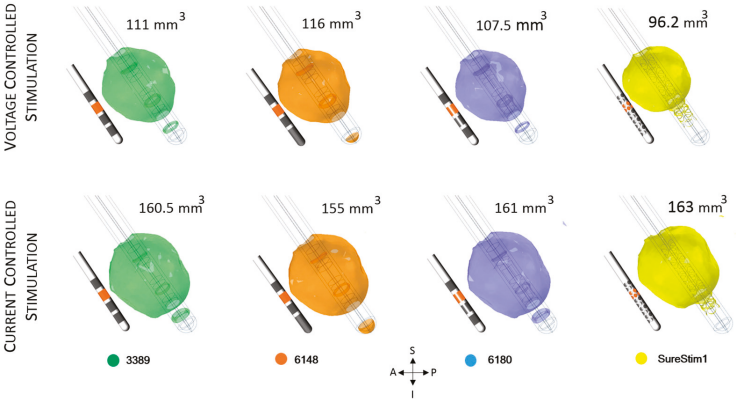

Figure 8. Electric field (EF) simulated at VIM for each lead depicted with an isosurface of 0.2 V/mm. Active contacts (shown in orange in each lead schematic) set to 3 V (first row) and 3.4 mA (bottom row). EF volume within the selected isosurface shown to the right of the lead. A: anterior, P: posterior, S: superior, I: inferior, L: left, R: right.

Table 2. Electric field (EF) volume determined by the 0.2 V/mm isosurface achieved by 3 V and 3.4 mA. Relative difference between the targets calculated for each operating mode.

Lead	ZI (mm^3)		VIM (mm^3)		Relative Difference (%)	
	Voltage	Current	Voltage	Current	Voltage	Current
3389	118.0	177.4	111.0	160.5	5.9	9.5
6148	127.4	174.2	116.0	155.0	8.9	11.0
6180	113.0	177.8	107.5	161.0	4.9	9.4
SureStim1	101.2	181.5	96.2	163.0	4.9	10.2

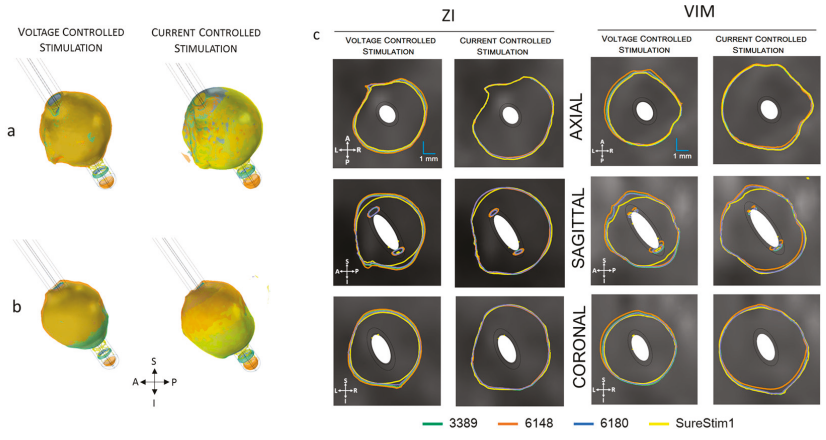

Figure 9. Electric field (EF) 0.2 V/mm isosurfaces achieved by each lead superimposed for each EF distribution of each lead operated in voltage (3 V) and current (3.4 mA). (**a**) EF isosurfaces at ZI in voltage (left) and current (right); (**b**) isosurfaces at VIM for voltage (left) and current (right); (**c**) Isocontours (0.2 V/mm) at the axial, sagittal and coronal planes. The cut planes for visualization were placed at the coordinates of the middle point of the active contacts. A: anterior, P: posterior, S: superior, I: inferior, L: left, R: right.

Table 3. Maximum spatial extension (mm) of the 0.2 V/mm electric field isolevel achieved at each plane for voltage (3 V) and current (3.4 mA) controlled stimulation for all leads. Measurements performed at the ZI.

Plane	3389		6148		6180		SureStim1	
	Voltage	Current	Voltage	Current	Voltage	Current	Voltage	Current
AXIAL	3.34	3.85	3.46	3.84	3.29	3.86	3.23	3.94
SAGITTAL	3.40	3.87	3.50	3.85	3.35	3.90	3.17	3.90
CORONAL	3.50	3.83	3.55	3.80	3.32	3.84	3.23	3.88

3.4. Patient-Specific Stimulation Amplitude Setting

The patient-specific simulation for the ZI using lead 3389, is presented in Figure 10. The equivalent amplitude for the patient-specific voltage of 1.6 V was 1.3 mA in current mode. This value achieved the most similar EF extension (~2.5 mm) and volume (46 mm^3) (Figure 10).

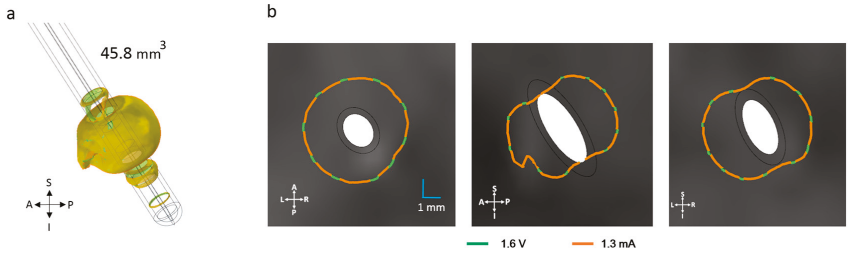

Figure 10. (**a**) Electric field (EF) distribution when the contact is set to 1.6 V and the equivalent current 1.3 mA (superimposed); (**b**) Isocontours for voltage and current superimposed. The maximal EF extent using an isolevel of 0.2 V/mm measured from the middle point of the active contact was 2.5 mm in all planes for both operating modes. A: anterior, P: posterior, S: superior, I: inferior, L: left, R: right.

3.5. Steering Function

The EF volumes within the 0.2 V/mm isosurface and the corresponding isocontours (Figure 11, Table 4) show that the EF distribution was notably different between operating modes for both leads. The spatial extension of the electric field was around 50% smaller in voltage mode. The smaller EF volumes are shown in Figure 11a,b. The axial and coronal views (first and third columns of Figure 11e) show the steering effect on the EF. The large EF distribution achieved by 3.4 mA did not show the steering effect (second and fourth columns of Figure 11e). The diamond configuration used for SureStim1 (1.6 mm^2 surface area) achieved larger EF volume (Figure 11b) than that using one contact of the 6180 lead (1.8 mm^2) for voltage mode. The opposite relation was observed in current mode, where 6180 lead achieved a larger EF volume (Figure 11d).

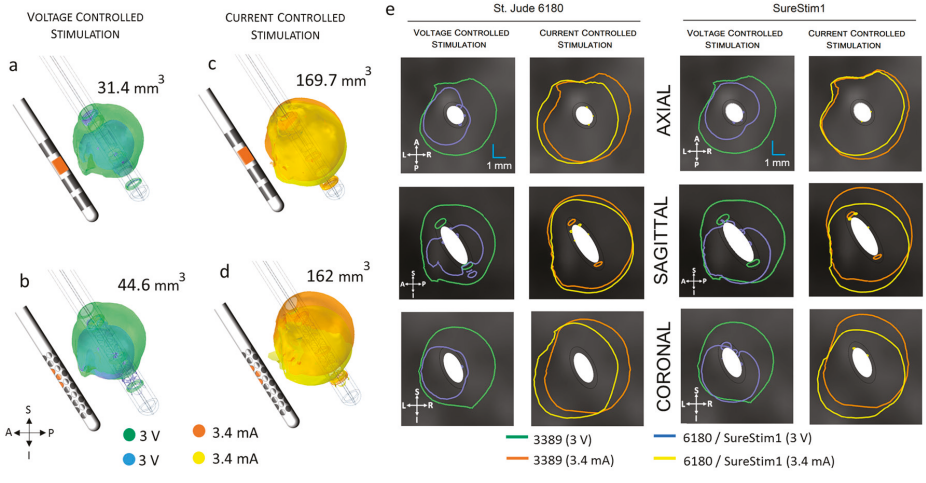

Figure 11. Comparison of the electric field (EF) isosurfaces (0.2 V/mm) at the zona incerta between the standard lead 3389 and the steering leads (active contacts shown in orange in the lead schematic). EF superimposed for lead 3389 (green/orange volumes) and (**a**) lead 6180 contact 5 active; (**b**) SureStim1 lead using the diamond configuration, operated in voltage mode (smaller volumes in blue); (**c**) Lead 6180 and (**d**) SureStim1 setting the contacts to current mode (EF volumes in yellow); (**e**) EF isocontours (0.2 V/mm) at the axial, sagittal and coronal planes for both leads operated in voltage and current mode. A: anterior, P: posterior, S: superior, I: inferior, L: left, R: right.

Table 4. Maximum spatial extension of the 0.2 V/mm electric field isolevel (mm) achieved by steering configurations. Relative difference between operating modes calculated for each lead.

Plane	6180		SureStim1		Relative Difference (%)	
	Voltage	Current	Voltage	Current	6180	SureStim1
AXIAL	2.80	4.18	2.51	3.65	49	45
SAGITTAL	2.92	3.95	3.18	4.46	36	40
CORONAL	2.68	4.54	3.15	4.69	69	49

4. Discussion

In this study, the influence on the electric field around DBS leads, from surrounding tissue and lead design, has been investigated by means of computer simulations. Both symmetrical and steering functions were considered and compared in current and voltage modes.

4.1. FEM and Neuron Modelling

The FEM models in this study have considered constant voltage and current amplitudes instead of the actual biphasic pulse used for the stimulation. This implies a quasi-static solution for the electric potential decoupled from the capacitive, inductive and wave propagation effects. Nevertheless, the conductivity values, for this FEM simulation method, took into consideration the frequency and pulse length components of the stimulation pulse [20]. The comparison of the leads relied on setting as many variables (e.g., isolevel, neuron diameter, pulse width, frequency, tissue variability, time points) to constant values. This results in an evaluation in a fixed environment where the differences in the achieved EF is sufficient to assess the leads. The selection of the 0.2 V/mm isolevel was initially based on previous studies by Hemm et al. [5] and Åström et al. [14]. However, the FEM model used by Åström did not consider the PES and used a homogenous model with a slightly different conductivity value for the grey matter. Therefore, the electric potential lines imported to the neuron model showed minor deviations compared to the previous study. The neuron simulations in the present study indicated that for neurons of 4 μm diameter, a 3 V drive potential reaches an activation distance of 3.2 mm. These results were tested against the FEM simulated EF extensions for one direction and plane, which support the EF isolevel of 0.2 V/mm in the patient-specific model.

Neuron diameter results were in the range of those found in [14,23–25], with consideration for driving parameter variations i.e., pulse width. FEM simulated EF extensions ranged from 3.3 to 3.5 mm in voltage mode. The FEM simulation values would imply a neuronal diameter between 4 and 5 μm. These diameters are at present a best guess at the true neuronal diameters in the vicinity of the electrode and should encompass a range of small diameters. As expected, the activation distance for the patient-specific model is distinct from that of the homogeneous model for all leads (Figures 5 and A1–A3).

A variation of 1 mm in activation distance with the working assumption of a 4 μm diameter neuron would result in an increase in neuron recruitment of approximately 250 extra neurons along a radius. For example, if the activation distance increases by 1 mm from 3 mm, the recruitment volume would change to the power of three, i.e., neuron activation expands significantly. An equivalent decrease in activation distance would result in a possible reduction of activated neurons along any radius from the centre of the volume. Calculating the activation distance in different directions (medial, posterior, anterior, lateral) allowed us to assess the influence of the lead's angle (trajectory) and thus the sensitivity to the direction (Figures 5 and A1–A3).

4.2. Homogeneous vs. Patient-Specific Tissue Models

The initial part of the study encompasses a comparison between homogeneous and patient-specific models for the standard 3389 lead in voltage and current modes. Several studies have shown the impact of the anisotropy and heterogeneity of the brain model. The McIntyre group [17] compared the axonal activation during monopolar DBS for different types of models, and concluded that simplistic models, such as the homogeneous model, overestimate the extent of neural activation. Åström et al. [12] observed an alteration of the electric field when the brain was modelled as heterogeneous isotropic tissue as opposed to homogeneous grey matter. These studies, however, were limited to voltage control stimulation. The novelty of the present study relies on the inclusion of current controlled stimulation. Our results show distinct behavior for each operating mode. The 3389 lead EF volume is smaller for the patient-specific model than for the homogeneous model in voltage mode. In current mode, on the contrary, the volume is larger. Furthermore, when comparing the EF volume between targets, the EF difference is larger in current stimulation (12% vs. 5% for voltage). The interest in using current controlled stimulation [26] partly relies on the consideration that it is the capacitive current that determines the neuronal effect; maintaining a constant current presumably would avoid the reprogramming of the DBS which normally occur for voltage controlled systems due to changes in the tissue impedance around the lead [4]. In agreement, the review by Bronstein et al. [24] considers the stimulation field as the electrical delivery which is a function of the voltage divided by the impedance, i.e., current.

The fundamental difference of this study is that the leads are evaluated in terms of the achieved EF and not in the current delivery. The results are numerically obtained considering Equation (1), where the EF is directly proportional to the current density and inversely proportional to the electrical conductivity obeying Ohm's law. The anisotropy of the tissue has not been included in the model, nevertheless with the introduction of tractography and white matter tracing [7,27], this feature will be important to consider in future simulations. Given that white matter is anisotropic, then the white matter tracing can help make the tissue conductivity classification even better.

4.3. DBS Leads Comparison

In the second part of the study, only patient-specific models were used to investigate the EF achieved by four different lead designs operated in voltage and current modes. The results of the simulations showed a very similar EF distribution around each lead, however SureStim1 showed a more spherically shaped EF distribution. In general, the EF extension and volume were higher using current mode and lower for voltage mode. The total current delivered by the electrode is determined by the electrode surface area and the average of the current density. Thus, applying a fixed total current of 3.4 mA to a smaller active area, as SureStim1 lead (3.12 mm^2) increases the current density, leading to an increase of the EF (Equation (1)). An experimental evaluation of segmented electrodes by Wei and Grill [28] showed that the electrode impedance was inversely proportional to its surface area. This implies that larger contacts would require higher current intensities to achieve the same EF than smaller electrodes. Another example of this behavior is lead 6148, which electrodes have the largest surface area (6.6 mm^2) achieving the smallest EF in current mode.

Several studies have compared the conventional steering leads either experimentally [29] or based on computer models [2,30,31]. In the experimental study, Contarino et al. [29] temporally inserted a 32 contact lead (similar to SureStim1) which was set with different configurations and current stimulation amplitudes ranging from 0.5 to 8 mA. The steering lead was then replaced by the permanent conventional 3389 lead. The performance of the steering lead was assessed by the current thresholds required to either induce side effects or clinical benefits in comparison to the conventional lead outcome in patients undergoing DBS surgery. By setting 12 consecutive contacts, the Contarino group observed equivalent current thresholds between the steering and the conventional leads. In the present study, eight consecutive electrodes achieved a larger EF volume than the 3389 lead when set to 3.4 mA, implying that choosing 12 contacts instead of eight would increase the difference with the conventional lead even more. This result reflects the influence of the smaller electrodes of SureStim1 lead.

Other computer based studies compared the steering and the conventional leads operated in either voltage or current mode. Martens et al. [2], for instance, investigated a lead of 64 contacts using eight consecutive contacts set to 2.6 mA and observed that a potential field distribution very similar to the generated by the standard ring electrode; our results showed a larger EF for SureStim1 in current mode. The difference between Martens' model and ours, is the brain model. While they consider homogeneous tissue with a single value of conductivity (0.1 S/m), we include a heterogeneous matrix of electrical conductivities. Dijk et al. [28] also compared the steering lead (SureStim1) to the conventional 3389 lead, however they quantified the stimulation effect in terms of the maximum amount of subthalamic nucleus (STN) cells activated based on axon models. They observed equivalent results between the standard and the directional lead by activating 12 consecutive contacts on the latter lead. In addition, this group used biphasic current pulses and neuron diameters of 5.7 μm. Due to the differences in the evaluation methodology and the model itself, our results are not directly comparable to the results of other groups.

4.4. Patient-Specific Stimulation Amplitude Setting

For the actual amplitude programmed, 1.6 V, the EF volume within the 0.2 V/mm isosurface was around 46 mm^3, and the extension was approximately 2.5 mm measured from the lead axis in all

directions. The clinical effect was satisfactory according to the patient journal, however, considering the dimensions of the ZI which has an elongated shape of approximately 2 mm (latero-medial) and 4–5 mm (anterio-posterior), a symmetrical stimulation field could possibly be improved by steering the field in the desired direction. The current amplitude required to achieve the same EF was 1.3 mA, which in comparison to the equivalence for the homogeneous model, indicates a larger impedance for the patient-specific model.

4.5. Steering DBS Leads

The steering function of lead 6180 and SureStim1 was evaluated in voltage and current mode. As for the symmetrical configuration, the EF was larger for current control. Setting 3.4 mA to a single contact of lead 6180 (1.8 mm^2) and to 4 contacts in SureStim1 (1.6 mm^2) derived in a large EF which did not show the directionality of the configuration. By reducing the current stimulation amplitude to 1.3 mA, it was possible to see the same steered profile as that for 3 V. The reason for this behavior is also due to the increase of the current density for smaller contact surface areas. In a similar way, the directionality of the configuration is not observable by lower EF isolevels. For instance, an isolevel of 0.1 V/mm did not show the steered field of 3 V. This is particularly interesting due to the uncertainty of the EF intensity required to activate neighboring neurons. The EF volumes achieved by each lead in the steering configuration do not follow the rationale of smaller surface area, larger EF due to higher current density. One of the reasons for this behavior could be that the active contacts do not have the same orientation. While the electrodes for SureStim1 are oriented towards the anterior part of the model, the single active contact for lead 6180 is oriented towards the lateral side. In voltage mode, the larger EF volume obtained with smaller surface areas may respond to the increase of the current density due to the higher number of edges [28]. Further investigations focused on different configurations for the steering leads are necessary to satisfactorily assess the performance of directional leads.

5. Conclusions

In conclusion, the use of brain models based on patient-specific images and the comparison of two operating modes have enhanced the assessment of the influence from the different lead designs on the EF with a fixed isolevel. The results showed that the EF distribution is influenced by the heterogeneity of the tissue for both operating modes. Computer models can visualize the electric field and thus further increase understanding when switching the stimulation settings, lead designs and inter and intra-patient conductivity variability.

Acknowledgments: The study was supported by the Swedish Research Council (621-2013-6078), the European Union's Seventh Framework Programme IMPACT (Grant agreement No. 305814) and the Parkinson Foundation at Linköping University. MRI and CT scanning were done at Centre for Medical Image Science and Visualization (CMIV) at Linköping University. Hubert Martens (currently at Medtronic Eindhoven Design Centre) for the development of the Sapiens Steering Brain Stimulation neuron model used in this study.

Author Contributions: Karin Wårdell and Peter Zsigmond initiated the study and did the overall planning. Fabiola Alonso, Karin Wårdell and Malcolm Latorre conceived and designed the simulations and analysis methodology. Fabiola Alonso performed and analysed the electric field simulations, and did art work. Malcolm Latorre performed and analysed the neuron simulations and did art work. Peter Zsigmond and Nathanael Göransson were responsible for imaging, planned and performed surgery and calculated targets for simulations. Fabiola Alonso and Karin Wårdell were main responsible for the writing. All other authors contributed to the writing with their special competence.

Conflicts of Interest: The authors declare no conflict of interest.

Appendix A

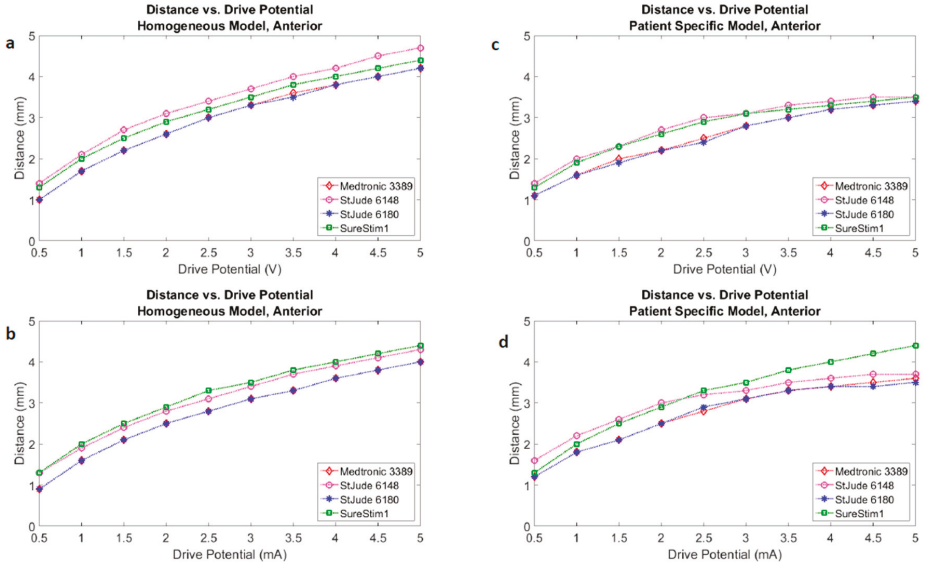

Figure A1. Neuron modelling: Distance vs. drive potential. Anterior.

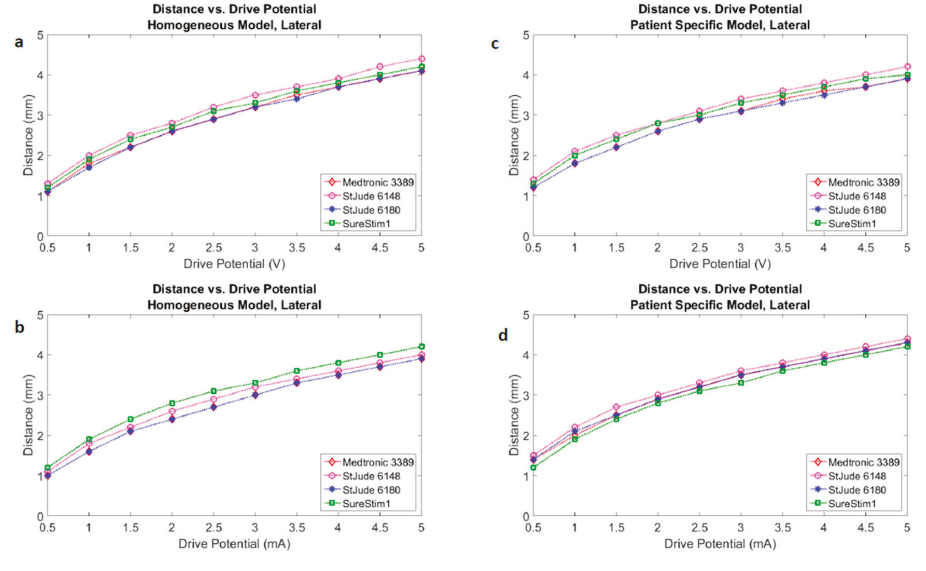

Figure A2. Neuron modelling: Distance vs. drive potential. Lateral.

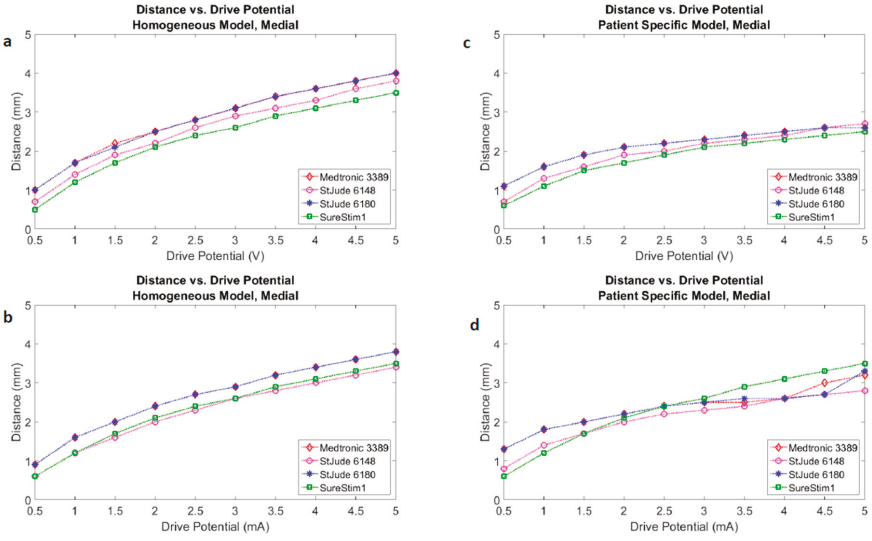

Figure A3. Neuron modelling: Distance vs. drive potential. Medial.

References

1. Hariz, M.; Blomstedt, P.; Zrinzo, L. Future of brain stimulation: New targets, new indications, new technology. *Mov. Disord.* **2013**, *28*, 1784–1792. [CrossRef] [PubMed]
2. Martens, H.C.; Toader, E.; Decre, M.M.; Anderson, D.J.; Vetter, R.; Kipke, D.R.; Baker, K.B.; Johnson, M.D.; Vitek, J.L. Spatial steering of deep brain stimulation volumes using a novel lead design. *Clin. Neurophysiol.* **2011**, *122*, 558–566. [CrossRef] [PubMed]
3. Mahlknecht, P.; Limousin, P.; Foltynie, T. Deep brain stimulation for movement disorders: Update on recent discoveries and outlook on future developments. *J. Neurol.* **2015**, *262*, 2583–2595. [CrossRef] [PubMed]
4. Gross, R.E.; McDougal, M.E. Technological advances in the surgical treatment of movement disorders. *Curr. Neurol. Neurosci. Rep.* **2013**, *13*, 371. [CrossRef] [PubMed]
5. Hemm, S.; Mennessier, G.; Vayssiere, N.; Cif, L.; El Fertit, H.; Coubes, P. Deep brain stimulation in movement disorders: Stereotactic coregistration of two-dimensional electrical field modeling and magnetic resonance imaging. *J. Neurosurg.* **2005**, *103*, 949–955. [CrossRef] [PubMed]
6. Åström, M.; Tripoliti, E.; Hariz, M.I.; Zrinzo, L.U.; Martinez-Torres, I.; Limousin, P.; Wårdell, K. Patient-specific model-based investigation of speech intelligibility and movement during deep brain stimulation. *Stereotact. Funct. Neurosurg.* **2010**, *88*, 224–233. [CrossRef] [PubMed]
7. Coenen, V.A.; Allert, N.; Paus, S.; Kronenburger, M.; Urbach, H.; Madler, B. Modulation of the cerebello-thalamo-cortical network in thalamic deep brain stimulation for tremor: A diffusion tensor imaging study. *Neurosurgery* **2014**, *75*, 657–669. [CrossRef] [PubMed]
8. Wårdell, K.; Kefalopoulou, Z.; Diczfalusy, E.; Andersson, M.; Astrom, M.; Limousin, P.; Zrinzo, L.; Hariz, M. Deep brain stimulation of the pallidum internum for gilles de la tourette syndrome: A patient-specific model-based simulation study of the electric field. *Neuromodulation* **2015**, *18*, 90–96. [CrossRef] [PubMed]
9. Butson, C.R.; Cooper, S.E.; Henderson, J.M.; McIntyre, C.C. Patient-specific analysis of the volume of tissue activated during deep brain stimulation. *NeuroImage* **2007**, *34*, 661–670. [CrossRef] [PubMed]
10. Chaturvedi, A.; Butson, C.R.; Lempka, S.F.; Cooper, S.E.; McIntyre, C.C. Patient-specific models of deep brain stimulation: Influence of field model complexity on neural activation predictions. *Brain Stimul.* **2010**, *3*, 65–67. [CrossRef] [PubMed]
11. Alonso, F.; Hemm-Ode, S.; Wårdell, K. Influence on deep brain stimulation from lead design, operating mode and tissue impedance changes—A simulation study. *Brain Disord. Ther.* **2015**, *4*, 3.
12. Åström, M.; Lemaire, J.J.; Wårdell, K. Influence of heterogeneous and anisotropic tissue conductivity on electric field distribution in deep brain stimulation. *Med. Biol. Eng. Comput* **2012**, *50*, 23–32. [CrossRef] [PubMed]

13. Schmidt, C.; van Rienen, U. Modeling the field distribution in deep brain stimulation: The influence of anisotropy of brain tissue. *IEEE Trans. Biomed. Eng.* **2012**, *59*, 1583–1592. [CrossRef] [PubMed]
14. Åström, M.; Diczfalusy, E.; Martens, H.; Wårdell, K. Relationship between neural activation and electric field distribution during deep brain stimulation. *IEEE Trans. Biomed. Eng.* **2015**, *62*, 664–672. [CrossRef] [PubMed]
15. Wårdell, K.; Hemm-Ode, S.; Rejmstad, P.; Zsigmond, P. High-resolution laser doppler measurements of microcirculation in the deep brain structures: A method for potential vessel tracking. *Stereotact. Funct. Neurosurg.* **2016**, *94*, 1–9. [CrossRef] [PubMed]
16. Wårdell, K.; Diczfalusy, E.; Åström, M. Patient-specific modeling and simulation of deep brain stimulation. In *Studies in Mechanobiology, Tissue Engineering and Biomaterials*; Springer Berlin Heidelberg: Heidelberg, Germeny, 2011; Volume 9, pp. 357–375.
17. Åström, M.; Zrinzo, L.U.; Tisch, S.; Tripoliti, E.; Hariz, M.I.; Wårdell, K. Method for patient-specific finite element modeling and simulation of deep brain stimulation. *Med. Biol. Eng. Comput.* **2009**, *47*, 21–28. [CrossRef] [PubMed]
18. Gabriel, S.; Lau, R.W.; Gabriel, C. The dielectric properties of biological tissues: II. Measurements in the frequency range 10 hz to 20 ghz. *Phys. Med. Biol.* **1996**, *41*, 2251–2269. [CrossRef] [PubMed]
19. Audreccetti, D.; Fossi, R.; Petrucci, C. Dielectric Properties of Body Tissue. Italian National Research Council. Available online: http://niremf.ifac.cnr.it/tissprop/htmlclie/htmlclie.htm#atsftag (accessed on 4 April 2016).
20. Wårdell, K.; Zrinzo, L.; Hariz, M.; Andersson, M. Patient-Specific Brain Modelling for Deep Brain Stimulation Simulation. In Proceedings of the 6th International IEEE/EMBS Conference on Neural Engineering proceedings, California, CA, USA, 6–8 November 2013.
21. Yousif, N.; Bayford, R.; Liu, X. The influence of reactivity of the electrode-brain interface on the crossing electric current in therapeutic deep brain stimulation. *Neuroscience* **2008**, *156*, 597–606. [CrossRef] [PubMed]
22. Nielsen, M.S.; Bjarkam, C.R.; Sorensen, J.C.; Bojsen-Moller, M.; Sunde, N.A.; Ostergaard, K. Chronic subthalamic high-frequency deep brain stimulation in Parkinson's disease—A histopathological study. *Eur. J. Neurol.* **2007**, *14*, 132–138. [CrossRef] [PubMed]
23. McIntyre, C.C.; Mori, S.; Sherman, D.L.; Thakor, N.V.; Vitek, J.L. Electric field and stimulating influence generated by deep brain stimulation of the subthalamic nucleus. *Clin. Neurophysiol.* **2004**, *115*, 589–595. [CrossRef] [PubMed]
24. Kuncel, A.M.; Cooper, S.E.; Grill, W.M. A method to estimate the spatial extent of activation in thalamic deep brain stimulation. *Clin. Neurophysiol.* **2008**, *119*, 2148–2158. [CrossRef] [PubMed]
25. Madler, B.; Coenen, V.A. Explaining clinical effects of deep brain stimulation through simplified target-specific modeling of the volume of activated tissue. *AJNR Am. J. Neuroradiol.* **2012**, *33*, 1072–1080. [CrossRef] [PubMed]
26. Bronstein, J.M.; Tagliati, M.; McIntyre, C.; Chen, R.; Cheung, T.; Hargreaves, E.L.; Israel, Z.; Moffitt, M.; Montgomery, E.B.; Stypulkowski, P.; et al. The rationale driving the evolution of deep brain stimulation to constant-current devices. *Neuromodulation* **2015**, *18*, 85–89. [CrossRef] [PubMed]
27. Ning, L.; Setsompop, K.; Michailovich, O.; Makris, N.; Shenton, M.E.; Westin, C.F.; Rathi, Y. A joint compressed-sensing and super-resolution approach for very high-resolution diffusion imaging. *Neuroimage* **2016**, *125*, 386–400. [CrossRef] [PubMed]
28. Wei, X.F.; Grill, W.M. Current density distributions, field distributions and impedance analysis of segmented deep brain stimulation electrodes. *J. Neural. Eng.* **2005**, *2*, 139–147. [CrossRef] [PubMed]
29. Contarino, M.F.; Bour, L.J.; Verhagen, R.; Lourens, M.A.; de Bie, R.M.; van den Munckhof, P.; Schuurman, P.R. Directional steering: A novel approach to deep brain stimulation. *Neurology* **2014**, *83*, 1163–1169. [CrossRef] [PubMed]
30. Cubo, R.; Åström, M.; Medvedev, A. Target coverage and selectivity in field steering brain stimulation. *Conf. Proc. IEEE Eng. Med. Biol Soc.* **2014**. [CrossRef]
31. Van Dijk, K.J.; Verhagen, R.; Chaturvedi, A.; McIntyre, C.C.; Bour, L.J.; Heida, C.; Veltink, P.H. A novel lead design enables selective deep brain stimulation of neural populations in the subthalamic region. *J. Neural. Eng.* **2015**, *12*, 046003. [CrossRef] [PubMed]

brain sciences

MDPI

Review

A Neurophysiological Perspective on a Preventive Treatment against Schizophrenia Using Transcranial Electric Stimulation of the Corticothalamic Pathway

Didier Pinault [1,2,3]

[1] INSERM U1114, Neuropsychologie Cognitive et Physiopathologie de la Schizophrénie, Strasbourg F-67085, France; pinault@unistra.fr; Tel.: +33-(0)3-6885-3245
[2] Unistra, Université de Strasbourg, Strasbourg F-67000, France
[3] Fédération de Médecine Translationnelle de Strasbourg (FMTS), Faculté de Médecine, Strasbourg F-67085, France

Academic Editors: Tipu Aziz and Alex Green
Received: 1 December 2016; Accepted: 24 March 2017; Published: 28 March 2017

Abstract: Schizophrenia patients are waiting for a treatment free of detrimental effects. Psychotic disorders are devastating mental illnesses associated with dysfunctional brain networks. Ongoing brain network gamma frequency (30–80 Hz) oscillations, naturally implicated in integrative function, are excessively amplified during hallucinations, in at-risk mental states for psychosis and first-episode psychosis. So, gamma oscillations represent a bioelectrical marker for cerebral network disorders with prognostic and therapeutic potential. They accompany sensorimotor and cognitive deficits already present in prodromal schizophrenia. Abnormally amplified gamma oscillations are reproduced in the corticothalamic systems of healthy humans and rodents after a single systemic administration, at a psychotomimetic dose, of the glutamate *N-methyl*-D-aspartate receptor antagonist ketamine. These translational ketamine models of prodromal schizophrenia are thus promising to work out a preventive noninvasive treatment against first-episode psychosis and chronic schizophrenia. In the present essay, transcranial electric stimulation (TES) is considered an appropriate preventive therapeutic modality because it can influence cognitive performance and neural oscillations. Here, I highlight clinical and experimental findings showing that, together, the corticothalamic pathway, the thalamus, and the glutamatergic synaptic transmission form an etiopathophysiological backbone for schizophrenia and represent a potential therapeutic target for preventive TES of dysfunctional brain networks in at-risk mental state patients against psychotic disorders.

Keywords: animal model; gamma frequency oscillations; glutamate; ketamine; network synchrony; *N-methyl*-D-aspartate; psychosis; sleep spindles; thalamic reticular nucleus; thalamus

1. Introduction

Neurobiological disorders of the brain are an immense burden with a rising cost in our societies [1,2]. In the European Union, about a third of the total population suffers from mental disorders [2], and we are still missing effective treatments, free of side-effects, against complex neuropsychiatric illnesses such as schizophrenia.

Schizophrenia is a progressive, debilitating mental illness characterized by a loss of contact with reality, personality disorders, mood symptoms, sensorimotor and cognitive impairments (DSM-5). This clinical disorganization and cognitive deficits are associated with abnormal anatomo-functional connectivity and disturbances in neural oscillations and synchrony in highly-distributed brain networks, including thalamus-related circuits [3–11]. Schizophrenia has a multifactorial etiology involving genetic,

neurodevelopmental, environmental and socio–cultural factors [12–15]. Therefore, the neurobiology of schizophrenia remains elusive. Its complex and multifactorial symptomatology has been driving multiple lines of research with diverse (genetic, immunological, metabolic, neurochemical, neurophysiological) hypotheses.

Most of the patients suffering from schizophrenia are treated with a combination of non-biological therapies (cognitive remediation, psychotherapies) and antipsychotic medications. These drugs are more effective against the positive than the negative symptoms of schizophrenia, and they induce serious adverse effects [16,17]. Because schizophrenia is characterized by multiple etiopathophysiological factors, does it make sense to have a treatment based principally on a "single receptor"? There is increasing evidence that the psychiatric disorders and the cognitive deficits of patients with schizophrenia are associated with and may be caused by dysfunction of highly-distributed systems displaying disturbed spatiotemporal activity patterns. Moreover, a recent meta-analysis demonstrated significant changes in whole brain network architecture associated with schizophrenia [18]. This supports the notion of functional interactions between multiple molecular, cellular and system pathways, which contribute to the multiple symptoms and cognitive deficits in schizophrenia [19]. So, would it not be more promising to use a therapeutic means that non-specifically modulates the ongoing global brain activity such as to re-establish normal brain function? The rationale behind the use of a non-specific therapeutic means in patients with schizophrenia is that the return to their normal brain function may especially alleviate the psychiatric disorders and dampen their emotion, sensorimotor and cognitive deficits. Deep brain stimulation (DBS) may be a promising alternative [20]. The challenge is immense given the complex symptomatology and pathophysiological mechanisms of schizophrenia (see below).

Davidson and colleagues [21] wrote: "To achieve the best therapeutic results in schizophrenia—like most other disorders—primary prevention is preferable to early and prompt treatment, which, in turn, is preferable to treatment of chronically established illness". This raises the questions when to apply the preventive treatment and what could be the appropriate treatment modality? Ideally, assuming that schizophrenia is caused by an aggressive agent (microbe, virus, parasite) during pregnancy, it would be great to have the infection type identified to proceed to the appropriate preventive asymptomatic treatment [22,23]. Moreover, there is increasing evidence suggesting that maternal immune stimulation during pregnancy can increase the risk of neurodevelopmental disorders such as schizophrenia [24–26]. Prenatal infection may lead to a developmental neuroinflammation, which would contribute to the disruption of the normal brain development leading to dysfunctional networks and abnormal behavior relevant to schizophrenia [27]. The corresponding neuroimmune and behavioral abnormalities might occur in response to stress in puberty [27,28]. Rodent models of maternal immune activation mimic both behavioral and neurobiological abnormalities, which are relevant to schizophrenia [28–31]. Interestingly, an early presymptomatic anti-inflammatory intervention during peripubertal stress exposure can prevent the schizophrenia-relevant behavioral and neurobiological abnormalities [28]. Nevertheless, there is a real need to treat high-risk patients for whom the causes of their mental state remain unknown. That is why in the present review, I will present a neurophysiological perspective on a preventive symptomatic treatment in patients with premorbid and/or prodromal manifestations and bioelectrical markers of latent schizophrenia.

A universal property of brain networks is to produce electric currents, conveyed by the movement of ions across cellular membranes, whatever the pathophysiological context may be. Moreover, both the normal and the unhealthy brain can generate normal and abnormal brain rhythms [32]. Importantly, almost every cognitive task is associated with event-related electroencephalographic (EEG) oscillations [33]. We will see that disturbances in brain rhythms are common in patients with schizophrenia. So, can exogenous electricity correct or re-normalize abnormal brain oscillations and, in parallel or as a result, the related mental, emotional, sensorimotor and cognitive disorders? Numerous clinical interventions have demonstrated the benefits of brain

electrical stimulation methods in patients with neurobiological disorders resistant to available pharmacological treatments.

There is increasing evidence that exogenous electric currents can modulate not only brain electrical activity but also behavioral and cognitive performance, giving hope for treating complex neuropsychiatric illnesses. Moreover, schizophrenia patients with auditory hallucinations that are unresponsive to antipsychotic medications can be treated with transcranial magnetic stimulation (TMS) [34,35] or transcranial electric stimulation (TES) [36–40]. Ongoing research aims to develop such noninvasive neurophysiological therapies as a routine therapy [40–42], which may be more promising than DBS (see below). The exponents of noninvasive technologies now face a huge challenge to develop and refine an efficient therapeutic, free of side-effects, neurophysiological method that treats schizophrenia in its entirety, that is, to treat all its core features, including positive, negative and mood symptoms, and the decline in cognitive abilities (memory and thinking skills). Although there is accumulating evidence that TES techniques are reliable and versatile therapeutic options, a certain number of questions remains open regarding their anatomical targets and the neural mechanisms underlying their clinical impact.

The development of the chronic character of schizophrenia takes years following the occurrence of prodromal symptoms with cognitive declines and first-episode psychosis [43–45]. Longitudinal studies in at-risk mental state individuals and the duration of untreated psychosis offer a time window to identify predictive biomarkers, to better understand the etiopathophysiology of schizophrenia and to develop innovative therapies [44]. It would be ideal to have a therapeutic neurophysiological modality, for instance, a weak TES (see below) applied in at-risk individuals, capable of stopping the occurrence of first-episode psychosis and chronic schizophrenia. This exciting idea has already received increasing interest during at least the last two decades [43,46–48].

Electro- and magneto-encephalographic oscillations are natural bioelectrical markers of the functional and dysfunctional state of brain networks [4,49]. Spontaneously-occurring gamma frequency (30–80 Hz) oscillations (GFO) of cortical origin, naturally implicated in attention and integration processes, are excessively amplified not only during hallucinations [50–53] but also in first-episode psychosis and in at-risk mental states for psychosis [54–57]. Such abnormally amplified GFO can be reproduced after a single systemic administration, at a psychotomimetic dose, of the glutamate *N-methyl*-D-aspartate receptor (NMDAR) antagonist ketamine in the corticothalamic (CT) systems of healthy humans [58] and rodents [59–62]. These translational models of first-episode psychosis highlight one important factor, glutamate synaptic transmission, which may be altered in individuals at high risk of developing psychotic disorders [63]. Also, disturbances in sleep and reductions in EEG sleep spindles in first-episode psychosis and early-onset schizophrenia [3,64–67] support the hypothesis that the thalamus plays a critical role in the pathogenesis of schizophrenia.

Therefore, in the present essay, I put forward the notion that the CT pathway, the thalamus, and glutamate synaptic transmission might together represent the backbone etiopathophysiological mechanism of chronic psychotic disorders. This mainstay mechanism may be a prime target for early therapeutic intervention using TES techniques, more specifically targeting the CT pathway. First of all, I will start with a discussion about possible anatomical targets for late therapeutic electrical stimulation in patients with advanced schizophrenia. Then, I will provide an overview of therapeutic neurophysiological procedures and will develop a theoretical proposal on how we may understand the mechanisms underlying the effects of TES of the cerebral cortex with a focus on the CT pathway. It is worth specifying that, in the present survey, the rodent is our predilection animal since its neural networks share common anatomo-functional properties with those of humans.

2. Is There an Anatomical Target for Advanced Schizophrenia?

It is extremely challenging to find the correct or best anatomical target(s) for the use of invasive or non–invasive electrical stimulation of brain networks as last resort treatment of complex mental-health disorders, such as schizophrenia. For instance, low-frequency TMS of

the left temporoparietal cortex can reduce positive symptoms, especially self-reported auditory hallucinations [34,68,69]. Although there is evidence that TMS can enhance cortical synchrony, improve cognitive performance [70,71], and is safe and free of cognitive side-effects, further investigations are however required to identify both the anatomical target(s) and the stimulation settings that would lead to an efficient treatment against both positive and negative symptoms of schizophrenia [72,73].

In contrast, applying DBS at the seemingly best anatomical target might not be free of side-effects. For instance, it is well known that DBS treatment in the subthalamic nucleus can not only alleviate essential and Parkinson disease tremors but also reduce symptoms in patients suffering from severe forms of obsessive compulsive disorders, providing encouraging findings that are corroborated by animal studies [74]. Even if the subthalamic nucleus might be an effective target for the treatment of behavioral disorders that include emotional, cognitive, and motor impairments [75], its use in patients experiencing severe psychiatric disorders with limited therapeutic options remains questionable.

Patients who severely suffer from advanced psychiatric disorders, and who are refractory to medication, must benefit from a new efficient therapeutic approach, and DBS may be a promising alternative. Goodman and Insel [20] recently put emphasis on the fact that the pace of DBS being used against seriously advanced neuropsychiatric disorders is accelerating, giving the incentive both basic and clinical researchers need to concentrate their efforts on the road ahead. However, are we actually ready to use DBS against severe and ultra-complex mental-health disorders? Schizophrenia, as a typical example, is a multidimensional and multifactorial illness, raising an important question as to whether or not DBS could alleviate both the negative and the positive symptoms in all schizophrenic patients who urgently need a new effective therapy [76]. Could both the anatomical target and the DBS settings used in any specific patient be also generally applied to other very problematic patients? The challenge is immense because of the existence of several types of schizophrenia [77]. Finding a unique effective therapy against all types of schizophrenia presupposes that they all share common etiopathophysiological mechanisms. In psychiatry, DBS may be effective in combination with commendable clinical practices [78,79]. Therefore, the use of non–human animal and network models remain a versatile means to develop therapeutic concepts and to understand the neural mechanisms of electrical neuromodulation used in diverse interventions.

Reliable and reproducible non-human animal models of schizophrenia do not exist, and any model for schizophrenia remains questionable with its strengths and limitations [80–83]. Indeed, schizophrenia belongs to a group of hyper-complex mental-health disorders. So, how to model the heterogeneity of the causes, the progression, the multiple clinical symptoms of chronic schizophrenia, and of the changes elicited by years of medication? The critical problem in finding an efficient treatment of schizophrenia is due to the challenge in modeling psychiatric disorders, which depends on the lack of information about their etiology and pathophysiology.

So, what would be a "good" model of or for advanced schizophrenia (untreatable using the currently available therapeutic means) suitable to develop a therapeutic concept based on the use of invasive or noninvasive electrical stimulation of the appropriate neural networks? In theory, one may believe that an animal model that is not validated as being a good model for schizophrenia but that is validated as being a good model for a measurable, singular pathophysiological behavioral trait (e.g., violent behavior, catatonia) similar to that observed in advanced schizophrenic patients and that often makes it to the headlines of newspapers [84–86], may have an added value to investigate the efficacy of a therapeutic treatment using DBS in clinical trials. Again, validation of such a concept (reversal of the behavioral/pathophysiological trait by DBS) should rest on well identified anatomo-pathophysiological mechanisms, and they should be conducted along with appropriate ethical guidelines.

Animal models are, however, all potentially useful as long as they are precisely described, and as the related working hypotheses are clearly formulated. This critical view is still a matter of discussion [80,81,83,87,88]. So, along these lines, any model can be a versatile tool to explore the multiple facets concealed by healthy and sick brains. The challenge is indeed to find

convergences across models and patients, at least in terms of symptoms and neural dysfunction. Then comes the question of how animal models can be used to discover the appropriate therapy? Neurodevelopmental rodent models, based on prenatal immune activation, which present at the adult stage schizophrenia-relevant behavioral and neurobiological abnormalities [89–91], may be promising. Indeed, it was recently demonstrated that a preventive, presymptomatic anti-inflammatory treatment during peripubertal stress exposure can prevent the abnormal behavior and the biomarkers of the neuroimmune abnormality [28]. However, there is a real need to find an appropriate treatment of psychosis for high-risk patients for whom the causes of their mental state remain unknown.

Also, if we have known the etiological cause(s) of a given patient suffering from schizophrenia for many years, would we be able to find the appropriate treatment that alleviates simultaneously the positive and negative symptoms and the cognitive and emotional disorders? For the time being, we face the absolute necessity to understand the etiology and pathophysiology of schizophrenia at the molecular, cellular and systems levels, with the dream to find an effective, asymptomatic or symptomatic treatment free of side-effects.

3. Overview of Therapeutic Neurophysiological Procedures: DBS versus TES

Since the middle of the 20th century, invasive and noninvasive neurophysiological approaches have been attracting increasing interest as means of last resort treatments against advanced neurological and mental illnesses that are resistant to currently available therapies. Deep brain electrical stimulation has evolved as an invasive, stereotaxic-guided [92] and neuroimaging-guided [93] neurophysiological treatment when drug therapy no longer provides relief from symptoms accompanying severe neurological and psychiatric disorders. It is now used to treat other severe brain disorders in patients resistant to pharmacological mono- and polytherapy, including Parkinson's disease [94,95] epilepsy [96], dystonia [97], obsessive-compulsive disorders [74], pain [98,99], multiple sclerosis [100], depression [101,102] and Tourette syndrome [103]. It is also used in brain-injured patients in vegetative and minimally conscious states [104]. Although therapeutic DBS is applied along with the rules of the art and ethics [105], its use can be accompanied by psychiatric complications [106,107]. The neural mechanisms underlying the effects of DBS are complex and little known [108,109].

Since the end of the 20th century, TMS has emerged as a tool to study the human brain and an efficient noninvasive therapeutic means against depression [110], schizophrenia [34,35], addiction [111] and other neurological and psychiatric disorders [42]. However, there is a need to optimize the TMS protocols for routine clinical practice. TMS excites or inhibits the activity of cortical nerve cells and the dynamics and plastic properties of neural networks through the influence of electric currents that are induced by changing magnetic fields. Repetitive TMS modulates in a frequency-dependent manner the excitability of the cortical circuits [112]. Regarding schizophrenia, although TMS is efficient in treating auditory hallucinations [34,68,69], a major issue is to find the anatomical target and the TMS settings that allow treating the disease in its entirety, that is, to alleviate all the negative and positive symptoms, mood disorders and cognitive deficits.

Since the beginning of the 21st century, three principal TES techniques, forms of noninvasive and less aggressive neurophysiological modulation, have been increasingly used in cognitive neurosciences and interventional approaches [37,40]: transcranial direct current stimulation (tDCS), alternating current stimulation (tACS), and random noise stimulation (tRNS). Transcranial electrical stimulations safely apply, via scalp electrodes, a weak electrical current to modulate the physiological or pathological cortical and subcortical activities of healthy subjects or patients suffering from severe mental disorders [113]. Such TES techniques can modulate synaptic plasticity and related genes [114]. It seems not yet clear whether the application of TES on the frontal cortex of patients with schizophrenia can bring significant beneficial effects [115]. However, tDCS applied over the left frontotemporal cortex of schizophrenia patients with disabling treatment-resistant symptoms reduces both the auditory verbal hallucinations (~30%) and the abnormal resting-state hyperactivity between the left temporoparietal junction and the anterior insula [116]. When applied to the temporoparietal cortex of schizophrenia

patients with medication-refractory auditory verbal hallucination, tDCS can not only decrease the severity of the hallucinations but also ameliorate some negative and positive symptoms [117]. tDCS is a static current that polarizes the membrane potential of the neuronal elements of the target cortical volume [118,119] whereas tACS modulates, in a frequency specific manner (within the EEG frequency range), ongoing cortical neural oscillations [120,121]. There is increasing evidence that tDCS can induce memory enhancement in healthy subjects, in patients with psychiatric and neurological disorders, and in animal models [122]. In contrast to tDCS, tACS can modulate, more directly, not only the firing of the nerve cells but also their oscillations and synchrony [40]. In a subpopulation of patients with schizophrenia, tDCS can be efficient in the reduction of refractory verbal hallucinations but also of positive and negative symptoms [116,117]. Interestingly, an imperceptible alternating current (peak-to-peak: 750 μA) applied at the gamma frequency (40 Hz) to the frontal cortex can enhance cognitive performance during logical reasoning [123]. Also, gamma frequency (25–40 Hz) tACS applied on the frontotemporal cortex of subjects during REM sleep influences ongoing brain activity and induces conscious awareness, making it possible for the dreamer to be lucid of his or her dream and to have control of its content [124]. Gamma frequency oscillations are well known to be prevalent during REM sleep [125]. It was recently shown that gamma tACS of the human motor cortex increases motor performance during a visuomotor task [126]. Concurrent functional magnetic resonance imaging has revealed neural activity changes underneath the stimulation electrode and in related brain networks, including the prefrontal cortex [126]. On the other hand, alpha frequency (10 Hz) tACS applied over the occipitoparietal cortex reduced cognitive performance in a visual task [127]. The effects of tACS on brain network oscillations and on behavior are critically discussed in a comprehensive review article [128]. tRNS is an alternating current stimulation technique with a wide-band stimulation frequency (up to 640 Hz) [129]. It has been shown to increase neuroplasticity during perceptual learning [130].

In summary, TES techniques appear promising for clinical interventions. They are safer than DBS techniques and less expensive than TMS. TES is also more appropriate than DBS as a preventive treatment modality against schizophrenia because it is noninvasive and almost free of side-effects. In addition, the efficacy of TES techniques to modulate brain activities and to influence cognitive performance have been demonstrated. The mechanisms underlying their effects, however, remain still elusive. Also, more research and clinical trials are necessary to attain, during routine clinical practice, consistent benefits for patients suffering from debilitating mental illnesses. Importantly, emerging clinical interventions have shown that TES therapeutic modalities can reduce essential tremors in patients suffering from Parkinson's disease [131,132]. So, one can easily imagine that the noninvasive and low-cost TES techniques might supplant invasive DBS methods.

4. Three Candidates for Preventive TES

As mentioned above, it is extremely challenging to make a decision for a late therapeutic neurophysiological intervention in treatment-resistant advanced schizophrenia. The development of chronic forms of schizophrenia takes years after the occurrence of prodromal symptoms, cognitive declines and first-episode psychosis [45,133–138]. So, would it be possible to prevent or to delay the progressive development of chronic schizophrenia? Early therapeutic intervention is a notion that has been around with increasing interest during the last two decades [44,46,47,139]. Indeed, the complex symptomatology of schizophrenia results from progressive abnormalities of brain networks, including the thalamus with its reciprocal connections with the cerebral cortex [11,140–142]. Even if cognitive impairments are relatively modest during the prodromal phase of schizophrenia [137,143], efficient early therapeutic intervention could stop or delay the onset of psychotic disorders, which might otherwise lead to further cognitive damage and impaired daily functioning [144–146].

A preventive treatment against schizophrenia of course requires a better understanding of the evolution of the clinical disorganization and of the cognitive changes that can be observed from premorbid to first-episode psychosis [136,143,147]. The great challenge is to

identify the time window when the very first clinical symptoms and cognitive declines start to occur in individuals who will actually develop schizophrenia [143]. The "primary" factor(s) responsible for the progressive neural changes leading to chronic forms of schizophrenia remain to be identified. Whatever the preventive neurophysiological therapy implies, it should target an etiopathophysiological mechanism that is at the root of the mental disorders. Multiple diverse (genetic, epigenetic, neurodevelopmental, immunological, environmental, socio-cultural) factors are thought to be (either in isolation or through interactions), the cause of schizophrenia [14,148–155]. This is a long–standing debate that is not discussed in the present essay. Here, I highlight recent findings supporting the glutamate neurotransmission hypothesis of schizophrenia, which implicates critical etiopathophysiological mechanisms that appear early during its progressive development. Here, it is assumed that these processes are common to several types of chronic schizophrenia during the prodromal phase.

Glutamate is one of the main neurotransmitters of the thalamus, an essential subcortical structure involved in sensory discrimination, motor and cognitive processes. It is worth mentioning that more than 80% of the thalamic neurons are glutamatergic and they are massively innervated by the CT neurons, which are also glutamatergic [156]. Importantly, there is compelling evidence that multiple and diverse abnormalities (glutamate receptors, transporters and associated proteins; NMDAR–associated intracellular signaling proteins, and glutamatergic enzymes) related to the glutamate transmission have been found in the thalamus of patients with schizophrenia [157]. Furthermore, in the following, we describe compelling evidence that the pathogenesis of first–episode psychosis can be better modeled translationally than chronic forms of schizophrenia. Therefore, we will also demonstrate that the thalamus might be an interesting target for TES, directly and indirectly via the glutamatergic CT pathway, designed for early therapeutic intervention against first-episode psychosis and chronic forms of schizophrenia.

4.1. The Corticothalamic Pathway and the Thalamus

The thalamus, located around the third ventricle, is reciprocally connected with the cerebral cortex and it receives inputs from the cerebellum, the basal ganglia, the brainstem and basal forebrain [158]. The thalamus is an essential relay and plays an integrative role for ongoing and function-related cortical activities [159]. It relays information to multiple regions of the cerebral cortex in a bottom-up (from the external world via the sensory receptors) and a top-down (from the cerebral cortex) fashion. During sensory discrimination, sensorimotor integration and cognitive processes, the information circulates along the glutamatergic CT and thalamocortical (TC) pathways [160]. The thalamus is implicated in multiple functions: sensory perception (visual, somatosensory, auditory), sleep, wakefulness (through the ascending activating system), pain, attention and consciousness [156]. It is also implicated in many neurological and psychiatric diseases, including Alzheimer's disease, Parkinson disease, epilepsy, schizophrenia, autism, bipolar disorders, chronic pain and major depression. Damage to the thalamus can cause very long-lasting (>3 years) or permanent coma [161,162]. The thalamus is also the anatomical target of therapeutic DBS methods [104,163,164]. The specific prethalamic (or peripheral) inputs of the sensory systems innervate both the specific or first-order (primary sensory) and the non-specific or higher-order (associative and cognitive) thalamic nuclei. First- and higher-order thalamic nuclei relay information to the granular and the supra- and infragranular layers of the neocortex, respectively [160].

TC neurons, the principal neurons of the thalamus, are glutamatergic and their axon relays thalamically processed signals to the cerebral cortex (Figure 1A). In contrast to the CT pyramidal neurons, the TC neurons do not communicate with each other. The TC axons give rise to en passant collaterals in the GABAergic thalamic reticular nucleus (TRN)—a thin layer that covers the lateral walls of the dorsal thalamus—which is the principal source of GABA receptor-mediated inhibition of TC neurons [165]. The TC-related information is also computed in vertical (within the cortical column) and horizontal (between columns) cortical networks, linked with other cortical (distant areas) and subcortical structures (e.g., striatum, amygdala, and hippocampus;

Figure 1B). Intracortically-computed information reaches the thalamus via CT axons. Thereby, both the thalamus and the cerebral cortex work together in concert through their topographically organized reciprocal connections, which form intermingled feed-forward and closed-loop CT-TC circuits [156,166]. The CT pathways are of two types, one originating in layer V and the other in layer VI.

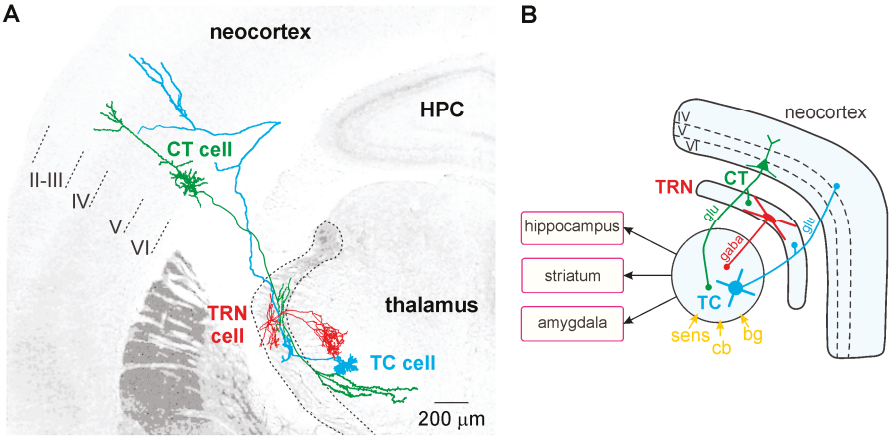

Figure 1. The principal anatomical features of the rodent cortico-reticulo-thalamocortical (CT-TRN-TC) system. This is the principal CT-TRN-TC system that is common to first- and higher-order thalamic nuclei. (**A**) Mounting of reconstructed juxtacellularly-labelled neurons of the rat primary somatosensory system. Both the CT (in green) and the TC (in blue) neurons are glutamatergic (glu) and their principal axon crosses the TRN where it gives rise to axon collaterals. The TRN neuron is GABAergic (gaba) and innervates only the TC neurons of the dorsal thalamus principally through lateral inhibition. (**B**) In this schematic drawing of this 3-neuron circuit, the principal afferents (bg, basal ganglia; cb, cerebellar; sens, sensory) and efferents of the dorsal thalamus are indicated, the TRN being part of the ventral thalamus.

The GABAergic TRN is an inhibitory interface strategically located between the thalamus and the neocortex [165,167]. It is innervated by glutamatergic TC and layer VI CT inputs (Figures 1 and 2). TRN cells have dendro-dendritic synapses to communicate among each other [168–171] (Figure 2). The TRN is also characterized by an important intrinsic network of chemical (GABAergic) and electrical synapses [172,173], which can effectively be influenced by the layer VI CT pathway [174–176]. The hodology and the innervation pattern of the CT-TRN-TC circuit strongly indicate that the GABAergic TRN neurons are implicated in both top-down and bottom-up processing, suggesting that the TRN might play a central role in attentional processes [165]. Moreover, lesions of the TRN lead to attentional deficit [177,178]. Their axonal projections are topographically organized and form open-loop connections with the related TC neurons, the anatomical substrate of lateral inhibition in the thalamus [179,180]. Thereby, TRN neurons can modulate, in a coordinated fashion, the TC activities that are relevant for attention and integration processes. In schizophrenia, disorders of thalamic lateral inhibition are thought to disturb the pattern of TC activity on the way to the cerebral cortex [8,181]. Importantly, GABAergic TRN neurons are endowed with powerful oscillatory properties (see below).

The layer V CT pathway selectively innervates the higher-order thalamic nuclei in a focal manner (like a driver input). Like the peripheral inputs, it does not innervate the TRN, in contrast to the layer VI CT pathway. This layer V CT pathway is an essential element in cortico-cortical (or transthalamic) circuits, which parallel direct cortico–cortical connections [159]. The principal axon of layer V CT neurons also innervates motor centers in the brainstem and spinal cord. The axonal branch that innervates the thalamus conveys corollary discharges used to modulate imminent sensorimotor

processing [159,182,183]. In fact, corollary discharges might be disturbed in schizophrenia [184–186]. Both layer V and VI CT pathways are assumed to work together in synergy from the very first stages of sensorimotor processing up to subsequent higher cognitive and motor processes.

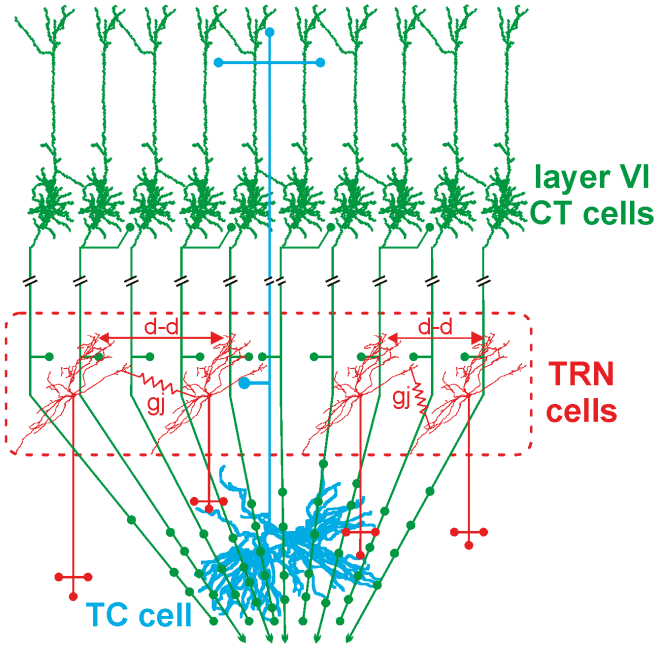

Figure 2. The layer VI corticothalamic (CT) neurons outnumber the thalamocortical (TC) neurons by a factor 10. As a consequence, the glutamatergic CT neurons exert a widespread and powerful excitatory influence on the first- and higher-order thalamic nuclei. Layer VI CT axons innervate other layer VI CT neurons via recurrent axon collaterals. In contrast, the glutamatergic TC neurons do not communicate among each other. The GABAergic TRN cells use dendro-dendritic chemical (d-d) and electrical (gj, gap-junction) synapses to communicate among each other.

The layer VI CT pathway plays an essential role in attentional and integrative processes [8,187–189]. This CT pathway innervates the TRN and the related first- and higher-order thalamic nuclei [156,159]. This pathway exerts a massive (about ten–fold stronger than the corresponding TC pathway) [190] and regional innervation within large thalamic territories (Figure 2). Cortical layer VI contains a heterogeneous population of neurons [191–193]. The layer VI CT pathway is the major glutamatergic output, which is reciprocally connected with TC neurons [188,194]. Layer VI CT apical dendrites and axon collaterals terminate in layer III–IV [188,193]. Their axon collaterals are implicated in both excitatory and inhibitory feedback mechanisms in layer IV [195,196]. Layer VI CT axons innervate other layer VI CT neurons [197,198]. Their apical dendrites can perform active integration of synaptic inputs via dendritic spiking [199]. There is anatomical evidence that some dendritic spines of neocortical pyramidal neurons are simultaneously innervated by GABAergic and glutamatergic inputs from local–circuit cells and TC neurons, respectively [200]. Thereby these GABAergic inputs can gate the synaptic impact of the incoming TC inputs on the pyramidal neurons. Layer VI CT neurons mediate most of their excitatory neuronal transmissions through the activation of ionotropic (NMDA and AMPA) and metabotropic glutamate receptors in both the cortex and the thalamus [201]. Interestingly, Layer VI CT neurons innervate not only the thalamus but also cortical layer IV, suggesting that layer VI CT neurons exert a dual, intrathalamic and intracortical,

feedback control of incoming TC activities [159,202]. Such a cortical feedback would have a facilitatory effect on the thalamus [203]. Thereby, the spatiotemporal dynamics of intracortical synaptic and intrinsic processes, especially in layer VI dendrites, are under the influence of the dialogue between the corresponding CT and TC neurons.

In the thalamus, NMDAR-mediated excitatory postsynaptic currents are much larger in CT than in prethalamic (sensory inputs) synapses [204–206]. Importantly, the corresponding NMDAR-related response is antagonized by the NMDAR antagonist ketamine or MK-801 [207], which significantly increases the power, and the synchrony, of ongoing GFO in the highly-distributed CT-TC systems [59–62]. Moreover, the CT pathway significantly contributes to thalamic GFO [59,208]. The layer VI CT pathway also exerts a great influence on the state of the membrane potential of the TC neurons, as well as on ongoing and function-related thalamic activities. More specifically, the CT neurons shape the spatiotemporal receptive fields of TC cells [209,210] and play an essential role in the coordination of widespread coherent oscillations [211]. Importantly, the CT innervation, mediated by both NMDA and non-NMDA receptors [212], is more effective to the TRN than to TC neurons [174]. In the TRN, the CT pathway involves not only monosynaptic excitations but also disynaptic and polysynaptic GABA(A)-mediated inhibitions [176]. Thereby, the layer VI CT pathway and the TRN work together as an attentional searchlight (focused attention) to salient sensory stimuli [165,213–215]. There is a large body of comprehensive anatomo-functional studies showing that CT neurons exert a simultaneous effect on both the center (excitation) and the surround (suppressive) of receptive fields [189,215–218]. The CT synapses would thus exert a crucial role in sharpening the thalamic receptive field via intensifying both the center and the surround mechanisms. The CT influence is dynamic with an excitation-inhibition balance changing in an activity-dependent manner [205]. Sustained cortical activity enhances thalamic activities, such as during states of focused attention [219,220]. Finally, CT neurons are thought to function similarly across species and across sensory modalities [218].

Thalamic rhythms: The thalamus plays a crucial role in the generation of brain rhythms [221,222] and it is implicated in a wide range of brain oscillations [223–225]. Indeed, the thalamic neurons are endowed with state-, time- and voltage-dependent properties, under the control of synaptic inputs, which allow them to fire a single action potential or a high-frequency (up to 600 Hz) burst of two to seven action potentials. The firing mode, tonic or bursting, is determined by low–threshold T-type calcium channels. They are inactivated at a membrane potential more positive than −60 mV and de-inactivated below for more negative values. This means that for a membrane potential hyperpolarized below −60 mV, any intrinsic depolarization or depolarizing input, including a reversed inhibitory postsynaptic potential, can trigger a low–threshold potential crowned by a high-frequency burst of action potentials. In short, when the T channels are inactive, the thalamic neurons fire in a tonic manner; they fire in the burst mode when the T channels are de-inactivated. These electrophysiological properties have been characterized in detail in a countless number of publications (for review see, e.g., [226–228]).

The GABAergic TRN cells are also endowed with state- and voltage-dependent pacemaker properties not only at the spindle frequency (7–12 Hz) [229–231] but also at the gamma frequency [232] oscillations. Indeed, the membrane of the GABAergic TRN neurons can generate intrinsic subthreshold and threshold GFO, which result in rhythmic GABA(A) receptor-mediated inhibitory postsynaptic potentials in related TC neurons [232]. The oscillating properties of TRN and TC neurons are influenced by the CT pathway [59,205,208,233,234]. Therefore, the TRN plays a key role in the state-dependent generation of thalamic GFO, which are under the powerful control of large populations of layer VI CT neurons.

In schizophrenia, the thalamus and its related networks present diverse (structural, chemical, physiological and metabolic) abnormalities [5,7,11,140,235–238]. Volumetric and structural studies using imaging have revealed a reduction in the volume of the thalamus not only in chronic schizophrenia [239] but also in first-episode psychosis and in antipsychotic-naive high-risk individuals

for psychosis [240]. These structural changes may be linked to a functional dysconnectivity between the thalamus and the cerebral cortex in both early and chronic stages of psychosis, which is associated with cognitive impairment [10,135,241–243]. A decrease of the thalamic glutamate level has also been measured [244,245], and almost all molecules implicated in the glutamate transmission pathway are altered in the thalamus of patients with schizophrenia (changes in the expression of glutamate receptors, transporters and associated proteins) [157]. The thalamic glutamate level, measured with the use of proton magnetic resonance spectroscopy, might also be a predictor of psychosis [244,245].

In first-episode and early–onset schizophrenia patients, disturbances in sleep represent a core pathophysiological feature. Cortical EEG studies conducted in such patients have revealed a significant deficit in sleep spindles, a marker of functional dysconnectivity [3,246]. This might be due to a reduced function of NMDAR, as an in vitro study, conducted in thalamic slices, demonstrated that a selective blockade of NMDAR or a diminished extracellular magnesium concentration significantly shortens spindle-like oscillations [247]. However, we do not know whether the reduction in sleep spindles in patients with schizophrenia is due to a presynaptic and/or postsynaptic dysfunction of TC or TRN neurons. It is tempting to speculate that the functional dysconnectivity recorded in schizophrenia also involves a reduction of NMDAR activity. This hypothesis is supported by the fact that, in rodents, the NMDAR antagonist ketamine, at a psychotomimetic dose, disrupts the functional state of the CT pathway [59].

In summary, the thalamic volume and glutamate level, sleep spindles and ongoing GFO are potentially useful biomarkers for the clinician to diagnose the prodromal phase of psychosis. Therefore, the thalamus with its structural, neurochemical and electrophysiological properties seems an essential structure in the etiopathophysiology of schizophrenia, as well as a prime target structure for preventive TES, directly and indirectly via the CT pathway.

4.2. Glutamatergic Transmission

In the light of our current knowledge, the term "glutamate hypothesis" mean that schizophrenia is caused by multiple variables and a stream of pathophysiological processes related to NMDAR–related synaptic functions [248,249]. NMDAR are well known to play, by means of synaptic plasticity, an essential role in the adequate neurodevelopment of cognitive abilities [250]. Here, the glutamate hypothesis does not negate the dopamine hypothesis and the other pathophysiological hypotheses of schizophrenia. Moreover, the disturbed dopaminergic and glutamatergic neurotransmissions might be causally related [44,251–253].

Glutamate is the predominant neurotransmitter in the brain. It is the precursor of GABA, the most prevalent inhibitory neurotransmitter that balances glutamate's actions. Glutamate works with ion channel–associated (ionotropic) or G protein–coupled (metabotropic) receptors. It is also well known that NMDARs play, by means of synaptic plasticity, an essential role in the adequate neurodevelopment of cognitive abilities [250]. Since 1980, there have been increasing lines of evidence suggesting that glutamate-based synaptic neurotransmission is altered in schizophrenia [254–256]. Kim and colleagues (1980) measured a decrease of glutamate in the cerebrospinal fluid of an untreated patient with schizophrenia. Then, studies performed on postmortem human brain samples demonstrated changes in glutamate receptor binding, transcription and subunit protein expression in the prefrontal cortex and subcortical structures, including the thalamus and hippocampus [257]. They also showed altered levels of the amino acids *N*-acetyl aspartate (NAA) and *N*-acetyl aspartyl glutamate (NAAG) and of the activity of the enzyme that cleaves NAA to NAAG and glutamate in the cerebral spinal fluid and postmortem tissues from patients suffering from schizophrenia [258,259]. Also, genetic studies have revealed that a majority of genes associated with schizophrenia are linked to the glutamatergic system [248,260–263]. Interestingly, an imaging study (SPECT tracer for the NMDAR) revealed a reduction in NMDAR binding in the hippocampus of medication–free patients [264]. Even when considering the possibility that schizophrenia is caused by an immune dysfunction due to infectious agents, a link is identified between immune alterations and disturbances of glutamate NMDA

receptors [153,265]. Interestingly, there is a growing body of findings indicating that glutamate synaptic transmission is significantly altered in schizophrenia since the premorbid phase [244,245,254,265–267].

A systemic single dose administration of non–competitive NMDAR antagonists (phencyclidine, ketamine or MK-801) elicits cognitive deficits and schizophreniform symptoms in healthy individuals and greatly exacerbates the symptoms in patients with schizophrenia [268–274]. The ketamine–induced schizophreniform symptoms are associated with a state of functional cortical–subcortical hyperconnectivity [275,276] and an abnormal amplification of baseline GFO, reminiscent of the increased GFO observed during hallucinations [50–53] and in at-risk mental state individuals for psychosis (untreated with ketamine) [56]. These clinical neurophysiological findings were predicted by comprehensive preclinical studies conducted in acute ketamine rodent models [60,62,277–280].

In summary, disturbances in glutamate synaptic transmission, involving a reduced function of NMDAR with multiple functional consequences, start to appear early during the development of schizophrenia. This may cause the dysfunctional neural plasticity in schizophrenia [281]. A certain number of genes (DISC-1, dysbindin, SHANK, and NRG-1) are well-known to modulate NMDAR-mediated glutamate transmission [282,283]. This notion is supported by patients with an autoimmune encephalitis because they produce antibodies against NMDAR and have a clinical disorganization that is similar to that of patients with schizophrenia [284]. Therefore, glutamate transmission appears a potential "primary" target for an early therapeutic intervention [285,286]. Of importance, the psychosis-relevant abnormal amplification of GFO is reliably reproduced in healthy humans and rodents under the acute influence of the NMDAR antagonist ketamine at a psychotomimetic dose [58,60]. So, these translational acute pharmacological models seem appropriate to develop an innovative preventive treatment against the development of chronic psychotic disorders. It is well recognized that reduced function of NMDAR is a crucial factor for the progression and symptoms of schizophrenia [284]. It is tempting to posit that an appropriate preventive treatment would correct the dysfunctional brain network plasticity.

5. Gamma Frequency (30–80 Hz) Oscillations, a Potential Pathophysiological and Therapeutic Bioelectrical Marker

In the present essay, I put emphasis on GFO because there is compelling evidence of functional links between GFO, NMDAR hypofunction and a reduction in the number and the function of cortical GABAergic interneurons in schizophrenia [287–290]. This implies that GFO are considered a common denominator of the above–presented three facets (CT pathway, thalamus, and glutamate transmission), which represent the etiopathophysiological backbone for premorbid, acute and chronic psychotic disorders. Indeed, (i) coherent GFO are recorded not only in the neocortex but also in the related thalamus; (ii) the layer VI CT pathway contributes to thalamic GFO; and (iii) GFO increase in amplitude and power not only during hallucinations, in at-risk individuals for psychosis, but also after the administration, at a psychotomimetic dose, of the NMDAR antagonist ketamine. It is worth remembering that, in humans, GFO start to emerge several months after birth [291]. It was demonstrated that, during rodent neural development, thalamic GFO play a crucial role in the mapping of the functional TC modules [292]. Both in humans and rodents, GFO are simultaneously present in cortex and thalamus [59,293]. In the following, we will see that GFO are also potential bioelectrical markers of psychosis, which could be used for the development of therapeutic interventions.

Coherent synchronized GFO emerge in large-scale cortical-subcortical networks spontaneously or during global brain operations such as attention, perception, and memory [294–297]. They are thought to play an essential role in synaptic plasticity [298], spatiotemporal coding (binding by synchronization), storage and recall of information [299–303]. Network GFO are ubiquitous and operate in combination with other brain rhythms [224,304,305]. Extracellular field GFO principally result from subthreshold, synaptic and intrinsic membrane potential oscillations that trigger action potentials at a precise phase during the oscillatory period. Their functions and mechanisms are still a matter of debate.

The functional interactions between GABAergic and glutamatergic neurons are thought to be responsible for the generation of GFO during attention and integration processes [304,306].

There is accumulating evidence that, in schizophrenia, the dysfunctional network connectivity between cerebral cortex and thalamus is accompanied by disturbances in GFO and by deficits in sensorimotor and cognitive performance [4,53,307–309]. There is also evidence of a correlation between schizophrenia–related symptoms and in particular cognitive and perceptual deficits with disturbances in cortical GFO [310–312], also in first-episode schizophrenia [6]. Gamma oscillations may be considered not only as neurophysiological markers of the functional state of brain networks but also as trait markers in schizophrenia [313]. Of importance, abnormally increased GFO are recorded in patients with first-episode schizophrenia [6,54,55,314,315] and in at-risk mental state patients for psychosis. Gamma oscillations are also abnormally excessive in amplitude during hallucinations [50–53]. Increased GFO are associated more with positive (such as hallucinations) than negative symptoms [4,316]. Therefore, hypersynchronized GFO look like a predictive bioelectrical marker for both psychosis and treatment outcome.

As reported above, such abnormally amplified GFO can consistently be reproduced in healthy humans and rodents following the systemic administration at a psychotomimetic dose of the NMDAR antagonist ketamine [58,60,317]. These translational acute ketamine models, which model the prodromal phase of psychotic disorders and first–episode psychosis, are thus appealing to work out a preventive treatment against the occurrence of chronic forms of schizophrenia. It may be worth specifying that a single low-dose (<10 mg/kg) application of ketamine in rats increases hyperfrontality, which can also be observed in first–episode schizophrenia [275,276,318]. In contrast, hypofrontality is diagnosed in patients with chronic schizophrenia. Therefore, the acute ketamine model may be more appropriate to mimic the pathogenesis of acute psychotic states in humans [268,271,273,275,276,317].

Abnormally amplified GFO in neural networks may contribute to the disruption of the integration of task–relevant information, which is part of psychotic symptoms [55,319]. Moreover, in rodents, a single systemic administration (at a subanesthetic dose) of ketamine disturbs the functional state of the somatosensory CT-TRN-TC circuit (Figure 3). Ketamine reliably increases the amplitude and power of spontaneously-occurring GFO and decreases the amplitude of the sensory-evoked potential and its related evoked GFO in both the thalamus and the neocortex. In other words, the NMDAR antagonist ketamine generates persistent and generalized hypersynchrony in GFO, which act as an aberrant diffuse network noise under these conditions, and represent a potential electrophysiological correlate of a psychosis-relevant state [60]. Such a generalized network gamma hypersynchrony thought to create a hyper-attentional state (see discussion in [59]), might be the force that disrupts the flow of sensorimotor and cognitive processes as observed in schizophrenia. Thereby, ketamine reduces the ability of the somatosensory CT-TRN-TC system to encode and integrate incoming information, perhaps by disrupting the center-surround receptive field properties in thalamic neurons [8]. The electrophysiological signals (ongoing and sensory-related potentials and GFO) appear as valuable neurophysiological markers to test the functional state of neural networks. Such quantifiable bioelectrical markers might thus be a promising translational tool to develop innovative therapies designed to prevent the occurrence of psychotic disorders. In short, ketamine decreases the signal-to-noise ratio at least in the CT-TRN-TC system [59,61,320]. Ketamine also transiently disrupts the expression of long-term potentiation in the TC system [61], disorganizes action potential firing in rat prefrontal cortex [321], increases the firing in fast-spiking neurons and decreases it in regular spiking neurons [322] and disturbs sensory-related cortical and thalamic GFO. Dizocilpine (MK-801) is, like its derivative ketamine, a well-known non-competitive NMDAR antagonist with psychotomimetic properties leading to similar but more sustained effects than ketamine [60–62]. It addition, dizocilpine modulates the expression of numerous genes in cortical and subcortical structures [323].

In summary, neural GFO represent a translational bioelectric marker. It may be considered a potential prognostic and therapeutic hallmark for cerebral network disorders underlying psychotic

symptoms. Such a quantifiable marker might be a promising translational tool for understanding the etiopathophysiological mechanisms of psychotic disorders and for developing innovative therapies. These include, for instance, noninvasive neurophysiological modalities such as TES, applied in at–risk mental state individuals to prevent the occurrence of first–episode psychosis and chronic forms of psychotic disorders.

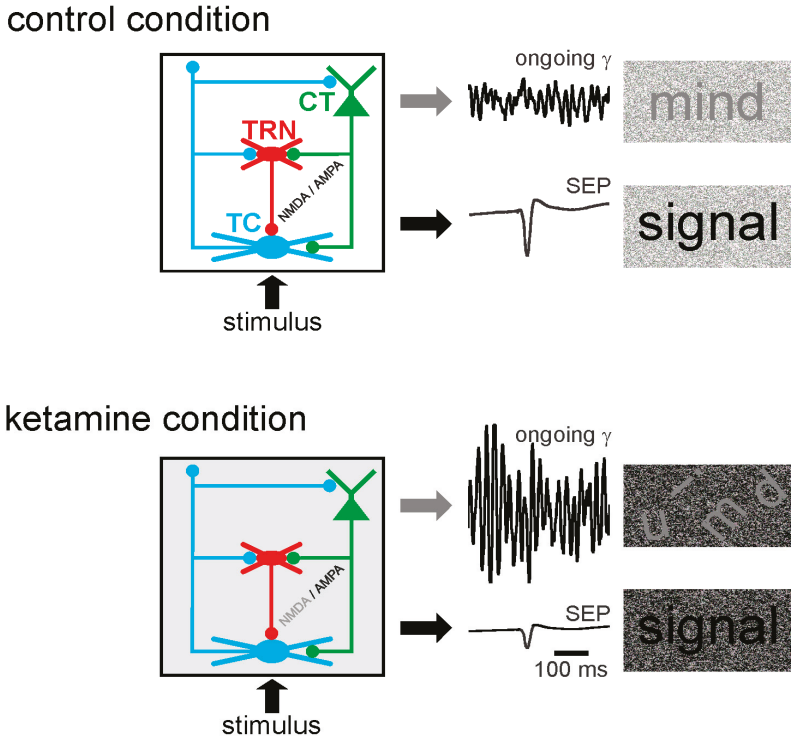

Figure 3. The NMDAR antagonist ketamine decreases the ability of the cortico-reticulo-thalamocortical (CT-TRN-TC) system to integrate incoming information. A single systemic administration of ketamine disturbs the functional state of the three-neuron circuit (layer VI CT-TRN-TC). Ketamine increases the amplitude of spontaneously occurring gamma frequency oscillations and decreases the amplitude of the sensory-evoked potential in both the thalamus and the neocortex. Layer VI CT neurons innervate the thalamic relay (TC) and reticular (TRN) neurons through the activation of glutamate ionotropic (NMDA and AMPA) and metabotropic receptors. Ketamine is expected to decrease the NMDA/AMPA ratio at least at CT synapses. Thereby, ketamine disturbs the mental state and decreases the gamma signal–to–noise ratio in the CT-TRN-TC system. The sensory-evoked potential (SEP) can be considered as an index of the sensory-related signal. Adapted from [61] and from [59].

6. Potential Mechanisms of TES

Little is known about the mechanisms underlying the clinical, acute and chronic effects of TES techniques, which are expected to re-establish the normal functional state in dysfunctional cortical-subcortical networks and/or to recruit compensatory networks. Whatever the technique and specific setting considered, it is difficult to perceive an integrated view of the mechanisms that are responsible for and contribute to the expected and the observed clinical effects. The possible mechanisms include genetic, molecular, cellular and systems pathways as well as long-lasting processes involving plasticity. The nerve cells are embedded in a conductive medium, the extracellular space,

an important interface between the exogenous and endogenous electric currents and the excitable and non–excitable elements involved in information processing. In addition, before reaching the excitable cellular and subcellular elements, the TES-induced electric currents cross several types of barriers, including the cranium, the meninges, the vascular network and the glial tissue [324–327]. Also, the applied electric field has two components, one parallel and the other one perpendicular to the brain surface [328]. The strength of these two components determines the relative influence of TES on the excitability of the neural and non-neuronal elements. All these barriers, as well as the ongoing changes in the brain state, are a source of interferences with the electric field. Taken together, TES is expected to target a large number of neuronal and glial elements over large cortical and subcortical regions.

The clinical effects of TES and the underlying short- and long-term mechanisms principally rely on the electrode type and stimulation parameters (stimulus location, intensity, duration, polarity) [329,330]. The TES effects on brain structures are non-selective, state-dependent [331], and the strongest impact is not necessarily exerted in neural structures that are located below the electrodes [332]. The TES effects on the cellular and subcellular excitable elements depend on their geometry and on their spatial orientation in the electric field [332,333]. Both the TES effects and the underlying mechanisms lie on a continuum of effects ranging from the stimulation settings to the ongoing genetic, molecular, cellular and network dynamics. The mechanisms underlying the effects of TES are the subject of intensive research (for a review see: [33,119,334–347]). Our current knowledge remains fragmented with multiple and diverse proposed mechanisms: conduction block [348], synaptic potentiation or depression [349–351], network resonance [352], modulation of brain oscillations [127,337,353–359], of ongoing cellular firing and subthreshold membrane potential oscillations [360,361], of dendritic inhibition [362], of the astrocytic Ca^{2+}/IP3 signaling [363] and of the synaptic efficacy in excitatory and inhibitory pathways [364]. It is reasonable to assume that multiple mechanisms are likely to operate in combination. The combination of these multiple mechanisms over time can be viewed as "meta-mechanisms" at the brain-network level.

In the following, I speculate on a few possible mechanisms that may, depending on the TES modality, be involved in the modulation of the layer VI CT pathway, which massively innervates both the dorsal thalamus and the TRN. As mentioned above, this glutamatergic pathway may be one of the prime targets for preventive TES in at-risk mental state individuals for psychotic disorders. In the present discussion, I take fundamental principles of neurophysiology into consideration. As the electrical field spreads at the speed of light, all neural and non-neural elements will be affected at the same time. The TES effects are expected to be attenuated with distance, obeying to the rule that the amount of current delivered by the electrode is proportional to the square of the distance between the brain elements and the stimulation electrode [365]. Figure 4 illustrates some of the anatomo-functional elements of the CT-TRN-TC system, which may somehow be impacted by TES electric fields.

TES entrains neuronal populations: Nerve cells operate on the basis of electrical charges, which makes them also responsive to weak electric currents [366–370]. Importantly, it was demonstrated that, in the rat, TES can directly entrain neurons in multiple neocortical areas and sub-neocortical structures, including the hippocampus [360]. Indeed, some of the cortical and hippocampal neurons were affected at similar phases of the TES oscillations, suggesting the contribution of non-synaptic mechanisms in the TES-induced direct entrainment of cortical and subcortical neurons. Of course, the directly activated neurons become a source for subsequent polysynaptic mechanisms, which represent a significant contribution in TES-induced entrainment over large cortical territories and the related subcortical structures. The percentage of TES phase-locked neurons depends on the state of brain networks and increases with TES intensity [360]. Furthermore, intracellular recordings revealed that both the firing and the underlying subthreshold and suprathreshold membrane potential oscillations are under the combined influence, through amplification, attenuation or interference, of TES fields and global network activities [360]. The mechanisms underlying the TES direct effects on ongoing neuronal activity are not well understood.

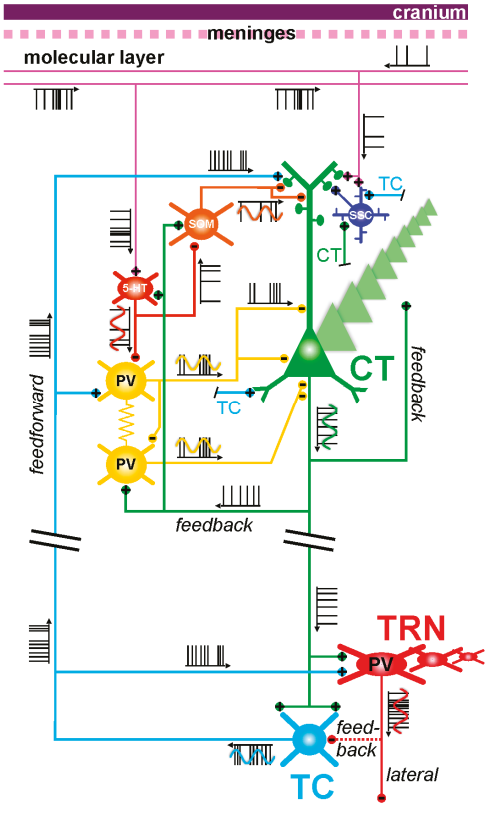

Figure 4. Potential mechanistic targets in the cortico-reticulo-thalamocortical (CT-TRN-TC) system for transcranial electrical stimulation. This model includes three parts, which are assumed to work together: (i) The innervation of the intracortical circuitry by both the descending axonal branches (top-down process) of the axons running within the molecular layer and the ascending TC inputs (bottom-up process); (ii) functional interactions between glutamatergic and GABAergic neurons of the intracortical circuitry, which includes feedback and feedforward excitations (from CT and TC axon collaterals, respectively); and (iii) the layer VI CT pathway, one of the outputs of the intracortical circuitry, which innervates simultaneously the thalamic GABAergic reticular (TRN) and glutamatergic relay (TC) neurons. In this model, the TRN cells generate more lateral than feedback inhibition in the dorsal thalamus, which contains only TC neurons. The layer VI CT axonal projections are about ten–fold higher in number than the TC projections, thereby generating a great excitatory pressure on TRN and TC neurons. Furthermore, the apical dendrites of layer VI pyramidal neurons terminate in layers III–IV. Each neuron exhibits its own firing pattern that is state-, voltage-, synaptic- and time-dependent. The action potentials (APs) are drawn like a code bar. Under physiological condition, it is assumed that the APs are initiated at the axon hillock, the initial segment of the axon. The axon can also transmit, in addition to APs, analog signals (generated in the somatodendritic domain and represented by sinusoidal waves) along the axon (at least several hundreds of micrometers away from the soma) and can modulate AP-evoked transmitter release at the corresponding synapses. In this model, it is assumed that axodendritic (chemical synapses) and dendrodentritic electrical (via gap junctions) coupling exist between the two types (basket and chandelier) of GABAergic parvalbumin (PV) expressing cells. 5-HT, 5-HT3A receptor; CT, corticothalamic; SOM, somatostatin; ssc, spiny stellate cells; TC, thalamocortical; TRN, thalamic reticular nucleus.

The axonal membrane, the more excitable element: The axonal membrane is generally more excitable than the somatic and dendritic membranes [371–373]. There is increasing evidence supporting the hypothesis that distal parts of the axon, remote from the axon initial segment, can autonomously integrate and generate action potentials, which could contribute to the emergence of field GFO involving synchronized GABAergic rhythmic activities [374–378]. So, it is predictable that the TES–induced electric field would create regional conditions in cortical tissue favorable for activating axons. Also, the number and the location of the activated axonal areas depend on both the neural tissue architecture and geometry, in relation to the direction of the electric field. The pattern of activated axons depends on the direction of the electric field and of the state of the cortical region being stimulated. The more numerous intersecting axons within an axonal bundle, the more numerous the axonal couplings [379]. An axon curvature would be as excitable as the initial segment [380]. Because the axonal membrane is more excitable than the somatodendritic membrane and is endowed with integrative properties [372,376,378], the TES-induced field may activate intracortical axons and axonal endings, where action potentials may be initiated. Dopamine and kainate can generate axon membrane depolarization leading to action potential initiation [381,382]. Also, oligodendrocytes, in addition to regulating myelination, would play a promoting role in synchronizing firing through axons [383]. Axo-axonal interactions can also involve glial cells [384]. Once triggered, ectopic axonal action potentials would run along the axons simultaneously both orthodromically up to the axon terminals and antidromically up to the parent somatodendritic domains. The orthodromically conducted action potentials would then activate local and distant postsynaptic neurons. A single orthodromically conducted action potential can even itself generate, for a while (a few tens of ms), a sequence of excitatory and inhibitory synaptic events in a subpopulation of interconnected glutamatergic and GABAergic neurons [385]. On the other hand, the antidromically conducted action potentials can activate directly the parent somatodendritic complex [376,378]. Moreover, TC neurons can spontaneously generate ectopic axonal action potentials, which subsequently modulate the parent soma's excitability [376,386].

Cortical neurons are excited when the electric field is directed from the dendrites toward the axon [328]. The impedance mismatch between the dendritic arbor and the principal axon represents a likely mechanism for TES-induced cortical excitation [328]. Moreover, low-intensity electric fields concurrent to suprathreshold synaptic inputs can modulate the timing of action potential initiation [387]. Therefore, TES has the potential to influence the functional input-output balance in neurons.

Electrical couplings: Couplings between neurons in the central nervous system can occur through electrical synapses, that is, gap junctions [388,389]. They represent another potential target for the TES electric field. An important feature of these synapses is that they are bidirectional. Axo-axonal electric coupling via gap junctions is thought to contribute to the oscillating and integrative properties of neural networks [389–394]. This is a possible mechanism through which periodic TES can entrain oscillating neural networks. Sparse electrical couplings through axo-axonal gap junctions play a key role in the initiation and spreading of network gamma and higher (>100 Hz) frequency oscillations [392,393,395]. The coupling action potentials occur in the axon prior to invading the parent somatodendritic tree [389]. Such a mechanism represents a fast device for signal transmission directly between the outputs of neurons, thereby leading to temporally precise firing during fast network synchrony [389]. This supports the notion that the axon and its branches are not only reliable transmission cables for action potentials but also functional entities with integrative properties [376,396,397]. In the presented CT-TRN-TC system (Figure 4), it is shown that intracortical GABAergic parvalbumin-expressing interneurons communicate with each other through electrical and chemical synapses, which are functional modalities of tight couplings that contribute to the generation of synchronized oscillations in cortical structures [398]. Such couplings may also be influenced by TES.

Electrical couplings between central nervous system neurons can also occur through direct electrical (or ephaptic: touch phenomenon through ion exchanges between two adjacent excitable membranes)

coupling [399,400]. Electrical couplings could also be mediated by the electric field generated jointly by many parallel axons. Such couplings might significantly be influenced not only by endogenous but also by exogenous electric fields independently of electrical and chemical synapses [401–403]. Therefore, ephaptic couplings may be one important target for TES. Ephaptic couplings between axons might be involved in the synchronization and the timing of action potentials as well. Endogenous or exogenous oscillating electric fields impose temporal windows, during which periodic ephaptically-induced membrane polarization can become the source of enhanced excitability in the corresponding neurons [401,404]. Thereby, ephaptic coupling leads to coordinated spiking activity among nearby neurons [401]. Ephaptic coupling influences the synchronization and timing of firing in neurons receiving suprathreshold synaptic inputs [360,387,405,406].

Combined digital and analog coding: It is usually taught that excitatory and inhibitory synaptic inputs modulate the integrative properties of the somatodendritic membrane areas, which lead to local voltage fluctuations (synaptic activity) that propagates up to the axon hillock, the non-myelinated segment of the principal axon, which will initiate a firing pattern (barcode) subsequently transmitted to the downstream synapses [407–412]. Once initiated, the action potentials simultaneously propagate orthodromically along the principal axon up to the presynaptic terminals, where they cause Ca^{2+} influx and transmitter release [413], and antidromically into the somatodendritic arbor, preventing the activation of the trigger zone at a proper time and/or triggering dendritic activities [414]. In vitro studies have demonstrated that, in the cerebral cortex and the hippocampus, somatodendritic voltage fluctuations can propagate over significant distances along the axon, change the amplitude and duration of the axonal action potential and, through a Ca^{2+}-dependent mechanism, change the amplitude of the corresponding postsynaptic potentials [415,416]. In short, axons can transmit analog signals in addition to action potentials (Figure 4). Such a combined digital and analog coding represents an additional mechanism for information processing in neural networks. This dual coding must be a functional target for TES. It can be predicted that a TES-induced field can, for instance, modulate (via amplification, attenuation or interference) the amplitude of the voltage fluctuations running along the axon with subsequent impact on the action potential-evoked transmitter release at the corresponding synapses.

Top–down control: The first neural elements that are intensely impacted by any TES technique are, by all likelihood, first located in the more superficial layers of the cerebral cortex. The layer I or molecular layer, which is situated just underneath the pial surface, contains dense bundles of axons and dendrites and a paucity of sparsely distributed cell bodies [417,418]. Some of these axons give rise to descending axonal branches that innervate cortical neurons, thereby exerting a top-down control on the cortical and subcortical networks. For instance, it was demonstrated that the electric current generated by TMS can activate a network of GABAergic interneurons that innervate, in the upper cortical layers, the apical dendrites of layer V pyramidal neurons [362]. This GABAergic inhibition would be mediated by GABA(B) receptors, and their activation would decrease or suppress dendritic Ca^{2+} currents implicated in the synaptically-mediated dendritic excitation, which is involved in the integration of information. Even if such a scenario could also apply to the dendrites of layer VI CT neurons, it remains a challenge to predict, from the inspection of individual mechanisms, the actual activity pattern of the CT neurons. Assuming that TES inhibits their somatodendritic activity and firing, reduced firing of layer VI CT neurons, which exert a massive excitatory pressure on both TC and TRN neurons (Figure 2), would lead to a disfacilitation of the thalamic activity. So, the proposed TES-induced CT disfacilitation would reduce first the monosynaptic excitation of the glutamatergic TC and GABAergic TRN neurons and, secondly, the disynaptic inhibition of the TC neurons (Figure 4). Furthermore, because of the presence of dendrodendritic synapses between TRN neurons [168,171] and because of their pacemaker properties for GFO [232], TES-induced disfacilitation would also reduce the multisynaptic intra-TRN inhibitions [176], a possible brake for the generation of thalamic GFO. It is thus tempting to hypothesize that such TES-induced intracortical dendritic inhibition can reduce the power of GFO in cortical and subcortical structures.

Bottom–up effect from the thalamus: So far, TES has been presented as a noninvasive therapeutic means exerting top-down effects from the current source. Such effects can be categorized into at least two principal types of mutual interactions: local type with top-down controls, for instance the one discussed above, and a highly–distributed type, which involves interconnected cortical and subcortical networks. Indeed, it was well demonstrated that TES can directly, likely through non–synaptic mechanisms, entrain/modulate subcortical neurons [360]. The TES-induced electric fields would act as endogenous electric fields, which are known to guide network activity, to modulate the timing of action potentials [419], and to enhance stochastic resonance [420]. This is valid for both tDCS (static electric field) and tACS (alternating electric field) with effects on brain function [387]. The TES–induced field effects would modulate the amplitude of subthreshold and suprathreshold membrane potential oscillations of the target neurons. Because of a large number of variables mentioned above, it is difficult to provide a precise picture of the direct effects of TES field on both GABAergic TRN and glutamatergic TC neurons. Whatever the differential effects, both types of neurons work together and mutually influence each other. TES would affect their threshold mechanisms equivalent to an integrate–and–fire model, which depends on a certain number of factors, including the ion channel kinetics, the weight of excitatory and inhibitory synaptic inputs and the shape of the membrane potential distribution near threshold [421,422]. However, as mentioned above, we should keep in mind that both TRN and TC neurons generate action potentials during sustained membrane potential depolarization and hyperpolarization.

The GABAergic TRN neurons can be considered a privileged cell-to-network target for TES indirectly through the CT pathway, as mentioned above, and directly. In the following, I will speculate on possible mechanisms underlying eventual direct effects at the thalamic level, more specifically in the GABAergic TRN cells. It is first important to know that, at a sufficiently hyperpolarized membrane potential, TRN cells are more excitable and electro-responsive than TC neurons. Indeed, high-frequency bursts of action potentials generated by excitatory inputs require a higher degree of convergence of excitatory inputs than TRN neurons [423]. Furthermore, TRN cells are endowed with low-threshold T-type calcium currents of longer duration than TC neurons [424,425]. These anatomofunctional properties suggest that TRN cells may be more electro-responsive to TES than TC neurons. Gap junctions-mediated electrical synapses is another important characteristic of GABAergic TRN neurons [172,426]. Such electrical synapses are implicated in diverse forms of cell-to-network signaling. Using a novel dye-coupling technique, Connors and colleagues [427] further demonstrated that, in the rodent, electrically coupled TRN cells form clusters with distinctive patterns and axonal projections. Unpredictably, TES would facilitate the synchronized generation and spread of electrically- and chemically-induced synaptic activities within TRN clusters. The presumed TES-induced TRN activity patterns would strongly influence network oscillations, which would generate inhibitory activities (principally lateral inhibition [179]) in the related populations of TC neurons. To sum up, alternating TES (or tACS) is expected to influence directly the thalamus, which is a well-known oscillator [221]. Here, in the present conceptual context, the thalamus is a reference. This means that the proposed mechanisms underlying direct subcortical effects could apply to other sub-neocortical structures, such as the hippocampus [360], along with their respective anatomofunctional properties.

Another direct influence relies on the fact that, as above mentioned, the axonal membrane is more excitable than the somatodendritic membrane. So, assuming that the ongoing state of the cortex allows TES-mediated triggering of action potentials on axonal terminations of TC neurons, the corresponding ectopically-generated axonal action potentials would backpropagate up to the parent somatodendritic complex of these TC neurons. Such antidromically conducted axonal action potentials would influence the somatodendritic excitability of the corresponding TC neurons [376]. If true, such an effect may, under suitable circumstances regarding the network state, short-circuit the CT-mediated thalamic multisynaptic effects. In theory, such an effect would be more efficient when the somatodendritic field is hyperpolarized (see Figure 35 in [376]). In short, TES would not only generate action potentials on

ectopic axonal membrane but also modulate the timing of action potential initiation in the axonal and somatodendritic membrane [387], thereby influencing the dynamics and plasticity of neural networks.

In summary, regarding its multiple and diverse mechanisms, TES would exert local and highly distributed influences on the ongoing thalamic activities through at least three principal ways. They would, over time, occur individually or in combination leading to polysynaptic effects (Figure 4): (1) Direct, intracortical synaptic and non-synaptic (especially electrical) mechanisms, thereby modulating the excitability of the CT axon (from the hillock to the ascending ramifying axon collaterals) and the integrative properties of the CT neurons' somatodendritic arbor; (2) direct, intracortical modulation of the excitability of TC axon terminals, which could initiate antidromic firing along the principal axon of TC neurons with subsequent effects on the TC neurons' somatodendritic membrane state-dependent excitability and a monosynaptic excitation of TRN cells; (3) direct forced TES field effect on thalamic neurons, especially on the GABAergic TRN cells because they are endowed with more "explosive" electrophysiological properties than TC neurons, leading for instance to phase–biased cellular firing. Whatever the TES-induced top-down and bottom-up (from presumed direct effect on thalamic neurons) mechanisms, the effect on the excitability and integrative properties of all the elements (including non-neuronal) that make up the CT-TRN-TC system would depend on its ongoing functional state. At any rate, TES-elicited modulation of the CT pathway should influence the thalamic neurons' spatiotemporal properties, which are related to the center-surround receptive field [428]. The predictions and hypotheses presented in the present essay need to be validated through appropriate experiments.

7. Conclusions and Perspectives

In the present essay, I began with a neurophysiological perspective on early therapeutic intervention (TES) in at-risk mental state individuals against the occurrence of FE psychosis, chronic psychotic disorders, and schizophrenia. Because of their noninvasiveness, low-cost and safety, the use of TES therapeutic modalities, which are almost free of side-effects, is increasing over years with encouraging and promising clinical outcomes. Furthermore, there is accumulating evidence that static (DC field) or alternating (AC field) TES exerts an effect on brain function. On the other hand, the underlying mechanisms still remain elusive. There is accumulating evidence that exogenous electric currents can modulate not only brain electrical activity but also behavioral and cognitive performance. All the proposed mechanisms belong to a continuum that can be considered "meta-mechanisms" at the brain-network level. The use of TES may be seen as a "natural" treatment as it can influence, like endogenous electric fields, the excitability and the integrative properties of the brain nerve cells and subcellular elements. TES can, through the extensive CT and cortico-cortical systems, nonselectively affect, directly and through multisynaptic pathways, global brain activity. This is not surprising since electrical modulation of a single neuron can modify not only the global brain state [429] but also motor behavior [430], and that a single action potential can itself generate sequences of excitatory and inhibitory synaptic events in subnetworks [385].

On the basis of our current knowledge, it is tempting to put forward that noninvasive therapeutic interventions using TES might turn out to be very promising in the future as there is emerging evidence that TES might supplant surgical DBS therapy against neurobiological disorders, including Parkinson's disease. This might also be the case for epilepsy, dystonia, obsessive compulsive disorders, pain, multiple sclerosis, addiction, depression, Tourette syndrome, and in brain–injured patients in vegetative and minimally conscious states. That TES (with settings adjusted on the basis of cortical-subcortical oscillations) can be applied to treat any neurobiological disorder rests on the notion that TES would set into action highly-distributed networks, which would help the brain, in case of dysfunctional networks associated with disturbed oscillations, to retrieve its fundamental capability to self-organize, self-calibrate and self-correct [431,432].

In the present essay, there is a bias toward rodent models merely because the CT-TRN-TC system of rodents and humans share common anatomo-functional properties. The CT-TRN-TC system was

put on the stage since the widespread CT pathway, the thalamus and the glutamatergic synaptic transmission together form an etiopathophysiological backbone for schizophrenia and, therefore, may represent a prime therapeutic target for preventive TES of dysfunctional brain networks in at-risk mental state individuals against the occurrence of first-episode psychosis and schizophrenia. Importantly, the one common denominator is cortical GFO, which are amplified not only during hallucinations but also in at-risk individuals for psychosis and during first-episode psychosis. Furthermore, abnormal network gamma hypersynchrony is likewise recorded in the CT systems of healthy humans and rodents after a single systemic administration, at a psychotomimetic dose, of the NMDAR antagonist ketamine. These translational ketamine models of prodromal to first-episode psychosis are thus promising means not only to work out a preventive treatment against the occurrence of chronic schizophrenia but also to investigate the TES mechanisms.

An important question remains open as to whether TES is capable of replacing the generalized cortical-to-subcortical ongoing gamma hypersynchrony for normal gamma synchrony. Importantly, alpha frequency (10 Hz) tACS can reduce the power of cortical GFO [433]. This is interesting since ongoing alpha oscillations are often associated to cortical idling whereas GFO are associated to an attentional state [128]. Because of its activity-dependent dynamic properties, the CT pathway is expected to play a crucial role in the modulation of the ongoing activity in the CT-TRN-TC system. Indeed, a comprehensive in vitro study performed in rodent CT-TRN-TC slices demonstrated that a low-frequency optogenetic stimulation ($\leq$10 Hz) exerts a suppressive effect on TC neurons' activity [205]. In other words, we predict that TES of the extensive CT pathway can re-normalize/improve its key attentional role to generate in the dysfunctional CT-TRN-TC circuits, more specifically in at-risk mental state individuals, "normal" prediction models that guide the flow and sequences of sensorimotor and cognitive processes. Such mechanisms would operate in combination with the TRN, strategically located at the interface between the dorsal thalamus and the neocortex, through the modulation of the excitatory and suppressive components of the receptive fields in the appropriate and related cortical and thalamic territories. Thereby, principally under the influence of the TC pathway, the TRN may fine-tune the responsiveness of sensory, motor and cognitive TC neurons, depending on the ongoing functional brain state and on the relative timing of the multiple and diverse thalamic inputs.

Now, if TES were able to suppress the psychosis-relevant CT-TRN-TC gamma hypersynchrony, thought to be the electrophysiological correlate of a hyper-attentional state, would it stop the occurrence of the schizophrenia-relevant clinical disorganization and the emotional, sensorimotor and cognitive abnormalities? This is a fundamental issue that certainly needs further investigation.

Also, should TES be systematically applied, along with ethical guidelines, in a standard fashion to all at-risk mental state patients for psychotic disorders? Probably not. This is an important issue because its efficiency depends on multiple variables, more specifically on the brain state and longitudinal outcomes. Also, in an attempt to effectively apply TES at the right time, it might be necessary to use a closed-loop feedback system able to trigger the stimulation on the basis of the pattern of the ongoing brain activity [434].

On the other hand, TES may be supplanted by, or combined with, other non-pharmacological therapies, for instance, with cognitive remediation and psychotherapies. These latter therapies are promising when it comes to helping individuals with impaired cognitive performance [146,435–437]. Mindfulness-based therapy may also be an interesting alternative or complement to TES [438]. All these alternatives mean that a good quality of life prevails for at–risk mental state and first-episode psychosis patients [44] with or without a rational use of TES in the frame of a personalized medicine.

Acknowledgments: The present work was supported by the Institut National de la Santé et de la Recherche Médicale (INSERM, the French National Institute of Health and Medical Research) and by Unistra, l'Université de Strasbourg. I thank Paul M Anderson and Stefan Rotter for a critical reading of the manuscript.

Conflicts of Interest: The author declares no conflict of interest.

References

1. Insel, T.R. Assessing the economic costs of serious mental illness. *Am. J. Psychiatry* **2008**, *165*, 663–665. [CrossRef] [PubMed]
2. Wittchen, H.U.; Jacobi, F.; Rehm, J.; Gustavsson, A.; Svensson, M.; Jonsson, B.; Olesen, J.; Allgulander, C.; Alonso, J.; Faravelli, C.; et al. The size and burden of mental disorders and other disorders of the brain in Europe 2010. *Eur. Neuropsychopharmacol.* **2011**, *21*, 655–679. [CrossRef] [PubMed]
3. Ferrarelli, F.; Tononi, G. Reduced sleep spindle activity point to a TRN-MD thalamus-PFC circuit dysfunction in schizophrenia. *Schizophr. Res.* **2017**, *180*, 36–43. [CrossRef] [PubMed]
4. Herrmann, C.S.; Demiralp, T. Human eeg gamma oscillations in neuropsychiatric disorders. *Clin. Neurophysiol.* **2005**, *116*, 2719–2733. [CrossRef] [PubMed]
5. Jones, E.G. Cortical development and thalamic pathology in schizophrenia. *Schizophr. Bull.* **1997**, *23*, 483–501. [CrossRef] [PubMed]
6. Minzenberg, M.J.; Firl, A.J.; Yoon, J.H.; Gomes, G.C.; Reinking, C.; Carter, C.S. Gamma oscillatory power is impaired during cognitive control independent of medication status in first-episode schizophrenia. *Neuropsychopharmacology* **2010**, *35*, 2590–2599. [CrossRef] [PubMed]
7. Pergola, G.; Selvaggi, P.; Trizio, S.; Bertolino, A.; Blasi, G. The role of the thalamus in schizophrenia from a neuroimaging perspective. *Neurosci. Biobehav. Rev.* **2015**, *54*, 57–75. [CrossRef] [PubMed]
8. Pinault, D. Dysfunctional thalamus-related networks in schizophrenia. *Schizophr. Bull.* **2011**, *37*, 238–243. [CrossRef] [PubMed]
9. Uhlhaas, P.J.; Haenschel, C.; Nikolic, D.; Singer, W. The role of oscillations and synchrony in cortical networks and their putative relevance for the pathophysiology of schizophrenia. *Schizophr. Bull.* **2008**, *34*, 927–943. [CrossRef] [PubMed]
10. Woodward, N.D.; Karbasforoushan, H.; Heckers, S. Thalamocortical dysconnectivity in schizophrenia. *Am. J. Psychiatry* **2012**, *169*, 1092–1099. [CrossRef] [PubMed]
11. Zhang, Y.; Su, T.P.; Liu, B.; Zhou, Y.; Chou, K.H.; Lo, C.Y.; Hung, C.C.; Chen, W.L.; Jiang, T.; Lin, C.P. Disrupted thalamo-cortical connectivity in schizophrenia: A morphometric correlation analysis. *Schizophr. Res.* **2014**, *153*, 129–135. [CrossRef] [PubMed]
12. Fatemi, S.H.; Folsom, T.D. The neurodevelopmental hypothesis of schizophrenia, revisited. *Schizophr. Bull.* **2009**, *35*, 528–548. [CrossRef] [PubMed]
13. Harrison, P.J. The neuropathology of schizophrenia. A critical review of the data and their interpretation. *Brain* **1999**, *122 Pt 4*, 593–624. [CrossRef] [PubMed]
14. Insel, T.R. Rethinking schizophrenia. *Nature* **2010**, *468*, 187–193. [CrossRef] [PubMed]
15. Ross, C.A.; Margolis, R.L.; Reading, S.A.; Pletnikov, M.; Coyle, J.T. Neurobiology of schizophrenia. *Neuron* **2006**, *52*, 139–153. [CrossRef] [PubMed]
16. Malhotra, A.K.; Litman, R.E.; Pickar, D. Adverse effects of antipsychotic drugs. *Drug Saf.* **1993**, *9*, 429–436. [CrossRef] [PubMed]
17. Muench, J.; Hamer, A.M. Adverse effects of antipsychotic medications. *Am. Fam. Physician* **2010**, *81*, 617–622. [PubMed]
18. Kambeitz, J.; Kambeitz-Ilankovic, L.; Cabral, C.; Dwyer, D.B.; Calhoun, V.D.; van den Heuvel, M.P.; Falkai, P.; Koutsouleris, N.; Malchow, B. Aberrant functional whole-brain network architecture in patients with schizophrenia: A meta-analysis. *Schizophr. Bull.* **2016**, *42* (Suppl. 1), S13–S21. [CrossRef] [PubMed]
19. Deng, C.; Dean, B. Mapping the pathophysiology of schizophrenia: Interactions between multiple cellular pathways. *Front. Cell. Neurosci.* **2013**, *7*, 238. [CrossRef] [PubMed]
20. Goodman, W.K.; Insel, T.R. Deep brain stimulation in psychiatry: Concentrating on the road ahead. *Biol. Psychiatry* **2009**, *65*, 263–266. [CrossRef] [PubMed]
21. Davidson, M.; Caspi, A.; Noy, S. The treatment of schizophrenia: From premorbid manifestations to the first episode of psychosis. *Dialogues Clin. Neurosci.* **2005**, *7*, 7–16. [PubMed]
22. Brown, A.S.; Patterson, P.H. Maternal infection and schizophrenia: Implications for prevention. *Schizophr. Bull.* **2011**, *37*, 284–290. [CrossRef] [PubMed]
23. Suvisaari, J.M.; Haukka, J.K.; Tanskanen, A.J.; Lonnqvist, J.K. Decline in the incidence of schizophrenia in finnish cohorts born from 1954 to 1965. *Arch. Gen. Psychiatry* **1999**, *56*, 733–740. [CrossRef] [PubMed]

24. Boksa, P. Effects of prenatal infection on brain development and behavior: A review of findings from animal models. *Brain Behav. Immun.* **2010**, *24*, 881–897. [CrossRef] [PubMed]
25. Brown, A.S.; Derkits, E.J. Prenatal infection and schizophrenia: A review of epidemiologic and translational studies. *Am. J. Psychiatry* **2010**, *167*, 261–280. [CrossRef] [PubMed]
26. Sorensen, H.J.; Mortensen, E.L.; Reinisch, J.M.; Mednick, S.A. Association between prenatal exposure to bacterial infection and risk of schizophrenia. *Schizophr. Bull.* **2009**, *35*, 631–637. [CrossRef] [PubMed]
27. Meyer, U. Developmental neuroinflammation and schizophrenia. *Prog. Neuropsychopharmacol. Biol. Psychiatry* **2013**, *42*, 20–34. [CrossRef] [PubMed]
28. Giovanoli, S.; Engler, H.; Engler, A.; Richetto, J.; Feldon, J.; Riva, M.A.; Schedlowski, M.; Meyer, U. Preventive effects of minocycline in a neurodevelopmental two-hit model with relevance to schizophrenia. *Transl. Psychiatry* **2016**, *6*, e772. [CrossRef] [PubMed]
29. Mandal, M.; Donnelly, R.; Elkabes, S.; Zhang, P.; Davini, D.; David, B.T.; Ponzio, N.M. Maternal immune stimulation during pregnancy shapes the immunological phenotype of offspring. *Brain Behav. Immun.* **2013**, *33*, 33–45. [CrossRef] [PubMed]
30. Reisinger, S.; Khan, D.; Kong, E.; Berger, A.; Pollak, A.; Pollak, D.D. The poly(i:C)-induced maternal immune activation model in preclinical neuropsychiatric drug discovery. *Pharmacol. Ther.* **2015**, *149*, 213–226. [CrossRef] [PubMed]
31. Zuckerman, L.; Rehavi, M.; Nachman, R.; Weiner, I. Immune activation during pregnancy in rats leads to a postpubertal emergence of disrupted latent inhibition, dopaminergic hyperfunction, and altered limbic morphology in the offspring: A novel neurodevelopmental model of schizophrenia. *Neuropsychopharmacology* **2003**, *28*, 1778–1789. [CrossRef] [PubMed]
32. Buzsaki, G. *Rhythms of the Brain*; Oxford University Press: New York, NY, USA, 2006.
33. Antal, A.; Herrmann, C.S. Transcranial alternating current and random noise stimulation: Possible mechanisms. *Neural Plast.* **2016**, *2016*, 3616807. [CrossRef] [PubMed]
34. Brunelin, J.; Poulet, E.; Bediou, B.; Kallel, L.; Dalery, J.; D'Amato, T.; Saoud, M. Low frequency repetitive transcranial magnetic stimulation improves source monitoring deficit in hallucinating patients with schizophrenia. *Schizophr. Res.* **2006**, *81*, 41–45. [CrossRef] [PubMed]
35. Puri, B.K.; Davey, N.J.; Ellaway, P.H.; Lewis, S.W. An investigation of motor function in schizophrenia using transcranial magnetic stimulation of the motor cortex. *Br. J. Psychiatry* **1996**, *169*, 690–695. [CrossRef] [PubMed]
36. Kallel, L.; Mondino, M.; Brunelin, J. Effects of theta-rhythm transcranial alternating current stimulation (4.5 Hz-tACS) in patients with clozapine-resistant negative symptoms of schizophrenia: A case series. *J. Neural Transm.* **2016**, *123*, 1213–1217. [CrossRef] [PubMed]
37. Mondino, M.; Brunelin, J.; Palm, U.; Brunoni, A.R.; Poulet, E.; Fecteau, S. Transcranial direct current stimulation for the treatment of refractory symptoms of schizophrenia. Current evidence and future directions. *Curr. Pharm. Des.* **2015**, *21*, 3373–3383. [CrossRef] [PubMed]
38. Mondino, M.; Haesebaert, F.; Poulet, E.; Suaud-Chagny, M.F.; Brunelin, J. Fronto-temporal transcranial direct current stimulation (tDCS) reduces source-monitoring deficits and auditory hallucinations in patients with schizophrenia. *Schizophr. Res.* **2015**, *161*, 515–516. [CrossRef] [PubMed]
39. Vercammen, A.; Rushby, J.A.; Loo, C.; Short, B.; Weickert, C.S.; Weickert, T.W. Transcranial direct current stimulation influences probabilistic association learning in schizophrenia. *Schizophr. Res.* **2011**, *131*, 198–205. [CrossRef] [PubMed]
40. Woods, A.J.; Antal, A.; Bikson, M.; Boggio, P.S.; Brunoni, A.R.; Celnik, P.; Cohen, L.G.; Fregni, F.; Herrmann, C.S.; Kappenman, E.S.; et al. A technical guide to tDCS, and related non-invasive brain stimulation tools. *Clin. Neurophysiol.* **2016**, *127*, 1031–1048. [CrossRef] [PubMed]
41. Ginhoux, R.; Renaud, P.; Zorn, L.; Goffin, L.; Bayle, B.; Foucher, J.; Lamy, J.; Armspach, J.P.; de Mathelin, M. A custom robot for transcranial magnetic stimulation: First assessment on healthy subjects. *Conf. Proc. IEEE Eng. Med. Biol. Soc.* **2013**, *2013*, 5352–5355. [PubMed]
42. Lefaucheur, J.P.; Andre-Obadia, N.; Antal, A.; Ayache, S.S.; Baeken, C.; Benninger, D.H.; Cantello, R.M.; Cincotta, M.; de Carvalho, M.; de Ridder, D.; et al. Evidence-based guidelines on the therapeutic use of repetitive transcranial magnetic stimulation (RTMS). *Clin. Neurophysiol.* **2014**, *125*, 2150–2206. [CrossRef] [PubMed]

43. Yung, A.R.; McGorry, P.D. The prodromal phase of first-episode psychosis: Past and current conceptualizations. *Schizophr. Bull.* **1996**, *22*, 353–370. [CrossRef] [PubMed]
44. Kahn, R.S.; Sommer, I.E. The neurobiology and treatment of first-episode schizophrenia. *Mol. Psychiatry* **2015**, *20*, 84–97. [CrossRef] [PubMed]
45. Perkins, D.O.; Gu, H.; Boteva, K.; Lieberman, J.A. Relationship between duration of untreated psychosis and outcome in first-episode schizophrenia: A critical review and meta-analysis. *Am. J. Psychiatry* **2005**, *162*, 1785–1804. [CrossRef] [PubMed]
46. Kulhara, P.; Banerjee, A.; Dutt, A. Early intervention in schizophrenia. *Indian J. Psychiatry* **2008**, *50*, 128–134. [CrossRef] [PubMed]
47. Larson, M.K.; Walker, E.F.; Compton, M.T. Early signs, diagnosis and therapeutics of the prodromal phase of schizophrenia and related psychotic disorders. *Expert Rev. Neurother.* **2010**, *10*, 1347–1359. [CrossRef] [PubMed]
48. Wyatt, R.J. Neuroleptics and the natural course of schizophrenia. *Schizophr. Bull.* **1991**, *17*, 325–351. [CrossRef] [PubMed]
49. Basar, E. Brain oscillations in neuropsychiatric disease. *Dialogues Clin. Neurosci.* **2013**, *15*, 291–300. [PubMed]
50. Baldeweg, T.; Spence, S.; Hirsch, S.R.; Gruzelier, J. Gamma-band electroencephalographic oscillations in a patient with somatic hallucinations. *Lancet* **1998**, *352*, 620–621. [CrossRef]
51. Becker, C.; Gramann, K.; Muller, H.J.; Elliott, M.A. Electrophysiological correlates of flicker-induced color hallucinations. *Conscious. Cogn.* **2009**, *18*, 266–276. [CrossRef] [PubMed]
52. Mulert, C.; Kirsch, V.; Pascual-Marqui, R.; McCarley, R.W.; Spencer, K.M. Long-range synchrony of gamma oscillations and auditory hallucination symptoms in schizophrenia. *Int. J. Psychophysiol.* **2011**, *79*, 55–63. [CrossRef] [PubMed]
53. Spencer, K.M.; Nestor, P.G.; Perlmutter, R.; Niznikiewicz, M.A.; Klump, M.C.; Frumin, M.; Shenton, M.E.; McCarley, R.W. Neural synchrony indexes disordered perception and cognition in schizophrenia. *Proc. Natl. Acad. Sci. USA* **2004**, *101*, 17288–17293. [CrossRef] [PubMed]
54. Andreou, C.; Nolte, G.; Leicht, G.; Polomac, N.; Hanganu-Opatz, I.L.; Lambert, M.; Engel, A.K.; Mulert, C. Increased resting-state gamma-band connectivity in first-episode schizophrenia. *Schizophr. Bull.* **2015**, *41*, 930–939. [CrossRef] [PubMed]
55. Flynn, G.; Alexander, D.; Harris, A.; Whitford, T.; Wong, W.; Galletly, C.; Silverstein, S.; Gordon, E.; Williams, L.M. Increased absolute magnitude of gamma synchrony in first-episode psychosis. *Schizophr. Res.* **2008**, *105*, 262–271. [CrossRef] [PubMed]
56. Ramyead, A.; Kometer, M.; Studerus, E.; Koranyi, S.; Ittig, S.; Gschwandtner, U.; Fuhr, P.; Riecher-Rossler, A. Aberrant current source-density and lagged phase synchronization of neural oscillations as markers for emerging psychosis. *Schizophr. Bull.* **2015**, *41*, 919–929. [CrossRef] [PubMed]
57. Ramyead, A.; Studerus, E.; Kometer, M.; Uttinger, M.; Gschwandtner, U.; Fuhr, P.; Riecher-Rossler, A. Prediction of psychosis using neural oscillations and machine learning in neuroleptic-naive at-risk patients. *World J. Biol. Psychiatry* **2016**, *17*, 285–295. [CrossRef] [PubMed]
58. Rivolta, D.; Heidegger, T.; Scheller, B.; Sauer, A.; Schaum, M.; Birkner, K.; Singer, W.; Wibral, M.; Uhlhaas, P.J. Ketamine dysregulates the amplitude and connectivity of high-frequency oscillations in cortical-subcortical networks in humans: Evidence from resting-state magnetoencephalography-recordings. *Schizophr. Bull.* **2015**, *41*, 1105–1114. [CrossRef] [PubMed]
59. Anderson, P.M.; Jones, N.C.; O'Brien, T.J.; Pinault, D. The n-methyl d-aspartate glutamate receptor antagonist ketamine disrupts the functional state of the corticothalamic pathway. *Cereb. Cortex* **2016**. [CrossRef] [PubMed]
60. Hakami, T.; Jones, N.C.; Tolmacheva, E.A.; Gaudias, J.; Chaumont, J.; Salzberg, M.; O'Brien, T.J.; Pinault, D. Nmda receptor hypofunction leads to generalized and persistent aberrant gamma oscillations independent of hyperlocomotion and the state of consciousness. *PLoS ONE* **2009**, *4*, e6755. [CrossRef] [PubMed]
61. Kulikova, S.P.; Tolmacheva, E.A.; Anderson, P.; Gaudias, J.; Adams, B.E.; Zheng, T.; Pinault, D. Opposite effects of ketamine and deep brain stimulation on rat thalamocortical information processing. *Eur. J. Neurosci.* **2012**, *36*, 3407–3419. [CrossRef] [PubMed]
62. Pinault, D. N-methyl d-aspartate receptor antagonists ketamine and MK-801 induce wake-related aberrant gamma oscillations in the rat neocortex. *Biol. Psychiatry* **2008**, *63*, 730–735. [CrossRef] [PubMed]

63. Treen, D.; Batlle, S.; Molla, L.; Forcadell, E.; Chamorro, J.; Bulbena, A.; Perez, V. Are there glutamate abnormalities in subjects at high risk mental state for psychosis? A review of the evidence. *Schizophr. Res.* **2016**, *171*, 166–175. [CrossRef] [PubMed]
64. Manoach, D.S.; Pan, J.Q.; Purcell, S.M.; Stickgold, R. Reduced sleep spindles in schizophrenia: A treatable endophenotype that links risk genes to impaired cognition? *Biol. Psychiatry* **2016**, *80*, 599–608. [CrossRef] [PubMed]
65. Tesler, N.; Gerstenberg, M.; Franscini, M.; Jenni, O.G.; Walitza, S.; Huber, R. Reduced sleep spindle density in early onset schizophrenia: A preliminary finding. *Schizophr. Res.* **2015**, *166*, 355–357. [CrossRef] [PubMed]
66. Monti, J.M.; Monti, D. Sleep disturbance in schizophrenia. *Int. Rev. Psychiatry* **2005**, *17*, 247–253. [CrossRef] [PubMed]
67. Kamath, J.; Virdi, S.; Winokur, A. Sleep disturbances in schizophrenia. *Psychiatr. Clin. N. Am.* **2015**, *38*, 777–792. [CrossRef] [PubMed]
68. Giesel, F.L.; Mehndiratta, A.; Hempel, A.; Hempel, E.; Kress, K.R.; Essig, M.; Schroder, J. Improvement of auditory hallucinations and reduction of primary auditory area's activation following tms. *Eur. J. Radiol.* **2012**, *81*, 1273–1275. [CrossRef] [PubMed]
69. Hoffman, R.E.; Gueorguieva, R.; Hawkins, K.A.; Varanko, M.; Boutros, N.N.; Wu, Y.T.; Carroll, K.; Krystal, J.H. Temporoparietal transcranial magnetic stimulation for auditory hallucinations: Safety, efficacy and moderators in a fifty patient sample. *Biol. Psychiatry* **2005**, *58*, 97–104. [CrossRef] [PubMed]
70. Luber, B.; Kinnunen, L.H.; Rakitin, B.C.; Ellsasser, R.; Stern, Y.; Lisanby, S.H. Facilitation of performance in a working memory task with rtms stimulation of the precuneus: Frequency- and time-dependent effects. *Brain Res.* **2007**, *1128*, 120–129. [CrossRef] [PubMed]
71. Luber, B.; Steffener, J.; Tucker, A.; Habeck, C.; Peterchev, A.V.; Deng, Z.D.; Basner, R.C.; Stern, Y.; Lisanby, S.H. Extended remediation of sleep deprived-induced working memory deficits using FMRI-guided transcranial magnetic stimulation. *Sleep* **2013**, *36*, 857–871. [CrossRef] [PubMed]
72. George, M.S.; Padberg, F.; Schlaepfer, T.E.; O'Reardon, J.P.; Fitzgerald, P.B.; Nahas, Z.H.; Marcolin, M.A. Controversy: Repetitive transcranial magnetic stimulation or transcranial direct current stimulation shows efficacy in treating psychiatric diseases (depression, mania, schizophrenia, obsessive-complusive disorder, panic, posttraumatic stress disorder). *Brain Stimul.* **2009**, *2*, 14–21. [CrossRef] [PubMed]
73. Lisanby, S.H.; Kinnunen, L.H.; Crupain, M.J. Applications of TMS to therapy in psychiatry. *J. Clin. Neurophysiol.* **2002**, *19*, 344–360. [CrossRef] [PubMed]
74. Haynes, W.I.; Mallet, L. High-frequency stimulation of deep brain structures in obsessive-compulsive disorder: The search for a valid circuit. *Eur. J. Neurosci.* **2010**, *32*, 1118–1127. [CrossRef] [PubMed]
75. Mallet, L.; Schupbach, M.; N'Diaye, K.; Remy, P.; Bardinet, E.; Czernecki, V.; Welter, M.L.; Pelissolo, A.; Ruberg, M.; Agid, Y.; et al. Stimulation of subterritories of the subthalamic nucleus reveals its role in the integration of the emotional and motor aspects of behavior. *Proc. Natl. Acad. Sci. USA* **2007**, *104*, 10661–10666. [CrossRef] [PubMed]
76. George, M.S.; Nahas, Z.; Borckardt, J.J.; Anderson, B.; Foust, M.J.; Burns, C.; Kose, S.; Short, E.B. Brain stimulation for the treatment of psychiatric disorders. *Curr. Opin. Psychiatry* **2007**, *20*, 250–254; discussion 247–259. [CrossRef] [PubMed]
77. Keller, W.R.; Fischer, B.A.; Carpenter, W.T., Jr. Revisiting the diagnosis of schizophrenia: Where have we been and where are we going? *CNS Neurosci. Ther.* **2011**, *17*, 83–88. [CrossRef] [PubMed]
78. Clausen, J. Ethical brain stimulation—Neuroethics of deep brain stimulation in research and clinical practice. *Eur. J. Neurosci.* **2010**, *32*, 1152–1162. [CrossRef] [PubMed]
79. Yamamoto, T.; Katayama, Y.; Kobayashi, K.; Oshima, H.; Fukaya, C.; Tsubokawa, T. Deep brain stimulation for the treatment of vegetative state. *Eur. J. Neurosci.* **2010**, *32*, 1145–1151. [CrossRef] [PubMed]
80. Forrest, A.D.; Coto, C.A.; Siegel, S.J. Animal models of psychosis: Current state and future directions. *Curr. Behav. Neurosci. Rep.* **2014**, *1*, 100–116. [CrossRef] [PubMed]
81. Jones, C.A.; Watson, D.J.; Fone, K.C. Animal models of schizophrenia. *Br. J. Pharmacol.* **2011**, *164*, 1162–1194. [CrossRef] [PubMed]
82. Low, N.C.; Hardy, J. What is a schizophrenic mouse? *Neuron* **2007**, *54*, 348–349. [CrossRef] [PubMed]
83. Powell, C.M.; Miyakawa, T. Schizophrenia-relevant behavioral testing in rodent models: A uniquely human disorder? *Biol. Psychiatry* **2006**, *59*, 1198–1207. [CrossRef] [PubMed]

84. Douglas, K.S.; Guy, L.S.; Hart, S.D. Psychosis as a risk factor for violence to others: A meta-analysis. *Psychol. Bull.* **2009**, *135*, 679–706. [CrossRef] [PubMed]
85. Hodgins, S.; Piatosa, M.J.; Schiffer, B. Violence among people with schizophrenia: Phenotypes and neurobiology. *Curr. Top. Behav. Neurosci.* **2014**, *17*, 329–368. [PubMed]
86. Iozzino, L.; Ferrari, C.; Large, M.; Nielssen, O.; de Girolamo, G. Prevalence and risk factors of violence by psychiatric acute inpatients: A systematic review and meta-analysis. *PLoS ONE* **2015**, *10*, e0128536. [CrossRef] [PubMed]
87. Marcotte, E.R.; Pearson, D.M.; Srivastava, L.K. Animal models of schizophrenia: A critical review. *J. Psychiatry Neurosci.* **2001**, *26*, 395–410. [PubMed]
88. Robertson, G.S.; Hori, S.E.; Powell, K.J. Schizophrenia: An integrative approach to modelling a complex disorder. *J. Psychiatry Neurosci.* **2006**, *31*, 157–167. [PubMed]
89. Bitanihirwe, B.K.; Peleg-Raibstein, D.; Mouttet, F.; Feldon, J.; Meyer, U. Late prenatal immune activation in mice leads to behavioral and neurochemical abnormalities relevant to the negative symptoms of schizophrenia. *Neuropsychopharmacology* **2010**, *35*, 2462–2478. [CrossRef] [PubMed]
90. Meyer, U.; Nyffeler, M.; Schwendener, S.; Knuesel, I.; Yee, B.K.; Feldon, J. Relative prenatal and postnatal maternal contributions to schizophrenia-related neurochemical dysfunction after in utero immune challenge. *Neuropsychopharmacology* **2008**, *33*, 441–456. [CrossRef] [PubMed]
91. Samuelsson, A.M.; Jennische, E.; Hansson, H.A.; Holmang, A. Prenatal exposure to interleukin-6 results in inflammatory neurodegeneration in hippocampus with nmda/gaba(a) dysregulation and impaired spatial learning. *Am. J. Physiol. Regul. Integr. Comp. Physiol.* **2006**, *290*, R1345–R1356. [CrossRef] [PubMed]
92. Spiegel, E.A.; Wycis, H.T.; Marks, M.; Lee, A.J. Stereotaxic apparatus for operations on the human brain. *Science* **1947**, *106*, 349–350. [CrossRef] [PubMed]
93. Williams, N.R.; Taylor, J.J.; Lamb, K.; Hanlon, C.A.; Short, E.B.; George, M.S. Role of functional imaging in the development and refinement of invasive neuromodulation for psychiatric disorders. *World J. Radiol.* **2014**, *6*, 756–778. [CrossRef] [PubMed]
94. Benabid, A.L.; Pollak, P.; Gervason, C.; Hoffmann, D.; Gao, D.M.; Hommel, M.; Perret, J.E.; de, R.J. Long-term suppression of tremor by chronic stimulation of the ventral intermediate thalamic nucleus. *Lancet* **1991**, *337*, 403–406. [CrossRef]
95. Benabid, A.L.; Pollak, P.; Louveau, A.; Henry, S.; de, R.J. Combined (thalamotomy and stimulation) stereotactic surgery of the vim thalamic nucleus for bilateral parkinson disease. *Appl. Neurophysiol.* **1987**, *50*, 344–346. [CrossRef] [PubMed]
96. Lockman, J.; Fisher, R.S. Therapeutic brain stimulation for epilepsy. *Neurol. Clin.* **2009**, *27*, 1031–1040. [CrossRef] [PubMed]
97. Mehdorn, H.M. Deep brain stimulation for dystonia: Review of the literature. *J. Neurosurg. Sci.* **2016**, *60*, 199–210. [PubMed]
98. Boccard, S.G.; Pereira, E.A.; Aziz, T.Z. Deep brain stimulation for chronic pain. *J. Clin. Neurosci.* **2015**, *22*, 1537–1543. [CrossRef] [PubMed]
99. Pereira, E.A.; Green, A.L.; Aziz, T.Z. Deep brain stimulation for pain. *Handb. Clin. Neurol.* **2013**, *116*, 277–294. [PubMed]
100. Roy, H.A.; Aziz, T.Z. Deep brain stimulation and multiple sclerosis: Therapeutic applications. *Mult. Scler. Relat. Disord.* **2014**, *3*, 431–439. [CrossRef] [PubMed]
101. Mayberg, H.S.; Lozano, A.M.; Voon, V.; McNeely, H.E.; Seminowicz, D.; Hamani, C.; Schwalb, J.M.; Kennedy, S.H. Deep brain stimulation for treatment-resistant depression. *Neuron* **2005**, *45*, 651–660. [CrossRef] [PubMed]
102. Hamani, C.; Nobrega, J.N. Deep brain stimulation in clinical trials and animal models of depression. *Eur. J. Neurosci.* **2010**, *32*, 1109–1117. [CrossRef] [PubMed]
103. Schrock, L.E.; Mink, J.W.; Woods, D.W.; Porta, M.; Servello, D.; Visser-Vandewalle, V.; Silburn, P.A.; Foltynie, T.; Walker, H.C.; Shahed-Jimenez, J.; et al. Tourette syndrome deep brain stimulation: A review and updated recommendations. *Mov. Disord.* **2015**, *30*, 448–471. [CrossRef] [PubMed]
104. Shah, S.A.; Schiff, N.D. Central thalamic deep brain stimulation for cognitive neuromodulation—A review of proposed mechanisms and investigational studies. *Eur. J. Neurosci.* **2010**, *32*, 1135–1144. [CrossRef] [PubMed]
105. Benabid, A.L.; Torres, N. New targets for dbs. *Parkinsonism Relat. Disord.* **2012**, *18* (Suppl. 1), S21–S23. [CrossRef]

106. Nassery, A.; Palmese, C.A.; Sarva, H.; Groves, M.; Miravite, J.; Kopell, B.H. Psychiatric and cognitive effects of deep brain stimulation for parkinson's disease. *Curr. Neurol. Neurosci. Rep.* **2016**, *16*, 87. [CrossRef] [PubMed]
107. Piasecki, S.D.; Jefferson, J.W. Psychiatric complications of deep brain stimulation for parkinson's disease. *J. Clin. Psychiatry* **2004**, *65*, 845–849. [CrossRef] [PubMed]
108. Kringelbach, M.L.; Jenkinson, N.; Owen, S.L.; Aziz, T.Z. Translational principles of deep brain stimulation. *Nat. Rev. Neurosci.* **2007**, *8*, 623–635. [CrossRef] [PubMed]
109. Deniau, J.M.; Degos, B.; Bosch, C.; Maurice, N. Deep brain stimulation mechanisms: Beyond the concept of local functional inhibition. *Eur. J. Neurosci.* **2010**, *32*, 1080–1091. [CrossRef] [PubMed]
110. Conca, A.; Koppi, S.; Konig, P.; Swoboda, E.; Krecke, N. Transcranial magnetic stimulation: A novel antidepressive strategy? *Neuropsychobiology* **1996**, *34*, 204–207. [CrossRef] [PubMed]
111. Gorelick, D.A.; Zangen, A.; George, M.S. Transcranial magnetic stimulation in the treatment of substance addiction. *Ann. N. Y. Acad. Sci.* **2014**, *1327*, 79–93. [CrossRef] [PubMed]
112. Kobayashi, M.; Pascual-Leone, A. Transcranial magnetic stimulation in neurology. *Lancet Neurol.* **2003**, *2*, 145–156. [CrossRef]
113. Bikson, M.; Grossman, P.; Thomas, C.; Zannou, A.L.; Jiang, J.; Adnan, T.; Mourdoukoutas, A.P.; Kronberg, G.; Truong, D.; Boggio, P.; et al. Safety of transcranial direct current stimulation: Evidence based update 2016. *Brain Stimul.* **2016**, *9*, 641–661. [CrossRef] [PubMed]
114. Chhabra, H.; Shivakumar, V.; Agarwal, S.M.; Bose, A.; Venugopal, D.; Rajasekaran, A.; Subbanna, M.; Kalmady, S.V.; Narayanaswamy, J.C.; Debnath, M.; et al. Transcranial direct current stimulation and neuroplasticity genes: Implications for psychiatric disorders. *Acta Neuropsychiatr.* **2016**, *28*, 1–10. [CrossRef] [PubMed]
115. Hasan, A.; Strube, W.; Palm, U.; Wobrock, T. Repetitive noninvasive brain stimulation to modulate cognitive functions in schizophrenia: A systematic review of primary and secondary outcomes. *Schizophr. Bull.* **2016**, *42* (Suppl. 1), S95–S109. [CrossRef] [PubMed]
116. Mondino, M.; Jardri, R.; Suaud-Chagny, M.F.; Saoud, M.; Poulet, E.; Brunelin, J. Effects of fronto-temporal transcranial direct current stimulation on auditory verbal hallucinations and resting-state functional connectivity of the left temporo-parietal junction in patients with schizophrenia. *Schizophr. Bull.* **2016**, *42*, 318–326. [CrossRef] [PubMed]
117. Brunelin, J.; Mondino, M.; Gassab, L.; Haesebaert, F.; Gaha, L.; Suaud-Chagny, M.F.; Saoud, M.; Mechri, A.; Poulet, E. Examining transcranial direct-current stimulation (tDCS) as a treatment for hallucinations in schizophrenia. *Am. J. Psychiatry* **2012**, *169*, 719–724. [CrossRef] [PubMed]
118. Priori, A.; Berardelli, A.; Rona, S.; Accornero, N.; Manfredi, M. Polarization of the human motor cortex through the scalp. *Neuroreport* **1998**, *9*, 2257–2260. [CrossRef] [PubMed]
119. Stagg, C.J.; Nitsche, M.A. Physiological basis of transcranial direct current stimulation. *Neuroscientist* **2011**, *17*, 37–53. [CrossRef] [PubMed]
120. Antal, A.; Boros, K.; Poreisz, C.; Chaieb, L.; Terney, D.; Paulus, W. Comparatively weak after-effects of transcranial alternating current stimulation (tACS) on cortical excitability in humans. *Brain Stimul.* **2008**, *1*, 97–105. [CrossRef] [PubMed]
121. Abd Hamid, A.I.; Gall, C.; Speck, O.; Antal, A.; Sabel, B.A. Effects of alternating current stimulation on the healthy and diseased brain. *Front. Neurosci.* **2015**, *9*, 391. [CrossRef] [PubMed]
122. Bennabi, D.; Pedron, S.; Haffen, E.; Monnin, J.; Peterschmitt, Y.; Van Waes, V. Transcranial direct current stimulation for memory enhancement: From clinical research to animal models. *Front. Syst. Neurosci.* **2014**, *8*, 159. [CrossRef] [PubMed]
123. Santarnecchi, E.; Polizzotto, N.R.; Godone, M.; Giovannelli, F.; Feurra, M.; Matzen, L.; Rossi, A.; Rossi, S. Frequency-dependent enhancement of fluid intelligence induced by transcranial oscillatory potentials. *Curr. Biol.* **2013**, *23*, 1449–1453. [CrossRef] [PubMed]
124. Voss, U.; Holzmann, R.; Hobson, A.; Paulus, W.; Koppehele-Gossel, J.; Klimke, A.; Nitsche, M.A. Induction of self awareness in dreams through frontal low current stimulation of gamma activity. *Nat. Neurosci.* **2014**, *17*, 810–812. [CrossRef] [PubMed]
125. Urbano, F.J.; D'Onofrio, S.M.; Luster, B.R.; Beck, P.B.; Hyde, J.R.; Bisagno, V.; Garcia-Rill, E. Pedunculopontine nucleus gamma band activity-preconscious awareness, waking, and rem sleep. *Front. Neurol.* **2014**, *5*, 210. [CrossRef] [PubMed]

126. Moisa, M.; Polania, R.; Grueschow, M.; Ruff, C.C. Brain network mechanisms underlying motor enhancement by transcranial entrainment of gamma oscillations. *J. Neurosci.* **2016**, *36*, 12053–12065. [CrossRef] [PubMed]
127. Brignani, D.; Ruzzoli, M.; Mauri, P.; Miniussi, C. Is transcranial alternating current stimulation effective in modulating brain oscillations? *PLoS ONE* **2013**, *8*, e56589. [CrossRef] [PubMed]
128. Herrmann, C.S.; Struber, D.; Helfrich, R.F.; Engel, A.K. Eeg oscillations: From correlation to causality. *Int. J. Psychophysiol.* **2016**, *103*, 12–21. [CrossRef] [PubMed]
129. Terney, D.; Chaieb, L.; Moliadze, V.; Antal, A.; Paulus, W. Increasing human brain excitability by transcranial high-frequency random noise stimulation. *J. Neurosci.* **2008**, *28*, 14147–14155. [CrossRef] [PubMed]
130. Fertonani, A.; Pirulli, C.; Miniussi, C. Random noise stimulation improves neuroplasticity in perceptual learning. *J. Neurosci.* **2011**, *31*, 15416–15423. [CrossRef] [PubMed]
131. Brittain, J.S.; Probert-Smith, P.; Aziz, T.Z.; Brown, P. Tremor suppression by rhythmic transcranial current stimulation. *Curr. Biol.* **2013**, *23*, 436–440. [CrossRef] [PubMed]
132. Hess, C.W. Modulation of cortical-subcortical networks in parkinson's disease by applied field effects. *Front. Hum. Neurosci.* **2013**, *7*, 565. [CrossRef] [PubMed]
133. Allen, P.; Luigjes, J.; Howes, O.D.; Egerton, A.; Hirao, K.; Valli, I.; Kambeitz, J.; Fusar-Poli, P.; Broome, M.; McGuire, P. Transition to psychosis associated with prefrontal and subcortical dysfunction in ultra high-risk individuals. *Schizophr. Bull.* **2012**, *38*, 1268–1276. [CrossRef] [PubMed]
134. Brans, R.G.; van Haren, N.E.; van Baal, G.C.; Staal, W.G.; Schnack, H.G.; Kahn, R.S.; Hulshoff Pol, H.E. Longitudinal mri study in schizophrenia patients and their healthy siblings. *Br. J. Psychiatry* **2008**, *193*, 422–423. [CrossRef] [PubMed]
135. Cho, K.I.; Shenton, M.E.; Kubicki, M.; Jung, W.H.; Lee, T.Y.; Yun, J.Y.; Kim, S.N.; Kwon, J.S. Altered thalamo-cortical white matter connectivity: Probabilistic tractography study in clinical-high risk for psychosis and first-episode psychosis. *Schizophr. Bull.* **2016**, *42*, 723–731. [CrossRef] [PubMed]
136. Howes, O.D.; Fusar-Poli, P.; Bloomfield, M.; Selvaraj, S.; McGuire, P. From the prodrome to chronic schizophrenia: The neurobiology underlying psychotic symptoms and cognitive impairments. *Curr. Pharm. Des.* **2012**, *18*, 459–465. [CrossRef] [PubMed]
137. Kahn, R.S.; Keefe, R.S. Schizophrenia is a cognitive illness: Time for a change in focus. *JAMA Psychiatry* **2013**, *70*, 1107–1112. [CrossRef] [PubMed]
138. Shah, J.; Eack, S.M.; Montrose, D.M.; Tandon, N.; Miewald, J.M.; Prasad, K.M.; Keshavan, M.S. Multivariate prediction of emerging psychosis in adolescents at high risk for schizophrenia. *Schizophr. Res.* **2012**, *141*, 189–196. [CrossRef] [PubMed]
139. Yung, A.R.; McGorry, P.D.; McFarlane, C.A.; Jackson, H.J.; Patton, G.C.; Rakkar, A. Monitoring and care of young people at incipient risk of psychosis. *Schizophr. Bull.* **1996**, *22*, 283–303. [CrossRef] [PubMed]
140. Cronenwett, W.J.; Csernansky, J. Thalamic pathology in schizophrenia. *Curr. Top. Behav. Neurosci.* **2010**, *4*, 509–528. [PubMed]
141. van Haren, N.E.; Cahn, W.; Hulshoff Pol, H.E.; Kahn, R.S. Schizophrenia as a progressive brain disease. *Eur. Psychiatry* **2008**, *23*, 245–254. [CrossRef] [PubMed]
142. Zipursky, R.B.; Reilly, T.J.; Murray, R.M. The myth of schizophrenia as a progressive brain disease. *Schizophr. Bull.* **2013**, *39*, 1363–1372. [CrossRef] [PubMed]
143. Harvey, P.D. When does cognitive decline occur in the period prior to the first episode of schizophrenia? *Psychiatry* **2009**, *6*, 12–14. [PubMed]
144. Simon, A.E.; Cattapan-Ludewig, K.; Zmilacher, S.; Arbach, D.; Gruber, K.; Dvorsky, D.N.; Roth, B.; Isler, E.; Zimmer, A.; Umbricht, D. Cognitive functioning in the schizophrenia prodrome. *Schizophr. Bull.* **2007**, *33*, 761–771. [CrossRef] [PubMed]
145. Tandon, N.; Shah, J.; Keshavan, M.S.; Tandon, R. Attenuated psychosis and the schizophrenia prodrome: Current status of risk identification and psychosis prevention. *Neuropsychiatry* **2012**, *2*, 345–353. [CrossRef] [PubMed]
146. Vidailhet, P. First-episode psychosis, cognitive difficulties and remediation. *Encephale* **2013**, *39* (Suppl. 2), S83–S92. [CrossRef]
147. Jahshan, C.; Heaton, R.K.; Golshan, S.; Cadenhead, K.S. Course of neurocognitive deficits in the prodrome and first episode of schizophrenia. *Neuropsychology* **2010**, *24*, 109–120. [CrossRef] [PubMed]
148. Riley, B.; Kendler, K.S. Molecular genetic studies of schizophrenia. *Eur. J. Hum. Genet.* **2006**, *14*, 669–680. [CrossRef] [PubMed]

149. Susser, E.; Neugebauer, R.; Hoek, H.W.; Brown, A.S.; Lin, S.; Labovitz, D.; Gorman, J.M. Schizophrenia after prenatal famine. Further evidence. *Arch. Gen. Psychiatry* **1996**, *53*, 25–31. [CrossRef] [PubMed]
150. Joyce, E. Origins of cognitive dysfunction in schizophrenia: Clues from age at onset. *Br. J. Psychiatry* **2005**, *186*, 93–95. [CrossRef] [PubMed]
151. Brown, A.S.; Susser, E.S. Prenatal nutritional deficiency and risk of adult schizophrenia. *Schizophr. Bull.* **2008**, *34*, 1054–1063. [CrossRef] [PubMed]
152. Brown, A.S. The risk for schizophrenia from childhood and adult infections. *Am. J. Psychiatry* **2008**, *165*, 7–10. [CrossRef] [PubMed]
153. Muller, N.; Schwarz, M.J. Immune system and schizophrenia. *Curr. Immunol. Rev.* **2010**, *6*, 213–220. [CrossRef] [PubMed]
154. Howes, O.D.; McDonald, C.; Cannon, M.; Arseneault, L.; Boydell, J.; Murray, R.M. Pathways to schizophrenia: The impact of environmental factors. *Int. J. Neuropsychopharmacol.* **2004**, *7* (Suppl. 1), S7–S13. [CrossRef] [PubMed]
155. Peters, E.; Day, S.; McKenna, J.; Orbach, G. Delusional ideation in religious and psychotic populations. *Br. J. Clin. Psychol.* **1999**, *38 Pt 1*, 83–96. [CrossRef] [PubMed]
156. Guillery, R.W.; Sherman, S.M. Thalamic relay functions and their role in corticocortical communication: Generalizations from the visual system. *Neuron* **2002**, *33*, 163–175. [CrossRef]
157. Watis, L.; Chen, S.H.; Chua, H.C.; Chong, S.A.; Sim, K. Glutamatergic abnormalities of the thalamus in schizophrenia: A systematic review. *J. Neural Transm.* **2008**, *115*, 493–511. [CrossRef] [PubMed]
158. Jones, E.G. *The Thalamus*, 2nd ed.; Cambridge University Press: Cambridge, UK; New York, NY, USA, 2007.
159. Sherman, S.M. Thalamus plays a central role in ongoing cortical functioning. *Nat. Neurosci.* **2016**, *19*, 533–541. [CrossRef] [PubMed]
160. Sherman, S.M.; Guillery, R.W. *Exploring the Thalamus*; Academic Press: San Diego, CA, USA, 2001; pp. xvii, 1312.
161. Castaigne, P.; Lhermitte, F.; Buge, A.; Escourolle, R.; Hauw, J.J.; Lyon-Caen, O. Paramedian thalamic and midbrain infarct: Clinical and neuropathological study. *Ann. Neurol.* **1981**, *10*, 127–148. [CrossRef] [PubMed]
162. Ingvar, D.H.; Sourander, P. Destruction of the reticular core of the brain stem. A patho-anatomical follow-up of a case of coma of three years' duration. *Arch. Neurol.* **1970**, *23*, 1–8. [CrossRef] [PubMed]
163. Hassler, R.; Ore, G.D.; Dieckmann, G.; Bricolo, A.; Dolce, G. Behavioural and eeg arousal induced by stimulation of unspecific projection systems in a patient with post-traumatic apallic syndrome. *Electroencephalogr. Clin. Neurophysiol.* **1969**, *27*, 306–310. [CrossRef]
164. Hardenacke, K.; Shubina, E.; Buhrle, C.P.; Zapf, A.; Lenartz, D.; Klosterkotter, J.; Visser-Vandewalle, V.; Kuhn, J. Deep brain stimulation as a tool for improving cognitive functioning in alzheimer's dementia: A systematic review. *Front. Psychiatry* **2013**, *4*, 159. [CrossRef] [PubMed]
165. Pinault, D. The thalamic reticular nucleus: Structure, function and concept. *Brain Res. Brain Res. Rev.* **2004**, *46*, 1–31. [CrossRef] [PubMed]
166. Deschenes, M.; Veinante, P.; Zhang, Z.W. The organization of corticothalamic projections: Reciprocity versus parity. *Brain Res. Brain Res. Rev.* **1998**, *28*, 286–308. [CrossRef]
167. Guillery, R.W.; Feig, S.L.; Lozsadi, D.A. Paying attention to the thalamic reticular nucleus. *Trends Neurosci.* **1998**, *21*, 28–32. [CrossRef]
168. Deschenes, M.; Madariaga-Domich, A.; Steriade, M. Dendrodendritic synapses in the cat reticularis thalami nucleus: A structural basis for thalamic spindle synchronization. *Brain Res.* **1985**, *334*, 165–168. [CrossRef]
169. Ide, L.S. The fine structure of the perigeniculate nucleus in the cat. *J. Comp. Neurol.* **1982**, *210*, 317–334. [CrossRef] [PubMed]
170. Montero, V.M.; Singer, W. Ultrastructure and synaptic relations of neural elements containing glutamic acid decarboxylase (GAD) in the perigeniculate nucleus of the cat. A light and electron microscopic immunocytochemical study. *Exp. Brain Res.* **1984**, *56*, 115–125. [CrossRef] [PubMed]
171. Pinault, D.; Smith, Y.; Deschenes, M. Dendrodendritic and axoaxonic synapses in the thalamic reticular nucleus of the adult rat. *J. Neurosci.* **1997**, *17*, 3215–3233. [PubMed]
172. Landisman, C.E.; Long, M.A.; Beierlein, M.; Deans, M.R.; Paul, D.L.; Connors, B.W. Electrical synapses in the thalamic reticular nucleus. *J. Neurosci.* **2002**, *22*, 1002–1009. [PubMed]

173. Deleuze, C.; Huguenard, J.R. Distinct electrical and chemical connectivity maps in the thalamic reticular nucleus: Potential roles in synchronization and sensation. *J. Neurosci.* **2006**, *26*, 8633–8645. [CrossRef] [PubMed]
174. Golshani, P.; Liu, X.B.; Jones, E.G. Differences in quantal amplitude reflect GluR4- subunit number at corticothalamic synapses on two populations of thalamic neurons. *Proc. Natl. Acad. Sci. USA* **2001**, *98*, 4172–4177. [CrossRef] [PubMed]
175. Wang, Z.; Neely, R.; Landisman, C.E. Activation of group i and group II metabotropic glutamate receptors causes LTD and LTP of electrical synapses in the rat thalamic reticular nucleus. *J. Neurosci.* **2015**, *35*, 7616–7625. [CrossRef] [PubMed]
176. Zhang, L.; Jones, E.G. Corticothalamic inhibition in the thalamic reticular nucleus. *J. Neurophysiol.* **2004**, *91*, 759–766. [CrossRef] [PubMed]
177. Bucherelli, C.; Tassoni, G.; Bures, J. Differential effect of functional ablation of thalamic reticular nucleus on the acquisition of passive and active avoidance. *Int. J. Neurosci.* **1993**, *73*, 77–84. [CrossRef] [PubMed]
178. Weese, G.D.; Phillips, J.M.; Brown, V.J. Attentional orienting is impaired by unilateral lesions of the thalamic reticular nucleus in the rat. *J. Neurosci.* **1999**, *19*, 10135–10139. [PubMed]
179. Pinault, D.; Deschenes, M. Anatomical evidence for a mechanism of lateral inhibition in the rat thalamus. *Eur. J. Neurosci.* **1998**, *10*, 3462–3469. [CrossRef] [PubMed]
180. Willis, A.M.; Slater, B.J.; Gribkova, E.D.; Llano, D.A. Open-loop organization of thalamic reticular nucleus and dorsal thalamus: A computational model. *J. Neurophysiol.* **2015**, *114*, 2353–2367. [CrossRef] [PubMed]
181. Pratt, J.A.; Morris, B.J. The thalamic reticular nucleus: A functional hub for thalamocortical network dysfunction in schizophrenia and a target for drug discovery. *J. PsychoPharmacol.* **2015**, *29*, 127–137. [CrossRef] [PubMed]
182. Sherman, S.M.; Guillery, R.W. Distinct functions for direct and transthalamic corticocortical connections. *J. Neurophysiol.* **2011**, *106*, 1068–1077. [CrossRef] [PubMed]
183. Veinante, P.; Lavallee, P.; Deschenes, M. Corticothalamic projections from layer 5 of the vibrissal barrel cortex in the rat. *J. Comp. Neurol.* **2000**, *424*, 197–204. [CrossRef]
184. Feinberg, I.; Guazzelli, M. Schizophrenia—A disorder of the corollary discharge systems that integrate the motor systems of thought with the sensory systems of consciousness. *Br. J. Psychiatry* **1999**, *174*, 196–204. [CrossRef] [PubMed]
185. Ford, J.M.; Mathalon, D.H. Corollary discharge dysfunction in schizophrenia: Can it explain auditory hallucinations? *Int. J. Psychophysiol.* **2005**, *58*, 179–189. [CrossRef] [PubMed]
186. Lisman, J. Excitation, inhibition, local oscillations, or large-scale loops: What causes the symptoms of schizophrenia? *Curr. Opin. Neurobiol.* **2012**, *22*, 537–544. [CrossRef] [PubMed]
187. Behuret, S.; Deleuze, C.; Bal, T. Corticothalamic synaptic noise as a mechanism for selective attention in thalamic neurons. *Front. Neural Circuits* **2015**, *9*, 80. [CrossRef] [PubMed]
188. Briggs, F. Organizing principles of cortical layer 6. *Front. Neural Circuits* **2010**, *4*, 3. [CrossRef] [PubMed]
189. Sillito, A.M.; Jones, H.E. Corticothalamic interactions in the transfer of visual information. *Philos. Trans. R. Soc. Lond. B Biol. Sci.* **2002**, *357*, 1739–1752. [CrossRef] [PubMed]
190. Sherman, S.M.; Koch, C. The control of retinogeniculate transmission in the mammalian lateral geniculate nucleus. *Exp. Brain Res.* **1986**, *63*, 1–20. [CrossRef] [PubMed]
191. Sirota, M.G.; Swadlow, H.A.; Beloozerova, I.N. Three channels of corticothalamic communication during locomotion. *J. Neurosci.* **2005**, *25*, 5915–5925. [CrossRef] [PubMed]
192. Tsumoto, T.; Suda, K. Three groups of cortico-geniculate neurons and their distribution in binocular and monocular segments of cat striate cortex. *J. Comp. Neurol.* **1980**, *193*, 223–236. [CrossRef] [PubMed]
193. Zhang, Z.W.; Deschenes, M. Intracortical axonal projections of lamina VI cells of the primary somatosensory cortex in the rat: A single-cell labeling study. *J. Neurosci.* **1997**, *17*, 6365–6379. [PubMed]
194. Da Costa, N.M.; Martin, K.A. Selective targeting of the dendrites of corticothalamic cells by thalamic afferents in area 17 of the cat. *J. Neurosci.* **2009**, *29*, 13919–13928. [CrossRef] [PubMed]
195. Kim, J.; Matney, C.J.; Blankenship, A.; Hestrin, S.; Brown, S.P. Layer 6 corticothalamic neurons activate a cortical output layer, layer 5a. *J. Neurosci.* **2014**, *34*, 9656–9664. [CrossRef] [PubMed]
196. Staiger, J.F.; Zilles, K.; Freund, T.F. Recurrent axon collaterals of corticothalamic projection neurons in rat primary somatosensory cortex contribute to excitatory and inhibitory feedback-loops. *Anat. Embryol.* **1996**, *194*, 533–543. [CrossRef] [PubMed]

197. Briggs, F.; Callaway, E.M. Layer-specific input to distinct cell types in layer 6 of monkey primary visual cortex. *J. Neurosci.* **2001**, *21*, 3600–3608. [PubMed]
198. Staiger, J.F.; Kotter, R.; Zilles, K.; Luhmann, H.J. Laminar characteristics of functional connectivity in rat barrel cortex revealed by stimulation with caged-glutamate. *Neurosci. Res.* **2000**, *37*, 49–58. [CrossRef]
199. Ledergerber, D.; Larkum, M.E. Properties of layer 6 pyramidal neuron apical dendrites. *J. Neurosci.* **2010**, *30*, 13031–13044. [CrossRef] [PubMed]
200. Kubota, Y.; Hatada, S.; Kondo, S.; Karube, F.; Kawaguchi, Y. Neocortical inhibitory terminals innervate dendritic spines targeted by thalamocortical afferents. *J. Neurosci.* **2007**, *27*, 1139–1150. [CrossRef] [PubMed]
201. Lee, C.C.; Sherman, S.M. Glutamatergic inhibition in sensory neocortex. *Cereb. Cortex* **2009**, *19*, 2281–2289. [CrossRef] [PubMed]
202. Lee, C.C.; Lam, Y.W.; Sherman, S.M. Intracortical convergence of layer 6 neurons. *Neuroreport* **2012**, *23*, 736–740. [CrossRef] [PubMed]
203. Yuan, B.; Morrow, T.J.; Casey, K.L. Corticofugal influences of s1 cortex on ventrobasal thalamic neurons in the awake rat. *J. Neurosci.* **1986**, *6*, 3611–3617. [PubMed]
204. Miyata, M.; Imoto, K. Different composition of glutamate receptors in corticothalamic and lemniscal synaptic responses and their roles in the firing responses of ventrobasal thalamic neurons in juvenile mice. *J. Physiol.* **2006**, *575*, 161–174. [CrossRef] [PubMed]
205. Crandall, S.R.; Cruikshank, S.J.; Connors, B.W. A corticothalamic switch: Controlling the thalamus with dynamic synapses. *Neuron* **2015**, *86*, 768–782. [CrossRef] [PubMed]
206. Salt, T.E. Mediation of thalamic sensory input by both nmda receptors and non-nmda receptors. *Nature* **1986**, *322*, 263–265. [CrossRef] [PubMed]
207. Salt, T.E.; Wilson, D.G.; Prasad, S.K. Antagonism of n-methylaspartate and synaptic responses of neurones in the rat ventrobasal thalamus by ketamine and mk-801. *Br. J. Pharmacol.* **1988**, *94*, 443–448. [CrossRef] [PubMed]
208. Pinault, D.; Deschenes, M. Control of 40-hz firing of reticular thalamic cells by neurotransmitters. *Neuroscience* **1992**, *51*, 259–268. [CrossRef]
209. Hillenbrand, U.; van Hemmen, J.L. Does corticothalamic feedback control cortical velocity tuning? *Neural Comput.* **2001**, *13*, 327–355. [CrossRef] [PubMed]
210. Yousif, N.; Denham, M. The role of cortical feedback in the generation of the temporal receptive field responses of lateral geniculate nucleus neurons: A computational modelling study. *Biol. Cybern* **2007**, *97*, 269–277. [CrossRef] [PubMed]
211. Destexhe, A. Modelling corticothalamic feedback and the gating of the thalamus by the cerebral cortex. *J. Physiol. Paris* **2000**, *94*, 391–410. [CrossRef]
212. Liu, X.B. Subcellular distribution of ampa and nmda receptor subunit immunoreactivity in ventral posterior and reticular nuclei of rat and cat thalamus. *J. Comp. Neurol.* **1997**, *388*, 587–602. [CrossRef]
213. Crick, F. Function of the thalamic reticular complex: The searchlight hypothesis. *Proc. Natl. Acad. Sci. USA* **1984**, *81*, 4586–4590. [CrossRef] [PubMed]
214. Sillito, A.M.; Jones, H.E.; Gerstein, G.L.; West, D.C. Feature-linked synchronization of thalamic relay cell firing induced by feedback from the visual cortex. *Nature* **1994**, *369*, 479–482. [CrossRef] [PubMed]
215. Temereanca, S.; Simons, D.J. Functional topography of corticothalamic feedback enhances thalamic spatial response tuning in the somatosensory whisker/barrel system. *Neuron* **2004**, *41*, 639–651. [CrossRef]
216. Murphy, P.C.; Sillito, A.M. Corticofugal feedback influences the generation of length tuning in the visual pathway. *Nature* **1987**, *329*, 727–729. [CrossRef] [PubMed]
217. Ghazanfar, A.A.; Krupa, D.J.; Nicolelis, M.A. Role of cortical feedback in the receptive field structure and nonlinear response properties of somatosensory thalamic neurons. *Exp. Brain Res.* **2001**, *141*, 88–100. [CrossRef] [PubMed]
218. Alitto, H.J.; Usrey, W.M. Corticothalamic feedback and sensory processing. *Curr. Opin. Neurobiol.* **2003**, *13*, 440–445. [CrossRef]
219. O'Connor, D.H.; Fukui, M.M.; Pinsk, M.A.; Kastner, S. Attention modulates responses in the human lateral geniculate nucleus. *Nat. Neurosci.* **2002**, *5*, 1203–1209. [CrossRef] [PubMed]
220. McAlonan, K.; Cavanaugh, J.; Wurtz, R.H. Guarding the gateway to cortex with attention in visual thalamus. *Nature* **2008**, *456*, 391–394. [CrossRef] [PubMed]
221. Steriade, M.; Deschenes, M. The thalamus as a neuronal oscillator. *Brain Res.* **1984**, *320*, 1–63. [CrossRef]

222. Steriade, M.; Llinas, R.R. The functional states of the thalamus and the associated neuronal interplay. *Physiol. Rev.* **1988**, *68*, 649–742. [PubMed]
223. Timofeev, I.; Chauvette, S. Thalamocortical oscillations: Local control of eeg slow waves. *Curr. Top. Med. Chem.* **2011**, *11*, 2457–2471. [CrossRef] [PubMed]
224. Steriade, M. Grouping of brain rhythms in corticothalamic systems. *Neuroscience* **2006**, *137*, 1087–1106. [CrossRef] [PubMed]
225. Steriade, M.; McCormick, D.A.; Sejnowski, T.J. Thalamocortical oscillations in the sleeping and aroused brain. *Science* **1993**, *262*, 679–685. [CrossRef] [PubMed]
226. Crunelli, V.; Cope, D.W.; Hughes, S.W. Thalamic T-type Ca2+ channels and NREM sleep. *Cell. Calcium* **2006**, *40*, 175–190. [CrossRef] [PubMed]
227. Kim, U.; Sanchez-Vives, M.V.; McCormick, D.A. Functional dynamics of gabaergic inhibition in the thalamus. *Science* **1997**, *278*, 130–134. [CrossRef] [PubMed]
228. Sherman, S.M. A wake-up call from the thalamus. *Nat. Neurosci.* **2001**, *4*, 344–346. [CrossRef] [PubMed]
229. Bal, T.; McCormick, D.A. Mechanisms of oscillatory activity in guinea-pig nucleus reticularis thalami in vitro: A mammalian pacemaker. *J. Physiol.* **1993**, *468*, 669–691. [CrossRef] [PubMed]
230. Fuentealba, P.; Steriade, M. The reticular nucleus revisited: Intrinsic and network properties of a thalamic pacemaker. *Prog. Neurobiol.* **2005**, *75*, 125–141. [CrossRef] [PubMed]
231. Luthi, A. Sleep spindles: Where they come from, what they do. *Neuroscientist* **2014**, *20*, 243–256. [CrossRef] [PubMed]
232. Pinault, D.; Deschenes, M. Voltage-dependent 40-Hz oscillations in rat reticular thalamic neurons in vivo. *Neuroscience* **1992**, *51*, 245–258. [CrossRef]
233. McCormick, D.A.; von Krosigk, M. Corticothalamic activation modulates thalamic firing through glutamate "metabotropic" receptors. *Proc. Natl. Acad. Sci. USA* **1992**, *89*, 2774–2778. [CrossRef] [PubMed]
234. Pinault, D. Cellular interactions in the rat somatosensory thalamocortical system during normal and epileptic 5–9 hz oscillations. *J. Physiol.* **2003**, *552*, 881–905. [CrossRef] [PubMed]
235. Andreasen, N.C.; Paradiso, S.; O'Leary, D.S. "Cognitive dysmetria" as an integrative theory of schizophrenia: A dysfunction in cortical-subcortical-cerebellar circuitry? *Schizophr. Bull.* **1998**, *24*, 203–218. [CrossRef] [PubMed]
236. Dorph-Petersen, K.A.; Lewis, D.A. Postmortem structural studies of the thalamus in schizophrenia. *Schizophr. Res.* **2017**, *180*, 28–35. [CrossRef] [PubMed]
237. Sim, K.; Cullen, T.; Ongur, D.; Heckers, S. Testing models of thalamic dysfunction in schizophrenia using neuroimaging. *J. Neural Transm.* **2006**, *113*, 907–928. [CrossRef] [PubMed]
238. Van Haren, N.E.; Bakker, S.C.; Kahn, R.S. Genes and structural brain imaging in schizophrenia. *Curr. Opin. Psychiatry* **2008**, *21*, 161–167. [CrossRef] [PubMed]
239. Adriano, F.; Spoletini, I.; Caltagirone, C.; Spalletta, G. Updated meta-analyses reveal thalamus volume reduction in patients with first-episode and chronic schizophrenia. *Schizophr. Res.* **2010**, *123*, 1–14. [CrossRef] [PubMed]
240. Harrisberger, F.; Buechler, R.; Smieskova, R.; Lenz, C.; Walter, A.; Egloff, L.; Bendfeldt, K.; Simon, A.E.; Wotruba, D.; Theodoridou, A.; et al. Alterations in the hippocampus and thalamus in individuals at high risk for psychosis. *NPJ Schizophr.* **2016**, *2*, 16033. [CrossRef] [PubMed]
241. Anticevic, A.; Cole, M.W.; Repovs, G.; Murray, J.D.; Brumbaugh, M.S.; Winkler, A.M.; Savic, A.; Krystal, J.H.; Pearlson, G.D.; Glahn, D.C. Characterizing thalamo-cortical disturbances in schizophrenia and bipolar illness. *Cereb. Cortex* **2014**, *24*, 3116–3130. [CrossRef] [PubMed]
242. Janssen, J.; Aleman-Gomez, Y.; Reig, S.; Schnack, H.G.; Parellada, M.; Graell, M.; Moreno, C.; Moreno, D.; Mateos-Perez, J.M.; Udias, J.M.; et al. Regional specificity of thalamic volume deficits in male adolescents with early-onset psychosis. *Br. J. Psychiatry* **2012**, *200*, 30–36. [CrossRef] [PubMed]
243. Woodward, N.D.; Heckers, S. Mapping thalamocortical functional connectivity in chronic and early stages of psychotic disorders. *Biol. Psychiatry* **2016**, *79*, 1016–1025. [CrossRef] [PubMed]
244. Allen, P.; Chaddock, C.A.; Egerton, A.; Howes, O.D.; Barker, G.; Bonoldi, I.; Fusar-Poli, P.; Murray, R.; McGuire, P. Functional outcome in people at high risk for psychosis predicted by thalamic glutamate levels and prefronto-striatal activation. *Schizophr. Bull.* **2015**, *41*, 429–439. [CrossRef] [PubMed]

245. Fusar-Poli, P.; Stone, J.M.; Broome, M.R.; Valli, I.; Mechelli, A.; McLean, M.A.; Lythgoe, D.J.; O'Gorman, R.L.; Barker, G.J.; McGuire, P.K. Thalamic glutamate levels as a predictor of cortical response during executive functioning in subjects at high risk for psychosis. *Arch. Gen. Psychiatry* **2011**, *68*, 881–890. [CrossRef] [PubMed]
246. Manoach, D.S.; Demanuele, C.; Wamsley, E.J.; Vangel, M.; Montrose, D.M.; Miewald, J.; Kupfer, D.; Buysse, D.; Stickgold, R.; Keshavan, M.S. Sleep spindle deficits in antipsychotic-naive early course schizophrenia and in non-psychotic first-degree relatives. *Front. Hum. Neurosci.* **2014**, *8*, 762. [CrossRef] [PubMed]
247. Jacobsen, R.B.; Ulrich, D.; Huguenard, J.R. Gaba(b) and nmda receptors contribute to spindle-like oscillations in rat thalamus in vitro. *J. Neurophysiol.* **2001**, *86*, 1365–1375. [PubMed]
248. Moghaddam, B. Bringing order to the glutamate chaos in schizophrenia. *Neuron* **2003**, *40*, 881–884. [CrossRef]
249. Stephan, K.E.; Baldeweg, T.; Friston, K.J. Synaptic plasticity and dysconnection in schizophrenia. *Biol. Psychiatry* **2006**, *59*, 929–939. [CrossRef] [PubMed]
250. Behar, T.N.; Scott, C.A.; Greene, C.L.; Wen, X.; Smith, S.V.; Maric, D.; Liu, Q.Y.; Colton, C.A.; Barker, J.L. Glutamate acting at nmda receptors stimulates embryonic cortical neuronal migration. *J. Neurosci.* **1999**, *19*, 4449–4461. [PubMed]
251. Floresco, S.B.; Blaha, C.D.; Yang, C.R.; Phillips, A.G. Dopamine d1 and nmda receptors mediate potentiation of basolateral amygdala-evoked firing of nucleus accumbens neurons. *J. Neurosci.* **2001**, *21*, 6370–6376. [PubMed]
252. Lisman, J.E.; Coyle, J.T.; Green, R.W.; Javitt, D.C.; Benes, F.M.; Heckers, S.; Grace, A.A. Circuit-based framework for understanding neurotransmitter and risk gene interactions in schizophrenia. *Trends Neurosci.* **2008**, *31*, 234–242. [CrossRef] [PubMed]
253. Schwartz, T.L.; Sachdeva, S.; Stahl, S.M. Genetic data supporting the nmda glutamate receptor hypothesis for schizophrenia. *Curr. Pharm. Des.* **2012**, *18*, 1580–1592. [CrossRef] [PubMed]
254. Kim, J.S.; Kornhuber, H.H.; Schmid-Burgk, W.; Holzmuller, B. Low cerebrospinal fluid glutamate in schizophrenic patients and a new hypothesis on schizophrenia. *Neurosci. Lett.* **1980**, *20*, 379–382. [CrossRef]
255. Kim, J.S.; Kornhuber, H.H.; Brand, U.; Menge, H.G. Effects of chronic amphetamine treatment on the glutamate concentration in cerebrospinal fluid and brain: Implications for a theory of schizophrenia. *Neurosci. Lett.* **1981**, *24*, 93–96. [CrossRef]
256. Moghaddam, B.; Javitt, D. From revolution to evolution: The glutamate hypothesis of schizophrenia and its implication for treatment. *Neuropsychopharmacology* **2012**, *37*, 4–15. [CrossRef] [PubMed]
257. Clinton, S.M.; Meador-Woodruff, J.H. Thalamic dysfunction in schizophrenia: Neurochemical, neuropathological, and in vivo imaging abnormalities. *Schizophr. Res.* **2004**, *69*, 237–253. [CrossRef] [PubMed]
258. Bergeron, R.; Coyle, J.T. Naag, nmda receptor and psychosis. *Curr. Med. Chem.* **2012**, *19*, 1360–1364. [CrossRef] [PubMed]
259. Molina, V.; Sanchez, J.; Reig, S.; Sanz, J.; Benito, C.; Santamarta, C.; Pascau, J.; Sarramea, F.; Gispert, J.D.; Misiego, J.M.; et al. N-acetyl-aspartate levels in the dorsolateral prefrontal cortex in the early years of schizophrenia are inversely related to disease duration. *Schizophr. Res.* **2005**, *73*, 209–219. [CrossRef] [PubMed]
260. Harrison, P.J.; Owen, M.J. Genes for schizophrenia? Recent findings and their pathophysiological implications. *Lancet* **2003**, *361*, 417–419. [CrossRef]
261. Kendler, K.S. What psychiatric genetics has taught us about the nature of psychiatric illness and what is left to learn. *Mol. Psychiatry* **2013**, *18*, 1058–1066. [CrossRef] [PubMed]
262. Richard, E.A.; Khlestova, E.; Nanu, R.; Lisman, J.E. Potential synergistic action of 19 schizophrenia risk genes in the thalamus. *Schizophr. Res.* **2017**, *180*, 64–69. [CrossRef] [PubMed]
263. Swerdlow, N.R.; Gur, R.E.; Braff, D.L. Consortium on the genetics of schizophrenia (cogs) assessment of endophenotypes for schizophrenia: An introduction to this special issue of schizophrenia research. *Schizophr. Res.* **2015**, *163*, 9–16. [CrossRef] [PubMed]
264. Pilowsky, L.S.; Bressan, R.A.; Stone, J.M.; Erlandsson, K.; Mulligan, R.S.; Krystal, J.H.; Ell, P.J. First in vivo evidence of an nmda receptor deficit in medication-free schizophrenic patients. *Mol. Psychiatry* **2006**, *11*, 118–119. [CrossRef] [PubMed]

265. Steiner, J.; Bogerts, B.; Sarnyai, Z.; Walter, M.; Gos, T.; Bernstein, H.G.; Myint, A.M. Bridging the gap between the immune and glutamate hypotheses of schizophrenia and major depression: Potential role of glial nmda receptor modulators and impaired blood-brain barrier integrity. *World J. Biol. Psychiatry* **2012**, *13*, 482–492. [CrossRef] [PubMed]
266. Egerton, A.; Stone, J.M.; Chaddock, C.A.; Barker, G.J.; Bonoldi, I.; Howard, R.M.; Merritt, K.; Allen, P.; Howes, O.D.; Murray, R.M.; et al. Relationship between brain glutamate levels and clinical outcome in individuals at ultra high risk of psychosis. *Neuropsychopharmacology* **2014**, *39*, 2891–2899. [CrossRef] [PubMed]
267. Stone, J.M.; Day, F.; Tsagaraki, H.; Valli, I.; McLean, M.A.; Lythgoe, D.J.; O'Gorman, R.L.; Barker, G.J.; McGuire, P.K.; OASIS. Glutamate dysfunction in people with prodromal symptoms of psychosis: Relationship to gray matter volume. *Biol. Psychiatry* **2009**, *66*, 533–539. [CrossRef] [PubMed]
268. Corlett, P.R.; Honey, G.D.; Fletcher, P.C. From prediction error to psychosis: Ketamine as a pharmacological model of delusions. *J. Psychopharmacol.* **2007**, *21*, 238–252. [CrossRef] [PubMed]
269. Lodge, D.; Anis, N.A. Effects of phencyclidine on excitatory amino acid activation of spinal interneurones in the cat. *Eur. J. Pharmacol.* **1982**, *77*, 203–204. [CrossRef]
270. Tricklebank, M.D.; Singh, L.; Oles, R.J.; Preston, C.; Iversen, S.D. The behavioural effects of mk-801: A comparison with antagonists acting non-competitively and competitively at the nmda receptor. *Eur. J. Pharmacol.* **1989**, *167*, 127–135. [CrossRef]
271. Hetem, L.A.; Danion, J.M.; Diemunsch, P.; Brandt, C. Effect of a subanesthetic dose of ketamine on memory and conscious awareness in healthy volunteers. *Psychopharmacology* **2000**, *152*, 283–288. [CrossRef] [PubMed]
272. Javitt, D.C.; Zukin, S.R. Recent advances in the phencyclidine model of schizophrenia. *Am. J. Psychiatry* **1991**, *148*, 1301–1308. [PubMed]
273. Krystal, J.H.; Karper, L.P.; Seibyl, J.P.; Freeman, G.K.; Delaney, R.; Bremner, J.D.; Heninger, G.R.; Bowers, M.B., Jr.; Charney, D.S. Subanesthetic effects of the noncompetitive NMDA antagonist, ketamine, in humans. Psychotomimetic, perceptual, cognitive, and neuroendocrine responses. *Arch. Gen. Psychiatry* **1994**, *51*, 199–214. [CrossRef] [PubMed]
274. Lahti, A.C.; Koffel, B.; LaPorte, D.; Tamminga, C.A. Subanesthetic doses of ketamine stimulate psychosis in schizophrenia. *Neuropsychopharmacology* **1995**, *13*, 9–19. [CrossRef]
275. Anticevic, A.; Corlett, P.R.; Cole, M.W.; Savic, A.; Gancsos, M.; Tang, Y.; Repovs, G.; Murray, J.D.; Driesen, N.R.; Morgan, P.T.; et al. *N*-methyl-D-aspartate receptor antagonist effects on prefrontal cortical connectivity better model early than chronic schizophrenia. *Biol. Psychiatry* **2015**, *77*, 569–580. [CrossRef] [PubMed]
276. Driesen, N.R.; McCarthy, G.; Bhagwagar, Z.; Bloch, M.; Calhoun, V.; D'souza, D.C.; Gueorguieva, R.; He, G.; Ramachandran, R.; Suckow, R.F.; et al. Relationship of resting brain hyperconnectivity and schizophrenia-like symptoms produced by the nmda receptor antagonist ketamine in humans. *Mol. Psychiatry* **2013**, *18*, 1199–1204. [CrossRef] [PubMed]
277. Ma, J.; Leung, L.S. The supramammillo-septal-hippocampal pathway mediates sensorimotor gating impairment and hyperlocomotion induced by MK-801 and ketamine in rats. *Psychopharmacology* **2007**, *191*, 961–974. [CrossRef] [PubMed]
278. Ehrlichman, R.S.; Gandal, M.J.; Maxwell, C.R.; Lazarewicz, M.T.; Finkel, L.H.; Contreras, D.; Turetsky, B.I.; Siegel, S.J. *N*-methyl-D-aspartic acid receptor antagonist-induced frequency oscillations in mice recreate pattern of electrophysiological deficits in schizophrenia. *Neuroscience* **2009**, *158*, 705–712. [CrossRef] [PubMed]
279. Kocsis, B. State-dependent increase of cortical gamma activity during rem sleep after selective blockade of nr2b subunit containing nmda receptors. *Sleep* **2012**, *35*, 1011–1016. [CrossRef] [PubMed]
280. Wood, J.; Kim, Y.; Moghaddam, B. Disruption of prefrontal cortex large scale neuronal activity by different classes of psychotomimetic drugs. *J. Neurosci.* **2012**, *32*, 3022–3031. [CrossRef] [PubMed]
281. Daskalakis, Z.J.; Christensen, B.K.; Fitzgerald, P.B.; Chen, R. Dysfunctional neural plasticity in patients with schizophrenia. *Arch. Gen. Psychiatry* **2008**, *65*, 378–385. [CrossRef] [PubMed]
282. Harrison, P.J.; Weinberger, D.R. Schizophrenia genes, gene expression, and neuropathology: On the matter of their convergence. *Mol. Psychiatry* **2005**, *10*, 40–68. [CrossRef] [PubMed]

283. Hahn, C.G.; Wang, H.Y.; Cho, D.S.; Talbot, K.; Gur, R.E.; Berrettini, W.H.; Bakshi, K.; Kamins, J.; Borgmann-Winter, K.E.; Siegel, S.J.; et al. Altered neuregulin 1-erbb4 signaling contributes to nmda receptor hypofunction in schizophrenia. *Nat. Med.* **2006**, *12*, 824–828. [CrossRef] [PubMed]
284. Snyder, M.A.; Gao, W.J. Nmda hypofunction as a convergence point for progression and symptoms of schizophrenia. *Front. Cell. Neurosci.* **2013**, *7*, 31. [CrossRef] [PubMed]
285. Lane, H.Y.; Liu, Y.C.; Huang, C.L.; Chang, Y.C.; Liau, C.H.; Perng, C.H.; Tsai, G.E. Sarcosine (n-methylglycine) treatment for acute schizophrenia: A randomized, double-blind study. *Biol. Psychiatry* **2008**, *63*, 9–12. [CrossRef] [PubMed]
286. Singh, S.P.; Singh, V. Meta-analysis of the efficacy of adjunctive nmda receptor modulators in chronic schizophrenia. *CNS Drugs* **2011**, *25*, 859–885. [CrossRef] [PubMed]
287. Coyle, J.T. The gaba-glutamate connection in schizophrenia: Which is the proximate cause? *Biochem. Pharmacol.* **2004**, *68*, 1507–1514. [CrossRef] [PubMed]
288. Gonzalez-Burgos, G.; Cho, R.Y.; Lewis, D.A. Alterations in cortical network oscillations and parvalbumin neurons in schizophrenia. *Biol. Psychiatry* **2015**, *77*, 1031–1040. [CrossRef] [PubMed]
289. Lewis, D.A.; Hashimoto, T.; Volk, D.W. Cortical inhibitory neurons and schizophrenia. *Nat. Rev. Neurosci.* **2005**, *6*, 312–324. [CrossRef] [PubMed]
290. Lewis, D.A.; Curley, A.A.; Glausier, J.R.; Volk, D.W. Cortical parvalbumin interneurons and cognitive dysfunction in schizophrenia. *Trends Neurosci.* **2012**, *35*, 57–67. [CrossRef] [PubMed]
291. Uhlhaas, P.J.; Roux, F.; Rodriguez, E.; Rotarska-Jagiela, A.; Singer, W. Neural synchrony and the development of cortical networks. *Trends Cogn. Sci.* **2010**, *14*, 72–80. [CrossRef] [PubMed]
292. Minlebaev, M.; Colonnese, M.; Tsintsadze, T.; Sirota, A.; Khazipov, R. Early gamma oscillations synchronize developing thalamus and cortex. *Science* **2011**, *334*, 226–229. [CrossRef] [PubMed]
293. Brucke, C.; Bock, A.; Huebl, J.; Krauss, J.K.; Schonecker, T.; Schneider, G.H.; Brown, P.; Kuhn, A.A. Thalamic gamma oscillations correlate with reaction time in a go/nogo task in patients with essential tremor. *Neuroimage* **2013**, *75*, 36–45. [CrossRef] [PubMed]
294. Joliot, M.; Ribary, U.; Llinas, R. Human oscillatory brain activity near 40 Hz coexists with cognitive temporal binding. *Proc. Natl. Acad. Sci. USA* **1994**, *91*, 11748–11751. [CrossRef] [PubMed]
295. Tallon-Baudry, C.; Bertrand, O. Oscillatory gamma activity in humans and its role in object representation. *Trends Cogn. Sci.* **1999**, *3*, 151–162. [CrossRef]
296. Varela, F.; Lachaux, J.P.; Rodriguez, E.; Martinerie, J. The brainweb: Phase synchronization and large-scale integration. *Nat. Rev. Neurosci.* **2001**, *2*, 229–239. [CrossRef] [PubMed]
297. Zhang, Z.G.; Hu, L.; Hung, Y.S.; Mouraux, A.; Iannetti, G.D. Gamma-band oscillations in the primary somatosensory cortex—A direct and obligatory correlate of subjective pain intensity. *J. Neurosci.* **2012**, *32*, 7429–7438. [CrossRef] [PubMed]
298. Buzsaki, G.; Draguhn, A. Neuronal oscillations in cortical networks. *Science* **2004**, *304*, 1926–1929. [CrossRef] [PubMed]
299. Buzsaki, G.; Chrobak, J.J. Temporal structure in spatially organized neuronal ensembles: A role for interneuronal networks. *Curr. Opin. Neurobiol.* **1995**, *5*, 504–510. [CrossRef]
300. Engel, A.K.; Roelfsema, P.R.; Fries, P.; Brecht, M.; Singer, W. Role of the temporal domain for response selection and perceptual binding. *Cereb. Cortex* **1997**, *7*, 571–582. [CrossRef] [PubMed]
301. Fries, P. Neuronal gamma-band synchronization as a fundamental process in cortical computation. *Annu. Rev. Neurosci.* **2009**, *32*, 209–224. [CrossRef] [PubMed]
302. Gray, C.M.; Konig, P.; Engel, A.K.; Singer, W. Oscillatory responses in cat visual cortex exhibit inter-columnar synchronization which reflects global stimulus properties. *Nature* **1989**, *338*, 334–337. [CrossRef] [PubMed]
303. Singer, W. Time as coding space? *Curr. Opin. Neurobiol.* **1999**, *9*, 189–194. [CrossRef]
304. Buzsaki, G.; Wang, X.J. Mechanisms of gamma oscillations. *Annu. Rev. Neurosci.* **2012**, *35*, 203–225. [CrossRef] [PubMed]
305. Roux, F.; Wibral, M.; Singer, W.; Aru, J.; Uhlhaas, P.J. The phase of thalamic alpha activity modulates cortical gamma-band activity: Evidence from resting-state meg recordings. *J. Neurosci.* **2013**, *33*, 17827–17835. [CrossRef] [PubMed]
306. Bartos, M.; Vida, I.; Jonas, P. Synaptic mechanisms of synchronized gamma oscillations in inhibitory interneuron networks. *Nat. Rev. Neurosci.* **2007**, *8*, 45–56. [CrossRef] [PubMed]

307. Uhlhaas, P.J.; Singer, W. Neural synchrony in brain disorders: Relevance for cognitive dysfunctions and pathophysiology. *Neuron* **2006**, *52*, 155–168. [CrossRef] [PubMed]
308. Stephan, K.E.; Friston, K.J.; Frith, C.D. Dysconnection in schizophrenia: From abnormal synaptic plasticity to failures of self-monitoring. *Schizophr. Bull.* **2009**, *35*, 509–527. [CrossRef] [PubMed]
309. Uhlhaas, P.J.; Roux, F.; Singer, W. Thalamocortical synchronization and cognition: Implications for schizophrenia? *Neuron* **2013**, *77*, 997–999. [CrossRef] [PubMed]
310. Cho, R.Y.; Konecky, R.O.; Carter, C.S. Impairments in frontal cortical gamma synchrony and cognitive control in schizophrenia. *Proc. Natl. Acad. Sci. USA* **2006**, *103*, 19878–19883. [CrossRef] [PubMed]
311. Hirano, Y.; Oribe, N.; Kanba, S.; Onitsuka, T.; Nestor, P.G.; Spencer, K.M. Spontaneous gamma activity in schizophrenia. *JAMA Psychiatry* **2015**, *72*, 813–821. [CrossRef] [PubMed]
312. Leicht, G.; Vauth, S.; Polomac, N.; Andreou, C.; Rauh, J.; Mussmann, M.; Karow, A.; Mulert, C. Eeg-informed fmri reveals a disturbed gamma-band-specific network in subjects at high risk for psychosis. *Schizophr. Bull.* **2016**, *42*, 239–249. [CrossRef] [PubMed]
313. Mitra, S.; Nizamie, S.H.; Goyal, N.; Tikka, S.K. Evaluation of resting state gamma power as a response marker in schizophrenia. *Psychiatry Clin. Neurosci.* **2015**, *69*, 630–639. [CrossRef] [PubMed]
314. Leicht, G.; Andreou, C.; Polomac, N.; Lanig, C.; Schottle, D.; Lambert, M.; Mulert, C. Reduced auditory evoked gamma band response and cognitive processing deficits in first episode schizophrenia. *World J. Biol. Psychiatry* **2015**. [CrossRef] [PubMed]
315. Tada, M.; Nagai, T.; Kirihara, K.; Koike, S.; Suga, M.; Araki, T.; Kobayashi, T.; Kasai, K. Differential alterations of auditory gamma oscillatory responses between pre-onset high-risk individuals and first-episode schizophrenia. *Cereb. Cortex* **2016**, *26*, 1027–1035. [CrossRef] [PubMed]
316. Basar, E. A review of gamma oscillations in healthy subjects and in cognitive impairment. *Int. J. Psychophysiol.* **2013**, *90*, 99–117. [CrossRef] [PubMed]
317. De la Salle, S.; Choueiry, J.; Shah, D.; Bowers, H.; McIntosh, J.; Ilivitsky, V.; Knott, V. Effects of ketamine on resting-state eeg activity and their relationship to perceptual/dissociative symptoms in healthy humans. *Front. Pharmacol.* **2016**, *7*, 348. [CrossRef] [PubMed]
318. Callicott, J.H.; Bertolino, A.; Mattay, V.S.; Langheim, F.J.; Duyn, J.; Coppola, R.; Goldberg, T.E.; Weinberger, D.R. Physiological dysfunction of the dorsolateral prefrontal cortex in schizophrenia revisited. *Cereb. Cortex* **2000**, *10*, 1078–1092. [CrossRef] [PubMed]
319. Gandal, M.J.; Edgar, J.C.; Klook, K.; Siegel, S.J. Gamma synchrony: Towards a translational biomarker for the treatment-resistant symptoms of schizophrenia. *Neuropharmacology* **2012**, *62*, 1504–1518. [CrossRef] [PubMed]
320. Pinault, D. *N*-methyl-D-aspartate receptor antagonists amplify network baseline gamma frequency (30–80 Hz) oscillations: Noise and signal. *AIMS Neurosci.* **2014**, *1*, 169–182. [CrossRef]
321. Molina, L.A.; Skelin, I.; Gruber, A.J. Acute nmda receptor antagonism disrupts synchronization of action potential firing in rat prefrontal cortex. *PLoS ONE* **2014**, *9*, e85842. [CrossRef] [PubMed]
322. Homayoun, H.; Moghaddam, B. Nmda receptor hypofunction produces opposite effects on prefrontal cortex interneurons and pyramidal neurons. *J. Neurosci.* **2007**, *27*, 11496–11500. [CrossRef] [PubMed]
323. Kobayashi, Y.; Kulikova, S.P.; Shibato, J.; Rakwal, R.; Satoh, H.; Pinault, D.; Masuo, Y. DNA microarray unravels rapid changes in transcriptome of mk-801 treated rat brain. *World J. Biol. Chem.* **2015**, *6*, 389–408. [CrossRef] [PubMed]
324. Lopez-Quintero, S.V.; Datta, A.; Amaya, R.; Elwassif, M.; Bikson, M.; Tarbell, J.M. Dbs-relevant electric fields increase hydraulic conductivity of in vitro endothelial monolayers. *J. Neural Eng.* **2010**, *7*, 16005. [CrossRef] [PubMed]
325. Watanabe, K.; Watanabe, T.; Takahashi, A.; Saito, N.; Hirato, M.; Sasaki, T. Transcranial electrical stimulation through screw electrodes for intraoperative monitoring of motor evoked potentials. Technical note. *J. Neurosurg.* **2004**, *100*, 155–160. [CrossRef] [PubMed]
326. Fenoy, A.J.; Goetz, L.; Chabardes, S.; Xia, Y. Deep brain stimulation: Are astrocytes a key driver behind the scene? *CNS Neurosci. Ther.* **2014**, *20*, 191–201. [CrossRef] [PubMed]
327. Gutierrez, J.C.; Seijo, F.J.; Alvarez Vega, M.A.; Fernandez Gonzalez, F.; Lozano Aragoneses, B.; Blazquez, M. Therapeutic extradural cortical stimulation for parkinson's disease: Report of six cases and review of the literature. *Clin. Neurol. Neurosurg.* **2009**, *111*, 703–707. [CrossRef] [PubMed]

328. Roth, B.J. Mechanisms for electrical stimulation of excitable tissue. *Crit. Rev. Biomed. Eng.* **1994**, *22*, 253–305. [PubMed]
329. Kanai, R.; Paulus, W.; Walsh, V. Transcranial alternating current stimulation (TACS) modulates cortical excitability as assessed by TMS-induced phosphene thresholds. *Clin. Neurophysiol.* **2010**, *121*, 1551–1554. [CrossRef] [PubMed]
330. Struber, D.; Rach, S.; Neuling, T.; Herrmann, C.S. On the possible role of stimulation duration for after-effects of transcranial alternating current stimulation. *Front. Cell. Neurosci.* **2015**, *9*, 311. [CrossRef] [PubMed]
331. Feurra, M.; Pasqualetti, P.; Bianco, G.; Santarnecchi, E.; Rossi, A.; Rossi, S. State-dependent effects of transcranial oscillatory currents on the motor system: What you think matters. *J. Neurosci.* **2013**, *33*, 17483–17489. [CrossRef] [PubMed]
332. Cabral-Calderin, Y.; Anne Weinrich, C.; Schmidt-Samoa, C.; Poland, E.; Dechent, P.; Bahr, M.; Wilke, M. Transcranial alternating current stimulation affects the bold signal in a frequency and task-dependent manner. *Hum. Brain Mapp.* **2016**, *37*, 94–121. [CrossRef] [PubMed]
333. Tauc, L.; Hughes, G.M. Modes of initiation and propagation of spikes in the branching axons of molluscan central neurons. *J. Gen. Physiol.* **1963**, *46*, 533–549. [CrossRef] [PubMed]
334. De Raedt, R.; Vanderhasselt, M.A.; Baeken, C. Neurostimulation as an intervention for treatment resistant depression: From research on mechanisms towards targeted neurocognitive strategies. *Clin. Psychol. Rev.* **2015**, *41*, 61–69. [CrossRef] [PubMed]
335. Fertonani, A.; Miniussi, C. Transcranial electrical stimulation: What we know and do not know about mechanisms. *Neuroscientist* **2016**. [CrossRef] [PubMed]
336. Frohlich, F. Experiments and models of cortical oscillations as a target for noninvasive brain stimulation. *Prog. Brain Res.* **2015**, *222*, 41–73. [PubMed]
337. Herrmann, C.S.; Rach, S.; Neuling, T.; Struber, D. Transcranial alternating current stimulation: A review of the underlying mechanisms and modulation of cognitive processes. *Front. Hum. Neurosci.* **2013**, *7*, 279. [CrossRef] [PubMed]
338. Hill, A.T.; Rogasch, N.C.; Fitzgerald, P.B.; Hoy, K.E. Tms-eeg: A window into the neurophysiological effects of transcranial electrical stimulation in non-motor brain regions. *Neurosci. Biobehav. Rev.* **2016**, *64*, 175–184. [CrossRef] [PubMed]
339. Jackson, M.P.; Rahman, A.; Lafon, B.; Kronberg, G.; Ling, D.; Parra, L.C.; Bikson, M. Animal models of transcranial direct current stimulation: Methods and mechanisms. *Clin. Neurophysiol.* **2016**, *127*, 3425–3454. [CrossRef] [PubMed]
340. Knotkova, H.; Nitsche, M.A.; Cruciani, R.A. Putative physiological mechanisms underlying tDCS analgesic effects. *Front. Hum. Neurosci.* **2013**, *7*, 628. [CrossRef] [PubMed]
341. Lewis, P.M.; Thomson, R.H.; Rosenfeld, J.V.; Fitzgerald, P.B. Brain neuromodulation techniques: A review. *Neuroscientist* **2016**, *22*, 406–421. [CrossRef] [PubMed]
342. Lisanby, S.H.; Belmaker, R.H. Animal models of the mechanisms of action of repetitive transcranial magnetic stimulation (rTMS): Comparisons with electroconvulsive shock (ECS). *Depress. Anxiety* **2000**, *12*, 178–187. [CrossRef]
343. Medeiros, L.F.; de Souza, I.C.; Vidor, L.P.; de Souza, A.; Deitos, A.; Volz, M.S.; Fregni, F.; Caumo, W.; Torres, I.L. Neurobiological effects of transcranial direct current stimulation: A review. *Front. Psychiatry* **2012**, *3*, 110. [CrossRef] [PubMed]
344. Nitsche, M.A.; Cohen, L.G.; Wassermann, E.M.; Priori, A.; Lang, N.; Antal, A.; Paulus, W.; Hummel, F.; Boggio, P.S.; Fregni, F.; et al. Transcranial direct current stimulation: State of the art 2008. *Brain Stimul.* **2008**, *1*, 206–223. [CrossRef] [PubMed]
345. Reato, D.; Rahman, A.; Bikson, M.; Parra, L.C. Effects of weak transcranial alternating current stimulation on brain activity—A review of known mechanisms from animal studies. *Front. Hum. Neurosci.* **2013**, *7*, 687. [CrossRef] [PubMed]
346. Terao, Y.; Ugawa, Y. Basic mechanisms of tms. *J. Clin. Neurophysiol.* **2002**, *19*, 322–343. [CrossRef] [PubMed]
347. Zaghi, S.; Acar, M.; Hultgren, B.; Boggio, P.S.; Fregni, F. Noninvasive brain stimulation with low-intensity electrical currents: Putative mechanisms of action for direct and alternating current stimulation. *Neuroscientist* **2010**, *16*, 285–307. [CrossRef] [PubMed]
348. Kilgore, K.L.; Bhadra, N. Nerve conduction block utilising high-frequency alternating current. *Med. Biol. Eng. Comput.* **2004**, *42*, 394–406. [CrossRef] [PubMed]

349. Fritsch, B.; Reis, J.; Martinowich, K.; Schambra, H.M.; Ji, Y.; Cohen, L.G.; Lu, B. Direct current stimulation promotes bdnf-dependent synaptic plasticity: Potential implications for motor learning. *Neuron* **2010**, *66*, 198–204. [CrossRef] [PubMed]
350. Monte-Silva, K.; Kuo, M.F.; Hessenthaler, S.; Fresnoza, S.; Liebetanz, D.; Paulus, W.; Nitsche, M.A. Induction of late LTP-like plasticity in the human motor cortex by repeated non-invasive brain stimulation. *Brain Stimul.* **2013**, *6*, 424–432. [CrossRef] [PubMed]
351. Suppa, A.; Huang, Y.Z.; Funke, K.; Ridding, M.C.; Cheeran, B.; Di Lazzaro, V.; Ziemann, U.; Rothwell, J.C. Ten years of theta burst stimulation in humans: Established knowledge, unknowns and prospects. *Brain Stimul.* **2016**, *9*, 323–335. [CrossRef] [PubMed]
352. Ali, M.M.; Sellers, K.K.; Frohlich, F. Transcranial alternating current stimulation modulates large-scale cortical network activity by network resonance. *J. Neurosci.* **2013**, *33*, 11262–11275. [CrossRef] [PubMed]
353. D'Atri, A.; De Simoni, E.; Gorgoni, M.; Ferrara, M.; Ferlazzo, F.; Rossini, P.M.; De Gennaro, L. Electrical stimulation of the frontal cortex enhances slow-frequency eeg activity and sleepiness. *Neuroscience* **2016**. [CrossRef] [PubMed]
354. Frohlich, F. Endogenous and exogenous electric fields as modifiers of brain activity: Rational design of noninvasive brain stimulation with transcranial alternating current stimulation. *Dialogues Clin. Neurosci.* **2014**, *16*, 93–102. [PubMed]
355. Helfrich, R.F.; Schneider, T.R.; Rach, S.; Trautmann-Lengsfeld, S.A.; Engel, A.K.; Herrmann, C.S. Entrainment of brain oscillations by transcranial alternating current stimulation. *Curr. Biol.* **2014**, *24*, 333–339. [CrossRef] [PubMed]
356. Marshall, L.; Helgadottir, H.; Molle, M.; Born, J. Boosting slow oscillations during sleep potentiates memory. *Nature* **2006**, *444*, 610–613. [CrossRef] [PubMed]
357. Rosanova, M.; Casali, A.; Bellina, V.; Resta, F.; Mariotti, M.; Massimini, M. Natural frequencies of human corticothalamic circuits. *J. Neurosci.* **2009**, *29*, 7679–7685. [CrossRef] [PubMed]
358. Schmidt, S.L.; Iyengar, A.K.; Foulser, A.A.; Boyle, M.R.; Frohlich, F. Endogenous cortical oscillations constrain neuromodulation by weak electric fields. *Brain Stimul.* **2014**, *7*, 878–889. [CrossRef] [PubMed]
359. Vossen, A.; Gross, J.; Thut, G. Alpha power increase after transcranial alternating current stimulation at alpha frequency (alpha-tACS) reflects plastic changes rather than entrainment. *Brain Stimul.* **2015**, *8*, 499–508. [CrossRef] [PubMed]
360. Ozen, S.; Sirota, A.; Belluscio, M.A.; Anastassiou, C.A.; Stark, E.; Koch, C.; Buzsaki, G. Transcranial electric stimulation entrains cortical neuronal populations in rats. *J. Neurosci.* **2010**, *30*, 11476–11485. [CrossRef] [PubMed]
361. Moliadze, V.; Zhao, Y.; Eysel, U.; Funke, K. Effect of transcranial magnetic stimulation on single-unit activity in the cat primary visual cortex. *J. Physiol.* **2003**, *553*, 665–679. [CrossRef] [PubMed]
362. Murphy, S.C.; Palmer, L.M.; Nyffeler, T.; Muri, R.M.; Larkum, M.E. Transcranial magnetic stimulation (TMS) inhibits cortical dendrites. *Elife* **2016**, *5*. [CrossRef] [PubMed]
363. Monai, H.; Ohkura, M.; Tanaka, M.; Oe, Y.; Konno, A.; Hirai, H.; Mikoshiba, K.; Itohara, S.; Nakai, J.; Iwai, Y.; et al. Calcium imaging reveals glial involvement in transcranial direct current stimulation-induced plasticity in mouse brain. *Nat. Commun.* **2016**, *7*, 11100. [CrossRef] [PubMed]
364. Reato, D.; Bikson, M.; Parra, L.C. Lasting modulation of in vitro oscillatory activity with weak direct current stimulation. *J. Neurophysiol.* **2015**, *113*, 1334–1341. [CrossRef] [PubMed]
365. Tehovnik, E.J. Electrical stimulation of neural tissue to evoke behavioral responses. *J. Neurosci. Methods* **1996**, *65*, 1–17. [CrossRef]
366. Bishop, G.H.; O'Leary, J.L. The effects of polarizing currents on cell potentials and their significance in the interpretation of central nervous system activity. *Electroencephalogr. Clin. Neurophysiol.* **1950**, *2*, 401–416. [CrossRef]
367. Francis, J.T.; Gluckman, B.J.; Schiff, S.J. Sensitivity of neurons to weak electric fields. *J. Neurosci.* **2003**, *23*, 7255–7261. [PubMed]
368. Jefferys, J.G. Nonsynaptic modulation of neuronal activity in the brain: Electric currents and extracellular ions. *Physiol. Rev.* **1995**, *75*, 689–723. [PubMed]
369. McIntyre, C.C.; Grill, W.M. Excitation of central nervous system neurons by nonuniform electric fields. *Biophys J.* **1999**, *76*, 878–888. [CrossRef]

370. Terzuolo, C.A.; Bullock, T.H. Measurement of imposed voltage gradient adequate to modulate neuronal firing. *Proc. Natl. Acad. Sci. USA* **1956**, *42*, 687–694. [CrossRef] [PubMed]
371. Nowak, L.G.; Bullier, J. Axons, but not cell bodies, are activated by electrical stimulation in cortical gray matter. I. Evidence from chronaxie measurements. *Exp. Brain Res.* **1998**, *118*, 477–488. [CrossRef] [PubMed]
372. Nowak, L.G.; Bullier, J. Axons, but not cell bodies, are activated by electrical stimulation in cortical gray matter. Ii. Evidence from selective inactivation of cell bodies and axon initial segments. *Exp. Brain Res.* **1998**, *118*, 489–500. [CrossRef] [PubMed]
373. Rapp, M.; Yarom, Y.; Segev, I. Modeling back propagating action potential in weakly excitable dendrites of neocortical pyramidal cells. *Proc. Natl. Acad. Sci. USA* **1996**, *93*, 11985–11990. [CrossRef] [PubMed]
374. Bahner, F.; Weiss, E.K.; Birke, G.; Maier, N.; Schmitz, D.; Rudolph, U.; Frotscher, M.; Traub, R.D.; Both, M.; Draguhn, A. Cellular correlate of assembly formation in oscillating hippocampal networks in vitro. *Proc. Natl. Acad. Sci. USA* **2011**, *108*, E607–E616. [CrossRef] [PubMed]
375. Dugladze, T.; Schmitz, D.; Whittington, M.A.; Vida, I.; Gloveli, T. Segregation of axonal and somatic activity during fast network oscillations. *Science* **2012**, *336*, 1458–1461. [CrossRef] [PubMed]
376. Pinault, D. Backpropagation of action potentials generated at ectopic axonal loci: Hypothesis that axon terminals integrate local environmental signals. *Brain Res. Brain Res. Rev.* **1995**, *21*, 42–92. [CrossRef]
377. Sasaki, T. The axon as a unique computational unit in neurons. *Neurosci. Res.* **2013**, *75*, 83–88. [CrossRef] [PubMed]
378. Sheffield, M.E.; Best, T.K.; Mensh, B.D.; Kath, W.L.; Spruston, N. Slow integration leads to persistent action potential firing in distal axons of coupled interneurons. *Nat. Neurosci.* **2011**, *14*, 200–207. [CrossRef] [PubMed]
379. Markin, V.S. Electric interaction of parallel non-myelinated nerve fibers. Iv. Role of anatomic non-uniformities of the nerve trunks. *Biofizika* **1973**, *18*, 512–518. [PubMed]
380. Tranchina, D.; Nicholson, C. A model for the polarization of neurons by extrinsically applied electric fields. *Biophys. J.* **1986**, *50*, 1139–1156. [CrossRef]
381. Bucher, D.; Thirumalai, V.; Marder, E. Axonal dopamine receptors activate peripheral spike initiation in a stomatogastric motor neuron. *J. Neurosci.* **2003**, *23*, 6866–6875. [PubMed]
382. Semyanov, A.; Kullmann, D.M. Kainate receptor-dependent axonal depolarization and action potential initiation in interneurons. *Nat. Neurosci.* **2001**, *4*, 718–723. [CrossRef] [PubMed]
383. Fields, R.D. Oligodendrocytes changing the rules: Action potentials in glia and oligodendrocytes controlling action potentials. *Neuroscientist* **2008**, *14*, 540–543. [CrossRef] [PubMed]
384. Halassa, M.M.; Dal Maschio, M.; Beltramo, R.; Haydon, P.G.; Benfenati, F.; Fellin, T. Integrated brain circuits: Neuron-astrocyte interaction in sleep-related rhythmogenesis. *ScientificWorldJournal* **2010**, *10*, 1634–1645. [CrossRef] [PubMed]
385. Molnar, G.; Olah, S.; Komlosi, G.; Fule, M.; Szabadics, J.; Varga, C.; Barzo, P.; Tamas, G. Complex events initiated by individual spikes in the human cerebral cortex. *PLoS Biol.* **2008**, *6*, e222. [CrossRef] [PubMed]
386. Pinault, D.; Pumain, R. Antidromic firing occurs spontaneously on thalamic relay neurons: Triggering of somatic intrinsic burst discharges by ectopic action potentials. *Neuroscience* **1989**, *31*, 625–637. [CrossRef]
387. Radman, T.; Su, Y.; An, J.H.; Parra, L.C.; Bikson, M. Spike timing amplifies the effect of electric fields on neurons: Implications for endogenous field effects. *J. Neurosci.* **2007**, *27*, 3030–3036. [CrossRef] [PubMed]
388. Bennett, M.V.; Zukin, R.S. Electrical coupling and neuronal synchronization in the mammalian brain. *Neuron* **2004**, *41*, 495–511. [CrossRef]
389. Schmitz, D.; Schuchmann, S.; Fisahn, A.; Draguhn, A.; Buhl, E.H.; Petrasch-Parwez, E.; Dermietzel, R.; Heinemann, U.; Traub, R.D. Axo-axonal coupling. A novel mechanism for ultrafast neuronal communication. *Neuron* **2001**, *31*, 831–840. [CrossRef]
390. Cuntz, H.; Haag, J.; Forstner, F.; Segev, I.; Borst, A. Robust coding of flow-field parameters by axo-axonal gap junctions between fly visual interneurons. *Proc. Natl. Acad. Sci. USA* **2007**, *104*, 10229–10233. [CrossRef] [PubMed]
391. Draguhn, A.; Traub, R.D.; Schmitz, D.; Jefferys, J.G. Electrical coupling underlies high-frequency oscillations in the hippocampus in vitro. *Nature* **1998**, *394*, 189–192. [CrossRef] [PubMed]
392. Lewis, T.J.; Rinzel, J. Self-organized synchronous oscillations in a network of excitable cells coupled by gap junctions. *Network* **2000**, *11*, 299–320. [CrossRef] [PubMed]

393. Maex, R.; De Schutter, E. Mechanism of spontaneous and self-sustained oscillations in networks connected through axo-axonal gap junctions. *Eur. J. Neurosci.* **2007**, *25*, 3347–3358. [CrossRef] [PubMed]
394. Traub, R.D.; Bibbig, A. A model of high-frequency ripples in the hippocampus based on synaptic coupling plus axon-axon gap junctions between pyramidal neurons. *J. Neurosci.* **2000**, *20*, 2086–2093. [PubMed]
395. Traub, R.D.; Schmitz, D.; Jefferys, J.G.; Draguhn, A. High-frequency population oscillations are predicted to occur in hippocampal pyramidal neuronal networks interconnected by axoaxonal gap junctions. *Neuroscience* **1999**, *92*, 407–426. [CrossRef]
396. Debanne, D. Information processing in the axon. *Nat. Rev. Neurosci.* **2004**, *5*, 304–316. [CrossRef] [PubMed]
397. Waxman, S.G. Integrative properties and design principles of axons. *Int. Rev. Neurobiol.* **1975**, *18*, 1–40. [PubMed]
398. Fukuda, T.; Kosaka, T. Gap junctions linking the dendritic network of gabaergic interneurons in the hippocampus. *J. Neurosci.* **2000**, *20*, 1519–1528. [PubMed]
399. Arvanitaki, A. Effects evoked in an axon by the activity of a contiguous one. *J. Neurophysiol.* **1942**, *5*, 89–108.
400. Katz, B.; Schmitt, O.H. Electric interaction between two adjacent nerve fibres. *J. Physiol.* **1940**, *97*, 471–488. [CrossRef] [PubMed]
401. Anastassiou, C.A.; Perin, R.; Markram, H.; Koch, C. Ephaptic coupling of cortical neurons. *Nat. Neurosci.* **2011**, *14*, 217–223. [CrossRef] [PubMed]
402. Chan, C.Y.; Nicholson, C. Modulation by applied electric fields of purkinje and stellate cell activity in the isolated turtle cerebellum. *J. Physiol.* **1986**, *371*, 89–114. [CrossRef] [PubMed]
403. Jefferys, J.G. Gap junctions and diseases of the nervous system. *Trends Neurosci.* **1995**, *18*, 520–521. [CrossRef]
404. Womelsdorf, T.; Schoffelen, J.M.; Oostenveld, R.; Singer, W.; Desimone, R.; Engel, A.K.; Fries, P. Modulation of neuronal interactions through neuronal synchronization. *Science* **2007**, *316*, 1609–1612. [CrossRef] [PubMed]
405. Chan, C.Y.; Hounsgaard, J.; Nicholson, C. Effects of electric fields on transmembrane potential and excitability of turtle cerebellar purkinje cells in vitro. *J. Physiol.* **1988**, *402*, 751–771. [CrossRef] [PubMed]
406. Deans, J.K.; Powell, A.D.; Jefferys, J.G. Sensitivity of coherent oscillations in rat hippocampus to ac electric fields. *J. Physiol.* **2007**, *583*, 555–565. [CrossRef] [PubMed]
407. Bishop, P.O. Synaptic transmission; an analysis of the electrical activity of the lateral geniculate nucleus in the cat after optic nerve stimulation. *Proc. R. Soc. Lond. B Biol. Sci.* **1953**, *141*, 362–392. [CrossRef] [PubMed]
408. Carras, P.L.; Coleman, P.A.; Miller, R.F. Site of action potential initiation in amphibian retinal ganglion cells. *J. Neurophysiol.* **1992**, *67*, 292–304. [PubMed]
409. Clark, B.D.; Goldberg, E.M.; Rudy, B. Electrogenic tuning of the axon initial segment. *Neuroscientist* **2009**, *15*, 651–668. [CrossRef] [PubMed]
410. Edwards, C.; Ottoson, D. The site of impulse initiation in a nerve cell of a crustacean stretch receptor. *J. Physiol.* **1958**, *143*, 138–148. [CrossRef] [PubMed]
411. Stuart, G.; Hausser, M. Initiation and spread of sodium action potentials in cerebellar purkinje cells. *Neuron* **1994**, *13*, 703–712. [CrossRef]
412. Tauc, L. Site of origin and propagation in spike in the giant neuron of aplysia. *J. Gen. Physiol.* **1962**, *45*, 1077–1097. [CrossRef] [PubMed]
413. Augustine, G.J.; Charlton, M.P.; Smith, S.J. Calcium entry and transmitter release at voltage-clamped nerve terminals of squid. *J. Physiol.* **1985**, *367*, 163–181. [CrossRef] [PubMed]
414. Stuart, G.J.; Sakmann, B. Active propagation of somatic action potentials into neocortical pyramidal cell dendrites. *Nature* **1994**, *367*, 69–72. [CrossRef] [PubMed]
415. Alle, H.; Geiger, J.R. Combined analog and action potential coding in hippocampal mossy fibers. *Science* **2006**, *311*, 1290–1293. [CrossRef] [PubMed]
416. Shu, Y.; Hasenstaub, A.; Duque, A.; Yu, Y.; McCormick, D.A. Modulation of intracortical synaptic potentials by presynaptic somatic membrane potential. *Nature* **2006**, *441*, 761–765. [CrossRef] [PubMed]
417. Hestrin, S.; Armstrong, W.E. Morphology and physiology of cortical neurons in layer i. *J. Neurosci.* **1996**, *16*, 5290–5300. [PubMed]
418. Ina, A.; Sugiyama, M.; Konno, J.; Yoshida, S.; Ohmomo, H.; Nogami, H.; Shutoh, F.; Hisano, S. Cajal-retzius cells and subplate neurons differentially express vesicular glutamate transporters 1 and 2 during development of mouse cortex. *Eur. J. Neurosci.* **2007**, *26*, 615–623. [CrossRef] [PubMed]
419. Frohlich, F.; McCormick, D.A. Endogenous electric fields may guide neocortical network activity. *Neuron* **2010**, *67*, 129–143. [CrossRef] [PubMed]

420. deng, B.; Wang, L.; Wang, J.; Wei, X.L.; Yu, H.T. Endogenous fields enhanced stochastic resonance in a randomly coupled neuronal network. *Chaos Solitons Fractals* **2014**, *68*, 30–39. [CrossRef]
421. Helias, M.; Deger, M.; Diesmann, M.; Rotter, S. Equilibrium and response properties of the integrate-and-fire neuron in discrete time. *Front. Comput. Neurosci.* **2010**, *3*, 29. [CrossRef] [PubMed]
422. Smith, G.D.; Sherman, S.M. Detectability of excitatory versus inhibitory drive in an integrate-and-fire-or-burst thalamocortical relay neuron model. *J. Neurosci.* **2002**, *22*, 10242–10250. [PubMed]
423. Destexhe, A.; Sejnowski, T.J. The initiation of bursts in thalamic neurons and the cortical control of thalamic sensitivity. *Philos. Trans. R. Soc. Lond. B Biol. Sci.* **2002**, *357*, 1649–1657. [CrossRef] [PubMed]
424. Huguenard, J.R.; Prince, D.A. A novel T-type current underlies prolonged Ca(2+)-dependent burst firing in gabaergic neurons of rat thalamic reticular nucleus. *J. Neurosci.* **1992**, *12*, 3804–3817. [PubMed]
425. Destexhe, A.; Contreras, D.; Steriade, M.; Sejnowski, T.J.; Huguenard, J.R. In vivo, in vitro, and computational analysis of dendritic calcium currents in thalamic reticular neurons. *J. Neurosci.* **1996**, *16*, 169–185. [PubMed]
426. Landisman, C.E.; Connors, B.W. Long-term modulation of electrical synapses in the mammalian thalamus. *Science* **2005**, *310*, 1809–1813. [CrossRef] [PubMed]
427. Lee, S.C.; Patrick, S.L.; Richardson, K.A.; Connors, B.W. Two functionally distinct networks of gap junction-coupled inhibitory neurons in the thalamic reticular nucleus. *J. Neurosci.* **2014**, *34*, 13170–13182. [CrossRef] [PubMed]
428. Cudeiro, J.; Sillito, A.M. Looking back: Corticothalamic feedback and early visual processing. *Trends Neurosci.* **2006**, *29*, 298–306. [CrossRef] [PubMed]
429. Li, C.Y.; Poo, M.M.; Dan, Y. Burst spiking of a single cortical neuron modifies global brain state. *Science* **2009**, *324*, 643–646. [CrossRef] [PubMed]
430. Brecht, M.; Schneider, M.; Sakmann, B.; Margrie, T.W. Whisker movements evoked by stimulation of single pyramidal cells in rat motor cortex. *Nature* **2004**, *427*, 704–710. [CrossRef] [PubMed]
431. Haken, H. *Synergetic Computers and Cognition*, 2nd ed.; Springer: Berlin, Germany, 2004.
432. Kelso, J.A.S. *Dynamic Patterns: The Self-Organization of Brain and Behavior*, 1995th ed.; MIT Press: Cambridge, MA, USA, 1995.
433. Wach, C.; Krause, V.; Moliadze, V.; Paulus, W.; Schnitzler, A.; Pollok, B. The effect of 10 hz transcranial alternating current stimulation (TACS) on corticomuscular coherence. *Front. Hum. Neurosci.* **2013**, *7*, 511. [CrossRef] [PubMed]
434. Berenyi, A.; Belluscio, M.; Mao, D.; Buzsaki, G. Closed-loop control of epilepsy by transcranial electrical stimulation. *Science* **2012**, *337*, 735–737. [CrossRef] [PubMed]
435. Elgamal, S.; McKinnon, M.C.; Ramakrishnan, K.; Joffe, R.T.; MacQueen, G. Successful computer-assisted cognitive remediation therapy in patients with unipolar depression: A proof of principle study. *Psychol. Med.* **2007**, *37*, 1229–1238. [CrossRef] [PubMed]
436. Mueser, K.T.; Penn, D.L.; Addington, J.; Brunette, M.F.; Gingerich, S.; Glynn, S.M.; Lynde, D.W.; Gottlieb, J.D.; Meyer-Kalos, P.; McGurk, S.R.; et al. The navigate program for first-episode psychosis: Rationale, overview, and description of psychosocial components. *Psychiatr. Serv.* **2015**, *66*, 680–690. [CrossRef] [PubMed]
437. Wykes, T.; Reeder, C.; Landau, S.; Everitt, B.; Knapp, M.; Patel, A.; Romeo, R. Cognitive remediation therapy in schizophrenia: Randomised controlled trial. *Br. J. Psychiatry* **2007**, *190*, 421–427. [CrossRef] [PubMed]
438. Van der Valk, R.; van de Waerdt, S.; Meijer, C.J.; van den Hout, I.; de Haan, L. Feasibility of mindfulness-based therapy in patients recovering from a first psychotic episode: A pilot study. *Early Interv. Psychiatry* **2013**, *7*, 64–70. [CrossRef] [PubMed]

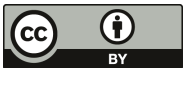

Section 3:
Deep Brain Stimulation for Pain and Autonomic Dysfunction

brain sciences

MDPI

Review

Single Electrode Deep Brain Stimulation with Dual Targeting at Dual Frequency for the Treatment of Chronic Pain: A Case Series and Review of the Literature

Milo Hollingworth [1], Hugh P. Sims-Williams [2], Anthony E. Pickering [3], Neil Barua [1] and Nikunj K. Patel [1,*]

1 Department of Neurosurgery, North Bristol Trust, Bristol BS10 5NB, UK; milo.hollingworth@gmail.com (M.H.), neil.barua@nbt.nhs.uk (N.B.)
2 Department of Neurosurgery, Sheffield Teaching Hospital, Sheffield S10 2JF, UK; simswilliams@doctors.org.uk
3 School of Physiology, Pharmacology & Neuroscience, University of Bristol, Bristol BS8 1TD, UK; tony.pickering@bristol.ac.uk
* Correspondence: nik.patel@nbt.nhs.uk; Tel.: +44-011-7414-6706

Academic Editors: Tipu Aziz and Alex Green
Received: 9 November 2016; Accepted: 9 January 2017; Published: 13 January 2017

Abstract: Deep Brain Stimulation (DBS) has been used to target many deep brain structures for the treatment of chronic pain. The periaqueductal grey and periventricular grey (PAG/PVG) is an effective target but results are variable, sometimes short-lived or subject to tolerance. The centromedian intra-laminar parafascicular complex (CMPf) modulates medial pain pathways and CMPf DBS may address the affective aspects of pain perception. Stimulation of multiple deep brain targets may offer a strategy to optimize management of patients with complex pain symptomatology. However, previous attempts to stimulate multiple targets requires multiple trajectories and considerable expense. Using a single electrode to stimulate multiple targets would help overcome these challenges. A pre-requisite of such a technique is the ability to use different stimulation parameters at different contacts simultaneously on the same electrode. We describe a novel technique in 3 patients with chronic pain syndromes for whom conventional medical and/or neuromodulation therapy had failed using a single electrode technique to stimulate PVG/PAG and CMPf at dual frequencies.

Keywords: deep brain stimulation; CMPf; PAG/PVG; pain; pain pathways

1. Introduction

1.1. Deep Brain Targets for the Treatment of Pain

For over 60 years deep brain stimulation (DBS) has demonstrated significant analgesic benefits. James Olds and Peter Milner found stimulation of septal regions in rodents elicited self-stimulation overwriting normal survival behaviours [1]. In attempts to treat patients with schizophrenia, stimulation of septal structures yielded serendipitous pain relief [2]. Sufferers of malignant oncological diseases and rheumatoid arthritis provided a willing and ethically justifiable cohort and, indeed, septal region DBS proved moderately effective in early studies. However, due to variable and non-sustained responses, finding alternative deep brain targets became a priority. Consequently targets range from the internal capsule (IC) [3] to thalamic structures such as the somatosensory thalamus, centromedian intralaminar parafascicular complex (CMPf) [4], to the periventricular and

periacqueductal grey (PVG/PAG) [5], to the nucleus accumbens (NAc) [6] and anterior cingulate cortex (AC) [7]. However, despite this array of deep brain targets, the complexity of pain management is a persistent challenge demanding new approaches. We provide a technical note of a novel technique and a review of the literature. Stimulation of PVG/PAG and CMPf is the focus of this review and technical note and will be described separately. The rationale and effects of targeting the other deep brain nuclei are important to place the treatment of chronic pain by DBS in context.

1.2. Anterior Cingulate

The first published case of AC DBS was reported by Spooner et al. [8] in a patient with neuropathic pain secondary to spinal cord injury. He received bilateral and unilateral DBS to the AC and PVG respectively. Pain relief was assessed using the Visual Analogue Scale for pain (VAS) and by tracking pain medication usage. Bilateral cingulate stimulation resulted in improved affect and was associated with improved subjective analgesic properties relative to PVG stimulation alone. Boccard et al., in 2014 [7] presented a case series of AC stimulation in 15 patients with chronic pain with a range of aetiologies including failed back surgery syndrome, poststroke pain, brachial plexus injury, cervical spinal cord injury, head injury, and pain of unknown origin. Using several pre- and post-operative pain measures they detected statistically significant overall improvement in reported pain. In 5 patients VAS decreased to less than 4 on a scale of 1 (no pain)–10 (very severe pain). No major adverse events were reported. Although, this study is limited by its heterogenous population and assessment measures that under emphasize the affective components of pain, this study demonstrates that AC stimulation is a useful option. As such, preclinical and clinical studies have explored the importance of the AC in pain perception, which has been subject to comprehensive review [9].

1.3. Nucleus Accumbens

NAc, forms an extension of the ventral striatum, which is involved in reward processing. DBS of the NAc is used in the treatment of depression and obsessive-compulsive disorder [10,11]. NAc also projects inhibitory projections to the medial thalamus [12] and thereafter to dorsal horn neurons to modulate pain perception [13]. The NAc together with the prefrontal cortex, insula and AC mediates the affective component of pain [12,13]. One case of post-stoke pain has been treated using DBS targeting the NAc and PVG simultaneously to great effect [6]. In our case of post-stroke pain described herein, stimulation of the NAc was combined with dual targeting of the PVG/PAG, however this was not found to be helpful.

1.4. The Somatosensory Thalamus

Somatosensory thalamus consisting of the ventroposterior lateral (VPL) and medial (VPM) nuclei have been targeted to treat chronic pain for over 40 years [14,15] Hosobuchi et al., in 1973 treated five patients with facial pain secondary to retrogasserian rhizotomy. Chronic stimulation of the contralateral VPM induced a paresthesia, which improved pain tolerance in 4 out of 5 patients [14]. The explanation for targeting the somatosensory thalamus is its aberrant neuronal firing observed in chronic pain [16] presumably driven by the absence of normal sensory input [17]. Melzack and Wall support this idea in their gate control theory [18], postulating that low threshold somatosensory pathways inhibit pain perception. Stimulation of this pathway was expected to reduce neuropathic pain. This has been supported in animal models where VPL stimulation inhibited spinothalamic nociceptive neurons [16,19]. Indeed, in a series of 12 patients with neuropathic pain secondary to brachial plexus injuries and phantom limb pain, 11 demonstrated improvement in pain scores following stimulation of VPL [20].

1.5. PVG/PAG

The PVG/PAG (see Figure 1a) is the most promising target in DBS for chronic pain [21]. The first descriptions of PVG/PAG DBS in humans demonstrated relief of somatoform and nociceptive

pain in both the acute and chronic settings [22,23]. This was consistent with descriptions of a PAG- derived descending inhibitory system modulating nociceptive inputs at a spinal level [24]. Indeed, recent evidence demonstrates PAG DBS causes a focal reduction of opioid binding in areas of electrostimulation consistent with the release of endogenous opioid peptides [25]. This is in keeping with several studies implicating opioids in PAG/PVG mediated attenuation of nociception. The analgesic effect of PAG DBS in both animal models and humans is reversible with the opioid antagonist naloxone [26] and opioid receptor binding density is also remarkably high [27]. However, the picture is complicated by blinded studies of DBS PAG patients whose analgesia was not fully reversed by naloxone and similarly failed to show cross-tolerance to systemically administered opioids [5]. Such findings raise the possibility of non-opioidergic mechanisms of PAG analgesia [28,29] painting a more complex picture of pain control. Indeed, although stimulation of the PAG/PVG provides long-term relief in 79% of patients with nociceptive pain, it is less effective in central and de-afferentation pain syndromes [28]. Taken together although PAG/PVG stimulation are an important focus, its mechanism of action is complex and innovation is still required to design better treatments for patients.

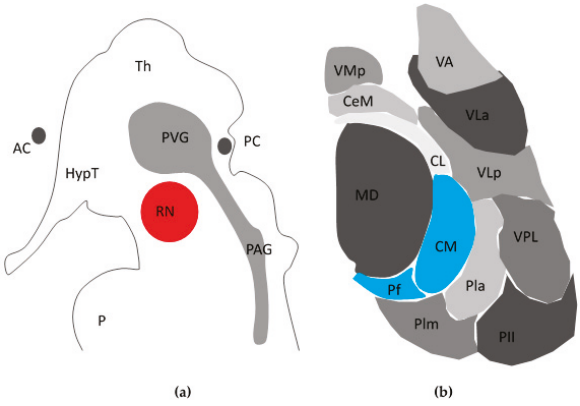

Figure 1. Schematic view of peri-aqueductal grey/Periventricular grey (PAG/PVG) and centromedian intralaminar parafasciular complex (CMPf). (**a**) Sagittal cross-sectional schema of PVG/PAG within midbrain/diencephalon; (**b**) Axial cross section of left thalamus demonstrating CMPf (**blue**) adapted from Weigel and Kraus, 2004 [30]. AC: Anterior Commissure; HypT: Hypothalamus; RN: Red Nucleus; PC: Posterior Commissure; Th: Thalamus; P: Pons; MD: Mediodorsal nucleus; VMp: Ventral Posteromedial nucleus; CeM: Central Medial nucleus; CL: Centrolateral; Plm: Medial nucleus of Pulvinar; Pll: Lateral nucleus of Pulvinar; Pla: Anterior nucleus of Pulvinar; VPL: Ventral Posterior Lateral nucleus; VLp: Ventrolateral Posterior nucleus; VLa: Ventrolateral Anterior nucleus; VA: Ventral Anterior nucleus.

1.6. Centromedian Parafasciculus Complex (CMPf)

Intra-operative stimulation of the CMPf and the intra-laminar zone achieves variable results [30,31], which may explain why it has received less attention compared to other targets. The CMPf (Figure 1b) was first described by Jules Bernard Luys [32], a 19th century Neurologist who also was first to describe the subthalamic nucleus. Dividing the medial and lateral thalamus, the internal medullary lamina contains anterior nuclei and posterior nuclei, the latter of which contains the CMPf [31]. The CMPf has afferents from the ventral posterolateral thalamus (VPL), spinothalamic tract (STT) and trigeminal lemniscus, and efferents to the striatum, cortex, and AC. It is responsive to noxious stimuli in rodents, large animals and primates [30]. However, neurones in the CMPf do not respond in a binary fashion but differentiate stimulus intensity. Firing of the VPL to nociceptive inputs carried within the STT actually inhibit activity in the CMPf, giving rise to a "thalamic gate theory"

akin to Melzack and Wall's ideas of pain modulation in the spinal cord [19]. Inputs to the striatum and the anterior cingulate also suggest the CMPf may modulate affective and behavioural responses suggesting that the CMPf is central to the concept of the medial pain pathway [33].

In human studies, the CMPf demonstrates increased background activity in neuropathic pain [34]. Similarly, the CMPf also expresses a high density of opiate receptors in the rested state [35,36]. Rinaldi et al. found that the intra-laminar thalamic nuclei, including the CMPf are also active in de-afferentation pain [37] and moreover, stimulation of the PVG reduces CMPf firing suggesting critical connectivity of the CMPf to pain-encoding structures [38]. Hariz and Bergenheim found that CMPf stimulation or ablation was helpful in the treatment of central pain and de-afferentation pain [39]. However in a prospective study of bilateral thalamic stimulation, CMPf stimulation only provided short-term relief from neuropathic pain [40]. Despite this it remains a promising target due to its anatomical and electrophysiological profile.

1.7. Dual Stimulation

The interconnectivity within the central nervous system prompts the consideration of stimulating multiple brain structures simultaneously to recruit complex neuronal processes involved in pain sensation and perception. In a meta-analysis the most successful technique to provide long term analgesia in 87% of cases reported was stimulation of both the PVG/PAG and Sensory thalamus/IC [21]. In the same way, stimulation of PVG and NAc have been used to treat post-stroke pain successfully [6].

We have previously published outcome data (n = 3) for dual stimulation of PAG/PVG and CMPf in the treatment of trigeminal anaesthesia dolorosa (TAD) [41]. The mean VAS was acutely reduced from 55 mm to 24 mm for PAG stimulation and from 67 mm to 22 mm for CMPf stimulation. PAG/PVG and CMPf stimulation were associated with pleasant warmth and improved pain tolerance respectively. Dual stimulation elicited both these features and was ultimately associated with reduction in analgesia requirements. This study by our group [41] and those reviewed by Bittar et al., [21] demonstrate the non-antagonistic effects of dual stimulation in the treatment of chronic pain. However, dual stimulation has practical considerations. For example, in our case series of 3 patients receiving dual stimulation for TAD, all patients required separate generators and trajectories per target to deliver dual stimulation parameters [41]. This is in itself multiplies the risk of haemorrhagic and infective complications as well as the financial cost. However, whilst treating a patient with phantom limb pain (not included in this series), stimulation of the proximal contacts of a PAG/PVG-targeted electrode yielded surprisingly favourable results. Closer inspection of these proximal contacts demonstrated their location within the CMPf lying along the trajectory directed toward the PAG/PVG (Personal Communication N.P.). The ability to target both the CMPf and PAG/PVG simultaneously along a single trajectory provided a solution to the increased cost and risk of surgical morbidity associated with dual stimulation by "striking two birds with one stone".

Single electrode dual targeting offers a practical solution to a risky and expensive problem and may encourage others to further explore the potential of dual stimulation. The ultimate aim would be to exploit different pain circuitry to provide synergistic modulation of complex pain symptomatology. However, such synergism can only be achieved by stimulating targets at their optimal parameters. Hence, single electrode dual targeting techniques require generators equipped to deliver different frequencies simultaneously. Through collaboration with Boston Scientific® (Marlborough, MA, USA), we exploited the versatility of the Boston Scientific Vercise™ generator (Boston Scientific Inc, Marlborough, MA, USA) to perform single electrode dual target dual stimulation PVG/PAG and CMPf DBS in 3 cases with chronic pain who either failed or were not amenable to conventional spinal cord stimulation.

2. The Technique

The technique previously developed by this group is based on magnetic resonance imaging (MRI) directed electrode implantation using implantable guide tubes [42]. Pre-operative planning scans

including T1 and T2 MRI and Computer Tomography Angiogram (CTA) are co-registered on in-house adapted Neuroinspire^{TM} software (Renishaw PLC., Wotton-under-Edge, UK). Deep brain trajectories to the CMPf and PAG are planned with proximal electrode contacts positioned within CMPf and distal contacts within PAG/PVG (see Figure 2a,b). Simultaneous targeting of both structures with a single trajectory requires the use of a DBS system with contacts spanning a sufficient distance and with the facility to use different stimulation parameters at each target. We have therefore opted to use the Boston Scientific Vercise^{TM} system to achieve these aims.

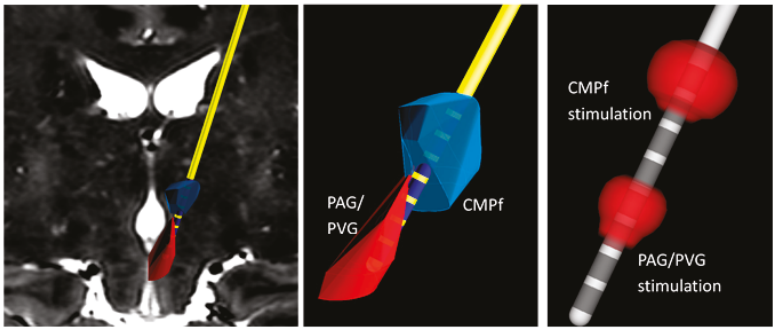

Figure 2. Dual frequency stimulation using a single electrode technique to target the Periaqueductal Grey/Periventricular Grey (PAG/PVG) and Centromedian Intralaminar Parafasciular complex (CMPf) in the treatment of chronic pain. (**a**) Tracings of the CMPf (**blue**) and PAG/PVG (**red**) in coronal plane undergo volumetric reconstruction using NeuroInspire^{TM} software to create 3-dimensional structures for robot-guided DBS electrode implantation; (**b**) Contacts 1–3 and 5–8 are embedded within the PAG/PVG and CMPf respectively along the same trajectory; (**c**) Spherical electrical fields (**red**) at contacts 4 and 8 stimulate the PAG/PVG and CMPf respectively yielding analgesia in a case of refractory phantom limb pain.

In the operating theatre, the patient is placed under general anaesthetic and a Leksell frame fitted. The patient is then placed in the head-holder of the Neuromate stereotactic robot (Renishaw PLC., Wotton-under-Edge, UK). Using intra-operative post-contrast three-dimensional fluoroscopy (O-Arm, Medtronic, Minneapolis, MN, USA), the patient position is registered and stereotactic co-ordinates outputted to the robot. A linear scalp incision is made and the periosteum retracted. The robot is driven to the first position on the skull and a multi-featured burr hole drilled. Using custom-made tooling a track is dissected using 1.3 mm and 1.7 mm outer diameter (OD) guide rods which traverse both CmPf and PAG. Prior to implantation of the electrode, a radio-opaque carbothane guide tube and stylet (Renishaw PLC, Wooton-under-Edge, UK) are inserted to target. The guide tube is cut 20 mm shorter than the stylet in order to ensure exposure of the electrode contacts within the deep brain targets. Insertion of guide tubes and stylets are visualized without the metal artifact and targeting accuracy verified by performing O-arm imaging after electrode insertion.

Once targeting accuracy is confirmed by co-registering the on-table imaging with the pre-operative plan, the stylet is removed and replaced with a Boston Scientific Vercise DBS system (model DB2201). Integration of the Boston Vercise^{TM} DBS with Neuroinspire^{TM} software (Renishaw PLC, Wooton-under-Edge, UK) allows visualization of electrode contacts within the target structures to 0.3 mm accuracy (Figure 2a,b).

Through personal collaboration between this group and Boston Scientific®, Boston Scientific Vercise^{TM}, model DB1110 generator was optimised for dual frequencies output (each ranging from 2 to 225 Hz) at two separate locations along the electrode (Figure 2c, Table 1). Our robot-guided technique co-registered with pre-and perioperative imaging allows precise knowledge of contact location so

contacts within the PAG/PVG and CMPf can be selectively activated. We performed this procedure in 3 patients with different aetiologies of intractable chronic pain.

Table 1. Stimulation parameters and overall Visual Analogue Scales (VAS) at pre-operative assessment and 3 years' follow-up (FU) in single electrode dual targeting of the Periaqueductal grey/Periventricular grey (PAG/PVG) and Centromedian Intralaminar Parafasciular complex (CMPf) for three patients with chronic pain syndromes.

	Diagnosis	PAG/PVG Stimulation			CMPf Stimulation			Overall VAS (mm)		Medication, Total Daily Dose	
		mA	µs	Hz	mA	µs	Hz	Pre-op	3 Years' FU	Pre-op	3 Years' FU
Case 1	Trigeminal anaethetica dolorsa	4.5	60	10	4.5	60	128	44	5	Gabapentin 4800 mg	Gabapentin 1800 mg
Case 2	Phantom limb pain	4.0	90	10	4.0	90	132	94	56	Tramadol 400 mg, Gabapentin 2700 mg, Temazapam 10 mg, Amitriptyline 150 mg	Mirtazepine 30 mg Tramadol 400 mg Baclofen 40 mg, Temazapam 10 mg, Amitriptyline 150 mg
Case 3	Post-stroke Pain	3.5	110	10	4	90	132	98	32	Carbamazepine 800 mg, Duloxetine 120 mg, Pregabalin 450 mg	Carbamazepine 800 mg, Duloxetine 120 mg, Pregabalin 450 mg

2.1. Case 1

52-year old scientist with a 2 year history of progressive left-sided facial pain secondary to Lyme's Disease contracted during field work was reviewed by neurosurgery following extensive contact with pain services. Her symptoms consisted of complete hypoesthesia to the left face with associated paraesthesia and allodynia. Supramaximal dosing of gabapentin at 5.4 g daily reduced her symptoms but was associated with significant cognitive disturbance and sedation. Pulsed radiofrequency therapy of the trigeminal ganglion failed to achieve benefit. The patient suffered persistent paraesthesia and irritation interfering with her activities of daily living. The patient was admitted for single electrode dual target surgery, which was performed under general anaesthetic with robot assistance as described above [27]. Implantation of a guide tube via a right transfrontal approach allowed delivery of an electrode to 96.6 mm passing through the right CMPF terminating in the right PAG. Stimulation of the CMPf and PAG/PVG resulted in a pleasant facial paresthesia and cold sensation respectively, dual stimulation subjectively provided preferable analgesic effects. Two days following surgery the generator was activated using dual frequencies (Table 1). At 3 years post-surgery, the patient only suffered minimal symptoms with full return to her activities using concomitant DBS stimulation and gabapentin therapy weaned to 1.8 g daily (Table 1).

2.2. Case 2

A 35-year old woman with left arm phantom pain was treated with DBS. Her pain developed after a severe episode of self-harm 10 years prior. Her tendons and nerves were cut at the proximal forearm resulting in contractures and de-afferentation pain. Above elbow amputation was eventually required; however, this resulted in worsening pain. Despite successful neuroma excision, a prosthesis was not tolerated. After input from a specialist pain team and multiple pharmacological trials, the patient underwent a trial of spinal cord (dorsal column) stimulation, which was ineffective. Her predominant complaint was cold pain centered over her phantom elbow requiring 2.7 g Gabapentin, 400 mg Tramadol, Baclofen 20 mg, and Amytriptyline 150 mg daily for pain control. To control her symptoms, the patient had become reliant on a hot compress applied to her stump fixed in place with a bandage. Keeping the compress hot had become a pre-occupation leading to significant limitation of her outdoor activities, even making attendance of her hospital follow-up problematic. Following thorough psychiatric assessment, the patient was admitted for single electrode dual target surgery as described. Via a right transfrontal approach a guide-tube was implanted and an electrode passed along the trajectory to a depth of 96.5 mm passing through the CMPf and PAG/PVG. Following activation of the generator (Table 1) the patient's predominant cold pain was reduced. PAG/PVG stimulation alone

achieved a warm glowing sensation throughout the phantom arm, hand and fingers, leaving only a cool sensation in her finger nails. The addition of CMPf stimulation resulted in reconfiguration of the phantom limb leading to dissipation of her pain at the elbow (Figure 3, Table 1). The elbow pain was however later replaced by a less severe pain in her phantom wrist (5/10 severity). It was not possible to control the new wrist pain without a return of the elbow pain. At 3 years follow-up, the patient was no longer reliant on her hot compress, which allowed her to leave her home and return to independent living.

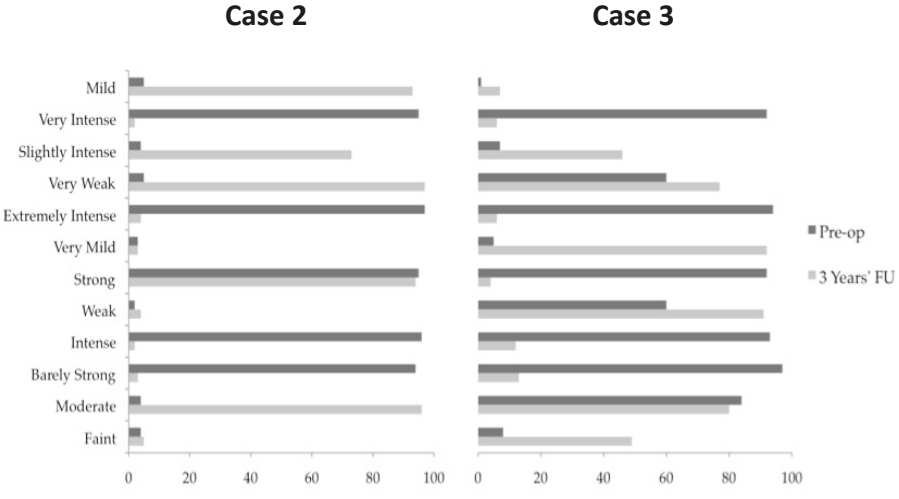

Figure 3. Pre-operative and post-operative Descriptor Differential Scale (DDS) [43] for Cases 2 and 3. Pre-operative and post-operative DDS measurements were performed for Case 2 and Case 3. Patients were asked to mark along each line the extent to which the description applies to their symptoms between 0 and 100. Single electrode dual target dual stimulation at 3 years follow-up decreased the severity of pain consistently in patients 2 and 3 compared to pre-operative assessments. Post-operative DDS measurements were not available for Case 1.

2.3. Case 3

A 49-year old man presented with an 8-year history of repeated strokes. At 41 years of age he suffered a right middle cerebral artery infarct resulting in contralateral hemiparesis. At the time of his infarct, the patient reported pain in the left upper limb, neck and leg with sparing of the face, which failed to abate following his recovery. The pain was described as burning/pulling sensation that was present all the time and it was associated with hypoesthesia. The patient was diagnosed with central pain syndrome and received extensive input from pain physicians over the intervening eight years with little alleviation in his symptoms. He was referred for consideration of DBS to treat his chronic pain. He underwent single electrode right CMPf and PAG/PVG targeting combined with targeting of his right NAc via a separate trajectory. NAc stimulation was found to be unhelpful and its stimulation was quickly terminated. Stimulation of the CMPf and PAG/PVG separately resulted in a warm paresthesia and reduced allodynia respectively. The patient continued dual CMPf PAG/PVG stimulation with improvement in his pain severity at 3 years follow-up (Figure 3, Table 1).

2.4. Testing and Optimization of Dual Frequency Dual Stimulation

Testing was performed at 2.5-min intervals during each assessment. Baseline pain was established prior to the next target being stimulated. Each patient had both pulse generators switched off prior to testing. Pain was allowed to stabilize, which took up to 60 min. CMPf monostimulation was

performed and descriptions of pain were recorded. The pulse generator was then switched off to allow pain to re-stabilise. The PVG/PAG was then stimulated singly; the process was repeated before finally assessing dual stimulation. Extensive description of this method is previously described by our group [41].

3. Discussion

Dual target stimulation with a single electrode represents a natural progression from dual target stimulation with multiple electrodes. This strategy requires the use of DBS technology with the flexibility to deliver different stimulation parameters at the proximal and distal contacts of an electrode. Such requirements may necessitate the use of multiple generators or a specially adapted generator, such as the Boston Scientific Versize™ DBS system, to deliver more than one set of stimulation parameters simultaneously.

This technique may be a potential solution to a complex condition such as intractable pain where even recent advances in neuromodulation, such as spinal cord stimulation and intrathecal therapy, have failed. Dual stimulation of the PVG/PAG and CMPf could help to modulate different symptom components including affective and nociceptive features in order to optimise long-term response and reduce tolerance. Dual targeting with one trajectory can also offer improved safety and cost-effectiveness by minimising the number of electrode insertions, use of operating time and resources. In this article, we describe 3 cases of robot-guided single electrode DBS to stimulate the CMPf and PAG/PVG and the methodological steps required to provide adequate accuracy, safety and efficacy. This further establishes the combined roles of CMPf and PAG/PVG in the control of chronic pain particularly those with de-afferentation and central pain syndromes. This also may allow us to improve the care of patients with increasingly complex pain conditions, and perhaps even neurological conditions beyond the current horizons of "standard" functional neurosurgery. Treatments for epilepsy, disordered consciousness, psychiatric illness and neurodegenerative diseases could potentially all be augmented using such a technique. Already, dual targeting has been explored outside the realms of chronic pain by way of simultaneous stimulation of globus pallidus internus (GPi) and externus stimulation in Parkinson's disease [44], GPi and subthalamic nucleus in Huntington's disease [45] and ventral intermediate nucleus and the subthalamic area in Holme's tremor [46]. Indeed, many promising applications of DBS such as Tourette's syndrome [47], epilepsy [48] and minimally conscious states [49] boast a selection of possible deep brain targets. Single electrode dual target dual stimulation DBS, either unilaterally or bilaterally, could be used to exploit two targets simultaneously and, with necessary developments in electrode and generator design, possibly more. Such developments could help explore conditions more ethically and more comprehensively allowing patients multiple therapeutic options, whilst providing opportunities to compare the efficacy of stimulating different structures without the need for further operations. In our case series, we describe a novel concept overcoming the safety and financial implications of multiple targeting in DBS. This technique will hopefully encourage others to consider its potential in chronic pain and other neurological diseases in both pre-clinical and clinical studies. Single electrode dual target dual stimulation DBS may also facilitate further research previously restricted by single target DBS, as dual targeting can be used to compare the stimulation effects of different brain targets without increasing surgical morbidity or multiplying costs.

4. Limitations

DBS for chronic pain remains a challenging area for both patient and physician. Accumulative evidence from hundreds of patients is available; however, it is observational in nature and derived from cohort studies, case-series and reports describing heterogeneous groups of patients, using various stimulation and neuroimaging technologies to target different deep brain structures. This case series does little to clarify the best way to treat chronic pain, but as a technological development it raises the possibility of treating chronic pain, and maybe other neurological diseases, in a new way. We cannot make assertions regarding the efficacy of our therapy

versus other treatment options owing to the small number of patients, the absence of a control group and the subjectivity of our recorded outcomes. Our series would be improved by being able to demonstrate assessments of affective, as well as nociceptive, aspects of pain before and after surgery in all patients. However, this was not possible. We can show that our technique was safe and well tolerated. It also provided preferable analgesic relief for three patients who failed to benefit from conventional approaches.

Acknowledgments: We would like to acknowledge Ann Rich for her support.

Author Contributions: M.H. wrote the paper and collected data supported by N.B. H.S.-W. performed data collection for the article. A.P. helped conceive of the 'Two Birds with One Stone' concept. N.K.P. developed the single electrode dual target technique.

Conflicts of Interest: N.K.P. has been medical advisor to Boston Scientific and has held consultancies to Medtronic, St Jude Medical (now Abbott) and Nevro; he is the chief medical officer at Bioinduction Ltd. (Bristol, United Kingdom). N.B. is a clinical consultant for Renishaw (Gloucestershire, PLC). H.S.-W, A.P. and M.H. declare no conflicts of interest.

References

1. Olds, J.; Milner, P. Positive reinforcement produced by electrical stimulation of septal area and other regions of rat brain. *J. Comp. Physiol. Psychol.* **1954**, *47*, 419–427. [CrossRef] [PubMed]
2. Heath, R. *Studies in Schizophrenia: A Multidisciplinary Approach to Mind-Brain Relationships*; Harvard University Press: Cambridge, MA, USA, 1954.
3. Adam, J.; Hosobuchi, Y.; Fields, H. Stimulation of the internal capsule for relief of chronic pain. *J. Neurosurg.* **1974**, *4*, 740–744. [CrossRef] [PubMed]
4. Hécaen, H.; Talairach, J.; David, M.; Dell, M. Coagulations limitées du thalamus dans les algies du syndrome thalamique. *Rev. Neurol.* **1949**, *81*, 917–931.
5. Duncan, G.; Bushnell, M.; Marchand, S. Deep brain stimulation: A review of basic research and clinical studies. *Pain* **1991**, *45*, 49–59. [CrossRef]
6. Mallory, G.; Abulseoud, O.; Hwang, S.; Gorman, D.; Stead, S.; Klassen, B.; Sandroni, P.; Watson, J.; Lee, K. The nucleus accumbens as a potential target for central poststroke pain. *Mayo Clin. Proc.* **2012**, *87*, 1025–1031. [CrossRef] [PubMed]
7. Boccard, S.; Fitzgerald, J.; Pereira, E.; Moir, L.; Van Hartevelt, T.; Kringelback, M.; Green, A.; Aziz, T. Targeting the affective component of chronic pain: A case series of deep brain stimulation of the anterior cingulate cortex. *Neurosurgery* **2014**, *74*, 628–635. [CrossRef] [PubMed]
8. Spooner, J.; Yu, H.; Kao, C.; Sillay, K.; Konrad, P. Neuromodulation of the cingulum for neuropathic pain after spinal cord injury. *J. Neurosurg.* **2012**, *117*, 169–172. [CrossRef] [PubMed]
9. Russo, R.F.; Sheth, S.A. Deep brain stimulation of the dorsal anterior cingulate cortex for the treatment of chronic neuropathic pain. *Neurosurg. Focus* **2015**, *38*, E1. [CrossRef] [PubMed]
10. Hauptman, J.S.; DeSalles, A.A.; Espinoza, R.; Sedrak, M.; Ishida, W. Potential surgical targets for deep brain stimulation in treatment-resistant depression. *Neurosurg. Focus* **2008**, *25*, E9. [CrossRef] [PubMed]
11. Franzini, A.; Messina, G.; Gambini, O. Deep-brain stimulation of the nucleus accumbens in obsessive compulsive disorder: Clinical, surgical and electrophysiological considerations in two consecutive patients. *Neurol. Sci.* **2010**, *31*, 353–359. [CrossRef] [PubMed]
12. Albe-Fessard, D.; Berkley, K.J.; Kruger, L.; Ralston, H.J.; Willis, W.D. Diencephalic mechanisms of pain sensation. *Brain Res.* **1985**, *356*, 217–296. [CrossRef]
13. Lorenz, J.; Minoshima, S.; Casey, K.L. Keeping pain out of mind: The role of the dorsolateral prefrontal cortex in pain modulation. *Brain* **2003**, *126*, 1079–1091. [CrossRef] [PubMed]
14. Hosobuchi, Y.; Adams, J.E.; Rutkin, B. Chronic thalamic stimulation for the control of facial anesthesia dolorosa. *Arch. Neurol.* **1973**, *29*, 158–161. [CrossRef] [PubMed]
15. Mazars, G.; Merienne, L.; Cioloca, C. Traitement de certains types de douleurs par des stimulateurs thalamiques implantables. *Neuro-Chirurgie* **1974**, *2*, 117–124.
16. Gerhart, K.D.; Yezierski, R.P.; Fang, Z.R.; Willis, W.D. Inhibition of primate spinothalamic tract neurons by stimulation in ventral posterior lateral (VPLc) thalamic nucleus: Possible mechanisms. *J. Neurophysiol.* **1983**, *49*, 406–423. [PubMed]

17. Mazars, G.J.; Merienne, L.; Ciolocca, C. Stimulations thalmiques intermittentes antalgiques. *Note Prelim. Rev. Neurol.* **1973**, *128*, 273–279.
18. Melzack, R.; Wall, P.D. Pain mechanisms: A new theory. *Surv. Anaesthesiol.* **1967**, *2*, 89. [CrossRef]
19. Benabid, A.; Henriksen, S.; McGinty, J.; Bloom, F. Thalamic nucleus ventro-posterolateralis inhibits nucleus parafascicularis response to noxious stimuli through a non-opioid pathway. *Brain Res.* **1983**, *280*, 217–231. [CrossRef]
20. Pereira, E.A.; Boccard, S.G.; Linhares, P.; Chamadoira, C.; Rosas, M.J.; Abreu, P.; Rebelo, V.; Vaz, R.; Aziz, T.Z. Thalamic deep brain stimulation for neuropathic pain after amputation or brachial plexus avulsion. *Neurosurg. Focus* **2013**, *35*, E7. [CrossRef] [PubMed]
21. Bittar, R.; Kar-Purkayastha, I.; Owen, S.; Bear, R.; Green, A.; Wand, S.; Aziz, T. Deep brain stimulation for pain relief: A meta-analysis. *J. Clin. Neurosci.* **2005**, *12*, 515–519. [CrossRef] [PubMed]
22. Richardson, D.; Akil, H. Pain reduction by electrical stimulation in man. Part 1: Acute administration in periaqueductal and perventricular sites. *J. Neurosurg.* **1977**, *47*, 178–183. [CrossRef] [PubMed]
23. Richardson, D.; Akil, H. Pain reduction by electrical stimulation in man. Part 2: Chronic self-administration in periaqueductal grey matter. *J. Neurosurg.* **1977**, *47*, 184–194. [CrossRef] [PubMed]
24. Mayer, D.; Liebeskind, J. Pain reduction by focal electrical stimulation of the brain: An anatomical and behavioral analysis. *Brain Res.* **1974**, *68*, 73–93. [CrossRef]
25. Sims-Williams, H.P.; Matthews, J.; Talbot, P.; Love-Jones, S.; Brooks, J.; Patel, N.K.; Pickering, A.E. Deep brain stimulation of periaqueductal gray releases endogenous opioids in humans. *Neuroimage* **2016**. [CrossRef] [PubMed]
26. Akil, H.; Mayer, D.; Liebeskind, J. Antagonism of stimulation-produced analgesia by naloxone, a narcotic antagonist. *Science* **1976**, *191*, 961–962. [CrossRef] [PubMed]
27. Kuhar, M.; Pert, C.; Snyder, S. Regional Distribution of opiate receptor binding in the monkey and human brain. *Nature* **1973**, *245*, 447–450. [CrossRef] [PubMed]
28. Bandler, R.; Shipley, M. Columnar organisation in the midbrain periaqueductal gray: Modules for emotional expression? *Trends Neurosci.* **1994**, *17*, 379–389. [CrossRef]
29. Heinricher, M.; Tavares, I.; Leith, J.; Lumb, B. Descending control of nociception: Specificity, recruitment and plasticity. *Brain Res. Rev.* **2009**, *60*, 214–225. [CrossRef] [PubMed]
30. Weigel, R.; Krauss, J. Center median parafascicular complex and pain control. *Sterotact. Funct. Neurosurg.* **2004**, *82*, 115–126. [CrossRef] [PubMed]
31. Davis, K.; Lozano, A.; Tasker, R.; Dostrovsky, J. Brain targets for pain control. *Stereotact. Funct. Neurosurg.* **1998**, *71*, 173–179. [CrossRef] [PubMed]
32. Luys, J. *Recherches sur la Système Nerveux Cerébrospinal: Sa Structure, ses Functions, et ses Maladies*; J.-B. Baillière et Fils: Paris, France, 1865.
33. Bushnell, M.; Duncan, G. Sensory and affective aspects of pain perception: Is medial thalamus restricted to emotional issues? *Exp. Brain Res.* **1989**, *78*, 415–418. [CrossRef] [PubMed]
34. Hirato, M.; Kawashima, Y.; Shibazaki, T.; Shibasaki, T.; Ohye, C. Pathophysiology of central (thalamic) pain: A possible role of the intralaminar nuclei in superficial pain. *Acta Neurochir.* **1991**, *52*, 133–136.
35. Pert, A.; Yaksh, T. Sites of morphine-induced analgesia in the primate brain: Relation to pain pathways. *Brain Res.* **1974**, *80*, 135–140. [CrossRef]
36. Pert, A.; Yaksh, T. Localization of the anti-nociceptive action of morphine in primate brain. *Pharmacol. Biochem. Behav.* **1975**, *3*, 133–138. [CrossRef]
37. Rinaldi, P.; Young, R.; Albe-Fessard, D.; Chodakiewitz, J. Spontaneous neuronal hyperactivity in the medial and intralaminar thalamic nuclei of patients with de-afferentation pain. *J. Neurosurg.* **1991**, *174*, 415–421. [CrossRef] [PubMed]
38. Gura, E.; Garkavenko, V.V.; Limansky, Y.P. Influences of central gray matter stimulation on thalamic neuron responses to high- and low threshold stimulation of trigeminal nerve structures. *Neuroscience* **1991**, *41*, 681–693. [CrossRef]
39. Hariz, M.I.; Bergenheim, A.T. Thalamic stereotaxis for chronic pain: Ablative lesion or stimulation? *Stereotact. Funct. Neurosurg.* **1995**, *64*, 47–55. [PubMed]
40. Krauss, J.K.; Pohle, T.; Weigel, R.; Kalbarczyk, A. Somatosensory thalamic stimulation versus center median-parafascicular complex stimulation in 11 patients with neuropathic pain. *Stereotact. Funct. Neurosurg.* **2001**, *77*, 194–195.

41. Sims-Williams, H.; Javed, S.; Pickering, A.; Patel, N. Characterising the analgesic effect of different targets for deep brain stimulation in trigeminal anaesthesia dolorosa. *Sterotact. Funct. Neurosurg.* **2016**, *94*, 174–181. [CrossRef] [PubMed]
42. Patel, N.; Plaha, P.; Gill, S. Magnetic resonance imaging-directed method for functional neurosurgery using implantable guide tubes. *Neurosurgery* **2007**, *61*, 358–365. [CrossRef] [PubMed]
43. Gracely, R.H.; Kwilosz, D.M. The Descriptor Differential Scale: Applying psychophysical principals to clinical pain. *Pain* **1988**, *35*, 279–288. [CrossRef]
44. Angeli, A.; Akram, H.; Zacharia, A.; Limousin, P.; Hariz, M.; Zrinzo, L.; Foltynie, T. Varying timecourse of effects of high frequency stimulation of sub-regions of the globus pallidus in patients with Parkinson's disease. *Parkinsonism Relat. Disord.* **2015**, *21*, 597–602. [CrossRef] [PubMed]
45. Gruber, D.; Kuhn, A.; Schoenecker, T.; Kopp, U.A.; Kivi, A.; Huebl, J.; Lobsien, E.; Mueller, B.; Schneider, G.H.; Kupsch, A. Quadruple deep brain stimulation in Huntington's disease, targeting pallidum and subthalamic nucleus: Case report and review of the literature. *J. Neural Transm.* **2014**, *121*, 1303. [CrossRef] [PubMed]
46. Kobayashi, K.; Katayama, Y.; Oshima, H.; Watanabe, M.; Sumi, K.; Obuchi, T.; Fukaya, C.; Yamamoto, T. Multitarget, dual-electrode deep brain stimulation of the thalamus and subthalamic area for treatment of Holmes' tremor. *J. Neurosurg.* **2014**, *120*, 1025–1032. [CrossRef] [PubMed]
47. Laxpati, N.G.; Kasoff, S.F.; Gross, R.E. Deep brain stimulation for the treatment of epilepsy: Circuits, targets, and trials. *Neurotherapeutics* **2014**, *11*, 508–526. [CrossRef] [PubMed]
48. Viswanathan, A.; Jimenez-Shahed, J.; Baizabal Carvallo, J.F.; Jankovic, J. Deep brain stimulation for Tourette syndrome: Target selection. *Stereotact. Funct. Neurosurg.* **2012**, *90*, 213–224. [CrossRef] [PubMed]
49. Lemaire, J.J.; Sontheimer, A.; Nezzar, H.; Pontier, B.; Luauté, J.; Roche, B.; Gillart, T.; Gabrillargues, J.; Rosenberg, S.; Sarret, C.; et al. Electrical modulation of neuronal networks in brain-injured patients with disorders of consciousness: A systematic review. *Ann. Fr Anesth. Reanim.* **2014**, *2*, 88–97. [CrossRef] [PubMed]

brain sciences

MDPI

Review

Surgical Neurostimulation for Spinal Cord Injury

Aswin Chari [1,2], Ian D. Hentall [3], Marios C. Papadopoulos [1] and Erlick A. C. Pereira [1,*]

1 Academic Neurosurgery Unit, St George's, University of London, London SW17 0RE, UK; aswinchari@gmail.com (A.C.); eacp@eacp.co.uk (E.A.C.P.)
2 Division of Brain Sciences, Faculty of Medicine, Imperial College London, London W6 8RF, UK
3 The Miami Project to Cure Paralysis and Department of Neurological Surgery, Miller School of Medicine, University of Miami, Miami, FL 33101, USA; ihentall@med.miami.edu
* Correspondence: eacp@eacp.co.uk; Tel.: +44-208-725-4173

Academic Editors: Tipu Aziz and Alex Green
Received: 21 December 2016; Accepted: 2 February 2017; Published: 10 February 2017

Abstract: Traumatic spinal cord injury (SCI) is a devastating neurological condition characterized by a constellation of symptoms including paralysis, paraesthesia, pain, cardiovascular, bladder, bowel and sexual dysfunction. Current treatment for SCI involves acute resuscitation, aggressive rehabilitation and symptomatic treatment for complications. Despite the progress in scientific understanding, regenerative therapies are lacking. In this review, we outline the current state and future potential of invasive and non-invasive neuromodulation strategies including deep brain stimulation (DBS), spinal cord stimulation (SCS), motor cortex stimulation (MCS), transcutaneous direct current stimulation (tDCS) and repetitive transcranial magnetic stimulation (rTMS) in the context of SCI. We consider the ability of these therapies to address pain, sensorimotor symptoms and autonomic dysregulation associated with SCI. In addition to the potential to make important contributions to SCI treatment, neuromodulation has the added ability to contribute to our understanding of spinal cord neurobiology and the pathophysiology of SCI.

Keywords: spinal cord injury; spinal cord stimulation; deep brain stimulation; neuromodulation

1. Introduction

Traumatic spinal cord injury (SCI) is a devastating neurological disorder with a reported incidence in various countries and regions ranging from 10 to 80 million per population per year [1–3]. It is most commonly caused by road traffic accidents, falls, violence and sports injuries. The incidence and distribution of causes, and long-term survival rates, vary significantly across the globe, depending upon a wide range of complex social and economic factors [1,3,4]. It has a 2.5–5 fold higher incidence in males, with a peak in young adults (age 20–30) [1].

SCI is characterized by a constellation of symptoms including paralysis, paraesthesia, pain, cardiovascular, bladder, bowel and sexual dysfunction. The level of physical disability depends on the severity of the injury and the level of injury. The severity of the injury is commonly assessed by the International Standards for Neurological Classification of Spinal Cord Injury (ISCNSCI) developed by the American Spinal Injury Association (ASIA). This can be classified into different grades on the ASIA impairment scale (Table 1). Epidemiological studies suggest that more injuries occur at the cervical levels than thoracic levels, although the exact distribution varies based on the geographic location of the studies [1]. SCI has been shown to cause significant autonomic dysfunction, with neurogenic shock one of the leading causes of death [5].

Arguably at least as important as the physical and physiological disability caused by SCI are its psychological and economic impacts. SCI predominantly affects a young adult population and the psychological impact of rendering an independent, healthy individual paraplegic or tetraplegic

without bladder, bowel or sexual function can be devastating. In addition to the costs associated with medical care in SCI patients, there is an immense secondary economic burden associated with individuals incapacitated for most of their prospective career and the subsequent impact upon their families. One study estimated the lifetime economic burden of 1.5 million 2011 Canadian dollars per tetraplegic individual [6].

Table 1. The American Spinal Injury Association (ASIA) Impairment Scale.

ASIA Impairment Scale	Definition	Explanation
A	Complete	No motor or sensory function is preserved in the sacral segments S4–S5.
B	Incomplete	Sensory but not motor function is preserved below the neurological level and includes the sacral segments S4–S5.
C	Incomplete	Motor function is preserved below the neurological level, and more than half of the key muscles below the neurological level have a muscle grade less than 3.
D	Incomplete	Motor function is preserved below the neurological level, and more than half of the key muscles below the neurological level have a muscle grade of 3 or more.
E	Normal	Motor and sensory function are normal.

In this review, we briefly outline the current management of acute and chronic SCI and focus on the potential of neuromodulation strategies in its treatment. In particular, we review the available clinical evidence for strategies such as deep brain stimulation (DBS), spinal cord stimulation (SCS), motor cortex stimulation (MCS), transcutaneous direct current stimulation (tDCS) and repetitive transcranial magnetic stimulation (rTMS) in affecting pain, sensorimotor symptoms and autonomic dysregulation, all of which are important sequelae in SCI.

2. Current Management of Acute Spinal Cord Injury

The mainstay of current management of acute spinal cord injury involves acute resuscitation and the prevention of secondary injury to the spinal cord. Acute resuscitation follows Advanced Trauma Life Support principles with particular importance to the airway and breathing in high cervical injuries that can impair diaphragmatic function, along with early spinal immobilisation. Circulatory resuscitation is also of paramount importance due to the phenomenon of neurogenic shock, which can cause profound bradycardia, hypotension and vasodilatation due to the loss of sympathetic tone. Standard first procedures include acute stabilisation, clinical assessment (ASIA score) and computerised tomography and magnetic resonance imaging (CT and MRI). Secondary injury to the spinal cord may be prevented by maintaining adequate perfusion to the cord [7,8] and early decompressive surgery [9–11]. There is also a growing body of evidence supporting intra-spinal cord pressure monitoring and expansion duraplasty for refractory intra-spinal hypertension, drawing parallels from intracranial pressure monitoring paradigms in traumatic brain injury [12–15].

There are currently no generally approved medical therapies to improve outcomes in acute SCI [8], although a number of major trials are ongoing. Riluzole, a blocker of voltage-gated sodium channels, has shown promise in improving motor function following cervical injury and is currently the subject of a phase III randomised controlled trial [16–18]. A substance of long-term interest has been the voltage-gated potassium channel blocker 4-aminopyridine [19], but this has given mostly disappointing results in acute and chronic human trials examining motor improvement [20–22]. Likewise, steroid treatment (methyl-prednisolone), which some practitioners viewed favourably in the previous two decades, now appears to offer little benefit and non-negligible risk [8,23]. Induced hypothermia remains a moderately promising therapy for acute SCI [24]. This was

explored over many decades to treat early traumatic brain injury, although with variable results. Unfortunately, its critical dependence on both the timing of cooling post-injury and the level of temperature drop appear to be largely responsible for its variable efficacy in central nervous system (CNS) neurotrauma [25,26]. Hypothermia is a typical acute sequela of spinal cord trauma, and is proposed to be an input to brainstem centers controlling repair, as described below.

Subsequent management involves a combination of intense rehabilitation to optimise functional outcomes and medical therapies, designed either to prevent complications, such as venous thromboembolic events, infections associated with indwelling catheters and pressure ulcers and osteoporosis or to treat specific symptoms such as neuropathic pain.

3. Current Management of Chronic Spinal Cord Injury

Despite the advances of modern molecular and cellular science, there has been little clinical progress in regenerative and restorative therapies for chronic SCI. In vitro and in vivo models have often looked promising, but no disease modifying therapies have been successfully translated to humans [27]. Following SCI, structurally damaged axons are unable to regenerate due to a combination of a glial inhibitory environment and a fundamental lack of neuronal intrinsic regeneration potential. These factors contribute to persisting functional neurological impairment. A number of promising restorative and regenerative therapies, including the delivery of olfactory ensheathing cells to act as a scaffold [28,29], chondroitinase therapy to limit the glial scar [30] and taxol therapy to promote microtubule stabilization [31], have sought to target these mechanisms, with limited clinical success [27].

The various proposals for using CNS stimulation in SCI and other neurotrauma are in part prompted by the apparent obstacles to other approaches. Electrical stimulation of a discrete anatomical pathway elicits a natural response that can be helpful, whereas the ultimate benefits of administering a mixture of slow-acting, powerful drugs with an array of adverse effects and issues of receptor specificity, timing of actions, dosing regimen, tolerance and spatial targeting remain unclear. Neurotrophic substances of potential interest additionally run the risk of uncontrolled deleterious axonal sprouting [32]. The testing of restorative pharmacotherapies to satisfy scientific standards and regulatory demands can also present major difficulties. Cell transplantation may be free of some of these problems, but safe functional integration of exogenous cells within solid tissue is also a formidable task, and there is the potential for tumor formation with some cell types [33,34]. The routine clinical use of cell transplantation therefore seems to be well beyond the immediate horizon.

4. The Potential Roles for Neurostimulation in SCI

The indications for functional neurosurgery, including deep brain stimulation (DBS), cerebral cortical stimulation and spinal cord stimulation (SCS), have expanded drastically over the last decade and now encompass a whole host of neurological disorders including movement disorders, psychological and psychiatric disorders, pain (including neuropathic pain and primary headache disorders), epilepsy, disorders of consciousness and cognitive disorders [35,36].

In the context of SCI, functional procedures have the potential to impact upon a number of different domains, including pain, functional motor/sensory recovery, bladder/bowel function and cardiovascular autonomic dysregulation. Many of these have been highlighted as important symptoms to address in large surveys of SCI patients [37,38].

There are three broad strategies for chronic SCI: (i) using technology to restore function without restoring neural architecture; (ii) taking advantage of plasticity to harness residual circuitry; and (iii) encouraging active regeneration of injured neurons. These are depicted in Figure 1.

The first strategy involves suppressing or inducing immediate effects. Pain suppression is an obvious example, and the most clinically developed (see next section). Less obviously, one can try to evoke or improve some specific movements that have been lost. For example, to facilitate locomotor movements in incompletely injured individuals, the mesencephalic locomotor region can

be stimulated, thus overcoming weakness in the spinal central pattern generator [39]. This positive approach requires in practice some integration with patient input or feedback so that it is turned on only when safe and needed. A more complex way to provide control signals to stimulators is by brain-machine interfaces tapping neuronal firing in neocortex that represents motor commands [40]. This has been successfully implemented via wireless control connecting cortical microelectrodes to lumbar epidural stimulators in monkeys [41]. However, a key obstacle that must be understood and overcome is the so-called "foreign body response" that reduces the efficacy of implants over time [42].

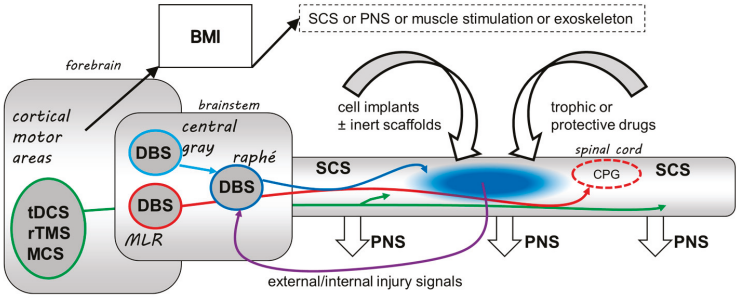

Figure 1. Diagram of possible sites for therapeutic electrical stimulation and other common interventions in spinal cord injury (SCI). Deep brain stimulation (DBS) of a brainstem restorative feedback loop is proposed to augment restorative effects around the injury site. This treatment resembles cell implantation or drug treatments in that it aims for non-specific recovery of visceral and sensory-motor deficits. Most forms of stimulation are concerned with narrowly specified functions. Thus DBS in brainstem central grey may also be used to block neuropathic pain. The nearby mesencephalic locomotor region (MLR) can be stimulated to activate descending pathways that boost the locomotor central pattern generator (CPG) in lower thoracic and upper lumbar segments. Cortical stimulation activating corticospinal tracts, whether non-invasively via transcutaneous direct current stimulation (tDCS) or repetitive transcranial magnetic stimulation (rTMS), or invasively with direct motor cortex stimulation (MCS), can be used for immediate production of movement or to induce adaptive plastic changes in motor output. Cortical commands may also be fed to a brain-machine interface (BMI) to control variously situated electrodes for peripheral nerve stimulation (PNS) or spinal cord stimulation (SCS). SCS distal to the injury has been used for bladder control; proximal SCS can be used block pain; and stimulation at any spinal location can be used to generate movements, depending on the degree of completeness of functional loss. The simplicity and comprehensiveness of restorative DBS in the brainstem are points in its favour.

The second strategy focuses on stimulation of pathways assumed to possess considerable neuroplasticity in their normal functioning, pre-eminently the cortico-spinal tract [43]. This propensity for axonal growth and sprouting can perhaps be exploited by the application of stimulation, but it is unclear how exactly to use this to shape a valid, adaptive repair.

A final strategy that has met with some preclinical success assumes that certain brain regions are specifically adapted as centres for repairing recent mild neurotrauma [44–47]. Thus the serotonergic raphe nuclei of the brainstem release a cocktail of trophic substances from their ubiquitous axon terminals in response to injury-correlated sensory or chemical stimuli (e.g., nociception, unconsciousness, hypothermia, circulating cytokines). Stimulation of this feedback loop, or the regions that feed into it, such as the midbrain periaqueductal grey (PAG), have been shown to enhance early histological and sensory-motor recovery in rats with incomplete thoracic SCI [35–37]. A potential advantage of these brain centres is that they are non-eloquent, that is, the applied stimulus intensities evoked no observable motor responses or arousal changes, facilitating continuous long-term stimulation.

5. Neurostimulation for Pain Following SCI

Pain is defined by the International Association for the Study of Pain (IASP) as "an unpleasant sensory and emotional experience associated with actual or potential tissue damage, or described in terms of such damage" [48]. In the context of SCI, pain is common, affecting over 70% of SCI patients, and can be categorised as neuropathic or nociceptive (musculoskeletal) in origin, affecting 34% and 64% of long-term survivors respectively [49–55]. Pain following SCI is thought to occur due a combination of abnormal inputs from the injured spinal cord and aberrant reorganisation of cortical circuitry [56,57] and has been shown to be more common at one year following injury than immediately after [55]. The multifactorial aetiology of SCI-related pain makes it notoriously difficult to treat, especially with traditional pharmacotherapy [58,59] and the IASP's Neuropathic Pain Special Interest Group is unable to currently recommend any interventional strategies for the management of SCI-related pain [60].

The use of neurostimulation to treat pain was reported as early as 1960 [61], predating the Melzack & Wall gate theory [62]. Current indications of neurostimulation for pain include pain from failed back surgery syndrome (FBSS), neuropathic pain secondary to peripheral nerve injury (e.g., amputation, brachial plexus injury), facial pain and headache disorders [63,64]. Interventions can target any part of an impaired nociceptive pathway, including at the level of the spinal cord, deep brain nuclei or motor cortex [65,66].

Evidence for the efficacy of DBS in the context of SCI-related pain is limited to a few patients that form part of small series which have had varying results [63,64,67–73]. The main sites targeted have been ventralis posterior lateralis (VPL) nucleus of the thalamus and the midbrain central gray, comprising the periaqueductal grey (PAG) and periventricular grey (PVG). A systematic review by Previnaire in 2009 recorded 19 cases of the successful implantation of DBS electrodes in SCI patients following trial stimulation in 36 patients to the VPL ± central gray. Only three (16%) of these cases reported "long-term success" [69]. DBS of VPL may also have a role in the management of phantom sensations and pain following SCI [74]. More recently, DBS electrodes in the central gray in two SCI patients were optimised to provide best analgesia; this study found that very low frequency stimulation (effectively <0.67 Hz) was most effective in these two patients; added benefits included a reduction in side effects and a long battery life and the authors emphasized the importance of allowing time (hours to days) before assessing the efficacy of new stimulation parameters [75]. Improving knowledge of the somatotopic organisation of the PAG may aid optimal electrode targeting, and given the bilateral pain often experienced by SCI patients, it is likely that most SCI patients will need bilateral electrodes [76,77]. Based on evidence of the success on cingulotomy for cancer related pain, Spooner et al. reported a single case of effective analgesia in SCI following DBS to the rostral anterior cingulate cortex, although this patient was only followed up for four months [78]. A subsequent case series of patients treated with anterior cingulate cortex DBS for chronic pain of various aetiologies (including 1 with SCI) illustrates its potential for long-term control [79]. Over the years, the lack of randomised controlled clinical trial evidence has led to a decrease in the number of studies reporting on DBS for pain [57] and this has been confounded by the US Food and Drug Administration giving DBS for pain "off label" status [80], so that the International Neuromodulation Society still views intracranial modulation for pain as "investigational" [81].

Another option for SCI-related pain is epidural motor cortex stimulation (MCS), although the limited reports in the literature suggest that SCI-related pain responds poorly to MCS compared with other pain syndromes [68,82]. However, the systematic review by Previnaire concluded that MCS may be more effective than DBS in the context of SCI, providing "long-term success" in four out of seven patients [69].

SCS has been used to treat a variety of pain syndromes for over 40 years and the first reports of its use for spinal cord injury date back to 1972 [83]. It is based upon the Melzack and Wall gate theory that stimulation of the large dorsal column fibres will inhibit some of the activity produced by smaller myelinated and unmyelinated fibres in the dorsal horn [62]. Nashold's series of 30 patients includes five with traumatic SCI (three from spinal fractures, one with a gunshot wound and one with a cord contusion), none of whom had an "excellent" response to the treatment [83]. Since then, reports of

the utility of SCS for SCI-related pain have been limited and suggest poorer responses in SCI patients compared to other indications such as failed back surgery and peripheral neuropathy pain [84–86]. This may be explained by injury to the neural circuits underlying its efficacy but we are still far from understanding the mechanisms underlying the efficacy and failure of SCS, especially in the context of SCI. Newer modalities of SCS such as burst and high frequency stimulation are yet to be evaluated in their efficacy for chronic pain after SCI.

Non-invasive neuromodulatory strategies include repetitive transcranial magnetic stimulation (rTMS) and transcranial direct current stimulation (tDCS), both of which are purported to work on the basis of altering maladaptive plasticity within pain circuits, affecting nuclei in the thalamus and subthalamic regions [59,87,88]. A recent systematic review identified six studies assessing 127 patients with neuropathic pain treated with rTMS following SCI. It concluded that although there was some reduction in pain indices following rTMS, this did not reach statistical significance [89]. There are many unresolved controversies within the field of rTMS including the location (motor cortex versus premotor cortex/dorsolateral prefrontal cortex), type and orientation of coil, schedule of repetitive stimulation and persistence of therapeutic response [90–93]. However, given the non-invasive nature of rTMS, it could prove a useful tool both in terms of mechanistic understanding and therapeutic benefit for pain following SCI. It may have a role in predicting responsiveness to MCS and the ability to influence phantom sensations after SCI, which could provide significant functional benefits for these patients [94,95]. tDCS is less well characterised, and differs from rTMS in that it does not result in neuronal firing but changes the resting membrane potential, thereby altering neuronal excitability. It has long-term effects that are thought to be caused by altered neurotransmitter systems [96]. The largest clinical study to date utilised the anode over the primary motor cortex and showed a reduction in pain VAS scores in 16 patients following SCI. The tDCS was found to alter metabolism in the subgenual anterior cingulate cortex, left dorsolateral prefrontal cortex and insula, suggesting an effect of tDCS on the emotional and cognitive components of pain [97]. The evidence in support of tDCS has led to it being included as part of third-line therapies for neuropathic pain for SCI in the CanPain guidelines; it is the only neuromodulatory strategy to be included in the guidelines [98].

The future of neurostimulation for pain in SCI lies in improving the level of evidence for each intervention and identifying subsets of patients and types of pain that benefit from specific interventions. Presently, DBS for various types of pain can yield a range of effects in different patients from dramatic and highly pleasing success to disheartening failure, and the factors leading to these variable outcomes are entirely unclear, although there are some weak statistical predictors [77]. This task will no doubt be aided by homogenisation of the measurement of pre-intervention and post-intervention data sets, such as the International Spinal Cord Injury Pain Basic and Extended Data Sets [99,100]. In addition to the rigorous assessment of outcomes, surgical complications must also be taken into consideration; studies have highlighted the burden of complications associated with implanted stimulators, which can impact upon quality of life and overall outcomes [69].

6. Neurostimulation for Sensorimotor Recovery Following SCI

There is little in the way of clinical evidence for the efficacy of neuromodulation for locomotor and sensory recovery following spinal cord injury. Perhaps the best evidence for efficacy of DBS in animal models comes from two landmark studies, showing the efficacy of DBS in improving gait in cord injured rats. The two studies used different targets, the mesencephalic locomotor region (MLR) and the nucleus raphe magnus and the PAG [39,47], and deliver improvement in different time frames (immediate or long-term). The correlates of this circuitry in humans need to be better understood, especially since the efficacy of stimulation for motor responses depends on the number of residual fibres within the injured cord [101].

Similar rodent and mammalian evidence also exists for SCS, which has been improved by the use of closed-loop feedback systems to refine stimulation parameters and improve gait [102–104]. The putative role for SCS can also be extrapolated from studies observing motor benefit in patients

and animals with Parkinson's disease [105,106] and multiple sclerosis [107,108] undergoing SCS. There is preliminary human evidence to suggest that epidural SCS may be efficacious in producing electrophysiological improvements in patients with SCI [109–111]. Further work is necessary to translate these electrophysiological improvements into functional benefits. Developing a better understanding of the pattern generator for human gait may also indicate a use for lumbosacral epidural stimulation, obviating the need for supraspinal inputs [112]. This concept of using stimulation to replace lost supraspinal input has recently been demonstrated in a primate model, which relies on real-time input of cortical signals to optimise lumbar epidural stimulation [41,113]. However, this model is limited by the lack of a sensory feedback system, which would further optimise motor functional recovery.

Animal evidence also exists for the utility of combined MCS and spinal tDCS in promoting motor recovery after pyramidotomy, suggesting that stimulation proximal and distal to the injury could facilitate the improvement in function following SCI [114]. TMS may also have a role in motor recovery, as it has been shown to elicit EMG responses below the level of injury in individuals with motor-complete SCI; it may therefore have a role in identifying individuals who may benefit from neuromodulatory therapies or have a therapeutic role in its own right [115,116].

7. Neurostimulation for Autonomic Recovery Following SCI

Autonomic functions, including bladder, bowel and sexual function, have consistently been highlighted as priorities for recovery in patients with SCI [37,38]. In the acute phase, bladder dysfunction often manifests as a "flaccid paralysis" resulting in urinary retention requiring catheterisation. In the chronic phase, this progresses into detrusor hyperreflexia and detrusor-sphincter dyssynergia resulting in incontinence and incomplete voiding; the mainstay of current treatment is intravesical botulinum toxin injection which requires repeated treatments every few months and does not address the dyssynergia [117,118]. Sexual dysfunction can manifest in a number of different ways in males and females, depending upon the level and completeness of the injury [117]. In addition to the physical impact, sexual dysfunction in particular may impact psychological wellbeing and overall quality of life [119,120]. Gastrointestinal disturbances in SCI are common (>60%) and wide-ranging, including delayed gastric emptying, abnormal colonic myoenteric activity and sphincter/defecation dysfunction [117,121,122]. The lower GI disturbances are consistent with a "spastic" paresis of the bowel. The increased colonic muscle tone, abnormal rectal compliance and tight external sphincters require laxatives and digital reflex stimulation to promote bowel emptying [117,123].

Cardiovascular autonomic dysfunction is a major problem in SCI, and contributes to the excess cardiovascular mortality in SCI [124]. In the acute phase, the loss of sympathetic outflow can lead to devastating hypotension, hypothermia and dysrhythmias [125]. In the chronic phase, especially after cervical or high thoracic injuries, disturbances such as orthostatic hypotension and autonomic dysreflexia (sudden drastic episodes of elevated blood pressure and bradycardia) have been shown to be common in SCI patients, which may contribute to the increased cardiovascular disease risk and also affect other aspects of recovery such as rehabilitation and cognitive function [5,125–128]. SCI can also lead to thermoregulatory dysfunction.

Although there is little in the way of evidence for autonomic manipulation in the context of SCI, evidence from other conditions indicate that neuromodulation strategies may have a role [129]. There is evidence that DBS can affect urinary symptoms and control in Parkinson's disease, dystonia, essential tremor and chronic pain [130–133]. These studies show a predominant effect on lower urinary tract symptoms and mechanistic studies have shown that this might be due to enhanced processing of bladder information following subthalamic nucleus DBS. In the context of SCI, this could prove beneficial in patients with incomplete SCI, where enhancement of residual sensory inputs could improve continence. In one study where patients had PAG stimulators for chronic pain, the maximum cystometric capacity increased during saline infusion into the bladder when the stimulators were switched on, indicating a switch to the "filling" state over the "voiding" state [134]. However, a deeper

understanding of the subcortical networks involved in urinary continence in health and how they are disturbed in SCI are required. A single patient has also been reported in the literature to have improved bowel symptoms following subthalamic nucleus DBS for Parkinson's, which may provide benefit via a similar mechanism [135].

DBS has also been shown to affect blood pressure with dorsal central gray stimulation resulting in an increase in blood pressure and ventral central gray stimulation resulting in a decrease in blood pressure [136–141]. There are therefore potential avenues to treat both the orthostatic hyptension and autonomic dysreflexia seen in SCI patients. Ventral versus dorsal DBS in the central gay has also been shown to alter different frequency components of heart rate variability, suggesting differential contributions of parasympathetic and sympathetic nervous systems to its mechanisms of action [142].

A number of other neuromodulatory strategies have also been reported for autonomic recovery, specifically for bladder, bowel and sexual function [118]. Although the sacral anterior root stimulator (Brindley device) has been shown to be successful at overcoming detrusor-sphincter dyssynergia and achieving and sustaining continence in 88% of 500 patients at a mean of four years follow-up [143], the negative impacts of deafferentation of the posterior nerve roots on bladder, bowel and sexual function has seen its use decline [118]. More recent evidence of using the same device for anterior and posterior root stimulation has shown promise [144,145]. Sievert and colleagues present compelling data that early (median 2.9 months following injury) insertion of sacral nerve modulators into the S3 nerve roots can improve urinary continence, bowel function and even help achieve erection in patients with complete SCI [144].

8. The Future of Neurostimulation in SCI

The plethora of applications for neuromodulation in SCI provides promise in a field currently devoid of disease-modifying therapies. The physiological, psychological and economic benefits associated with addressing issues such as pain, mobility and autonomic symptoms in SCI patients is large. Given the current dearth of treatment options, neuromodulation is an attractive emerging option. However, there are a number of outstanding questions that first need to be answered.

Apart from the need to identify evidence-based indications for deep brain, motor cortex and spinal cord stimulation and the non-invasive strategies in the context of SCI, we also need a more nuanced understanding of the patient, injury and treatment factors that influence success. Specifically, the timing of interventions seems a crucial variable. The interventions for pain have thus far been performed many months to years after the injury once aberrant circuitry has become established and it remains to be explored whether more acute interventions could be more beneficial at preventing the development of maladapted circuits or promote regeneration [146]. Another key variable are the stimulation parameters. As recent studies have shown, parameters that are vastly different to what is commonly used may be more beneficial [75] and optimisation of parameters may be aided by closed-loop feedback systems, as has been tentatively shown in Parkinson's disease [147,148].

The potential, in particular, of PAG DBS for addressing multiple symptoms is intriguing. The animal and human evidence presented earlier in this review have illustrated the potential to address pain, autonomic features and facilitate motor recovery in SCI. The fact that PAG is already a target in human DBS for pain makes it an ideal candidate for further investigation to target the disabling triad of pain, autonomic dysreflexia (both cardiovascular and sphincteric) and paralysis.

Mechanistic insight studies, both in humans and animals, will also aid progress in the field. In particular, human electrophysiological and imaging studies in spinal cord injury both before and after neurostimulator implantation will allow us to develop a better understanding the biological processes underlying symptomatic improvement. For example, despite the use of DBS in the central gray for pain, the mechanism of action remains unclear [149]. Theories implicating endorphins and opioid pathways have since been disproven [150–152]. More recent evidence has shown that DBS and SCS may modulate gene expression [153,154]. An understanding of these modifications may provide

insight into the failure of CNS regeneration following injury. However, as with other SCI studies, translation of mechanistic understanding in animals to humans must be approached with caution [27].

Technological advances will also be of direct relevance to this field. Smaller nanodevices for stimulation may improve the specificity and reduce the side-effect profile. Such devices have also been reported to promote axonal regeneration in the cord [155] and may allow access to previously inaccessible nuclei, such as the nucleus raphe magnus that has been shown to improve gait in rats [47]. Crucial to providing conclusive evidence of efficacy is well designed clinical trials with relevant outcome measures that are able to be consistently replicated. Much is to be learnt from the failure of medical therapies such as steroids [156]. Trials in SCI will never be able to recruit large numbers, which places added importance on trial design. An abundance of prognostic factors (ASIA score on admission, age, level of injury, rehabilitation) increases heterogeneity in SCI trials. Adaptive trial designs or n-of-1 trials [157] may be important in the context of neuromodulation, as will be improving our understanding of factors influencing outcome in SCI patients. Using established frameworks such as the IDEAL recommendations and using homogenised core outcome sets will be important to systematic evaluation of these new technologies [158,159].

Despite the potential of neuromodulation strategies, the limitations must also be taken into consideration. All implants and surgical procedures are associated complications such as the foreign body response that reduces efficacy over time [42]. Specifically, the risks of functional compromise associated with damage to residual neural structures in SCI patients may be higher than in other disorders.

9. Conclusions

Despite the current paucity of clinical evidence for efficacy, functional neurosurgery has the potential to make contributions to the treatment of SCI. It can immediately relieve some of the many visceral and sensory-motor deficits and has the potential to effectuate some useful degree of reversal of the underlying neurodegeneration, albeit partially, by exploiting the capacity of electrical activity to increase sprouting or induce other plastic changes in neural pathways, such as maturation and integration of endogenous neural progenitor cells.

Acknowledgments: Support to IDH was provided by the United States Department of Defense Spinal Cord Injury Research Program award W81XWH-12-1-0559.

Author Contributions: A.C. wrote the manuscript under supervision of E.P.; I.R., M.P. and E.P. edited the paper. I.R. created figure 1.

Conflicts of Interest: The authors declare no conflict of interest.

References

1. Singh, A.; Tetreault, L.; Kalsi-Ryan, S.; Nouri, A.; Fehlings, M.G. Global prevalence and incidence of traumatic spinal cord injury. *Clin. Epidemiol.* **2014**, *6*, 309–331. [PubMed]
2. Jazayeri, S.B.; Beygi, S.; Shokraneh, F.; Hagen, E.M.; Rahimi-Movaghar, V. Incidence of traumatic spinal cord injury worldwide: A systematic review. *Eur. Spine J.* **2015**, *24*, 905–918. [CrossRef] [PubMed]
3. Rahimi-Movaghar, V.; Sayyah, M.K.; Akbari, H.; Khorramirouz, R.; Rasouli, M.R.; Moradi-Lakeh, M.; Shokraneh, F.; Vaccaro, A.R. Epidemiology of traumatic spinal cord injury in developing countries: A systematic review. *Neuroepidemiology* **2013**, *41*, 65–85. [CrossRef] [PubMed]
4. Cripps, R.A.; Lee, B.B.; Wing, P.; Weerts, E.; Mackay, J.; Brown, D. A global map for traumatic spinal cord injury epidemiology: Towards a living data repository for injury prevention. *Spinal Cord* **2011**, *49*, 493–501. [CrossRef] [PubMed]
5. Phillips, A.A.; Krassioukov, A.V. contemporary cardiovascular concerns after spinal cord injury: Mechanisms, maladaptations, and management. *J. Neurotrauma* **2015**, *32*, 1927–1942. [CrossRef] [PubMed]
6. Krueger, H.; Noonan, V.K.; Trenaman, L.M.; Joshi, P.; Rivers, C.S. The economic burden of traumatic spinal cord injury in Canada. *Chronic Dis. Inj. Can.* **2013**, *33*, 113–122. [PubMed]

7. Hawryluk, G.; Whetstone, W.; Saigal, R.; Ferguson, A.; Talbott, J.; Bresnahan, J.; Dhall, S.; Pan, J.; Beattie, M.; Manley, G. Mean arterial blood pressure correlates with neurological recovery after human spinal cord injury: Analysis of high frequency physiologic data. *J. Neurotrauma* **2015**, *32*, 1958–1967. [CrossRef] [PubMed]
8. Walters, B.C.; Hadley, M.N.; Hurlbert, R.J.; Aarabi, B.; Dhall, S.S.; Gelb, D.E.; Harrigan, M.R.; Rozelle, C.J.; Ryken, T.C.; Theodore, N. Guidelines for the management of acute cervical spine and spinal cord injuries: 2013 update. *Neurosurgery* **2013**, *60*, 82–91. [CrossRef] [PubMed]
9. Anderson, K.K.; Tetreault, L.; Shamji, M.F.; Singh, A.; Vukas, R.R.; Harrop, J.S.; Fehlings, M.G.; Vaccaro, A.R.; Hilibrand, A.S.; Arnold, P.M. Optimal timing of surgical decompression for acute traumatic central cord syndrome: A systematic review of the literature. *Neurosurgery* **2015**, *77*, S15–S32. [CrossRef] [PubMed]
10. Fehlings, M.G.; Vaccaro, A.; Wilson, J.R.; Singh, A.; David, W.C.; Harrop, J.S.; Aarabi, B.; Shaffrey, C.; Dvorak, M.; Fisher, C.; et al. Early versus delayed decompression for traumatic cervical spinal cord injury: Results of the Surgical Timing in Acute Spinal Cord Injury Study (STASCIS). *PLoS ONE* **2012**, *7*, e32037. [CrossRef] [PubMed]
11. Liu, J.M.; Long, X.H.; Zhou, Y.; Peng, H.W.; Liu, Z.L.; Huang, S.H. Is Urgent decompression superior to delayed surgery for traumatic spinal cord injury? A meta-analysis. *World Neurosurg.* **2016**, *87*, 124–131. [CrossRef] [PubMed]
12. Phang, I.; Papadopoulos, M.C. Intraspinal pressure monitoring in a patient with spinal cord injury reveals different intradural compartments: Injured Spinal Cord Pressure Evaluation (ISCoPE) study. *Neurocrit. Care* **2015**, *23*, 414–418. [CrossRef] [PubMed]
13. Saadoun, S.; Chen, S.; Papadopoulos, M.C. Intraspinal pressure and spinal cord perfusion pressure predict neurological outcome after traumatic spinal cord injury. *J. Neurol. Neurosurg. Psychiatry* **2016**. [CrossRef] [PubMed]
14. Werndle, M.C.; Saadoun, S.; Phang, I.; Czosnyka, M.; Varsos, G.; Czosnyka, Z.; Smielewski, P.; Jamous, A.; Bell, B.A.; Zoumprouli, A.; et al. Measurement of intraspinal pressure after spinal cord injury: technical note from the injured spinal cord pressure evaluation study. *Acta Neurochir. Suppl.* **2016**, *122*, 323–328. [PubMed]
15. Werndle, M.C.; Saadoun, S.; Phang, I.; Czosnyka, M.; Varsos, G.V.; Czosnyka, Z.H.; Smielewski, P.; Jamous, A.; Bell, B.A.; Zoumprouli, A.; et al. Monitoring of spinal cord perfusion pressure in acute spinal cord injury: Initial findings of the injured spinal cord pressure evaluation study. *Crit. Care Med.* **2014**, *42*, 646–655. [CrossRef] [PubMed]
16. Fehlings, M.G.; Kopjar, B.; Grossman, R.G. 329 efficacy and safety of riluzole in acute spinal cord injury: Rationale and design of aospine phase III multicenter double-blinded Randomized Controlled Trial (RISCIS). *Neurosurgery* **2016**, *63*, 196. [CrossRef] [PubMed]
17. Fehlings, M.G.; Nakashima, H.; Nagoshi, N.; Chow, D.S.; Grossman, R.G.; Kopjar, B. Rationale, design and critical end points for the Riluzole in Acute Spinal Cord Injury Study (RISCIS): A randomized, double-blinded, placebo-controlled parallel multi-center trial. *Spinal Cord* **2016**, *54*, 8–15. [CrossRef] [PubMed]
18. Grossman, R.G.; Fehlings, M.G.; Frankowski, R.F.; Burau, K.D.; Chow, D.S.; Tator, C.; Teng, A.; Toups, E.G.; Harrop, J.S.; Aarabi, B.; et al. A prospective, multicenter, phase I matched-comparison group trial of safety, pharmacokinetics, and preliminary efficacy of riluzole in patients with traumatic spinal cord injury. *J. Neurotrauma* **2014**, *31*, 239–255. [CrossRef] [PubMed]
19. Waxman, S.G. Aminopyridines and the treatment of spinal cord injury. *J. Neurotrauma* **1993**, *10*, 19–24. [CrossRef] [PubMed]
20. Domingo, A.; Al-Yahya, A.A.; Asiri, Y.; Eng, J.J.; Lam, T. A systematic review of the effects of pharmacological agents on walking function in people with spinal cord injury. *J. Neurotrauma* **2012**, *29*, 865–879. [CrossRef] [PubMed]
21. DeForge, D.; Nymark, J.; Lemaire, E.; Gardner, S.; Hunt, M.; Martel, L.; Curran, D.; Barbeau, H. Effect of 4-aminopyridine on gait in ambulatory spinal cord injuries: A double-blind, placebo-controlled, crossover trial. *Spinal Cord* **2004**, *42*, 674–685. [CrossRef] [PubMed]
22. Haghighi, S.S.; Pugh, S.L.; Perez-Espejo, M.A.; Oro, J.J. Effect of 4-aminopyridine in acute spinal cord injury. *Surg. Neurol.* **1995**, *43*, 443–447. [CrossRef]
23. Hurlbert, R.J. Methylprednisolone for acute spinal cord injury: An inappropriate standard of care. *J. Neurosurg.* **2000**, *93*, 1–7. [CrossRef] [PubMed]

24. Levi, A.D.; Green, B.A.; Wang, M.Y.; Dietrich, W.D.; Brindle, T.; Vanni, S.; Casella, G.; Elhammady, G.; Jagid, J. Clinical application of modest hypothermia after spinal cord injury. *J. Neurotrauma* **2009**, *26*, 407–415. [CrossRef] [PubMed]
25. Madden, L.K.; DeVon, H.A. A systematic review of the effects of body temperature on outcome after adult traumatic brain injury. *J. Neurosci. Nurs.* **2015**, *47*, 190–203. [CrossRef] [PubMed]
26. Ahmed, A.I.; Bullock, M.R.; Dietrich, W.D. Hypothermia in traumatic brain injury. *Neurosurg. Clin. N. Am.* **2016**, *27*, 489–497. [CrossRef] [PubMed]
27. Ramer, L.M.; Ramer, M.S.; Bradbury, E.J. Restoring function after spinal cord injury: Towards clinical translation of experimental strategies. *Lancet Neurol.* **2014**, *13*, 1241–1256. [CrossRef]
28. Tabakow, P.; Jarmundowicz, W.; Czapiga, B.; Fortuna, W.; Miedzybrodzki, R.; Czyz, M.; Huber, J.; Szarek, D.; Okurowski, S.; Szewczyk, P.; et al. Transplantation of autologous olfactory ensheathing cells in complete human spinal cord injury. *Cell Transplant.* **2013**, *22*, 1591–1612. [CrossRef] [PubMed]
29. Tabakow, P.; Raisman, G.; Fortuna, W.; Czyz, M.; Huber, J.; Li, D.; Szewczyk, P.; Okurowski, S.; Miedzybrodzki, R.; Czapiga, B.; et al. Functional regeneration of supraspinal connections in a patient with transected spinal cord following transplantation of bulbar olfactory ensheathing cells with peripheral nerve bridging. *Cell Transplant.* **2014**, *23*, 1631–1655. [CrossRef] [PubMed]
30. Bradbury, E.J.; Moon, L.D.; Popat, R.J.; King, V.R.; Bennett, G.S.; Patel, P.N.; Fawcett, J.W.; McMahon, S.B. Chondroitinase ABC promotes functional recovery after spinal cord injury. *Nature* **2002**, *416*, 636–640. [CrossRef] [PubMed]
31. Popovich, P.G.; Tovar, C.A.; Lemeshow, S.; Yin, Q.; Jakeman, L.B. Independent evaluation of the anatomical and behavioral effects of Taxol in rat models of spinal cord injury. *Exp. Neurol.* **2014**, *261*, 97–108. [CrossRef] [PubMed]
32. Deumens, R.; Joosten, E.A.; Waxman, S.G.; Hains, B.C. Locomotor dysfunction and pain: The scylla and charybdis of fiber sprouting after spinal cord injury. *Mol. Neurobiol.* **2008**, *37*, 52–63. [CrossRef] [PubMed]
33. Dlouhy, B.J.; Awe, O.; Rao, R.C.; Kirby, P.A.; Hitchon, P.W. Autograft-derived spinal cord mass following olfactory mucosal cell transplantation in a spinal cord injury patient: Case report. *J. Neurosurg. Spine* **2014**, *21*, 618–622. [CrossRef] [PubMed]
34. Lee, A.S.; Tang, C.; Rao, M.S.; Weissman, I.L.; Wu, J.C. Tumorigenicity as a clinical hurdle for pluripotent stem cell therapies. *Nat. Med.* **2013**, *19*, 998–1004. [CrossRef] [PubMed]
35. Hariz, M.; Blomstedt, P.; Zrinzo, L. Future of brain stimulation: New targets, new indications, new technology. *Mov. Disord.* **2013**, *28*, 1784–1792. [CrossRef] [PubMed]
36. Pereira, E.A.; Green, A.L.; Nandi, D.; Aziz, T.Z. Deep brain stimulation: Indications and evidence. *Expert Rev. Med. Devices* **2007**, *4*, 591–603. [CrossRef] [PubMed]
37. Anderson, K.D. Targeting recovery: Priorities of the spinal cord-injured population. *J. Neurotrauma* **2004**, *21*, 1371–1383. [CrossRef] [PubMed]
38. Simpson, L.A.; Eng, J.J.; Hsieh, J.T.; Wolfe, D.L. The health and life priorities of individuals with spinal cord injury: A systematic review. *J. Neurotrauma* **2012**, *29*, 1548–1555. [CrossRef] [PubMed]
39. Bachmann, L.C.; Matis, A.; Lindau, N.T.; Felder, P.; Gullo, M.; Schwab, M.E. Deep brain stimulation of the midbrain locomotor region improves paretic hindlimb function after spinal cord injury in rats. *Sci. Transl. Med.* **2013**, *5*, 208ra146. [CrossRef] [PubMed]
40. Donati, A.R.; Shokur, S.; Morya, E.; Campos, D.S.; Moioli, R.C.; Gitti, C.M.; Augusto, P.B.; Tripodi, S.; Pires, C.G.; Pereira, G.A.; et al. Long-term training with a brain-machine interface-based gait protocol induces partial neurological recovery in paraplegic patients. *Sci. Rep.* **2016**, *6*, 30383. [CrossRef] [PubMed]
41. Capogrosso, M.; Milekovic, T.; Borton, D.; Wagner, F.; Moraud, E.M.; Mignardot, J.B.; Buse, N.; Gandar, J.; Barraud, Q.; Xing, D.; et al. A brain-spine interface alleviating gait deficits after spinal cord injury in primates. *Nature* **2016**, *539*, 284–288. [CrossRef] [PubMed]
42. Groothuis, J.; Ramsey, N.F.; Ramakers, G.M.; van der Plasse, G. Physiological challenges for intracortical electrodes. *Brain Stimul.* **2014**, *7*, 1–6. [CrossRef] [PubMed]
43. Jiang, Y.Q.; Zaaimi, B.; Martin, J.H. competition with primary sensory afferents drives remodeling of corticospinal axons in mature spinal motor circuits. *J. Neurosci.* **2016**, *36*, 193–203. [CrossRef] [PubMed]
44. Carballosa-Gonzalez, M.M.; Blaya, M.O.; Alonso, O.F.; Bramlett, H.M.; Hentall, I.D. Midbrain raphe stimulation improves behavioral and anatomical recovery from fluid-percussion brain injury. *J. Neurotrauma* **2013**, *30*, 119–130. [CrossRef] [PubMed]

45. Carballosa-Gonzalez, M.M.; Vitores, A.; Hentall, I.D. Hindbrain raphe stimulation boosts cyclic adenosine monophosphate and signaling proteins in the injured spinal cord. *Brain Res.* **2014**, *1543*, 165–172. [CrossRef] [PubMed]
46. Hentall, I.D.; Burns, S.B. Restorative effects of stimulating medullary raphe after spinal cord injury. *J. Rehabil. Res. Dev.* **2009**, *46*, 109–122. [CrossRef] [PubMed]
47. Hentall, I.D.; Gonzalez, M.M. Promotion of recovery from thoracic spinal cord contusion in rats by stimulation of medullary raphe or its midbrain input. *Neurorehabil. Neural Repair* **2012**, *26*, 374–384. [CrossRef] [PubMed]
48. International Association for the Study of Pain. IASP Taxonomy. 2012. Available online: http://www.iasp-pain.org/Taxonomy (accessed on 5 January 2017).
49. Bryce, T.N.; Biering-Sorensen, F.; Finnerup, N.B.; Cardenas, D.D.; Defrin, R.; Lundeberg, T.; Norrbrink, C.; Richards, J.S.; Siddall, P.; Stripling, T.; et al. International spinal cord injury pain classification: Part I. Background and description. March 6–7, 2009. *Spinal Cord* **2012**, *50*, 413–417. [CrossRef] [PubMed]
50. Bryce, T.N.; Biering-Sorensen, F.; Finnerup, N.B.; Cardenas, D.D.; Defrin, R.; Ivan, E.; Lundeberg, T.; Norrbrink, C.; Richards, J.S.; Siddall, P.; et al. International Spinal Cord Injury Pain (ISCIP) Classification: Part 2. Initial validation using vignettes. *Spinal Cord* **2012**, *50*, 404–412. [CrossRef] [PubMed]
51. Adriaansen, J.J.; Post, M.W.; de Groot, S.; van Asbeck, F.W.; Stolwijk-Swuste, J.M.; Tepper, M.; Lindeman, E. Secondary health conditions in persons with spinal cord injury: A longitudinal study from one to five years post-discharge. *J. Rehabil. Med.* **2013**, *45*, 1016–1022. [CrossRef] [PubMed]
52. Adriaansen, J.J.; van Asbeck, F.W.; Lindeman, E.; van der Woude, L.H.; de Groot, S.; Post, M.W. Secondary health conditions in persons with a spinal cord injury for at least 10 years: Design of a comprehensive long-term cross-sectional study. *Disabil. Rehabil.* **2013**, *35*, 1104–1110. [CrossRef] [PubMed]
53. Jorgensen, S.; Iwarsson, S.; Lexell, J. Secondary health conditions, activity limitations, and life satisfaction in older adults with long-term spinal cord injury. *PM&R* **2016**. [CrossRef]
54. Turner, J.A.; Cardenas, D.D.; Warms, C.A.; McClellan, C.B. Chronic pain associated with spinal cord injuries: A community survey. *Arch. Phys. Med. Rehabil.* **2001**, *82*, 501–509. [CrossRef] [PubMed]
55. Burke, D.; Fullen, B.M.; Stokes, D.; Lennon, O. Neuropathic pain prevalence following spinal cord injury: A systematic review and meta-analysis. *Eur. J. Pain* **2017**, *21*, 29–44. [CrossRef] [PubMed]
56. Nardone, R.; Holler, Y.; Brigo, F.; Seidl, M.; Christova, M.; Bergmann, J.; Golaszewski, S.; Trinka, E. Functional brain reorganization after spinal cord injury: Systematic review of animal and human studies. *Brain Res.* **2013**, *1504*, 58–73. [CrossRef] [PubMed]
57. Nardone, R.; Holler, Y.; Leis, S.; Holler, P.; Thon, N.; Thomschewski, A.; Golaszewski, S.; Brigo, F.; Trinka, E. Invasive and non-invasive brain stimulation for treatment of neuropathic pain in patients with spinal cord injury: A review. *J. Spinal Cord Med.* **2014**, *37*, 19–31. [CrossRef] [PubMed]
58. Saulino, M.; Averna, J.F. Evaluation and Management of SCI-Associated Pain. *Curr. Pain Headache Rep.* **2016**, *20*, 53. [CrossRef] [PubMed]
59. Moreno-Duarte, I.; Morse, L.R.; Alam, M.; Bikson, M.; Zafonte, R.; Fregni, F. Targeted therapies using electrical and magnetic neural stimulation for the treatment of chronic pain in spinal cord injury. *Neuroimage* **2014**, *85 Pt. 3*, 1003–1013. [CrossRef] [PubMed]
60. Dworkin, R.H.; O'Connor, A.B.; Kent, J.; Mackey, S.C.; Raja, S.N.; Stacey, B.R.; Levy, R.M.; Backonja, M.; Baron, R.; Harke, H.; et al. Interventional management of neuropathic pain: NeuPSIG recommendations. *Pain* **2013**, *154*, 2249–2261. [CrossRef] [PubMed]
61. Heath, R.G.; Mickle, W.A. Evaluation of seven years' experience with depth electrode studies in human patients. In *Electrical Studies on the Unanesthetized Brain*; PB Hoeber: New York, NY, USA, 2013; pp. 214–247.
62. Melzack, R.; Wall, P.D. Pain mechanisms: A new theory. *Science* **1965**, *150*, 971–979. [CrossRef] [PubMed]
63. Boccard, S.G.; Pereira, E.A.; Moir, L.; Aziz, T.Z.; Green, A.L. Long-term outcomes of deep brain stimulation for neuropathic pain. *Neurosurgery* **2013**, *72*, 221–230. [CrossRef] [PubMed]
64. Kumar, K.; Toth, C.; Nath, R.K. Deep brain stimulation for intractable pain: A 15-year experience. *Neurosurgery* **1997**, *40*, 736–746. [CrossRef] [PubMed]
65. Romanelli, P.; Esposito, V. The functional anatomy of neuropathic pain. *Neurosurg. Clin. N. Am.* **2004**, *15*, 257–268. [CrossRef] [PubMed]
66. Canavero, S.; Bonicalzi, V. Neuromodulation for central pain. *Expert Rev. Neurother.* **2003**, *3*, 591–607. [CrossRef] [PubMed]

67. Pereira, E.A.; Boccard, S.G.; Aziz, T.Z. Deep brain stimulation for pain: Distinguishing dorsolateral somesthetic and ventromedial affective targets. *Neurosurgery* **2014**, *61*, 175–181. [CrossRef] [PubMed]
68. Im, S.H.; Ha, S.W.; Kim, D.R.; Son, B.C. Long-term results of motor cortex stimulation in the treatment of chronic, intractable neuropathic pain. *Stereotact. Funct. Neurosurg.* **2015**, *93*, 212–218. [CrossRef] [PubMed]
69. Previnaire, J.G.; Nguyen, J.P.; Perrouin-Verbe, B.; Fattal, C. Chronic neuropathic pain in spinal cord injury: Efficiency of deep brain and motor cortex stimulation therapies for neuropathic pain in spinal cord injury patients. *Ann. Phys. Rehabil. Med.* **2009**, *52*, 188–193. [CrossRef] [PubMed]
70. Levy, R.M.; Lamb, S.; Adams, J.E. Treatment of chronic pain by deep brain stimulation: Long term follow-up and review of the literature. *Neurosurgery* **1987**, *21*, 885–893. [CrossRef] [PubMed]
71. Rasche, D.; Rinaldi, P.C.; Young, R.F.; Tronnier, V.M. Deep brain stimulation for the treatment of various chronic pain syndromes. *Neurosurg. Focus* **2006**, *21*, E8. [CrossRef] [PubMed]
72. Hamani, C.; Schwalb, J.M.; Rezai, A.R.; Dostrovsky, J.O.; Davis, K.D.; Lozano, A.M. Deep brain stimulation for chronic neuropathic pain: Long-term outcome and the incidence of insertional effect. *Pain* **2006**, *125*, 188–196. [CrossRef] [PubMed]
73. Owen, S.L.; Green, A.L.; Nandi, D.; Bittar, R.G.; Wang, S.; Aziz, T.Z. Deep brain stimulation for neuropathic pain. *Neuromodulation* **2006**, *9*, 100–106. [CrossRef] [PubMed]
74. Katayama, Y.; Yamamoto, T.; Kobayashi, K.; Kasai, M.; Oshima, H.; Fukaya, C. Motor cortex stimulation for phantom limb pain: Comprehensive therapy with spinal cord and thalamic stimulation. *Stereotact. Funct. Neurosurg.* **2001**, *77*, 159–162. [CrossRef] [PubMed]
75. Hentall, I.D.; Luca, C.C.; Widerstrom-Noga, E.; Vitores, A.; Fisher, L.D.; Martinez-Arizala, A.; Jagid, J.R. The midbrain central gray best suppresses chronic pain with electrical stimulation at very low pulse rates in two human cases. *Brain Res.* **2016**, *1632*, 119–126. [CrossRef] [PubMed]
76. Pereira, E.A.; Wang, S.; Owen, S.L.; Aziz, T.Z.; Green, A.L. Human periventricular grey somatosensory evoked potentials suggest rostrocaudally inverted somatotopy. *Stereotact. Funct. Neurosurg.* **2013**, *91*, 290–297. [CrossRef] [PubMed]
77. Pereira, E.A.; Green, A.L.; Aziz, T.Z. Deep brain stimulation for pain. *Handb. Clin. Neurol.* **2013**, *116*, 277–294. [PubMed]
78. Spooner, J.; Yu, H.; Kao, C.; Sillay, K.; Konrad, P. Neuromodulation of the cingulum for neuropathic pain after spinal cord injury. Case report. *J. Neurosurg.* **2007**, *107*, 169–172. [CrossRef] [PubMed]
79. Boccard, S.G.; Pereira, E.A.; Moir, L.; Van Hartevelt, T.J.; Kringelbach, M.L.; FitzGerald, J.J.; Baker, I.W.; Green, A.L.; Aziz, T.Z. Deep brain stimulation of the anterior cingulate cortex: Targeting the affective component of chronic pain. *Neuroreport* **2014**, *25*, 83–88. [CrossRef] [PubMed]
80. Coffey, R.J. Deep brain stimulation for chronic pain: Results of two multicenter trials and a structured review. *Pain Med.* **2001**, *2*, 183–192. [CrossRef] [PubMed]
81. Deer, T.R.; Mekhail, N.; Petersen, E.; Krames, E.; Staats, P.; Pope, J.; Saweris, Y.; Lad, S.P.; Diwan, S.; Falowski, S.; et al. The appropriate use of neurostimulation: Stimulation of the intracranial and extracranial space and head for chronic pain. Neuromodulation Appropriateness Consensus Committee. *Neuromodulation* **2014**, *17*, 551–570. [CrossRef] [PubMed]
82. Saitoh, Y.; Yoshimine, T. Stimulation of primary motor cortex for intractable deafferentation pain. *Acta Neurochir. Suppl.* **2007**, *97 Pt. 2*, 51–56. [PubMed]
83. Nashold, B.S., Jr.; Friedman, H. Dorsal column stimulation for control of pain. Preliminary report on 30 patients. *J. Neurosurg.* **1972**, *36*, 590–597. [CrossRef] [PubMed]
84. Spiegelmann, R.; Friedman, W.A. Spinal cord stimulation: A contemporary series. *Neurosurgery* **1991**, *28*, 65–70. [CrossRef] [PubMed]
85. Kumar, K.; Toth, C.; Nath, R.K.; Laing, P. Epidural spinal cord stimulation for treatment of chronic pain—Some predictors of success. A 15-year experience. *Surg. Neurol.* **1998**, *50*, 110–120. [CrossRef]
86. Taylor, R.S.; van Buyten, J.P.; Buchser, E. Spinal cord stimulation for chronic back and leg pain and failed back surgery syndrome: A systematic review and analysis of prognostic factors. *Spine (Phila Pa 1976)* **2005**, *30*, 152–160. [CrossRef]
87. Strafella, A.P.; Vanderwerf, Y.; Sadikot, A.F. Transcranial magnetic stimulation of the human motor cortex influences the neuronal activity of subthalamic nucleus. *Eur. J. Neurosci.* **2004**, *20*, 2245–2249. [CrossRef] [PubMed]

88. Lang, N.; Siebner, H.R.; Ward, N.S.; Lee, L.; Nitsche, M.A.; Paulus, W.; Rothwell, J.C.; Lemon, R.N.; Frackowiak, R.S. How does transcranial DC stimulation of the primary motor cortex alter regional neuronal activity in the human brain? *Eur. J. Neurosci.* **2005**, *22*, 495–504. [CrossRef] [PubMed]
89. Gao, F.; Chu, H.; Li, J.; Yang, M.; Du, L.; Li, J.; Chen, L.; Yang, D.; Zhang, H.; Chan, C. Repetitive transcranial magnetic stimulation for pain after spinal cord injury: A systematic review and meta-analysis. *J. Neurosurg. Sci.* **2016**. Available online: https://www.ncbi.nlm.nih.gov/labs/articles/27603408/ (accessed on 5 January 2017).
90. Cruccu, G.; Garcia-Larrea, L.; Hansson, P.; Keindl, M.; Lefaucheur, J.P.; Paulus, W.; Taylor, R.; Tronnier, V.; Truini, A.; Attal, N. EAN guidelines on central neurostimulation therapy in chronic pain conditions. *Eur. J. Neurol.* **2016**, *23*, 1489–1499. [CrossRef] [PubMed]
91. Cruccu, G.; Aziz, T.Z.; Garcia-Larrea, L.; Hansson, P.; Jensen, T.S.; Lefaucheur, J.P.; Simpson, B.A.; Taylor, R.S. EFNS guidelines on neurostimulation therapy for neuropathic pain. *Eur. J. Neurol.* **2007**, *14*, 952–970. [CrossRef] [PubMed]
92. Lefaucheur, J.P.; Andre-Obadia, N.; Antal, A.; Ayache, S.S.; Baeken, C.; Benninger, D.H.; Cantello, R.M.; Cincotta, M.; de Carvalho, M.; De Ridder, D.; et al. Evidence-based guidelines on the therapeutic use of repetitive transcranial magnetic stimulation (rTMS). *Clin. Neurophysiol.* **2014**, *125*, 2150–2206. [CrossRef] [PubMed]
93. Lefaucheur, J.P.; Drouot, X.; Menard-Lefaucheur, I.; Zerah, F.; Bendib, B.; Cesaro, P.; Keravel, Y.; Nguyen, J.P. Neurogenic pain relief by repetitive transcranial magnetic cortical stimulation depends on the origin and the site of pain. *J. Neurol. Neurosurg. Psychiatry* **2004**, *75*, 612–616. [CrossRef] [PubMed]
94. Osenbach, R.K. Motor cortex stimulation for intractable pain. *Neurosurg. Focus* **2006**, *21*, E7. [CrossRef] [PubMed]
95. Nardone, R.; Holler, Y.; Langthaler, P.B.; Lochner, P.; Golaszewski, S.; Schwenker, K.; Brigo, F.; Trinka, E. rTMS of the prefrontal cortex has analgesic effects on neuropathic pain in subjects with spinal cord injury. *Spinal Cord* **2016**, *55*, 20–25. [CrossRef] [PubMed]
96. Lefaucheur, J.P. Cortical neurostimulation for neuropathic pain: State of the art and perspectives. *Pain* **2016**, *157*, S81–S89. [CrossRef] [PubMed]
97. Yoon, E.J.; Kim, Y.K.; Kim, H.R.; Kim, S.E.; Lee, Y.; Shin, H.I. Transcranial direct current stimulation to lessen neuropathic pain after spinal cord injury: A mechanistic PET study. *Neurorehabil. Neural Repair* **2014**, *28*, 250–259. [CrossRef] [PubMed]
98. Guy, S.D.; Mehta, S.; Casalino, A.; Cote, I.; Kras-Dupuis, A.; Moulin, D.E.; Parrent, A.G.; Potter, P.; Short, C.; Teasell, R.; et al. The CanPain SCI Clinical Practice Guidelines for Rehabilitation Management of Neuropathic Pain after Spinal Cord: Recommendations for treatment. *Spinal Cord* **2016**, *54*, S14–S23. [CrossRef] [PubMed]
99. Widerstrom-Noga, E.; Biering-Sorensen, F.; Bryce, T.N.; Cardenas, D.D.; Finnerup, N.B.; Jensen, M.P.; Richards, J.S.; Richardson, E.J.; Siddall, P.J. The international spinal cord injury pain extended data set (Version 1.0). *Spinal Cord* **2016**, *54*, 1036–1046. [CrossRef] [PubMed]
100. Widerstrom-Noga, E.; Biering-Sorensen, F.; Bryce, T.; Cardenas, D.D.; Finnerup, N.B.; Jensen, M.P.; Richards, J.S.; Siddall, P.J. The international spinal cord injury pain basic data set. *Spinal Cord* **2008**, *46*, 818–823. [CrossRef] [PubMed]
101. Richardson, M. Deep brain stimulation for locomotor recovery following spinal cord injury. *Neurosurgery* **2014**, *74*, N18–N19. [CrossRef] [PubMed]
102. Wenger, N.; Moraud, E.M.; Raspopovic, S.; Bonizzato, M.; DiGiovanna, J.; Musienko, P.; Morari, M.; Micera, S.; Courtine, G. Closed-loop neuromodulation of spinal sensorimotor circuits controls refined locomotion after complete spinal cord injury. *Sci. Transl. Med.* **2014**, *6*, 255ra133. [CrossRef] [PubMed]
103. Courtine, G.; Gerasimenko, Y.; van den Brand, R.; Yew, A.; Musienko, P.; Zhong, H.; Song, B.; Ao, Y.; Ichiyama, R.M.; Lavrov, I.; et al. Transformation of nonfunctional spinal circuits into functional states after the loss of brain input. *Nat. Neurosci.* **2009**, *12*, 1333–1342. [CrossRef] [PubMed]
104. Holinski, B.J.; Everaert, D.G.; Mushahwar, V.K.; Stein, R.B. Real-time control of walking using recordings from dorsal root ganglia. *J. Neural Eng.* **2013**, *10*, 056008. [CrossRef] [PubMed]
105. Fenelon, G.; Goujon, C.; Gurruchaga, J.M.; Cesaro, P.; Jarraya, B.; Palfi, S.; Lefaucheur, J.P. Spinal cord stimulation for chronic pain improved motor function in a patient with Parkinson's disease. *Parkinsonism Relat. Disord.* **2012**, *18*, 213–214. [CrossRef] [PubMed]
106. Fuentes, R.; Petersson, P.; Siesser, W.B.; Caron, M.G.; Nicolelis, M.A. Spinal cord stimulation restores locomotion in animal models of Parkinson's disease. *Science* **2009**, *323*, 1578–1582. [CrossRef] [PubMed]

107. Cook, A.W. Electrical stimulation in multiple sclerosis. *Hosp. Pract.* **1976**, *11*, 51–58. [CrossRef] [PubMed]
108. Cook, A.W.; Weinstein, S.P. Chronic dorsal column stimulation in multiple sclerosis. Preliminary report. *N. Y. State J. Med.* **1973**, *73*, 2868–2872. [PubMed]
109. Angeli, C.A.; Edgerton, V.R.; Gerasimenko, Y.P.; Harkema, S.J. Altering spinal cord excitability enables voluntary movements after chronic complete paralysis in humans. *Brain* **2014**, *137 Pt. 5*, 1394–1409. [CrossRef] [PubMed]
110. Sayenko, D.G.; Angeli, C.; Harkema, S.J.; Edgerton, V.R.; Gerasimenko, Y.P. Neuromodulation of evoked muscle potentials induced by epidural spinal-cord stimulation in paralyzed individuals. *J. Neurophysiol.* **2014**, *111*, 1088–1099. [CrossRef] [PubMed]
111. Harkema, S.; Gerasimenko, Y.; Hodes, J.; Burdick, J.; Angeli, C.; Chen, Y.; Ferreira, C.; Willhite, A.; Rejc, E.; Grossman, R.G.; et al. Effect of epidural stimulation of the lumbosacral spinal cord on voluntary movement, standing, and assisted stepping after motor complete paraplegia: A case study. *Lancet* **2011**, *377*, 1938–1947. [CrossRef]
112. Minassian, K.; McKay, W.B.; Binder, H.; Hofstoetter, U.S. Targeting lumbar spinal neural circuitry by epidural stimulation to restore motor function after spinal cord injury. *Neurotherapeutics* **2016**, *13*, 284–294. [CrossRef] [PubMed]
113. Mayr, W.; Krenn, M.; Dimitrijevic, M.R. Epidural and transcutaneous spinal electrical stimulation for restoration of movement after incomplete and complete spinal cord injury. *Curr. Opin. Neurol.* **2016**, *29*, 721–726. [CrossRef] [PubMed]
114. Song, W.; Amer, A.; Ryan, D.; Martin, J.H. Combined motor cortex and spinal cord neuromodulation promotes corticospinal system functional and structural plasticity and motor function after injury. *Exp. Neurol.* **2016**, *277*, 46–57. [CrossRef] [PubMed]
115. Squair, J.W.; Bjerkefors, A.; Inglis, J.T.; Lam, T.; Carpenter, M.G. Cortical and vestibular stimulation reveal preserved descending motor pathways in individuals with motor-complete spinal cord injury. *J. Rehabil. Med.* **2016**, *48*, 589–596. [CrossRef] [PubMed]
116. Cha, H.G.; Ji, S.G.; Kim, M.K. Effect of high-frequency repetitive transcranial magnetic stimulation on motor cortical excitability and sensory nerve conduction velocity in subacute-stage incomplete spinal cord injury patients. *J. Phys. Ther. Sci.* **2016**, *28*, 2002–2004. [CrossRef] [PubMed]
117. Hou, S.; Rabchevsky, A.G. Autonomic consequences of spinal cord injury. *Compr. Physiol.* **2014**, *4*, 1419–1453. [PubMed]
118. Wyndaele, J.J. The management of neurogenic lower urinary tract dysfunction after spinal cord injury. *Nat. Rev. Urol.* **2016**, *13*, 705–714. [CrossRef] [PubMed]
119. Park, S.E.; Elliott, S.; Noonan, V.K.; Thorogood, N.P.; Fallah, N.; Aludino, A.; Dvorak, M.F. Impact of bladder, bowel and sexual dysfunction on health status of people with thoracolumbar spinal cord injuries living in the community. *J. Spinal Cord Med.* **2016**. [CrossRef] [PubMed]
120. Cobo Cuenca, A.I.; Sampietro-Crespo, A.; Virseda-Chamorro, M.; Martin-Espinosa, N. Psychological impact and sexual dysfunction in men with and without spinal cord injury. *J. Sex. Med.* **2015**, *12*, 436–444. [CrossRef] [PubMed]
121. Krassioukov, A. Autonomic function following cervical spinal cord injury. *Respir. Physiol. Neurobiol.* **2009**, *169*, 157–164. [CrossRef] [PubMed]
122. Karlsson, A.K. Autonomic dysfunction in spinal cord injury: Clinical presentation of symptoms and signs. *Prog. Brain Res.* **2006**, *152*, 1–8. [PubMed]
123. Trivedi, P.M.; Kumar, L.; Emmanuel, A.V. Altered colorectal compliance and anorectal physiology in upper and lower motor neurone spinal injury may explain bowel symptom pattern. *Am. J. Gastroenterol.* **2016**, *111*, 552–560. [CrossRef] [PubMed]
124. Garshick, E.; Kelley, A.; Cohen, S.A.; Garrison, A.; Tun, C.G.; Gagnon, D.; Brown, R. A prospective assessment of mortality in chronic spinal cord injury. *Spinal Cord* **2005**, *43*, 408–416. [CrossRef] [PubMed]
125. Partida, E.; Mironets, E.; Hou, S.; Tom, V.J. Cardiovascular dysfunction following spinal cord injury. *Neural Regen. Res.* **2016**, *11*, 189–194. [PubMed]
126. Dance, D.L.; Chopra, A.; Campbell, K.; Ditor, D.S.; Hassouna, M.; Craven, B.C. Exploring daily blood pressure fluctuations and cardiovascular risk among individuals with motor complete spinal cord injury: A pilot study. *J. Spinal Cord Med.* **2016**. [CrossRef] [PubMed]

127. Lee, A.H.; Phillips, A.A.; Krassioukov, A.V. Increased central arterial stiffness after spinal cord injury: contributing factors, implications and possible interventions. *J. Neurotrauma* **2016**. [CrossRef] [PubMed]
128. West, C.R.; Squair, J.W.; McCracken, L.; Currie, K.D.; Somvanshi, R.; Yuen, V.; Phillips, A.A.; Kumar, U.; McNeill, J.H.; Krassioukov, A.V. Cardiac consequences of autonomic dysreflexia in spinal cord injury. *Hypertension* **2016**, *68*, 1281–1289. [CrossRef] [PubMed]
129. Hyam, J.A.; Kringelbach, M.L.; Silburn, P.A.; Aziz, T.Z.; Green, A.L. The autonomic effects of deep brain stimulation—A therapeutic opportunity. *Nat. Rev. Neurol.* **2012**, *8*, 391–400. [CrossRef] [PubMed]
130. Herzog, J.; Weiss, P.H.; Assmus, A.; Wefer, B.; Seif, C.; Braun, P.M.; Herzog, H.; Volkmann, J.; Deuschl, G.; Fink, G.R. Subthalamic stimulation modulates cortical control of urinary bladder in Parkinson's disease. *Brain* **2006**, *129 Pt. 12*, 3366–3375. [CrossRef] [PubMed]
131. Herzog, J.; Weiss, P.H.; Assmus, A.; Wefer, B.; Seif, C.; Braun, P.M.; Pinsker, M.O.; Herzog, H.; Volkmann, J.; Deuschl, G.; et al. Improved sensory gating of urinary bladder afferents in Parkinson's disease following subthalamic stimulation. *Brain* **2008**, *131 Pt. 1*, 132–145. [CrossRef] [PubMed]
132. Kessler, T.M.; Burkhard, F.C.; Z'Brun, S.; Stibal, A.; Studer, U.E.; Hess, C.W.; Kaelin-Lang, A. Effect of thalamic deep brain stimulation on lower urinary tract function. *Eur. Urol.* **2008**, *53*, 607–612. [CrossRef] [PubMed]
133. Mordasini, L.; Kessler, T.M.; Kiss, B.; Schupbach, M.; Pollo, C.; Kaelin-Lang, A. Bladder function in patients with dystonia undergoing deep brain stimulation. *Parkinsonism Relat. Disord.* **2014**, *20*, 1015–1017. [CrossRef] [PubMed]
134. Halim, A.; Baumgartner, L.; Binder, D.K. Switching off micturition using deep brain stimulation at midbrain sites. *Ann. Neurol.* **2012**, *72*, 144–147.
135. Halim, A.; Baumgartner, L.; Binder, D.K. Effect of deep brain stimulation on autonomic dysfunction in patients with Parkinson's disease. *J. Clin. Neurosci.* **2011**, *18*, 804–806. [CrossRef] [PubMed]
136. Green, A.L.; Paterson, D.J. Identification of neurocircuitry controlling cardiovascular function in humans using functional neurosurgery: Implications for exercise control. *Exp. Physiol.* **2008**, *93*, 1022–1028. [CrossRef] [PubMed]
137. Pereira, E.; Green, A. Autonomic neurosurgery: From microvascular decompression to image guided stimulation. *Biomed. Imaging Interv. J.* **2007**, *3*, e14. [CrossRef] [PubMed]
138. Green, A.L.; Hyam, J.A.; Williams, C.; Wang, S.; Shlugman, D.; Stein, J.F.; Paterson, D.J.; Aziz, T.Z. Intra-operative deep brain stimulation of the periaqueductal grey matter modulates blood pressure and heart rate variability in humans. *Neuromodulation* **2010**, *13*, 174–181. [CrossRef] [PubMed]
139. Green, A.L.; Wang, S.; Bittar, R.G.; Owen, S.L.; Paterson, D.J.; Stein, J.F.; Bain, P.G.; Shlugman, D.; Aziz, T.Z. Deep brain stimulation: A new treatment for hypertension? *J. Clin. Neurosci.* **2007**, *14*, 592–595. [CrossRef] [PubMed]
140. Green, A.L.; Wang, S.; Owen, S.L.; Paterson, D.J.; Stein, J.F.; Aziz, T.Z. Controlling the heart via the brain: A potential new therapy for orthostatic hypotension. *Neurosurgery* **2006**, *58*, 1176–1183. [CrossRef] [PubMed]
141. Pereira, E.A.; Wang, S.; Paterson, D.J.; Stein, J.F.; Aziz, T.Z.; Green, A.L. Sustained reduction of hypertension by deep brain stimulation. *J. Clin. Neurosci.* **2010**, *17*, 124–127. [CrossRef] [PubMed]
142. Pereira, E.A.; Lu, G.; Wang, S.; Schweder, P.M.; Hyam, J.A.; Stein, J.F.; Paterson, D.J.; Aziz, T.Z.; Green, A.L. Ventral periaqueductal grey stimulation alters heart rate variability in humans with chronic pain. *Exp. Neurol.* **2010**, *223*, 574–581. [CrossRef] [PubMed]
143. Brindley, G.S. The first 500 patients with sacral anterior root stimulator implants: General description. *Paraplegia* **1994**, *32*, 795–805. [CrossRef] [PubMed]
144. Sievert, K.D.; Amend, B.; Gakis, G.; Toomey, P.; Badke, A.; Kaps, H.P.; Stenzl, A. Early sacral neuromodulation prevents urinary incontinence after complete spinal cord injury. *Ann. Neurol.* **2010**, *67*, 74–84. [CrossRef] [PubMed]
145. Kirkham, A.P.; Knight, S.L.; Craggs, M.D.; Casey, A.T.; Shah, P.J. Neuromodulation through sacral nerve roots 2 to 4 with a Finetech-Brindley sacral posterior and anterior root stimulator. *Spinal Cord* **2002**, *40*, 272–281. [CrossRef] [PubMed]
146. Andrade, D.C.; Borges, I.; Bravo, G.L.; Bolognini, N.; Fregni, F. Therapeutic time window of noninvasive brain stimulation for pain treatment: Inhibition of maladaptive plasticity with early intervention. *Expert Rev. Med. Devices* **2013**, *10*, 339–352. [CrossRef] [PubMed]

147. Little, S.; Beudel, M.; Zrinzo, L.; Foltynie, T.; Limousin, P.; Hariz, M.; Neal, S.; Cheeran, B.; Cagnan, H.; Gratwicke, J.; et al. Bilateral adaptive deep brain stimulation is effective in Parkinson's disease. *J. Neurol. Neurosurg. Psychiatry* **2016**, *87*, 717–721. [CrossRef] [PubMed]
148. Little, S.; Pogosyan, A.; Neal, S.; Zavala, B.; Zrinzo, L.; Hariz, M.; Foltynie, T.; Limousin, P.; Ashkan, K.; FitzGerald, J.; et al. Adaptive deep brain stimulation in advanced Parkinson disease. *Ann. Neurol.* **2013**, *74*, 449–457. [CrossRef] [PubMed]
149. Keifer, O.P., Jr.; Riley, J.P.; Boulis, N.M. Deep brain stimulation for chronic pain: Intracranial targets, clinical outcomes, and trial design considerations. *Neurosurg. Clin. N. Am.* **2014**, *25*, 671–692. [CrossRef] [PubMed]
150. Hosobuchi, Y.; Rossier, J.; Bloom, F.E.; Guillemin, R. Stimulation of human periaqueductal gray for pain relief increases immunoreactive beta-endorphin in ventricular fluid. *Science* **1979**, *203*, 279–281. [CrossRef] [PubMed]
151. Hosobuchi, Y.; Adams, J.E.; Linchitz, R. Pain relief by electrical stimulation of the central gray matter in humans and its reversal by naloxone. *Science* **1977**, *197*, 183–186. [CrossRef] [PubMed]
152. Fessler, R.G.; Brown, F.D.; Rachlin, J.R.; Mullan, S.; Fang, V.S. Elevated beta-endorphin in cerebrospinal fluid after electrical brain stimulation: Artifact of contrast infusion? *Science* **1984**, *224*, 1017–1019. [CrossRef] [PubMed]
153. Mohammadi, A.; Mehdizadeh, A.R. Deep brain stimulation and gene expression alterations in Parkinson's disease. *J. Biomed. Phys. Eng.* **2016**, *6*, 47–50.
154. Tilley, D.M.; Cedeno, D.L.; Kelley, C.A.; Benyamin, R.; Vallejo, R. Spinal cord stimulation modulates gene expression in the spinal cord of an animal model of peripheral nerve injury. *Reg. Anesth. Pain Med.* **2016**, *41*, 750–756. [CrossRef] [PubMed]
155. Andrews, R.J. Neuroprotection at the nanolevel—Part II: Nanodevices for neuromodulation—Deep brain stimulation and spinal cord injury. *Ann. N. Y. Acad. Sci.* **2007**, *1122*, 185–196. [CrossRef] [PubMed]
156. Lammertse, D.P. Clinical trials in spinal cord injury: Lessons learned on the path to translation. The 2011 International Spinal Cord Society Sir Ludwig Guttmann Lecture. *Spinal Cord* **2013**, *51*, 2–9. [CrossRef] [PubMed]
157. Green, A.L.; Shad, A.; Watson, R.; Nandi, D.; Yianni, J.; Aziz, T.Z. N-of-1 Trials for assessing the efficacy of deep brain stimulation in neuropathic pain. *Neuromodulation* **2004**, *7*, 76–81. [CrossRef] [PubMed]
158. McCulloch, P.; Altman, D.G.; Campbell, W.B.; Flum, D.R.; Glasziou, P.; Marshall, J.C.; Nicholl, J.; Aronson, J.K.; Barkun, J.S.; Blazeby, J.M.; et al. No surgical innovation without evaluation: The IDEAL recommendations. *Lancet* **2009**, *374*, 1105–1112. [CrossRef]
159. Williamson, P.R.; Altman, D.G.; Blazeby, J.M.; Clarke, M.; Devane, D.; Gargon, E.; Tugwell, P. Developing core outcome sets for clinical trials: Issues to consider. *Trials* **2012**, *13*, 132. [CrossRef] [PubMed]

brain sciences

MDPI

Review

Effects of Deep Brain Stimulation on Autonomic Function

Adam Basiago [1] and Devin K. Binder [2,*]

[1] School of Medicine, University of California, Riverside, CA 92521, USA; adam.basiago@email.ucr.edu
[2] Division of Biomedical Sciences, School of Medicine, University of California, 1247 Webber Hall, Riverside, CA 92521, USA
* Correspondence: dbinder@ucr.edu; Tel.: +1-951-827-2224; Fax: +1-951-827-5504

Academic Editors: Tipu Aziz and Alex Green
Received: 30 June 2016; Accepted: 10 August 2016; Published: 16 August 2016

Abstract: Over the course of the development of deep brain stimulation (DBS) into a well-established therapy for Parkinson's disease, essential tremor, and dystonia, its utility as a potential treatment for autonomic dysfunction has emerged. Dysfunction of autonomic processes is common in neurological diseases. Depending on the specific target in the brain, DBS has been shown to raise or lower blood pressure, normalize the baroreflex, to alter the caliber of bronchioles, and eliminate hyperhidrosis, all through modulation of the sympathetic nervous system. It has also been shown to improve cortical control of the bladder, directly induce or inhibit the micturition reflex, and to improve deglutition and gastric emptying. In this review, we will attempt to summarize the relevant available studies describing these effects of DBS on autonomic function, which vary greatly in character and magnitude with respect to stimulation target.

Keywords: deep brain stimulation; autonomic dysfunction; subthalamic nucleus; periaqueductal or periventricular gray; globus pallidus interna; thalamus; blood pressure; sweating; micturition; gastrointestinal motility

1. Introduction

Deep brain stimulation (DBS) has evolved into a well-established therapy for Parkinson's disease [1], essential tremor [2], and dystonia [2], as well as a therapy for multiple sclerosis [3], cluster headache [4], Tourette syndrome [5], and obsessive-compulsive disorder [6]. DBS is even being investigated as a surgical intervention for obesity, major depression, and a therapy for restoring memory to patients with Alzheimer disease [7–11]. In addition to the primary symptoms treated by DBS, many groups have investigated its effect on autonomic functions at various target sites in the brain [12,13]. Dysfunction of autonomic processes is common in neurological diseases [14–18]. In Parkinson's disease and multiple sclerosis, for example, patients are afflicted with varying manifestations of dysautonomia including orthostatic and cardiovascular dysregulation, lower urinary tract dysfunction, sudomotor dysfunction, and gastrointestinal disturbances [15,17,19–21]. In this review, we will attempt to summarize the research available describing the effects of DBS on autonomic function.

2. Methodology

A PubMed search of the available literature describing the autonomic effects of DBS was conducted through EndNote using the keywords listed above; along with any applicable iterations; in order to capture as many relevant references as possible. A total of 99 references were found with this method. Those references were then categorized by the affected autonomic function and then further by DBS target. 75 of 99 references were used in the final reference list.

3. Sympathetic Autonomic Modulation

3.1. DBS and Cardiorespiratory Control

DBS has shown significant effects on hypertension and hypotension. Depending on the target in the brain, DBS can cause a decrease or increase in blood pressure, and a decrease in orthostatic hypotension [22–24]. What makes this variable outcome possible is precise placement of the electrodes into their targets. The region of the brain that has shown the most promise as a target for DBS blood pressure regulation is the periventricular/periaqueductal gray matter (PVG/PAG) of the midbrain, as described by Green et al. [25] in 2005. In a study of 15 patients undergoing PVG/PAG DBS for uncontrolled neuropathic pain, they observed variable changes in BP depending on whether PVG/PAG stimulation was dorsal or ventral. In six patients with ventral PVG/PAG stimulation, a mean reduction of systolic BP of 14.2 $\pm$ 3.6 mmHg (13.9%), a mean reduction of diastolic BP of 4.9 $\pm$ 2.9 mmHg (6%), and a mean reduction of pulse pressure of 9.3 $\pm$ 3.16 mmHg were observed [25]. In seven patients with dorsal PVG/PAG stimulation, a mean increase in systolic BP of 16.73 $\pm$ 5.9 mmHg (16.4%), a mean increase in diastolic BP of 4.9 $\pm$ 2.8 mmHg (6%), and a mean increase in pulse pressure of 11.83 $\pm$ 5.4 mmHg were observed [25]. There were patients in whom the electrodes did not produce any BP alteration, but it was determined that electrode location was not in the PVG/PAG. Green et al. [25] determined these effects to be due to modulation of sympathetic activity, due to the presence of changes in both total peripheral resistance (TPR) and myocardial contractility [25]. Later publications, reviews, and case reports by Green et al. and other groups all report similar findings in humans and in animal models [12,13,22,23,26–32].

Posterior hypothalamic area (PHA) DBS, PVG/PAG DBS and subthalamic nucleus (STN) DBS have all been shown to affect orthostatic hypotension (OH) and baroreflex sensitivity (BRS), most likely through changes in sympathetic activity. During head-up tilt testing (HUTT), PHA DBS can increase diastolic BP and TPR without changing the effect of the baroreflex on other cardiovascular parameters or resting supine BP and heart rate (HR) [33]. In 2006, Green et al. [24] showed that through an increase in BRS, PVG/PAG DBS can prevent the drop in BP on standing in patients diagnosed with OH and mild orthostatic intolerance, but does not cause resting hypertension in those patients or hypertension in the control group with no postural BP problems. A later 2014 publication by Sverisdóttir et al. [34] reported differential changes in patients with dorsolateral versus ventrolateral PAG DBS; that same publication also showed an increase in orthostatic tolerance in Parkinson's disease (PD) patients with STN DBS. Neither BRS nor BP were influenced with stimulation of the motor thalamus, globus pallidus interna (GPi), pedunculopontine nucleus (PPN), sensory thalamus, or anterior cingulate cortex (ACC) [34]. This seems to confirm prior research by Stemper et al. [35] that showed that with stimulation during HUTT, PD patients with STN DBS had stable BP and BRS, yet without simulation during HUTT, the same patients experienced significant orthostatic hypotension. Therefore, the available data indicate some anatomic specificity to the effects of DBS on BP and BRS.

In spite of evidence supporting the sympathetically-mediated improvement of OH caused by STN DBS, its direct effects on the cardiovascular system remain unclear. A recent report of STN DBS in PD patients by Furgala et al. [36] found that STN DBS results in activation of the sympathetic nervous system resulting in changes to BP and heart rate variability. However, Trachani et al. [37] reported the opposite in 2012. Several other publications also offer conflicting opinions on the cardiovascular effects of STN DBS [38–40]. Sumi et al. [41] imply that the cardiovascular improvements seen with STN DBS are due not to the stimulation itself, but rather to an increased ability to exercise, thus improving overall cardiovascular health and lower extremity muscle strength. One explanation for the conflicting reports may be that the autonomic effects are not a direct result of the stimulation at all, but are rather the result of reduced need for pharmacotherapy to combat motor symptoms of PD [42]. Hyam et al. [12] suggest that because STN DBS generally requires higher frequencies and higher total energy delivery than DBS of other targets, a spread of stimulation to nearby components of the central autonomic network could be the cause rather than stimulation of the STN itself. This conclusion seems to be supported

by the earlier findings of Lipp et al. [43] in 2005. In a study of five patients undergoing bilateral STN DBS for Parkinson's disease, four patients with magnetic resonance imaging (MRI)-confirmed correct placement of their electrodes within the STN experienced no autonomic symptoms. However, in the fifth patient whose electrodes were shown by MRI to extend into the posteromedial and lateral hypothalamic areas, significant autonomic changes were observed including changes to blood pressure regulation, sweating, and breathing pattern [44]. This report emphasizes the importance of precise placement of the electrodes and the tuning of stimulation frequency and total energy delivery when autonomic effects are desired or not desired, regardless of other clinical goals.

For DBS modulation of autonomic respiratory control, the evidence is relatively new. In 2012, Hyam et al. [45] studied the effects on two pulmonary function tests—peak expiratory flow rate (PEFR) and forced expiratory volume in one second (FEV_1)—of PAG DBS in ten neuropathic pain (NP) patients, sensory thalamus DBS in seven NP patients, STN DBS in 10 movement disorder patients, and GPi DBS in 10 movement disorder patients. Using sensory thalamus DBS to control for the effect of pain relief, and GPi DBS to control for improvement in general motor function (both with no change in PEFR), they showed that PAG DBS and STN DBS both increase PEFR [45]. There was no change in FEV_1 with any of the stimulated targets, indicating that the increase in PEFR was likely due to bronchodilation of the large airways [45]. Further research into these effects could lead to DBS-mediated treatment of both asthma and obstructive sleep apnea through dilation of bronchioles and maintenance of upper airway patency, respectively [9]. DBS has also been implicated in increasing the respiratory rate in human and animal studies through stimulation of the anterior limb of the internal capsule and the caudal dorsal PAG [9,46,47]. A report by Vigneri et al. [48] claimed to show that DBS of the STN or PHA does not affect respiratory rate, HR or BP, but they were not able to precisely localize the electrode placement, a significant confounding factor as shown by numerous reports described above.

3.2. DBS and Sudomotor Control

Sudomotor dysfunction, most often hyperhidrosis, is extremely common in PD patients and has been shown to be alleviated by STN DBS [43,49–51]. In 2007, Witjas et al. [43] conducted a study of 30 male and 10 female patients with PD lasting an average of 12.4 ± 4.5 years, in which their nonmotor symptoms (NMS) were analyzed before and after bilateral STN DBS. One year after surgery, 34 of 35 patients were completely relieved of the drenching sweats they had experienced prior to STN DBS [43]. This effect was again seen in a later case report by Sanghera et al. [50], in which a STN DBS patient would experience whole body drenching sweats that would be alleviated with stimulation, and would return when stimulation was turned off. A study of nineteen STN DBS patients by Trachani et al. [49] observed a post-implantation reduction in hyperhidrosis in four patients, as well as an improvement of hypohidrosis in two patients. In a 2011 study of PD patients with STN DBS, Halim et al. [52] observed complete resolution of sudomotor dysfunction (and other autonomic dysfunction to be discussed later) in the three patients with early onset PD (EOPD), whereas the other eight patients with late onset PD (LOPD) did not experience any improvement in their dysautonomia. One of the three EOPD patients experienced bilateral resolution of his excessive sweating even though he only had unilateral left STN DBS [51]. Although STN DBS appears to dramatically help sudomotor dysfunction, DBS of other targets can also make it worse. A DBS electrode mistakenly placed in the thalamus or posterolateral hypothalamus can actually cause hyperhidrosis in patients who did not suffer from it prior to surgery [44,53].

4. Parasympathetic Autonomic Control

4.1. DBS and Micturition

Lower urinary tract symptoms (LUTS) are extremely common in neurological diseases like PD [54–56] and multiple sclerosis (MS) [3], and are a significant source of morbidity [52]. In parallel with the other dysautonomias above, DBS can either induce or inhibit micturition, dependent upon

the brain target. Basal ganglia and brainstem targets (STN and PAG) appear to inhibit micturition and improve urinary incontinence, while thalamic targets (ventral intermediate and ventral posterolateral nuclei—VIM and VPL, respectively) induce micturition [3]. The vast majority of studies on DBS and micturition are on STN DBS. In 2003, Finazzi-Argò et al. [57] studied urodynamics in 5 patients with PD and LUTS following STN DBS and found that all patients experienced increased volumes for initial desire to void (V_{ID}) and bladder capacity (V_{BC}), as well as decreased hyperreflexive detrusor contraction. In their study of sixteen STN DBS patients with PD but no preexisting urinary problems, Seif et al. [58] in 2004 found similar changes to urodynamic parameters. Herzog et al. [59,60] in 2006 and 2008 reported similar results while showing through PET studies that STN DBS may be achieving these effects by improving cortical control over the micturition pathway. Pietraszko et al. [61] demonstrated that in addition to the quantitative change in volumes, these patients can experience significant qualitative improvements to urgency, frequency, nocturia, and hesitancy as well. In the case series by Halim et al. [51] discussed previously, the same EOPD patients who experienced improvements in hyperhidrosis also reported subjective improvements in bladder function. As with hyperhidrosis, the LOPD patients did not experience urinary improvement either. Fritsche et al. [62] reported two cases of acute urinary retention as a complication of STN DBS in patients who did not have LUTS prior to surgery. Winge et al. [63] in 2012 reported that STN DBS is at least comparable to medication in relieving LUTS, and superior in relieving nocturia.

Other targets for modulating micturition and urodynamic parameters include the GPi, the PAG, the VPL, and the VIM [64–66]. While GPi DBS can also ameliorate detrusor overactivity in patients with dystonia, it has been shown to worsen maximum flow rate and post-void residual volume [64]. In cystometric experiments on NP patients in which bladders are filled with isotonic saline via catheter infusion, Green et al. showed that PAG DBS dramatically increases the maximum cystometric capacity (MCC), the volume at which the patients would ask for the saline infusion to be stopped, but does not affect the volumes at which voiding is desired: V_{ID}, strong desire (V_{SD}), very strong desire (V_{VSD}). By controlling for bladder sensation and pain, which were unchanged between stimulation on and off, they showed that the mechanism is most likely due to interruption of micturition directly [65]. In the same study, there were two VPL DBS patients who experienced smaller MCC volumes with stimulation on [65]. This is in agreement with a prior 2008 study by Kessler et al. [66] in which it was shown that VIM DBS results in reduced volumes for V_{ID}, V_{SD}, and MCC. These results suggest an induction of the micturition pathway by thalamic DBS.

4.2. DBS and Gastrointestinal Dysfunction

There has also been some evidence for DBS-mediated improvement of gastrointestinal dysmotility, which is a common symptom in PD [15,67]. In a study of PD patients with STN DBS by Ciucci et al. [68] in 2008, it was shown that STN DBS can improve the pharyngeal stage of deglutition, with faster pharyngeal transit times and degrees of bolus clearance, but does not improve the oral stage of deglutition. This resulted in less aspiration during swallowing with stimulation on versus off, perhaps due to greater coordination of the swallowing process [68]. Silbergleit et al. [69] suggested that STN DBS improves the patients' perception of improved swallowing, in addition to improved motor control during the swallowing of solid foods. In a randomized cross-over study of sixteen PD patients with bilateral STN DBS either on or off at random, Derrey et al. [70] determined that STN DBS can improve bolus transport in the esophagus by causing amplified peristalsis of the distal esophagus and improved relaxation of the lower esophageal sphincter. They suggested that this is mediated by a cholinergic effect. Using ^{13}C-acetate breath testing in a study of 16 bilateral STN DBS PD patients, Arai et al. [71] demonstrated improved gastric emptying with STN stimulation on versus off. In a recent study of twenty PD patients, Krygowska-Wajs et al. [72] demonstrated that STN DBS can improve gastrointestinal motility. They observed frequency reductions from 50% to 25% for dysphagia, 35% to 15% for sialorrhea, 95% to 75% for constipation, and 85% to 50% for difficulties with defecation. The patients in the study by Pietraszko et al. [61] also reported significant improvements in the same

parameters as well as abdominal pain and rectal burning during or after defecation. One of the EOPD patients from the study by Halim et al. [51] also reported marked improvement in her bowel function, consistent with the findings above.

5. Conclusions

In addition to its current status as the primary surgical treatment for movement disorders, DBS has emerging potential for use as a surgical therapy for various dysautonomias. At the very least, the autonomic effects of DBS mandate careful assessment of autonomic dysfunction in patients requiring the treatment in order to choose the appropriate target—when a choice is available—to avoid undesirable effects that may lead to significant morbidity. Beyond that careful target selection, DBS offers the opportunity for novel therapy modalities that are not possible with conventional medical therapy. Autonomic drugs, while some are "selective," generally target receptors throughout the whole body when only a specific organ or tissue type is desired, such as the heart or the bladder. DBS has the potential to add more precision to the arsenal available to physicians. Patients with orthostatic hypotension, for example, often are normotensive when supine. Pharmaceutical treatment includes α/β-agonists and adrenergic prodrugs such as droxidopa, which all can cause supine hypertension in these patients. DBS in concert with an accelerometer or mercury switch activator (that can detect when the patient is upright) can raise the patient's blood pressure only while standing, deactivating the stimulation while the patient is supine [28]. In patients with urinary retention or urinary incontinence, self-control over activation/deactivation of the pulse generator could allow the patients to turn the stimulation on or off depending on whether inhibition or induction of micturition is desired given their condition and where their electrodes have been placed. The technology of DBS is continuing to evolve, and adaptive DBS (aDBS) will soon be able to adjust stimulation intensity based on a patient's real-time clinical condition [73–75]. In addition, there are several ongoing government- and privately-funded projects aimed at enhancing the specificity of brain electrical stimulation (e.g., DARPA ElectRx, GSK electroceuticals).

Author Contributions: A.B. and D.K.B. conceived of the manuscript and discussed its outline. A.B. did a complete literature search and drafted the manuscript. D.K.B. extensively reviewed and edited the manuscript into its final form.

Conflicts of Interest: The authors declare no conflict of interest.

References

1. Hickey, P.; Stacy, M. Deep brain stimulation: A paradigm shifting approach to treat Parkinson's disease. *Front. Neurosci.* **2016**. [CrossRef] [PubMed]
2. Crowell, J.L.; Shah, B.B. Surgery for dystonia and tremor. *Curr. Neurol. Neurosci. Rep.* **2016**. [CrossRef] [PubMed]
3. Roy, H.A.; Aziz, T.Z. Deep brain stimulation and multiple sclerosis: Therapeutic applications. *Mult. Scler. Relat. Disord.* **2014**, *3*, 431–439. [CrossRef] [PubMed]
4. Leone, M.; Franzini, A.; Cecchini, A.P.; Broggi, G.; Bussone, G. Hypothalamic deep brain stimulation in the treatment of chronic cluster headache. *Ther. Adv. Neurol. Disord.* **2010**, *3*, 187–195. [CrossRef] [PubMed]
5. Baldermann, J.C.; Schüller, T.; Huys, D.; Becker, I.; Timmermann, L.; Jessen, F.; Visser-Vandewalle, V.; Kuhn, J. Deep brain stimulation for tourette-syndrome: A systematic review and meta-analysis. *Brain Stimul.* **2016**, *9*, 296–304. [CrossRef] [PubMed]
6. Van Westen, M.; Rietveld, E.; Figee, M.; Denys, D. Clinical outcome and mechanisms of deep brain stimulation for obsessive-compulsive disorder. *Curr. Behav. Neurosci. Rep.* **2015**, *2*, 41–48. [CrossRef] [PubMed]
7. Kumar, R.; Simpson, C.V.; Froelich, C.A.; Baughman, B.C.; Gienapp, A.J.; Sillay, K.A. Obesity and deep brain stimulation: An overview. *Ann. Neurosci.* **2015**, *22*, 181–188. [CrossRef] [PubMed]
8. Ho, A.L.; Sussman, E.S.; Zhang, M.; Pendharkar, A.V.; Azagury, D.E.; Bohon, C.; Halpern, C.H. Deep brain stimulation for obesity. *Cureus* **2015**, *7*, e259. [CrossRef] [PubMed]

9. Hyam, J.A.; Aziz, T.Z.; Green, A.L. Control of the lungs via the human brain using neurosurgery. *Prog. Brain Res.* **2014**, *209*, 341–366. [PubMed]
10. Bick, S.K.; Eskandar, E.N. Neuromodulation for restoring memory. *Neurosurg. Focus* **2016**, *40*, E5. [CrossRef] [PubMed]
11. Mirsaeedi-Farahani, K.; Halpern, C.H.; Baltuch, G.H.; Wolk, D.A.; Stein, S.C. Deep brain stimulation for Alzheimer disease: A decision and cost-effectiveness analysis. *J. Neurol.* **2015**, *262*, 1191–1197. [CrossRef] [PubMed]
12. Hyam, J.A.; Kringelbach, M.L.; Silburn, P.A.; Aziz, T.Z.; Green, A.L. The autonomic effects of deep brain stimulation—A therapeutic opportunity. *Nat. Rev. Neurol.* **2012**, *8*, 391–400. [CrossRef] [PubMed]
13. Lovick, T. Deep brain stimulation and autonomic control. *Exp. Physiol.* **2014**, *99*, 320–325. [CrossRef] [PubMed]
14. Ailani, J. A practical approach to autonomic dysfunction in patients with headache. *Curr. Neurol. Neurosci. Rep.* **2016**, *16*, 1–6. [CrossRef] [PubMed]
15. Pinter, A.; Cseh, D.; Sárközi, A.; Illigens, B.M.; Siepmann, T. Autonomic dysregulation in multiple sclerosis. *Int. J. Mol. Sci.* **2015**, *16*, 16920–16952. [CrossRef] [PubMed]
16. Palma, J.A.; Kaufmann, H. Autonomic disorders predicting Parkinson's disease. *Parkinsonism Relat. Disord.* **2014**, *20*, S94–S98. [CrossRef]
17. Goldstein, D.S. Dysautonomia in Parkinson disease. *Compr. Physiol.* **2014**, *4*, 805–826. [PubMed]
18. Goetz, C.G.; Lutge, W.; Tanner, C.M. Autonomic dysfunction in Parkinson's disease. *Neurology* **1986**, *36*, 73–75. [CrossRef] [PubMed]
19. Swinn, L.; Schrag, A.; Viswanathan, R.; Bloem, B.R.; Lees, A.; Quinn, N. Sweating dysfunction in Parkinson's disease. *Mov. Disord.* **2003**, *18*, 1459–1463. [CrossRef] [PubMed]
20. Santos-Garcia, D.; de Deus, T.; Tejera-Perez, C.; Exposito-Ruiz, I.; Suarez-Castro, E.; Carpintero, P.; Macias-Arribi, M. Gastroparesis and other gastrointestinal symptoms in Parkinson's disease. *Rev. Neurol.* **2015**, *61*, 261–270. [PubMed]
21. Marrinan, S.; Emmanuel, A.V.; Burn, D.J. Delayed gastric emptying in Parkinson's disease. *Mov. Disord.* **2014**, *29*, 23–32. [CrossRef] [PubMed]
22. O'Callaghan, E.L.; McBryde, F.D.; Burchell, A.E.; Ratcliffe, L.E.; Nicolae, L.; Gillbe, I.; Carr, D.; Hart, E.C.; Nightingale, A.K.; Patel, N.K.; et al. Deep brain stimulation for the treatment of resistant hypertension. *Curr. Hypertens. Rep.* **2014**, *16*, 493. [CrossRef] [PubMed]
23. Pereira, E.; Green, A. Autonomic neurosurgery: From microvascular decompression to image guided stimulation. *Biomed. Imaging Interv. J.* **2007**, *3*, e14. [CrossRef] [PubMed]
24. Green, A.L.; Wang, S.; Owen, S.L.; Paterson, D.J.; Stein, J.F.; Aziz, T.Z. Controlling the heart via the brain: A potential new therapy for orthostatic hypotension. *Neurosurgery* **2006**, *58*, 1176–1183. [CrossRef] [PubMed]
25. Green, A.L.; Wang, S.; Owen, S.L.; Xie, K.; Liu, X.; Paterson, D.J.; Stein, J.F.; Bain, P.G.; Aziz, T.Z. Deep brain stimulation can regulate arterial blood pressure in awake humans. *Neuroreport* **2005**, *16*, 1741–1745. [CrossRef] [PubMed]
26. Green, A.L.; Wang, S.; Owen, S.L.; Xie, K.; Bittar, R.G.; Stein, J.F.; Paterson, D.J.; Aziz, T.Z. Stimulating the human midbrain to reveal the link between pain and blood pressure. *Pain* **2006**, *124*, 349–359. [CrossRef] [PubMed]
27. Green, A.L.; Wang, S.; Bittar, R.G.; Owen, S.L.; Paterson, D.J.; Stein, J.F.; Bain, P.G.; Shlugman, D.; Aziz, T.Z. Deep brain stimulation: A new treatment for hypertension? *J. Clin. Neurosci.* **2007**, *14*, 592–595. [CrossRef] [PubMed]
28. Green, A.L.; Wang, S.; Owen, S.L.; Aziz, T.Z. The periaqueductal grey area and the cardiovascular system. *Acta Neurochir. Suppl.* **2007**, *97*, 521–528. [PubMed]
29. Green, A.L.; Hyam, J.A.; Williams, C.; Wang, S.; Shlugman, D.; Stein, J.F.; Paterson, D.J.; Aziz, T.Z. Intra-operative deep brain stimulation of the periaqueductal grey matter modulates blood pressure and heart rate variability in humans. *Neuromodulation* **2010**, *13*, 174–181. [CrossRef] [PubMed]
30. Pereira, E.A.; Wang, S.; Paterson, D.J.; Stein, J.F.; Aziz, T.Z.; Green, A.L. Sustained reduction of hypertension by deep brain stimulation. *J. Clin. Neurosci.* **2010**, *17*, 124–127. [CrossRef] [PubMed]
31. Patel, N.K.; Javed, S.; Khan, S.; Papouchado, M.; Malizia, A.L.; Pickering, A.E.; Paton, J.F. Deep brain stimulation relieves refractory hypertension. *Neurology* **2011**, *76*, 405–407. [CrossRef] [PubMed]

32. Carter, H.H.; Dawson, E.A.; Cable, N.T.; Basnayake, S.; Aziz, T.Z.; Green, A.L.; Paterson, D.J.; Lind, C.R.; Thijssen, D.H.; Green, D.J. Deep brain stimulation of the periaqueductal grey induces vasodilation in humans. *Hypertension* **2011**, *57*, e24–e25. [CrossRef] [PubMed]
33. Cortelli, P.; Guaraldi, P.; Leone, M.; Pierangeli, G.; Barletta, G.; Grimaldi, D.; Cevoli, S.; Bussone, G.; Baruzzi, A.; Montagna, P. Effect of deep brain stimulation of the posterior hypothalamic area on the cardiovascular system in chronic cluster headache patients. *Eur. J. Neurol.* **2007**, *14*, 1008–1015. [CrossRef] [PubMed]
34. Sverrisdottir, Y.B.; Green, A.L.; Aziz, T.Z.; Bahuri, N.F.; Hyam, J.; Basnayake, S.D.; Paterson, D.J. Differentiated baroreflex modulation of sympathetic nerve activity during deep brain stimulation in humans. *Hypertension* **2014**, *63*, 1000–1010. [CrossRef] [PubMed]
35. Stemper, B.; Beric, A.; Welsch, G.; Haendl, T.; Sterio, D.; Hilz, M.J. Deep brain stimulation improves orthostatic regulation of patients with Parkinson disease. *Neurology* **2006**, *67*, 1781–1785. [CrossRef] [PubMed]
36. Furgala, A.; Górecka-Mazur, A.; Fiszer, U.; Pietraszko, W.; Thor, P.; Moskała, M.; Potasz, K.; Bukowczan, M.; Polak, J.; Krygowska-Wajs, A. Evaluation of heart rate and blood pressure variability in Parkinson's disease patients after bilateral subthalamic deep brain stimulation. *Prz. Lek.* **2015**, *72*, 246–252. [PubMed]
37. Trachani, E.; Constantoyannis, C.; Sakellaropoulos, G.C.; Stavrinou, M.L.; Nikiforidis, G.; Chroni, E. Heart rate variability in Parkinson's disease unaffected by deep brain stimulation. *Acta Neurol. Scand.* **2012**, *126*, 56–61. [CrossRef]
38. Erola, T.; Haapaniemi, T.; Heikkinen, E.; Huikuri, H.; Myllyä, V. Subthalamic nucleus deep brain stimulation does not alter long-term heart rate variability in Parkinson's disease. *Clin. Auton. Res.* **2006**, *16*, 286–288. [CrossRef] [PubMed]
39. Chen, S.Y.; Yang, C.C.; Kuo, T.B.; Harnod, T. Association of heart rate variability with clinical outcome in parkinsonian patients after subthalamic deep brain stimulation: A retrospective cohort study. *J. Formos. Med. Assoc.* **2011**, *110*, 593–599. [CrossRef] [PubMed]
40. Liu, K.D.; Shan, D.E.; Kuo, T.B.; Yang, C.C. The effects of bilateral stimulation of the subthalamic nucleus on heart rate variability in patients with Parkinson's disease. *J. Neurol.* **2013**, *260*, 1714–1723. [CrossRef] [PubMed]
41. Sumi, K.; Katayama, Y.; Otaka, T.; Obuchi, T.; Kano, T.; Kobayashi, K.; Oshima, H.; Fukaya, C.; Yamamoto, T.; Ogawa, Y.; et al. Effect of subthalamic nucleus deep brain stimulation on the autonomic nervous system in Parkinson's disease patients assessed by spectral analyses of R-R interval variability and blood pressure variability. *Stereotact. Funct. Neurosurg.* **2012**, *90*, 248–254. [CrossRef] [PubMed]
42. Ludwig, J.; Remien, P.; Guballa, C.; Binder, A.; Binder, S.; Schattschneider, J.; Herzog, J.; Volkmann, J.; Deuschl, G.; Wasner, G.; et al. Effects of subthalamic nucleus stimulation and levodopa on the autonomic nervous system in Parkinson's disease. *J. Neurol. Neurosurg. Psychiatry* **2007**, *78*, 742–745. [CrossRef] [PubMed]
43. Witjas, T.; Kaphan, E.; Régis, J.; Jouve, E.; Chérif, A.A.; Péragut, J.C.; Azulay, J.P. Effects of chronic subthalamic stimulation on nonmotor fluctuations in Parkinson's disease. *Mov. Disord.* **2007**, *22*, 1729–1734. [CrossRef] [PubMed]
44. Lipp, A.; Tank, J.; Trottenberg, T.; Kupsch, A.; Arnold, G.; Jordan, J. Sympathetic activation due to deep brain stimulation in the region of the STN. *Neurology* **2005**, *65*, 774–775. [CrossRef] [PubMed]
45. Hyam, J.A.; Brittain, J.S.; Paterson, D.J.; Davies, R.J.; Aziz, T.Z. Controlling the lungs via the brain: A novel neurosurgical method to improve lung function in humans. *Neurosurgery* **2012**, *70*, 469–478. [CrossRef] [PubMed]
46. Okun, M.S.; Mann, G.; Foote, K.D.; Shapira, N.A.; Bowers, D.; Springer, U.; Knight, W.; Martin, P.; Goodman, W.K. Deep brain stimulation in the internal capsule and nucleus accumbens region: Responses observed during active and sham programming. *J. Neurol. Neurosurg. Psychiatry* **2007**, *78*, 310–314. [CrossRef] [PubMed]
47. Zhang, W.; Hayward, L.F.; Davenport, P.W. Respiratory responses elicited by rostral versus caudal dorsal periaqueductal gray stimulation in rats. *Auton. Neurosci.* **2007**, *134*, 45–54. [CrossRef] [PubMed]
48. Vigneri, S.; Guaraldi, P.; Calandra-Buonaura, G.; Terlizzi, R.; Cecere, A.; Barletta, G.; Cortelli, P. Switching on the deep brain stimulation: Effects on cardiovascular regulation and respiration. *Auton. Neurosci.* **2012**, *166*, 81–84. [CrossRef] [PubMed]

49. Trachani, E.; Constantoyannis, C.; Sirrou, V.; Kefalopoulou, Z.; Markaki, E.; Chroni, E. Effects of subthalamic nucleus deep brain stimulation on sweating function in Parkinson's disease. *Clin. Neurol. Neurosurg.* **2010**, *112*, 213–217. [CrossRef] [PubMed]
50. Sanghera, M.K.; Ward, C.; Stewart, R.M.; Mewes, K.; Simpson, R.K.; Lai, E.C. Alleviation of drenching sweats following subthalamic deep brain stimulation in a patient with Parkinson's disease—A case report. *J. Neurol. Sci.* **2009**, *285*, 246–249. [CrossRef] [PubMed]
51. Halim, A.; Baumgartner, L.; Binder, D.K. Effect of deep brain stimulation on autonomic dysfunction in patients with Parkinson's disease. *J. Clin. Neurosci.* **2011**, *18*, 804–806. [CrossRef] [PubMed]
52. Sakakibara, R.; Shinotoh, H.; Uchiyama, T.; Sakuma, M.; Kashiwado, M.; Yoshiyama, M.; Hattori, T. Questionnaire-based assessment of pelvic organ dysfunction in Parkinson's disease. *Auton. Neurosci.* **2001**, *92*, 76–85. [CrossRef]
53. Diamond, A.; Kenney, C.; Almaguer, M.; Jankovic, J. Hyperhidrosis due to deep brain stimulation in a patient with essential tremor. *J. Neurosurg.* **2007**, *107*, 1036–1038. [CrossRef] [PubMed]
54. Sakakibara, R.; Panicker, J.; Finazzi-Agro, E.; Iacovelli, V.; Bruschini, H. A guideline for the management of bladder dysfunction in Parkinson's disease and other gait disorders. *Neurourol. Urodyn.* **2015**, *35*, 551–563. [CrossRef] [PubMed]
55. Sakakibara, R.; Tateno, F.; Nagao, T.; Yamamoto, T.; Uchiyama, T.; Yamanishi, T.; Yano, M.; Kishi, M.; Tsuyusaki, Y.; Aiba, Y. Bladder function of patients with Parkinson's disease. *Int. J. Urol.* **2014**, *21*, 638–646. [CrossRef] [PubMed]
56. Winge, K.; Skau, A.M.; Stimpel, H.; Nielsen, K.K.; Werdelin, L. Prevalence of bladder dysfunction in Parkinsons disease. *Neurourol. Urodyn.* **2006**, *25*, 116–122. [CrossRef] [PubMed]
57. Finazzi-Agro, E.; Peppe, A.; D'Amico, A.; Petta, F.; Mazzone, P.; Stanzione, P.; Micali, F.; Caltagirone, C. Effects of subthalamic nucleus stimulation on urodynamic findings in patients with Parkinson's disease. *J. Urol.* **2003**, *169*, 1388–1391. [CrossRef] [PubMed]
58. Seif, C.; Herzog, J.; van der Horst, C.; Schrader, B.; Volkmann, J.; Deuschl, G.; Juenemann, K.P.; Braun, P.M. Effect of subthalamic deep brain stimulation on the function of the urinary bladder. *Ann. Neurol.* **2004**, *55*, 118–120. [CrossRef] [PubMed]
59. Herzog, J.; Weiss, P.H.; Assmus, A.; Wefer, B.; Seif, C.; Braun, P.M.; Herzog, H.; Volkmann, J.; Deuschl, G.; Fink, G.R. Subthalamic stimulation modulates cortical control of urinary bladder in Parkinson's disease. *Brain* **2006**, *129*, 3366–3375. [CrossRef] [PubMed]
60. Herzog, J.; Weiss, P.H.; Assmus, A.; Wefer, B.; Seif, C.; Braun, P.M.; Pinsker, M.O.; Herzog, H.; Volkmann, J.; Deuschl, G.; et al. Improved sensory gating of urinary bladder afferents in Parkinson's disease following subthalamic stimulation. *Brain* **2008**, *131*, 132–145. [CrossRef] [PubMed]
61. Pietraszko, W.; Furgala, A.; Gorecka-Mazur, A.; Thor, P.; Moskala, M.; Polak, J.; Surowka, A.D.; Krygowska-Wajs, A. Efficacy of deep brain stimulation of the subthalamic nucleus on autonomic dysfunction in patients with Parkinson's disease. *Folia Med. Crac.* **2013**, *53*, 15–22.
62. Fritsche, H.M.; Ganzer, R.; Schlaier, J.; Wieland, W.F.; Brawanski, A.; Lange, M. Acute urinary retention in two patients after subthalamic nucleus deep brain stimulation (STN-DBS) for the treatment of advanced Parkinson's disease. *Mov. Disord.* **2009**, *24*, 1553–1554. [CrossRef] [PubMed]
63. Winge, K.; Nielsen, K.K. Bladder dysfunction in advanced Parkinson's disease. *Neurourol. Urodyn.* **2012**, *31*, 1279–1283. [CrossRef] [PubMed]
64. Mordasini, L.; Kessler, T.M.; Kiss, B.; Schüpbach, M.; Pollo, C.; Kaelin-Lang, A. Bladder function in patients with dystonia undergoing deep brain stimulation. *Parkinsonism Relat. Disord.* **2014**, *20*, 1015–1017. [CrossRef] [PubMed]
65. Green, A.L.; Stone, E.; Sitsapesan, H.; Turney, B.W.; Coote, J.H.; Aziz, T.Z.; Hyam, J.A.; Lovick, T.A. Switching off micturition using deep brain stimulation at midbrain sites. *Ann. Neurol.* **2012**, *72*, 144–147. [CrossRef] [PubMed]
66. Kessler, T.M.; Burkhard, F.C.; Z'Brun, S.; Stibal, A.; Studer, U.E.; Hess, C.W.; Kaelin-Lang, A. Effect of thalamic deep brain stimulation on lower urinary tract function. *Eur. Urol.* **2008**, *53*, 607–612. [CrossRef] [PubMed]
67. Cersosimo, M.G.; Benarroch, E.E. Neural control of the gastrointestinal tract: Implications for Parkinson disease. *Mov. Disord.* **2008**, *23*, 1065–1075. [CrossRef] [PubMed]

68. Ciucci, M.R.; Barkmeier-Kraemer, J.M.; Sherman, S.J. Subthalamic nucleus deep brain stimulation improves deglutition in Parkinson's disease. *Mov. Disord.* **2008**, *23*, 676–683. [CrossRef] [PubMed]
69. Silbergleit, A.K.; LeWitt, P.; Junn, F.; Schultz, L.R.; Collins, D.; Beardsley, T.; Hubert, M.; Trosch, R.; Schwalb, J.M. Comparison of dysphagia before and after deep brain stimulation in Parkinson's disease. *Mov. Disord.* **2012**, *27*, 1763–1768. [CrossRef] [PubMed]
70. Derrey, S.; Chastan, N.; Maltete, D.; Verin, E.; Dechelotte, P.; Lefaucheur, R.; Proust, F.; Freger, P.; Leroi, A.M.; Weber, J. Impact of deep brain stimulation on pharyngo-esophageal motility: A randomized cross-over study. *Neurogastroenterol. Motil.* **2015**, *27*, 1214–1222. [CrossRef] [PubMed]
71. Arai, E.; Arai, M.; Uchiyama, T.; Higuchi, Y.; Aoyagi, K.; Yamanaka, Y.; Yamamoto, T.; Nagano, O.; Shiina, A.; Maruoka, D.; et al. Subthalamic deep brain stimulation can improve gastric emptying in Parkinson's disease. *Brain* **2012**, *135*, 1478–1485. [CrossRef] [PubMed]
72. Krygowska-Wajs, A.; Furgala, A.; Gorecka-Mazur, A.; Pietraszko, W.; Thor, P.; Potasz-Kulikowska, K.; Moskala, M. The effect of subthalamic deep brain stimulation on gastric motility in Parkinson's disease. *Parkinsonism Relat. Disord.* **2016**, *26*, 35–40. [CrossRef] [PubMed]
73. Priori, A.; Foffani, G.; Rossi, L.; Marceglia, S. Adaptive deep brain stimulation (aDBS) controlled by local field potential oscillations. *Exp. Neurol.* **2013**, *245*, 77–86. [CrossRef] [PubMed]
74. Alamri, A.; Ughratdar, I.; Samuel, M.; Ashkan, K. Deep brain stimulation of the subthalamic nucleus in Parkinson's disease 2003–2013: Where are we another 10 years on? *Br. J. Neurosurg.* **2015**, *29*, 319–328. [CrossRef] [PubMed]
75. Rosa, M.; Giannicola, G.; Marceglia, S.; Fumagalli, M.; Barbieri, S.; Priori, A. Neurophysiology of deep brain stimulation. *Int. Rev. Neurobiol.* **2012**, *107*, 23–55. [PubMed]

brain sciences

MDPI

Review

DBS for Obesity

Ruth Franco [1], Erich T. Fonoff [2], Pedro Alvarenga [3], Antonio Carlos Lopes [3], Euripides C. Miguel [3], Manoel J. Teixeira [2], Durval Damiani [1] and Clement Hamani [2,4,5,*]

1 Division of Pediatric Endocrinology, Children's Hospital, University of São Paulo Medical School, São Paulo 05403-000, Brazil; franco.ruth@icloud.com (R.F.); durvald@iconet.com.br (D.D.)
2 Division of Functional Neurosurgery of Institute of Psychiatry, Department of Neurology, University of São Paulo Medical School, São Paulo 01060-970, Brazil; erich.fonoff@gmail.com (E.T.F.); manoeljacobsen@gmail.com (M.J.T.)
3 Department of Psychiatry, Institute of Psychiatry, University of São Paulo Medical School, São Paulo 01060-970, Brazil; pedrodealvarenga@gmail.com (P.A.); antonioclopesmd@gmail.com (A.C.L.); ecmiguel7@gmail.com (E.C.M.)
4 Division of Neurosurgery, Toronto Western Hospital, University of Toronto, Toronto, ON M5T 1R8, Canada
5 Division of Neuroimaging, Centre for Addiction and Mental Health, Toronto, ON M5T 1R8, Canada
* Correspondence: Clement.Hamani@camh.ca; Tel.: +1-416-603-5771

Academic Editors: Tipu Aziz and Alex Green
Received: 21 June 2016; Accepted: 12 July 2016; Published: 18 July 2016

Abstract: Obesity is a chronic, progressive and prevalent disorder. Morbid obesity, in particular, is associated with numerous comorbidities and early mortality. In patients with morbid obesity, pharmacological and behavioral approaches often have limited results. Bariatric surgery is quite effective but is associated with operative failures and a non-negligible incidence of side effects. In the last decades, deep brain stimulation (DBS) has been investigated as a neurosurgical modality to treat various neuropsychiatric disorders. In this article we review the rationale for selecting different brain targets, surgical results and future perspectives for the use of DBS in medically refractory obesity.

Keywords: deep brain stimulation; obesity; hypothalamus; nucleus accumbens

1. Introduction

Obesity is a chronic and progressive disorder with a prevalence of 600 million individuals worldwide [1]. In 2014, approximately 39% of the adult population was considered to be overweight and 13% obese [1]. Unfortunately, this number is on the rise [2]. Such an increased incidence is problematic due to the associated comorbidity and the reduced life expectancy in patients bearing the disease [3].

Morbid obesity is defined as a body mass index (mass/height^2) >40 kg/m^2. It affects more than eight million Americans with a prevalence of approximately 14% [4]. Morbidly obese patients not only die prematurely, but they also have a poor quality of life [5]. This is due in part to the numerous co-morbidities associated with the disease, including diabetes, cardiovascular disorders, osteoarthritis, hepatic steatosis, among others.

A major problem in patients with morbid obesity is that pharmacological and behavioral approaches often have limited results [6,7]. Surgical interventions, including bariatric procedures, are currently being used with variable outcomes and a non-negligible incidence of side effects [8]. That said, bariatric surgery is currently the most efficacious treatment for rapid weight loss in morbid obesity, with overall clinical results superior to those achieved with the best medical management [9,10]. In addition to side effects, a common problem with the bariatric surgery is the relatively high incidence of recurrence [11]. In fact, recent long-term follow-up studies have shown that up to 46% of patients may regain weight in the postoperative period [12]. One of the main factors associated with disease

recurrence is compulsive eating [13,14]. It has now been suggested that patients who present binge eating disorders or loss of control eating have less weight loss and/or more weight regain after bariatric surgery [14]. This stresses the fact that obesity cannot be simply regarded as an endocrinological condition, but as a disease with a strong neuropsychiatric component.

Deep brain stimulation (DBS) involves the delivery of electrical current to the brain parenchyma. This is accomplished by implanting electrodes into specific brain targets and connecting them to a pacemaker (i.e., implantable pulse generator) [15]. The latter is programmed so that current may be delivered at different amplitudes, pulse widths and frequencies in monopolar or bipolar configurations. The electrodes most commonly used today have four different contacts, which may be activated alone or in combination. Depending on the stimulation parameters and brain target, different neural elements or circuits may be involved in a DBS response [16]. In recent years, a few reports have been published using DBS to treat obesity [17–19]. In this article we review the rationale for selecting different brain targets, surgical results and future perspectives of using DBS for treating medically refractory obesity.

2. Anatomical Targets

The pathophysiology of obesity involves not only altered patterns of eating and satiety but also reward and compulsive aspects of food intake. As such, DBS targets currently proposed to treat obesity include the hypothalamus and nucleus accumbens (NAc) [20,21].

The hypothalamus may be subdivided in various anatomical and functional subregions/nuclei. Some of the most commonly involved in mechanisms of feeding and energy balance are the arcuate nucleus (ARC), the dorsal medial nucleus, the paraventricular nucleus, the lateral hypothalamus (LH) and the ventral medial nucleus (VM). An in-depth review of the neurocircuitry of feeding and satiety, including all the cell types and peptides involved, may be found elsewhere [22–24]. Of particular interest are the VM and LH, as these nuclei are being considered as potential targets for DBS surgery. The VM is a relatively large nucleus with an abundance of leptin receptors [22]. Leptin and insulin provide the hypothalamus with peripheral signals of adiposity [25]. If levels of these hormones are high, the organism reduces feeding. In the hypothalamus, prominent levels of leptin and insulin receptors may also be found in ARC [22,24]. In this nucleus, these hormones modulate activity of populations of cells expressing neuropeptide Y/agouti gene-related protein and cocaine- and amphetamine-related transcript (CART)/pro-opiomelanocortin (POMC) [22,26]. In general, states of negative energy deficit (e.g., starvation) increase the activity of ARC NPY/AGRP neurons, ultimately favoring food consumption. Overall, ARC NPY/AGRP neurons project to most hypothalamic nuclei involved in feeding control [22].

The LH extends through most of the anteropoesterior axis of the hypothalamus [27]. It is composed of diffuse populations of neurons intermingled with fibers, largely from the medial forebrain bundle (MFB) [27]. Subpopulations of cells in LH express different peptides and hormones, including orexins and melanin-concentrating hormone (MCH). Both have orexigenic effects and tend to increase food consumption [22,27].

In contrast to the hypothalamus, the NAc has been suggested to play a role in rewarding aspects of food intake and compulsive feeding. Some of the evidence suggesting an involvement of the NAc in the pathophysiology of obesity includes the following: the pattern of compulsive eating shown in some forms of clinical and preclinical obesity often resembles that of drug addiction [28–30]. Food craving and the anticipation of food reward in preclinical models are associated with changes in D2 striatal receptors [31]. In rodents, binging on sugar and the ingestion of fat diets increase the release of dopamine in the NAc [32,33]. In addition to the above-mentioned evidence, numerous neuroimaging studies using positron emission tomography or functional magnetic resonance imaging have been conducted in obese patients at baseline and during activation tasks (for a review see [34, 35]). Overall, sensory stimuli related to palatable foods seem to activate cortical regions and the reward circuitry, including the ventral striatum [34,35]. In some studies, hyper-responsiveness of reward-related regions has been suggested to forecast a poor outcome to weight-loss programs [36].

Though not a consensus, studies in obese patients treated with bariatric surgery have shown that the response of the ventral striatum to images of caloric food is less pronounced than that recorded prior to surgery [37]. Also commonly investigated with neuroimaging is the status of the dopaminergic system. Though results are not consistent across trials, a few studies have shown that food-related sensory stimuli elicit dopamine release and that obese individuals have a low D2 binding in the striatum [34,35,38–40].

3. Preclinical Studies

Based on studies in which lesions, pharmacological agents and electrical stimulation were applied to the hypothalamus, as well as on clinical cases of patients with brain tumors, the VM and LH have been suggested as being "satiety" and "feeding" hypothalamic centers, respectively [41–43]. Though this "dual center hypothesis" is somewhat outdated, much has been learned from experiments manipulating hypothalamic regions to investigate mechanisms and neurocircuits of food intake and satiety. Early preclinical work in which either the VM or LH were lesioned or pharmacologically inhibited has shown an increase in feeding or satiety, respectively [44,45]. In contrast to the relative uniformity of conclusions reached by the above-mentioned studies, results with the use of electrical stimulation are far more complex. As the hypothalamus is involved in numerous physiological functions, stimulation of different nuclei may influence multiple physiologic processes. In addition, current may spill over and modulate activity in adjacent nuclei and nearby structures, including the fornix and medial forebrain bundle. Stimulation delivered to the VM of rodents [46–49], dogs [50], mini-pigs [51], and nonhuman primates [52] at settings known to drive neurons and axonal projections has been shown to alter feeding behavior, the type of food ingested and/or has slowed down weight gain over time. However, these results are not consistent with a few studies in these same species showing that stimulation may not be effective [53] or even increase food consumption [54]. Though part of the discrepancies across studies may be explained by the use of different stimulation settings (e.g., 50 vs. 130 Hz and targeted regions), this is still not able to fully explain why studies using similar paradigms, targeting somewhat analogous regions, reached different conclusions. As for the LH, initial studies in rodents [55,56] and felines [57] have largely shown that stimulation induced feeding. Part of those findings, however, has been attributed to the stimulation of structures adjacent to the LH, such as the medial forebrain bundle [27]. The MFB is comprised of axonal projections that interconnect over 50 brainstem, subcortical and cortical regions, including those involved in mechanisms of reward (e.g., LH, nucleus accumbens and ventral tegmental area). In contrast to earlier reports, however, recent studies in rodents using high frequency stimulation (e.g., above 100 Hz) have shown that LH DBS may reduce weight gain over time [58,59].

In contrast to the long history of hypothalamic stimulation for obesity, studies in which the nucleus accumbens was targeted in animal models are much more recent. Lesions of the NAc in rodents decrease food-hoarding behavior and are associated with weight loss [60]. Stimulation of the NAc shell delivered for 14 days to diet-induced obese rats led to significant reductions in total energy intake and weight gain, an effect that was associated with an up-regulation of the D2 receptor and increased DA levels [61]. Mice treated with NAc shell DBS were found to have a decrease in binge eating and an increase in immediate early gene expression in this same region [62]. D2 receptor antagonists attenuated DBS effects. In diet-induced obese mice, chronic NAc shell DBS has been found to reduce caloric intake and lead to weight loss. In rodents, stimulation of the accumbens core has also been shown to reduce binge eating [63].

4. Clinical Studies

Stereotactic ablative surgery targeting the hypothalamus for the treatment of obesity was initially been carried 40 years ago [64,65]. Overall, the procedure was proven to be safe, resulting in significant, though transient (e.g., few weeks), reductions in appetite and weight loss.

In 2008, Hamani et al. reported on a single patient with obesity treated with hypothalamic DBS [17]. Postoperative reconstruction of the electrode placement has shown that contacts used for stimulation were located near the fornix. While no weight changes were observed with high frequency DBS (130 Hz), when stimulated at 3.0–4.0 V, 210 μsec and 50 Hz, the patient lost 12 kg over five months. This was not due to significant dietary changes but to a reduction in food craving [17]. Over time, however, the patient reported that he was unable to sleep with the system activated and started turning it off at night. Without stimulation, he began nighttime binging and regained the weight he had lost [17].

In a more recent trial, Whiting et al. reported on the safety, efficacy and calorimetric effects of LH DBS in patients with obesity followed for an average of 35 months [18]. The three individuals in that study were diagnosed with refractory morbid obesity, which included a failure of bariatric surgery. Several scales were applied to assess the effects of DBS on eating and quality of life, including the Gormally Binge Eating Scale, the Cognitive Restraint subscale (used to assess dieting skills), a hunger scale, the Body Shape Questionnaire, and the Impact of Weight on Quality of Life–Lite Questionnaire. Though one of the participants had postoperative improvements in some of these scales, overall testing suggested that DBS did not induce significant changes. Also unchanged after DBS were blood tests to measure nutritional status, pituitary hormones, and neuroendocrine/neuropeptide studies. The most striking aspect of the trial was that DBS significantly increased resting metabolic state (RMR) in two patients. In these subjects, RMR improvement was in the order of 28% and 9%. Despite this fact, no consistent weight changes were noticed. DBS settings were 90 μsec, 185 Hz at different stimulation voltages [18].

In 2016, Harat and colleagues implanted NAc DBS electrodes in a 19-year-old patient who developed hypothalamic obesity following the onset and surgery for the removal of a craniopharyngioma [19]. Her weight before surgery was 151.4 kg. Three months after DBS she weighed 132 kg. Over time, her weight fluctuated due to a few instances in which the pacemaker was accidentally switched off. At the last follow-up visit (14 months after DBS), her weight was 138 kg. During periods in which the electrodes were found to be off, she reported increased food craving. This is of importance, as reductions in food craving and compulsive eating are some of the mechanisms through which NAc DBS has been postulated to exert its effects. Settings used in that study were 2–3.75 mA, 130 Hz and 208 μsec [19].

5. Future Perspectives and Applications of DBS in Obesity

To date, experience with DBS for obesity is quite limited. Overall, surgery has been proven to be safe, but no definitive conclusions can be made as to whether it is effective. Despite the number of studies published in animal models, several clinical aspects are still unclear, including target selection, the kinetics of DBS, or ideal stimulation parameters. Also unknown is whether DBS will work on genetic forms of obesity.

Prader Willi Syndrome (PWS) is one of the main causes of genetic obesity during childhood. Approximately 70% of patients have a deletion in chromosome 15 (15q11–q13) [66,67]. Of the remainder of patients, 25% have maternal uniparental disomy and 5% have imprinting defects. In infants and children, PWS is characterized by hypotonia, delayed neuropsychological development, lower-than-expected growth, hypogonadism, and hyperphagia [68,69]. Severe to morbid obesity is the most relevant problem of the syndrome due to associated comorbidities and early mortality. Hyperphagia in PWS is often refractory to pharmacological and psychotherapeutic approaches, as well as bariatric surgery [70]. Several factors suggest that the increased appetite in PWS may be associated with hypothalamic dysfunction [71]. First, the disease is comprised of a spectrum of hormonal problems (e.g., low levels of growth hormone, hypogonadotropic hypogonadism, temperature dysregulation). Post-mortem studies in patients with PWS have shown a reduced number of cells in the paraventricular nucleus, including neurons that synthesize anorexigenic hormones and oxytocin [72]. In PWS, imaging studies have shown an increased activation of reward circuits when patients are presented with food stimuli [73]. Bearing these facts in mind, DBS in either the

hypothalamus or NAc has been hypothesized as a suitable alternative for the treatment of patients with PWS [74,75].

Another aspect that deserves to be discussed is the advancement of DBS technology, which may improve the delivery of stimulation to some of the targets discussed above. The hypothalamus is a small structure responsible for modulating various physiological functions. In this target, directional leads could certainly be of help to steer current into specific regions while avoiding spread to adjacent undesirable structures [76,77]. This may, in theory, improve safety and reduce the incidence of stimulation-induced side effects.

6. Conclusions

Data from animal studies and preliminary reports in humans suggest that DBS may be a promising alternative for the treatment of obesity. Structures involved in mechanisms of feeding and rewarding aspects of food intake, namely the hypothalamus and NAc, have been considered as potential targets. Though surgery was shown to be safe in the few patients treated so far, further studies are still needed not only to better characterize the side effect profile of these procedures but also their actual efficacy.

As in previous functional neurosurgery studies, trials on DBS for obesity have to take several issues into account. Inclusion criteria should be strict, with a clearly defined diagnosis, measures of refractoriness and recruitment of patients with severe forms of the disease. In addition, trials need to be carried out in an ethical manner [78–80], with particular attention paid to the informed consent process, long-term follow up, clinical care and support. Ideally, patients should be assessed by a multidisciplinary team of endocrinologists, neurosurgeons, psychiatrists and neuropsychologists, so that comprehensive care may be provided.

In summary, results of preclinical and early clinical trials using DBS for obesity have been promising. However, numerous questions remain unanswered, including the optimal target, stimulation parameters, and clinical aspects of the patients to be included (e.g., previous failure to bariatric surgery, compulsive eating, among other). Further work is certainly needed to address these issues.

Acknowledgments: No funding was required for conducting this work.

Author Contributions: All authors either wrote parts of the text or provided insights on the manuscript.

Conflicts of Interest: The authors declare no conflict of interest.

Abbreviations

DBS	deep brain stimulation
NAc	nucleus accumbens
LH	lateral hypothalamus
PWS	Prader Willi syndrome
VM	ventromedial nucleus of the hypothalamus

References

1. World Health Organization (WHO). Obesity and Overweight. Available online: http://www.who.int/mediacentre/factsheets/fs311/en/ (accessed on 11 July 2016).
2. Finucane, M.M.; Stevens, G.A.; Cowan, M.J.; Danaei, G.; Lin, J.K.; Paciorek, C.J.; Singh, G.M.; Gutierrez, H.R.; Lu, Y.; Bahalim, A.N.; et al. National, regional, and global trends in body-mass index since 1980: Systematic analysis of health examination surveys and epidemiological studies with 960 country-years and 9.1 million participants. *Lancet* **2011**, *377*, 557–567. [CrossRef]
3. Fontaine, K.R.; Redden, D.T.; Wang, C.; Westfall, A.O.; Allison, D.B. Years of life lost due to obesity. *JAMA* **2003**, *289*, 187–193. [CrossRef] [PubMed]
4. Flegal, K.M.; Carroll, M.D.; Ogden, C.L.; Curtin, L.R. Prevalence and trends in obesity among US adults, 1999–2008. *JAMA* **2010**, *303*, 235–241. [CrossRef] [PubMed]

5. Must, A.; Spadano, J.; Coakley, E.H.; Field, A.E.; Colditz, G.; Dietz, W.H. The disease burden associated with overweight and obesity. *JAMA* **1999**, *282*, 1523–1529. [CrossRef] [PubMed]
6. Shi, X.; Karmali, S.; Sharma, A.M.; Birch, D.W. A review of laparoscopic sleeve gastrectomy for morbid obesity. *Obes. Surg.* **2010**, *20*, 1171–1177. [CrossRef] [PubMed]
7. Connelly, J.B.; Duaso, M.J.; Butler, G. A systematic review of controlled trials of interventions to prevent childhood obesity and overweight: A realistic synthesis of the evidence. *Public Health* **2007**, *121*, 510–517. [CrossRef] [PubMed]
8. Chang, S.H.; Stoll, C.R.; Song, J.; Varela, J.E.; Eagon, C.J.; Colditz, G.A. The effectiveness and risks of bariatric surgery: An updated systematic review and meta-analysis, 2003–2012. *JAMA Surg.* **2014**, *149*, 275–287. [CrossRef] [PubMed]
9. Cheng, J.; Gao, J.; Shuai, X.; Wang, G.; Tao, K. The comprehensive summary of surgical versus non-surgical treatment for obesity: A systematic review and meta-analysis of randomized controlled trials. *Oncotarget* **2016**. [CrossRef] [PubMed]
10. Gloy, V.L.; Briel, M.; Bhatt, D.L.; Kashyap, S.R.; Schauer, P.R.; Mingrone, G.; Bucher, H.C.; Nordmann, A.J. Bariatric surgery versus non-surgical treatment for obesity: A systematic review and meta-analysis of randomised controlled trials. *BMJ* **2013**, *347*, f5934. [CrossRef] [PubMed]
11. Ells, L.J.; Mead, E.; Atkinson, G.; Corpeleijn, E.; Roberts, K.; Viner, R.; Baur, L.; Metzendorf, M.I.; Richter, B. Surgery for the treatment of obesity in children and adolescents. *Cochrane Database Syst. Rev.* **2015**. [CrossRef]
12. Kalarchian, M.A.; Marcus, M.D.; Wilson, G.T.; Labouvie, E.W.; Brolin, R.E.; LaMarca, L.B. Binge eating among gastric bypass patients at long-term follow-up. *Obes. Surg.* **2002**, *12*, 270–275. [CrossRef] [PubMed]
13. Saunders, R. Compulsive eating and gastric bypass surgery: What does hunger have to do with it? *Obes. Surg.* **2001**, *11*, 757–761. [CrossRef] [PubMed]
14. Meany, G.; Conceicao, E.; Mitchell, J.E. Binge eating, binge eating disorder and loss of control eating: Effects on weight outcomes after bariatric surgery. *Eur. Eat Disord. Rev.* **2014**, *22*, 87–91. [CrossRef] [PubMed]
15. Hamani, C.; Lozano, A.M. Hardware-related complications of deep brain stimulation: A review of the published literature. *Stereotact. Funct. Neurosurg.* **2006**, *84*, 248–251. [CrossRef] [PubMed]
16. Hamani, C.; Temel, Y. Deep brain stimulation for psychiatric disease: Contributions and validity of animal models. *Sci. Trans. Med.* **2012**, *4*, 142–148. [CrossRef] [PubMed]
17. Hamani, C.; McAndrews, M.P.; Cohn, M.; Oh, M.; Zumsteg, D.; Shapiro, C.M.; Wennberg, R.A.; Lozano, A.M. Memory enhancement induced by hypothalamic/fornix deep brain stimulation. *Ann. Neurol.* **2008**, *63*, 119–123. [CrossRef] [PubMed]
18. Whiting, D.M.; Tomycz, N.D.; Bailes, J.; de Jonge, L.; Lecoultre, V.; Wilent, B.; Alcindor, D.; Prostko, E.R.; Cheng, B.C.; Angle, C.; et al. Lateral hypothalamic area deep brain stimulation for refractory obesity: A pilot study with preliminary data on safety, body weight, and energy metabolism. *J. Neurosurg.* **2013**, *119*, 56–63. [CrossRef] [PubMed]
19. Harat, M.; Rudas, M.; Zielinski, P.; Birska, J.; Sokal, P. Nucleus accumbens stimulation in pathological obesity. *Neurol. Neurochir. Pol.* **2016**, *50*, 207–210. [CrossRef] [PubMed]
20. Halpern, C.H.; Torres, N.; Hurtig, H.I.; Wolf, J.A.; Stephen, J.; Oh, M.Y.; Williams, N.N.; Dichter, M.A.; Jaggi, J.L.; Caplan, A.L.; et al. Expanding applications of deep brain stimulation: A potential therapeutic role in obesity and addiction management. *Acta Neurochir.* **2011**, *153*, 2293–2306. [CrossRef] [PubMed]
21. Tomycz, N.D.; Whiting, D.M.; Oh, M.Y. Deep brain stimulation for obesity–from theoretical foundations to designing the first human pilot study. *Neurosurg. Rev.* **2012**, *35*, 37–42. [CrossRef] [PubMed]
22. Williams, G.; Bing, C.; Cai, X.J.; Harrold, J.A.; King, P.J.; Liu, X.H. The hypothalamus and the control of energy homeostasis: Different circuits, different purposes. *Physiol. Behav.* **2001**, *74*, 683–701. [CrossRef]
23. Atasoy, D.; Betley, J.N.; Su, H.H.; Sternson, S.M. Deconstruction of a neural circuit for hunger. *Nature* **2012**, *488*, 172–177. [CrossRef] [PubMed]
24. Simpson, K.A.; Martin, N.M.; Bloom, S.R. Hypothalamic regulation of food intake and clinical therapeutic applications. *Arq. Bras. Endocrinol. Metabol.* **2009**, *53*, 120–128. [CrossRef] [PubMed]
25. Elmquist, J.K.; Elias, C.F.; Saper, C.B. From lesions to leptin: Hypothalamic control of food intake and body weight. *Neuron* **1999**, *22*, 221–232. [CrossRef]
26. Elmquist, J.K. Hypothalamic pathways underlying the endocrine, autonomic, and behavioral effects of leptin. *Physiol. Behav.* **2001**, *74*, 703–708. [CrossRef]

27. Stuber, G.D.; Wise, R.A. Lateral hypothalamic circuits for feeding and reward. *Nat. Neurosci.* **2016**, *19*, 198–205. [CrossRef] [PubMed]
28. Rospond, B.; Szpigiel, J.; Sadakierska-Chudy, A.; Filip, M. Binge eating in pre-clinical models. *Pharmacol. Rep.* **2015**, *67*, 504–512. [CrossRef] [PubMed]
29. DiLeone, R.J.; Taylor, J.R.; Picciotto, M.R. The drive to eat: Comparisons and distinctions between mechanisms of food reward and drug addiction. *Nat. Neurosci.* **2012**, *15*, 1330–1335. [CrossRef] [PubMed]
30. Hone-Blanchet, A.; Fecteau, S. Overlap of food addiction and substance use disorders definitions: Analysis of animal and human studies. *Neuropharmacology* **2014**, *85*, 81–90. [CrossRef] [PubMed]
31. Johnson, P.M.; Kenny, P.J. Dopamine D2 receptors in addiction-like reward dysfunction and compulsive eating in obese rats. *Nat. Neurosci.* **2010**, *13*, 635–641. [CrossRef] [PubMed]
32. Rada, P.; Avena, N.M.; Hoebel, B.G. Daily bingeing on sugar repeatedly releases dopamine in the accumbens shell. *Neuroscience* **2005**, *134*, 737–744. [CrossRef] [PubMed]
33. Rada, P.; Avena, N.M.; Barson, J.R.; Hoebel, B.G.; Leibowitz, S.F. A high-fat meal, or intraperitoneal administration of a fat emulsion, increases extracellular dopamine in the nucleus accumbens. *Brain. Sci.* **2012**, *2*, 242–253. [CrossRef] [PubMed]
34. Val-Laillet, D.; Aarts, E.; Weber, B.; Ferrari, M.; Quaresima, V.; Stoeckel, L.E.; Alonso-Alonso, M.; Audette, M.; Malbert, C.H.; Stice, E. Neuroimaging and neuromodulation approaches to study eating behavior and prevent and treat eating disorders and obesity. *Neuroimage Clin.* **2015**, *8*, 1–31. [CrossRef] [PubMed]
35. Iozzo, P. Metabolic imaging in obesity: Underlying mechanisms and consequences in the whole body. *Ann. N. Y. Acad. Sci.* **2015**, *1353*, 21–40. [CrossRef] [PubMed]
36. Murdaugh, D.L.; Cox, J.E.; Cook, E.W., 3rd; Weller, R.E. fMRI reactivity to high-calorie food pictures predicts short- and long-term outcome in a weight-loss program. *Neuroimage* **2012**, *59*, 2709–2721. [CrossRef] [PubMed]
37. Ochner, C.N.; Kwok, Y.; Conceicao, E.; Pantazatos, S.P.; Puma, L.M.; Carnell, S.; Teixeira, J.; Hirsch, J.; Geliebter, A. Selective reduction in neural responses to high calorie foods following gastric bypass surgery. *Ann. Surg.* **2011**, *253*, 502–507. [CrossRef] [PubMed]
38. Wang, G.J.; Volkow, N.D.; Fowler, J.S. The role of dopamine in motivation for food in humans: Implications for obesity. *Expert Opin. Ther. Targets* **2002**, *6*, 601–609. [CrossRef] [PubMed]
39. Volkow, N.D.; Wang, G.J.; Fowler, J.S.; Logan, J.; Jayne, M.; Franceschi, D.; Wong, C.; Gatley, S.J.; Gifford, A.N.; Ding, Y.S.; Pappas, N. "Nonhedonic" food motivation in humans involves dopamine in the dorsal striatum and methylphenidate amplifies this effect. *Synapse* **2002**, *44*, 175–180. [CrossRef] [PubMed]
40. Wang, G.J.; Volkow, N.D.; Logan, J.; Pappas, N.R.; Wong, C.T.; Zhu, W.; Netusll, N.; Fowler, J.S. Brain dopamine and obesity. *Lancet* **2001**, *357*, 354–357. [CrossRef]
41. Ahima, R.S.; Antwi, D.A. Brain regulation of appetite and satiety. *Endocrinol. Metab. Clin. N. Am.* **2008**, *37*, 811–823. [CrossRef] [PubMed]
42. Bernardis, L.L. Ventromedial and dorsomedial hypothalamic syndromes in the weanling rat: Is the "center" concept really outmoded? *Brain Res. Bull.* **1985**, *14*, 537–549. [CrossRef]
43. Bernardis, L.L.; Bellinger, L.L. The lateral hypothalamic area revisited: Neuroanatomy, body weight regulation, neuroendocrinology and metabolism. *Neurosci. Biobehav. Rev.* **1993**, *17*, 141–193. [CrossRef]
44. Stricker, E.M.; Swerdloff, A.F.; Zigmond, M.J. Intrahypothalamic injections of kainic acid produce feeding and drinking deficits in rats. *Brain Res.* **1978**, *158*, 470–473. [CrossRef]
45. Anand, B.K.; Brobeck, J.R. Localization of a "feeding center" in the hypothalamus of the rat. *Proc. Soc. Exp. Biol. Med.* **1951**, *77*, 323–324. [CrossRef] [PubMed]
46. Bielajew, C.; Stenger, J.; Schindler, D. Factors that contribute to the reduced weight gain following chronic ventromedial hypothalamic stimulation. *Behav. Brain Res.* **1994**, *62*, 143–148. [CrossRef]
47. Krasne, F.B. General Disruption Resulting from Electrical Stimulus of Ventromedial Hypothalamus. *Science* **1962**, *138*, 822–823. [CrossRef] [PubMed]
48. Ruffin, M.; Nicolaidis, S. Electrical stimulation of the ventromedial hypothalamus enhances both fat utilization and metabolic rate that precede and parallel the inhibition of feeding behavior. *Brain Res.* **1999**, *846*, 23–29. [CrossRef]
49. Stenger, J.; Fournier, T.; Bielajew, C. The effects of chronic ventromedial hypothalamic stimulation on weight gain in rats. *Physiol. Behav.* **1991**, *50*, 1209–1213. [CrossRef]

50. Brown, F.D.; Fessler, R.G.; Rachlin, J.R.; Mullan, S. Changes in food intake with electrical stimulation of the ventromedial hypothalamus in dogs. *J. Neurosurg.* **1984**, *60*, 1253–1257. [CrossRef] [PubMed]
51. Melega, W.P.; Lacan, G.; Gorgulho, A.A.; Behnke, E.J.; De Salles, A.A. Hypothalamic deep brain stimulation reduces weight gain in an obesity-animal model. *PLoS ONE* **2012**, *7*, e30672. [CrossRef] [PubMed]
52. Torres, N.; Chabardes, S.; Piallat, B.; Devergnas, A.; Benabid, A.L. Body fat and body weight reduction following hypothalamic deep brain stimulation in monkeys: An intraventricular approach. *Int. J. Obes. (Lond.)* **2012**, *36*, 1537–1544. [CrossRef] [PubMed]
53. Ettrup, K.S.; Sorensen, J.C.; Rodell, A.; Alstrup, A.K.; Bjarkam, C.R. Hypothalamic deep brain stimulation influences autonomic and limbic circuitry involved in the regulation of aggression and cardiocerebrovascular control in the Gottingen minipig. *Stereotact. Funct. Neurosurg.* **2012**, *90*, 281–291. [CrossRef] [PubMed]
54. Lacan, G.; De Salles, A.A.; Gorgulho, A.A.; Krahl, S.E.; Frighetto, L.; Behnke, E.J.; Melega, W.P. Modulation of food intake following deep brain stimulation of the ventromedial hypothalamus in the vervet monkey. Laboratory investigation. *J. Neurosurg.* **2008**, *108*, 336–342. [CrossRef] [PubMed]
55. Mendelson, J. Lateral hypothalamic stimulation in satiated rats: The rewarding effects of self-induced drinking. *Science* **1967**, *157*, 1077–1079. [CrossRef] [PubMed]
56. Mendelson, J.; Chorover, S.L. Lateral Hypothalamic Stimulation in Satiated Rats: T-Maze Learning for Food. *Science* **1965**, *149*, 559–561. [CrossRef] [PubMed]
57. Delgado, J.M.; Anand, B.K. Increase of food intake induced by electrical stimulation of the lateral hypothalamus. *Am. J. Physiol.* **1953**, *172*, 162–168. [PubMed]
58. Sani, S.; Jobe, K.; Smith, A.; Kordower, J.H.; Bakay, R.A. Deep brain stimulation for treatment of obesity in rats. *J. Neurosurg.* **2007**, *107*, 809–813. [CrossRef] [PubMed]
59. Soto-Montenegro, M.L.; Pascau, J.; Desco, M. Response to deep brain stimulation in the lateral hypothalamic area in a rat model of obesity: In vivo assessment of brain glucose metabolism. *Mol. Imaging Biol.* **2014**, *16*, 830–837. [CrossRef] [PubMed]
60. Kelley, A.E.; Stinus, L. Disappearance of hoarding behavior after 6-hydroxydopamine lesions of the mesolimbic dopamine neurons and its reinstatement with L-dopa. *Behav. Neurosci.* **1985**, *99*, 531–545. [CrossRef] [PubMed]
61. Zhang, C.; Wei, N.L.; Wang, Y.; Wang, X.; Zhang, J.G.; Zhang, K. Deep brain stimulation of the nucleus accumbens shell induces anti-obesity effects in obese rats with alteration of dopamine neurotransmission. *Neurosci. Lett.* **2015**, *589*, 1–6. [CrossRef] [PubMed]
62. Halpern, C.H.; Tekriwal, A.; Santollo, J.; Keating, J.G.; Wolf, J.A.; Daniels, D.; Bale, T.L. Amelioration of binge eating by nucleus accumbens shell deep brain stimulation in mice involves D2 receptor modulation. *J. Neurosci.* **2013**, *33*, 7122–7129. [CrossRef] [PubMed]
63. Doucette, W.T.; Khokhar, J.Y.; Green, A.I. Nucleus accumbens deep brain stimulation in a rat model of binge eating. *Trans. Psychiatry* **2015**, *5*, e695. [CrossRef] [PubMed]
64. Quaade, F.; Vaernet, K.; Larsson, S. Stereotaxic stimulation and electrocoagulation of the lateral hypothalamus in obese humans. *Acta Neurochir. (Wien.)* **1974**, *30*, 111–117. [CrossRef] [PubMed]
65. Quaade, F. Letter: Stereotaxy for obesity. *Lancet* **1974**, *1*, 267. [CrossRef]
66. Goldstone, A.P. Prader-Willi syndrome: Advances in genetics, pathophysiology and treatment. *Trends Endocrinol. Metab.* **2004**, *15*, 12–20. [CrossRef] [PubMed]
67. Saitoh, S.; Buiting, K.; Cassidy, S.B.; Conroy, J.M.; Driscoll, D.J.; Gabriel, J.M.; Gillessen-Kaesbach, G.; Glenn, C.C.; Greenswag, L.R.; Horsthemke, B.; et al. Clinical spectrum and molecular diagnosis of Angelman and Prader-Willi syndrome patients with an imprinting mutation. *Am. J. Med. Genet.* **1997**, *68*, 195–206. [CrossRef]
68. Cassidy, S.B. Prader-Willi syndrome. *J. Med. Genet.* **1997**, *34*, 917–923. [CrossRef] [PubMed]
69. Cassidy, S.B.; Schwartz, S.; Miller, J.L.; Driscoll, D.J. Prader-Willi syndrome. *Genet. Med.* **2012**, *14*, 10–26. [CrossRef] [PubMed]
70. Scheimann, A.O.; Butler, M.G.; Gourash, L.; Cuffari, C.; Klish, W. Critical analysis of bariatric procedures in Prader-Willi syndrome. *J. Pediatr. Gastroenterol. Nutr.* **2008**, *46*, 80–83. [CrossRef] [PubMed]
71. Swaab, D.F. Prader-Willi syndrome and the hypothalamus. *Acta Paediatr. Suppl.* **1997**, *423*, 50–54. [CrossRef] [PubMed]

72. Swaab, D.F.; Purba, J.S.; Hofman, M.A. Alterations in the hypothalamic paraventricular nucleus and its oxytocin neurons (putative satiety cells) in Prader-Willi syndrome: A study of five cases. *J. Clin. Endocrinol. Metab.* **1995**, *80*, 573–579. [PubMed]
73. Miller, J.L.; James, G.A.; Goldstone, A.P.; Couch, J.A.; He, G.; Driscoll, D.J.; Liu, Y. Enhanced activation of reward mediating prefrontal regions in response to food stimuli in Prader-Willi syndrome. *J. Neurol. Neurosurg. Psychiatry* **2007**, *78*, 615–619. [CrossRef] [PubMed]
74. Ho, A.L.; Sussman, E.S.; Zhang, M.; Pendharkar, A.V.; Azagury, D.E.; Bohon, C.; Halpern, C.H. Deep Brain Stimulation for Obesity. *Cureus* **2015**, *7*, e259. [CrossRef] [PubMed]
75. Ho, A.L.; Sussman, E.S.; Pendharkar, A.V.; Azagury, D.E.; Bohon, C.; Halpern, C.H. Deep brain stimulation for obesity: Rationale and approach to trial design. *Neurosurg. Focus* **2015**, *38*, E8. [CrossRef] [PubMed]
76. Bour, L.J.; Lourens, M.A.; Verhagen, R.; de Bie, R.M.A.; Van Den Munckhof, P.; Schuurman, P.R.; Contarino, M.F. Directional Recording of Subthalamic Spectral Power Densities in Parkinson's Disease and the Effect of Steering Deep Brain Stimulation. *Brain Stimul.* **2015**, *8*, 730–741. [CrossRef] [PubMed]
77. Contarino, M.F.; Bour, L.J.; Verhagen, R.; Lourens, M.A.; de Bie, R.M.; van den Munckhof, P.; Schuurman, P.R. Directional steering: A novel approach to deep brain stimulation. *Neurology* **2014**, *83*, 1163–1169. [CrossRef] [PubMed]
78. Gilbert, F. The burden of normality: From 'chronically ill' to 'symptom free'. New ethical challenges for deep brain stimulation postoperative treatment. *J. Med. Ethics.* **2012**, *38*, 408–412. [CrossRef] [PubMed]
79. Grant, R.A.; Halpern, C.H.; Baltuch, G.H.; O'Reardon, J.P.; Caplan, A. Ethical considerations in deep brain stimulation for psychiatric illness. *J. Clin. Neurosci.* **2014**, *21*, 1–5. [CrossRef] [PubMed]
80. Pisapia, J.M.; Halpern, C.H.; Muller, U.J.; Vinai, P.; Wolf, J.A.; Whiting, D.M.; Wadden, T.A.; Baltuch, G.H.; Caplan, A.L. Ethical considerations in deep brain stimulation for the treatment of addiction and overeating associated with obesity. *AJOB Neurosci.* **2013**, *4*, 35–46. [CrossRef]

Section 4:
Brain Stimulation for Psychiatric Disease

brain sciences

MDPI

Review

Deep Brain Stimulation Frequency—A Divining Rod for New and Novel Concepts of Nervous System Function and Therapy

Erwin B. Montgomery Jr. * and Huang He

Greenville Neuromodulation Center, 179 Main St., Greenville, PA 16125, USA; Hehuang@grnneuromod.com
* Correspondence: ebmontgomery@wisc.edu; Tel.: +1-724-588-1324

Academic Editors: Tipu Aziz and Alex Green
Received: 9 June 2016; Accepted: 5 August 2016; Published: 17 August 2016

Abstract: The efficacy of Deep Brain Stimulation (DBS) for an expanding array of neurological and psychiatric disorders demonstrates directly that DBS affects the basic electroneurophysiological mechanisms of the brain. The increasing array of active electrode configurations, stimulation currents, pulse widths, frequencies, and pulse patterns provides valuable tools to probe electroneurophysiological mechanisms. The extension of basic electroneurophysiological and anatomical concepts using sophisticated computational modeling and simulation has provided relatively straightforward explanations of all the DBS parameters except frequency. This article summarizes current thought about frequency and relevant observations. Current methodological and conceptual errors are critically examined in the hope that future work will not replicate these errors. One possible alternative theory is presented to provide a contrast to many current theories. DBS, conceptually, is a noisy discrete oscillator interacting with the basal ganglia–thalamic–cortical system of multiple re-entrant, discrete oscillators. Implications for positive and negative resonance, stochastic resonance and coherence, noisy synchronization, and holographic memory (related to movement generation) are presented. The time course of DBS neuronal responses demonstrates evolution of the DBS response consistent with the dynamics of re-entrant mechanisms. Finally, computational modeling demonstrates identical dynamics as seen by neuronal activities recorded from human and nonhuman primates, illustrating the differences of discrete from continuous harmonic oscillators and the power of conceptualizing the nervous system as composed on interacting discrete nonlinear oscillators.

Keywords: Deep Brain Stimulation (DBS); stimulation frequency; discrete nonlinear oscillators; stochastic resonance; basal ganglia–thalamic–cortical system of oscillators; Principle of Causational Synonymy; Principle of Informational Synonymy

1. The Conundrum of Deep Brain Stimulation (DBS) Frequency

The effects of specific electrode configurations, the set of active cathodes and anodes, can be understood to relate to the regional anatomy and the volume of tissue activation. While the effects of stimulation parameters, such as stimulation current (voltage) and pulse width, can be understood as related to activation of neuronal axonal elements mediated by the presence or absence of myelin, axonal diameter, and chronaxie, how DBS frequency controls the response is much more problematic [1]. From the perspective of information transfer between neurons, such as those activated directly by the DBS pulse and the subsequent postsynaptic neurons, DBS frequency could have an effect on temporal summation. Such temporal summation would be important in propagating the DBS effect through a long sequence of interactions, ultimately affecting the orchestration of motor unit activities that mediate the clinical motor responses to DBS. However, the frequencies used typically in DBS are not

very effective at temporal summation [2], and thus the mechanisms by which DBS frequencies affect motor control likely are through some other mechanism(s).

The neurophysiology of the DBS frequency effect is an enigma and likely will require novel attempts to explicate. This article takes on this challenge, proceeding from the hypothesis that DBS can be considered a nonlinear discrete noise oscillator that is interjected into the nonlinear polysynaptic re-entrant discrete oscillators that comprise the basal ganglia–thalamic–cortical system. Whether this will illuminate the issue of DBS frequency effects requires the test of time. However, the theory requires the introduction of novel or, at the very least, unfamiliar concepts—hence the review-like nature of the article; these will be in addition to novel observations, hence the presentation of experiments. The format provides a significant advantage in the opportunity to make a full proposal with the mutual reinforcement or consilience of the many parts not typically available in most journals.

The first effort is to demonstrate just how complex the effect of varying DBS frequencies is, in this case the effect of various DBS frequencies in the vicinity of the subthalamic nucleus on bradykinesia in patients with Parkinson's disease, and to account for the failure of such complexity to be appreciated previously. There is considerable experience that demonstrates benefits from low-frequency DBS, for example of the STN for gait disturbances and for dystonia. Further, there may be differences in the frequency-dependent responses for different symptoms and signs of Parkinson's disease. The failure to appreciate this complexity, although it has long been suspected by astute clinicians, is both methodological and due to conceptual presuppositions. Thus, the review aspects of this article necessarily have an epistemological and historical bent. Also, it will be necessary to provide evidence of highly complex neural oscillators intrinsic to the basal ganglia–thalamic–cortical systems. Further, these oscillations are tied to the orchestration of motor unit behaviors that necessarily mediate the motoric effects of DBS. Next, the power of DBS to induce oscillations is discussed. Finally, preliminary evidence of complex interactions between the DBS oscillator and intrinsic oscillators in the subthalamic nucleus is presented.

The authors ask the indulgence of the reader. This is not a systematic review of all the publications that address the issue of DBS frequency. Such an effort is far beyond the opportunity reasonably offered by the editors. Thus, it is impossible to acknowledge the individual contributions made by many clinicians and scientists. This should not be taken as a judgment of their contributions or as a slight of any kind, rather a practical necessity. Second, this is a critique in the robust sense of the term. The critique recognizes that the issue of DBS frequency-based mechanisms is far from a complete understanding. Rather, considerable more research and scholarly efforts will be necessary. The strong critique is not a matter of fault-finding but more an effort so that future scientists and clinicians do not make the same mistakes that these authors and others have made. The term "error" as applied to any finding, inference, or conclusion is not a pejorative term. It is a wise person who learns from their mistakes; it a wiser person who learns from the mistakes of others. If one wants to change the future then one must see the present and the best way to see the present is to clearly see the past.

No theory or hypothesis arises spontaneously but rather is the consequence of a long history of reasoning. Reasoning laboriously worked through, perhaps centuries ago—for example by Aristotle (384–322 B.C.E.), now may be forgotten or taken for granted as a presupposition but is no less relevant. This fact was not lost on some of the greatest neuroscientists, such as Sir Charles Sherrington. Any competent critique must trace the conceptual antecedents as far back as is necessary to fully inform the review. It would be naïve, at best, or petulant, at worse, to discount analyses and wisdom from any age.

2. Conceptual History

Historically, the study of the effects of DBS frequencies has dichotomized the frequencies into high and low. This article demonstrates that such dichotomization is the result of a methodological error reinforced by highly intuitive conceptual appeal, also probably in error. This is not to say that clinicians did not see a difference when they stimulated at high frequencies compared to low frequencies. Rather,

one error lies in undersampling in the frequency domain, resulting in aliasing. This is not a matter of opinion but rather a direct consequence of the Nyquist theorem. Another error lies in the pooling of results across subjects when the intersubject variability is high. The result is information loss according to the Second Law of Thermodynamics. The study by Huang et al. [3] demonstrates the effects of these errors.

Results of the study by Huang et al. [3] demonstrate that a number of DBS frequencies over a wide range for any individual subject resulted in improved bradykinesia as measured by hand opening–closing (Figure 1). If only a few DBS frequencies are studied, the result would likely demonstrate aliasing, and it will appear as though the relationship between improvement and DBS frequency is a monotonically increasing function, which it is not in reality. Further, there was considerable intersubject variability, suggesting that pooling subjects would have obscured the true relationship between improvement and DBS frequency.

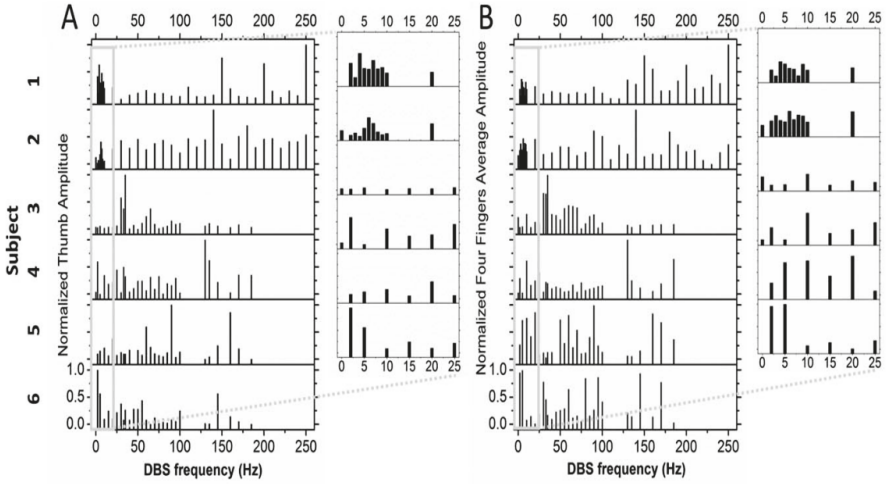

Figure 1. Patients with Parkinson's disease executed rapid hand opening and closing while wearing a glove that recorded finger and thumb movements. Following an overnight fast, these patients received their first dose of medications used to treat Parkinson's. Movements of the fingers were separated from those of the thumb. The movement amplitudes were normalized by scaling from 0 to 1 where 1 represents the maximum amplitude. The mean over all the movements was analyzed: (**A**) for the thumb and (**B**) for the fingers (pooled across all the fingers) for each subject. Absence of a column indicates that the associated stimulation frequency was unavailable with the subject's Implanted Pulse Generator (IPG). Multiple peaks in amplitude movements are found across multiple frequencies, including low frequencies. (Inserts) Amplitudes for the lower range of stimulation frequencies are shown in the expanded window [3].

The implications of the study by Huang et al. [3] go beyond the methodological (epistemological) to the reality (ontology) of the physiology of relevant parts of the nervous system, such as the basal ganglia–thalamic–cortical system. It is at least interesting that many years have passed since Cooper and colleagues' description of DBS as presently implemented in 1980 [4] and popularized by Benabid and colleagues in 1987 [5] before the issue of DBS frequency was evaluated systematically over a range of frequencies. One wonders why.

Perhaps the need to study the range of frequencies systematically did not raise sufficient concern. However, this could only be the case if the prior concept of a dichotomous effect of DBS frequency was thought to be sufficient. Further, there is nothing in past observations that would be evidence that such a dichotomous effect is sufficient. At the very least, it could demonstrate the Fallacy of Limited

Alternatives, where one explanation is considered more certain (falsely) when some alternatives are eliminated or not considered. However, for the one explanation to be certain, all reasonable alternatives would have to be considered and excluded, which, in the case of the effects of DBS frequencies, was not done.

Perhaps it was that the dichotomization of the effects of DBS frequencies seemed valid because of the analogy between pallidotomy and DBS in the vicinity of the globus pallidus interna. The logical fallacy of this analogy has been discussed elsewhere [6]. Interestingly, the contemporaneous theory of the pathophysiology of movement disorders, at theory positing excessive or reduced activity in the neurons of the globus pallidus interna (Globus Pallidus Interna (GPi Rate Theory)), was used to argue in favor of the analogy [7]. Considerable evidence shows that this notion of pathophysiology is no longer tenable [8].

The concerns raised here are more than historical. Successor theories likely share the same fatal flaw as the GPi Rate theory and therefore are at risk of delaying better theories. Current theories that posit excessive oscillations in the beta frequency range or excessive synchronization, along with the GPi Rate theory, share one-dimensional push–pull dynamics. At the very least, alternative theories that do not share these dynamics should be considered, particularly in view of the risks associated with the Fallacy of Limited Alternatives.

Given the lack of direct evidence, the presupposition of a dichotomous effect of DBS frequency then appears to be a default. Actually, dichotomization of phenomena and inferred causes marks human reasoning for millennia. Dichotomization is a consequence of the human epistemic condition. The inherent tendency to such a dichotomy, in appropriate circumstances, represents a pitfall only avoided if appreciated. Below the case is made for the ubiquity of dichotomization and, ultimately, its relevance to the consideration of DBS frequencies.

These dynamics were codified by Aristotle in his notion of *contraries*, where Aristotle wrote:

> "The physicists (. . .) have two modes of explanation. The first set make the underlying body one—either one of the three or something else which is denser than fire and rarer than air—then generate everything else from this, and obtain in multiplicity by condensation and rarefaction. Now these are contraries which may be generalized into '*excess and defect*' (italics added)" [9].

Aristotle's notion was extended by Galen (129–c. 200/c. 216, C.E.) in his notion of one-dimensional push–pull dynamics of relative excess or deficiencies of the humors. Galen's dynamics continue underlying neurological and psychiatric therapeutics [10]. John Hughlings Jackson (1835–1911), one of history's preeminent and defining neurologists, held a notion of positive and negative symptoms mediated by facilitation, inhibition, and inhibition of inhibition to release facilitation, continues to underlie mainstream neurological thinking. As neurology was the source of neuroscience, historically, it is not unexpected that the conceptual foundations of neurology would influence those of neuroscience. This inheritance is evident in the facilitation and inhibition of a hierarchy of reflex mechanisms in the work of Sir Charles Sherrington (1857–1952) in his Integrative Action of the Nervous System [11]. The one-dimensional push–pull dynamics are apparent in the descriptions of Phineas Gauge, where damage to the frontal lobes impaired the ability to suppress antisocial behavior, although the source or mechanism that produces antisocial behavior, thought to be released, has never been made clear.

Needed now is a Kuhnian paradigm shift [12] away from paradigms that presuppose one-dimensional push–pull dynamics. Despite celebrations written in *Science* and *Nature* 50 years after publication of *The Structure of Scientific Revolutions* [12], Kuhn's work continues to invite critique, fairly, but outright rejection by reasonable thinkers would be to make an oxymoron of the latter. Kuhn's work was first and foremost a historical analysis. The uneven progress of science, even to the point of "getting stuck," is a matter of historical fact. Such is the case as it relates to current theories of the pathophysiology of the basal ganglia–thalamic–cortical system as it informs hypotheses of the mechanisms of action of DBS, particularly as it relates to frequency.

Thomas Kuhn (1922–1996) argued that a paradigm shift occurs when observations unexplainable by the dominant paradigm—anomalies—accumulate to some breaking point. Kuhn left unexplained what the dynamics of the breaking point were, but many critics of science argue that the breaking point is a polemical issue. At what point do editors of scientific journals and grant administrators stop being accepting of failed paradigms? For example, almost since the inception of the GPi Rate theory, there have been contrary observations and anomalies, including the production of Parkinsonism in nonhuman primates with *N*-methyl-4-phenyl-1,2,3,6-tetrahydropyridine, that fail to demonstrate predictions of the GPi Rate theory [13], as well as demonstrating that pallidotomy improves hyperkinetic disorders contrary to the predictions. However, the GPi Rate theory persists even today, attesting to the ability of an intuitively appealing theory to trump fact [14].

3. Some Principles for Developing Alternative Theories

This critique is written with an eye to the future in the hope that much better hypotheses and theories will arise that, when vindicated, will extend our knowledge. There are some generic principles that may be helpful. Any theory is more than a set of facts and includes hypotheses that bridge gaps (interpolate) and extrapolate from observations to predictions. Hypotheses invoke notions of necessity and causality that go beyond correlations. However, the generation and evaluation of hypotheses in themselves are poorly understood and have been explained as happenstance, psychological, or aesthetic. However, Aristotle and other ancient Greek philosophers offered an important requirement called the Principle of Causational Synonymy that imposes constraints on any hypothesis and theory that posits some causal mechanism, such as changes in neuronal activities that cause, denigrate, or restore normal behavior. The Principle of Causational Synonymy holds that the means by which a cause acts to generate an effect must match the means in the effect that generates an effect. For example, when one pushes an object, the electrons in the outer orbit of the atoms on the surface of the hand repel the electrons in the other orbit of the atoms on the surface of the object. In the case of understanding the motor effects of DBS, these effects are through the recruitment and de-recruitment of motor units, as is discussed latter. As per the Principle of Causational Synonymy, no theory of the mechanisms of action of DBS can be considered complete or satisfactory without full explication of motor unit activities. Indeed, the inability of any theory or explanation to do so is evidence of serious shortcomings.

The Principle of Causational Synonymy can be extended to a Principle of Informational Synonymy. Considering information as nonrandom state changes, the nonrandom state changes, such as the frequency by which electrostatic charges are placed, reversed, and then stopped on the electrical contact of the DBS lead (the cause), must be synonymous with the neuronal changes in the vicinity of the DBS target that generate the DBS effect. Thus, both with the Principle of Causational Synonymy and the Principle of Informational Synonymy, there must be precise mapping of the dynamics of the causal agent with the effector agent.

Consider the situation of a person pushing a child on a swing. In addition to the repulsive forces in the appropriate electrons in the person and the child, there also is informational content in terms of the movements of the person pushing and the child swing. This is evident in the fact that the person pushing cannot push at any random time. Rather, the person pushing must be in phase with the child's swing. Further, the pushing and swinging must be at the same frequencies, consistent with the Principle of Information Synonymy.

Applying these principles to the theories of DBS mechanisms of action, particularly as it relates to the stimulation pattern, in this case frequency, shows that current concepts are inadequate. Start with the effect, in this case the normalization of movement in the case of DBS for Parkinson's disease. Ultimately, any changes in the movement must be implemented by orchestrating the recruitment and de-recruitment of motor units over a number of muscles. This orchestration is very complex and operates over multiple levels over varying time scales. This includes the recruitment of motor units by size. Reciprocal coordination exists between muscles agonistic and antagonistic to the intended joint

rotation. Synergistic coordination of motor unit recruitments and de-recruitments in muscles spanning the same joint can be extended to motor unit orchestration simultaneously over multiple joints. Each of these operates at different time scales, and if related to oscillators in the nervous system (as will be demonstrated), then each time scale implies multiple oscillators at corresponding frequencies. Further, the operations at different frequencies are organized simultaneously. These issues are addressed in detail in Montgomery [15].

The fact that DBS improves motor control at specific frequencies argues that the frequency of the DBS is interacting in a nonrandom oscillatory manner with analogous oscillators within the basal ganglia-thalamic-cortical system. Indeed, as will be argued for, DBS can be considered as introducing an additional oscillator into the network of oscillators that comprises the basal ganglia-thalamic-cortical system. As discussed later, these oscillators are a specific kind that endows them with very important and interesting properties. The fact that multiple DBS frequencies exist shows that there are multiple oscillators of corresponding frequencies within the basal ganglia-thalamic-cortical system.

A possible alternative theory is presented here. The purpose here is to highlight alternative conceptions and not necessarily to champion any one particular theory. This is consistent with the intent of providing a critique rather than a review. To the authors' knowledge, the proposed theory is rather novel, at least in literature searches of various databases, thus providing a study of contrast. For example, there is no other publication searchable in PubMed that discusses motor unit recruitment abnormalities in Parkinson's disease or the effects of DBS. Nor are there any publications on discrete neural oscillators. Understandably, research bearing on the alternative theory largely will be those pursued by the authors. The theory advanced here includes the following:

1. The basal ganglia–thalamic–cortical system is involved in the recruitment and de-recruitment of motor units through oscillators within the system that then drive the motor cortex and brainstem structures that project to the lower motor neurons of the spinal cord and brainstem.
2. The basal ganglia-thalamic-cortical system is composed of multiple loosely coupled re-entrant, nonlinear polysynaptic discrete oscillators (Figure 2). Note that the term "discrete" is emphasized, as nearly all discussions of oscillators within the context of DBS, physiology, and pathophysiology do not make a distinction between continuous harmonic oscillators and discrete oscillators. These two types of oscillators have very different properties and dynamics. This theory was described previously in general terms [16] and in more detail in Montgomery [1].

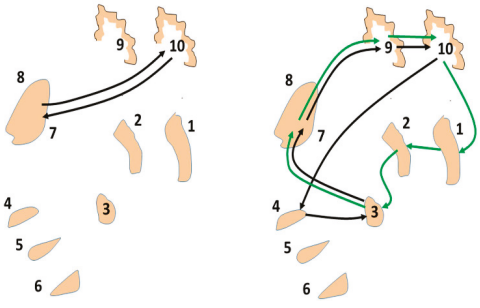

Figure 2. Schematic representation of the various components of the basal ganglia–thalamic–cortical system, demonstrating three oscillator architectures out of a greater number of possible oscillators. Represented are the following various structures: 1, putamen (as representative of the striatum); 2, globus pallidus externa; 3, globus pallidus interna; 4, subthalamic nucleus; 5, substantia nigra pars reticulata; 6, substantia nigra pars compacta (location of the cell bodies that utilize dopamine as their neurotransmitter); 7, ventral thalamus pars oralis; 8, parafasicular and centromedian nuclei of the thalamus; 9, supplementary motor area; and 10, primary motor cortex. Note that the GPi participates in two different oscillators, each of which is associated with a different fundamental frequency—a five-node loop and a six-node loop [1].

3. Oscillatory states consist of oscillators representing different frequencies simultaneously and that oscillatory states can shift dynamically, in the manner of a bifurcation in Complex Systems.
4. DBS acts as a noisy discrete oscillator when introduced into the basal ganglia-thalamic-cortical system, which interacts with oscillators inherent to the basal ganglia-thalamic-cortical system.
5. Interaction of the DBS oscillator within the oscillatory network is a model of mechanisms inherent in the basal ganglia-thalamic-cortical system, both in normal and in pathological circumstances. These interactions include the following:

    a. Positive and negative stochastic resonance
    b. Noisy synchronization
    c. Phase control such as advancement and entrainment

4. Evidence for a Role of the Basal Ganglia-Thalamic-Cortical System in Motor Unit Recruitment and De-Recruitment

Oscillator activities in motor unit behaviors have been known, and perhaps underappreciated, since described by Piper in 1907 [17]. At high muscle contractions, a 40-Hz signal can be appreciated, not only by electromyographic (EMG) recordings but also by auscultation using a stethoscope [18]. The genesis of such oscillatory activity is not known but likely is of central nervous system origin [19,20]. The question arises whether the basal ganglia via the motor cortex plays a role in these motor unit oscillations specifically, as suggested by abnormalities of the Piper rhythm in patients with Parkinson's and motor unit orchestration generally.

Motor unit recruitment normally is organized based on the muscular force at which a motor unit becomes active. The phenomenology of motor unit recruitment order is the recruitment of small motor units with low force requirements followed by a recruitment of larger motor units with a greater force requirement and is known as the Henneman Size Principle. Small motor units generated are thought to provide the small forces necessary for fine resolution of the forces generated, whereas large motor units supply the strength.

Another important extrapolation from the phenomenology is to the underlying mechanisms. Initially, it was hypothesized that motor unit recruitment was determined by the local biophysical properties of the lower motor neuron with large lower motor neurons, corresponding to larger motor units, being harder to excite. Subsequently, differential synaptic inputs with respect to lower motor neuron size, particularly peripheral afferents, were postulated to play a role. Nevertheless, most studies have not discussed or have discounted the role of descending inputs. Indeed, Enoka writes, "The great advantage of a spinally based control scheme (recruitment order determined by motor neuron biophysics—authors), such as orderly recruitment, is that it relieves higher centers (for example, the basal ganglia—authors) of the responsibility to select the motor neurons that must be activated for a specific task" [21]. Thus, it is not surprising that Parkinson's disease's effects on motor unit recruitment order have not received much attention.

In a study of motor unit recruitment [22], subjects were recruited from patients implanted previously with DBS systems in the vicinity of the subthalamic nucleus (STN). Following an overnight fast from their usual medications used to treat Parkinson's disease, subjects placed their extended finger and wrists into a manipulandum through which they could exert an isometric flexor force about the wrist. The task was to exert a force starting at rest to their maximum voluntary force over 60 s. Fine wire hook electrodes were inserted into the flexor carpi ulnaris. An example is shown in Figure 3. A raw EMG is shown in the top panel of Figure 3 under the condition of therapeutic DBS in the vicinity of the subthalamic nucleus. The therapeutic DBS electrode configuration and stimulation parameters were those determined optimal during prior routine clinical care with frequencies at least greater than 100 pps. As can be appreciated readily, there is a step-like increase in the amplitudes of the motor unit potentials with increasing force, clearly consistent with the Henneman Size Principle. However, under the condition of no DBS in the same subject, the step-like increase

is not seen. Further, large amplitude motor unit potentials are seen early in the task at low forces, clearly inconsistent with the Henneman Size Principle.

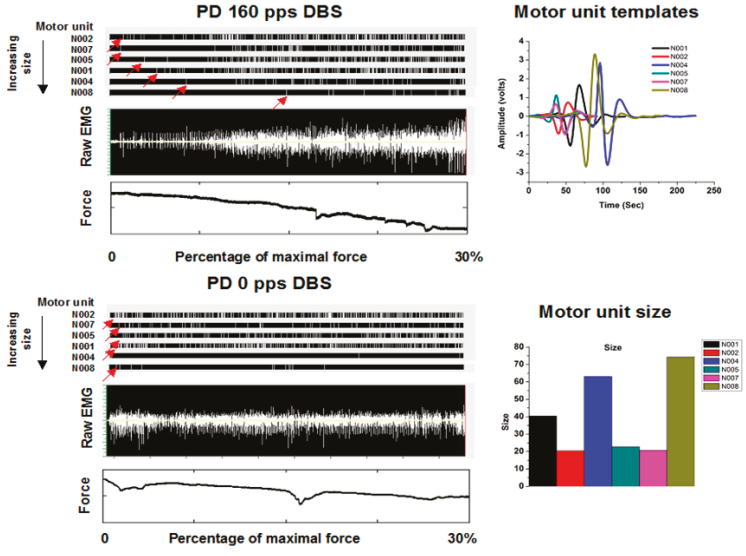

Figure 3. Representative example of raw intramuscular electromyographic (EMG) activities in a subject with Parkinson's disease under conditions of 160 pulses per second (pps) DBS (therapeutic) and 0 pps DBS. The raw EMG under 160 pps DBS has a stair-step appearance. Each step is associated with recruitment of a larger motor unit. The same six motor units were identified under both conditions and their waveforms and size are shown. The waveform associated with each motor unit is distinct and varies in size from its fellows. The size was determined by measuring the area under the curve. The time of occurrence of a motor unit discharge appears in the raster, with one row for each motor unit. The red arrow indicates onset of activities as the force generated increases progressively. In the 160-pps DBS condition, an orderly recruitment is shown (indicated by red arrows): Consistent with the Henneman Size Principle, smaller units are recruited first, followed by progressively larger motor units. Under the 0-pps DBS condition, the orderly recruitment of motor units is lost and the units are recruited nearly simultaneously. Large motor units are recruited early in the task and at small forces.

The EMG signals associated with individual motor units were extracted using a template-matching algorithm [23] to identify individual waveforms. Subsequently, another computer program used these waveforms as the basis to decompose superimposed signals into the elemental waveforms, allowing discrimination of individual motor units to higher percentages of maximal force production. Curve fitting of a sigmoidal function to cumulative discharge histograms over the ramp force allowed determination of the force at which the motor unit was recruited. The force at recruitment was correlated with the motor unit size determined by the area under the curve of the motor unit potential waveform (Figure 4). A positive slope indicates consistency with the Henneman Size Principle.

As can be seen in Figure 4 for a subject with Parkinson's disease, the slopes are near or less than 0 with the stimulator off or at 20 pps. With higher frequency DBS, the slopes become more positive. Indeed, the therapeutic DBS frequency resulted in the greatest positive slope. The reasonable conclusion is that the Henneman Size Principle is violated without treatment but is restored with higher frequencies of DBS. Figure 5 shows results comparing slopes for patients in the DBS Off (0 pps) and DBS On (therapeutic pps) for another patient. As can be seen, there was a near reversal of the normal recruitment pattern. Large motor units were recruited at the lowest forces generated and the small motor units only at the highest force. The motor recruitment changed to what would normally be

expected with therapeutic DBS. Slopes under the different conditions for 14 subjects with Parkinson's disease and 10 normal subjects are shown in Figure 6.

The question is what accounts for restoration of the normal motor unit recruitment profile with high-frequency therapeutic DBS and the dependence on frequency as shown in Figure 4. Changes in the recruitment order may be mediated by the motor cortex, whose upper motor neurons project to the lower motor neurons of the motor unit. Studies in nonhuman primates and in humans demonstrate a short latency highly temporally consistent with antidromic activations in motor cortex neurons in response to DBS pulses applied in the vicinity of the subthalamic nucleus. Evidence also shows an antidromic activation of the cortex in response to DBS in the vicinity of the subthalamic nucleus in humans with Parkinson's disease [24]. However, there were subsequent responses at longer latencies that suggest the possibility of re-entrant oscillations. Such an effect is demonstrated more clearly in the recording of neurons in the ventral thalamus pars oralis in response to DBS in the vicinity of the globus pallidus interna (Figure 7). The buildup of responses at approximately 5 ms following the DBS pulse suggests a resonance effect.

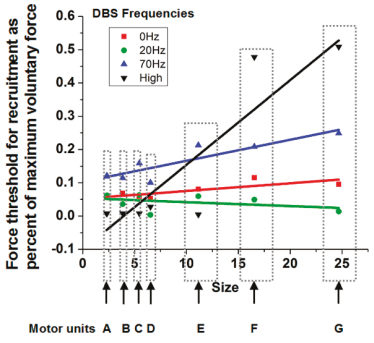

Figure 4. Relationship between percent of maximum force at which each of the seven motor units were recruited and the size of the motor units for different DBS conditions for a representative subject with Parkinson's disease. The seven motor units (A–G) are ordered according to motor unit size: A is the smallest and G is the largest. Different symbols and colors represent the various DBS conditions. A flat or small slope indicates that the Henneman Size Principle did not hold under that DBS condition. An initially relatively flat slope for the untreated patient (0 Hz DBS) increases greatly with therapeutic (high) DBS, suggesting that motor unit recruitment has become normalized.

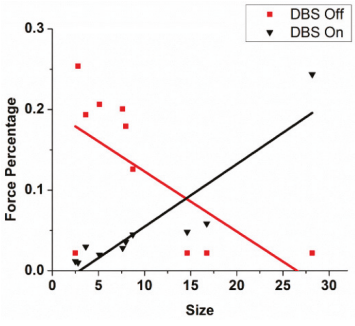

Figure 5. An example of the relationship between the size of the motor units and the percentages of maximum voluntary force at which the motor unit was recruited. In the DBS Off condition, the recruitment is opposite that predicted by the Henneman Size Principle. The recruitment became what would normally be expected by the principle.

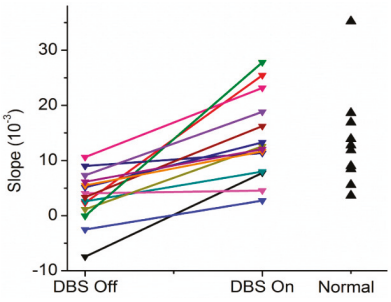

Figure 6. Summary of the changes in slopes of the motor unit recruitment order for 14 patients off and on therapeutic DBS compared to 10 normal controls.

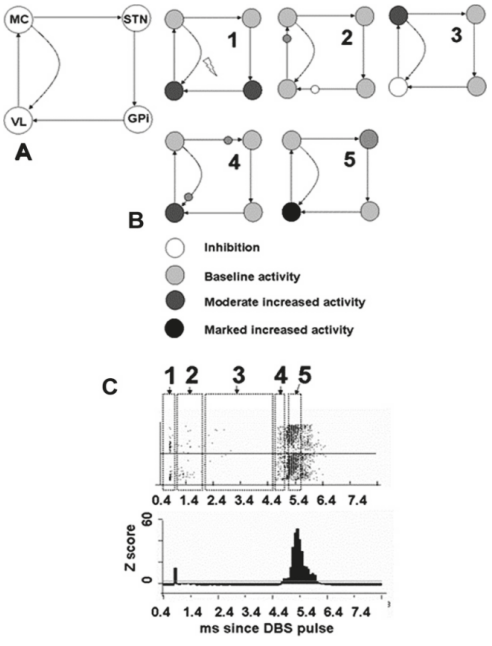

Figure 7. Some ventral thalamus pars oralis neurons (designated VL) demonstrate a remarkable posthyperpolarization (postinhibitory) rebound increased excitability (**C**). A potential mechanism is represented schematically (**B**); a nested two oscillator system is shown (**A**). The first oscillator is the disynaptic feedback loop between the motor cortex (MC) and the ventral thalamus pars oralis, the basal ganglia relay nucleus of the thalamus. The second loop consists of the MC to the subthalamic nucleus (STN), globus pallidus interna (GPi), Vop, and motor cortex once again. Each numbered step (**B**) shows subsequent activations, which begin with synchronized activation of the ventral thalamus pars oralis and GPi neurons in step 1. The activity in Vop is then transmitted to MC, and the activity in GPi is transmitted to the ventral thalamus pars oralis in step 2. This results in excitation of the MC and inhibition of the ventral thalamus pars oralis (VL) in step 3. MC activity is then transmitted back to the ventral thalamus pars oralis coincides with a posthyperpolarization rebound-increased activity in Vop following GPi axonal influences on the thalamic neurons in step 4. Excitation from the MC in step 4 combines with the postinhibitory rebound-increased excitability in the ventral thalamus pars oralis to produce a marked increase in activity, as shown in step 5 (modified from Montgomery [25]).

One possible explanation is that an action potential generated in the axon of the thalamic neuron passing in the vicinity of the DBS contact proceeds in an antidromic manner, as demonstrated in the recording of extracellular action potentials (Figure 7), as well as orthodromically to the cortex. There, the stimulated motor cortex neurons sent action potentials back to the thalamic neurons. The timing is such that the action potentials generated in the thalamic neurons consequent to driving by cortical neurons collided with the antidromic action potentials. This process could be modeled as the activity traversing one-half of the pathway from the thalamus to the cortex and the entire pathway from the cortex to the thalamus. Estimating from the latency of the resonant buildup of 5 ms, the total transit time in the thalamic–cortical feedback loop would be on the order of 6.7 ms. This would correspond to a frequency within the thalamic–cortical feedback loop of approximately 150 Hz.

These considerations suggest that one possible mechanism for motor improvements with DBS in the vicinity of both the subthalamic nucleus and the globus pallidus interna may reflect resonance interactions between the oscillator composed of the thalamic-cortical loop and the oscillator in the manner of DBS. The resonant interactions between the DBS oscillator and the thalamic-cortical oscillator are thought to improve the signal-to-noise ratio by stochastic resonance, thereby reducing the misinformation exiting from the motor cortex to the lower motor neurons and restoring the normal order of motor unit recruitment.

5. Stochastic Resonance

The next question is whether the model described here could account for the improvement in bradykinesia at other DBS frequencies, as demonstrated in Figure 1. The basal ganglia-thalamic-cortical system can be considered a network of interconnected polysynaptic re-entrant nonlinear discrete oscillators (Figure 2). There are a number of different oscillators with differing numbers of nodes; thus, the DBS at several different frequencies could interact via stochastic resonance with any of the multiple oscillators. Evidence in support of this hypothesis is given here.

Improvement in motor control can be considered increased information in the effectors, which is in the orchestration of motor unit recruitments and de-recruitments. Recordings of extracellular action potentials were obtained as a nonhuman primate preformed an arm-reaching task. Peri-event rasters and histograms show neuronal activities before and after a behavioral event (Figure 8). As can be seen, under the condition of no stimulation, there is no change or modulation of the neuronal activities. However, with DBS-like stimulation in the vicinity of the subthalamic nucleus at 150 pps, there is a consistent modulation of the neuronal activities with the behavior. The modulation was less at 100 pps and still less at 50 pps. Again, it is not likely that the information represented by the modulation of neuronal activities at 150 pps DBS originated in the DBS pulse train (a violation of the Principle of Informational Synonymy). Rather, modulation was present there, although not observable over the "noise". Thus, the signal, being the underlying modulation of neuronal activities, was not seen above the noise; in other words, there was a poor signal-to-noise ratio. The reverse has been observed, in which a signal in the neuronal responses with no DBS was progressively lost with higher DBS frequencies (Figure 9). The DBS at 150 pps affects the signal relative to the noise, but in different directions and dependent on DBS frequency.

If this model holds for DBS, then the observation that multiple but specific DBS frequencies improve hand opening-closing bradykinesia argues for multiple oscillators involved in the hand opening-closing behavior. Indeed, it is likely that there is an orchestration of motor unit recruitment and that de-recruitment operates over multiple time scales, each related to an oscillator within the basal ganglia-thalamic-cortical system [15].

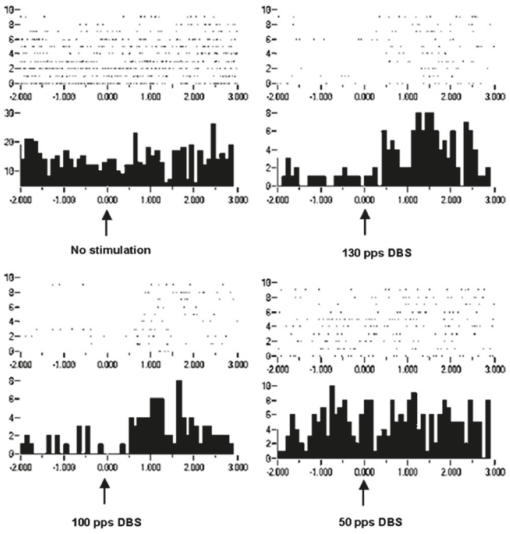

Figure 8. Peri-event rasters and histograms for a neuron recorded in the putamen of a non-human primate. Each dot in the rasters represents a neuronal discharge and each row represents a trial. Summing a column in the raster produces the histogram. There is no meaningful modulation of neuronal activity with behavior (appearance of the commencement signal at time zero is indicated by the up arrow) under the no stimulation condition. However, consistent modulation occurs at 130 pps and, to a lesser extent, at 100 pps DBS, suggesting that the DBS has enlisted the neuron into being meaningfully related to the behavior. It bears noting that the baseline activity prior to the commencement signal is reduced [25].

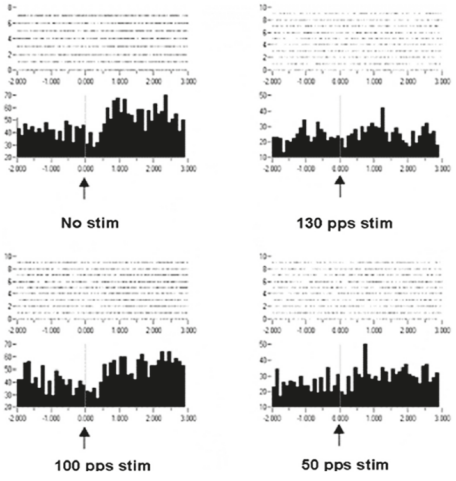

Figure 9. Peri-event rasters and histogram showing activity of a caudate nucleus neuron before and after onset of the commencement signal, indicated by the up arrow. Each dot in the rasters represents a neuronal discharge and each row represents a trial. Summing a column in the raster produces the histogram. With no stimulation, with 100 pps DBS, and, to a lesser degree, with 50 pps DBS, there is an increase in neuronal discharge following the onset of the commencement signal. This dynamic modulation is lost with the 130-pps DBS [25].

6. Evidence for Oscillations in the Basal Ganglia–Thalamic–Cortical System

The Schuster periodogram [26] is an alternative to a Fourier transform of detecting periodic (oscillatory) activity in a time series. A variant of the Schuster periodogram has been demonstrated as mathematically equivalent to the Fourier transform but is easier to implement (Figure 10) [27]. This method was used to analyze neuronal spike trains from neurons in the basal ganglia-thalamic-cortical system from two nonhuman primates at rest [28]; an example of the spectrogram is shown in Figure 11. The color of the pixels in the image represents the *z*-score difference from the same spike train where the interspike intervals (ISI) were randomized. A 2-s window of the spike train was sampled and the *z*-score change was calculated. The window was then moved over the entire spike train at 0.2-s steps.

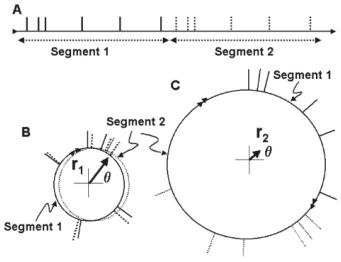

Figure 10. Schematic representation of the Schuster periodogram utilizing circular statistics. (**A**) A spike train is divided into segments; (**B**) each of the two segments is closed to form a circle, and the time of occurrence of each action potential is plotted as a unit vector on the circumference. As can be seen, the unit vectors are not distributed randomly over the circumference. A resultant vector is determined (r_1), which, in the situation depicted by B, will be nonzero. The magnitude of the resultant vector indicates the statistical significance of the power at the frequency corresponding to the lengths of the segments. The resultant vectors can be calculated for segments of any size, thus corresponding to a specific frequency analogous to the power at any frequency in a Fourier transform. The angle, θ indicates the phase of the periodic or oscillatory activity.

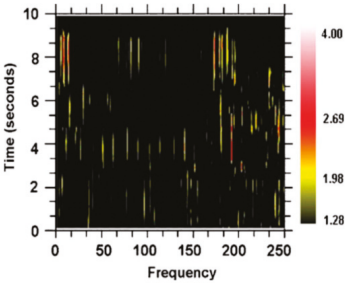

Figure 11. Spectrogram relative power indicated as a *z*-score change over the randomized spike train using a 2-s window moved through time in 0.2-s steps. As can be appreciated, many frequencies are represented simultaneously in the neuronal spike train. Further, it appears that there are sets of frequencies that change over time, suggesting bifurcations from metastable states associated with each set of frequencies [25].

As can be seen, there are multiple and high-frequency oscillatory activities in the neuronal spike train simultaneously. This multiplicity of frequencies and changes in the sets of frequencies can be seen in the following: 24 neurons were recorded in the globus pallidus externa, 15 in the globus pallidus interna, 16 in the putamen, 49 in the sensory cortex, 9 in the subthalamic nucleus, and 25 in the motor cortex [28]. The average frequency for each structure ranged from 135 to

140 Hz. Mathematical modeling demonstrates that the individual spike trains in loosely coupled nonlinear oscillators operating at noncommensurate frequencies can entrain multiple frequencies simultaneously [1,29].

The theory is offered that each oscillator of different frequencies affects different physiological mechanisms over different time scales, for example, the orchestration of motor unit recruitment and de-recruitment as described previously. Thus, it would not be unexpected that DBS at different frequencies would have multiple effects on motor behavior as shown previously in Figure 1. However, it is not just any frequencies but specific and precise frequencies, perhaps reflecting the specific frequencies entrained in the neuronal spike trains of the basal ganglia-thalamic-cortical system.

7. Evidence for DBS-Induced Oscillations

7.1. Direct Observations

Studying the effects of DBS in the vicinity of the subthalamic nucleus in a nonhuman primate on neuronal action potentials provided an example where DBS could induce oscillations in the basal ganglia-thalamic-cortical system [28]. An example is shown in the peri-event raster and histogram of the time interval between DBS pulses for a cortical neuron (Figure 12). As can be seen, there are three peaks in the post-DBS response with 50 pps DBS. This would correspond to a frequency of oscillation of 150 Hz. Two peaks are noted in the interval between pulses with stimulation at 100 and 130 pps. Of note, the second peak at 100 pps occurs sooner that at 50 pps and the second peak is even earlier at 130 pps. These findings could be explained if the DBS pulses induced an inherent oscillation of approximately 150 Hz. Thus, the inherent frequency would resonate with DBS at 50 pps. However, the effect at 100 and 130 pps would be a combination of the response driven by the DBS pulses at those frequencies and the inherent oscillations phase entrained at 50 pps DBS. Nonetheless, this observation supports the hypothesis that DBS can induce ongoing oscillations.

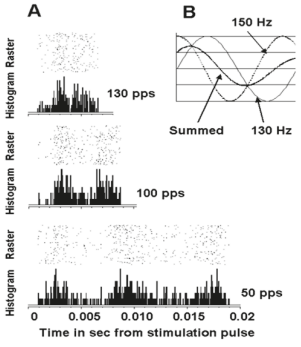

Figure 12. (**A**) A post-stimulus raster and histogram of a cortical neuron recorded in a nonhuman primate using a 50-pps DBS-like stimulation delivered in the vicinity of the STN. The stimulus pulse occurred at time 0, and the raster and histogram show the periodic neuronal activities during the interstimulus pulse intervals. Each dot in the raster represents the onset of an action potential. Each row represents responses to a single DBS pulse. The number of dots in columns across the raster appears in the histogram below each raster. The lengths of the raster and histogram represent the time interval between DBS pulses. In the raster and histogram associated with the 50-pps DBS, a recurring peak of increased neuronal activity is evident. The truncated appearance of the third peak suggests that the time period associated with the frequency of the re-entrant oscillatory activity is not an integer multiple of the time interval between the DBS pulses. This suggests an interaction between the oscillator generating the recurrent activity and the oscillator composed of the DBS spike train (**B**). This observation may be explained by an interaction between a 130-Hz DBS oscillator and a 150-Hz oscillator intrinsic to the neuron.

7.2. Resonance Effects to Pair-Pulse Stimulation

The basic concept is that if the basal ganglia-thalamic-cortical system represents a closed loop or feedback system of oscillators, then a single pulse might reverberate in an oscillatory manner through the loop. If a second pulse is timed precisely to the returning effect from the prior pulse, these effects should be additive (Figure 13). Thus, an experiment was conducted using pairs of DBS pulses. The first pulse was hypothesized to initiate a re-entrant oscillation, and the second pulse was timed to interact with the re-entrant activity generated by the first pulse. The time interval between the first and the second pulse of the pair corresponds to the cycle time of the oscillator.

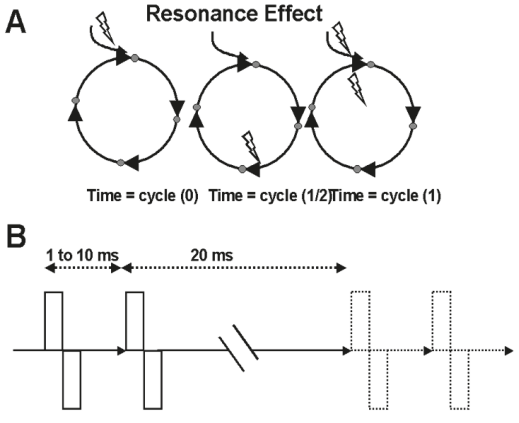

Figure 13. (**A**) A schematic representation of the resonance effect. The first stimulation (conditioning pulse) causes an excitation to traverse the closed loop. If the second stimulation (test pulse) is delivered just as the excitation effect from the first or conditioning pulse returns to the original site, the temporal summation on the neuronal cell membrane will amplify the response. (**B**) Paired-pulse stimulus trains represented schematically. The interstimulus interval represents a specific frequency (1/interval). This study examined the frequencies represented by the intervals from 1 to 10 ms (1000 Hz to 100 Hz) at 1-ms increments.

Two nonhuman primates (*Macaca mulatta*) were trained using only positive reinforcement to sit quietly in a loosely restraining chair and to allow passive movement of their arms. After training, a recording chamber was implanted surgically over a craniotomy site such that microelectrodes could be passed through the intact dura into the basal ganglia as described previously [30]. The protocol received prior approval by the Institutional Animal Care and Use Committee of the Cleveland Clinic Foundation.

A reduced scale model of the human DBS lead (NuMed Inc., 2880 Main St. Hopkinton, NY, USA) was placed such that the deepest contact was at the bottom of the subthalamic nucleus using stereotactic methods confirmed by microelectrode recordings of extracellular action potentials. Locations of the DBS-like leads, as well as other microelectrode recordings, were later confirmed by histological analyses. The leads had four contacts, each 0.525 mm in diameter, 0.5 mm long, and with a 0.5-mm space between contacts, giving a total surface area of 0.82 mm^2 per contact. Using biphasic square-wave pulses, constant current electrical stimulations, using biphasic square-wave pulses, were delivered using the most distal contact (contact No. 0) referenced to the most proximal contact (contact No. 3). The morphology of the pulses was such that, at contact No. 0, the cathodic phase preceded the anodic phase. The reverse was true at contact No. 3. A pulse width of 90 μs per phase was used. The amplitude selected was 80% of the current that produced tonic contraction, presumably from the current spread to the internal capsule.

Standard methods of microelectrode recordings of neuronal extracellular action potentials were used. As is standard in electrophysiological studies, autocorrelograms for all neurons were inspected for the absence of a refractory period as evidenced by a high probability of a neuronal discharge within 3 ms of the index discharge. Lack of a refractory period would indicate that the waveforms isolated and attributed to a single neuron were an admixture of two or more neurons. Data from these neurons were discarded. Also, all pair-wise cross-correlograms for neurons isolated from a single microelectrode recording site were constructed. Any cross-correlograms showing a refractory period effect were interpreted as the two neurons actually represented a single neuron that was isolated incorrectly. If found, data for these pairs of neurons were pooled. Loss of signal related to the effects of the stimulator artifact was accounted for and corrected.

Continuous recordings of neuronal activity before and during trains of paired-pulse stimuli were made. Resonance effects were demonstrated by constructing post-stimulus rasters, and histograms that were indexed to the second of the pulse pair, test pulse. Rasters and histograms were constructed by taking segments of data immediately after the second or test pulse for 20 ms (Figure 14). This corresponds to the period between each pair of pulses. Post-stimulus histograms were constructed where each sequential time bin (0.4 ms) contained counts of neuronal discharge for the 20 ms that followed the second test pulse. These time bins were then averaged across the number of stimulus pairs applied, giving a neuronal discharge probability in 0.4-ms time increments following the second test pulse.

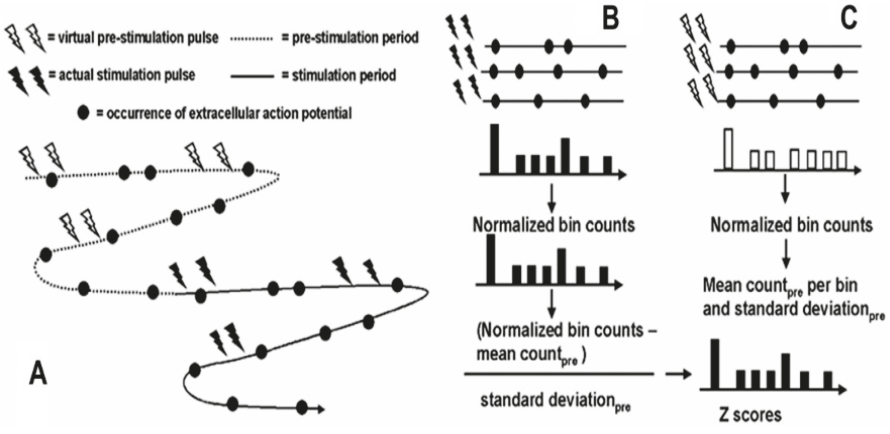

Figure 14. Schematic representation of analysis methods for detecting a resonance effect for paired-pulse stimulation. A set of virtual stimulus pulse pairs was created during the prestimulation period by translating the timing of the actual stimulation pulse pairs into the prestimulation period (**A**). Post-stimulus rasters and histograms were constructed indexed to the second pulse of the actual (**B**) and virtual (**C**) stimulation pulses. The rasters were collapsed across rows into the time bins (0.4 ms) of the histograms, resulting in counts of extracellular action potentials. This was normalized by dividing by the number of sets of paired pulse stimuli, resulting in probabilities of neuronal discharge in each time interval following the second stimulus pair. The mean probabilities per bin and the standard deviation were calculated for the virtual stimulation histograms (**C**). The mean was then subtracted from each time bin probability during the actual stimulation and divided by the standard deviation, resulting in a *z* score (**B**).

For comparison across different neurons and different structures, these post-stimulus histograms of neuronal discharge probabilities were normalized by expressing the neuronal discharge counts in bins as a *z* score based on the mean and standard deviation of neuronal discharges during the baseline prior to stimulation. Because of the short interstimulus intervals, it was not possible to compare

neuronal activities following the first pulse to activities following the second pulse. Sampling of the prestimulation period values was determined by creating virtual stimulation pulses so that neuronal activity during the prestimulation period could be analyzed exactly as the neuronal activity during the stimulation period (Figure 14). This was chosen as a means to sample the prestimulation baseline randomly.

Although the interstimulation pulse intervals were not random and therefore the virtual stimulation train was not random, neuronal activity in the prestimulation period is independent of the subsequent virtual stimulation pulse train and therefore can be considered random with respect to the time of neuronal discharge. The mean and standard deviation of the neuronal discharge probability in the time bins during the prestimulation baseline were calculated as described previously for the stimulation period. In this case, histograms were indexed to the second virtual pulse. The probability of neuronal discharge in each time bin in the post-actual stimulus histogram was converted to a z score by subtracting the mean discharge probability per bin in the post-virtual stimulation histogram and dividing the difference by the standard deviation of the bin probabilities in the post-virtual stimulation histogram. This method was chosen over other techniques such as absolute or percent change in discharge frequency because (1) the z score normalizes data, thus allowing comparisons between different neurons in different structures; and (2) the z score accounts for the variability of neuronal discharge activity, thus allowing inferences as to statistical significance.

One hundred and eighteen neurons were recorded in the basal ganglia-thalamic-cortical system in two nonhuman primates (in one nonhuman primate, only 15 neurons studied were in the motor cortex). Forty neurons were recorded in the motor cortex, 25 in the somatosensory cortex, 16 in the caudate and putamen, 14 in the globus pallidus internal segment, and 23 in the globus pallidus external segment. While the number of neurons analyzed within each structure was relatively small, the intent was to study the dynamics of the basal ganglia-thalamic-cortical system such that consistency of observations across different nuclei was the primary interest. As such, the number of neurons for the system studied is similar to other published studies. Analyses within each structure were secondary.

An example of a response in a motor cortex neuron is shown in Figure 15. Each colored bar represents a change in the probability of a neuronal discharge after the second or test pulse compared to the prestimulation baseline associated with a z score equal to or greater than 1.96. As can be seen, the significant resonance effects for longer interstimulus intervals had different latencies than the response to the interstimulus interval of 1 ms. Consequently, it is not likely that these other responses were mediated by the same mechanism or that they represent a direct response to the second pulse. Figure 15 also shows that this neuron had multiple resonance effects at longer latencies that were associated with 4-, 5-, 7-, and 8-ms interstimulus intervals, corresponding to a resonance frequency of 250, 200, 143, and 125 Hz, respectively. Interestingly, such high-frequency oscillations also have been noted in local field potential recordings in the subthalamic nucleus of patients with Parkinson's disease through implanted DBS leads [31]. However, inferences from local field potentials are problematic given that these represent the summed activities of a large number of dendrites, some of which may be irrelevant yet interact to affect the local field potential in any event.

Results shown in Figure 15 suggest evidence of a periodic excitability arising within the single neuron. The first response with the 1-ms interstimulus interval pulses occurs 3.8 ms after the test pulse, suggesting that this was not a direct antidromic effect, but probably that the neuron being analyzed was at least one synapse from the neuron being stimulated. Interestingly, after the 1-ms interstimulus interval test pulse, the neuronal discharge probability increased significantly at 7.6 and 15.2 ms during the 20 ms after the test pulse; these probably are harmonics of the initial latency of 3.8 ms. Analyses were conducted on 118 neurons, all of which showed at least one resonance effect with paired-pulse stimulation at different interstimulus intervals. The median number of significant resonance frequencies (25th to 75th percentile; number of neurons) in the pooled caudate and putamen was five (2 to 7.5, n = 16); globus pallidus externa, 9 (5.5 to 11.75, n = 23); globus pallidus interna, 6 (1 to 9, n = 14); somatosensory cortex, 7 (3.5 to 8.5, n = 25); and motor cortex, 7 (4.5 to 12, n = 40). Thus, most neurons had multiple resonance effects at different frequencies.

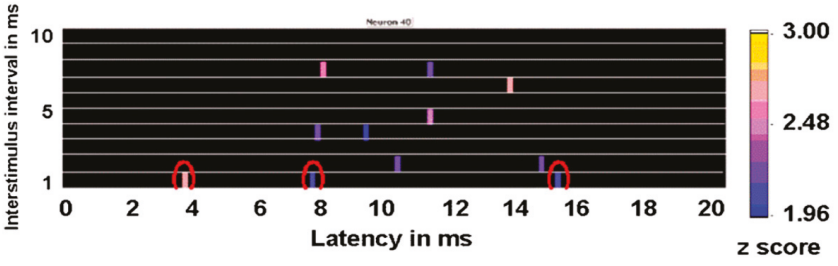

Figure 15. Results from paired-pulse experiments for a neuron recorded in the motor cortex of a nonhuman primate. Each row represents changes in the probability of a neuronal discharge from baseline for each interstimulus interval of the paired-pulse stimuli. Colored bars represent any change that has a *z* score greater than 1.96 compared to baseline. The horizontal axis represents the latency of the resonance effect after the second or test pulse of the pair.

8. Evidence of DBS Oscillatory Interactions with Intrinsic Oscillators within the Basal Ganglia-Thalamic-Cortical System

Recent studies demonstrate antidromic action potentials in the subthalamic nucleus neuronal in response to DBS in the vicinity of the contralateral STN [32]. Interestingly, only a small percentage of DBS pulses resulted in antidromic action potentials. This result is consistent with other studies [32–36]. One wonders whether this result indicates a purely stochastic process or some underlying determining mechanism such as the specific dynamics in the neuronal membrane potentials in the soma. STN neuronal microelectrode recordings were used in subjects with Parkinson's disease made during DBS in the vicinity of the contralateral STN in a manner described elsewhere [32]. Stimulation was at 160 and 30 pps. Fifty-eight neurons were recorded from eight STNs in eight subjects.

Spike trains containing only antidromic action potentials (antidromic-only spike trains) were constructed from the original spike trains by retaining only those time stamps of antidromic action potentials. Fifty-two of the 58 neurons demonstrated antidromic action potentials. Randomized antidromic-only spike trains were created by shuffling the order of the antidromic action potentials in the antidromic-only spike trains. This was accomplished by dividing the antidromic-only spike trains into segments between successive stimulation pulses. Each interstimulus pulse interval may or may not have an antidromic action potential.

The hypothesis to be addressed is that sequence of antidromic action potentials are not random. Thus, it is necessary to compare the actual sequence of antidromic action potentials to what would be a random sequence. The orders of the consecutive interstimulus pulse intervals were randomized (shuffled) in order to affect a breaking up of any periodicity in intervals containing an antidromic action potential, creating a randomized antidromic-only spike train. If the probability of an antidromic action potential is not random, the interspike interval histogram of the randomized antidromic-only spike train would differ from the ISI of the corresponding antidromic-only spike train.

Periodicity in the antidromic-only spike train was examined by comparing the antidromic-only spike train to the randomized antidromic-only spike train using power spectral densities (PSDs). It is important to note that the antidromic action potentials are time-locked to the stimulation pulse. The frequencies of the antidromic action potentials thus stand in complex relation to the DBS frequencies.

Figures 16 and 17 show representative antidromic-only spike trains and randomized antidromic-only spike train ISI histograms for two neurons for DBS at 160 and 30 pps, respectively. As can be seen, an antidromic action potential occurs only after a stimulation pulse. The time resolution is thus the interstimulus pulse interval. Importantly, the varying magnitude of the peaks suggests that different probabilities of an antidromic action potential follow different stimulation pulses. Such would not be the case, however, if every stimulation pulse was associated with an antidromic action potential or if the probability of an antidromic action potential was random relative to the stimulation pulses.

Rather, there appears to be "structure" in the probabilities of an antidromic action potential. This is further supported by the lack of peaks at such times when the sequential order of the antidromic action potentials is randomized. Of the 52 neurons demonstrating antidromic action potentials studied, 24 showed a significant difference between the antidromic-only spike train and the randomized antidromic spike train ISI. These latter neurons received additional study.

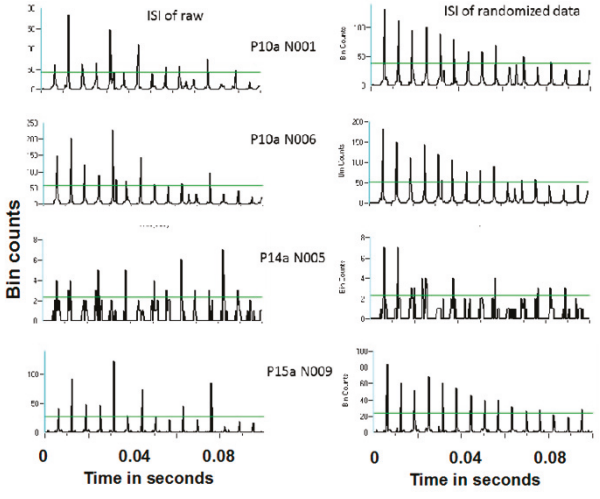

Figure 16. Representative interspike interval histogram of a antidromic-only spike train and its randomized-only spike train counterpart for 160 pps DBS.

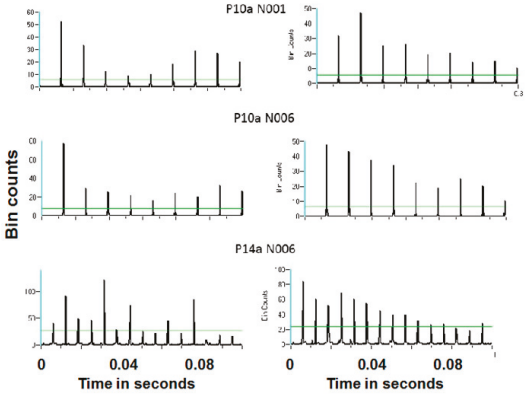

Figure 17. Representative interspike interval histogram of a antidromic-only spike train and its randomized-only spike train counterpart for 30 pps DBS.

Power spectral densities (PSDs) were constructed on antidromic spike trains from antidromic-only spike train and randomized antidromic-only spike train data. Figure 18 shows a representative example. A strong peak appears at 66 Hz, a lesser peak at 26 Hz, and a small peak appears at 92 Hz in the antidromic-only spike trains. This latter peak is not present in the randomized antidromic-only spike train. The clear distinction in these peaks from the rest of the frequencies in the PSD attests to their significance. Figure 19 shows the PSD for the same neuron that appears in Figure 6 but does not appear under the 30-pps DBS condition. Peaks are observed at 30 Hz (DBS frequency), 26 Hz, 22 Hz, 6 Hz,

and 3 Hz. Original spike trains demonstrated no peaks in the PSD of neuronal activity during the baseline before DBS; a representative example is shown in Figure 20.

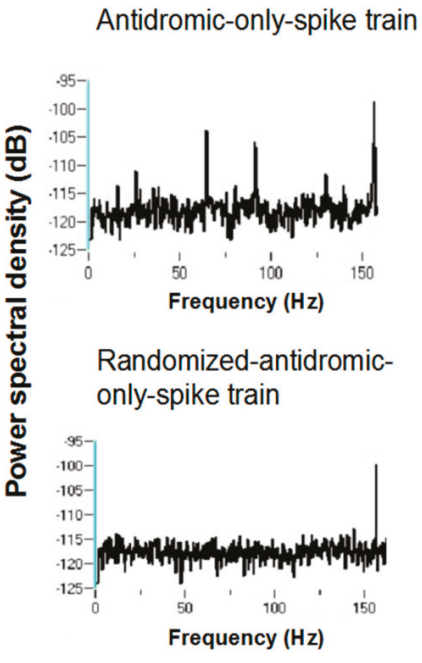

Figure 18. Representative power spectral density of a antidromic-only spike train and its randomized-only spike train counterpart for 160 pps DBS.

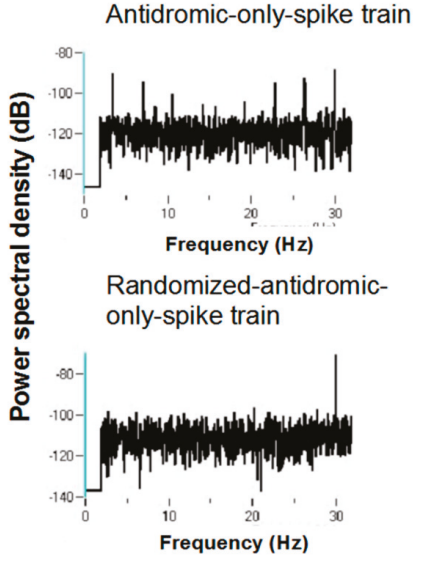

Figure 19. Representative power spectral density of a antidromic-only spike train and its randomized-only spike train counterpart for 30 pps DBS.

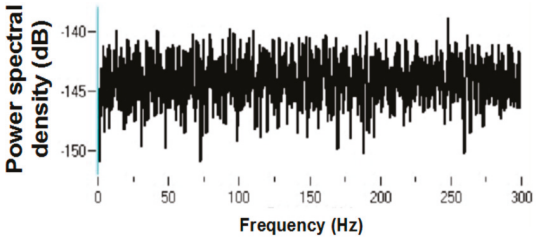

Figure 20. Representative power spectral density of an original train prior to DBS.

The various peaks are listed in Table 1. Oscillations at 66 and 26 Hz occurred independently of other frequencies, which suggests that these oscillators are fundamental to the subthalamic nucleus. In addition, the 26-Hz oscillations were seen at both 160 and 30 pps DBS. These are not a consequence of the stimulation frequency. They likely represent, rather, a fundamental oscillator involving the subthalamic nucleus. Also, the peaks at 26 and 66 Hz are not harmonics of the DBS frequencies. Interestingly, several neurons had both 66- and 26-Hz oscillators. Other peaks probably represent beat frequencies that result from the interaction of the fundamental frequencies and the DBS frequency. For example, peaks detected at 92 Hz probably are the result of interactions between the 66-Hz fundamental oscillator and the 160-pps DBS (the actual stimulation frequency was measured at 157.5 pps). As can be seen, the 92-Hz peak was never present without the peak at 66 Hz. Similarly, the 3-Hz peak likely represents the beat frequency from the interaction of the fundamental 26-Hz frequency and the 30-pps DBS, as the 3-Hz peak was never seen at the 160-pps DBS and was never independent of the 26-Hz peak under the 30-pps DBS. By virtue of the fact that the 30-pps DBS is closer to the fundamental frequency at 26 Hz than the 160-pps DBS, which would produce high-frequency harmonics and beat interactions, other peaks under the 30-pps DBS likely represent beat interactions among harmonics of the DBS and the fundamental frequencies.

Table 1. Results of power spectral densities on antidromic-only-spike trains. Frequencies associated with the peaks are reported (in Hz).

Subject	Neuron	160 pps DBS	30 pps DBS
15a	N001	66	
	N002	66	
	N003	66	
	N004	66, 92	
	N006	66, 92	
	N007	66, 92	
	N008	66, 92	
	N009	26, 66, 92, 136	
	N014	26, 66, 92, 136	
p10a	N001	26, 66, 92, 136	3, 26, 23
	N002	26, 66, 92, 136	3, 26, 23,6
	N004	26	
	N005	26, 66, 92, 136	3, 26
	N006	26, 66, 92, 136	3, 26, 22, 6, 10, 19
	N011	26, 66, 92, 136	3, 26, 6, 22
	N019	26, 66, 92, 136	3, 26, 6, 22
p03a	N001	26, 66, 92	3, 26
	N005	26, 66, 92 136	3, 26
	N008	66, 92	
	N016	26, 66, 92 136	3, 26

The relatively few neurons available for analyses mean that any conclusions are tentative, and the difficulty of these experiments makes it unlikely that significantly more data are forthcoming.

As one awaits future confirmation or refutation, these remarkable findings—their implications in particular—warrant reporting, albeit with the appropriate caveats kept in mind.

The study led to the following conclusions: For many neurons, occurrence of an antidromic action potential is not random. The probability of an antidromic action potential reflects the underlying state of the neuronal excitability, which means that the antidromic action potential can be used as a probe of the underlying neuronal dynamics. The probability of an antidromic action potential and the underlying neuronal state of excitability appear periodic or oscillatory. Not simple harmonics of the DBS frequency, the frequencies of the underlying oscillatory neuronal states are, rather, independent of the latter. One cannot exclude the possibility that the actual frequency of these oscillators is not some integer multiple of the 26- or 66-Hz oscillators. The beat frequencies of 3 and 92 Hz for some of the neurons suggest that 26 and 66 Hz are the fundamental frequencies for the involved oscillators. The key finding for the purpose of this article is that DBS can be considered a discrete nonlinear oscillator, which interacts with independent oscillators within the subthalamic nucleus, possibly arising from oscillators intrinsic to the basal ganglia-thalamic-cortical system.

9. Computational Simulations of the Basal Ganglia-Thalamic-Cortical System as a Network of Loosely Coupled, Nonlinear Re-Entrant Discrete Oscillators

As a proof of concept, although not of biological fact, computational simulations were conducted using an architecture derived from the theory that the basal ganglia-thalamic-cortical system is organized as large, loosely coupled, nonlinear polysynaptic discrete re-entrant oscillators (Figure 21), details of which are discussed elsewhere [1,16]. A detailed description of discrete neural oscillators can be found in Montgomery [1]. Briefly, a node is defined as a collection of local neurons that generally share the same inputs and project to same neurons in another node. For example, a node may be confined to a single anatomical structure and each anatomical nucleus (and region of cortex) consists of a number of nodes. An oscillator consists of a set of nodes whose neurons are connected with previous and subsequent nodes of neurons. During any cycle of reentrant activities within the oscillator, a subset of neurons within each node may discharge sufficient to maintain the oscillations yet not leading to saturation or collapse of the oscillator. The simulations are designed to determine whether neural oscillators of the general architecture shown in Figure 21 are capable of sustained oscillatory activities, what would be the nature of those activities and what if any similarity of the oscillations in the simulation to analyses of neuronal activities recorded in human and non-human primates.

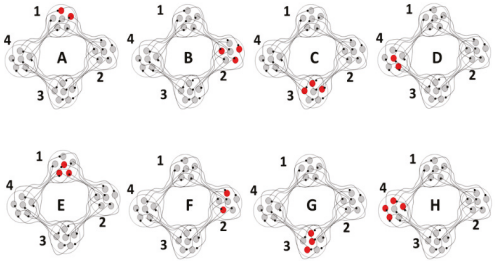

Figure 21. Schematic representation of the basic architecture of the computer simulations. Represented is one oscillator to show the structure of neurons within each node and how information is transmitted via subsets of neurons within each node. A four-node oscillator (nodes 1–4) whose nodes contain five neurons each is illustrated. A series of time intervals (A–H) are represented. Neurons become active in node 1 at time A. The activity then propagates to neurons in subsequent nodes. For any part of the cycle, a subset of neurons in each node becomes active and the specific neurons that are active vary with each cycle. Thus the neurons active at time B in node 2 are different than the neurons active in node 2 at time F. Multiple oscillators of different numbers of nodes, thus different inherent fundamental frequencies, can be linked [1].

The operations of neurons in the simulation are depicted in Figure 22. Each neuron is of the integrate-and-fire type. Postsynaptic potentials resulting from synaptic inputs are modeled as decaying exponential functions. The output is a discrete pulse representing an action potential based on the summed synaptic inputs exceeding a threshold. The threshold is dynamic so as to account for changes in ionic conductances with subthreshold changes in the neuronal membrane potential, for example, depolarization blockade (elevated threshold) and post-hyperpolarization rebound (decreased threshold). A probability function determines whether an action potential arriving at the presynaptic terminal induces a postsynaptic potential change and reflects the known inefficiency of synaptic transmission. Conduction times and synaptic delays were established based on studies described previously.

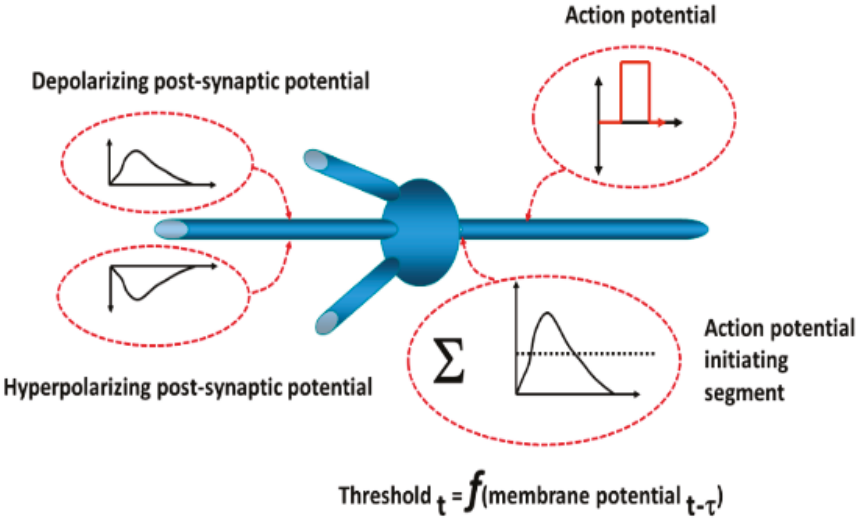

Figure 22. Model neurons consist of multiple dendritic inputs affecting the postsynaptic transmembrane electrical potentials. These inputs are summed at the action potential-initiating segment. If the summed potentials exceed a dynamic threshold, an action potential is generated. The postsynaptic potentials are modeled on as either a depolarizing or a hyperpolarizing decaying exponential function. The threshold, for example, at time t_i, varies with the previous transmembrane electrical potential just prior at time t_{i-1}. This allows changes in Na^+ voltage-gated ionic conductance channel activation and inactivation. In this manner, post-hyperpolarization excitation and depolarization blockade are modeled [1].

One instantiation of the computational modeling is shown in Figure 23. There are three interconnected oscillators with different numbers of nodes and thus different inherent fundamental frequencies. The inherent frequency is defined as number of times a "bit of information", such as an action potential, can traverse the oscillator in one second and depends on the number of nodes within the oscillator. A spectrogram showing the frequency contents over time for a representative neuron in the computational network is shown in Figure 24, along with spectrograms obtained from a globus pallidus externa of a nonhuman primate and from a neuron recorded in the subthalamic nucleus of a human with Parkinson's disease. As can be seen, the outputs are very similar and consist of multiple frequencies entrained simultaneously, sets of frequencies that are stable over brief periods of time between bifurcations.

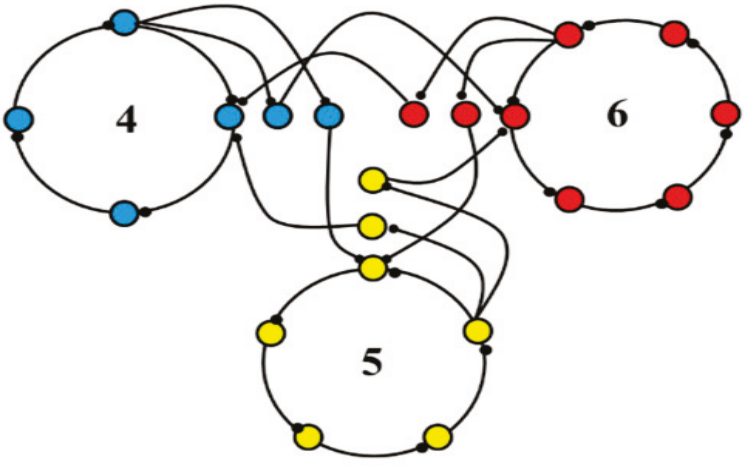

Figure 23. One instantiation of the four-oscillator network. There are three oscillators that consist of four, five, and six nodes, respectively. Each node contains 100 neurons. In each oscillator, a designative node is also connected to the corresponding node in the other oscillators, creating a loosely coupled network. The neurons in each node received inputs from all neurons in the previous node and sent outputs to each neuron in the subsequent node [1].

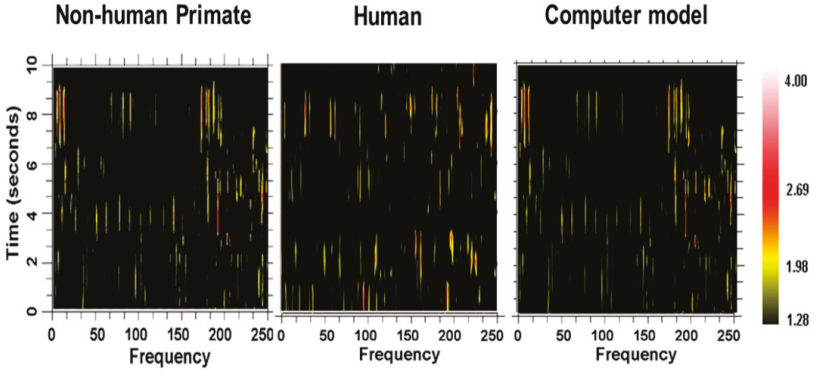

Figure 24. Spectrograms showing the amount of activity (power) at different frequencies over time. The power is represented as the *z*-score difference (color scale) over a randomized train of action potentials (spike train). At each point in time, the train of action potentials has a specific set of frequencies over a range of frequencies. Also, the train of action potentials appears to be stable in their frequency content and then change (bifurcate) to other sets of frequencies. Spectrograms of actual recordings in the globus pallidus externa of a nonhuman primate, the subthalamic nucleus in a human, and a neuron in the computer model of the network are shown.

10. Conclusions

The physiological mechanism underlying the effect of DBS frequency remains an enigma, particularly as the complexities of the relationship between the DBS frequencies and motor effects are more fully recognized. However, addressing the enigma is a great opportunity because, typically, new knowledge is needed in order to solve it. New knowledge can only come from new hypotheses, which most often require new perspectives. New perspectives require letting go of old

perspectives, at least those aspects that are counterproductive. This requires exercise in epistemological analysis as well as experiments.

It is likely that the effects of DBS frequency have a great deal to say about the underlying dynamics of the pathophysiology and physiology of the basal ganglia-thalamic-cortical system. A better understanding of those dynamics could provide a metaphor for research that extends beyond the basal ganglia-thalamic-cortical system.

Acknowledgments: Funding was provided in its entirety by the Greenville Neuromodulation Center, which is a nonprofit corporation dedicated to the advancement of neuromodulation therapies.

Author Contributions: Erwin B. Montgomery Jr. was responsible for all efforts related to the article; He Huang: data acquisition and analyses, computational modeling and simulations

Conflicts of Interest: The author declares no conflict of interest. The founding sponsors had no role in the design of the study; in the collection, analyses, or interpretation of data; in the writing of the manuscript; and in the decision to publish the results.

References

1. Montgomery, E.B., Jr. *Deep Brain Stimulation Programming: Mechanisms, Principle and Practice*, 2nd ed.; Oxford University Press: Oxford, UK, 2016.
2. Schultz, W.; Montgomery, E.B., Jr.; Marini, R. Proximal limb movements in response to microstimulation of primate dentate and interpositus nuclei mediated by brain-stem structures. *Brain* **1979**, *102*, 127–146. [CrossRef] [PubMed]
3. Huang, H.; Watts, R.L.; Montgomery, E.B., Jr. Effects of deep brain stimulation frequency on bradykinesia of Parkinson's disease. *Mov. Disord.* **2014**, *29*, 203–206. [CrossRef] [PubMed]
4. Cooper, I.S.; Upton, A.R.; Amin, I. Reversibility of chronic neurologic deficits. Some effects of electrical stimulation of the thalamus and internal capsule in man. *Appl. Neurophysiol.* **1980**, *43*, 244–258. [CrossRef] [PubMed]
5. Benabid, A.-L.; Pollak, P.; Louveau, A.; Henry, S.; De Rougemont, J. Combined (thalamotomy and stimulation) stereotactic surgery of the VIM thalamic nucleus for bilateral Parkinson disease. *Appl. Neurophysiol.* **1987**, *50*, 344–346. [CrossRef] [PubMed]
6. Montgomery, E.B., Jr. The epistemology of Deep Brain Stimulation and neuronal pathophysiology. *Front. Integr. Neurosci.* **2012**, *6*. [CrossRef] [PubMed]
7. Goetz, C.G.; Delong, M.R.; Penn, R.D.; Bakay, R.A. Neurosurgical horizons in Parkinson's disease. *Neurology* **1993**, *43*, 1–7. [CrossRef] [PubMed]
8. Montgomery, E.B., Jr. Basal ganglia physiology and pathophysiology: A reappraisal. *Parkinsonism Relat. Disord.* **2007**, *13*, 455–465. [CrossRef] [PubMed]
9. Aristotle, A. *The Basic Works of Aristotle*; McKeon, R., Ed.; The Modern Library: New York, NY, USA, 2001.
10. Arikha, N. *Passions and Tempers: A History of the Humours*; Harper Perennial: New York, NY, USA, 2007.
11. Sherrington, C.S. *The Integrative Action of the Nervous System*; Oxford University Press: Oxford, UK, 1906.
12. Kuhn, T. *The Structure of Scientific Revolutions*; The University of Chicago Press: Chicago, IL, USA, 1962.
13. Montgomery, E.B., Jr.; Buchholz, S.R.; Delitto, A.; Collins, R.C. Alterations in basal ganglia physiology following MPTP in monkeys. In *MPTP: A Neurotoxin Producing a Parkinsonian Syndrome*; Markey, S.P., Castagnoli, A.J., Jr., Trevor, A.J., Kopin, I.J., Eds.; Academic Press, Inc.: Orlando, FL, USA, 1986; pp. 679–682.
14. Johnson-Laird, P. *How We Reason*; Oxford University Press: Oxford, UK, 2006.
15. Montgomery, E.B., Jr. Neurophysiology. In *Handbook of Parkinson's Disease*, 5th ed.; Pahwa, R., Lyons, K.E., Eds.; CRC Press: Boca Raton, FL, USA, 2013; p. 258.
16. Montgomery, E.B., Jr. Dynamically coupled, high-frequency reentrant, non-linear oscillators embedded in scale-free basal ganglia-thalamic-cortical networks mediating function and deep brain stimulation effects. *Nonlinear Stud.* **2004**, *11*, 385–421.
17. Piper, H. Uber den willkiirlichen Muskeltetanus. *Arch. Gesamte Physiol. Menschen Tiere* **1907**, *119*, 301–338. [CrossRef]
18. Brown, P. Muscle sounds in Parkinson's disease. *Lancet* **1997**, *349*, 533–535. [CrossRef]

19. Hagbarth, K.E.; Jessop, J.; Eklund, G.; Wallin, E.U. The Piper rhythm: A phenomenon related to muscle resonance characteristics? *Acta Physiol. Scand.* **1983**, *117*, 263–271. [CrossRef] [PubMed]
20. Brown, P.; Salenius, S.; Rothwell, J.C.; Hari, R. Cortical correlate of the Piper rhythm in humans. *J. Neurophysiol.* **1998**, *80*, 2911–2917. [PubMed]
21. Enoka, R.M. Morphological features and activation patterns of motor units. *J. Clin. Neurophysiol.* **1995**, *12*, 538–559. [CrossRef] [PubMed]
22. Huang, H.; Watts, R.L.; Guthri, B.L.; Walker, H.C.; Montgomery, E.B., Jr. Reversal of size principle in Parkinson's Disease and normalization with Deep Brain Stimulation. In Proceedings of the International Motor Units Conference, Sydney, Australia, 23–26 July 2012; p. 45.
23. Montgomery, E.B., Jr.; Gale, J.T.; Huang, H. Methods for isolating extracellular action potentials and removing stimulus artifacts from microelectrode recordings of neurons requiring minimal operator intervention. *J. Neurosci. Methods* **2005**, *144*, 107–125. [CrossRef] [PubMed]
24. Walker, H.C.; Huang, H.; Gonzalez, C.L.; Bryant, J.E.; Killen, J.; Cutter, G.R.; Knowlton, R.C.; Montgomery, E.B.; Guthrie, B.L.; Watts, R.L. Short latency activation of cortex during clinically effective subthalamic deep brain stimulation for Parkinson's disease. *Mov. Disord.* **2012**, *27*, 864–873. [CrossRef] [PubMed]
25. Montgomery, E.B., Jr.; Gale, J.T. Mechanisms of action of deep brain stimulation (DBS). *Neurosci. Biobehav. Rev.* **2008**, *32*, 388–407. [CrossRef] [PubMed]
26. Schuster, A. The periodogram and its optical analogy. *Proc. Roy. Soc. Lond.* **1905**, *77*, 136–140. [CrossRef]
27. Takeshita, D.; Gale, J.T.; Montgomery, E.B., Jr.; Bahar, S.; Moss, F. Analyzing spike trains with circular statistics. *Am. J. Phys.* **2009**, *77*, 424–429. [CrossRef]
28. Gale, J.T. Basis of Periodic Activities in the Basal Ganglia–Thalamic–Cortical System of the Rhesus Macaque. Ph. D. Thesis, Kent State University, Kent, OH, USA, 2004.
29. Hoppensteadt, F.C.; Izhikevic, E.M. *Weakly Connected Neural Networks*; Springer-Verlag New York Inc.: New York, NY, USA, 1997; p. 126.
30. Buchholz, S.R.; Montgomery, E.B., Jr. Head restraint device for chronic recording of neural activity in the awake monkey. *J. Neurosci. Methods* **1988**, *25*, 139–141. [CrossRef]
31. Hirschmann, J.; Butz, M.; Hartmann, C.J.; Hoogenboom, N.; Özkurt, T.E.; Vesper, J.; Wojtecki, L.; Schnitzler, A. Parkinsonian rest tremor is associated with modulations of subthalamic high-frequency oscillations. *Mov. Disord.* **2016**. [CrossRef] [PubMed]
32. Walker, H.C.; Watts, R.L.; Schrandt, C.J.; Huang, H.; Guthrie, S.L.; Guthrie, B.L.; Montgomery, E.B., Jr. Activation of subthalamic neurons by contralateral subthalamic deep brain stimulation in Parkinson disease. *J. Neurophysiol.* **2011**, *105*, 1112–1121. [CrossRef] [PubMed]
33. Montgomery, E.B., Jr. Effects of GPi stimulation on human thalamic neuronal activity. *Clin. Neurophysiol.* **2006**, *117*, 2691–2702. [CrossRef] [PubMed]
34. Chomiak, T.; Hu, B. Axonal and somatic filtering of antidromically evoked cortical excitation by simulated deep brain stimulation in rat brain. *J. Physiol.* **2007**, *579*, 403–412. [CrossRef] [PubMed]
35. Rosen, A.D. Nonlinearity in the generation of antidromic activity during evoked cortical activity. *Exp. Neurol.* **1981**, *71*, 269–277. [CrossRef]
36. Li, S.; Arbuthnott, G.W.; Jutras, M.J.; Goldberg, J.A.; Jaeger, D. Resonant antidromic cortical circuit activation as a consequence of high-frequency subthalamic deep-brain stimulation. *J. Neurophysiol.* **2007**, *98*, 3525–3537. [CrossRef] [PubMed]

brain sciences

MDPI

Opinion

Deep Brain Stimulation: In Search of Reliable Instruments for Assessing Complex Personality-Related Changes

Christian Ineichen [1,*], Heide Baumann-Vogel [2] and Markus Christen [1]

[1] Institute of Biomedical Ethics and History of Medicine, University of Zurich, Winterthurerstrasse 30, Zurich 8006, Switzerland; christen@ethik.uzh.ch

[2] Department of Neurology, University Hospital Zurich, Frauenklinikstrasse 26, Zurich 8091, Switzerland; Heide.baumann-vogel@usz.ch

* Correspondence: christian.ineichen@uzh.ch; Tel.: +41-446-348-439

Academic Editors: Tipu Aziz and Alex Green
Received: 20 July 2016; Accepted: 1 September 2016; Published: 7 September 2016

Abstract: During the last 25 years, more than 100,000 patients have been treated with Deep Brain Stimulation (DBS). While human clinical and animal preclinical research has shed light on the complex brain-signaling disturbances that underpin e.g., Parkinson's disease (PD), less information is available when it comes to complex psychosocial changes following DBS interventions. In this contribution, we propose to more thoroughly investigate complex personality-related changes following deep brain stimulation through refined and reliable instruments in order to help patients and their relatives in the post-surgery phase. By pursuing this goal, we first outline the clinical importance DBS has attained followed by discussing problematic and undesired non-motor problems that accompany some DBS interventions. After providing a brief definition of complex changes, we move on by outlining the measurement problem complex changes relating to non-motor symptoms currently are associated with. The latter circumstance substantiates the need for refined instruments that are able to validly assess personality-related changes. After providing a brief paragraph with regard to conceptions of personality, we argue that the latter is significantly influenced by certain competencies which themselves currently play only a tangential role in the clinical DBS-discourse. Increasing awareness of the latter circumstance is crucial in the context of DBS because it could illuminate a link between competencies and the emergence of personality-related changes, such as new-onset impulse control disorders that have relevance for patients and their relatives. Finally, we elaborate on the field of application of instruments that are able to measure personality-related changes.

Keywords: deep brain stimulation; personality; instruments; competencies

1. Introduction

Deep Brain Stimulation (DBS) is a neurosurgical intervention that involves electrode implantation to apply electrical currents to target structures aiming at alleviating symptoms. More precisely, the surgical method involves a stereotactical implantation of usually quadripolar electrodes including an extracerebral "pacemaker" that modulates the activity of selected regions in the brain with electric impulses. The key advantages of this procedure are (1) its potential reversibility and (2) the possibility to postoperatively optimize treatment effects via an external programming device. So far, a great number of patients suffering from various neurological and neuropsychiatric disorders have been treated with DBS. DBS unquestionably is a remarkable therapy that has provided hope for many patients and that has been shown to be more effective than best medical treatment for some disorders. Among those, patients suffering from Parkinson's disease (PD) and who are refractory to drug treatment represent by far the largest patient group.

In the meantime, the rapid development reached a non-undisputed broadening of the therapeutic spectrum [1]. DBS of the subthalamic nucleus (STN) has been established in randomized, controlled trials as an effective therapy for the motor symptoms of PD [2–4] and, consequently, the'number of patients being treated by DBS has steadily increased. Along this increase, challenges arose with regard to appropriate patient selection and side-effects, to name a few. With some delay, the systematic investigation of neuropsychiatric changes observed in patients treated with DBS for movement disorders found their way into the scientific literature, first as anecdotal reports and later in the form of quantitative research studies [5].

In sum, DBS has demonstrated dramatic symptom relief for a multitude of patients. However, complex non-motor changes following DBS interventions have been described. Because there is only a very limited number of instruments that are able to validly measure complex personality-related changes, there is great need for the development of new and reliable instruments in order to collect information and to evaluate these changes. As will be seen, there is a need to more thoroughly explore e.g., morally relevant behaviours (such as impulse control disorders, ICDs) with a particular emphasis on psychosocial competencies. The underlying competencies that might be dysfunctional secondary to disease, pharmacological therapy or neuromodulation interventions aiming to treat patients suffering from diseases, however, are hardly the focus of current DBS-research. In turn, new instruments that are able to quantify and depict such competencies might be highly relevant because they can yield explanatory power regarding psychosocial changes that are decisive for patients and their relatives.

2. Complex Changes after DBS Interventions

2.1. Non-Motor Problems Following DBS in Movement Disorders

In what will follow and for the sake of clarity, we restrict the argumentation of this contribution to the context of movement disorders and especially PD, even though we are aware of the fact that strictly speaking, PD has a well-documented neuropsychiatric impact on patients. Because STN-DBS in PD is, apart from stimulation of the globus pallidus internus (GPi), most frequently performed, the argumentation below takes up studies that investigated basal-ganglia dysfunction. Furthermore, a recent study provides Class II evidence that STN DBS offers more off-phase motor improvement than GPi DBS with similar risk for behavioural, affective and cognitive complications [6].

Whilst DBS aims primarily at improving motor symptoms in PD, accumulating knowledge points toward non-motor complications. Because a large number of fibers converge in the basal ganglia nuclei on a very small area, it is not surprising that targeting specific functions and manipulating them in an isolated fashion is tremendously difficult. In fact, intervening into basal ganglia physiology bears the risk of modulating non-motor functions [7–9]. The difficulty of specific targeting is even greater when factoring in recent notions of re-entrant or interconnected cortico-striato-pallido-thalamo-cortical loops representing different frequencies [10]. In fact, by manipulating a specific node in the network, one might influence as many different functions, depending on the degree of shared functionality with other circuits. Hence, DBS intervenes with a very complex network [11], the shear complexity of which has probably only started to be deciphered.

A large body of evidence implicates the role of the basal ganglia (BG) in the processing of non-motor signals and several psychiatric disorders such as schizophrenia, obsessive compulsive disorder (OCD), phobias and panic attacks, depressive states, addiction and eating disorders [12–14]. Similarly, neuropsychological changes in humans following DBS interventions have been observed [15], denoting the characterization of the BG as centers of convergence encoding motor, cognitive, associative and affective processes. Notably, the STN, one of the most commonly targeted structures for DBS in PD, has a strategic position due to its connections to both BG output structures (the GPi and substantia nigra pars reticulata (SNr)). Unsurprisingly, modulation of STN-signaling has therefore demonstrated to result in impulsive responding and dysfunctional inhibitory control, such as perseveration, obsessions and compulsions [16]. Hence, it is very well possible that interference with basal ganglia nuclei and the STN specifically, by disease or interventions, can modulate associative

and limbic processing. Notably, interventions not only include DBS but also e.g., pharmacological treatment. The latter has demonstrated the potential of causing unintended side-effects either in combination with DBS or by itself e.g., when drugs are reduced too promptly after DBS initiation or in case of dopamine agonists [17]. In addition, the dopamine agonist withdrawal syndrome (DAWS) and dopamine dysregulation syndrome (DDS) leading to neuropsychiatric symptoms and decreased self-control, respectively, have been described in PD. Therefore, it is widely appreciated that pathological processes and pharmacological treatment alike can lead to alterations in the processing of emotional, cognitive and behavioural stimuli [18].

More generally, a number of behavioural and affective sequelae, such as hypomania, new onset impulse control disorders (ICDs including hypersexuality, pathological buying, pathological gambling, and addiction to levodopa), logorrhea, irritability, impatience and aggression, distractibility and attention problems, egocentrism, obstinacy, and lying have been described following DBS treatment in humans [15,16,19,20]. In the meanwhile, there is also evidence for changes that can be evaluated positively such as increased emotional wellbeing that results in increased Quality of Life (QoL) (see Section 2.2).

Undisputedly, complex non-motor changes have been described following DBS. In this contribution, we extend the topic of non-motor problems and deliberate on complex, non-motor changes for which the evaluation is unclear (i.e., such changes are not per se problematic and can even be positively evaluated). Patients who experience substantial symptom relief may develop new interests and behave differently. While the evaluation of whether these changes are problematic is important, we may first have to make sure that complex changes can reliably be measured. This includes the possibility that strictly differentiating between the measurement and evaluation process is eventually not possible, in particular when measuring personality changes where a positive or negative evaluation could be intrinsic to the measurement process. Nevertheless, and as will be seen, sensitive instruments are highly needed. First, however, we will investigate the nature of complex changes and the fundamental problem they are associated with.

2.2. Complex Changes: In Search of Reliable Instruments

Complex changes can be described as side-effects characterized by two gradual, qualitatively described dimensions. They include measurement complexity of side-effect on the one side and relative life impact of the side-effect weighted by its incidence in the natural disease history on the other side (see [20], Figure 2, for detailed information). Hence, complex changes represent side-effects that are associated with a high level of measurement complexity—an indirect evidence for it being an above average variance of the documented prevalence of a specific side-effect—and a correspondingly high level of relative life impact for the patient but also his/her social surrounding. Unfortunately, our own research provides evidence that the third-person perspective is almost never assessed in current practice (the usage of test scores that emerge from persons affiliated with the patient, are basically nonexistent [21], with the exception of some few recent studies (e.g., [22,23]). Paradigmatic examples of complex changes include changes in personality and moral behaviour. Because there is the problem of measurement complexity, predicting side-effects relating to psychosocial functioning of the patient is currently difficult. Despite the fact that patients raise their concern over the propensity of DBS to cause personality-related changes and that cases in which sudden alterations of personality after DBS have been described (see next paragraph), less emphasis has been put on the construction of instruments for quantifying personality-related changes. It thus stands to reason that complex changes in general (i.e., not limited to stimulation-induced changes) are generally underreported and hence affect the patient population to a much greater extent than assumed. The relative life-impact, in the meanwhile, depends on not only the type of side-effect but also on factors such as, among others, the pre-operative psychosocial status of the individual and premorbid personality traits.

As listed above, non-motor problems following DBS interventions—factors that clearly constrain the effectiveness of this type of intervention—often comprise a neuropsychiatric dimension. While some studies investigated non-motor problems following DBS interventions, few if any have focused on more demanding notions of personality and psychosocial competency [15],

probably because of the complexity of the subject matter. For example, STN-DBS has been associated with deficits on a variety of tasks that require inhibition of prepotent responses and response selection during situations of high conflict (for a review, see [16]; for augmented impulsivity, see [24–26]; for a study demonstrating increased impulsivity assessed by the Barratt Impulsiveness Scale (BIS), see [27]), but few investigations included more profound notions of personality (see next paragraph). With regard to changes in mood and behaviour, a meta-analysis involving 1398 patients and 82 studies by Temel et al. [28] outlined that 8% suffer from depression, while activities of daily living (ADL) score improved by 52%, consistent with other reports documenting an improvement in QoL that is only related to physical aspects but not to mood ([29]: prospective study with non-implanted PD patients as control group). The latter study also highlighted 9% psychiatric complications (compared to 3% in the control group). Another more recent study found few changes in mood and behaviour with unilateral STN or GPi DBS, relating to worsened anxiety, depression and mania [30]. Other studies also revealed an increase in QoL including emotional well-being (for improvements of anxiety and depression see [31–33], in case of stigma and bodily discomfort see [34,35]). Particularly, the study of Witt and colleagues [19] found an improvement in anxiety, otherwise psychiatric adverse events in 16.7% of patients (compared to 12.7% for best medical treatment group) and a decrease in frontal cognitive functioning with no consequences on improvements in QoL. Finally, alterations in decision-making of PD patients measured by the Iowa gambling task (IGT) have been demonstrated by Pagonabarraga and colleagues [36] (with results pointing at similar decision-making deficits as seen in ventromedial prefrontal cortex (PFC) lesioned patients and pathological gamblers). Even though incorporating only a small sample size, Bentrup et al. [37] found an increase in "novelty seeking" in two out of 15 patients besides a decrease of sociomoral judgment on the six-level Kohlberg scale. On the contrary, Brandt et al. found that DBS may temper the tendency of risk-taking on risky decision making tasks with DBS patients being more risk-averse in ambiguous-risk situations [38].

With regard to personality changes mirroring temperament and character, Houeto and colleagues [39] have examined, in an earlier study and retrospectively, adjustment disorders (using the social adjustment scale (SAS)), personality changes (using the Iowa rating scale of personality change (IRSPC)) and psychiatric disorders (using psychiatric interviews and the mini international neuropsychiatric inventory). Results indicated moderately to severely impaired social adjustment by 62.5% while personality traits were improved by 35% and aggravated by another 35%. Table 1 lists these and the forthcoming outcomes of some recently performed DBS-studies together with a brief test description, overall revealing that more studies and new instruments would be desirable. Another retrospective study of the same researchers [34], however, observed very different results including unmodified personality traits (as assessed by the Temperament and Character Inventory-revised (TCI-R) and this contrary to [40], who found increased scores on two Novelty-Seeking subscales of the same measure) and social adjustment apart from improved depression, anxiety and QoL. Denheyer and colleagues [41], on the other hand, used the Frontal Systems Behavior Scale (FrSBE) in order to assess behavioural changes including apathy, disinhibition and executive dysfunction. In a retrospective study with a non-representative sample, all scores increased significantly. Notably, most of the above-listed instruments have important limitations, such as, for example, the subjective nature of the FrSBE that is influenced by e.g., preconceived expectations about the outcome of DBS. Taken together, these outcomes imply relatively contradictory results. To be clear, psychosocial dysfunction and changes relating to altered character after DBS, potentially resulting in difficulties of social adjustment, satisfaction gaps and conflicting outcome interpretations between patients, their relatives and practitioners, have vaguely been described ([42,43], or studies using e.g., the SAS), but have not been investigated focusing on causal elements leading to such changes. Because few empirical studies that investigate personality changes exist, recently Lewis and colleagues [22] have examined the latter by use of semi-structured interviews and a neuropsychiatric battery (Parkinson's disease questionnaire-PDQ-39, Beck depression inventory (BDI-II), apathy evaluation scale (AES), state-trait anxiety inventory

(STAI-state), self-report manic inventory (SRMI), Barratt impulsiveness scale (BIS-11), hypomanic personality scale (HPS) and mini mental status examination (MMSE)), highlighting that personality changes occur between 22% (self-evaluation) and 44% (evaluation by caregiver, e.g., spouses), with another 57% perceiving mood changes as positively, thereby emphasizing the relevance of such investigations. However, higher apathy and anxiety levels were found in the negative change group. The fact that the used standard measurement scales were unsuccessful in adequately reflecting personality and mood changes in this study, substantiates the need for better and refined instruments. One more recent study investigated personality changes after DBS [23]: the 125-item version of the TCI (TCI-125), the urgency-premeditation-perseverance-sensation seeking (UPPS) impulsive behaviour scale and the Eysenck Personality Questionnaire (EPQ) have been used with findings relating to increased impulsivity and personality changes in Persistence- and Self-Transcendence test scores (see Table 1). Notably, the previously listed non-motor problems are likely to be associated with other fine-grained changes which may reach far into the domain of personal convictions, values and sensitivities. These changes might be so nuanced that they will slip through current assessment of psychiatric test batteries (for example, see [22]). Hence, even though there are a number of tests for investigating e.g., impulsivity (e.g., Eriksen flanker and Simon task, the Stroop color word interference task and random number generation; [16]), less emphasis has been put on the construction of instruments for quantifying nuanced personality-related changes [5,44], including instruments depicting personal competencies in sociomoral information processing in order to have instruments at one's disposal that pick up relevant topics that matter to patients and caregivers.

Addressing complex personality-related changes with the requisite rigour may explain causal elements for the emergence of conflicting outcome interpretations and social maladjustment that are relevant for patients and their relatives. Clearly, such instruments need to rely on newer insights of psychological research (see Section 4.2). While in the large majority of patients, symptoms relating to dominant expressions of behavioural phenotypes such as impulse control disorders or hypomania can be controlled (either they vanish spontaneously or by adjusting stimulation and/or drug treatment), more subtle changes have rarely been addressed so far due to the lack of sensitive instruments that measure complex changes beyond standard test-psychology. Given that some behavioural changes listed above had long-lasting social effects and damaged relationships that often only came to the fore through in-depth qualitative research [45], and given that patients express their concern over personality-related changes secondary to deep brain stimulation—as clinical experience at our clinic shows—together with the magnitude of the life impact for patients and their relatives, it is staggering that, if any, only a very limited set of data e.g., [22,23,46] and few established instruments apart from very general personality assessment tools of standard test psychology (e.g., the big five personality test, but see Table 1) are currently available that deal with the topic of personality-related changes. The limited data is surprising also when considering that changes in personality and mood under DBS in PD are discussed both in the clinical but also the ethical literature [47–50]. In addition to the problem of measuring complex changes, there is also the evaluation difficulty relating to the problem of how to evaluate such changes. As Kraemer [51] pointed out, "alienation from alienating conditions" can occur. The latter denotes the difficulty of how to evaluate changes in personality. Are marital problems following DBS implantations categorically social maladjustments or may they, in a proportion of patients, reflect a changed personality denoting to more fundamental desires and thoughts that are at the core of the patients' true self? Does a given change in personality symbolize alienation or approach to a patient's pre-morbid personality? Without going into the details of such difficult questions, it is enough to stress that instruments and their ability to measure complex changes are a necessary precondition in order to move on and evaluate whether complex changes are problematic (including e.g., notions of felt-authenticity and felt-alienation). This includes the very possibility that not all changes are per se negative and that also positive personality changes following DBS surgery can occur. The latter is particularly important in the context of psychiatric DBS intervention where the positive change of ones' personality is at the core of the therapeutic aim. These strategies may inform ethically responsible decision making in e.g., the referral practice of DBS interventions (see Section 4.3).

Table 1. Outline of some of the recently used measures of personality in deep brain stimulation (DBS) studies, including measurement description and study outcome with reference numbers in brackets.

Name of Test/Scale	Short-Description	Study & Main Study Results
Social adjustment scale (SAS)	Semistructured interview, performed in the presence of the spouse, that evaluates current social adjustment in terms of 44 items	Houeto et al., 2002 [39]: moderately to severely impaired social adjustment by 62.5%; Houeto et al., 2006 [34]: SAS global score and subscores (work, social life and leisure activities, family life, marital relations, and interaction with children) unmodified
Iowa rating scale of personality change (IRSPC)	30 characteristics are assessed, ratings are gathered from family members with regular contact with the patient	Houeto et al., 2002 [39]: personality traits were improved by 35% aggravated by 35% und unchanged by another 30%
Temperament and Character Inventory-revised (TCI-R)	Self-evaluation, four temperaments (Novelty Seeking (NS), Harm Avoidance (HA), Reward Dependence (RD), Persistence (PS)) and three characters (Self-Directedness (SD), Cooperativeness (CO), Self-Transcendence (ST))	Fassino et al., 2010 [40]: higher scores emerged on two Novelty-Seeking subscales; Houeto et al., 2006 [34]: unmodified personality traits; Pham et al., 2015 (TCI-125) [23]: patients reported lower score on the TCI Persistence and Self-Transcendence scales, after three months of subthalamic nucleus stimulation (STN-DBS), compared to baseline
Eysenck Personality Questionnaire (EPQ)	Self-report questionnaire: Extraversion, Neuroticism, Psychoticism and Lie scale	Pham et al., 2015 [23] (Neuroticism and Lie subscales (EPQ-N, EPQ-L)): no changes
Frontal Systems Behavior Scale (FrSBE)	Behavioral assessment of frontal lobe syndromes, includes items related to apathy, disinhibition, and executive dysfunction; 46-item behavior rating scale, self-evaluation and family evaluation	Denheyer et al., 2009 [41]: apathy, disinhibition and executive dysfunction increased
X	Semi-structured interviews, developed by the ELSA-DBS study group (a project that examines Ethical, Legal and Social Aspects of Deep Brain Stimulation with respect to health, quality of life and personal identity) to investigate motor, emotional, social, behavioural and cognitive functioning, activities of daily living and QoL	Lewis et al., 2015 [22]: personality changes occurred between 22% (self-evaluation) and 44% (evaluation by caregiver, e.g., spouses)

In sum, we argue that there is currently a lack of valid instruments that adequately depict changes in psychosocial processing. Even though a limited number of standardized questionnaires and tests are available, they may not reflect sufficiently the behavioural and affective changes and their effects in real life. Therefore, new avenues for the better description of complex personality-related changes that may explain causal elements for the emergence of conflicting outcome interpretations, in addition to social maladjustment that are relevant for patients and their relatives, need to involve instruments that rely on newer insights of psychological research.

3. Psychosocial Competencies

3.1. Individual Identity, Personality and Psychosocial Competencies: Conceptualizations and Interconnections

As proposed elsewhere [5], a conceptual clarification of individual identity and personality is decisive for evaluating and measuring potential personality-related changes in the future. Even though the focus of this contribution is empirical rather than conceptual, a brief conceptual clarification is necessary. While "individual identity" may be understood as a philosophical concept, "personality" refers to a psychological one [5]. Because the latter is empirical in nature, it is part of this work. Personality can briefly be described as the combination of certain characteristics or qualities that form an individual's idiosyncratic character. It is commonly defined as "the organized set of characteristics possessed by a person that uniquely influences his or her cognitions, motivations, and behaviours in various situations" [52]. Psychosocial competencies are one class of examples that can influence and guide a person's cognition, motivation and behaviour and hence align with the previous definition of personality. They include, among others, self-regulatory skills, the ability to identify issues linked to personal desires and values and to align one's behaviour according to one's self-conception, the desire to orient oneself towards and strive for one's ideals, skills to resolve conflicting (internal or external) tendencies and the ability to act consistently with one's internal thoughts and ideas. They furthermore guide human cognition through schemas and scripts (i.e., cognitive representations, e.g., [53,54]). Personality changes as understood in current psychology refer to alterations in the "Big Five" personality traits (i.e., extraversion, neuroticism, agreeableness, conscientiousness, openness to experience; see [55]), representing a very vague sum of a set of traits that can be altered. Notably, the latter concept has recently been expanded by the HEXACO model that adds a sixth trait circumscribing ones' personality. That this sixth personality trait is precisely moral in nature (honesty-humility-dimension) is certainly an interesting development that aligns with the requested emphasis on morality and its associated competencies expressed in this contribution (see Section 4.1).

While a whole plethora of different competencies are necessary and amalgamate in interpersonal human conduct, the time is rife for investigating basic mechanisms of psychosocial competencies and to start developing instruments for measuring the underlying competencies. The fact that psychological competencies are needed in situations of complex decision making and behaviour, together with the likely potential of DBS to influence such competencies, corroborates the need of instruments to document and evaluate changes of psychosocial functioning in order to better support patients and their social surrounding. Moreover, DBS provides a possibility to investigate changes depending on type of stimulation and anatomical target.

3.2. Human Behaviour as an Expression of Social Competencies

With the emergence of psychology as a scientific discipline, questions arose regarding the identification of psychological skills that are necessary for social interaction but also regarding the extent and interplay of biological determinants that affect psychological processes. Broadly speaking, human behaviour includes processing external and internal stimuli and interacting with the external world. Hence, an interactionist view is mandatory in order to explain and understand behaviour.

The same holds with regard to moral behaviour where analogously personal and environmental or contextual factors operate interactively in determining behaviour. Personal factors include a specific set of competencies while environmental factors involve conditions promoting or obscuring moral conduct (e.g., through priming by family pictures, time pressure, economic incentives, [56–59]). In addition, moral behaviour involves a normative reference frame to which the subject has at least partial access [60]. Thus, apart from environmental factors as well as ones' personal moral identity, personal competencies significantly influence human action. Because it is likely that disorders and treatment approaches when interfering with the central nervous systems integrity directly or indirectly alike, might influence psychosocial competencies, the investigation of abilities of patients is genuinely pertinent. In line with this, it might be possible that DBS detrimentally influences a specific subset of competencies in a way that facilitates the emergence of behavioural disorders, such as ICDs, consequently leading to complex changes including e.g., psychosocial maladjustment. Unfortunately, the potentially dysfunctional competencies secondary to DBS interventions are hardly the focus of current research. So far, socio-moral behaviour and moral information processing following deep brain stimulation interventions has received little attention, even though problems in social adjustment raise questions that refer to psychosocial competences and abilities of the patient. New instruments that are able to quantify and depict such competencies might be highly relevant because they can yield explanatory power regarding psychosocial changes that are decisive for patients and their relatives.

4. Moral Psychological Competencies, Requirements for Instrument Implementation Strategies and Future Use of Instruments in DBS Research and Therapy

4.1. Moral Psychological Relevance for Assessing Complex Changes in Moral Information Processing as an Exemplary Case

The field with the richest empirical knowledge on how agents reason, decide and act morally is still moral psychology. Undisputedly, moral behaviour in everyday situations reposes critically on specific skills moral agents imperatively have to be equipped with. Many of those competencies and abilities are psychological in nature. Apart from earlier approaches (see e.g., [61]) Tanner and Christen [62] proposed an adapted framework termed "Moral Intelligence" that describes the process logic of moral behaviour by taking into account fundamental knowledge about implicit and explicit psychological processes and theoretical insights into morality, and superimposed on this, aiming at translating these processes into competencies. The framework includes a content-related component along a set of motivational, perceptive, decisional and action-related abilities. Besides that, progress in cognitive and social neuroscience has led to investigations of other important social constructs such as empathy and morality (see e.g., Jefferson Scale of Empathy, the multifaceted empathy test with one study revealing reduction of the "negativity bias" in patients with treatment-resistant depression by DBS [63], or the moral foundation scale by Haidt and the moral attentiveness scale by Reynolds). These and other strains of research, therefore, bear witness to the importance of identifying key competencies of human moral ability and how those competencies are rooted within and affected by psychological processes. Because moral competencies, such as the ability to recognize ethical issues in everyday situations, influences a person's cognitions, motivations, and behaviours, changes in these competencies can lead to complex, personality-related changes. Other moral-related competencies include the possession of a more distinct desire to strive for moral goals, self-regulatory skills, the ability to resolve conflicting tendencies or being more prone to act consistently and courageously despite internal or external barriers. This rich variety of different skills that can be expressed in different degrees in part account for why people act uniquely and why they display unique personalities.

4.2. Thinking Ahead: Operationalization of Moral Competencies as an Exemplary Case

As an example, one particular psychological competency that is relevant in the context of moral behaviour is moral sensitivity (MS) [64], the ability to recognize (moral) issues in a given

situation. Being conceptualizes as the first competency in the process logic of human moral behaviour (see Rest's (1986) multi stage model of moral functioning [61] or the framework of Moral Intelligence [62]), moral sensitivity is an indispensable competence to enter decision-making processes and moral behaviour in general. Hypothetically, it might be possible that DBS constrains the sensitivity of an individual in such a way that makes it difficult for the patient to recognize that a given person might be harmed by certain actions, even though he is generally of the opinion that one should abstain from harming others. To be sure, changes in moral information processing are likely to occur also secondary to pathological processes and (e.g., pharmacological) treatment approaches. The use of refined instruments that depict neuropsychological competencies is, therefore, not limited to DBS. The decreased sensitivity to recognize e.g., the harming nature of certain actions following DBS intervention could symbolize a basis for explaining complex personality-related changes. Notably, there is a difference between the inability to subconsciously recognize that a given value might be harmed and the deliberate convictions somebody holds. While such fine-grained changes can sometimes be assessed by conducting qualitative semi-structured interviews in patients [20], the latter are often impracticable due to the time-consuming steps of post-coding. Often enough, in times of evidence-based medicine, and hence a quantitatively oriented medical discipline, effects are only becoming a relevant aspect of research if they can reliably be measured. Hence, quantitative instruments should supplement qualitative research, thereby emphasizing the prima facie importance of more vigorously investigating personality. Most importantly, and in order to safeguard clinical meaningfulness, abstract clinical scale-improvements have to be associated with an actual improvement in the individual patient's life. While there were e.g., reports documenting measurable cognitive declines, the latter were found not to be very relevant for patients' QoL. That the same holds for slight changes in personality is less likely, since changes in one's personality are more probable to have an impact on daily life by being able to endanger relationships and family life [22]. They often affect interpersonal relations and inflict greater burden on caregivers [65], apart from the fact that changes can be subtle so that patients themselves may be unaware of them [66]. Statistically significant efficacy is, therefore, only a necessary, but not a sufficient condition, as it does not always correspond to meaningful changes. QoL assessments are one way to document clinical meaningfulness, but the construct itself is very difficult to assess (e.g., unrealistic expectations about DBS outcomes can fundamentally influence QoL in that no improvement is seen in QoL despite motor improvement). By aligning our own research to the mentioned need, we recently have built a computerized instrument to measure MS by taking into account recent insights from moral psychology [67]. Needless to say, instruments need to satisfy common psychodiagnostic standards including reliability, validity and other quality characteristics of psychological test-theory in order to guarantee that these instruments measure what they intend to measure and with the requisite precision.

Challenges of the instrument development process are multifaceted and include e.g., the incorporation of vague quantifiers in the context of psychosocial functioning. The step of specifying basic components is therefore utterly important. In addition, the delicate nature of the instruments' content, covering morality including e.g., anti-social compulsions or sexual urges, poses implicit challenges to instrument development and data acquisition. Besides that, there might be the problem of overlapping functions denoting the difficulty of dissociating competencies that result in moral action. Instruments should likewise, to some degree, adhere to the criterion of generalizability or, as a minimum criterion, context-dependent instruments would need some form of justification. They are also expected to refrain from provoking biased responses by e.g., avoiding including the terms "ethical" and "moral". In addition, instruments should take up recent insights of moral-psychological research. Correspondingly, instruments that are entirely based on self-reports are susceptible to bias, due to the provocation of social-desirable answer tendencies or e.g., reduced awareness based on frontal-subcortical circuit dysfunction. Finally, the methodological requirements should be as low as possible: because the categorization (post-coding) of issues (mentioned by participants) is time-consuming and requires the analysis of inter-rater-reliabilities, and because some implicit

measurements impose participants to work on computers and in controlled environments, they are unsuited for quantitative research approaches.

In sum, in the context of neuropsychological competencies of socio-moral information processing, even fewer instruments exist at present. Future instruments that focus on socio-moral functioning should comply with the requirements of psychological test theory besides taking up recent insights of (moral) psychological research.

4.3. Future Use and Advantage of Instruments Measuring Moral Competencies

Generally, the deployment of instruments that measure psychosocial functioning are conceivable for the referral practice in DBS interventions and as diagnostic outcome-measures in order to measure pre-post DBS effects. The prospective measurement of complex changes may help with making predictions regarding who is likely to experience clinically significant personality-related alterations, making individualized counselling possible, and aiming at minimizing negative impacts on patients and their families.

Because competencies are believed to be flexible entities that evolve and change over time, the focus on psychosocial competencies might encourage investigating means for modulating such competencies for the better, as a potential form of therapeutic interventions. By such an approach, subjects have the opportunity to inimitably learn more about as well as specifically train ones' own competencies.

5. Conclusions

Whilst DBS has provided hope for a large number of patients and while a number of scales for e.g., assessing motor changes have been developed during the last years, there is a conspicuous lack of instruments that target and adequately depict personality-related changes specifically. Standardized questionnaires and tests are available, but they may not reflect sufficiently the behavioural changes and their effects in real life. Together with the highlighted lack of sensitive instruments, an appreciation of the concrete incidence of personality-related changes (evoked by DBS or other treatment approaches) is impossible. Therefore, there is great need for refined instruments that quantify complex, personality-related changes at a satisfactory level. While the clinical significance of any measured change has to be demonstrated, the frequency of such changes has to be investigated by representative samples and prospective study designs in order to systematically investigate these changes in patients relative to controls. Because such instruments may explain causal elements for the emergence of conflicting outcome interpretations and social maladjustment that are relevant for patients and their relatives, such research is desperately needed. Integrating caregivers and families' perceptions of the patient and the impact on their life would complement this complex investigation, thereby safeguarding clinical meaningfulness. Given the challenge patients may face when finding a "new" personality after being freed from the motor symptoms, and the subsequent loss of (motor) autonomy that kept them fettered to PD, it is utterly important to give patients, their relatives and clinicians means for granting ways for measuring and assessing changes in an appropriate way. Hence, the time is rife for advancing DBS treatment along both the technological axis, and an axis that involves the holistic assessment including personality in its full intricacy in order to provide further help to many patients. Besides empirical research that includes the development of instruments and the systematic and longitudinal investigation of complex changes that relate to personality, conceptual investigation on identity and qualitative research with patients, their relatives and clinicians are highly relevant. It is only with the construction of sensitive instruments, allowing a subtle measurement of the type of change, that an evaluation of the positive or negative nature of change is possible. Finally, besides a clinical, it is also an ethical requirement to further investigate complex changes in order to responsibly apply DBS.

Author Contributions: C.I. wrote the paper, M.C. and H.B.V. provided valuable feedback.

Conflicts of Interest: The authors declare no conflict of interest.

Abbreviations

The following abbreviations are used in this manuscript:

DBS	Deep Brain Stimulation
PD	Parkinson's Disease
STN	Subthalamic Nucleus
GPi	Globus Pallidus Internus
SNr	Substantia Nigra Pars Reticulata
ICD	Impulse Control Disorders
OCD	Obsessive Compulsive Disorder
BG	Basal Ganglia
QoL	Quality of Life
DDS	Dopamine Dysregulation Syndrome
DAWS	Dopamine Agonist Withdrawal Syndrome
ADL	Activities of Daily Living
SAS	Social Adjustment Scale
FrSBE	Frontal Systems Behavior Scale
PDQ-39	Parkinson's Disease Questionnaire-(PDQ-39)
BDI-II	Beck Depression Inventory-II
AES	Apathy Evaluation Scale
STAI-state	State-Trait Anxiety Inventory
SRMI	Self-Report Manic Inventory
BIS-11	Barratt Impulsiveness Scale
HPS	Hypomanic Personality Scale
MMSE	Mini Mental Status Examination
BIS	Barratt Impulsiveness Scale
TCI-R	Temperament and Character Inventory-Revised
TCI-125	125-Item Version of The Temperament and Character Inventory (Including Dimensions of Temperament (Novelty Seeking, Harm Avoidance, Reward Dependence, Persistence) and Character (Self-Directedness, Cooperativeness and Self-transcendence))
UPPS	Impulsive Behaviour Scale
EPQIGT	Eysenck Personality QuestionnaireIowa Gambling Task
IRSPC	Iowa Rating Scale of Personality Change

References

1. Hariz, M.; Blomstedt, P.; Zrinzo, L. Future of brain stimulation: New targets, new indications, new technology. *Mov. Disord.* **2013**, *28*, 1784–1792. [CrossRef] [PubMed]
2. Deuschl, G.; Schade-Brittinger, C.; Krack, P.; Volkmann, J.; Schäfer, H.; Bötzel, K.; Daniels, C.; Deutschländer, A.; Dillmann, U.; Eisner, W.; et al. A randomized trial of deep-brain stimulation for Parkinson's disease. *N. Engl. J. Med.* **2006**, *355*, 896–908. [CrossRef] [PubMed]
3. Follett, K.A.; Weaver, F.M.; Stern, M.; Hur, K.; Harris, C.L.; Luo, P.; Marks, W.J., Jr.; Rothlind, J.; Sagher, O.; Moy, C.; et al. Pallidal versus subthalamic deep-brain stimulation for Parkinson's disease. *N. Engl. J. Med.* **2010**, *362*, 2077–2091. [CrossRef] [PubMed]
4. Weaver, F.M.; Follett, K.; Stern, M.; Hur, K.; Harris, C.; Marks, W.J.; Rothlind, J.; Sagher, O.; Reda, D.; Moy, C.S.; et al. Bilateral deep brain stimulation vs best medical therapy for patients with advanced Parkinson disease: A randomized controlled trial. *JAMA* **2009**, *301*, 63–73. [CrossRef] [PubMed]
5. Witt, K.; Kuhn, J.; Timmermann, L.; Zurowski, M.; Woopen, C. Deep brain stimulation and the search for identity. *Neuroethics* **2013**, *6*, 499–511. [CrossRef] [PubMed]
6. Odekerken, V.J.; Boel, J.A.; Schmand, B.A.; de Haan, R.J.; Figee, M.; van den Munckhof, P.; Schuurman, P.R. GPi vs STN deep brain stimulation for Parkinson disease Three-year follow-up. *Neurology* **2016**, *86*, 755–761. [CrossRef] [PubMed]

7. Frank, M.J.; Samanta, J.; Moustafa, A.A.; Sherman, S.J. Hold your horses: Impulsivity, deep brain stimulation, and medication in Parkinsonism. *Science* **2007**, *318*, 1309–1312. [CrossRef] [PubMed]
8. Castrioto, A.; Lhommee, E.; Moro, E.; Krack, P. Mood and behavioural effects of subthalamic stimulation in Parkinson's disease. *Lancet Neurol.* **2014**, *13*, 287–305. [CrossRef]
9. Temel, Y.; Blokland, A.; Steinbusch, H.W.; Visser-Vandewalle, V. The functional role of the subthalamic nucleus in cognitive and limbic circuits. *Prog. Neurobiol.* **2005**, *76*, 393–413. [CrossRef] [PubMed]
10. Montgomery, E.B. *Deep Brain Stimulation Programming: Principles and Practice*; Oxford University Press: Oxford, UK, 2010.
11. Herrington, T.M.; Cheng, J.J.; Eskandar, E.N. Mechanisms of deep brain stimulation. *J. Neurobiol.* **2016**, *115*, 19–38. [CrossRef] [PubMed]
12. Kopell, B.H.; Greenberg, B.D. Anatomy and physiology of the basal ganglia: Implications for DBS in psychiatry. *Neurosci. Biobehav. Rev.* **2008**, *32*, 408–422. [CrossRef] [PubMed]
13. Sesack, S.R.; Grace, A.A. Cortico-basal ganglia reward network: Microcircuitry. *Neuropsychopharmacology* **2010**, *35*, 27–47. [CrossRef] [PubMed]
14. Tremblay, L.; Worbe, Y.; Thobois, S.; Sgambato-Faure, V.; Féger, J. Selective dysfunction of basal ganglia subterritories: From movement to behavioral disorders. *Mov. Disord.* **2015**, *30*, 1155–1170. [CrossRef] [PubMed]
15. Müller, S. *Implanted Minds: The Neuroethics of Intracerebral Stem Cell Transplantation and Deep Brain Stimulation*; Transcript-Verlag: Bielefeld, Germany, 2011.
16. Jahanshahi, M.; Obeso, I.; Baunez, C.; Alegre, M.; Krack, P. Parkinson's disease, the subthalamic nucleus, inhibition, and impulsivity. *Mov. Disord.* **2015**, *30*, 128–140. [CrossRef] [PubMed]
17. Schüpbach, W.M. Impulsivity, impulse control disorders, and subthalamic stimulation in Parkinson's disease. *Basal Ganglia* **2012**, *2*, 205–209. [CrossRef]
18. Jule, S.; Egloff, B.; Schmukle, S.C. Stability and change of personality across the life course: The impact of age and major life events on mean-level and rank-order stability of the Big Five. *J. Personal. Soc. Psychol.* **2011**, *101*, 862.
19. Witt, K.; Daniels, C.; Reiff, J.; Krack, P.; Volkmann, J.; Pinsker, M.O.; Krause, M.; Tronnier, V.; Kloss, M.; Schnitzler, A.; et al. Neuropsychological and psychiatric changes after deep brain stimulation for Parkinson's disease: A randomised, multicentre study. *Lancet Neurol.* **2008**, *7*, 605–614. [CrossRef]
20. Müller, S.; Christen, M. Deep brain stimulation in Parkinsonian patients—Ethical evaluation of cognitive, affective, and behavioural sequelae. *AJOB Neurosci.* **2011**, *2*, 3–13. [CrossRef]
21. Christen, M.; Bittlinger, M.; Walter, H.; Brugger, P.; Müller, S. Dealing with side effects of deep brain stimulation: Lessons learned from stimulating the STN. *AJOB Neurosci.* **2012**, *3*, 37–43. [CrossRef]
22. Lewis, C.J.; Maier, F.; Horstkötter, N.; Zywczok, A.; Witt, K.; Eggers, C.; Meyer, T.D. Subjectively perceived personality and mood changes associated with subthalamic stimulation in patients with Parkinson's disease. *Psychol. Med.* **2015**, *45*, 73–85. [CrossRef] [PubMed]
23. Uyen, P.; Solbakk, A.-K.; Skogseid, I.-M.; Toft, M.; Pripp, A.H.; Konglund, A.E.; Andersson, S. Personality changes after deep brain stimulation in Parkinson's disease. *Parkinson's Dis.* **2015**. [CrossRef]
24. Plessow, F.; Fischer, R.; Volkmann, J.; Schubert, T. Subthalamic deep brain stimulation restores automatic response activation and increases susceptibility to impulsive behavior in patients with Parkinson's disease. *Brain Cogn.* **2014**, *87*, 16–21. [CrossRef] [PubMed]
25. Wylie, S.A.; Ridderinkhof, K.R.; Elias, W.J.; Frysinger, R.C.; Bashore, T.R.; Downs, K.E.; van Wouwe, N.C.; van den Wildenberg, W.P.M. Subthalamic nucleus stimulation influences expression and suppression of impulsive behaviour in Parkinson's disease. *Brain* **2010**, *133*, 3611–3624. [CrossRef] [PubMed]
26. Florin, E.; Müller, D.; Pfeifer, J.; Barbe, M.T.; Fink, G.R.; Timmermann, L. Subthalamic stimulation modulates self-estimation of patients with Parkinson's disease and induces risk-seeking behaviour. *Brain* **2013**. [CrossRef] [PubMed]
27. Hälbig, T.D.; Frisina, P.G.; Tse, W.; Baker, B.R.; Shapiro, H.; Hollander, E.; Tagliati, M.; Olanow, C.W. Subthalamic deep brain stimulation and obsessive-compulsive symptoms in Parkinson's disease. *Aktuelle Neurol.* **2008**, *35*, P742. [CrossRef]
28. Temel, Y.; Kessels, A.; Tan, S.; Topdag, A.; Boon, P.; Visser-Vandewalle, V. Behavioural changes after bilateral subthalamic stimulation in advanced Parkinson disease: A systematic review. *Parkinsonism Relat. Disord.* **2006**, *12*, 265–272. [CrossRef] [PubMed]

29. Smeding, H.M.M.; Speelman, J.D.; Koning-Haanstra, M.; Schuurman, P.R.; Nijssen, P.; van Laar, T.; Schmand, B. Neuropsychological effects of bilateral STN stimulation in Parkinson disease A controlled study. *Neurology* **2006**, *66*, 1830–1836. [CrossRef] [PubMed]
30. Okun, M.S.; Wu, S.S.; Fayad, S.; Ward, H.; Bowers, D.; Rosado, C.; Bowen, L.; Jacobson, C.; Butson, C.; Foote, K.D. Acute and chronic mood and apathy outcomes from a randomized study of unilateral STN and GPi DBS. *PLoS ONE* **2014**, *9*, e114140. [CrossRef] [PubMed]
31. Funkiewiez, A.; Ardouin, C.; Krack, P.; Fraix, V.; Van Blercom, N.; Xie, J.; Moro, E.; Benabid, A.-L.; Pollak, P. Acute psychotropic effects of bilateral subthalamic nucleus stimulation and levodopa in Parkinson's disease. *Mov. Disord.* **2003**, *18*, 524–530. [CrossRef] [PubMed]
32. Funkiewiez, A.; Ardouin, C.; Caputo, E.; Krack, P.; Fraix, V.; Klinger, H.; Chabardes, S.; Foote, K.; Benabid, A.L.; Pollak, P. Long term effects of bilateral subthalamic nucleus stimulation on cognitive function, mood, and behaviour in Parkinson's disease. *J. Neurol. Neurosurg. Psychiatry* **2004**, *75*, 834–839. [CrossRef] [PubMed]
33. Witt, K.; Daniels, C.; Herzog, J.; Lorenz, D.; Volkmann, J.; Reiff, J.; Mehdorn, M.; Deuschl, G.; Krack, P. Differential effects of L-dopa and subthalamic stimulation on depressive symptoms and hedonic tone in Parkinson's disease. *J. Neuropsychiatry Clin. Neurosci.* **2006**, *18*, 397–401. [CrossRef] [PubMed]
34. Houeto, J.-L.; Mallet, L.; Mesnage, V.; Du Montcel, S.T.; Béhar, C.; Gargiulo, M.; Torny, F.; Pelissolo, A.; Welter, M.-L.; Agid, Y. Subthalamic stimulation in Parkinson disease: Behavior and social adaptation. *Arch. Neurol.* **2006**, *63*, 1090–1095. [CrossRef] [PubMed]
35. Martínez-Martín, P.; Valldeoriola, F.; Tolosa, E.; Pilleri, M.; Molinuevo, J.L.; Rumià, J.; Ferrer, E. Bilateral subthalamic nucleus stimulation and quality of life in advanced Parkinson's disease. *Mov. Disord.* **2002**, *17*, 372–377. [CrossRef] [PubMed]
36. Pagonabarraga, J.; García-Sánchez, C.; Llebaria, G.; Pascual-Sedano, B.; Gironell, A.; Kulisevsky, J. Controlled study of decision-making and cognitive impairment in Parkinson's disease. *Mov. Disord.* **2007**, *22*, 1430–1435. [CrossRef] [PubMed]
37. Brentrup, A.; Ohrmann, P.; Weckesser, M.; Tombach, H.; Bothe, H.W. Alterations of sociomoral judgement and glucose utilization in the frontomedial cortex induced by electrical stimulation of the subthalamicus nucleus (STN) in Parkinsonian patients. *Meet. Abstr. Ed* **2004**, *55*.
38. Brandt, J.; Rogerson, M.; Al-Joudi, H.; Reckess, G.; Shpritz, B.; Umeh, C.C.; Aljehani, N.; Mills, K.; Mari, Z. Betting on DBS: Effects of subthalamic nucleus deep brain stimulation on risk taking and decision making in patients with Parkinson's disease. *Neuropsychology* **2015**, *29*, 622. [CrossRef] [PubMed]
39. Houeto, J.L.; Mesnage, V.; Mallet, L.; Pillon, B.; Gargiulo, M.; Tezenas Du Moncel, S.; Bonnet, A.M. Behavioural disorders, Parkinson's disease and subthalamic stimulation. *J. Neurol. Neurosurg. Psychiatry* **2002**, *72*, 701–707. [CrossRef] [PubMed]
40. Fassino, S.; Daga, G.A.; Gramaglia, C.; Pierò, A.; Zibetti, M.; Castelli, L.; Cinquepalmi, A.; la Notte, M.; Lopiano, L. Novelty-seeking in Parkinson's disease after deep brain stimulation of the subthalamic nucleus: A case–control study. *Psychosomatics* **2010**, *51*, 62–67. [PubMed]
41. Denheyer, M.; Kiss, Z.H.; Haffenden, A.M. Behavioral effects of subthalamic deep brain stimulation in Parkinson's disease. *Neuropsychologia* **2009**, *47*, 3203–3209. [CrossRef] [PubMed]
42. Schüpbach, W.M.; Agid, Y. Psychosocial adjustment after deep brain stimulation in Parkinson's disease. *Nat. Clin. Pract. Neurol.* **2008**, *4*, 58–59. [CrossRef] [PubMed]
43. Christen, M.; Ineichen, C.; Bittlinger, M.; Bothe, H.W.; Müller, S. Ethical focal points in the international practice of deep brain stimulation. *AJOB Neurosci.* **2014**, *5*, 65–80. [CrossRef]
44. Cyron, D. Mental side effects of deep brain stimulation (DBS) for movement disorders: The futility of denial. *Front. Integr. Neurosci.* **2016**, *10*. [CrossRef] [PubMed]
45. Schüpbach, M.; Gargiulo, M.; Welter, M.L.; Mallet, L.; Behar, C.; Houeto, J.L.; Maltete, D.; Mesnage, V.; Agid, Y. Neurosurgery in Parkinson disease A distressed mind in a repaired body? *Neurology* **2006**, *66*, 1811–1816. [CrossRef] [PubMed]
46. Fumagalli, M.; Marceglia, S.; Cogiamanian, F.; Ardolino, G.; Picascia, M.; Barbieri, S.; Pravettoni, G.; Pacchetti, C.; Priori, A. Ethical safety of deep brain stimulation: A study on moral decision-making in Parkinson's disease. *Parkinsonism Related Disord.* **2015**, *21*, 709–716. [CrossRef] [PubMed]
47. Glannon, W. Stimulating brains, altering minds. *J. Med. Ethics* **2009**, *35*, 289–292. [CrossRef] [PubMed]

48. Mathews, D.J.H. Deep brain stimulation, personal identity and policy. *Int. Rev. Psychiatry* **2011**, *23*, 486–492. [CrossRef] [PubMed]
49. Gilbert, F. The burden of normality: From "chronically ill" to "symptom free". New ethical challenges for deep brain stimulation postoperative treatment. *J. Med. Ethics* **2012**, *38*, 408–412. [CrossRef] [PubMed]
50. Lipsman, N.I.R.; Glannon, W. Brain, mind and machine: What are the implications of deep brain stimulation for perceptions of personal identity, agency and free will? *Bioethics* **2013**, *27*, 465–470. [CrossRef] [PubMed]
51. Kraemer, F. Me, myself and my brain implant: Deep brain stimulation raises questions of personal authenticity and alienation. *Neuroethics* **2013**, *6*, 483–497. [CrossRef] [PubMed]
52. Ryckman, R.M. *Theories of Personality*; Cengage Learning: Massachusetts, MA, USA, 2000.
53. Eitam, B.; Higgins, E.T. Motivation in mental accessibility: Relevance of a representation (ROAR) as a new framework. *Soc. Personal. Psychol. Compass* **2010**, *4*, 951–967. [CrossRef] [PubMed]
54. Higgins, E.T. Knowledge activation: Accessibility, applicability and salience. In *Social Psychology: Handbook of Basic Principles*; Higgins, E.T., Kruglanski, A.W., Eds.; Guilford: New York, NY, USA, 1996; pp. 133–168.
55. Costa, P.T.; McCrae, R.R. *Revised NEO Personality Inventory (NEOPI-R) and NEO Five Factor Inventory (NEO-FFI)*; Psychological Assessment Resources: Odessa, FL, USA, 1992.
56. Bargh, J.A.; Chartrand, T.L. The mind in the middle. In *Handbook of Research Methods in Social and Personality Psychology*; Cambridge University Press: Cambridge, UK, 2000.
57. Kay, A.C.; Wheeler, S.C.; Bargh, J.A.; Ross, L. Material priming: The influence of mundane physical objects on situational construal and competitive behavioral choice. *Organ. Behav. Hum. Decis. Process.* **2004**, *95*, 83–96. [CrossRef]
58. Kouchaki, M.; Smith-Crowe, K.; Brief, A.P.; Sousa, C. Seeing green: Mere exposure to money triggers a business decision frame and unethical outcomes. *Organ. Behav. Hum. Decis. Process.* **2013**, *121*, 53–61. [CrossRef]
59. Vohs, K.D.; Mead, N.L.; Goode, M.R. The psychological consequences of money. *Science* **2006**, *314*, 1154–1156. [CrossRef] [PubMed]
60. Christen, M.; Van Schaik, C.; Fischer, J.; Huppenbauer, M.; Tanner, C. *Empirically Informed Ethics: Morality Between Facts and Norms*; Springer International Publishing: Cham, Switzerland, 2014.
61. Rest, J.R. *Moral Development: Advances in Research and Theory*; Praeger: New York, NY, USA, 1986.
62. Tanner, C.; Christen, M. Moral Intelligence: A framework for understanding moral competences. In *Empirically Informed Ethics: Morality between Facts and Norms*; Christen, M., Fischer, J., Huppenbauer, M., Tanner, C., van Schaik, C., Eds.; Springer: Berlin, Germay, 2013; pp. 119–136.
63. Merkl, A.; Neumann, W.-J.; Huebl, J.; Aust, S.; Horn, A.; Krauss, J.K.; Dziobek, I. Modulation of beta-band activity in the subgenual anterior cingulate cortex during emotional empathy in treatment-resistant depression. *Cereb. Cortex* **2015**. [CrossRef] [PubMed]
64. Clarkeburn, H. A test for ethical sensitivity in science. *J. Moral Educ.* **2002**, 439–453. [CrossRef]
65. Leroi, I.; Harbishettar, V.; Andrews, M.; McDonald, K.; Byrne, E.J.; Burns, A. Carer burden in apathy and impulse control disorders in Parkinson's disease. *Int. J. Geriatr. Psychiatry* **2012**, *27*, 160–166. [CrossRef] [PubMed]
66. Voon, V.; Kubu, C.; Krack, P.; Houeto, J.-L.; Tröster, A.I. Deep brain stimulation: Neuropsychological and neuropsychiatric issues. *Mov. Disord.* **2006**, *21*, S305–S327. [CrossRef] [PubMed]
67. Ineichen, C.; Christen, M.; Tanner, C. Measuring value sensitivity in medicine. *BMC Med Ethics*. Manuscript under review.

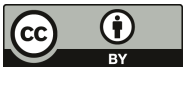

brain sciences

MDPI

Review

The Use of Deep Brain Stimulation in Tourette Syndrome

Ladan Akbarian-Tefaghi [1], Ludvic Zrinzo [2] and Thomas Foltynie [2,*]

[1] Institute of Neurology, University College London (UCL), Queen Square, London WC1N 3BG, UK; ladan.akbarian-tefaghi.15@ucl.ac.uk

[2] Sobell Department of Motor Neuroscience, University College London (UCL) Institute of Neurology, London WC1N 3BG, UK; l.zrinzo@ucl.ac.uk

* Correspondence: t.foltynie@ucl.ac.uk; Tel.: +44-0203-4488-726

Academic Editors: Tipu Aziz and Alex Green
Received: 30 June 2016; Accepted: 15 August 2016; Published: 19 August 2016

Abstract: Tourette syndrome (TS) is a childhood neurobehavioural disorder, characterised by the presence of motor and vocal tics, typically starting in childhood but persisting in around 20% of patients into adulthood. In those patients who do not respond to pharmacological or behavioural therapy, deep brain stimulation (DBS) may be a suitable option for potential symptom improvement. This manuscript attempts to summarise the outcomes of DBS at different targets, explore the possible mechanisms of action of DBS in TS, as well as the potential of adaptive DBS. There will also be a focus on the future challenges faced in designing optimized trials.

Keywords: Tourette syndrome; TS deep brain stimulation; DBS

1. Introduction

Tourette syndrome (TS) is a childhood neurobehavioural disorder affecting approximately 0.3%–0.8% of the paediatric population [1]. It is defined by the presence of at least one vocal and two motor tics starting before the age of 18, lasting longer than one year, with the exclusion of other causes [2]. Tics are often preceded by a premonitory urge [3] tend to occur daily in variable bouts and follow a waxing and waning course. The typical age of onset is five to seven years [4] with symptoms peaking at puberty and often remitting into early adulthood. In around 20% of patients, symptoms persist and have a detrimental effect on quality of life including social, professional and educational development [5]. Psychiatric co-morbidities are experienced in approximately 50%–90% of TS individuals, particularly obsessive compulsive disorder (OCD/OCB), attention deficit hyperactivity disorder (ADHD), deliberate self-injurious behaviours (SIBs) along with disturbances in mood and anxiety [6]. Current treatments include a combination of pharmacological and behavioural therapies. However, in patients with disabling refractory symptoms, surgical intervention, such as deep brain stimulation (DBS), may be considered a potential option for symptom improvement.

DBS has been applied to patients with both hypokinetic and hyperkinetic movement disorders including Parkinson's disease, dystonia and essential tremor, as well as neuropsychiatric disorders such as treatment-resistant depression and OCD [7]. Targets of DBS for TS are based on the postulated dysfunction of the basal ganglia-thalamo-cortical loops. A simplistic proposal is that aberrant activity in groups of striatal medium spiny neurons [8] lead to a decrease in the inhibitory output of the globus pallidus internus (GPi), resulting in disinhibition and the execution of involuntary cortical motor commands in the form of repetitive, stereotyped movements. A variety of methods, such as structural imaging in longitudinal studies of TS patients, have correlated smaller caudate nucleus volumes with severity of tics, as well as changes in the diffusivity of water molecules in the frontal lobe and thalamus as measured by diffusion tensor magnetic resonance imaging [9]. Decreased connectivity between

caudate nucleus and lateral frontal cortex has been observed, supporting a cortical disinhibition theory for the disorder [10] though contradictory findings have also been reported [11] and the precise pathophysiology of TS remains unknown.

The current manuscript attempts to provide an updated review of the published literature regarding the use of DBS for severe, medication refractory Tourette syndrome. A particular focus has been (1) to understand the potential mechanisms of action of this therapy based on neurophysiological recordings and neuroanatomical knowledge of the basal ganglia circuity; and (2) to make recommendations for the future evaluation of the use of DBS in TS.

2. Methods

A broad search was carried out using the databases Pubmed and OVID Medline with a variety of terms including "Tourette syndrome", "GTS", combined with "deep brain stimulation" or "DBS". Each target region for DBS, including the "thalamus" "globus pallidus internus" "anterior limb internal capsule" "nucleus accumbens", "globus pallidus externus" were combined with the above terms. Only references in the English language were included.

3. Literature Review

Currently, nine targets have been used in DBS for TS, including the thalamic centromedian parafascicular complex (CMPf), the cross point of the centromedian nucleus-substantia periventricularis-nucleus ventro-oralis nucleus (CM-Spv-Voi), the target of the nucleus ventro-oralis posterior-ventro oralis anterior-Voi complex (Vop-Voa-Voi), the globus pallidus internus (GPi) (anteromedial AND posteroventral regions), the nucleus accumbens (NA), the anterior limb of the internal capsule (ALIC), the subthalamic nucleus (STN) and the globus pallidus externus (GPe) [12]. Known connections between nuclei targeted by TS DBS, as well as other structures in the cortico-basal ganglia network are illustrated in Figure 1.

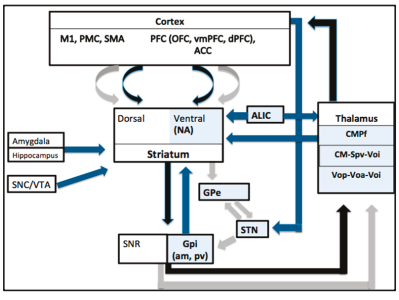

Figure 1. Simplified schematic showing the main connections of the cortico-thalamo-cortical network, with the nuclei targeted in TS DBS in blue boxes (NA = nucleus accumbens, ALIC = anterior limb internal capsule, CMPf centromedian parafasciular complex, CM Sp Voi, centromedian nucleus-substantia periventricularis-nucleus ventro-oralis nucleus, the nucleus ventro-oralis posterior-ventro oralis anterior ventro-oralis complex (Vop-Voa-Voi), GPe = globus pallidus externus, STN = subthalamic nucleus, GPi (am, pv = anteromedial, posteroventral globus pallidus internus). The direct pathway is shown with black arrows, the indirect pathway with grey arrows and other connections shown with blue arrows. Projections from the primary motor cortex (M1), the pre-motor cortex (PMC) and the supplementary motor area (SMA) are predominantly directed to the dorsal striatum (putamen and caudate) whereas fibers from the prefrontal cortex (PFC) including the orbitofrontal cortex (OFC), ventromedial PFC (vmPFC) and the dorsal PFC (dPFC) as well as the anterior cingulate cortex (ACC) mostly project to the ventral striatum (nucleus accumbens and rostroventral most aspects of caudate and putamen). The main output nuclei are the GPi and the substantia nigra pars reticulata (SNR). Other regions, such as the substantia nigra pars compacta (SNC), also have connections with the striatum.

The rationale behind target choice has varied depending on whether tics are considered a movement disorder in which case sensorimotor areas such as the posteroventral pallidum have been stimulated or if they are considered to be a compulsion or a failure of inhibition wherein associative/limbic areas have been targeted [13]. The thalamus and GPi have been the most widely stimulated with a combination of targets used in some studies. A summary of the results of open label trials is presented in Table 1, and blinded trials in Table 2. The outcome measures in these studies relate to tics or co-morbidities and include the Yale global tic severity scale (YGTSS) [14] as well as the Modified Rush video rating scale (MRVRS) [15] which measure tic frequency, severity and impairment levels. The Yale Brown Obsessive Compulsive scale (Y-BOCS) [16] assesses the severity of OCD/OCB symptoms whilst measures of quality of life, anxiety and depression commonly include the Gilles de la Tourette quality of life (GTS-QOL) scale [17] State Trait Anxiety Inventory (STAI) and Beck depression inventory (BDI), respectively, which have been validated for use in TS.

3.1. Thalamic Targets

Motor patterns in TS are postulated to result in part from an increased thalamocortical drive due to inappropriate activation of striatal neurons [18]. There is an excitatory feedback loop from the thalamus to the striatum originating in the CMPf and midline thalamic nuclei [19], which are the most common thalamic targets for TS DBS.

The first report of DBS for the treatment of refractory TS by Visser-Vandewalle, used the same thalamic nuclei (centromedian-parafasciucular complex (CM/Pf), and ventral oral internus nuclei (Voi)) that Hassler and Dieckmann had targeted in stereotactic ablation in 1970. This individual was a 42 years old male who subsequently experienced a 90% improvement in his tics at 12 months [20] although using stimulation parameters with extremely high charge density, in comparison to those used in Parkinson's disease. In 2003, the same group reported three patients including the above who showed a 72%–90% improvement in tics over a follow up of between eight months and five years [21]. In two of three patients the co-morbidities of SIB and OCD were also no longer present. The main adverse effects reported were either a reduction or increase in sexual drive in two patients along with reduced energy levels. In the larger series of 18 patients who were followed up between 3 and 18 months [22] YGTSS improvement varied between 24% and 79% in 15 of 18 patients with a concurrent improvement in co-morbidities. A longer follow up study [23] of 15 males after five to six years showed a mean YGTSS improvement of 73% and YBOCS of 42%. Adverse effects included a scalp erosion due to compulsive picking, and an abdominal haematoma. These and other open label studies [24–38] are outlined in Table 1 and strongly indicated that thalamic stimulation may have a beneficial therapeutic role in TS for both tic severity as well as comorbid symptoms.

However, the results of two randomised controlled trials showed a more variable response. In 2007, the anterior part of the CMPf complex was targeted in five male patients, with only a mean improvement in tics of 17% in the YGTSS when blindly comparing ON vs. OFF stimulation. However, three of the five responded with a 50% average reduction of tics following open label stimulation at three months, though no biomarker could distinguish responders from non-responders. Measures of OCD, depression and anxiety demonstrated a trend towards improvement, with a 44% increase in the YBOCS whilst one patient experienced a psychotic episode [39]. A more recent double blind crossover study targeted the CM-Spv-Voi assessing 6 male patients who were randomly assigned to three months on stimulation and three months off or vice versa. At a group level improvement in tic control during the off and on condition was 2.8% and 39.4% respectively. After one year open label follow up, these levels were maintained at 49.2% on YGTSS and 35.5% on the MRVRS [40].

Table 1. Summary of open label trials.

Study	Target	Sample Size, Sex (Age, Years)	Follow up (Months)	Stimulation Parameters	Tic outcome (Improvement in YGTSS or MRVRS)	Comoribidity Outcome	Adverse Effects/Comments
Vandewalle et al. (1999) [20], Visser-Vandewalle (2003) [21]	CMPf, SPv Voi	Three males (42, 28, 45)	60, 12, 8	Bipolar all contacts 100 Hz, 210 μs, 2.4 V right, 2.2 V left; Right double monopolar 65 Hz, 210 μs, 3 V; left monopolar 100 Hz, 210 μs; Right monopolar 2.8 V, 130 Hz, 210 μs; left one monopolar 2.4 V, 100 Hz 200 μs	90%, 72%, 83%	OCD and SIB disappeared in all 3.	A slight sedative effect in all three; 2 had increased or decreased libido.
Diederich et al. (2005) [41]	pvGPi	One male (27)	14	Monopolar 2 V, 185 Hz, 60 μs	73% (previous YGTSS 83)	No apparent change in the mild compulsions of the patient. Significant reduction of anxiety/depression.	Small symptomatic haematoma right pallidum bradykinesia of left extremities
Flaherty et al. (2005) [42], Shields et al (2008) [43]	Anterior capsule CMPf, SPv Voi	One female (37), same patient operated at different target	18, 3	Bipolar 4.1 V, 185 Hz, 210 μs, 7 V, 90 μs, 185 Hz	YGTSS 25%, 32%	Self-injury stopped (previous retinal detachment led to blindness in one eye), but vision stabilized post DBS	Electrode breakage therefore same patient had stimulation at different target. The AC site caused altered mood and impulse control disturbance.
Ackermans et al. 2006 [24]	CMPf, Voi pvGpi	One male (45), one male (27)	12	Monopolar 6.4 V, 130 Hz, 120 μs bilaterally; Monopolar 3.1 V, 170 Hz, 210 μs bilaterally	Tics 20 to 3/min, Tics 28 to 2/min	Obssessions and compulsions (measured by the revised Padua inventory) improved by 62% in the ON than OFF condition	CMPf patient is the same as in Vandewalle study- he experienced vertical gaze palsy and decreased libido. Both patients complained of reduced energy.
Kuhn et al. 2007 [44]	NAC, internal capsule	One male (26)	30	Tetra monopolar 90 μs, 130 Hz, 7 V	41% with YGTSS, 50% MRVRS (Previous YGTSS 90 and MRVRS 18)	Reduction in SIB, reduction in OCD by 52% based on Y-BOCS	No significant adverse effects
Bajwa et al. 2007 [25]	CMPf, SPv Voi	One male (48)	24	Bipolar 2 V, 130 Hz and 90 μs	66% (Previous YGTSS score 35.5 and overall 83)	YBOCS improved 75%	Approximately 14 programming sessions required over 2 years. No serious adverse effects.
Shahed et al. 2007 [45]	pvGPi	One male (16)	6	Monopolar 5 V, 160 Hz right, 145 Hz left, 90 μs	84% (YGTSS)	YBOCS improved 69% (only obsessions not compulsions).	No surgical adverse effects
Dehning et al. 2008 [46]	pvGPi	One female (44)	12	Monopolar 4.2 V, 145 Hz, 210 μs	YGTSS 88%	Patient did have SIB including self-biting and beating but outcome not reported.	Complaints of depression. Vertigo and stomach aches in first few months. No serious adverse effects.
Zabek et al. 2008 [47]	Right NAC	One male (31)	28	Not reported	80% (15-minute videotaped exams)	None reported	Unilateral right side only.
Neuner et al. 2009 [48]	NAC	One male (38)	36	Double monopolar 6 V, 145 Hz, 90 μs	YGTSS 44% mRVTRS 58%	YBOCS 56%	Rapid IPG depletion-2 replacements in 36 months. Incidental finding was that patient no longer wanted to smoke.
Dueck 2009 [49]	pvGPi	One male (16)	12	Monopolar 4 V, 130 Hz, 120 μs	No improvement	Co-morbidity was severe mental retardation which was not affected	Not reported
Servello et al. 2008 [22]	CMPf Voi	15 males, 3 females (17–47)	3-18	Bipolar 2.5–4 V, 90–120 μs, 130 Hz	YGTSS 65%	None reported	Transient stimulation induced vertigo, poor scalp incision healing due to repetitive touching requiring body shield.

Table 1. *Cont.*

Study	Target	Sample Size, Sex (Age, Years)	Follow up (Months)	Stimulation Parameters	Tic outcome (Improvement in YGTSS or MRVRS)	Comoribidity Outcome	Adverse Effects/Comments
Servello et al. 2009 [50]	CMPF + ALIC/NA in 3, 1 had only ALIC/NA	Three males, one female (25, 31 ,37, 47)	10–26	3 monopolar, 1 bipolar 4–4.5 V, 130–160 Hz, 150–180 μs	Variable, mostly slight improvement in tics	Sight improvement in OCD	None reported
Servello et al. 2010 [26]	Total 79 procedures 36 patients) CMPf/Voi (67) pvGPi (2)ALIC-NA (10)	25 males, 6 females (17–57). 4 additional patients received leads in multiple targets and one in ALIC/NA	3–48	At last follow up 2–5 V, 90–140 μs, 60–180 Hz	YGTSS 47% mean improvement	17% mean improvement in YBOCS	2 patients had stimulator switched off, reporting unsatisfactory results, 2 had surgical revision of pulse generator due to infection, and one had hardware failure.
Martinez-Torres et al. 2009 [51]	STN	One male (38)	12	Monopolar 3 and 3.2 V, 130 Hz, 60 μs	76%	Not reported	Patient also had Parkinson's disease which was the indication for DBS in STN
Martinez-Fernandez et al. 2011 [52]	pvGPi (2), amGPi (2), pvGPi (1) (then changed to anteromedial region after 18 months)	4 males (21–60), 1 female (35)	3–24	PL GPi: Monopolar 2.5 V, 150 μs, 170 Hz, 2.5 V, 60 μs, 130 Hz; AM GPi: Monopolar 4.2 V, 60 μs, 160 Hz, Monopolar 4 V, 210 μs, 130 Hz; PL then AM GPi: Bipolar 3.6 V, 60 μs, 20 Hz for both	Anteromedial group: MRVRS 54% , Posterolateral group (3 patients, with one experiencing worsening symptoms and responders average 37% improvement). YGTSS 38% improvement versus 20% for amGPi and pvGPi.	YBOCS mean change of 26% at last follow up	Complaints of agitation in 1, anxiety in 2, weight gain in 1, infection in 1 requiring repeat removal of battery.
Idris et al. 2010 [27]	CMPf, Voa	1 male (24)	2	3.5 V, 120 μs, 130 Hz	No scales reported, but tics noted to improve	Not reported	Postoperative bilateral subcortical haematomas attributed to low factor XIIIA
Ackermans et al. 2010 [28]	CMPf, SPv, Voi	2 males (42,45)	72–120	Amplitude L1, 8 R1, 5 130 Hz, 90 μs Amplitude L8, 5 R8, 5 100 Hz 150 μs At long-term follow up	Patient 1 (5 years) tic improvement 90.1%, maintained at 10 years (92.6%). In patient 2, after 8 months 82% slightly decreased at 6 years (78%). Video tic rating scale used measuring vocal and motor tics/10minutes.	Not reported, but in one patient "psychopathology" reported to remain. Compulsions said to have disappeared in both patients. In one patient with depression, only slight decrease after surgery.	Both patients reported reduced energy. Both experienced traction of the lead in neck. One patient experienced a decrease in erectile function whilst the other had increased sexual drive. Both reported some visual blurring. One patient reported decreased verbal fluency and learning.
Burdick et al. 2010 [53]	ALIC/NA	One male (33)	30	Not reported	YGTSS 15% reduction at 6 months and thereafter until 30 months of last follow up remained unchanged. Initially had mild tics with a pre-operative MRVRS score of 5.	Not reported	No reported adverse effects.
Kaido et al. 2011 [19]	CMPf	One male (20) ,two females (19, 21)	14–21	Tetrapolar bilateral 2.3 V, 210 μs, 130 Hz; Tetrapolar Left 2.1 V, right 2.3 V, left 210 μs, right 180 μs, 130 Hz; bilaterally Tripolar Right 2.6 V, left 2.5 V, 180 μs, 80 Hz	Tics (52%–71%) Social impairment (56%–71%)	Not reported	No reported side effects.

Table 1. *Cont.*

Study	Target	Sample Size, Sex (Age, Years)	Follow up (Months)	Stimulation Parameters	Tic outcome (Improvement in YGTSS or MRVRS)	Comoribidity Outcome	Adverse Effects/Comments
Kuhn et al. 2011 [29]	Vop-Voa-Voi (unilateral)	One male (39), one female (27)	12	Bipolar 4.5 V, 130 Hz, 120 μs; Bipolar 3.1 V, 90 Hz, 120 μs	YGTSS 75%–100% MRVRS 77%–100%	BDI-no negative impact	Reduced verbal fluency at one year in both patients.
Dehning et al. 2011 [54] (one patient previously reported in Dehning 2008 [46])	pvGPi	Three females (25–44), one male (38)	5–13	4.2 V, 4 V, 3.8 V; 210 μs, 150 μs, 150 μs, 145 Hz, 130 Hz, 130 Hz (3 females) 3.5 V, 180 Ms, 130 Hz	2 patients responders (64% and 88% improvement YGTSS) 2 patients non-responders 1 female 2 male	Not reported	Lead revision was done in a non-responder without improvement.
Dong et al. 2012 [55]	pvGpi (unilateral R)	Two males (41, 22)	12	Quadripolar, 3.5 V, 2.8 V, 90 μs, 160, 130 Hz	YGTSS 53.1%–58.5%	None reported	No apparent adverse effects.
Cannon et al. 2012 [56]	amGPi	8 males (22–50), 3 females (18–34)	4–30	Quadripolar, initial stimulation 1 V, 60 μs, 130 Hz, adjusted at follow ups	YGTSS motor 48% vocal 56.5%	Mean YBOCS reduction 59%, HDRS 74%, GTS-QLS 102%	Complications from hardware malfunctions in 3 (due to SIB, MVA, and unknown). 1 patient did not tolerate DBS and switched it off. Anxiety in 2 patients
Duits et al. 2012 [30]	CM-Spv-Voi	One male (21)	23	Not reported	YGTSS- worse with DBS Pre-op-42 Stim OFF-12 Stim on-39	Y-BOCS Pre-op: 20 Stim OFF-8 Stim ON-7	Severe post-operative complications including psychogenic paroxysmal hypertonia.The patient may have had a somatoform disorder, that may contra-indicate DBS.
Savica et al. 2012 [31]	CMPf	2 males, one female (17, 17, 35)	1	17 years old males: Bipolar 3.7 V, 120 μs, 117 Hz; Monopolar 2.5 V, 90 μs, 130 Hz. 35 years old female: Bipolar 4.1 V, 120 μs, 107 Hz	YGTSS 70% mean improvement	No formal assessment, but co-morbid symptoms appeared stable or slightly improved.	Adverse effects related to stimulation such as mild paraesthesias but corrected with programming changes.
Okun et al. 2013 [32]	CM (scheduled stimulation)	3 females, 2 males (28–39)	6	Not reported	YGTSS 19% mean improvement mRVRS 36% mean improvement	YBOCS, HDRS, QOLAS did not improve.	No serious side effects.
Porta et al. 2012 [23]	Cm-Pfc-Voa	15 male, 3 females (17–47)	5–6 years	2.5–4 V, 60–120 μs, 130 Hz	YGTSS 73%	YBOCS 42% ($p = 0.003$), STAI-46%, BDI−55%	One patient developed poor healing of scalp scar due to compulsion to touch, the other developed abdominal haematoma where pulse generator was located. Majority had some minor side effects if voltage> 4 such as vertigo or blurring of vision.
Motlagh et al. 2013 [33]	Midline thalamic	4 males (16–44)	6–95	0.1–5 V, 60–120 μs, 60–200 Hz (4 bipolar one tripolar)	YGTSS- Greater improvement in the 2 younger patients (67%–85%), compared to older patients (7%–20%).	YBOCS-100% improvement in on patient but minimal change or worsening in others, HDRS and HARS-no change	44 year old male picked compulsively at chest and cranial incisions so DBS was removed due to infection. 42 year old male had DBS system removed due to lack of therapeutic effect.
Dong et al. 2014 [57]	pvGpi	1 male (33)	39	Monopolar 2.8 V, 90 μs, 130 Hz (frequency then reduced to 65 Hz 33 months)	YGTSS 92.9% at 33 and 39 months	YBOCS went from 18 to 0HAS and HDS markedly reduced	Supports that low frequency stimulation may be an optional therapeutic strategy in some patients
Zhang et al. 2014 [58]	pvGpi	12 males (16–34), 1 female (21)	13–80	Not reported	YGTSS Mean 52.1% (13–80 months).	GTS-QOL improved by a mean of 45.7% (range, 11.0%–77.2%).	Not reported
Sachdev et al. 2014 [59]	amGPi	14 males, 3 females (17–51)	8–46	Mean at follow up: 4.14 V, 95.2 μs, 139.4 Hz	Overall 48.3% reduction motor tics, 41.3% in phonic, 1 month 70.6% of patients had >50% reduction in YGTSS	YBOCS average 62% improvement ($p = 0.001$), 39% improvement in GTS-QOL ($p < 0.001$)	Lead breakage in 4 patients, one patient had infection, 2 transient anxiety, 1 dizziness, 1 poor balance.

Table 1. *Cont.*

Study	Target	Sample Size, Sex (Age, Years)	Follow up (Months)	Stimulation Parameters	Tic outcome (Improvement in YGTSS or MRVRS)	Comoribidity Outcome	Adverse Effects/Comments
Huasen et al. 2014 [60]	amGPi	One female (19)	12	Bipolar 2.9 V, 180 Hz, 180 μs	YGTSS 55% improvement	Not formally assessed	Patient had a cervical cord contusion secondary to violent cervical tics, with DBS used to preserve limb function and led to improvement in her neck extension tics
Zekaj et al. 2015 [38]	CMPf, Vo	1 male (17)	84	Not reported	At 12 months YGTSS 58.2%	Not reported	5 years post surgery DBS removed, and patient had stabilized despite stimulation. 2 year later continues stable. Symptoms may have resolved spontaneously. However, supports DBS in younger patients.
Huys et al. 2016 [34]	Ventro- anterior and ventrolateral motor parts of thalamus	Three female, five male (19–56)	12	1.3–3.7 V, 80–130 Hz, 60–150 μs	YGTSS and mRVRS at last follow up average 58%	In 5 no OCD at baseline, 2 mild and 1 severe. No significant effect on OCD comorbidity. Significant effect on quality of life improvement.	One patient had mild infection of subcutaneous pulse generator one patient had disturbance of eye motility, tremor of lower jaw. 1 patient had suicidal thoughts, 1 dysarthria.
Smeets et al. 2016 [61]	Anterior GPi	Three males and two females (35–57)	5–38	Tetrapolar 2.2–5.6 V, 180-360 μs, 100–180 Hz	YGTSS 71.5% average	In the three patients with baseline OCB (12%, 35% and 100%).	Two males had previous CMPf stimulation but due to side effects such as gaze disturbance, switched to GPi after 6 and 8 years after infection with IPG replacement. Other adverse effects included apathy in 2 patients, weight loss and agitation in 1 patient
Cury et al. 2016 [35]	CMPf	One male (23)	18	Not reported	YGTSS 70.5% Subscore impairment 60%	Patient did not have OCD 53% improvement on hospital anxiety scale (HAS)	None reported
Servello et al. 2016 [36], Testini et al. 2016 [37]	Vo-Cm-Pf-30, Vo-Cm-Pf and NA-ALIC-2, NA-ALIC (in 3 patients as single target, 3 as rescue therapy) amGPi (1 patient and 2 as rescue) CMPf	14 females, 34 males (total 48), 37 included in final analysis (17–57) 18 males, 3 females (17–46)	Up to 4 years 2–91	130 Hz initally in all patients, 60–120 μs, 2.5–4.5 V Bilateral quadripolar, specific parameters not reported	For remaining 37 patients Mean postoperative decrease in YGTSS 63% Reduction of more than 50% seen in 78.4% patients Average YGTSS 54% (46% motor, 52% vocal and 59% impairment). All but two patients reported marked reduction in tic severity and quality of life	35 OCD, 25 both OCD and depressive disorder. In 4 patients with moderate/severe depression, BDI improved by 45%, in the other 2 only slightly or inconsistently. All patients had psychiatric co-morbidities but outcome not reported.	In 11 patients the device was removed due to inflammatory complications or poor compliance and these were not included in final analysis. NA-ALIC was the single target in 3 patients, joint target in another 3, and rescue for further 3 patients. PvGPi targeted in one patient who then required rescue surgery in NA-ALIC. 12 patients had skin erosions requiring surgical intervention. 1 patient underwent wound revision due to scalp erosion and wound infection. Three years before, one patient had pallidal DBS with no apparent benefit. Postsurgical adverse effects reported on neuropsychological evaluation included occipital headache, and memory loss (including temporary anterograde amnesia)

Table 2. Summary of randomised trials.

Study	Target	Sample Size, Sex (Age, Years)	Follow up	Stimulation Parameters	Effect on Tics Severity/YGTSS or MRVRS	Effect on Comorbidity	Adverse Effects/Comments
Maciunas et al. 2007 [39]	CMPf, Voi	Five males (18–34)	3	Variable polarity 3.5–3.6 V, 90–210 μs,130–180 Hz	Double blind comparison during first 4 weeks showed a 17% improvement. At 3 months 44% (mean) Non-responders with 4.3%–260% tic exacerbation	Mean score improvements: YBOCS 44%, BDI-2 60%, Hamilton anxiety scale, (HAS) 51%	One patient experienced acute psychosis during randomised period which was successfully treated. Overall three responders and two non-responders
Houeto et al. 2005 [62], Welter et al. 2008 [63]	CMPF and anteromedial GPi	Two females, one male (36, 30, 30)	60, 27, 20	CMPf: double monopolar 1.5–1.7 V, 60 μs, 130 Hz, Gpi: Single or double monopolar 1.5–3.5 V, 60 μs, 130 Hz	YGTSS cross-over period, (a)-AmGPi: (65%, 96%, 74%, (b)-CMPf: 30%, 40%, 64%, (c)-Gpi and CMPF 43%, 60%, 76% (after 60 months)	One patient previously had major depressive disorder and self-injurious behaviours and impulsiveness. Depressive mood, anxiety and impulsiveness tended to decrease with thalamic and pallidal stimulation but not paillidal sitmulation alone. None of the patients had OCD.	Reduced libido in one patient having thalamic stimulation. Lethargy, anxiety reported under pallidal stimulation and vertigo under higher intensity stimulation; arm paraesthesia under thalamic. Pallidal better than thalamic stimulation and both better than sham stimulation.
Ackermans et al. 2011 [40]	CM-Spv-Voi	6 males (completed full trial) (35–48 years)	36	1.3–7 V, 60–210 μs, 70–130 Hz. Monopolar stimulation in three patients and bipolar stimulation in the other three patients.	YGTSS at blinded ON compared to OFF stimulation was significantly lower (37%). After one year 49% and MRVRS 35%.	No significant difference found between the behavioural disorders and mood in the ON and OFF stimulation conditions.	One small haemorrhage ventral to electrode, one infection of pulse generator, subjective gaze disturbances which resolved after 6 months; all patient reported reduced energy levels. All patients when further questioned had subtle changes in oculomotor function, from visual disturbance to blurred vision and fixation problems, with no objective abnormalities detected with investigations. One younger patient with very severe SIB and life-threatening tics developed hypertonia, mutism and repeated fainting which needed extensive diagnostic evaluation- she was not randomised and considered loss to follow up. Only two patients completed the full 3 months on and of stimulation periods.
Kefalopoulou et al. 2015 [64]	AmGPi (13 patients), pvGPi (2 patients due to dystonic features).	11 males 4 females (25–55 years), 14 randomly assigned 13 completed assessments in both blinded periods. All 15 received stimulation in open-label phase	20–60	In blinded phase, 9 patients had monopolar and double monopolar in 4	YGTSS from off to on stimulation during blinded crossover period was 15.3%. Increased to 40.1% in open label phase	YBOCS-modest non-significant improvements Significant improvement in BDI GTS-QOL 38.9%	2 patients experienced infection of hardware requiring removal of leads and pulse generator with antibiotic treatment who were re-implanted 22 months later. One patient experienced deterioration of tics and hypomanic behaviour during on-stimulation periods, requiring stimulation parameter alterations and benzodiazepine treatment. 23 non-serious adverse events occurred, 15 of which resolved. During blinded phase, 6 patients had no clear benefit (<10% improvement in YGTSS) but most of these had more significant improvement in open label phase when parameters could be optimized. In open-label phase, 4 patients had less than 20% improvement n YGTSS.

3.2. Globus Pallidus Internus (GPi)

The GPi is considered to be functionally segregated into an anteromedial region which is part of the associative/limbic loop of the cortico-striato-thalamo-cortical circuit, while the posteroventral region is involved in the motor loop of the parallel circuit. However, there is much convergence of both limbic and motor inputs in both segments of the GPi [65]. Therefore, there has been much debate as to which sub-region might respond best to DBS for TS. The posteroventral target is familiar territory to functional neurosurgeons as it has been stimulated in other hyperkinetic movement disorders, such as Parkinson's disease (PD) and various forms of dystonia.

3.2.1. Posteroventral GPi

The results of open label studies of DBS of the posteroventral GPi region in TS patients [24,41,45,46,49,52,54,55,57,58] are also listed in Table 1. The range of tic improvement has been 20%–92.9% at 6–39 months follow up [41,45,46,52,54,55,57], with serious side effects including a small haemorrhage in the right GPi at surgery resulting in a persistent bradykinesia of the left hand in one 27 year old male [41] and complaints of depression [46]. In a four patient cohort [52], two patients were non-responders and two experienced an improvement in YGTSS of up to 88%, whilst in a long-term outcome study of 13 patients YGTSS improved by 52.1% with a wide range of 4.3%–83.6% over a mean follow up of 13–80 months) [58]. Stimulation in a 16 year old boy with TS and severe mental retardation led to lack of symptom improvement, attributed to his severe co-morbidity [49]. Despite the variable response at this target it may be preferred in patients with dystonic tics [66].

3.2.2. Anteromedial GPi

The rationale for targeting the anteromedial GPi region is based on the associative-limbic connections that may impact the underlying urge driving the expression of motor and phonic tics. A summary of the results of open label trials is also presented in Table 1 [52,56,59–61] with the amGPi demonstrating tic improvement ranging from 38% to 71.5% [52,56,59–61] in patients followed up between 4 and 46 months, with anxiety reported as an adverse effect [56,59].

However, when evaluated using a randomised crossover trial methodology in 15 patients, comparison of blinded ON stimulation vs. OFF stimulation periods showed a mean YGTSS improvement of only 15.3% although with substantial variability between patients. With long-term follow up assessment, patients showed a 40.1% improvement in tics and 38.9% improvement in quality of life [64] leading to discussion about factors which may influence the outcome of DBS surgery when evaluated using blinded trial methods [67].

3.3. Other Targets

The Subthalamic nucleus (STN), External Globus pallidus (GPe), Anterior limb of Internal capsule (ALIC) and Nucleus Accumbens (NA) have been less frequent targets for stimulation [26,36,42–44,47,48,50,51,53,54,68]. The result of STN stimulation has only been reported in one patient who had both PD and TS with DBS resulting in a 97% improvement in tics along with relief of PD symptoms [51]. One male patient stimulated in the GPe region showed a 70.5% increase in YGTSS and a 75% improvement in anxiety [68]. Although limited by study design and sample size, the above results certainly suggest that the STN and GPe show promise as targets of stimulation and warrant further study.

The NA and ALIC have been used as a target in treatment-resistant OCD and have been chosen as potential stimulation targets in some circumstances owing to the frequent OCD comorbidity seen in TS [69]. Open label studies have shown tic improvement of between 25% and 45% [42–44,48,50] at up to 34 months follow up with adverse effects including rapid internal pulse generator depletion in one patient requiring 2 replacement in 36 months [48]. However, in one case report there was no benefit from NA stimulation [47].

3.4. Comparative Studies

In a randomised crossover study, three patients had electrodes placed in both the thalamus and the anteromedial GPi, stimulation resulting in a YGTSS improvement of 65%–96% for amGPi, 30%–64% for CMPf and 43%–76% in combination stimulation. Follow up for as long as 60 months in 1 patient demonstrated maintenance of tic improvement. Pallidal stimulation appeared to be more effective for tic reduction than thalamic or even combination stimulation. However, depressive mood, anxiety and impulsiveness were not affected by pallidal stimulation alone, whilst they showed improvement in thalamic or combination stimulation. The thalamic and pallidal targets gave rise to varying adverse effects with the former including arm paraesthesia and reduced libido whilst the latter included increased anxiety [62,63].

The ALIC, which has been used for sterotactic lesioning in OCD patients and contains fibers that travel between the orbitofrontal cortex and the anterodorsal thalamus was stimulated in a 37 year old female with TS. This resulted in a 25% improvement on the YGTSS, but caused apathy or hypomania as side effects. The target was subsequently switched to the CMPf of the thalamus [42,43] resulting in a YGTSS improvement of 32% with cessation of SIBs that had led to retinal detachment. In a four patient cohort, two patients who had previous surgery at the CM-Pf-Vo, subsequently had ALIC/NA stimulation as rescue surgery with combined stimulation demonstrating superior tic reduction (82.6% than ALIC/NA only (68.1%)) [43]. These comparative studies can inform whether specific targets have a differential effect on tics and co-morbid symptoms which could impact target selection for TS patients with different co-morbidities.

3.5. Clinical Outcome and Targets

In a recent systematic review the thalamic targets of DBS were found to improve YGTSS scores by an average of 47.62% $p < 0.001$ with comparable results for GPi (55.32%), whilst the ALIC/NA regions showed a 44% improvement ($p = 0.017$) albeit in a smaller number of patients [70]. Direct comparisons between targets generally also indicate a lesser effect with ALIC stimulation [50,53]. The co-morbidity outcome across targets revealed a median 31.25% reduction in YBOCS and 38.89% in BDI, but without any statistically significant difference in the outcome of tics or co-morbidity. It should be considered that clinical outcomes are attributed to the target yet the anatomical brain regions ultimately stimulated by DBS depend on precise electrode placing, stimulation parameters, as well as individual anatomical variation [70]. The development of computer models using electrode location and extent of current spread has enabled investigation of the electric field distribution in individual patients using proton-density magnetic resonance imaging (MRI) scans. In one such study of five patients who had DBS targeting the amGPi, patient-specific stimulation confirmed this region to be the main stimulation field. However, three patients showed possible extension into GPe and internal capsule and in two patients with clear extension into the anterior GPe, there was a superior clinical effect. This highlights the importance of analysing the exact position of effective stimulation contacts and correlating outcome with patient specific stimulation fields in order to obtain more valid results about optimal target [71].

Although no definitive predictive factors for improved tic outcome have been identified, a positive correlation was observed between pre-operative YGTSS impairment score and tic reduction following amGPi DBS ($p = 0.01$), whilst the opposite effect was seen for pre-operative YGTSS tic severity and outcome following thalamic DBS. Furthermore there was no correlation between severity of co-morbidity symptoms or with stimulation parameters and tic outcome [70]. This meta-analysis did find a trend towards younger age and improved outcome, suggesting that the neurobiological underpinnings of TS are better impacted by stimulation in the younger population. Interpretation is limited by pooling of results from sub-regions of the thalamus or ventral striatum which could be improved by using individual co-ordinates and settings though these are not always available. These findings nevertheless remain informative and suggest that higher YGTSS impairment scores,

tic severity, patient age and choice of preferred target should all be considered in the selection of patients for DBS.

3.6. Inclusion and Exclusion Criteria

The suitability of DBS in TS patients depends on many factors yet there is much variability around specific inclusion and exclusion criteria across studies. Typically, core criteria focus on accurate diagnosis, high tic severity (typically a YGTSS score >35/50) and resistance to at least three different pharmacological agents [72]. Although psychiatric co-morbidity is a common component of TS, motor and vocal tics should be the main source of disability [7]. In addition, realistic expectations of DBS outcome and adequate social support [22], as well as compliance in attending appointments for outcome assessment or alteration of parameter settings is crucial when selecting patients for DBS. These should all be considered in a multidisciplinary team setting including a neurologist, psychiatrist, neurosurgeon and psychologist.

Exclusion criteria typically include major psychiatric disorders, pregnancy, current substance abuse or dependence and severe cognitive impairment, (supported by a study showing a lack of benefit in a 16 year old boy with TS and mental retardation undergoing DBS, although the outcome of this single case report should not be over-interpreted [49]). Other factors warranting exclusion include structural abnormalities on MRI, general contra-indications for surgery and patients with somatoform disorder [61] which have also been outlined in the European guidelines for TS [73]. Some centres have also used age as an exclusion criteria, restricting DBS to patients over 18 or 25 [73], based on the premise that TS may subside into adulthood and that there are ethical implications for placing patients under potentially unnecessary surgical risk. Nonetheless, adolescence is a crucial period for social, emotional and educational development and preventing younger patients with severe debilitating TS receiving treatment could impact negatively on independence and wellbeing into adult life. This is supported by beneficial reports in younger patients including a 17 year old with SIBs that prevented full time school attendance who showed markedly improved social integration post DBS [37]. Consequently, recent recommendations argue against strict age criteria and suggest that younger patients should be reviewed on a case by case basis, involving a local ethics committee.

3.7. Adverse Effects

Adverse effects can be classified into procedure or stimulation related events with some stimulation effects varying between targets. Stimulating the thalamic CM-Spv-Voi region has been associated with gaze disturbances or visual symptoms which are less often seen when targeting motor regions of the thalamus [34]. Other adverse effects include increased or decreased libido, which can result from modulating certain parts of intra-laminar thalamic nuclei involved in controlling sexual function [74]. In addition, arm paraesthesia, dysarthria and a case of psychosis have been reported.

Stimulation of the pvGPi has been associated with increased anxiety, depression and memory impairment [33], whilst that of the amGPi has also been related to higher anxiety levels, dyskinetic limb movements and a case of hypomania [64]. Stimulation of the ALIC/NA was linked to side effects such as depression, hypomania, as well as a suicide attempt reported in an NA patient with known depressive episodes. The adverse effects of apathy, fatigue, dizziness and weight changes are more common across targets and in many instances adjustment of the stimulation parameters can diminish or eradicate these but target selection should aim to limit their effects.

Procedure related adverse effects mostly centre around hardware malfunction and infections with the latter appearing to be higher in TS compared to other movement disorders. This was suggested by a retrospective study of 272 DBS patients, 39 of whom were treated for TS and showed an overall 3.7% infection rate whilst for TS this was 18 [75]. The higher rate of infection in TS patients was attributed to the compulsive picking at surgical scars in some patients [75] though altered immune function has also been postulated including lower T cell count [76], dysgammaglobulinemia, or an altered immunomodulatory effect of dopamine [77], though this requires further investigation.

3.8. Mechanisms of DBS Action in TS

DBS has demonstrated improvement in patient symptoms across targets yet much remains to be elucidated about its mechanism of action. Some studies have investigated the role of DBS in the dopaminergic modulation of striatothalamic pathways, supported by the postulated hyper-dopaminergic innervation in TS pathology and the use of dopamine antagonists in TS treatment. The first report of modulation of dopaminergic transmission with DBS was in a 22 years old patient who had undergone bilateral thalamic stimulation with a resultant improvement in tics [78]. Six months post surgery [^{8}F] fallypride (FP) positron emission tomography (PET) scans, which quantified the striatal and extrastriatal dopamine 2/3 (D2/3) receptors, showed a 16.3% decrease in dopamine binding potential during on-stimulation compared to off-stimulation conditions, suggesting that DBS may indirectly cause a decrease in dopamine release. In addition, there was an increase in D2/3 receptor availability in the baseline on condition compared to healthy control subjects (n = 20) based on a published control group. A further study using FP PET scans on three patients receiving thalamic DBS demonstrated similar results in dopamine binding during DBS [79]. Although these studies are limited by small sample size and potential anaesthetic effect, they indicate that dopamine modulation may be a component of the therapeutic impact of DBS.

It had previously been shown using electroencephalography that premotor potentials did not precede simple motor tics in TS suggesting that the cortex was not their site of origin [80,81] though more recent contradictory findings have also been published [82]. Microelectrode recordings in thalamic nuclei during DBS surgery has typically shown a burst-firing pattern with an interburst interval ranging from 0.12 to 0.4 s within the low frequency (delta/theta) range (2.5–8 Hz) [83]. Similar results were obtained in a study that demonstrated oscillatory activity at low frequencies [84], which has also been observed in other hyperkinetic movement disorders, such as dystonia [85] suggesting that low-frequency activity and decreased thalamic beta activity could contribute to the pathophysiology of TS. This is supported by correlation with clinical phenotype in a patient who had few tics but severe OCD showing significantly fewer low-frequency oscillations than in local field potentials (LFPs) recorded in patients with severe tics. Further, increased gamma activity (25–45 Hz) recorded from the CM in awake patients with TS (n = 5) correlated with tic improvement and demonstrated that DBS increases the power of LFP gamma oscillations [86]. Therefore, shifting basal ganglia thalamic oscillation power from low to high frequency may be one of the effects of DBS in TS patients, supported by the correlation between increased CM gamma activity and clinical tic reduction [86]. Short-term neuronal mechanisms of DBS in TS have also been investigated using primate models of basal ganglia-mediated motor tics [87]. High frequency stimulation in the anteromedial GPi was shown to significantly reduce the amplitude of tic related phasic changes in the pallidum most likely caused by cellular activity temporally locking with the stimulation pulse [87].

Neuroplasticity is also being recognised as relevant to the effects of DBS supported by the reported shift in magnitude of long-latency response components across stimulation blocks [87]. However in a study investigating thalamic LFP recordings in a 48 years old male with Tourette syndrome 12 months after DBS, LFPs remained in the low frequency range as observed a few days after initial DBS implantation, suggesting that DBS may not cause a persistent change in LFP oscillation pattern [88] though this requires investigation in more patients. Evidence has implicated microglia in the modification of synaptic connections and plasticity which could contribute to functionally immature control networks typical of that seen in TS. The role of DBS in altering the immunobiology of the brain in TS is an interesting avenue of research [89].

Mechanisms of DBS in TS should continue to be explored as they inform both the pathophysiology of the disorder and ways in which DBS delivery can be optimized in patients. When considering the search for an optimal target, the high interconnectivity of basal ganglia structures means it is likely that stimulation in one area will have profound downstream or upstream effects in others and rather than the target being a specific focus of pathology, it may instead block propagation of aberrant signals through a local network [87]. As DBS currents spread through anatomical connections, it may be

useful to consider the effect of target stimulation on these different brain networks through a variety of imaging techniques. Functional magnetic resonance imaging (fMRI) compatible DBS systems could be used to map cortical-subcortical circuits [90] and patient specific tractography activation models (TAMs) could identify white matter pathways and monitor the projections being activated by DBS in individual patients [91]. Resting state functional connectivity MRI, which has previously been used to identify thalamic DBS targets based on connectivity to brain regions in tremor could be applied in a similar way to tics in TS [92]. These methods may help motivate a shift to the stimulation of specific brain networks and potentially customise treatment for varying patient phenotypes.

3.9. Adaptive DBS in TS

Further research into neurophysiological recordings in TS patients can also inform the potential future application of adaptive rather than continuous DBS which may be particularly relevant due to the paroxysmal nature of TS [93]. An adaptive DBS system would allow the pathological neural activity of patients to be used as feedback through variables, such as LFPs recorded by DBS electrodes, informing when tics will arise and leading to a responsive alteration in stimulation to suppress their onset.

The finding that increased gamma band activity and reduced alpha band power in the CM complex of the thalamus correlated with superior clinical outcome [86] could be the starting point for developing specific neural markers correlating with tic onset. Moreover, the GPi has been seen to exhibit low frequency oscillations that precede the electromyographic recording of tics by 50 ms or more, and may mark the premonitory urge of motor tics [88], whilst LFP recordings in ALIC/NA, have shown high beta power oscillations, a potential physiological indicator of OCD activity [88]. However, the reliability of feedback algorithms and the accuracy of correlation of variables such as LFPs with clinical symptoms requires much investigation, particularly as the latter can differ between tic types and individual patients [94] A proof of principle study showed the beneficial effects of scheduled DBS in TS patients [32] and though a closed loop system was not employed it may provide the foundation for applying neuromodulatory approaches. The benefits of an adaptive DBS system pertain to the reduced energy expenditure leading to a prolonged battery life [95], as well as a reduction in stimulation related side effects, such as fatigue or anxiety, potentially further improving patient quality of life.

Nonetheless, the use of adaptive DBS remains highly experimental in all conditions, not least until a consistent neurophysiological biomarker for tic urge is identified and issues of sustained efficacy and potential side effects have been thoroughly investigated in future trials and studies.

4. Discussion

Stimulation applied to different cortico-basal ganglia thalamic network structures appears to improve motor and non-motor symptoms in TS. However, over-interpretation of 'between target comparisons' of these results is unwise as most data are derived from case reports and small prospective series with wide variability in methodology. Although more double-blind controlled studies are required, designing these to ensure adequate optimization of stimulation settings as well as maintenance of patient and investigator blinding can be a challenge [67].

Therefore, study design and patient selection should be carefully considered in the future in order to investigate the relative strength of treatments across studies.

Establishing an optimal target has been controversial as the precise pathophysiology of TS is not yet elucidated and stimulated structures have high interconnectivity. To date, the most commonly used targets have been the thalamus and GPi, which have shown variable but overall promising results. Many patients with electrodes targeting the GPi will have electrode trajectories that also straddle the GPe. Reviewing the data in Tables 1 and 2, the optimal stimulation parameters often include the more dorsal electrodes therefore potentially also preferentially delivering stimulation to the GPe fibres.

Only single studies have investigated the STN and the GPe despite demonstrating beneficial effects in tic reduction. Further, the STN is known to have an excitatory influence on the GPi, which could be

manipulated to affect both the limbic and sensorimotor circuits to a greater extent than using the GPi or thalamus alone. Further insight into the cortico-subcortical networks stimulated by DBS through different imaging modalities will further inform optimal targeting.

Looking closer at patient specific factors related to variability of response could help reveal predictive factors for improved outcome. Results of a meta-analysis suggesting that higher pre-operative YGTSS impairment and younger age in patients targeted in the GPi region, correlated with better tic outcome in the may also inform future inclusion and exclusion criteria. Furthermore, correlating clinical outcome to specific fields of stimulation based on patient specific computer models, may contribute to a more accurate mapping of the optimal target within structures like the GPi/GPe.

Study outcomes have focused on tic reduction using rating scales, such as the YGTSS, and although these are validated and include measures of overall impairment, they are not always an accurate reflection of tic impact on self-esteem and socio-professional life. The social integration of TS patients should be a considered a vital aim of the DBS procedure, determined not only by a reduction in tics, but often more importantly, by that of co-morbid symptoms. Consequently, it is crucial that studies uniformly use scales such as the GTS-QOL, STAI and BDI in order to compare quality of life and co-morbidity outcomes across targets. Further, supportive accounts from caregivers can also increase the accuracy of clinical evaluation.

In order to further assess the efficacy of thalamic DBS there is a need for larger, multi-centre trials with careful consideration of optimal trial design to ensure the outcome of this intervention can be objectively assessed. One proposal would be to perform a direct comparison of thalamic (CMPf) DBS against anteromedial GPI/GPe DBS with the latter electrodes deliberately straddling both GPi and GPe targets. Intraoperative and post-operative recordings from externalized electrodes will continue to be informative regarding the neurophysiological changes associated with tics and OCD/OCB. Confirmation of dopaminergic receptor occupancy post DBS using functional imaging techniques would be useful.

To compare the clinical efficacy of two targets requires a sufficiently long period of time for resolution of surgical swelling and wound healing and stimulation parameters can require long periods before considered optimized. Objective confirmation of efficacy must also include an off stimulation assessment, brief if necessary to allow the impact of stimulation to be distinguished from placebo effects. There is now a worldwide consortium of clinicians including functional neurosurgeons interested in DBS and the design of such future trials are the subject of ongoing discussions.

5. Conclusions

Despite variable outcomes between patients, DBS for TS has shown much promise across targets. The careful design of randomised trials, use of comparative studies and imaging modalities in DBS systems can inform target selection. Considering that the ultimate aim of this procedure is the social integration of patients, future studies should continue to address the treatment of both tics and co-morbidities. Further elucidating the mechanisms of DBS action can help enable its optimization, inform the pathophysiology of TS and future potential applications of adaptive DBS.

Acknowledgments: The Unit of Functional Neurosurgery, Queen Square, receives funding from the Monument trust and the Parkinson's Appeal and receives support from UCL NIHR Biomedical Research Centre.

Author Contributions: Ladan Akbarian-Tefaghi drafted manuscript and Thomas Foltynie and Ludvic Zrinzo edited and revised manuscript.

Conflicts of Interest: The authors declare no conflicts of interest.

References

1. Scharf, J.M.; Miller, L.L.; Mathews, C.A.; Ben-Shlomo, Y. Prevalence of Tourette syndrome and chronic tics in the population-based Avon longitudinal study of parents and children cohort. *J. Am. Acad. Child Adolesc. Psychiatry* **2012**, *51*, 192–201. [CrossRef]

2. American Psychiatric Association. *Diagnostic and Statistical Manual of Mental Disorders*, 5th ed.; American Psychiatric Publishing: Arlington, VA, USA, 2013.
3. Leckman, J.F. Tourette's syndrome. *Lancet* **2002**, *360*, 1577–1586. [CrossRef]
4. Porta, M.; Servello, D.; Sevello, D.; Sassi, M.; Brambilla, A.; Defendi, S.; Priori, A.; Robertson, M. Issues related to deep brain stimulation for treatment-refractory Tourette's syndrome. *Eur. Neurol.* **2009**, *62*, 264–273. [CrossRef] [PubMed]
5. Bloch, M.H.; Leckman, J.F. Clinical course of Tourette syndrome. *J. Psychosom. Res.* **2009**, *67*, 497–501. [CrossRef] [PubMed]
6. Eapen, V.; Cavanna, A.E.; Robertson, M.M. Comorbidities, social impact, and quality of life in Tourette syndrome. *Front. Psychiatry* **2016**, *7*, 97. [CrossRef] [PubMed]
7. Cavanna, A.E.; Eddy, C.M.; Mitchell, R.; Pall, H.; Mitchell, I.; Zrinzo, L.; Foltynie, T.; Jahanshahi, M.; Limousin, P.; Hariz, M.I.; et al. An approach to deep brain stimulation for severe treatment-refractory Tourette syndrome: The UK perspective. *Br. J. Neurosurg.* **2011**, *25*, 38–44. [CrossRef] [PubMed]
8. Alam, M.; Schwabe, K.; Lütjens, G.; Capelle, H.H.; Manu, M.; von Wrangel, C.; Müller-Vahl, K.; Schrader, C.; Scheinichen, D.; Blahak, C.; et al. Comparative characterization of single cell activity in the globus pallidus internus of patients with dystonia or Tourette syndrome. *J. Neural Transm.* **2015**, *122*, 687–699. [CrossRef] [PubMed]
9. Müller-Vahl, K.R.; Grosskreutz, J.; Prell, T.; Kaufmann, J.; Bodammer, N.; Peschel, T. Tics are caused by alterations in prefrontal areas, thalamus and putamen, while changes in the cingulate gyrus reflect secondary compensatory mechanisms. *BMC Neurosci.* **2014**, *15*, 2–11. [CrossRef] [PubMed]
10. Makki, M.I.; Govindan, R.M.; Wilson, B.J.; Behen, M.E.; Chugani, H.T. Altered fronto-striato-thalamic connectivity in children with tourette syndrome assessed with diffusion tensor MRI and probabilistic fiber tracking. *J. Child Neurol.* **2009**, *24*, 669–678. [CrossRef] [PubMed]
11. Tinaz, S.; Malone, P.; Hallett, M.; Horovitz, S.G. Role of the right dorsal anterior insula in the urge to tic in tourette syndrome. *Mov. Disord.* **2015**, *30*, 1190–1197. [CrossRef] [PubMed]
12. Fraint, A.; Pal, G. Deep brain stimulation in Tourette's syndrome. *Front. Neurol.* **2015**, *6*, 170. [CrossRef] [PubMed]
13. Hariz, M.I.; Robertson, M.M. Gilles de la Tourette syndrome and deep brain stimulation. *Eur. J. Neurosci.* **2010**, *32*, 1128–1134. [CrossRef] [PubMed]
14. Leckman, J.F.; Riddle, M.A.; Hardin, M.T.; Ort, S.I.; Swartz, K.L.; Stevenson, J.; Cohen, D.J. The Yale Global Tic Severity Scale: Initial testing of a clinician-rated scale of tic severity. *J. Am. Acad. Child Adolesc. Psychiatry* **1989**, *28*, 566–573. [CrossRef] [PubMed]
15. Goetz, C.G.; Pappert, E.J.; Louis, E.D.; Raman, R.; Leurgans, S. Advantages of a modified scoring method for the Rush video-based tic rating scale. *Mov. Disord.* **1999**, *14*, 502–506. [CrossRef]
16. Goodman, W.K.; Price, L.H.; Rasmussen, S.A.; Mazure, C.; Fleischmann, R.L.; Hill, C.L.; Heninger, G.R.; Charney, D.S. The Yale-Brown obsessive compulsive scale. I. Development, use, and reliability. *Arch. Gen. Psychiatry* **1989**, *46*, 1006–1011. [CrossRef]
17. Cavanna, A.E.; Schrag, A.; Morley, D.; Orth, M.; Robertson, M.M.; Joyce, E.; Critchley, H.D.; Selai, C. The Gilles de la Tourette syndrome-quality of life scale (GTS-QOL): Development and validation. *Neurology* **2008**, *71*, 1410–1416. [CrossRef] [PubMed]
18. Mink, J.W. Basal ganglia dysfunction in Tourette's syndrome: A new hypothesis. *Pediatr. Neurol.* **2001**, *25*, 190–198. [CrossRef]
19. Kaido, T.; Otsuki, T.; Kaneko, Y.; Takahashi, A.; Omori, M.; Okamoto, T. Deep brain stimulation for Tourette syndrome: A prospective pilot study in Japan. *Neuromodulation* **2011**, *14*, 123–129. [CrossRef] [PubMed]
20. Vandewalle, V.; Van Der Linden, C.; Groenewegen, H.J.; Caemaert, J. Stereotactic treatment of Gilles de la Tourette syndrome by high frequency stimulation of thalamus. *Lancet* **1999**, *353*, 724. [CrossRef]
21. Visser-Vandewalle, V.; Temel, Y.; Boon, P.; Vreeling, F.; Colle, H.; Hoogland, G.; Groenewegen, H.J.; van der Linden, C. Chronic bilateral thalamic stimulation: A new therapeutic approach in intractable Tourette syndrome: Report of three cases. *J. Neurosurg.* **2003**, *99*, 1094–1100. [CrossRef] [PubMed]
22. Servello, D.; Porta, M.; Sassi, M.; Brambilla, A.; Robertson, M.M. Deep brain stimulation in 18 patients with severe Gilles de la Tourette syndrome refractory to treatment: The surgery and stimulation. *J. Neurol. Neurosurg. Psychiatry* **2008**, *79*, 136–142. [CrossRef] [PubMed]

23. Porta, M.; Servello, D.; Zanaboni, C.; Anasetti, F.; Menghetti, C.; Sassi, M.; Robertson, M.M. Deep brain stimulation for treatment of refractory Tourette syndrome: Long-term follow-up. *Acta Neurochir.* **2012**, *154*, 2029–2041. [CrossRef] [PubMed]
24. Ackermans, L.; Temel, Y.; Cath, D.; van der Linden, C.; Bruggeman, R.; Kleijer, M.; Nederveen, P.; Schruers, K.; Colle, H.; Tijssen, M.A.J.; et al. Deep brain stimulation in Tourette's syndrome: Two targets? *Mov. Disord.* **2006**, *21*, 709–713. [CrossRef] [PubMed]
25. Bajwa, R.J.; de Lotbiniere, A.J.; King, R.A.; Jabbari, B.; Quatrano, S.; Kunze, K.; Scahill, L.; Leckman, J.F. Deep brain stimulation in Tourette's syndrome. *Mov. Disord.* **2007**, *22*, 1346–1350. [CrossRef] [PubMed]
26. Servello, D.; Sassi, M.; Brambilla, A.; Defendi, S.; Porta, M. Long-term, post-deep brain stimulation management of a series of 36 patients affected with refractory gilles de la tourette syndrome. *Neuromodulation* **2010**, *13*, 187–194. [CrossRef] [PubMed]
27. Idris, Z.; Ghani, A.R.I.; Mar, W.; Bhaskar, S.; Wan Hassan, W.N.; Tharakan, J.; Abdullah, J.M.; Omar, J.; Abass, S.; Hussin, S.; et al. Intracerebral haematomas after deep brain stimulation surgery in a patient with Tourette syndrome and low factor XIIIA activity. *J. Clin. Neurosci.* **2010**, *17*, 1343–1344. [CrossRef] [PubMed]
28. Ackermans, L.; Duits, A.; Temel, Y.; Winogrodzka, A.; Peeters, F.; Beuls, E.A.M.; Visser-Vandewalle, V. Long-term outcome of thalamic deep brain stimulation in two patients with Tourette syndrome. *J. Neurol. Neurosurg. Psychiatry* **2010**, *81*, 1068–1072. [CrossRef] [PubMed]
29. Kuhn, J.; Bartsch, C.; Lenartz, D.; Huys, D.; Daumann, J.; Woopen, C.; Hunsche, S.; Maarouf, M.; Klosterkötter, J.; Sturm, V. Clinical effectiveness of unilateral deep brain stimulation in Tourette syndrome. *Transl. Psychiatry* **2011**, *1*, e52. [CrossRef] [PubMed]
30. Duits, A.; Ackermans, L.; Cath, D.; Visser-Vandewalle, V. Unfavourable outcome of deep brain stimulation in a Tourette patient with severe comorbidity. *Eur. Child. Adolesc. Psychiatry* **2012**, *21*, 529–531. [CrossRef] [PubMed]
31. Savica, R.; Stead, M.; Mack, K.J.; Lee, K.H.; Klassen, B.T. Deep brain stimulation in Tourette syndrome: A description of 3 patients with excellent outcome. *Mayo Clin. Proc.* **2012**, *87*, 59–62. [CrossRef] [PubMed]
32. Okun, M.S.; Foote, K.D.; Wu, S.S.; Ward, H.E.; Bowers, D.; Rodriguez, R.L.; Malaty, I.A.; Goodman, W.K.; Gilbert, D.M.; Walker, H.C.; et al. A trial of scheduled deep brain stimulation for Tourette syndrome: Moving away from continuous deep brain stimulation paradigms. *JAMA Neurol.* **2013**, *70*, 85. [CrossRef] [PubMed]
33. Motlagh, M.G.; Smith, M.E.; Landeros-Weisenberger, A.; Kobets, A.J.; King, R.A.; Miravite, J.; de Lotbinière, A.C.J.; Alterman, R.L.; Mogilner, A.Y.; Pourfar, M.H.; et al. Lessons learned from open-label deep brain stimulation for Tourette syndrome: Eight cases over 7 years. *Tremor Other Hyperkinetic Mov.* **2013**, *1*, 3.
34. Huys, D.; Bartsch, C.; Koester, P.; Lenartz, D.; Maarouf, M.; Daumann, J.; Mai, J.K.; Klosterkötter, J.; Hunsche, S.; Visser-Vandewalle, V.; et al. Motor improvement and emotional stabilization in patients with Tourette syndrome after deep brain stimulation of the ventral anterior and ventrolateral motor part of the thalamus. *Biol. Psychiatry* **2016**, *79*, 392–401. [CrossRef] [PubMed]
35. Cury, R.G.; Lopez, W.O.C.; Dos Santos Ghilardi, M.G.; Barbosa, D.C.; Barbosa, E.R.; Teixeira, M.J.; Fonoff, E.T. Parallel improvement in anxiety and tics after DBS for medically intractable Tourette syndrome: A long-term follow-up. *Clin. Neurol. Neurosurg.* **2016**, *144*, 33–35. [CrossRef] [PubMed]
36. Servello, D.; Zekaj, E.; Saleh, C.; Lange, N.; Porta, M. Deep brain stimulation in Gilles de la Tourette syndrome: What does the future hold? A cohort of 48 patients. *Neurosurgery* **2016**, *78*, 91–100. [CrossRef] [PubMed]
37. Testini, P.; Zhao, C.Z.; Stead, M.; Duffy, P.S.; Klassen, B.T.; Lee, K.H. Centromedian-parafascicular complex deep brain stimulation for Tourette syndrome: A retrospective study. *Mayo Clin. Proc.* **2016**, *91*, 218–225. [CrossRef] [PubMed]
38. Zekaj, E.; Saleh, C.; Porta, M.; Servello, D. Temporary deep brain stimulation in Gilles de la Tourette syndrome: A feasible approach? *Surg. Neurol. Int.* **2015**, *6*, 122.
39. Maciunas, R.J.; Maddux, B.N.; Riley, D.E.; Whitney, C.M.; Schoenberg, M.R.; Ogrocki, P.J.; Albert, J.M.; Gould, D.J. Prospective randomized double-blind trial of bilateral thalamic deep brain stimulation in adults with Tourette syndrome. *J. Neurosurg.* **2007**, *107*, 1004–1014. [CrossRef] [PubMed]
40. Ackermans, L.; Duits, A.; van der Linden, C.; Tijssen, M.; Schruers, K.; Temel, Y.; Kleijer, M.; Nederveen, P.; Bruggeman, R.; Tromp, S.; et al. Double-blind clinical trial of thalamic stimulation in patients with Tourette syndrome. *Brain* **2011**, *134*, 832–844. [CrossRef] [PubMed]
41. Diederich, N.J.; Kalteis, K.; Stamenkovic, M.; Pieri, V.; Alesch, F. Efficient internal pallidal stimulation in Gilles de la Tourette syndrome: A case report. *Mov. Disord.* **2005**, *20*, 1496–1499. [CrossRef] [PubMed]

42. Flaherty, A.W.; Williams, Z.M.; Amirnovin, R.; Kasper, E.; Rauch, S.L.; Cosgrove, G.R.; Eskandar, E.N. Deep brain stimulation of the anterior internal capsule for the treatment of Tourette syndrome: Technical case report. *Neurosurgery* **2005**, *57*, E403. [CrossRef] [PubMed]
43. Shields, D.C.; Cheng, M.L.; Flaherty, A.W.; Gale, J.T.; Eskandar, E.N. Microelectrode-guided deep brain stimulation for Tourette syndrome: Within-subject comparison of different stimulation sites. *Stereotact. Funct. Neurosurg.* **2008**, *86*, 87–91. [CrossRef] [PubMed]
44. Kuhn, J.; Lenartz, D.; Mai, J.K.; Huff, W.; Lee, S.-H.; Koulousakis, A.; Klosterkoetter, J.; Sturm, V. Deep brain stimulation of the nucleus accumbens and the internal capsule in therapeutically refractory Tourette-syndrome. *J. Neurol.* **2007**, *254*, 963–965. [CrossRef] [PubMed]
45. Shahed, J.; Poysky, J.; Kenney, C.; Simpson, R.; Jankovic, J. GPi deep brain stimulation for Tourette syndrome improves tics and psychiatric comorbidities. *Neurology* **2007**, *68*, 159–160. [CrossRef] [PubMed]
46. Dehning, S.; Mehrkens, J.H.; Müller, N.; Bötzel, K. Therapy-refractory tourette syndrome: Beneficial outcome with globus pallidus internus deep brain stimulation. *Mov. Disord.* **2008**, *23*, 1300–1302. [CrossRef] [PubMed]
47. Zabek, M.; Sobstyl, M.; Koziara, H.; Dzierzecki, S. Deep brain stimulation of the right nucleus accumbens in a patient with Tourette syndrome. Case report. *Neurol. Neurochir. Polska* **2008**, *42*, 554–559.
48. Neuner, I.; Podoll, K.; Janouschek, H.; Michel, T.M.; Sheldrick, A.J.; Schneider, F. From psychosurgery to neuromodulation: Deep brain stimulation for intractable Tourette syndrome. *World J. Biol. Psychiatry* **2009**, *10*, 366–376. [CrossRef] [PubMed]
49. Dueck, A.; Wolters, A.; Wunsch, K.; Bohne-Suraj, S.; Mueller, J.U.; Haessler, F.; Benecke, R.; Buchmann, J. Deep brain stimulation of globus pallidus internus in a 16-year-old boy with severe Tourette syndrome and mental retardation. *Neuropediatrics* **2009**, *40*, 239–242. [CrossRef] [PubMed]
50. Servello, D.; Sassi, M.; Brambilla, A.; Porta, M.; Haq, I.; Foote, K.D.; Okun, M.S. De novo and rescue DBS leads for refractory Tourette syndrome patients with severe comorbid OCD: A multiple case report. *J. Neurol.* **2009**, *256*, 1533–1539. [CrossRef] [PubMed]
51. Martinez-Torres, I.; Hariz, M.I.; Zrinzo, L.; Foltynie, T.; Limousin, P. Improvement of tics after subthalamic nucleus deep brain stimulation. *Neurology* **2009**, *72*, 1787–1789. [CrossRef] [PubMed]
52. Martínez-Fernández, R.; Zrinzo, L.; Aviles-Olmos, I.; Hariz, M.; Martinez-Torres, I.; Joyce, E.; Jahanshahi, M.; Limousin, P.; Foltynie, T. Deep brain stimulation for Gilles de la Tourette syndrome: A case series targeting subregions of the globus pallidus internus. *Mov. Disord.* **2011**, *26*, 1922–1930. [CrossRef] [PubMed]
53. Burdick, A.; Foote, K.D.; Goodman, W.; Ward, H.E.; Ricciuti, N.; Murphy, T.; Haq, I.; Okun, M.S. Lack of benefit of accumbens/capsular deep brain stimulation in a patient with both tics and obsessive—Compulsive disorder. *Neurocase* **2010**, *16*, 321–330. [CrossRef] [PubMed]
54. Dehning, S.; Feddersen, B.; Cerovecki, A.; Botzel, K.; Muller, N.; Mehrkens, J.-H. Globus pallidus internus-deep brain stimulation in Tourette's syndrome: Can clinical symptoms predict response? *Mov. Disord.* **2011**, *26*, 2440–2441. [CrossRef] [PubMed]
55. Dong, S.; Zhuang, P.; Zhang, X.-H.; Li, J.-Y.; Li, Y.-J. Unilateral deep brain stimulation of the right globus pallidus internus in patients with Tourette's syndrome: Two cases with outcomes after 1 year and a brief review of the literature. *J. Int. Med. Res.* **2012**, *40*, 2021–2028. [CrossRef] [PubMed]
56. Cannon, E.; Silburn, P.; Coyne, T.; O'Maley, K.; Crawford, J.D.; Sachdev, P.S. Deep brain stimulation of anteromedial globus pallidus interna for severe tourette's syndrome. *Am. J. Psychiatry* **2012**, *169*, 860–866. [CrossRef] [PubMed]
57. Dong, S.; Zhang, X.; Li, J.; Li, Y. The benefits of low-frequency pallidal deep brain stimulation in a patient with Tourette syndrome. *Parkinsonism Relat. Disord.* **2014**, *20*, 1438–1439. [CrossRef] [PubMed]
58. Zhang, J.-G.; Ge, Y.; Stead, M.; Zhang, K.; Yan, S.; Hu, W.; Meng, F.-G. Long-term outcome of globus pallidus internus deep brain stimulation in patients with Tourette syndrome. *Mayo Clin. Proc.* **2014**, *89*, 1506–1514. [CrossRef] [PubMed]
59. Sachdev, P.S.; Mohan, A.; Cannon, E.; Crawford, J.D.; Silberstein, P.; Cook, R.; Coyne, T.; Silburn, P.A. Deep brain stimulation of the antero-medial globus pallidus interna for Tourette syndrome. *PLoS ONE* **2014**, *9*, e104926. [CrossRef] [PubMed]
60. Huasen, B.; McCreary, R.; Evans, J.; Potter, G.; Silverdale, M. Cervical myelopathy secondary to Tourette's syndrome managed by urgent deep brain stimulation. *Mov. Disord.* **2014**, *29*, 452–453. [CrossRef] [PubMed]

61. Smeets, A.Y.J.M.; Duits, A.A.; Plantinga, B.R.; Leentjens, A.F.G.; Oosterloo, M.; Visser-Vandewalle, V.; Temel, Y.; Ackermans, L. Deep brain stimulation of the internal globus pallidus in refractory Tourette syndrome. *Clin. Neurol. Neurosurg.* **2016**, *142*, 54–59. [CrossRef] [PubMed]
62. Houeto, J.L.; Karachi, C.; Mallet, L.; Pillon, B.; Yelnik, J.; Mesnage, V.; Welter, M.L.; Navarro, S.; Pelissolo, A.; Damier, P.; et al. Tourette's syndrome and deep brain stimulation. *J. Neurol. Neurosurg. Psychiatry* **2005**, *76*, 992–995. [CrossRef] [PubMed]
63. Welter, M.-L.; Mallet, L.; Houeto, J.-L.; Karachi, C.; Czernecki, V.; Cornu, P.; Navarro, S.; Pidoux, B.; Dormont, D.; Bardinet, E.; et al. Internal pallidal and thalamic stimulation in patients with Tourette syndrome. *Arch. Neurol.* **2008**, *65*, 952–957. [CrossRef] [PubMed]
64. Kefalopoulou, Z.; Zrinzo, L.; Jahanshahi, M.; Candelario, J.; Milabo, C.; Beigi, M.; Akram, H.; Hyam, J.; Clayton, J.; Kass-Iliyya, L.; et al. Bilateral globus pallidus stimulation for severe Tourette's syndrome: A double-blind, randomised crossover trial. *Lancet Neurol.* **2015**, *14*, 595–605. [CrossRef]
65. Nair, G.; Evans, A.; Bear, R.E.; Velakoulis, D.; Bittar, R.G. The anteromedial GPi as a new target for deep brain stimulation in obsessive compulsive disorder. *J. Clin. Neurosci.* **2014**, *21*, 815–821. [CrossRef] [PubMed]
66. Viswanathan, A.; Jimenez-Shahed, J.; Baizabal Carvallo, J.F.; Jankovic, J. Deep brain stimulation for tourette syndrome: Target selection. *Stereotact. Funct. Neurosurg.* **2012**, *90*, 213–224. [CrossRef] [PubMed]
67. Jimenez-Shahed, J. Design challenges for stimulation trials of Tourette's syndrome. *Lancet Neurol.* **2015**, *14*, 563–565. [CrossRef]
68. Piedimonte, F.; Andreani, J.C.M.; Piedimonte, L.; Graff, P.; Bacaro, V.; Micheli, F.; Vilela Filho, O. Behavioral and motor improvement after deep brain stimulation of the globus pallidus externus in a case of Tourette's syndrome. *Neuromodulation* **2013**, *16*, 55–58. [CrossRef] [PubMed]
69. Huisman-van Dijk, H.M.; van de Schoot, R.; Rijkeboer, M.M.; Mathews, C.A.; Cath, D.C. The relationship between tics, OC, ADHD and autism symptoms: A cross-disorder symptom analysis in Gilles de la Tourette syndrome patients and family-members. *Psychiatry Res.* **2016**, *237*, 138–146. [CrossRef] [PubMed]
70. Baldermann, J.C.; Schuller, T.; Huys, D.; Becker, I.; Timmermann, L.; Jessen, F.; Visser-Vandewalle, V.; Kuhn, J. Deep brain stimulation for tourette-syndrome: A systematic review and meta-analysis. *Brain Stimul.* **2016**, *9*, 296–304. [CrossRef] [PubMed]
71. Wårdell, K.; Kefalopoulou, Z.; Diczfalusy, E.; Andersson, M.; Åström, M.; Limousin, P.; Zrinzo, L.; Hariz, M. Deep brain stimulation of the pallidum internum for Gilles de la Tourette syndrome: A patient-specific model-based simulation study of the electric field. *Neuromodulation* **2015**, *18*, 90–96. [CrossRef] [PubMed]
72. Schrock, L.E.; Mink, J.W.; Woods, D.W.; Porta, M.; Servello, D.; Visser-Vandewalle, V.; Silburn, P.A.; Foltynie, T.; Walker, H.C.; Shahed-Jimenez, J.; et al. Tourette syndrome deep brain stimulation: A review and updated recommendations. *Mov. Disord.* **2015**, *30*, 448–471. [CrossRef] [PubMed]
73. Muller-Vahl, K.R.; Cath, D.C.; Cavanna, A.E.; Dehning, S.; Porta, M.; Robertson, M.M.; Visser-Vandewalle, V. European clinical guidelines for Tourette syndrome and other tic disorders. Part IV: Deep brain stimulation. *Eur. Child. Adolesc. Psychiatry* **2011**, *20*, 209–217. [CrossRef] [PubMed]
74. Piedad, J.C.P.; Rickards, H.E.; Cavanna, A.E. What patients with Gilles de la Tourette syndrome should be treated with deep brain stimulation and what is the best target? *Neurosurgery* **2012**, *71*, 173–192. [CrossRef] [PubMed]
75. Servello, D.; Sassi, M.; Gaeta, M.; Ricci, C.; Porta, M. Tourette syndrome (TS) bears a higher rate of inflammatory complications at the implanted hardware in deep brain stimulation (DBS). *Acta Neurochir.* **2011**, *153*, 629–632. [CrossRef] [PubMed]
76. Kawikova, I.; Leckman, J.F.; Kronig, H.; Katsovich, L.; Bessen, D.E.; Ghebremichael, M.; Bothwell, A.L.M. Decreased numbers of regulatory T cells suggest impaired immune tolerance in children with tourette syndrome: A preliminary study. *Biol. Psychiatry* **2007**, *61*, 273–278. [CrossRef] [PubMed]
77. Ferrari, M.; Termine, C.; Franciotta, D.; Castiglioni, E.; Pagani, A.; Lanzi, G.; Marino, F.; Lecchini, S.; Cosentino, M.; Balottin, U. Dopaminergic receptor D5 mRNA expression is increased in circulating lymphocytes of Tourette syndrome patients. *J. Psychiatr. Res.* **2008**, *43*, 24–29. [CrossRef] [PubMed]
78. Vernaleken, I.; Kuhn, J.; Lenartz, D.; Raptis, M.; Huff, W.; Janouschek, H.; Neuner, I.; Schaefer, W.M.; Grunder, G.; Sturm, V. Bithalamical deep brain stimulation in tourette syndrome is associated with reduction in dopaminergic transmission. *Biol. Psychiatry* **2009**, *66*, e15–e17. [CrossRef] [PubMed]

79. Kuhn, J.; Janouschek, H.; Raptis, M.; Rex, S.; Lenartz, D.; Neuner, I.; Mottaghy, F.M.; Schneider, F.; Schaefer, W.M.; Sturm, V.; et al. In vivo evidence of deep brain stimulation-induced dopaminergic modulation in Tourette's syndrome. *Biol. Psychiatry* **2012**, *71*, 11–13. [CrossRef] [PubMed]
80. Obeso, J.A.; Marsden, C.D. Simple tics in Gilles de la Tourette' s syndrome are not prefaced by a normal premovement EEG potential. *J. Neurol. Neurosurg. Psychiatry* **1981**, *44*, 735–738. [CrossRef] [PubMed]
81. Karp, B.I.; Hallett, M. Extracorporeal "phantom" tics in Tourette's syndrome. *Neurology* **1996**, *46*, 38–40. [CrossRef] [PubMed]
82. Van der Salm, S.M.A.; Tijssen, M.A.J.; Koelman, J.H.T.M.; van Rootselaar, A.-F. The bereitschaftspotential in jerky movement disorders. *J. Neurol. Neurosurg. Psychiatry* **2012**, 1162–1167. [CrossRef] [PubMed]
83. Marceglia, S.; Servello, D.; Foffani, G.; Porta, M.; Sassi, M.; Mrakic-Sposta, S.; Rosa, M.; Barbieri, S.; Priori, A. Thalamic single-unit and local field potential activity in Tourette syndrome. *Mov. Disord.* **2010**, *25*, 300–308. [CrossRef] [PubMed]
84. Zauber, S.E.; Ahn, S.; Worth, R.M.; Rubchinsky, L.L. Oscillatory neural activity of anteromedial globus pallidus internus in Tourette syndrome. *Clin. Neurophysiol.* **2014**, *125*, 1923–1924. [CrossRef] [PubMed]
85. Barow, E.; Neumann, W.J.; Brucke, C.; Huebl, J.; Horn, A.; Brown, P.; Krauss, J.K.; Schneider, G.H.; Kuhn, A.A. Deep brain stimulation suppresses pallidal low frequency activity in patients with phasic dystonic movements. *Brain* **2014**. [CrossRef] [PubMed]
86. Maling, N.; Hashemiyoon, R.; Foote, K.D.; Okun, M.S.; Sanchez, J.C. Increased thalamic gamma band activity correlates with symptom relief following deep brain stimulation in humans with Tourette's syndrome. *PLoS ONE* **2012**, *7*, e44215. [CrossRef]
87. McCairn, K.W.; Iriki, A.; Isoda, M. Deep brain stimulation reduces tic-related neural activity via temporal locking with stimulus pulses. *J. Neurosci.* **2013**, *33*, 6581–6593. [CrossRef] [PubMed]
88. Priori, A.; Giannicola, G.; Rosa, M.; Marceglia, S.; Servello, D.; Sassi, M.; Porta, M. Deep brain electrophysiological recordings provide clues to the pathophysiology of Tourette syndrome. *Neurosci. Biobehav. Rev.* **2013**, *37*, 1063–1068. [CrossRef] [PubMed]
89. Leckman, J.F. Deep brain stimulation for tourette syndrome: Lessons learned and future directions. *Biol. Psychiatry* **2016**, *79*, 343–344. [CrossRef] [PubMed]
90. Gunduz, A.; Morita, H.; Rossi, P.J.; Allen, W.L.; Alterman, R.L.; Bronte-Stewart, H.; Butson, C.R.; Charles, D.; Deckers, S.; de Hemptinne, C.; et al. Proceedings of the second annual deep brain stimulation think tank: What's in the pipeline. *Int. J. Neurosci.* **2015**, *7454*, 1–11. [CrossRef] [PubMed]
91. Hartmann, C.J.; Lujan, J.L.; Chaturvedi, A.; Goodman, W.K.; Okun, M.S.; McIntyre, C.C.; Haq, I.U. Tractography activation patterns in dorsolateral prefrontal cortex suggest better clinical responses in OCD DBS. *Front. Neurosci.* **2016**, *9*, 519. [CrossRef] [PubMed]
92. Anderson, J.S.; Dhatt, H.S.; Ferguson, M.A.; Lopez-Larson, M.; Schrock, L.E.; House, P.A.; Yurgelun-Todd, D. Functional connectivity targeting for deep brain stimulation in essential tremor. *Am. J. Neuroradiol.* **2011**, *32*, 1963–1968. [CrossRef] [PubMed]
93. Almeida, L.; Martinez-Ramirez, D.; Rossi, P.J.; Peng, Z.; Gunduz, A.; Okun, M.S. Chasing tics in the human brain: Development of open, scheduled and closed loop responsive approaches to deep brain stimulation for tourette syndrome. *J. Clin. Neurol.* **2015**, *11*, 122–131. [CrossRef] [PubMed]
94. Rossi, P.J.; Gunduz, A.; Judy, J.; Wilson, L.; Machado, A.; Giordano, J.J.; Elias, W.J.; Rossi, M.A.; Butson, C.L.; Fox, M.D.; et al. Proceedings of the third annual deep brain stimulation think tank: A review of emerging issues and technologies. *Front. Neurosci.* **2016**, *10*, 119. [CrossRef] [PubMed]
95. Arlotti, M.; Rosa, M.; Marceglia, S.; Barbieri, S.; Priori, A. The adaptive deep brain stimulation challenge. *Parkinsonism Relat. Disord.* **2016**, *28*, 12–17. [CrossRef] [PubMed]

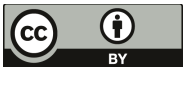

brain sciences

MDPI

Article

Deep Brain Stimulation of the Basolateral Amygdala: Targeting Technique and Electrodiagnostic Findings

Jean-Philippe Langevin [1,*], James W. Y. Chen [2], Ralph J. Koek [3], David L. Sultzer [3], Mark A. Mandelkern [4], Holly N. Schwartz [3] and Scott E. Krahl [5]

1 Neurosurgery Service, VA Greater Los Angeles Healthcare System, Los Angeles, CA 90073, USA
2 Neurology Service, VA Greater Los Angeles Healthcare System, Los Angeles, CA 90073, USA; james.chen1@va.gov
3 Psychiatry and Mental Health Service, VA Greater Los Angeles Healthcare System, Los Angeles, CA 90073, USA; ralph.koek@va.gov (R.J.K.); david.sultzer@va.gov (D.L.S.); holly.schwartz@va.gov (H.N.S.)
4 Radiology Service, Nuclear Medicine VA Greater Los Angeles Healthcare System, Los Angeles, CA 90073, USA; mark.mandelkern@va.gov
5 Research and Development Service, VA Greater Los Angeles Healthcare System, Los Angeles, CA 90073, USA; scott.krahl@va.gov
* Correspondence: jean-philippe.langevin@va.gov; Tel.: +1-310-478-3711

Academic Editors: Tipu Aziz and Alex Green
Received: 30 June 2016; Accepted: 5 August 2016; Published: 10 August 2016

Abstract: The amygdala plays a critical role in emotion regulation. It could prove to be an effective neuromodulation target in the treatment of psychiatric conditions characterized by failure of extinction. We aim to describe our targeting technique, and intra-operative and post-operative electrodiagnostic findings associated with the placement of deep brain stimulation (DBS) electrodes in the amygdala. We used a transfrontal approach to implant DBS electrodes in the basolateral nucleus of the amygdala (BLn) of a patient suffering from severe post-traumatic stress disorder. We used microelectrode recording (MER) and awake intra-operative neurostimulation to assist with the placement. Post-operatively, the patient underwent monthly surveillance electroencephalograms (EEG). MER predicted the trajectory of the electrode through the amygdala. The right BLn showed a higher spike frequency than the left BLn. Intra-operative neurostimulation of the BLn elicited pleasant memories. The monthly EEG showed the presence of more sleep patterns over time with DBS. BLn DBS electrodes can be placed using a transfrontal approach. MER can predict the trajectory of the electrode in the amygdala and it may reflect the BLn neuronal activity underlying post-traumatic stress disorder PTSD. The EEG findings may underscore the reduction in anxiety.

Keywords: amygdala; basolateral nucleus; deep brain stimulation; microelectrode recording; PTSD; targeting technique

1. Introduction

The amygdala is a critical node within a network that regulates emotions. Two functional zones of the amygdala are especially important in this role. The centromedial group is the output of the amygdala: through its efferent connections, it orchestrates the physiological and behavioral components of emotions [1]. The basolateral group receives sensory input and it links emotions to stimuli [2,3]. This function is particularly important because it defines the behavior manifested in response to a stimulus. To fulfill its role, the basolateral amygdala receives modulatory inputs from the medial prefrontal cortex (mPFC) and several other regions, such as the hippocampus and the ventral tegmental area [4,5].

Because it defines the emotional context of behavior, the amygdala has been surgically targeted for intractable psychiatric conditions. Bilateral transfrontal stereotactic amygdalotomies have been performed for patients suffering from intractable aggressiveness [6]. In these cases, aggression was targeted as a symptom regardless of the specific underlying psychiatric condition. The amygdala was understood as a center of fear and anger. Recent studies have shown that the amygdala links both positive as well as negative emotions to stimuli (for review [3]). The amygdala determines if a stimulus should elicit fear (association) or not (extinction). In fact, the basolateral nucleus of the amygdala BLn contains "fear cells" that are active during fear acquisition and consolidation and "extinction cells" that are active during fear extinction [4]. Emotional extinction is a delicate process by which the basolateral nucleus (BLn) learns to no longer elicit an emotion in response to a stimulus. This learning process likely requires plasticity in the BLn, in part induced by modulation from the mPFC [2], whereby a larger population of extinction cells is activated relative to fear cells. In this sense, the BLn can be seen as an emotional receptive field modulated by the mPFC, the hippocampus and several other regions [7]. The relative population of active fear cells and extinction cells can therefore determine the specific response to a reminder. An intense stimulus, such as a life-threatening event, may overwhelm this learning process by forming a stereotypical neurophysiological response in the BLn. In post-traumatic stress disorder (PTSD), a life-threatening event leads to a state of failure of fear extinction that may be understood as a neuroplasticity failure to re-engage extinction cells. In this context, neuromodulation could be focally applied to the BLn to restore fear extinction by modifying the relative volume of active fear cells compared to extinction cells.

Indeed, we have previously shown that BLn deep brain stimulation (DBS) can promote fear extinction in a rodent model of PTSD [8,9]. This effect could translate in patients suffering from PTSD. We are performing an early-phase trial evaluating BLn DBS for treatment-refractory PTSD [10]. In this paper, we aim to describe our targeting technique and intraoperative microelectrode recording (MER) results in a case of bilateral BLn DBS electrode placements. We are aware of only one other human BLn DBS case: a teenage boy was treated successfully for treatment-refractory self-mutilating behavior in the context of severe autism [11].

2. Materials and Methods

2.1. Subject

Our subject is a Gulf War veteran who developed PTSD from participation in a military assault and the subsequent exposure to the bodies of enemy combatants. His baseline Clinician Administered PTSD Scale (CAPS) [12] score was 119, classifying him among the most severely ill patients. He suffered from vivid nightmares during which charred corpses would surround him. Upon exposure to trauma reminders, he would enter an unresponsive, hyper-aroused, dissociated state. He often missed workdays after a triggered flashback and lost several jobs due to absenteeism. He remained severely symptomatic despite 20 years of antidepressant, antipsychotic, antiadrenergic (prazosin) and mood stabilizer pharmacotherapy and cognitive-behavioral psychotherapy. The patient met all the criteria for enrollment in our clinical trial [10], and he gave his informed consent for inclusion before participating in the study. The study was conducted in accordance with the Declaration of Helsinki, and the protocol was approved by the institutional review board of the Greater Los Angeles VA Healthcare System (IRB approval code is PCC#2016-040351).

2.2. Targeting

The patient underwent a stereotactic 3T MRI with gadolinium. The images were re-oriented along the anterior commissure/posterior commissure (AC/PC) in our planning software (FHC, Bowdoin, ME, USA). Targeting the BLn is complicated due to anatomical variations in this region. Using a stereotactic atlas [13], the inferior limit of the BLn is located 16 mm lateral to the AC, 4 mm posterior to the AC and 18 mm inferior to the AC-PC plane. However, these coordinates would

be incorrect for a large number of patients, and targeting has to be performed based on the local mesiotemporal anatomy.

The BLn is located in the inferior portion of the amygdala. It is at the center of the amygdala where it is flanked laterally by the lateral nucleus and medially by the basomedial and basolateral ventromedial part [14]. The central and medial nuclei of the amygdala are dorsal to the BLn. When the MRI is oriented along the AC-PC plane, the fornices can be seen crossing the hypothalamus in the same coronal plane as the BLn within the amygdala [14]. Within this coronal plane, the BLn is located in the center of the amygdala from a medial-to-lateral perspective. When studying the axial plane at this level, the BLn is located just anterior to the tip of the temporal horn, which thus serves as another important landmark [11]. Finally, the inferior border of the BLn is marked by the presence of the head of the hippocampus (Figure 1).

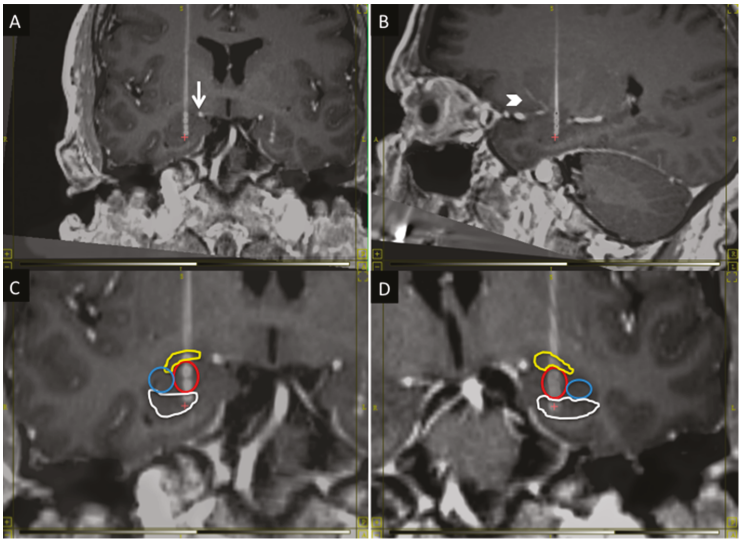

Figure 1. The figure shows the anatomical position of the BLn electrodes in the coronal plane (**A**,**C**,**D**) and sagittal plane (**B**): (**A**) The electrode must avoid the superior extent of the ambient cistern (arrow); (**B**) and the lenticulostriate vessels (arrowhead); (**C**,**D**) respectively show the right and left Bln electrodes with segmentation of the nuclei: in yellow, the central nucleus; in red, the basolateral nucleus; in blue, the lateral nucleus and, in white, the head of the hippocampus. The electrode contact distribution, from dorsal to ventral: Central nucleus (one contact); BLn (two contacts); Hippocampus (one contact). Laterally: Lateral nucleus (zero contacts).

The electrode trajectory must avoid critical structures to permit a safe transfrontal approach. It should be posterior to the lenticulostriate perforator vessels from the first segment of the middle cerebral artery and it should remain lateral to the superior aspect of the ambient cistern (Figure 1). Finally, the trajectory should be seen traversing just anterior to the tip of the temporal horn to confirm the location within the BLn [11]. The location of the entry point will vary depending on the anatomy of the critical structures. In general, it will have a lateral angle of 0–10° from midline and an anterior angle of 70–80° from the AC-PC plane.

2.3. Anesthesia and Microelectrode Recording

Induction was performed with fentanyl and propofol. Subsequently, the patient received sevoflurane until the burr holes were completed. At that point, sevoflurane was stopped, the patient

was awakened and the laryngeal mask was removed. The microelectrode recording (MER) was started on the right side, once the patient had fully regained consciousness, using a platinum-iridium differential electrode (DZAP, FHC). The patient received fentanyl (100 mcg) and midazolam (1 mg) during the right MER and he received fentanyl (50 mcg) and midazolam (1 mg) during the left MER. This medication was administered in order to assist the patient with symptoms of pain and anxiety that became clinically significant as the patient emerged from anesthesia.

The MER was started 20 mm above the target. The microelectrodes were advanced and the signal output was recorded for 30 s at 0.5 mm increments. The unit signals were sampled at 48,000 Hz and were recorded with low- and high-frequency cutoffs of 500 and 5000 Hz, respectively. The spike counts were calculated with a spike threshold set at 150 μvolt (MATLAB, MathWorks, Natick, MA, USA). The spike detection algorithm follows a few rules for automatic spike detection. It only detected spikes in unilateral direction (on the upward deflection) when the signal data point reaches above the threshold of 150 μvolt. It requires the signal data point to decrease below 150 μvolt before a new spike is counted. This algorithm biased toward a low estimate of the actual spike generated because in scenario that multiple discharging units were overlapping one after the other and the waveform stayed above the threshold, the multiple spikes were counted as the same spike. However, this algorithm could avoid a bigger bias by counting every data point above the threshold as a new spike. Spikes were counted per second over the 30 s period, and the mean and standard deviation ($n = 30$) of spike frequency was calculated per recording site.

2.4. EEG Recording

The EEG recording was performed using a clinical EEG machine (Nihon Kohden, Irvine, CA, USA). The electrodes were placed according to the standard international 10–20 system. The EEG tracings were displayed using a double-banana montage. The EEG was studied using conventional clinical analysis techniques.

2.5. Sleep and Nightmares Recording

The most distressing PTSD symptom reported by our patient was the occurrence of severe nightmares. Given the clinical relevance of those episodes for our subject, we elected to measure the impact of BLn DBS on sleep and nightmares. Upon enrollment, he was given a table on which he recorded the hours that he slept every night as well as the number and the subjective intensity (0 none, 10 most severe) of these nightmares. This method of measurement is inherently qualitative, subjective and non-validated. Our aim was to obtain a preliminary sense of the impact of our treatment on subjective sleep experience.

3. Results

3.1. Microelectrode and DBS Lead Positions

The positions of the DBS leads were confirmed using a stereotactic CT scan fused to the preoperative MRI using our planning software (WayPoint, FHC, Bowdoin, ME, USA). The location of microelectrode recordings in relation to the anatomy was extrapolated based on a stereotactic atlas [14], while taking into account the local anatomy and the AC-PC coordinates at each MER recording point.

3.2. Microelectrode Recording

The MER data correlated to the anatomy as predicted by a stereotactic atlas (Figure 2). The initial high-frequency signal was in the position of the ventral globus pallidus externa (GPe) (49 ± 17 Hz on the left and 114 ± 84 Hz on the right). This signal was followed by an area sparse in spikes in the region of the ventroamygdalofugal pathway dorsal to the amygdala. The entry into the amygdala was characterized by an increase in firing frequency in the region of the central nucleus of the amygdala CeA (2 ± 3 Hz on the left and 20 ± 18 Hz on the right). The BLn was characterized by a similar

neuronal firing frequency as the CeA. The dorsal BLn showed 3 ± 3 Hz on the left and 29 ± 19 Hz on the right. The ventral BLn had a spike frequency of 12 ± 13 Hz and 33 ± 30 Hz on the left and right, respectively. The ventral exit from the BLn was characterized with a drop of spikes and background activity consistent with white matter in the region separating the BLn from the hippocampus. The entry into the hippocampus was characterized by high-frequency activity on the right (85 ± 53 Hz), but not on the left (2 ± 4 Hz). Overall, the frequency was higher in the right hemisphere compared to the left.

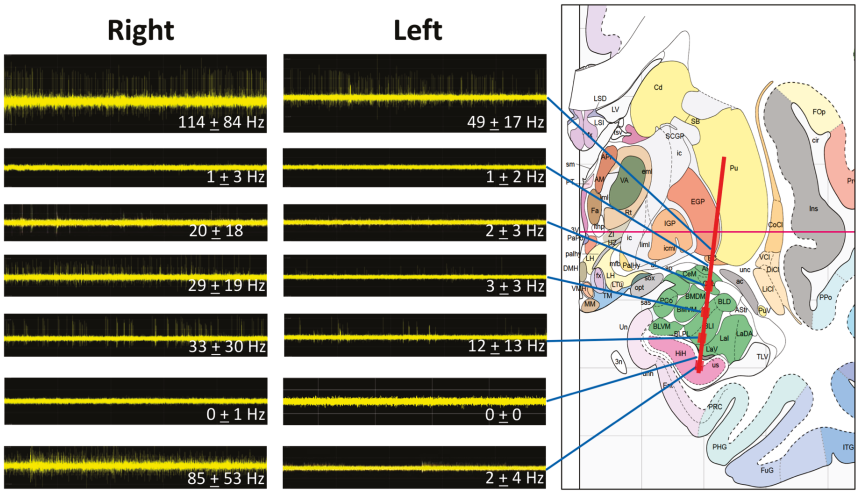

Figure 2. MER signals at different sites along the trajectory of the microelectrode. The predicted trajectory has been superimposed to a stereotactic brain atlas [14]. The MERs match the predicted anatomy with higher frequencies noted in the GPe, the amygdala and the hippocampus. The right side shows a higher frequency than the left side. The entrance and the exit from the amygdala are marked by a drop in background activity.

3.3. Intraoperative Neurostimulation

The patient was awake and able to correspond with the psychiatry team during testing of DBS electrode contacts. The intra-operative neurostimulation was conducted using the implant DBS electrode (3387, Medtronic, Minneapolis, MN, USA). The DBS electrodes were connected to an external neurostimulator (37022, Medtronic, USA) using an alligator clip wire (3550-67, Medtronic, USA) that allows for each contact to be activated individually. For each electrode contact, we used the following stimulation parameters: 120 μs of pulse width, 160 Hz of frequency and an amplitude of 0–5 V increased by increments of 0.5 V. The activation of the contacts located in the BLn triggered memories of places he had been, mainly in his childhood. Some of the scenes were experienced as if from a distance. These were generally experienced as pleasant or amusing. He also experienced emotions of calm. Since his diagnosis of PTSD, he had not had pleasant memories and this represented a new experience for him. The only unpleasant experience was a transient subjective sensation that he could not picture the examiner's face when he closed his eyes, despite accurate recognition by looking at the examiner in person or on an identification card. There were no other adverse events related to the stimulation at amplitudes up to 5 V. Electrical stimulation of the mesiotemporal structures has led to similar experiences in epilepsy patients [15].

3.4. Post-Operative Electroencephalogram

The patient underwent surveillance of a 30 min EEG at baseline and then monthly post-operatively. The predominant muscle artifacts that were noted in awake recordings attenuated significantly after

DBS stimulation. The persistent finding of being able to relax his frontalis muscles suggests that the patient was less anxious or hypervigilant. Over time, the EEG has demonstrated a reduction in the frequency of the posterior dominant rhythm (PDR) from 11 Hz to 9 Hz. Furthermore, the EEG showed progressively more sleep patterns and, by month 10, slow wave sleep was observed on all subsequent EEG studies (Figure 3). The patient reported improved duration and quality of sleep during the same interval. In particular, he reported an average gain of three hours of sleep and a marked reduction in nightmare frequency and severity (Figure 4). These nightmares were reported to the study team and many previous psychiatrists as horrifying re-experiences of combat events that woke him from sleep in an autonomically hyper-aroused state. For years he would get out of bed after these nightmares and stand in a cold shower for an hour or more, trying to "wash off" the residue of charred flesh he had experienced enveloping him during the nightmare. Upon enrollment in the study, given that this was the patient's most distressing PTSD symptom, he was given a recording sheet on which he recorded the number and subjective (0 none, 10 most severe) intensity of these nightmares. As shown in Figure 4, these experiences have decreased in frequency and severity with DBS, and have not recurred as of the time of this writing (18 months after initiation of DBS).

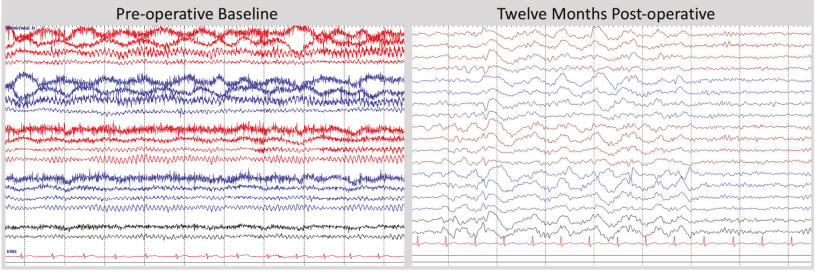

Figure 3. EEG at baseline and one year post-operatively. At baseline, the EEG shows robust PDR and muscle artifacts in the frontal channels, possibly related to anxiety. At one year post-operatively, the EEG shows a reduction in PDR and the presence of SWS, which may reflect a reduction in anxiety. Double Banana montage and a bandwidth of 1–70 Hz were used for displaying EEG tracings. Tracings from the right hemisphere were color-coded as red, and left hemisphere as blue, and sagittal line as black. The tracings from top to bottom in sequence were: F_p2-F8, F8-T4, T4-T6, T6-O2, F_p1-F7, F7-T3, T3-T5, T5-O1, F_p2-F4, F4-C4, C4-P4, P4-O2, F_p1-F3, F3-C3, C3-P3, P3-O1, Fz-Cz, Cz-Oz. One channel EKG tracing, which was in red color, was shown at the bottom.

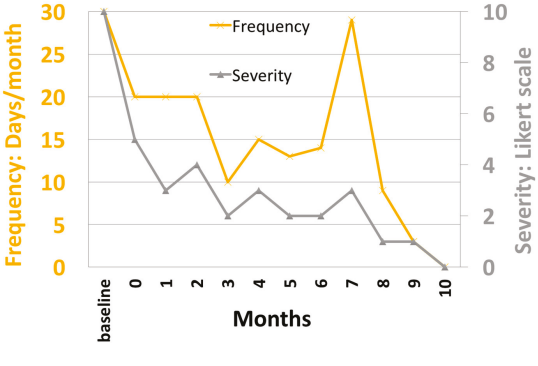

Figure 4. Graph showing the self-reported frequency and intensity of nightmares over time after BLn DBS. After month 10, the patient reported the occurrence of occasional bad dreams that were different from his typical nightmares in quality and intensity.

4. Discussion

BLn DBS may prove beneficial for psychiatric conditions characterized by the failure to extinguish the link between an emotion (fear, pleasure) and a stimulus. Thus far, our patient has shown a substantial clinical improvement [16]. This is the second reported case of BLn DBS [11]. In both cases, a transfrontal trajectory was safely employed. This approach allows for a DBS lead placement that spans the CeA, the BLn, and the head of the hippocampus. These structures are interconnected and have been implicated in PTSD. The transfrontal approach therefore allows us to modulate more than one target nucleus depending on the clinical response. In addition, this trajectory avoids the ventricle and the body of the hippocampus, both of which would be entered during a transoccipital approach. Finally, the transfrontal approach is comfortable for the patient and it permits a safe and tolerable subdermal implantation of the leads. A transtemporal approach would require dividing the temporalis muscle, thus causing pain and possibly interfering with subcutaneous tunneling. The neurostimulation in this acute setting triggered memories of childhood; this experience has been reported with mesiotemporal electrical stimulation in epilepsy patients [15] and may prove predictive of proper electrode placement.

The MER findings were concordant with the anatomy as predicted by a stereotactic atlas. There is a relative paucity of neuronal spikes at the dorsal and the ventral extent of the BLn corresponding to white matter tracts at the margins of the nucleus. MER may predict the trajectory and span of the lead within the BLn. Our MER data also suggested more neuronal spikes in the right subcortical structures compared to the left. Several factors could account for this discrepancy. For instance, differences in anesthesia may account for this finding, although efforts were made to maintain the level of consciousness and the medication administered as constant during the right and the left MERs. Nevertheless, a benzodiazepine and a narcotic agent had to be administered to help the patient with pain and anxiety which became significant as the anesthesia was lifted. Other factors could also explain some of the differences between the right and left MER recordings. The trajectories may have been slightly different and the left electrode may have passed through a region with relative paucity in neurons compared to the right side. Alternatively, our MER findings may represent an overall increase in neuronal activity in the right hemisphere and the right amygdala in the context of PTSD. Other authors have reported hemispheric laterality findings in PTSD. Using resting-state magnetoenceopahlography (MEG), Engdahl et al. [17] showed that PTSD patients have more synchronous neuronal interactions in the right hemisphere compared to normal controls or PTSD patients in remission. Using a SPECT scan, Pagani et al. [18] showed an increase in right hemisphere cerebral blood flow when PTSD patients were exposed to a traumatic reminder compared to normal controls. Our ability to draw any conclusions in regard to this right and left discrepancy in MERs is limited by the fact that we have data for only one subject thus far.

The EEG findings of reduced PDR frequency and increased presence of sleep may reflect an effect of BLn DBS on anxiety. The PDR frequency has been reported to be higher in anxious patients compared to normal controls [19]. This effect on the PDR can serve as a proxy for anxiety whether it is directly related to anxiety or related to the patient's inability to achieve a relaxed state [20]. Clinically, DBS of the amygdala reduced hyper-arousal symptoms and the underlying anxiety associated with PTSD. This effect may translate into an overall reduction in PDR and the appearance of slow-wave sleep SWS on the EEG since the patient is less anxious and is able to fall asleep easily. During the same interval, the patient reported a subjective improvement in duration and quality of sleep. By reducing anxiety, DBS may permit the activation of amygdala circuits critical to sleep. Anxiety can be understood as the psychological percept associated with the inability to activate those sleep circuits due to amygdala-mediated hypervigilance.

5. Conclusions

We describe our targeting technique and intraoperative findings for the placement of BLn DBS electrodes. BLn DBS may prove beneficial in conditions where emotional regulation mechanisms are

dysfunctional, leading to a pervasive state of emotional inflexibility. In severe PTSD, failure of fear extinction causes a generalized association of fear to benign stimuli. In substance abuse, dysfunction in pleasure control leads to a preoccupation with drug-seeking behavior due to a failure of reward extinction. We describe MER findings for a patient with severe PTSD. The MER data may predict the span of the DBS lead within the BLn. Furthermore, the increase in spike frequency can be explained by the increase in metabolism and cerebral blood flow seen in PTSD patients. On EEG, chronic BLn DBS was associated with an overall reduction in the PDR frequency and the presence of SWS. These findings may highlight a reduction in anxiety. Nevertheless, our study is limited to a single subject. In addition, MER in the clinical setting does not clearly distinguish the type and the exact number of neurons being recorded, limiting our analytic capability.

Author Contributions: Jean-Philippe Langevin conceptualized the use of BLn DBS for PTSD, performed the experiments and wrote the manuscript. W.Y. Chen designed the EEG surveillance portion of the protocol and he analyzed the EEG data. Ralph J. Koek designed the protocol, performed the experiments, gathered and analyzed the data. David L. Sultzer participated in the design of the protocol and the analysis of the data. Mark A. Mandelkern participated in the design of the protocol and the analysis of the data. Holly N. Schwartz performed the experiments, participated in gathering the data. Scott E. Krahl participated in the design of the protocol, he performed the experiments and participated in the analysis of the data.

Conflicts of Interest: The authors declare no conflict of interest.

References

1. Freese, J.L.; Amaral, D.G. Neuroanatomy of the primate amygdala. In *The Human Amygdala*; Whalen, P., Phelps, E.A., Eds.; The Guilford Press: New York, NY, USA, 2009; pp. 3–42.
2. Marek, R.; Strobel, C.; Bredy, T.W.; Sah, P. The amygdala and medial prefrontal cortex: Partners in the fear circuit. *J. Physiol.* **2013**, *591*, 2381–2391. [CrossRef] [PubMed]
3. Murray, E.A.; Izquierdo, A.; Malkova, L. Amygdala function in positive reinforcement. In *The Human Amygdala*; Whalen, P., Phelps, E.A., Eds.; The Guilford Press: New York, NY, USA, 2009; pp. 82–104.
4. Luthi, A.; Luscher, C. Pathological circuit function underlying addiction and anxiety disorders. *Nat. Neurosci.* **2014**, *17*, 1635–1643. [CrossRef] [PubMed]
5. Sotres-Bayon, F.; Sierra-Mercado, D.; Pardilla-Delgado, E.; Quirk, G. Gating of fear in prelimbic cortex by hippocampal and amygdala inputs. *Neuron* **2012**, *76*, 804–812. [CrossRef] [PubMed]
6. Mpakopoulou, M.; Gatos, H.; Brotis, A.; Paterakis, K.; Fountas, K. Stereotactic amygdalotomy in the management of severe aggressive behavioral disorders. *Neurosurg. Focus* **2008**, *25*. [CrossRef] [PubMed]
7. Koek, R.J.; Schwartz, H.N.; Scully, S.; Langevin, J.P.; Spangler, S.; Korotinsky, A.; Jou, K.; Leuchter, A. Treatment-refractory posttraumatic stress disorder (TRPTSD): A review and framework for the future. *Prog. Neuropsychopharmacol. Biol. Psychiatry* **2016**, *70*, 170–218. [CrossRef] [PubMed]
8. Langevin, J.P.; De Salles, A.A.F.; Kosoyan, H.; Krahl, S. Deep brain stimulation alleviates posttraumatic stress disorder in a rat model. *J. Psychiatr Res.* **2010**, *44*, 1241–1245. [CrossRef] [PubMed]
9. Stidd, D.A.; Vogelsang, K.; Krahl, S.E.; Langevin, J.P.; Fellous, J.M. Amygdala deep brain stimulation is superior to paroxetine treatment in a rat model of posttraumatic stress disorder. *Brain Stimul.* **2013**, *6*, 837–844. [CrossRef] [PubMed]
10. Koek, R.J.; Langevin, J.P.; Krahl, S.E.; Kosoyan, H.J.; Schwartz, H.N.; Chen, J.W.; Melrose, R.; Mandelkern, M.J.; Sultzer, D. Deep brain stimulation of the basolateral amygdala for treatment-refractory combat post-traumatic stress disorder (PTSD): Study protocol for a pilot randomized controlled trial with blinded, staggered onset of stimulation. *Trials* **2014**, *15*. [CrossRef] [PubMed]
11. Sturm, V.; Fricke, O.; Buhrle, C.P.; Lenartz, D.; Maarouf, M.; Treuer, H.; Mai, J.K.; Lehmkuhl, G. DBS in the basolateral amygdala improves symptoms of autism and related self-injurious behavior: A case report and hypothesis on the pathogenesis of the disorder. *Front. Hum. Neurosci.* **2013**, *6*, 1–10. [CrossRef] [PubMed]
12. Blake, D.D.; Weathers, F.W.; Nagy, L.M.; Kaloupek, D.G.; Gusman, F.D.; Charney, D.S.; Keane, T.M. The development of a clinician-administered PTSD Scale. *J. Trauma Stress* **1995**, *8*, 75–90. [CrossRef] [PubMed]
13. Schaltenbrand, G.; Wahren, W. *Atlas for Stereotaxy of the Human Brain*, 3rd ed.; Thieme: New York, NY, USA, 2005.
14. Mai, J.; Paxinos, G.; Voss, T. *Atlas of the Human Brain*, 3rd ed.; Elsevier: New York, NY, USA, 2008.

15. Bancaud, J.; Brunet-Bourgin, F.; Chauvel, P.; Halgren, E. Anatomical origin of déjà vu and vivid "memories" in human temporal lobe epilepsy. *Brain* **1994**, *117*, 71–90. [CrossRef] [PubMed]
16. Langevin, J.P.; Koek, R.J.; Schwartz, H.N.; Chen, J.W.; Sultzer, D.L.; Mandelkern, M.A.; Kulick, A.D.; Krahl, S.E. Deep brain stimulation of the basolateral amygdala for treatment-refractory posttraumatic stress disorder. *Biol. Psychiatry* **2015**, *79*, 82–84. [CrossRef] [PubMed]
17. Engdahl, B.; Leuthold, A.C.; Tan, H.R.M.; Lewis, S.M.; Winskowski, A.M.; Dikel, T.N.; Georgopoulos, A.P. Post-traumatic stress disorder: A right temporal lobe syndrome? *J. Neural. Eng.* **2010**, *7*. [CrossRef] [PubMed]
18. Pagani, M.; Hogberg, G.; Salmaso, D.; Tarnell, B.; Sanchez-Crespo, A.; Soares, J.; Aberg-Wistedt, A.; Jacobsson, H.; Hallstrom, T.; Larsson, S.A.; et al. Regional cerebral blood flow during auditory recall in 47 subjects exposed to assaultive and non-assaultive trauma and developing or not posttraumatic stress disorder. *Eur. Arch. Psychiatry Clin. Neurosci.* **2005**, *255*, 359–365. [CrossRef] [PubMed]
19. Brazier, M.A.B.; Finesinger, J.E.; Coob, S. A contrast between the electroencephalograms of 100 psychoneurotic patients and those of 500 normal adults. *Am. J. Psychiatry* **1945**, *101*, 443–448. [CrossRef]
20. Lader, M.H.; Wing, L. *Physiological Measures, Sedative Drugs and Morbid Anxiety*; Oxford University Press: London, UK, 1966.

MDPI AG
St. Alban-Anlage 66
4052 Basel, Switzerland
Tel. +41 61 683 77 34
Fax +41 61 302 89 18
http://www.mdpi.com

Brain Sciences Editorial Office
E-mail: brainsci@mdpi.com
http://www.mdpi.com/journal/brainsci

MDPI AG
St. Alban-Anlage 66
4052 Basel
Switzerland

Tel: +41 61 683 77 34
Fax: +41 61 302 89 18

www.mdpi.com

ISBN 978-3-03842-539-7